

ADPRL-TH-81-48

LEVEL

AIR FORCE

AD A110226

HUMAN RESOURCES

1981 IMAGE II CONFERENCE PROCEEDINGS

Compiled by

Eric G. Monroe

OPERATIONS TRAINING DIVISION
Williams Air Force Base, Arizona 85224

November 1981

Final Report

DTIC
SELECTED
JAN 20 1982
H

Approved for public release: distribution unlimited.

LABORATORY

FILE FILE COPY

**AIR FORCE SYSTEMS COMMAND
BROOKS AIR FORCE BASE, TEXAS 78235**

82 01 29 054

When Government drawings, specifications, or other data are used in any product or process in connection with a definitely Government-related purpose, the Government assumes no responsibility or any obligation whatsoever. The fact that the Government may have in any way supplied the said drawings, specifications, or other data, is not to be construed as implying, or otherwise in any manner construed, as licensing the rights in any patent, copyright, or otherwise in any manner construed, as conveying any rights or permission to manufacture, use, or sell any product or invention that may in any way be related thereto.

The Public Affairs Office has reviewed this report, and it is releasable to the National Technical Information Service, where it will be available to the general public, including foreign nationals.

This report has been reviewed and is approved for publication.

MILTON E. WOOD, Technical Director
Operations Training Division

RONALD W. TERRY, Colonel, USAF
Commander

Unclassified

SECURITY CLASSIFICATION OF THIS PAGE (When Data Entered)

REPORT DOCUMENTATION PAGE		READ INSTRUCTIONS BEFORE COMPLETING FORM
1. REPORT NUMBER AFHRL-TR-81-48	2. GOVT ACCESSION NO. AD-A110 286	3. RECIPIENT'S CATALOG NUMBER
4. TITLE (and Subtitle) 1981 IMAGE II CONFERENCE PROCEEDINGS		5. TYPE OF REPORT & PERIOD COVERED Final
		6. PERFORMING ORG. REPORT NUMBER
7. AUTHOR(s) Eric G. Monroe		8. CONTRACT OR GRANT NUMBER(s)
9. PERFORMING ORGANIZATION NAME AND ADDRESS Operations Training Division Air Force Human Resources Laboratory Williams Air Force Base, Arizona 85224		10. PROGRAM ELEMENT, PROJECT, TASK AREA & WORK UNIT NUMBERS 99830451
11. CONTROLLING OFFICE NAME AND ADDRESS HQ Air Force Human Resources Laboratory (AFSC) Brooks Air Force Base, Texas 78235		12. REPORT DATE November 1981
		13. NUMBER OF PAGES 500
14. MONITORING AGENCY NAME & ADDRESS (if different from Controlling Office)		15. SECURITY CLASS. (of this report) Unclassified
		15a. DECLASSIFICATION/DOWNGRADING SCHEDULE
16. DISTRIBUTION STATEMENT (of this Report) Approved for public release; distribution unlimited.		
17. DISTRIBUTION STATEMENT (of the abstract entered in Block 20, if different from Report)		
18. SUPPLEMENTARY NOTES		
19. KEY WORDS (Continue on reverse side if necessary and identify by block number)		
area of interest	computer simulation	flight simulation
behavioral visual research	data base environment	helmet mounted displays
CRT displays	digital landmass system	helmet mounted projectors
computer graphics	electro-optical displays	image generation
computer image generation	forward-looking infrared simulation	laser
20. ABSTRACT (Continue on reverse side, if necessary, and identify by block number)		
<p>These proceedings are a collection of papers presented at the 1981 Image Generation/Display Conference II. The Image Conference is devoted to issues relevant to the development and use of imagery generated and displayed for visual flight simulation. The purpose of the Conference is to provide a forum for presenting and discussing topics concerned with the imagery generated for out-of-the cockpit and sensor visual flight simulation. The Conference was attended by more than 215 representatives of industry, military, aerospace, government, and educational institutions from all the United States, Great Britain, Germany, France, and Canada. The 31 papers presented were compatible with the theme of the Conference, including both engineering research/development and behavioral research. In the engineering area, papers covered such topics as computer-simulated forward-looking infrared and low light-level television imagery, computer image generation (CIG) texturing of curved surfaces, shuttle mission simulation, nap of</p>		

DD FORM 1 JAN 73 1473

EDITION OF 1 NOV 65 IS OBSOLETE

Unclassified

SECURITY CLASSIFICATION OF THIS PAGE (When Data Entered)

Unclassified

SECURITY CLASSIFICATION OF THIS PAGE(When Data Entered)

Item 19 (Continued):

light valve projectors
low light level television simulation
optics
projectors
psychological aspects of visual research
psychophysical aspects of visual processing
sensor simulation
shuttle mission simulation
simulation
tactical combat simulation
visual cues
visual flight simulation
visual illusions
visual simulation
weapons delivery simulation

Item 20 (Continued):

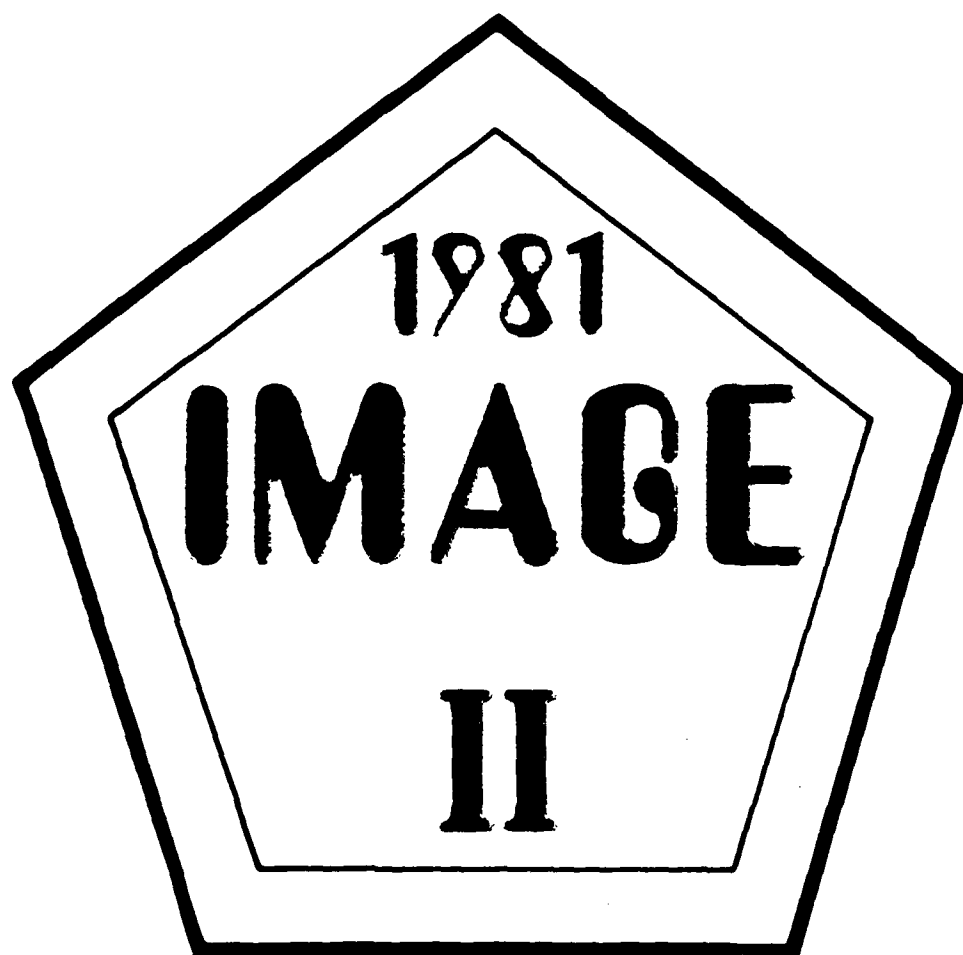
the earth flight simulation, light valve projectors, lasers in simulation, area-of-interest displays, tactical combat simulation, sensor simulation, and helmet-mounted displays. Topics in behavioral research included such items as effects of visual and motion cues, identification of targets in CIC displays, psychophysical aspects of visual processing, visual illusions, visually induced self-motion, determination of visual cue requirements, visual data base development for terrain flight simulation, transformation realism, and strategies to optimize CIC image content.

Accession For	
NTIS GRA&I	<input checked="checked" type="checkbox"/>
DTIC TAB	<input type="checkbox"/>
Unannounced	
Justification	
By	
Distribution	
Availability Codes	
Dist	Avail and/or Special
A	

DTIC
COPY
INSPECTED
8

Unclassified

SECURITY CLASSIFICATION OF THIS PAGE(When Data Entered)

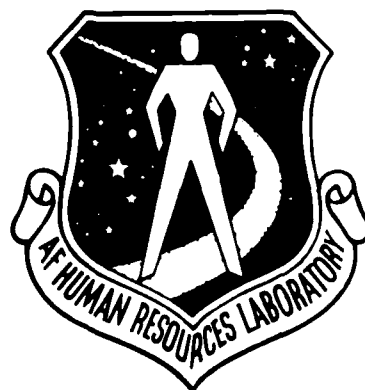


82 01 29 054

**THE
1981
IMAGE
GENERATION/DISPLAY
CONFERENCE
II**

June 10 - 12, 1981

Sponsored by:



**The
Air Force
Human Resources Laboratory**

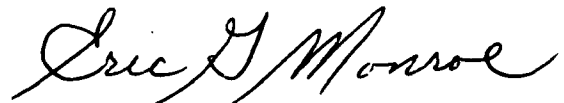
FOREWARD

The 1981 Image Generation/Display Conference II is the only conference devoted entirely to issues relevant to the development and use of imagery generated and displayed for visual flight simulation. The first Conference was held at Williams Air Force Base, Arizona, in May of 1977. The purpose of the Conference is to provide a forum for presenting and discussing topics concerned with the imagery generated for out of the cockpit and sensor visual flight simulation. The Air Force recognizes that the rapid technological advances and uses of real-time visual simulators requires that the interchange of information among the user organizations be expanded in order to promote new developments, applications, and techniques and avoid unnecessary duplication of efforts.

Papers are solicited in all areas compatible with the theme of the Conference; including engineering research and development, behavioral research, application and techniques, specific program's progress and status, as well as technical problems and potential solutions. Pertinent topics include but are not necessarily limited to:

1. Software/hardware developments directly resulting in an enhancement of image capabilities.
2. Psychological determination of visual cue requirements.
3. Environmental data base design and structure.

The Image Generation/Display Conference was conceived in 1977 at the Operations Training Division (formerly the Flying Training Division) of the Air Force Human Resources Laboratory at Williams Air Force Base, Arizona. Since its inception, the Conference has been sponsored by this Laboratory in a continuing effort to pioneer new methods and devices for aircrew training.



ERIC G. MONROE
Conference Chairman

Accession For	
NTIS	<input checked="checked" type="checkbox"/>
GRA&I	<input type="checkbox"/>
DTIC TAB	<input type="checkbox"/>
Unannounced	<input type="checkbox"/>
Justification	
By	
Distribution/	
Availability Codes	
Dist	Avail and/or Special

(Handwritten 'A' in the Dist box)

CONFERENCE COMMITTEE

Colonel Richard C. Needham
Chief, Operations Training Division
Air Force Human Resources Laboratory

Conference Chairman
Eric G. Monroe

Conference Secretary
Audrey L. Vasenko

Conference Treasurer
1Lt Caroline L. Hanson

Conference Subcommittees

Registration:

Audrey L. Vasenko
1Lt Caroline L. Hanson
Laura Miner
Evie Meduna Beyers

Papers:

Eric G. Monroe
Dr Robert S. Kellogg

Program:

Eric G. Monroe
Dr Robert S. Kellogg
Major George Buckland

Audio Visual:

William F. Brubaker
Richard O. Greateorex
SSgt Jeffrey T. Koogler
SrA Denis C. Helble

AFHRL Tour:

1Lt Caroline L. Hanson
1Lt Michael J. Jaskinski
A1C Bernadette Hill
SSgt Jeffrey T. Koogler
SrA Denis C. Helble

Photographer:

Don Fike

TABLE OF CONTENTS

	<u>Page</u>
Introduction Eric G. Monroe	1
Opening Remarks Colonel Richard C. Needham	2
Commander's Comments Colonel Ronald W. Terry	3
 <u>SESSION I</u> Chairman: Dr. Bernard A. Kulp	 4
"Computational Analysis: A Technique for Improving The Visual Simulation of Terrain" Kent A. Stevens	 5
"Simulated FLIR Imagery Using Computer Animated Photographic Terrain Views (CAPTV)" John T. Hooks and Venkat Devarajan	 25
"Simulated A-10 Combat Environment" Robert S. Kellogg, Dirk C. Prather, and Carl H. Castore	 35
"Effects of Visual and Motion Cues on Pilot Effectiveness During Engine-Out Training" George L. Cefeldo, Christopher J. Brady, and Robert K. Knapp	 45
"A Real-Time Computer Image Generation System Using Textured Curved Surfaces" Geoffrey Y. Gardner; Edwin P. Berlin, Jr.; and Robert M. Gelman	 59
 <u>SESSION II</u> Chairman: Capt Thornwell F. Rush, USN	 77
"A 3-D Synthetic Imagery Generator In Real-Time" Pascal Leray	 78
"Low Cost Air-to-Ground Weapons Delivery Simulation Using Microprocessor-Driven Displays" Dorwin L. Kilborn, William R. Phillips, J. Earl Bailey, and James E. Dudgeon	 90
"The Influence of Figural Complexity on the Detection, Recognition, and Identification of Targets in CGI Displays" Moria LeMay	 106
"All Natural Color--Cockpit Bright/Daylight Japanese CGI Systems (A Look at One Japanese Company)" Capt John L. Westland, USNR (Ret)	 121

TABLE OF CONTENTS
(continued)

	<u>Page</u>
<u>P A N E L D I S C U S S I O N</u>	137
<p style="margin-left: 40px;">"What You Always Wanted To Know About CIG But Were Afraid To Ask"</p> <div style="margin-left: 80px;"> <p>Chairman: Herbert A. Cooles</p> <p>Panelists: Colonel John Hall, USAF</p> <p> Colonel Art Deel, USA</p> <p> CDR William Jones, USN</p> <p> Lt Col Dennis Cole, USAF</p> </div>	
<u>S E S S I O N I I I</u>	141
Chairman: LTC Bobby R. Adams, USN	
"Turnkey CAD/CAM Systems in CIG Data Base Creation"	142
John L. Booker and Sam T. Giambarbaree	
"The Shuttle Mission Simulator Visual Databases"	156
Thomas H. Henderson	
"Nap-of-the-Earth (NOE) Maneuvering With Computer Generated Imagery (CGI)"	172
Frank Lewandowski	
"Increased Sensor Simulation Capability as a Result of Improvement to the Digital Landmass System (DLMS) Data Base"	181
Marshall B. Faintich and John Gough	
<u>S E S S I O N I V</u>	197
Chairman: John B. Sinacori	
"Project 2363: Liquid Crystal Light Valve Projector Investigations"	198
Peter C. Baron, Uzi Efron, and Jan Grinberg	
"Light Valve Projection Systems As An Alternate"	220
Fernando B. Neves, Jerome T. Carollo, Warren E. Richeson, and Joe A. Whisenhunt	
"Titus Light Valve Projection System"	233
Francois Desvignes and Jean R. Huriet	
"Helmet Mounted Laser Projector"	241
Denis R. Breglia, Michael Spooner, and Dan Lobb	
<u>S E S S I O N V</u>	259
Chairman: Dr Conrad L. Kraft	
"Some Psychophysical Aspects of Visual Processing of Displayed Information"	260
Yehoshua Y. Zeevi and John G. Daugman	

TABLE OF CONTENTS
(continued)

	<u>Page</u>
"Visual Illusions and Visual Simulation" Duncan L. Dieterly	278
"The Importance of Being Square" Dennis McCormick	286
"Visually Induced Self-Motion Sensation Adapts Rapidly To Left-Right Reversal of Vision" Charles M. Oman	295
"The Relevance of Channel Theory for the Design of Simulator Imagery" David R. Regan, Ronald Kruk, Kenneth Beverley, and Thomas Longridge	307
 <u>D E B A T E</u> Organizer: Dr Ralph Haber	 345
"Is The Eye Sufficient To See?"	
Moderator:	Dr Harry L. Snyder
<u>PRO:</u>	Dr David Regan Dr Ralph Haber
<u>CON:</u>	Dr Herschel Leibowitz Dr Josh Zeevi
 <u>S E S S I O N V I</u> Chairman: Colonel Robert F. Lopina	 349
"Flight Simulator Visual Development and Instructional Features for Terrain Flight Simulation" George H. Buckland, Bernell J. Edwards, and Steve Stephens	350
"A Model-Based Procedure for Determining Visual Cue Requirements" Greg L. Zacharias and William H. Levison	363
"Transformation Realism: An Interactive Evaluation of Optical Information Necessary for the Visual Simulation of Flight" Dean H. Owen	385
"Scaled Subjective Complexity of Low Light Level Television and Forward Looking Infra Red Displays Applied to Computer Image Generation Simulation" Sybil de Groot	401

TABLE OF CONTENTS
(continued)

	<u>Page</u>
<u>S E S S I O N V I I</u> Chairman: Dr Robert M. Howe	419
"Computrol -- A New Technique in Computer Image Generation to CRT Displays" Jerry T. Lewis	420
"A Continuous Wide-Angle Visual System Using Scanned Lasers" Bruce Barker and Paul Murray	430
"Investigation of Simulator Design Features for the Carrier Landing Task" Daniel P. Westra, Charles W. Simon, Stanley C. Collyer, and Walter S. Chambers	448
"Systems Strategies to Optimize CIG Image Content" Michael A. Cosman and Robert A. Schumacker	463
"Area of Interest -- Instantaneous Field of View Vision Model" Dorothy M. Baldwin	481
Closing Remarks Dr. Earl A. Alluisi	497

INTRODUCTION
to the
1981 Image Generation/Display Conference II



Eric G. Monroe
Conference Chairman

It is indeed a personal pleasure to welcome you to the second Image Generation/Display Conference. The participation in the first conference held in May of 1977 exceeded my original conception of a relatively small symposium, consisting primarily of project scientists and engineers interacting at a task level basis. A total of 21 behavioral and engineering papers were presented at that conference. This year, 31 papers will be presented and, upon examination of the Proceedings, I believe you will find the quality of the papers and expertise of their authors second to none in their field. In addition to the papers, a panel discussion entitled "What You Always Wanted To Know About CIG But Were Afraid To Ask" and a debate with the topic "Is the Eye Sufficient To See" have been established in order to encourage more audience participation. As you look around and observe your fellow conferees, I believe you will find them to be neither lacking in experience or credentials. In attendance this year are representatives of industry, military, aerospace, and governmental and educational institutions from all over the United States, Great Britain, Germany, France, and Canada. The result of bringing together this broad spectrum of intellectual talents focusing on the central theme of visual flight simulation should have a synergistic effect in achieving our goals. The primary objective of the Conference is to provide a forum for the exchange of information concerning engineering technology developments and behavioral research issues relative to effective and efficient pilot training with visual flight simulators. The objective of the Conference has not changed over the last four years, but many of the issues and technological capabilities have. Some of these will be raised in the papers, panel discussion, and debate over the next few days. Others will hopefully arise out of your personal interactions at some of the social functions. I believe you will find the environment at the beautiful Registry Resort here in Scottsdale, Arizona, provides an atmosphere conducive to stimulating thought and communication. May you find your attendance here most pleasant and productive.

OPENING REMARKS

Colonel Richard C. Needham
Chief, Operations Training Division
Air Force Human Resources Laboratory
Williams Air Force Base, Arizona



Colonel Richard C. Needham assumed his duties as Operations Training Division Chief in June 1978, after having served as Chief, Flying Training Branch, Deputy Chief of Staff for Personnel, Headquarters USAF, the Pentagon. In his current capacity, Colonel Needham is responsible for the operation and conduct of research on the world's most advanced aircrew training research device. A native of Phoenix, Arizona, he was commissioned a Second Lieutenant in 1955, receiving his initial Air Force assignment as a Radar Observer in the 75th Fighter Squadron at Presque Isle AFB, Maine. He attended pilot training at Moultrie AFB, Georgia and Webb AFB, Texas. After attending gunnery school in F-86F aircraft, he was assigned to Greenville AFB in 1959 as an instructor pilot in T-33 aircraft. He also served for five years as a T-37 instructor pilot at Williams AFB. He received his Bachelor of Science Degree in Political Science from the University of Nebraska in 1965. He is a command pilot with over 4500 flying hours. Military decorations include Silver Star, Distinguished Flying Cross, Air Medal with seven oak leaf clusters, three Presidential Unit Citations and numerous other awards and decorations.

COMMANDER'S COMMENTS

Colonel Ronald W. Terry
Commander, Air Force Human Resources Laboratory
Brooks Air Force Base, Texas



Colonel Ronald W. Terry is Commander, Air Force Human Resources Laboratory, Brooks AFB, TX. Colonel Terry enlisted in the Air Force in June 1952. He graduated from Aviation Cadets and was commissioned May 1954. The next 5 years were spent in operational assignments with the Tactical Air Command in F-86H and F-100 aircraft and a tour in Iceland with the Military Airlift Command.

After graduation from the School of Business at Indiana University in 1961, Colonel Terry was assigned to the Air Force Systems Command. He has served in a wide variety of assignments, including Flight Test as project pilot and test director, Aide to the Commander, ASD, HQ AFSC Monitor for the Air Force Project Shedlight (Night Attack Capability for the Air Force) and also assignments in the DCS/Personnel at HQ AFSC. He was previously assigned Assistant Deputy Chief of Staff/DCS Procurement and Manufacturing, Headquarters Air Force Systems Command.

Colonel Terry is best known as the originator and Director of the Air Force AC-47 and AC-130 Gunship programs. Not only were these systems designed and integrated by Air Force personnel, but these same people saw extensive combat operations throughout US involvement in Vietnam, Laos and Cambodia. The program office was the focal point of combat operations for each model until they were transitioned to the Tactical Air Command. A number of program office personnel (including Colonel Terry) are on the list of most missions and combat hours flown in SEA.

Colonel Terry was a distinguished graduate of the Aviation Cadets in 1954. He graduated with honors in (AFIT) Management at Indiana University in 1961. He was a distinguished graduate of ICAF in 1974. He was the first recipient of the USAF Harold Brown Award. He also received the Harvey C. Knowles Award from the American Ordnance Association and the Citation of Honor Award from the Air Force Association. From the Air Force he has been presented the Legion of Merit with three oak leaf clusters, the Distinguished Flying Cross with two oak leaf clusters, Air Medal with eight oak leaf clusters, the Bronze Star, and other decorations and awards.

SESSION I

Chairman

Dr. Bernard A. Kulp
Chief Scientist, Director of Laboratories
Headquarters, Air Force System Command
Andrews Air Force Base, D.C.



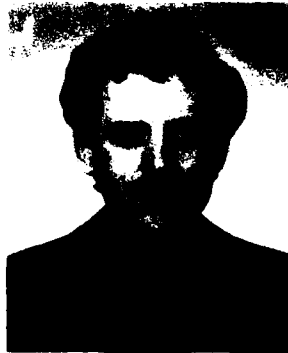
Dr. Bernard A. Kulp is a native of Ohio and received his Ph.D. in Physics from The Ohio State University. He spent eleven years in the Aerospace Research Labs of the Office of Aerospace Research at Wright-Patterson Air Force Base, Ohio, where he conducted research in radiation damage in semiconductors. He is the author of 20 articles in Physical Review, Journal of Applied Physics, and other scientific journals, and was Adjunct Professor of Physics at the Air Force Institute of Technology. From 1965 to 1969 he was engaged in design, development and testing of electro-optic devices and systems for night reconnaissance and guidance and control. He joined Air Force Armament Lab in 1969 as Chief Scientist to assist in the development of a Missile Systems Technology capability. He transferred to Air Force Systems Command in 1975 to be Chief Scientist to the Director of Laboratories.

He was awarded the Exceptional Civilian Service Medal for work in electro-optics.

He is a member of many professional and scientific societies and is a Fellow of the American Association for the Advancement of Science.

**COMPUTATIONAL ANALYSIS: A TECHNIQUE FOR
IMPROVING THE VISUAL SIMULATION OF TERRAIN:
(as applied to low level flight)**

Kent A. Stevens



Kent A. Stevens obtained his Ph.D. from the Massachusetts Institute of Technology in Artificial Intelligence, and his M.S. and B.S. are from the University of California, Los Angeles in Computer Science and in Engineering. His 12 years of experience has involved computer graphics at Hughes Aircraft Company and the National Institutes of Health, followed with academic involvement in robotics at California Institute of Technology, and for the past six years, research into human vision at the M.I.T. Artificial Intelligence Laboratory. His interests are primarily in surface perception and the detection and encoding of texture and contour information.

COMPUTATIONAL ANALYSIS: A TECHNIQUE FOR IMPROVING THE VISUAL SIMULATION OF TERRAIN: (as applied to low level flight)¹

Abstract

Images carry information, and for flight simulation one needs to understand how that information is conveyed in the image, relative to the human visual processes that utilize the information. Developing a useful definition of "information content", however, has been a frustrating enterprise. While images carry information, it is also true that images are ambiguous, and that additional information is necessary for their interpretation. Human vision interprets the image, in part, by utilizing properties of the natural world (such as those which Gibson [1950] brought to our attention) which constrain the possible interpretations. Those constraints are amenable to precise mathematical description, and their theoretical study within a larger computational framework (which we describe here) yields useful insights into "information content" and thus how visible surfaces might be better depicted in the simulator.

1. Introduction

The Air Force has asked the Committee on Vision of the National Research Council to recommend research strategies for improving the visual simulation of low level flight (LLF). Emphasis is placed on LLF because it is a flight regime of increasing importance in combat, and also a regime where significant difficulty has been experienced in its simulation. Pilots who are expert in actual LLF often cannot duplicate their performance in the simulator. When "on the deck" in the simulator they have difficulty both in following the contour of the terrain at low altitude (without crashing) and in judging altitude. In part, the difficulty is technological, for instance the very rapid motion of terrain detail across the display requires fast display processors. Other difficulties are perceptual: the visual displays must convey an adequate 3-D understanding of the terrain over which the pilot must fly. The combination of technological and perceptual problems has prompted some re-examination of the methods for terrain depiction. This article describes a new technique for improving the visual simulation of terrain, as applied to the simulation of LLF.

The introduction will discuss three background issues. The first concerns flight training. Research and development efforts regarding simulators for flight training should be evaluated in terms of their impact on training. However, LLF simulation presents some basic visual problems that must be solved regardless of whether the simulator is used for training or any other purpose. Hence we concentrate here solely on the visual problems of LLF simulation. Next, we show that although CIG displays caricature the real world, they can still convey useful 3-D information. With that observation we turn to problems of defining "information content". Finally, we discuss a computational methodology for studying human vision that approaches complex systems at several levels of detail or specificity, where different theoretical tools are appropriate at each level. This approach has led to succinct and precise descriptions of various processes of human vision (such as stereopsis and edge detection, see later). That point is crucial for its application to flight simulation: even though we currently have only a limited understanding of the overall visual system, many facts that we do know translate into important suggestions for simulator scene generation. The rest of the article attempts to show how that insight comes about.

1. This article will appear as an appendix to the forthcoming report by the Committee on Vision of the National Research Council on research strategies for the visual simulation of low level flight.

1.1 Some remarks regarding training

The flight simulator that we have in mind is a device for training low level flight. But the fact that simulated I.L.F. is difficult to fly for an experienced pilot, let alone a trainee, places the following training issues in a different perspective.

It is often said that a training device should be optimized for the particular training task it will be used for. Thus, for instance, the distinction between training a skill to a novice and training for performance or skill maintenance should be reflected by the simulator system. But it is doubtful that the state of the art of I.L.F. simulation is sufficiently advanced to make this distinction worthwhile. We need a visual simulation that is adequate for the experienced pilot before we may consider optimizing for particular sorts of training.

But one may argue that in emphasizing the visual simulation without regard for its role as a device for training pilots, one might inadvertently concentrate on visual problems that are unimportant to training, or overlook problems that are important to training. In those training tasks for which the visual simulation is at least adequate (as in landings, inflight refueling, and formation flying), the simulation should be optimized for training that task. But for I.L.F. the visual display is still inadequate, hence one needs to concentrate on improving it before addressing issues of training. The pragmatic view taken here is that there are two distinct problems facing simulation: making the display adequate in basic perceptual terms, and making it particularly useful for training. Effort on one problem should not be made at the exclusion of the other. However, we will not deal with issues of training here.

1.2 Simulation is often caricature

When the CIG simulation of I.L.F. is compared to the real world seen from a low flying aircraft, the simulation seems oversimplified and somewhat corrupted by artifacts, such as the stuttering effect that results when the CIG system cannot update the display in the periphery sufficiently often given the large angular velocities associated with I.L.F. One might conclude that the 3-D impression would be adequate if only one had greater display capability. But it is conceivable that even a hundred-fold improvement would not solve the problem.

Insufficiency of detail is not the whole story. A simulation scene is not merely a simplification of a real scene; there are dramatic and qualitative differences. In reducing the bandwidth of a real visual scene to manageable proportions, there is no straightforward sampling technique available -- we cannot merely take every n -th bit of information, as it were. Instead, we construct a novel and unique world out of a relatively few edges, and perhaps shading, color, points, and lines.

The visual world we construct in the simulator shares many similarities with the real world. The single most important similarity is that the rules of perspective geometry are preserved in the simulation. That means the visual world in the simulation behaves optically as we expect. This point should not be underrated, for it is responsible for much of the success of visual simulation. Specifically, the perspective transformation by which the simulator CIG system projects 3-D points, lines, and surfaces from the terrain model onto the 2-D display screen (and in turn, onto the retina so long as the display is viewed from the proper location) precisely corresponds to the way real 3-D points project onto the retina.¹ Consequently, any static view is reproduced with geometric precision (e.g. the proper "texture gradient" is generated because increasingly distant surface elements appear progressively smaller). Also, if the surfaces are modelled as opaque, the CIG system (usually) has the capability to make nearer surfaces occlude from view those that are farther. Moreover, if we move in space, the continuous changes in perspective of points and surfaces also corresponds geometrically to what happens in the real world. Consequently we also have geometrically correct "optic flow", "motion parallax", and so forth (see later). It is the fact that perspective projection is accurately duplicated by the CIG system that was responsible for the compelling effect of space in early night flight

1. But see [Kraft, *et al.* 1980] for engineering considerations

simulators, where only moving luminous dots (such as runway lights and city lights) were projected. As opaque surface shading was added and daytime scenes were simulated, the additional gains came, in part, from the visually apparent occlusion of distant objects by nearer ones. But along with attempts to simulate daytime scenes came the realization that the simulation is very different from the real thing.

One difference of probably minor importance is that the display is effectively a monocular presentation (see later). But just to note a few of the profound differences between the real scene and the simulated counterpart, observe that real surfaces have detail at all scales, and that new detail is continuously revealed as one approaches a surface. But the limited detail that most CIG systems can display, combined with their resolution limits, result in drastically simplified scenes. (This fact may be particularly relevant to the LLF question, as pilots in real flight conceivably use fine recognizable detail, of vegetation and rocks, in order to judge their distance from approaching terrain.) Another difference is that real surfaces are not restricted in their 3-D shape (consider a rolling desert floor, or an eroded canyon wall). But the usual computer representation of curved surfaces in terms of planes bounded by polygons results in a dramatically different sort of terrain than one that would be found in nature. It is not simply the fact that the surface is piecewise planar rather than continuously curved, it is also not true that sharp straight boundaries occur at every junction. Those straight boundaries are also used to denote field boundaries (such as the checkerboards which resemble agricultural land). In fact, the basic element in simulation for representing surfaces is an edge across which screen intensity is sharply discontinuous. That edge may represent a sharp physical feature such as a cliff, ridge, or corner of a building, or a place where the surface reflectance sharply changes such as the boarder of a runway or the edge of a checkerboard square. Some display systems have shading and modulation of contrast to approximate atmospheric haze or fog, but generally the CIG edges are equally sharp and homogeneous -- qualities that are not natural. Another point is that actual surfaces have physical texture in relief above the mean surface level (bushes above the ground, peaks and troughs of waves) but this is costly to generate in current simulator systems. One final difference should be pointed out: actual surfaces reflect light in a complex way depending upon the orientation of the light source (the sun and the overall sky illumination), the orientation of the viewer relative to the surface, and the physical properties of the surface. But generally the intensities of simulated surfaces are unnaturally constant and homogeneous -- even the most sophisticated techniques for shading surfaces are highly simplified.

This discussion is not intended to point out the already-known fact that simulator scenes are *unrealistic*. Its purpose is to show that a CIG display is not merely a simplification of the real world -- it is inevitably a *caricature*. Should we regard the caricature-like qualities of CIG display as detrimental? Not necessarily, for human vision has a remarkable ability to ignore simplifications in illustrations. For instance, we are all familiar with the strong visual impact that even simple line drawings provide, such as seen in engineering and mathematics texts, and in assembly instructions. While they are highly unrealistic, we seldom attend to that fact. Since they carry the necessary 3-D information, they serve their purpose; it does not matter that actual surfaces give rise to more complicated images. Similarly, it may be argued that simulation displays of terrain may be adequate (for purposes of training, etc.) and yet highly unrealistic and caricatured.

1.3 Problems with intuitive and geometric argument

Thus we have that the CIG display may carry the necessary 3-D information despite the unrealistic qualities just described. But we still have to formalize what we mean by "necessary 3-D information". In that pursuit it should be stressed that our intuition should not be trusted. Intuition is often wrong regarding the way the human visual system operates. In short, what we naively believe to govern our visual perceptions is often not the case. It is worthwhile examining one such example in detail. The example involves the familiar "texture gradient", specifically, that the texture *density* seems intuitively to be the crucial depth cue in texture gradients the higher the density, the greater the distance to the surface [Gibson 1950] (and see the geometric analysis in [Purdy 1960]). In fact, distance cannot be inferred directly from density (the following argument is summarized from [Stevens 1980]). The reason is that texture density is a function not only of the distance to

the surface but also of the slant of the surface relative to the viewer (the greater the slant, the greater the foreshortening and hence the greater the texture density). In the case of an arbitrary surface one cannot decouple the relative contributions to the density gradient caused by foreshortening from that due to distance. Consequently one cannot infer distance from texture density. This argument provides an explanation for the largely ignored psychophysical evidence (e.g., [Smith & Smith 1957; Braunstein 1968; Braunstein & Payne 1969]) that texture density is an ineffective cue to distance. This result is contrary to our intuitions. It points out that we must go beyond introspection.

In the same vein, it is not sufficient merely to examine the geometric properties of perspective projection. For instance, the analysis of texture gradients that Purdy [1960] performed set out to find geometric basis for the hypotheses that Gibson [1950] set forth (such as the one just discussed). But such geometric analyses must be carefully regarded, as they implicitly embody certain geometric assumptions, such as that the ground is globally planar (see [Purdy 1960]). The mathematical relations derived with those assumptions, of course, do not hold when the physical surfaces are not so constrained (e.g., when the textured surface is not planar). It is not a straightforward matter to set down the geometric relations that provide the basis for visual interpretation of the image. The relations necessarily incorporate constraints, and it is a separate and non-trivial matter to verify that those constraints are adopted by the actual perceptual processes of human vision. (For further discussion on the matter of constraints and its relation to Gibson's "direct perception" hypothesis, the reader is referred to [Ullman 1980])

1.4 How is information encoded in the image?

Image information content is usually discussed in terms of depth cues such as texture gradients, optic flow, and stereopsis. But to be useful, in particular to be useful for flight simulation, those terms must be defined more precisely than is usual in the psychological literature (see also [Hennesy *et al.* 1980; Semple *et al.* 1980]). To illustrate, consider the difficulty a simulator designer would have trying to apply a general fact about optic flow. For argument, suppose he reads that optic flow provides information about the direction of travel because of the streaming of detail radially away from the point he is approaching [Gibson 1950]. If the designer learns that pilots often lose visual orientation in the simulator (while maneuvering, say), the designer would recall that optic flow is relevant. But the designer is now stuck, in a word, because optic flow was not defined with sufficient specificity that the designer might translate that suggestion into an improved visual display. It is a rather subtle point that optic flow is *inevitable* whenever one moves through other than empty space. Optic flow is a consequence of perspective projection and motion, so regardless of how the terrain is depicted, if one moves across it, the resulting movement of detail across the visual field is optic flow.

The designer is faced with a terrain simulation that is apparently inadequate, seeks to improve it, and knows that optic flow is relevant. So he considers the variables that govern optic flow, those being the parameters of motion relative to the surface as well as the qualities of the surface texture itself. (The faster and lower the aircraft, the more pronounced the apparent optic flow; also, the more densely textured the surface, the greater the effect.) Of these variables, it is only the surface texture that the designer may manipulate, but how to do so? Insight would come from knowing something about how the human visual system measures and internally encodes moving texture and how it extracts 3-D information such as orientation from those measurements. We cannot dismiss this issue in a cavalier manner, trusting that the human visual system will extract what it needs so long as the CIG display is rich enough in detail. Current (and foreseeable) CIG display technology does not (and probably will not) have the capability of reproducing the complex visual texture presented by real LRF over natural terrain. Rather, we should devise more efficient uses of the CIG system's ability to generate texture. We might think of this as "impedance matching", of matching the type of texture that is displayed with the type of visual processing we make on that texture, so as to optimize the information transfer. For instance, the visual display might concentrate its detail at the (instantaneous) point of gaze and capitalize on the fact that visual resolution degrades with

eccentricity.¹ But much more thought is needed; it is not enough to discuss what might be omitted (such as detail in the periphery) but what might be included in the texture. Such thought requires that one examine the visual processes with more analytically than in simple "depth cue" terms.

1.5 A computational information processing approach

We now sketch an approach to the study of vision which has application to visual simulation. It is probably well to remark at the outset that this approach stands among many approaches to vision research. Later we will see how this approach, because of its different perspective, emphasizes certain issues of terrain depiction that have not been addressed previously.

It has long been regarded that vision embodies processes that derive information about the visual world from the interpretation of retinal images. To be sure, virtually every phrase in the previous statement has been contested, cast in a different light, or relatively emphasized by a particular theoretical viewpoint. For instance, Gibson [1950, 1979] characterizes human vision as direct registration of higher order variables in the visual stimuli, thereby downplaying the need for interpretation and information processing (but see [Ullman 1979]). There are some conflicting theories of visual processing, but largely the differences are of emphasis. For instance, some researchers concentrate on the fact that our perception is often as much a product of what we expect as what is objectively present in the image (e.g. [Rock 1977; Hochberg 1978]). Others concentrate on the fact that natural scenes have richly redundant and consistent sources of information, and argue that since human vision probably capitalizes on that fact, experiments using simplified stimuli must be carefully interpreted (e.g. [Haber & Hershenson 1980]).

Another theoretical viewpoint has been developed largely by Marr [1976, 1978, 1981; Marr & Poggio 1977] which examines the information processing aspects of vision. The value of this approach to vision research stems largely from recognizing (i) that human vision involves complex information processing, and (ii) that complex systems are feasibly understood by us only when described at several levels of detail and abstraction. The first point is well accepted by psychologists (in fact, some researchers find the complexity overwhelming and believe we will never understand the processes of vision because of their complexity). The second point is well accepted by engineers, and particularly computer scientists, that see the need for making clean distinctions between the purposes or goals of a complex device, the methods by which it achieves those goals, and the particular nuts-and-bolts details of how they are carried out. The vocabulary used for describing *what* a system accomplishes is very different than that used for describing *how* it does that (at various levels of detail, culminating in the physics of transistors, or whatever comprise the basic building blocks of the system). Complex information processing systems require this sort of multi-level description; any one level of description, alone, would be inadequate. For instance, the circuit diagram of a digital computer at the level of individual transistors and capacitors would be incomprehensible, if it were not for additional descriptions of how the electronic components implement logical functions such as "nand" and "or", and how those functions are sequenced to achieve processes, and so forth. Marr argues that biological information processing should be similarly approached. Neurophysiology and anatomy provide us some understanding of the detailed architecture of the visual system, but just as studying the physics of a transistor reveals nothing about operating systems or Fortran compilers, neither does study of neural synapses reveal the principles of stereopsis or motion perception.

This computational approach describes visual processes at several levels.² Ideally one like to would

1. One should be careful here, because while resolution degrades with eccentricity, temporal processing is still strong (e.g. flicker and motion is readily detected in the periphery).

2. See, e.g., [Marr & Hildreth 1980; Richter & Ullman 1980] for detailed theories of retinal processing and edge detection, [Marr & Poggio 1979; Mayhew & Frisby 1980; Grimson 1980] for computational theories of stereopsis, [Ullman 1979] for visual motion, [Stevens 1980, 1981] for texture gradients and surface contours.

understand some visual process (such as stereopsis) at all levels, from the abstract and mathematical down to the level of neural implementation. But it is only for certain very early stages of visual processing (such as retinal function) that neurophysiological details are feasibly incorporated into a computational theory as of yet (see [Marr & Hildreth 1980; Richter & Ullman 1980]). Of course, one can have significant and useful understanding of a complex mechanism without knowing its implementation details. By and large, the theories emerge "top-down", with the initial insights gained at the level of *what* the visual system computes (regarding, for instance, stereopsis) and the theoretical basis for that computation. This sort of research is reminiscent of Gibson and his followers, for one is concerned with geometric constraints and feasibility. But, in contrast, the computational approach concerns itself with the form in which visual information is encoded or made explicit within the visual system. The 3-D representations are described abstractly, not at the neural level (that sort of understanding is far from us at the present) [Marr 1976, 1978; Marr & Nishihara 1978; Stevens 1980].

In formalizing the computations that underlie vision, one makes rigorous the form in which the visual information is made explicit by the visual system, the sources of that information in the image and how that information is actually extracted and measured, and finally, the computational constraints that are necessary to interpret that information. This sort of vision research has relevance to simulation, therefore, because understanding how information is extracted tells us how it should be presented. Also, the constraints that visual processes incorporate are essentially perceptual assumptions about the nature of the visual world. Those assumptions are either always valid, because of the physics of solid objects, perspective, and optics, or the assumptions are usually valid because of the statistical properties of the world (see [Ullman 1979] for discussion of assumptions in computational terms, and [Gibson 1979] for the related notion of "ecological optics"). These assumptions have relevance to simulation, for in laying out a simulated 3-D environment it is important to have its properties match our visual assumptions, otherwise our perceptual reconstruction of that environment will not correspond to what was intended. A specific example will be given concerning the assumptions underlying our interpretation of surface contours. Those results are primarily geometric; other relevant contributions to simulator research pertain to efficient depictions of texture.

With this introduction, the rest of the article reflects on the problems of depicting terrain for flight simulation from the computational perspective.

2. Shape, orientation, and scale

Let us consider in general terms what the pilot's visual system must accomplish in order that an aircraft may be maneuvered at low altitude over actual terrain. Of course, the shape of the terrain must be perceived in 3-D, so that a close earth-hugging course might be followed. But not merely the shape must be known, but also its size or scale. A small hill and a mountain might have the same shape but differ significantly in scale. We will need to become more specific about shape and scale, but let us continue informally for a moment. One must also know his orientation and attitude relative to the terrain. The pilot, it is reported, envisions himself as following a path through space above the ground, where he keeps a mental trace of where he has been, where he is, and a projection in front of him of where he is going. In large part this must come from his visually perceiving his orientation relative to the terrain. We must also be specific about what this entails.

We have singled out *shape, scale, and orientation* as three classes of visual information necessary for flying over terrain. Although we are being informal in our use of the terms, these three notions seem amenable to a precise definition eventually. But is this decomposition of the visual requirements for LLF into the perception of shape, scale, and orientation the best decomposition for purposes of improving the visual simulation? It certainly seems that each form of information is basic and necessary. On the other hand, concern is perhaps warranted that the shape, scale, and orientation are not sufficiently inclusive; we might be omitting some different quality of 3-D information which is necessary for LLF. (Note that we are not considering information about tactical targets, navigation cues, and so forth. Rather, we are solely concerned with the information that must be gathered by the visual system so that the pilot might fly just above the

terrain.) We do not know the answer to that question; nonetheless, the shape-orientation-scale approach to describing necessary information should prove useful even if not the "whole story".

The distinction between shape and scale is important. Human vision is often surprisingly imprecise about scale: we appreciate the shape of a micro-organism from a scanning electron micrograph without any concern for (or appreciation of) its size; likewise an astrophotograph of a nebula imparts in us no sense of scale. This phenomenon is not difficult to explain theoretically: it is likely that the internal representations of visual shape are inherently scale-independent (see the notion of scales in [Haber & Hershenov 1980] and the representations of surface orientation in [Attneave 1972] and [Marr 1978]). Furthermore, the visual system probably treats as distinct perceptual problems the determination of an object's shape and size. This distinction between shape and scale is often non-intuitive because in everyday scenes we usually have rich sources to both forms of information; there are many convergent perceptual processes that provide information about shape, and there are many means by which we directly and indirectly determine the actual size and distance of visible objects. The scale of our immediate surrounds is usually so precisely known that we interact in it with grace and facility. But we are also faced with natural situations in which the scale information is relatively impoverished. One case with which most of us are familiar concerns viewing the earth from the air, where the shape of the mountains or canyons are clear to us, but their size is appreciated only if, say, we detect a cabin, or a car on a road. We then experience a sudden and sometimes shocking appreciation of the scale of the scene and simultaneously, of the actual distances involved. (The apparent shape remains unchanged, however, after we learn the scale, it is as if independent information is added to our perception.) The crucial points we should draw are two: (i) scale and shape are distinct forms of information about the 3-D world, and (ii) both forms of information are needed in order to interact precisely with the world.

The third class of 3-D information, orientation, has many facets and is closely intertwined with shape. First we will discuss what we mean by orientation, then show how shape and orientation relate. Gibson [1950] discusses two qualities of orientation, one local, the other global. The local orientation of surfaces is defined relative to the viewer, one's orientation in space is defined globally relative to the surrounding visual environment. Let us consider each in turn. It is natural to visualize the orientation of a patch of surface relative to oneself. The slant angle between the line of sight and the normal to the surface is one way of quantifying this. When viewing a large planar surface such as the ground seen from the air, there is a wide range of relative surface orientation (zero slant directly below the aircraft, slant approaching 90 degrees towards the horizon). But we think of the planar surface as having one orientation, not merely a local orientation that depends on which patch of the surface we view. If the plane rolls, we see the orientation of the ground change relative to us. We clearly have the ability to judge orientation more globally, e.g., relative to the horizon.

We have discussed two sorts of orientation information: information about the attitude of individual patches of surfaces relative to the viewer, and the overall orientation of a large surface such as the ground seen from the air. There is another related sort of information which also seems primitive and important: the direction of movement. Whether running through a forest or flying at low altitude, we are visually aware of which way we are travelling relative to the environment.

If we regard shape, orientation, and scale as three types of 3-D information necessary for flying relative to the terrain, we may approach the problems of improving the terrain simulation in these terms. The approach is as follows.

2.1 The basic approach

The visual deficiencies of the LLF simulation would be cast in terms of shape, orientation, and scale. In other words, one would ascertain where the performance problems lie in simulated LLF flight, to what extent the cause is inadequate perception of the shape of the terrain (*is that ridge sharp or is it smoothly rounded? what does the terrain do over to the right?*), inadequate perception of orientation (*is the aircraft yawing? is the ground*

ahead rising or horizontal?), and inadequate perception of scale (*how high am I above the ground? how far is the ridge?*). Insight into the underlying problems cast in these terms might be gained by many means. Pilots might even be verbally examined in these terms, because we all have strong (and similar) understanding of what is meant by shape, orientation, and scale. It was mentioned earlier that pilots commonly remark that judging altitude is difficult. That, for instance, is a matter of scale.

In addition to direct interview, there should be more quantitative psychophysical means for determining what 3-D information is deficient, but again, cast only in terms of shape, orientation, and scale, without attempting to uncover what "depth cues" are missing from the CIG display.

Note that we seem to attack what has been a thorny problem with only very informal and casual terminology. Be assured that the rigor comes later, when we apply knowledge about visual perception to suggest improvements to scale, or whatever. We will see an example of this analysis, when we discuss how shape is perceived from undulating surface contours. This would have importance in the CIG depiction of rolling terrain. First it will be useful to examine a wide range of visual processes so that we begin to sort out which processes concern shape, which concern orientation, and so forth. In a sense, we are abandoning the rather simple notion of "depth cue" for three types of surface information, not just depth. This has proven useful in vision research proper. To illustrate, stereopsis is not merely a "cue" to depth but also of shape, at least; shading also provides shape information but tells us nothing about scale (the shading of the moon is similar to that of an orange). We cannot expect a simple correspondence between process and either shape, or orientation, or scale -- vision is far too intertwined to be cast in such simple terms. But on the other hand, if we know that we need additional information about shape, we have many visual means for providing that information.

Given understanding of where the visual deficiencies lie, and where we might make improvements, we then examine the associated perceptual processes theoretically. It should be understood that our understanding of vision is not sufficiently mature that we might treat this task as a lookup procedure. We have no ready-made recipes in this regard.

As a final introductory remark, note that although we might treat scale, orientation and shape as substantially independent topics, we will probably find that improvements to the CIG display intended to enhance, say, the perception of shape will also improve the apparent orientation, and so forth. These side effects would be welcomed, of course. But the general strategy is to understand how one gains a perception of shape, orientation, and scale, in order to increase the effectiveness of the simulator in inducing those perceptions.

2.2 Shape: what are the sources?

There are several potential sources of information about the shape of a surface, including binocular disparity from stereopsis, visual motion, shading, texture gradients, and surface contours. Let us consider each in turn.

First, although stereopsis provides an acute sense for 3-D shape in our usual environment, it is not useful for large scale shape perception, *e.g.* of terrain a few miles away. The reason is that only the very near terrain causes detectable stereo disparities, and since that portion of the scene is also moving across the field of view at high angular velocity, one must track some near by surface feature; otherwise it is blurred. On the other hand, stereopsis cannot be ruled out as potentially determining *scale*, especially in the foreground (see later).

2.2.1 Motion: *parallax, optic flow, and shear*

Visual motion provides one of the dominant sources of information about shape. Several different aspects of motion have been distinguished, such as "shear" (discontinuities in projected angular velocity which arise, for example, along the edge of a physical object seen against a relatively distant background), "optic flow" (the wide-field visual effect from movement through the environment), and "motion parallax" (the changing projection of an object as it moves relative to us, from which we infer its 3-D shape).

Before discussing these aspects of motion, we reiterate that visual motion across the CIG display comes

automatically when the 3-D model is transformed by perspective projection while "continuously" (*i.e.* at a sufficient rate) updating the viewer's position in that model according to the speed and direction of motion relative to the model. Thus motion *per se* is given; it is *what* is in motion across the CIG display that is relevant to our discussion. For instance, are moving dots sufficient? (Luminous dots are particularly "cheap" to display on many CIG systems while surface patches are in relatively short supply.)

In fact, moving dots are effective: if a collection of 3-D points in some rigid arrangement (such as the runway marker lights and the lights of nearby buildings and streets) are projected in motion on the display as if we were moving relative to them (as in landing) the visual interpretation in 3-D is remarkably precise.¹ Of course, the designers of visual simulator night displays have long been familiar with this. Note the 3-D shape is accurately perceived, but not the scale, unless there are familiar cues such as the runway width (see later).

So we know that points are sufficient stimuli, what about lines and edges? What do they contribute over mere points of light? This perceptual issue has not been fully unravelled, but some relevant observations may be made. Our visual processes seem to require distinct and traceable image points in order to derive 3-D shape, but a curve or line only offers the endpoints or points of discontinuity in tangent; arbitrary intermediate points along the curve cannot be tracked (see [Wallach & O'Connell 1953]). Incidentally, this suggests that only the corner points of the checkerboard pattern (popularly used to depict terrain) contributes useful input to the motion interpretation process.²

When travelling across a textured surface there is an apparent streaming of detail across the visual field, commonly termed *optic flow*. This is regarded as a wide field phenomenon, while the previously discussed motion parallax is detailed and foveal. What 3-D information is derived from optic flow the periphery? Some hypotheses have been forwarded that the optic flow specifies distance up to a scalar [Gibson 1950; Nakayama & Loomis 1974] and even local surface orientation everywhere across the image [Koenderink & van Doorn 1976]. Those two proposals suggest that optic flow provides shape (but not scale) information, but they are largely theoretical; it remains to be seen what sort of 3-D information is derived, in fact, by the human visual system. It is possible that negligible shape information is derived from the periphery, even under the best conditions. Optic flow, particularly in the case of I.I.F., may only provide information about orientation and the direction of travel (this is discussed further later).

Another aspect of visual motion is *motion shear*. Whenever an opaque surface feature protrudes above the mean surface level, it occludes from view that which is behind it. Occlusion thereby provides information about relative distance -- it allow us to partition the visual world into surfaces segregated by distance. This is particularly striking in I.I.F. when the relative motion of nearby ridges against the background terrain causes them to be seen in relief. Since shear contributes to the apparent terrain shape, it deserves study. In particular, the question of *what* is shearing, whether it is a simple dot patterns or edges or lines, is of importance to CIG design. The perception of 3-D shape from motion was only briefly sketched here. Hopefully it shows that while studying the perceptual processes one can also derive specific implications for CIG display.

2.2.2 Shading, texture gradients, and contours

We have considered the dynamic aspects of the visual display. The other side of the coin are the static properties which carry information about shape. These include shading, texture gradients, and contours that lie across the surface.

The apparent 3-D shape of a surface is usually enhanced when shaded. The interpretation of shading

1. See [Ullman 1979] for a theorem proving how this interpretation is feasible solely by analysis of the images without requiring higher level knowledge.

2. But that does not mean one can replace the checkerboard with dots (placed where each corner was) and have an equally compelling 3-D impression. The checkerboard also provides a useful texture gradient, at least. This demonstrates a difficult aspect of this work: visual processes and their visual inputs are largely intertwined.

information is analytically a very difficult problem requiring knowledge of the illuminant directions, the reflectance functions of the various surfaces, and means for dealing with complex shadowing and mutual illumination conditions [Horn 1975]. But the human visual system probably does not attempt such a solution, instead extracts weaker inferences of 3-D shape that would be true without having to know the illumination conditions and the particular reflectance properties of the surface. This probably explains the success of even crude approximations to real shading that are adopted by CIG systems. Further research into human perception of shading should lead to understanding just how simple an approximation to shading can still be effective in the simulator display.

Another source of 3-D information which we will discuss only briefly is the texture gradient. A homogeneous distribution of physical texture across a surface results in a texture gradient in the image. Because of perspective projection, the image texture in every locality is both foreshortened and scaled. We recover shape information (specifically distance up to a scalar) from the texture gradient, but as discussed earlier, probably not from texture density. Further research is needed to determine how texture gradients are measured in order that we may gain insight into how best to depict texture for CIG display.

Contours that lie across a surface, as depicted in figure 1a, are useful for inferring the shape of the surface. To make sense of the contours in the image, however, we must make certain assumptions about their geometry.¹ We will turn this to our advantage by insuring that those assumptions are not violated when modelling terrain by means of contours.

Observe in figure 1a that the lines appear drawn across an undulating surface. The basic assumption that

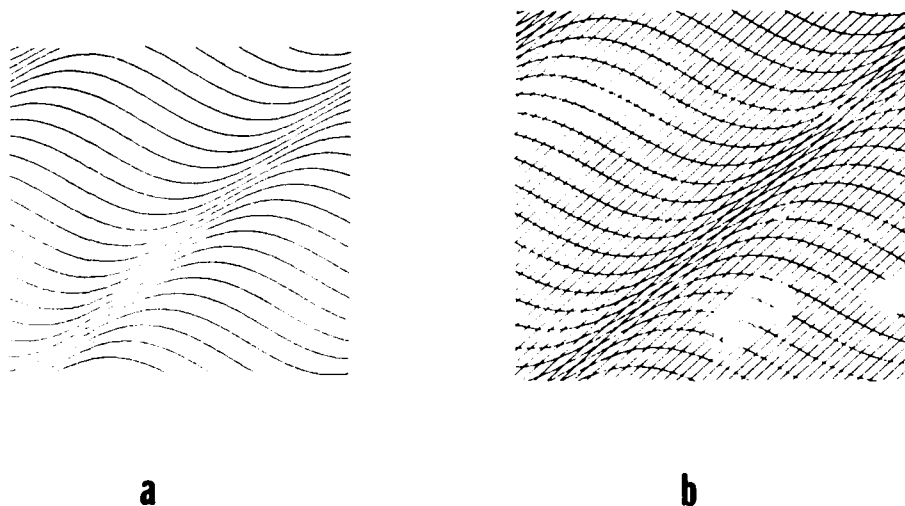


Figure 1. The curved surface in *a* resembles a rippled carpet. The straight lines lie parallel to the ridge, the curved lines are perpendicular. The curved lines are lines of greatest curvature and planar, the straight lines are lines of least curvature. Note that the curved lines alone tell us a great deal about the shape of the surface (*b*), but the straight lines alone carry virtually no information.

1. See [Stevens 1981] for a detailed discussion of surface contours.

we make is that the curvature of the lines reflects surface curvature.¹ It is as if the lines were straight lines on a carpet that became curved because the carpet was rippled. More formally, these contours are *geodesics* with the additional property of being *lines of greatest curvature* (see [Hilbert & Cohn-Vossen 1952] for a lucid discussion of these concepts).

A line of greatest curvature may be thought of as a path across a surface which experiences the greatest undulation. Note that in figure 1b the straight lines that follow the ridges are perpendicular to the lines of greatest curvature. The straight lines are lines of *least* curvature and the surface is singly curved. The perpendicularity of the two curves is very important -- it gives us constraint on the shape of the surface. Roughly speaking, our interpretation of surface contours embodies the following geometric reasoning (the various deductions follow from theorems in Differential Geometry, but they will not be elaborated upon here).

- (i) the physical curves are lines of curvature.
- (ii) intersecting curves meet at a right angle on the surface as a consequence of (i).
- (iii) where the surface contours are parallel the surface is singly curved (like a rippled carpet).
- (iv) because of (i) and (iii) the curves are geodesics and planar.

The above provides the likely basis for our perception of shape from surface contours in images such as figure 1. It may also act as the basis for design rules relevant to simulators.

When modelling terrain, especially undulating terrain, it is commonplace to use curves that resemble the edges of fields, roads, or fences. These curves carry information about the terrain shape just as figure 1 does, but only if they are restricted geometrically in the manner that the human visual system implicitly assumes. That is to say, the curves that a simulator engineer lays in the terrain model should have the following restrictions:

- (i) each curve should be planar, a line of curvature, and geodesic.
- (ii) any intersecting curves should meet at a right angle.
- (iii) if the surface is singly curved, like a smooth ridge, it is only necessary to depict a few lines of greatest curvature (as in figure 1a). The lines parallel to the ridge may be omitted in general.
- (iv) if the surface is doubly curved, like a round hill, it is important to place lines of curvature at close spacing. It is best to include both sets of lines of curvature, so the surface appears to have a net draped over it (figure 1a). Each intersection will then be a right angle, and the surface shape will be readily apparent.

These are a few rules which should be followed. Note that they may be "broken" and we might still correctly perceive the surface from motion, just as we can understand a strange piece of sculpture by walking about it and seeing it from different perspectives. For instance, suppose a ridge were depicted by a contour that climbs over it, but instead of following a line of greatest curvature (the "fall line" as a skier would put it) it climbs obliquely over the ridge. At a glance that curve would mislead us -- we would see the surface shape incorrectly, but with changing viewpoints we might later see the surface correctly and understand that the curve is not what we assumed.

1. Note that we do not easily see figure 1 for what it is, a collection of lines on a flat sheet of paper. Instead, we interpret the undulation as having been caused by the underlying surface.

Depicting surface shape by undulating lines, as just discussed, should be compared with the method of using checkerboards. First of all, checkerboards have been proposed because they are relatively economical in terms of edges, and squares seen in perspective are easily interpreted in 3-D. A checkerboard pattern, in fact, is probably optimal for depicting a *planar* surface, given the current limitations in displayable edges. But the straightforward extension of checkerboards to undulating surfaces may not be the best approach. First let us consider singly curved surfaces -- ripples in a carpet. Checkerboard patterns are useful for ridges so long as the rows are arranged parallel with the ridge. In that case we have the geometric arrangement of figure 1b where the edges of the squares that are parallel with the ridge (in other words, those that lie at constant elevation) are lines of least curvature, and the other edges climb over the ridge. But as stated earlier, the lines of least curvature may probably be omitted because they are redundant. In terms of edges, then, a series of stripes, rather than checkers, would be more economical and probably would be equally effective. For a doubly curved surface such as a round hill, the problem becomes somewhat more difficult, but solvable if sufficiently fine stripes or checkers are used. That is because a doubly curved surface, if sliced fine enough, can be treated as singly curved in general. Incidentally, the line defined by a column or row of checker squares has alternating contrast along its length. This tends to break up the lines, for the visual system has difficulty in aggregating into a line elements with opposite contrast sense. The checkerboard pattern is unlikely treated as a collection of long surface contours, therefore. Instead, each white or black square is seen jointly. For that reason, long stripes or lines may be more useful in depicting undulating terrain.

In sum, parallel undulating lines in an image provide a dramatic sense of 3-D shape, but to be useful they must correspond to 3-D lines that have particular geometric restrictions. So, provided these restrictions are met, we have a powerful method for depicting curved surfaces -- a method which may be more economical and more effective than the traditional checkerboard patterns.

2.3 Sources of information about orientation

The previous discussion covered the major sources of visual information about surface shape. Next is for us to discuss orientation. This discussion is more difficult, because 3-D shape is most naturally described *relative to the viewer* and therefore in representing shape one simultaneously captures several aspects of orientation. For instance, recall that in the night landing simulation, motion parallax involving mere luminous dots on a dark background can give a compelling impression of movement towards the solid earth during landing. Clearly we perceive the orientation of the terrain as well as its shape. While orientation and shape are intertwined, it is useful to approach visual processing from one or the other perspective, depending on the need.

The direction of movement and one's spatial orientation are two forms of orientation information that are relatively distinct from shape. Both are difficult to visually determine in LLF since uneven terrain often prevents one from using a distant horizon as an attitude reference. But optic flow seems useful [Gibson 1950], particularly in LLF, where the terrain appears smeared and blurred (see [Harker & Jones 1980]). However, the highly simplified CIG displays might not provide sufficiently dense surface texture moving with sufficient smoothness of motion to be effective. Again, we see that further research is needed to see how optic flow is visually processed. This research problem is of particular importance to LLF. A final point regarding optic flow should be made. Simply because the ground texture appears blurred and streaky in LLF does not mean that one can display a simple pattern of streaks in the periphery displays. When one tracks a detail on the ground, it becomes roughly stationary on the retina and the smearing of detail vanishes. We do not know what role tracking eye movements would play in LLF (certainly they are important when scrutinizing ground targets, but what importance they have in the basic problem of flying LLF is not yet known).

A local "cue" to orientation which has been incorporated in CIG displays is the simple geometric arrangement of two lines or edges that intersect at right angles on the surface (figure 2a). It is straightforward to show that the image of a right angle (which because of foreshortening in the perspective projection appears as an obtuse angle) carries some information about the surface orientation, but it alone does not specify a

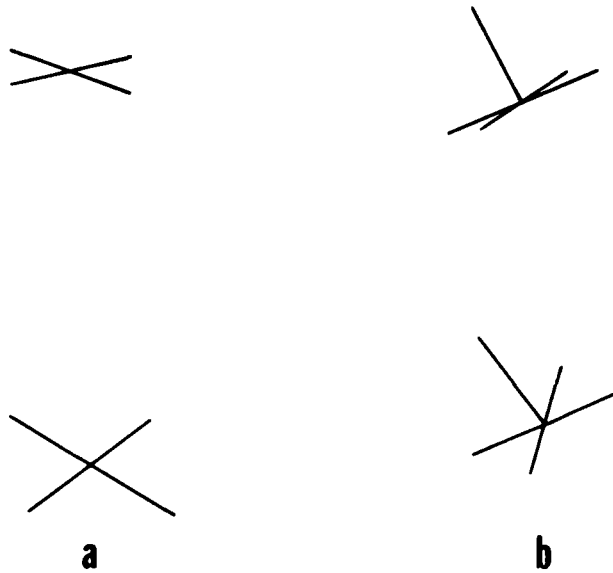


Figure 2. The intersecting lines in *a* appear to lie on planar surfaces in 3-D. The interpretation involves assuming the intersection is perpendicular and the two lines are of equal length on the surface. The intersections in *b* may be thought of as a signpost at a street intersection seen from different viewpoints. To interpret this configuration it is only necessary to assume the intersecting lines are mutually perpendicular in 3-D.

unique 3-D orientation; it could theoretically correspond to a large variety of differently oriented planes in 3-D. Additional constraint comes from assuming that the two lines are *equal length* in 3-D.¹ Note that these two constraints -- perpendicular intersections and equal length segments -- are neatly combined in the square checkerboard patterns which are often used in terrain simulation. Perpendicular intersections in general are useful indicators of surface orientation, provided the lines or edges are of equal length on the surface.

A point that has seldom been emphasized is that a trihedral intersection, three mutually perpendicular lines (figure 2b), actually carries enough information in its image to fix its surface orientation precisely.² The arrangement resembles a signpost at a street intersection -- note that the line segments no longer need to be equal length in 3-D. This configuration would be a very effective means for indicating orientation, even scattered across otherwise featureless terrain.

2.4 Sources of information about scale

Now let us suppose that the terrain simulation is adequate in terms of shape and orientation. The problem that would remain is to insure that he can judge the distance to the surface and his altitude above it with sufficient accuracy. What are the sources of information about *scale* that he might utilize? Scale may be inferred by several perceptual methods: directly from stereopsis, or indirectly from the known size of

1. There is still an ambiguity of the Necker cube variety. But when viewing this configuration within the larger context of the ground plane, that ambiguity is resolved.

2. Again, up to a Necker reversal which can be disregarded here.

recognizable objects, from known velocity, and several other methods that we will discuss. Scale is certainly necessary for various flying tasks; the difficulty that pilots often have in landing amphibious planes on water and maintaining low level flight over water and sand dunes suggests that there are real visual scenes that are deficient in information about scale.

2.4.1 Stereopsis

Stereopsis may, in theory, have a minor contribution at low altitude, but to see this we need to be somewhat quantitative for a moment. A generous estimate of the maximum distance which may be distinguished from infinity by stereopsis is on the order of 1800 ft. (computed from a stereoacuity of 24 arc seconds [Graham, *et al.* 1949]). Objects would be seen "in relief" against the distant horizon only when significantly closer, say 1000 ft. Of course, stereopsis is most useful in the very near environment, say within 30 ft., but since we are sensitive to stereo disparity at larger distances, it might serve a useful purpose in determining the size and distance of somewhat more distant objects. If that is the case, stereopsis might give the pilot a sense of his altitude when flying LLF (some pilots reportedly look out of the side canopy to judge their altitude [Harker & Jones 1980]). We examine that hypothesis here.

At roughly 100 foot altitude the pilot can see downward sufficiently well to be viewing surface detail within the useful range of stereopsis [Kennedy & McKechnie 1970], but because of the blurring and streaking which we have discussed, unless the pilot tracks some feature on the ground, stereopsis would probably fail. But a significant impression of depth might be derived, provided one tracks a surface feature for sufficient time to achieve stereopsis before it is out of view. Consider an aircraft travelling 500 kt. at 100 ft., and a surface feature that passes within 500 ft. of the aircraft at nearest approach. One may easily compute that approximately two seconds elapses from the time the point enters stereo range (1800 ft.) to when it passes directly by the side of the aircraft. Hence if it is still tracked after it is passed by, one has a reasonably long time to judge its distance by stereopsis. Thus it is possible, in theory, that stereopsis directly provides a sense of scale.

There is evidence that casts doubt on this hypothesis, however. The evidence is simple: recall that certain types of terrain are particularly difficult to fly over at low level -- specifically, sand dunes and open water. There is sufficient viewing time to achieve binocular fusion, sufficient visible detail on which to establish stereo fusion, and a large region of the surface is within stereo range at low altitude. Nonetheless LLF is difficult over that terrain. Apparently the sense of scale (if any) that one derives from stereopsis is insufficient for making the critical altitude judgments. Stated another way, stereopsis may play some role in LLF, but it is probably insignificant. It must be said, however, that the above is not conclusive -- the issue deserves careful experimental consideration.

2.4.2 Known size

One method to infer distance is from the measured retinal size of an object of known size. It is well known that the distance to an object varies inversely with the angle it subtends. Theoretically, if one knew that a tree were 20 ft. high, one could also know its absolute distance on the basis of its retinal size. Certainly the visual system capitalizes on this relation, and we even consciously search a novel scene for some cue to its scale (*n.b.* conscious attention is not required, as Helmholtz [1925] recognized in his terming it "unconscious inference"). There are phenomena which strongly suggest that we do infer distance from known size (e.g., [Enright 1970]), however, empirical studies of "size constancy" and absolute distance perception [Rock & McDermott 1964; Epstein & Landauer 1969; Gogel 1971; Hochberg 1971] have shown that the psychophysical relation between distance and retinal size is not as simple as might be expected. This is one place where simulator designers have experienced difficulty in interpreting the psychological literature. Many of the experiments were performed in artificially restricted viewing situations (e.g., darkened rooms with few reference objects) and those that were performed "in the field" would involve verbal judgments of distance, e.g., as a target being so-many feet away [Gibson & Bergman 1954] or comparison judgments between two distances [Foley 1972].

Few experiments reveal just how precisely we perceive the scale of the visual world from objects of known size.

It must be stressed that we are ultimately concerned with the visual judgments of absolute distances, and therefore, with providing sufficient information so that the pilot can fly 100 ft. above the terrain, for instance. The known-size method probably plays a role in this ability. This is another place where tightly-directed investigation is critically needed.

2.4.3 Known velocity

A potentially useful method for computing scale is quite similar to the known-size method just discussed. If one knew the velocity of travel past an object, one could infer the distance to that object from the induced angular velocity (e.g., retinal velocity given a fixed gaze, or velocity relative to some point on the cockpit canopy). The following relation between absolute distance d , absolute velocity V , and angular velocity ω was pointed out by Gibson and others (e.g., [Gibson 1950; Nakayama & Loomis 1974]):

$$d = \frac{V \sin \beta}{\omega}$$

where β is the angle from the direction of travel to the given point whose distance is to be measured. The relation presumes that the given point is stationary and the viewer is in pure translation. It is powerful in that it allows one to compute a depth map for the entire visual field (everywhere there is detail moving across the field of view) in terms of ω and β (measurable, in theory) and the single unknown V . That depth map would specify absolute distance if the absolute velocity V were known.

Conscious deduction is not necessary or even likely in this process. Instead, a pilot experienced in flight at low altitude and high velocity might come to expect a particular angular velocity in the periphery, in a manner analogous to driving a car and expecting the road to slip by at an appropriate rate for any given driving speed.¹ Then if the groundspeed is held constant but the altitude is lower than normal, the angular velocity would be higher than normal, and *vice versa*. This relation could, theoretically, account for the precision with which altitude may be held in I.I.F. by experienced pilots. It is not inconceivable that part of the skill that a pilot acquires through flight training is the unconscious calibration of retinal velocity according to ground speed and altitude, and furthermore the development of an effective feedback loop that attempts to control altitude according to actual retinal velocity at any instant.

It should be relatively straightforward to establish whether this is the case. The direct relationship between altitude and groundspeed predicts that as speed increases there should be a tendency to increase the cruise altitude, other factors being constant. The following evidence [J. Richter, personal communication] suggests that this occurs. Interestingly, it is most apparent when flying over open water (the situation we noted before as difficult). Perhaps the fact that water provides little evidence of scale, compared to a richly textured rural terrain containing familiar surface features, allows one to observe the weaker contribution of the known speed method. Over the ground, one's altitude tends to remain fairly constant as speed increases, but over water the altitude definitely tends to climb as the aircraft is accelerated. It is consistent with there being some unconscious process attempting to maintain an expected angular velocity, where an increase in angular velocity it is attributed to a loss of altitude rather than an increase in ground speed. These informal reports suggest that the known velocity method for computing scale may have some validity in actual flight, and therefore should be given careful experimental investigation. The experiments should probably be performed using unfamiliar surface textures to examine the relationship between speed and altitude. The problem must be addressed in conjunction with an investigation of texture, as there is undoubtedly the effect will vary in magnitude with texture variations.

1. It is noteworthy that when changing from a passenger car to a low sports car the apparent speed is greater merely because of the larger angular velocities associated with being nearer the ground.

2.4.4 Other methods

In addition to the two methods just discussed, there are other geometrical methods for gaining scale information. Several have been discussed by Harker and Jones [1980]. Typically they consist of some geometric quantity -- e.g., the ratio of angle subtended by some vertical surface feature compared to its angular distance below the horizon -- from which one may judge whether the altitude is maintained constant, or whether the aircraft will clear a vertical obstacle.¹ While strictly speaking these geometric quantities do not specify *scale* in the sense we mean, they are, nonetheless, potentially useful in flying. We probably should distinguish between qualitative problems that can be solved geometrically (such as obstacle clearance and maintaining constant altitude) and quantitative problems (such as clearing obstacles *by so many feet*, maintaining a *particular* altitude, and so forth). But it is not certain which sort of problem, the qualitative or the quantitative, deserves the greater attention at the moment.

3 Concluding remarks

Three types of 3-D information that must be gathered by the visual system in order that a pilot might fly close to the terrain are its scale, shape, and orientation. The visual deficiencies of the I.I.F. simulation can be discussed in such terms. Indications are that scale information requires the greatest improvement.

More rigorous analysis comes next. We gain insight into improving the display by learning how the human visual system determines scale (for example). There are many sources of scale information, but much more effort is required before we can make concrete suggestions regarding CIG improvements.

We did see an example of where the computational analysis of surface contours, a source of shape information, leads to rather specific suggestions regarding the visual display. For our visual systems to make sense of image curves in terms of actual contours lying across physical surfaces, a number of geometric assumptions have to be made. Analyzing what these might be, in theory, coupled with psychophysical verification that *those* particular assumptions are involved in our interpretation process, and not some other set of assumptions, leads to some design rules, as it were. The design rules are intended for the simulator engineer who depicts terrain using curves (one curve might be meant to depict a fence over a hill, another might depict the edge of a field). It is of course important that the pilot perceive the simulated world in the way that it was intended by the designer. To do so, the contours placed in the terrain model should be restricted in their geometry so that they match the geometric assumptions that govern their visual interpretation.

The surface contour example is a particularly clean demonstration of how understanding some aspect of vision has application to simulation. As should be evident from the previous discussions, much needs to be learned about vision. But the sorts of questions that we ask can be efficiently guided by applying the computational methodology.

Acknowledgments

A number of people made important contributions and suggestions: Prof. W. Richards and Drs. S. Collyer, D. Regan, J. Richter, and S. Ullman. The author gratefully acknowledges the useful comments on an earlier draft of this article provided by Drs. K. Dismukes, R. Haber, and J. Hochberg. The manuscript was prepared at the Artificial Intelligence Laboratory of the Massachusetts Institute of Technology, with support provided in part by the Advanced Research Projects Agency of the Department of Defense under Office of Naval Research contract N00014-75-C-0643 and in part by the AFOSR and NSF under MCS79-23110.

1. Some are well known and supposed to be consciously attended to. For instance, if the top of a tower is climbing in the visual field it is above the flight path and will not be cleared.

References

- Attneave, F. 1972 Representation of physical space. In *Coding processes in human memory*. A.W. Melton & E. Martin (Eds.). New York: John Wiley.
- Braunstein, M. 1968 Motion and texture as sources of slant information. *Journal of Experimental Psychology* 78, 247-253.
- Braunstein, M. & Payne, J.W. 1969 Perspective and form ratio as determinants of relative slant judgements. *Journal of Experimental Psychology* 81, 584-590.
- Enright, J.T. 1970 Distortions of apparent velocity: a new optical illusion. *Science* 168, 464-467
- Epstein, W. & Landauer, A.A. 1969 Size and distance judgments under reduced conditions of viewing. *Perception and Psychophysics* 6, 269-272.
- Foley, J.M. 1972 The size-distance relation and intrinsic geometry of visual space: implications for processing. *Vision Research* 12, 323-332.
- Gibson, J.J. 1950 *The perception of the visual world*. Boston: Houghton Mifflin.
- Gibson, J.J. 1979 *The ecological approach to visual perception*. Boston: Houghton Mifflin.
- Gibson, J.J. & Bergman R. 1954 The effect of training on absolute estimation of distance over the ground. *Journal of Experimental Psychology* 48, 473-482.
- Gogel, W.C. 1971 The validity of the size-distance invariance hypothesis with cue reduction. *Perception and Psychophysics* 9, 92-94.
- Graham, C.H., Riggs, L.A., Mueller, C.G., & Solomon, R.L. 1949 Precision of stereoscopic settings as influenced by distance of target from a fiducial line. *Journal of Psychology* 27, 203-207.
- Grimson, W.E.L. 1980 Computing shape using a theory of human stereo vision. Ph.D. thesis, M.I.T. (mathematics).
- Haber, R. & Hershenson, M. 1980 *The psychology of visual perception*, 2nd edition. New York: Holt.
- Harker, G.S. & Jones, P.D. 1980 Depth perception in visual simulation. AFHRL-TR-80-19.
- Hennessy, R.T., Sullivan, D.J., & Cooles, H.D. 1980 Critical research issues and visual systems for a V/STOL training research simulator. NAVTRAEQUIPCEN 78-C-0076-1.
- Helmholtz, H. 1925 *Physiological optics*, Vol. 3 (3rd edition translated by J.P. Southall) New York: Optical Society of America.
- Hilbert, D. & Cohn-Vossen 1952 *Geometry and the Imagination*. Chelsea Publishing.
- Hochberg, J. 1971 Perception II: Space and movement. In *Woodworth and Schlosberg's Experimental Psychology* (3rd ed.), J.W. Kling & L.A. Riggs (Eds.). New York: Holt, Rinehart and Wilson.
- Hochberg, J. 1978 Art and Perception. In *Handbook of perception*, Vol. 10, E.C. Carterette and H. Friedman (Eds.), New York: Academic Press.

- Horn, B.K.P. 1975 Obtaining shape from shading information. In *The psychology of computer vision*, P.H. Winston, ed. New York: McGraw-Hill.
- Kraft, C. L., Anderson, C.D. & Elworth, C.L. 1980 Psychophysical criteria for visual simulation systems. Final Report. AFHRL-TR-79-30.
- Koenderink, J.J. & van Dorn, A.J. 1976 Local structure of movement parallax of the plane. *J. Opt. Soc. Am.* **66**, 717-723.
- Kennedy, K.W. & McKechnie, D. 1970 Visibility toward the ground from selected tactical aircraft. AMRL Technical Memorandum No. AMRL-TR-69-123.
- Marr, D. 1976 Early processing of visual information. *Phil. Trans. R. Soc. Lond. B* **275**, 483-524.
- Marr, D. 1978 Representing visual information. A.A.A.S. 143rd Annual Meeting, Symposium on: Some mathematical questions in biology, February 1977. Published in *Lectures on mathematics in the life sciences* **10**, 10-180. Also available as *M.I.T. A.I. Lab. Memo 415*.
- Marr, D. 1981 *Vision: A computational investigation into the human representation and processing of visual information*. San Francisco: W.H. Freeman. (in press)
- Marr, D. & Hildreth, E. 1980 Theory of edge detection. *Proc. R. Soc. Lond. B* **207** 187-217.
- Marr, D. & Nishihara, K. 1978 Representation and recognition of the spatial organization of three-dimensional shapes. *Phil. Trans. Roy. Soc. B.* **200**, 269-294.
- Marr, D. & Poggio, T. 1977 From understanding computation to understanding neural circuitry. *Neuroscience Research Progress Bulletin* **15**(3), 470-488.
- Marr, D. & Poggio, T. 1979 A computational theory of human stereo vision. *Proc. R. Soc. Lond. B* **207**, 301-328.
- Mayhew, J.E.W. & Frisby, J.P. 1981 Psychophysical and computational studies towards a theory of human stereopsis. *Artificial Intelligence* **16** (in press).
- Nakayama, K. & Loomis, J.M. 1974 Optical velocity patterns, velocity-sensitive neurons, and space perception: a hypothesis. *Perception* **3**, 63-80.
- Purdy, W.C. 1960 The hypothesis of psychophysical correspondence in space perception. General Electric Technical Information Series, No. R60ELC56.
- Richter, J. & Ullman, S. 1980 A model for the spatio-temporal organization of x and y-type ganglion cells in the primate retina. *M.I.T. A.I. Lab. Memo 573*.
- Rock, I. 1977 In defense of unconscious inference. In *Stability and constancy in visual perception*, W. Epstein (Ed.), New York: Wiley, 321-373.
- Rock, I. & McDermott, W. 1964 The perception of visual angle. *Acta Psychol.* **22**, 119-134.
- Semple, C.A., Hennessy, R.T., Sanders, M.S., Cross, B.K., Beith, B.H., & McCauley, M.E. 1980 Aircrew training device fidelity features (final report). Canyon Research Group, Inc. CRG-TR-3041B.

Smith, O.W. & Smith, P.C. 1957 Interaction of the effects of cues involved in judgments of curvature. *Americal Journal of Psychology* 70, 361-375.

Stevens, K.A. 1980 Surface perception from local analysis of texture and contour. M.I.T. A.I. Lab. Technical Report 512.

Stevens, K.A. 1981 The visual interpretation of surface contours. *Artificial Intelligence* 16 (in press).

Ullman, S. 1979 *The interpretation of visual motion*. Cambridge, Ma.: M.I.T. Press.

Ullman, S. 1980 Against direct perception. *The Behavioral and Brain Sciences* 3, 373-415.

Wallach, H. & O'Connell, D.N. 1953 The kinetic depth effect. *Journal of Experimental Psychology* 45, 205-217.

SIMULATED FLIR IMAGERY USING COMPUTER ANIMATED

PHOTOGRAPHIC TERRAIN VIEWS (CAPTV)

J. T. Hooks and Venkat Devarajan



John Terry Hooks, Jr., obtained his MS in Mechanical Engineering from Southern Methodist University, Dallas. His 30 years of professional experience has been in industry and in the military. Most of the 25 years of his association with Vought Corporation has been in various aspects of Flight Simulation. He has been the principal investigator in the R&D effort that led to the development of CAPTV concept and the FLIR simulator and is currently the supervisor of the Image Processing section at Vought.



Venkat Devarajan obtained his Ph.D. from the University of Texas at Arlington. During the 7 years that he spent in Vought and academia, he has worked on digital image and speech processing, machine recognition of alphanumeric characters, orthogonal transforms and visual systems for flight simulators. He most recently has been involved with the photogrammetric applications to visual systems.

SIMULATED FLIR IMAGERY USING
COMPUTER ANIMATED PHOTOGRAPHIC
TERRAIN VIEWS (CAPTV)

J. T. Hooks, Jr.
Venkat Devarajan

ABSTRACT

In the first successful application of Vought's CAPTV technology the Navy has been provided a unique training capability for the forward looking infrared receiver (FLIR) system utilizing real world imagery. The CAPTV system employs monochrome aerial photographs stored in a large random access video data base, which, through computer processing, provides smooth high-detail simulated visual motion cues to the pilot trainee.

I. INTRODUCTION

Flight simulators have come to be recognized as important training components for several reasons. The rising cost of fuel and equipment, congestion over airports, the need to avoid accidents during training are some of the more important reasons. Computer Generated Imagery (CGI) is presently the most popular method of image generation for the visual systems in most flight simulation¹. This paper describes an alternative to CGI in that aerial photography of the gaming area is used instead of CGI as the database in our system. The approach achieves excellent scene realism for the student pilot besides providing the visual cues needed for most training requirements. The photographic database is a part of the unique Vought-developed concept called computer animated photographic terrain view (CAPTV).

The development of CAPTV has been a continuing effort by Vought in the last decade. Early systems were restricted by the unavailability of video bulk storage with fast random access. With the availability of the video disc, Vought has pioneered applications for simulated visual displays using oblique aerial photography. The recent delivery of two systems to the U.S. Navy to provide simulated Forward Looking Infrared (FLIR) imagery represents the first successful application of the CAPTV concept and the use of video disc.

The FLIR simulators have been added to the Navy's A-7E Weapon System Trainers (WST) (Device 2Fl11) at Cecil Field NAS in Florida and Lemoore NAS

in California. The real-time playback system, when added to the existing WST equipment, provides the student pilot with a continuous FLIR display of the gaming area as presented on the head-up display (HUD) in the cockpit. The scope of the gaming area is large enough and flexible enough for a simulator pilot to fly a mission with total maneuvering freedom within the gaming area. The derived FLIR scene can be selected in a 12-degree or a magnified 3-degree field of view. Finally, FLIR registration with the radar display in the WST is maintained regardless of the simulated aircraft maneuvers throughout the flight.

II. CAPTV CONCEPT

The basic CAPTV concept assumes an array of still photographs taken from an airplane that covers the gaming area defined by pilot training requirements. Photographs are taken at regular intervals along straight and/or cross tracks, the interval between the photos is proportional to the altitude. These photos are scanned, formatted, and stored in a bulk storage device. As these photos are retrieved from the storage medium for display, the pilot 'flies' through them using controls similar to the ones on the cockpit panels. At any given instant, knowing the pilot's eyepoint in space, the photo in the database nearest his location is stretched, skewed, rotated and translated in a mathematical transformation such that the transformed photo would overlay a different photo taken from the pilot's eyepoint. This process is a continuous one each frame time under computer control and allows the introduction of smooth translation into a basically still picture set for any direction of travel through that set. During the period in which translation is taking place using a given fixed scene, the computer is fetching a new appropriate view to be used as an overlay substitute. The new view is selected by a sophisticated prediction scheme that determines when the present photo must be discarded in favor of a new scene. It is important to understand that the transformation process does not cause unrealistic distortions of the viewed scene. The key to CAPTV lies in its unique capability to make one fixed photo serve in a dynamic translation situation long enough to fetch another view and incidentally perform many other functions as well.

III. OFF-LINE IMAGE GENERATION

The off-line image generation system of the FLIR simulation (Fig. 1) was used to develop the database for the playback system. The image generation consisted of the following subsystems:

(a) Aerial Camera: A Ziess/Hasselblad 38mm Biogon lens using 70mm Infrared film rigidly attached to an airplane that flew over two gaming areas (one on the West coast and one on the East coast). Each of the two gaming areas was partitioned to contain some 3000 to 4000 'eyepoints' distributed into several altitudes in straight and cross tracks.

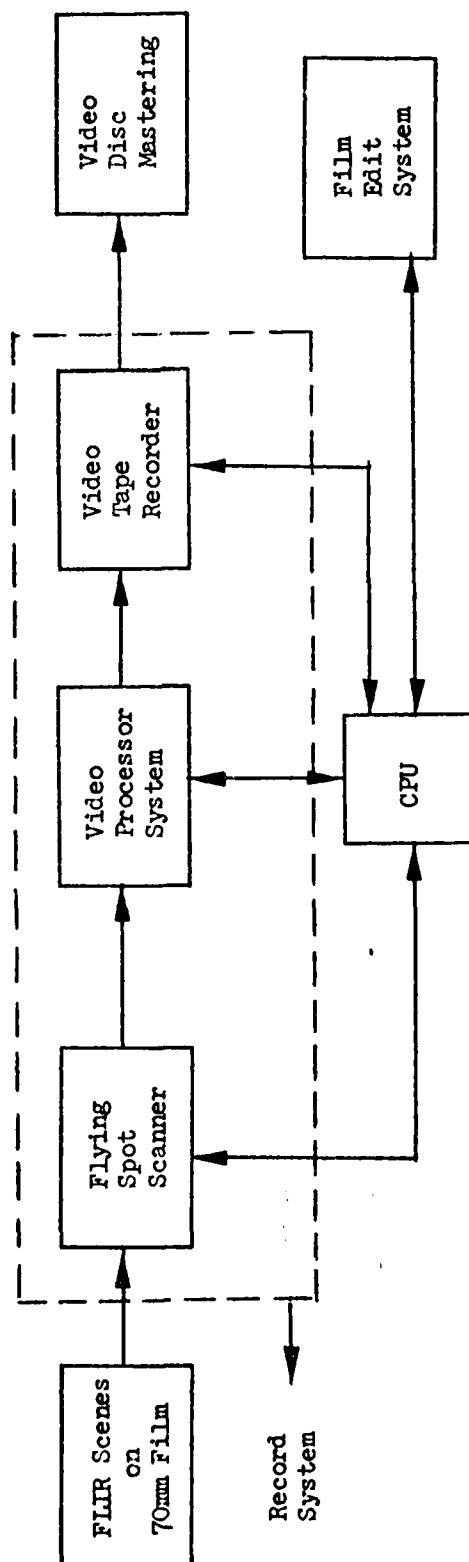


FIGURE 1 CAPTV - OFFLINE RECORD SYSTEM

Each of the photographs has a FOV of 60 degrees in both azimuth and elevation. Objects which moved as the terrain was photographed (e.g., vehicles on the road) were treated as stationary anomalies.

(b) Record System: The flying spot scanner was used to scan the 57mm square usable area of the 70mm frames to provide a pixel resolution of approximately 4000 x 4000 elements. The resulting analog video was uniquely formatted using the Video Processor System (VPS) such that each terrain scene was made up of (typically 72) NTSC frames. Appropriate sync signals were inserted to make the signals suitable for recording on video tape recorders and disks. During the recording process, opportunity was afforded for manipulating the video gain and bias of each scene to correct anomalies resulting from earlier photographic processes.

(c) Film Edit System: This system consisted of a digitizer and an analytical software package residing on the Harris Slash 6 digital computer (32K, 24 bit) that determined the approximate exposure station orientations (eyepoints) of each photograph. The calculations aided in the proper sequencing of the scanned scenes on the tape recorder and eventually facilitated fast random access of the scenes from the video disks during playback.

(d) Video Disk: The database recorded on the Ampex VPR-1 recorder was transferred by MCA to video disks suitable for playing on the MCA DiscoVision Model 700 industrial optical video disk player². Each of the video disks can hold up to 54000 standard NTSC frames - typically 600 FLIR scenes. Both frame identification numbers and Society of Motion Pictures and Television Engineers (SMPTE) codes were used for the proper sequencing of the frames. Such sequencing is optimized to provide minimal search times during playback.

IV. ON-LINE PLAYBACK SYSTEM

The deliverable real-time on-line playback system (Fig. 2) consisted of the following sub-systems:

(a) Video Storage System: Analog storage using television techniques is a practical and economical alternative to digital storage and is especially suited to pictorial data. The purpose of the storage system consisting of the four video disks was to provide large segments of the desired data under control of the host computer and in anticipation of the real time needs of the simulation. The bulk data was distributed over the four disks to optimize the retrieval of the desired data. Any randomly accessed TV frame on a single play-back unit could be located and made available in 2 to 8 secs. Adjacent or sequential frames required much less time than this, however. The players operated essentially independently and were rotationally synchronized to the system timing references for color subcarrier and horizontal/vertical raster scans (although the entire system was essentially monochrome, a color subcarrier was provided for synchronization and clocking within the VPS). In operation, these units were not supplying data at the same time. Data was transferred from only one player at a time while the others were searched for the anticipated subsequent scenes.

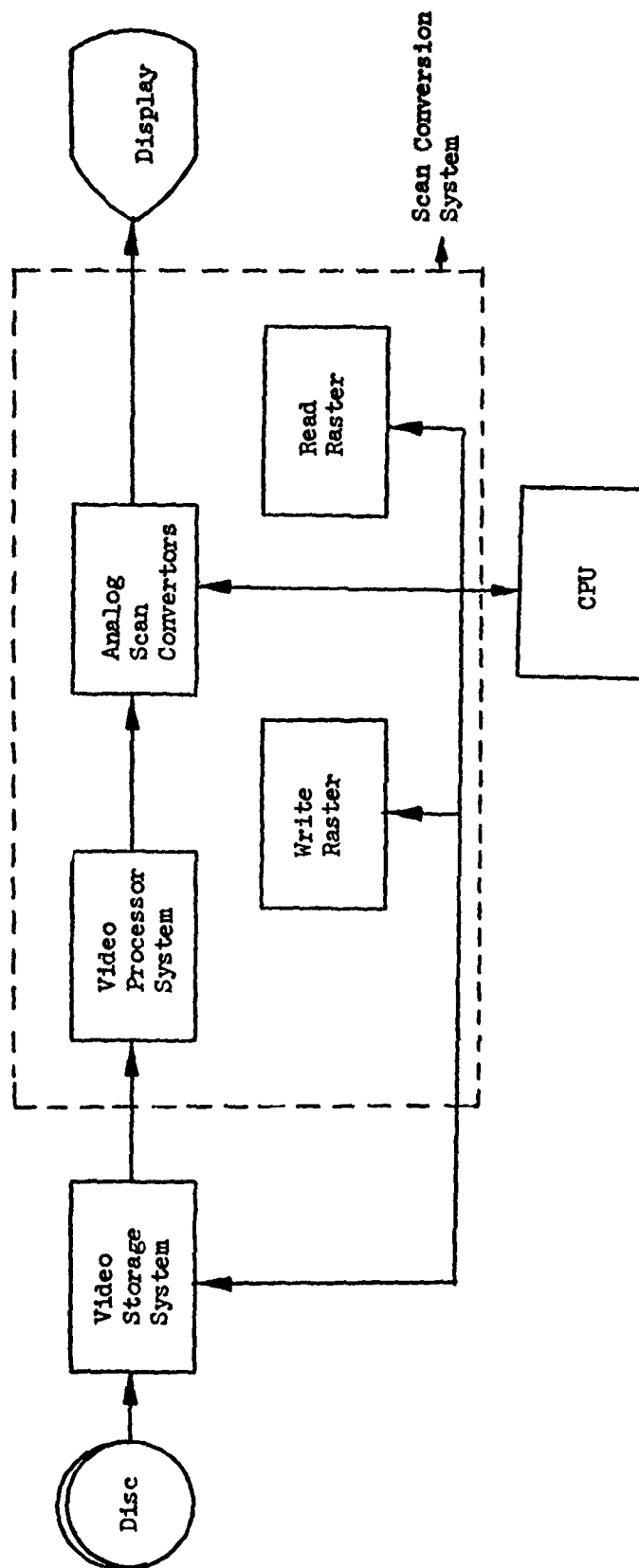


FIGURE 2 CAPTV - ON-LINE PLAYBACK SYSTEM

(b) Video Processor System: As the pilot determined the location and FOV of the database that he wanted to 'fly', the host computer CPU transferred an entire scene or a programmed fraction of the total scene to the video processor system. The analog video was stripped off of the NTSC sync, and was reformatted into the original FSS format. This signal was then converted into a digital stream of 8-bit pixels and stored in a 3-line internal storage. Based on the pilot's zoom rate and the resulting requirements on the HUD FOV, the video lines were appropriately interpolated on in the VPS. The resulting video was converted back into the analog form and under CPU control transferred to the scan conversion system.

(c) Scan Converter System: This system consisted essentially of two analog storage tubes. To achieve the requirement of the continuous display of video information, the two scan converters were utilized in a 'ping-pong' configuration; that is, while video information was being read from one scan converter, new video was being written on the other scan converter. Switching then enabled the newly written information to be read from the second scan converter while the older information on the first scan converter was erased and replaced.

(d) Write Raster: The usable scan converter memory had a normalized resolution of only 1200 lines of scanned FLIR video. The available resolution on the disk for each scene was approximately 4000 such lines. Therefore, a different write raster was obtained using a 2-dimensional re-sampling technique based on the slew rate, FOV to be displayed and the velocity of the aircraft.

(e) Read Raster: The Read Raster size was a fraction of the Write Raster size (Fig. 3) and this fact enabled the pilot to maneuver over a gaming area for a few seconds before he out-stepped the edge of the scan converter image. A new read raster was calculated every 1/30th of a second (Fig. 4) by generating a (3 x 3) transformation matrix which was used to skew and rotate a window off of the scan converter to obtain the off-nominal image.

(f) Display: An 875 line Conrac CRT display was used to display the FLIR images. A joystick and a switch box enabled the pilot to move into different modes of operation and flight. The FLIR simulator display was compatible with the FLIR imagery coming off the pod. The entire setup (Fig. 5) was designed to be added to the existing A-7E WST hardware at Cecil Field, Florida and Lemoore, California.

V. EXPANDABILITY OF DATABASE

One of the major advantages of the FLIR simulator system described above is the almost unlimited expandability of the database without changing the record/playback hardware. The terrain database delivered to the Navy was in fact expanded to include a database consisting of 'enemy' ships. This was accomplished by taking photographs of a model ship with enough density of photographs to perform an efficient eyepoint transformation. As explained earlier, the addition of databases involves taking aerial or model photos, scanning on the FSS, formatting, recording on the video tape recorder, and video disc mastering. A FLIR record system rack is permanently stationed in-house to accomplish this task. Thus, there are virtually no limits to the expansion of database.

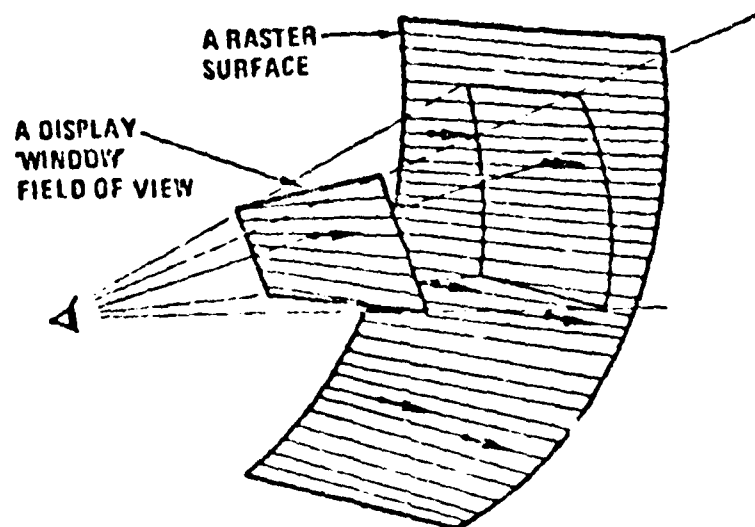


FIGURE 3 RELATIONSHIP OF READ RASTER TO WRITE RASTER

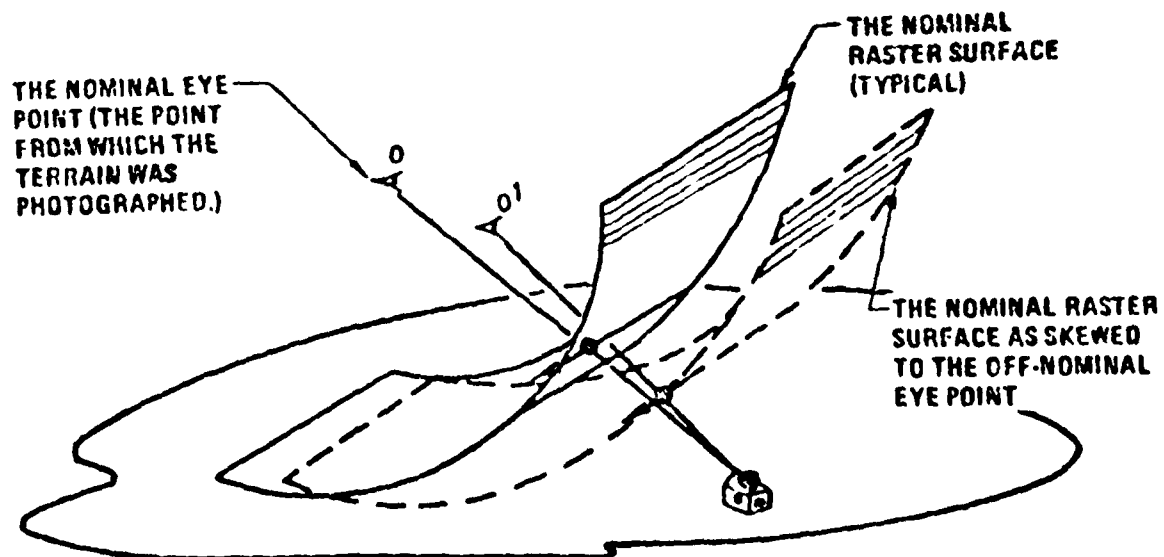


FIGURE 4 PRODUCTION OF MOVING SCENE FROM STILL SCENE

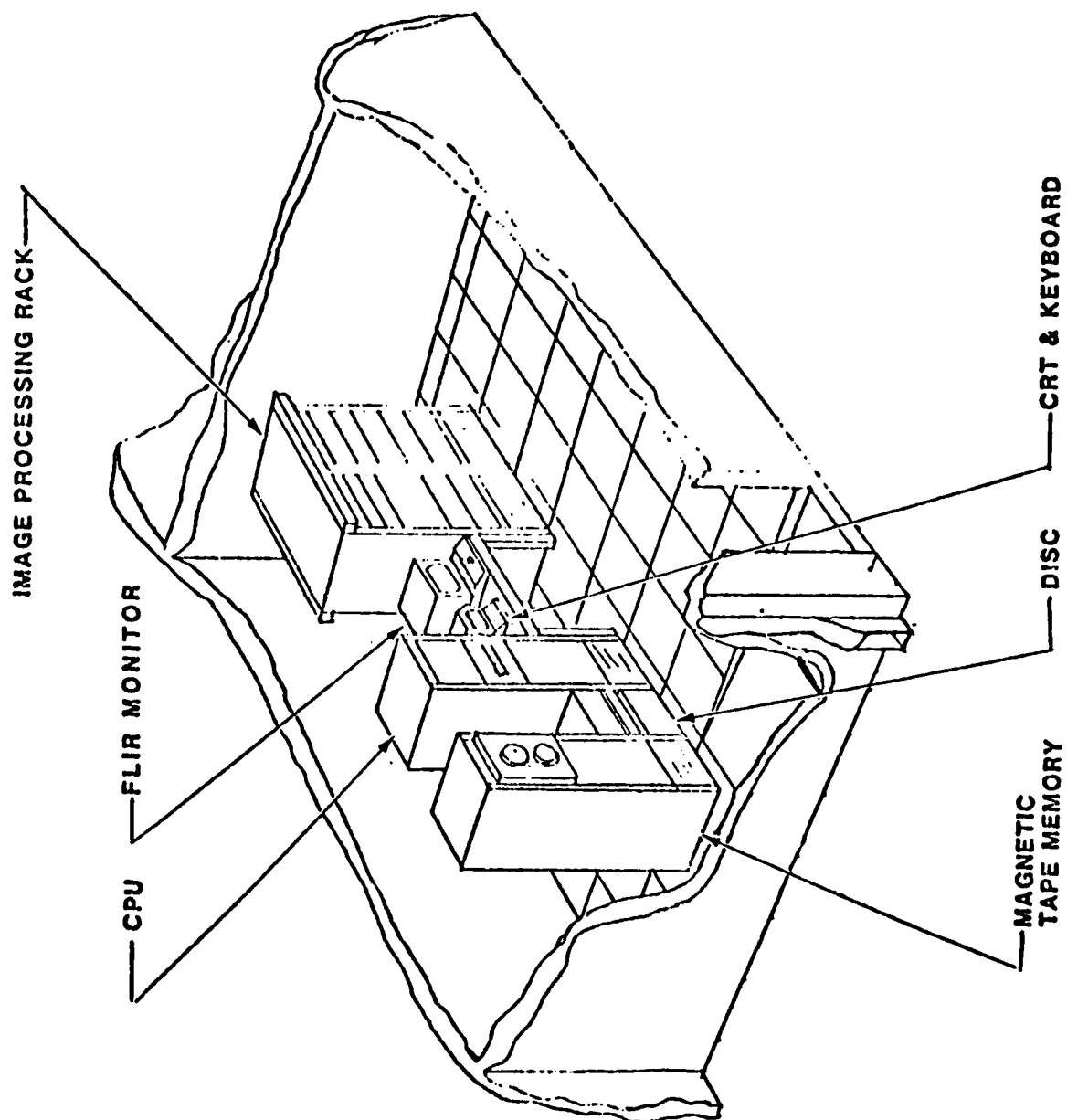


FIGURE 5 FLIR SIMULATION SYSTEM HARDWARE CONFIGURATION

VI. PHOTOGRAMMETRY

Photogrammetry is the science of obtaining extremely precise information about physical objects and the environment through the process of recording, measuring and interpreting photographic images³. Extensive use of photogrammetry was made in the FLIR simulator to pin-point accurately the eyepoints of the database photographs. The overlap between successive database photos was utilized to carefully pick pass points off the photos of discernible physical features of the terrain, and control points on the terrain obtained from the U. S. Geological Survey. Typical physical features were street intersections, building corners, edges of runways, etc. Sophisticated photogrammetric equipment also allows common points to be picked even where there are not many discernible physical features on the terrain. The pass points and control points were used as input data to a data reduction software package which calculated the eyepoint parameters to the desired accuracy.

VII. SUMMARY AND CONCLUSIONS

The Vought-developed CAPTV concept has resulted in a FLIR visual system for the A-7E WST simulator that has proved to be a valuable training device. CAPTV offers some major advantages in its ability to provide scene-realism, detail, 3-dimensionality, and texture that is limited only by photography and almost unlimited for expandability of database. The system components include such state-of-the-art technology as video discs and some of the best photogrammetric software packages for the preparation of the database. The FLIR simulator provides an 875-line display that is presently used by the Navy in full mission training application. As a follow-on effort, work is in progress at Vought to provide a full color out-the-window visual system using the principles proved by the FLIR simulation.

VIII. REFERENCES

1. Bruce Schachter and Narendra Ahuja, "A History of Visual Flight Simulation", Computer Graphics, May 1980. pp. 16-31.
2. Jules Street, "Video Disc Systems Come of Age", EOSD, December 1980. pp. 31-37.
3. Sanjib K Ghosh, "Analytical Photogrammetry", Pergamon Press, 1979.

SIMULATED A-10 COMBAT ENVIRONMENT



DR ROBERT S. KELLOGG is a research psychologist on the staff of the University of Dayton Research Institute, presently assigned to the Air Force Human Resources Laboratory, Williams AFB, Arizona. He is a retired Air Force officer with extensive research experience with the Aerospace Medical Research Laboratory, Wright-Patterson AFB, Ohio. His areas of interest include human operator control with special emphasis on vision and vestibular function.



COL DIRK C. PRATHER is Technical Advisor for the Operational Training Division, Air Force Human Resources Laboratory, Williams AFB, Arizona. He has been Chief of Exercise Plans, 314th Air Division, Korea; Tenure Associate Professor, Department of Behavioral Sciences and Leadership, USAF Academy, Colorado; Instructor Pilot F-104G, Luke AFB, Arizona; Direct Air Support Center Operations Officer, DaNang, Republic of Vietnam, during which time he flew 174 combat missions in the O1E as a forward air controller; and a US Navy fighter pilot. Col Prather is a naval aviation cadet graduate and has logged more than 3500 flight hours. He received a PhD in Educational Psychology from Arizona State University in 1969. He has been awarded the Distinguished Flying Cross, four Meritorious Service Medals, the Bronze Star, five Air Medals, and the Air Force Commendation Medal.

(no photo available)

DR CARL N. CASTORE is an associate professor at Purdue University Psychology Department. He has recently served as a visiting scientist for Air Force Systems Command at the Air Force Human Resources Laboratory at Williams AFB, Arizona. His research interests are in individual and group decision making and risk taking.

SIMULATED A-10 COMBAT ENVIRONMENT

Robert S. Kellogg, PhD
Dirk C. Prather, PhD
Carl H. Castore, PhD

Air Force Human Resources Laboratory
Williams AFB, Arizona

Abstract

The purpose of this study was to test the feasibility of using the Advanced Simulator for Pilot Training (ASPT) in training pilots for combat in a simulated hostile environment. A combat environment was developed in which the A-10 aircraft was flown. The environment included mountainous terrain, enemy surface-to-air missiles (SAM) and anti aircraft artillery (AAA). The offensive target was a tank located at random along the roadway. The pilots flew the mission in real time and were scored on offensive and defensive procedures. They showed clear learning for those procedures in the simulator.

INTRODUCTION:

The purpose of this study was to test the feasibility of using the Advanced Simulator for Pilot Training (ASPT) in training pilots for combat in a simulated hostile environment. It has been suggested (Ref 1) that in the future, complex flight simulators will not be limited simply to procedures and instrument training, but will serve the much more important and broader need of training combat ready pilots in the complex task of tactics development. NASA's experience in successfully training crews to perform moon landings, which could only be practiced through simulation, has demonstrated the value of simulating tasks which are impractical or impossible to practice in the real situation. Experiences of the Air Force and Navy during the Viet Nam era indicated that pilot performance in a combat situation could be improved considerably by providing the pilot with experience in flying mock air-to-air engagements against dissimilar aircraft and against the types of ground defenses he would be coming up against in combat (Ref. 2). This type of experience provided the pilot with the opportunity to develop his skills at offensive and defensive strategies. The success of this program led directly to the establishment of the Red Flag and Blue Flag exercises by TAC and similar training exercises by other commands. While such exercises are excellent test beds for new tactics on a squadron or wing level, they are frequently of too short a duration for the evolution of new tactical approaches or an exploration of the relative effectiveness of alternative strategies on an individual pilot level. With the use of a high fidelity full mission simulator such as the ASPT, it is possible to expose the pilot to a large number of combat simulations of sufficient fidelity in a short period of time to provide him an optimum situation for offensive and defensive skill development. Using such simulation will engender a more holistic view of the combat mission in which the pilot will be required to meet the ever changing mission requirements with flexibility and judgment, based on "experience". The present study is a first effort to demonstrate that the simulator can be used in this extended role.

Combat Environment

Existing visual environments on the ASPT were used and modified to produce the computer generated imagery (CGI) used in this study. The imagery was presented in an A-10 simulator which included the heads up display (HUD).

A map of the basic environment can be seen in Figure 1. It consists of an area of about 10 miles square. Twelve mountains are included in the area, ranging in height from 1400 to 6500 feet. Also, there were a number of small rock-like projections between the mountain ranges on the right. Three surface-to-air missile (SAM) sites were located in the central valley. Each SAM site had the following capabilities:

- a. Effective slant range of 40,000 feet
- b. Minimum tracking elevation of 2.5°
- c. Minimum tracking altitude of 50 feet
- d. Each site was limited to six firings during each trial
- e. Maximum 9-G turn capability
- f. Acceleration of 400 feet per sec^2
- g. Maximum velocity of 1600 feet per second

The SAM site closest to the aircraft was the one activated. If the aircraft was outside of its firing envelope, the other two SAM sites searched to see if the aircraft was within their range. When the aircraft was within range, a 3.5 seconds alternating 2025 Hz spaced tone indicated radar acquisition. Immediately after the acquisition warning, a three second alternating 2025 Hz tone indicated imminent launch. At the end of the tone, the SAM fired and a light illuminated to indicate launch. The missile could be seen by the pilot if he was in a position of proper viewing angle. A rapidly alternating tone continued for as long as the SAM was in flight. If a SAM had been launched and the aircraft subsequently exited the firing envelope of the site, the SAM would abort. If, during the time the SAM was in flight, the aircraft entered the firing envelope of another SAM site, the SAM in flight would continue its course unless the aircraft exited the envelope of the launching site, in which case the SAM aborted. If the aircraft was then being tracked by a new site, a new acquisition cycle was initiated. If hit by the SAM, the aircraft went out of control and crashed.

Co-located at each SAM site was an anti-aircraft artillery battery (AAA), consisting of four 23 mm guns as well as an isolated AAA site to the west of the battle area. Each AAA site had the following capabilities:

- a. Effective slant range of 8,000 feet
- b. Firing rate of 300 Rnd/Min
- c. Minimum tracking altitude of 50 feet

COMBAT ENVIRONMENT

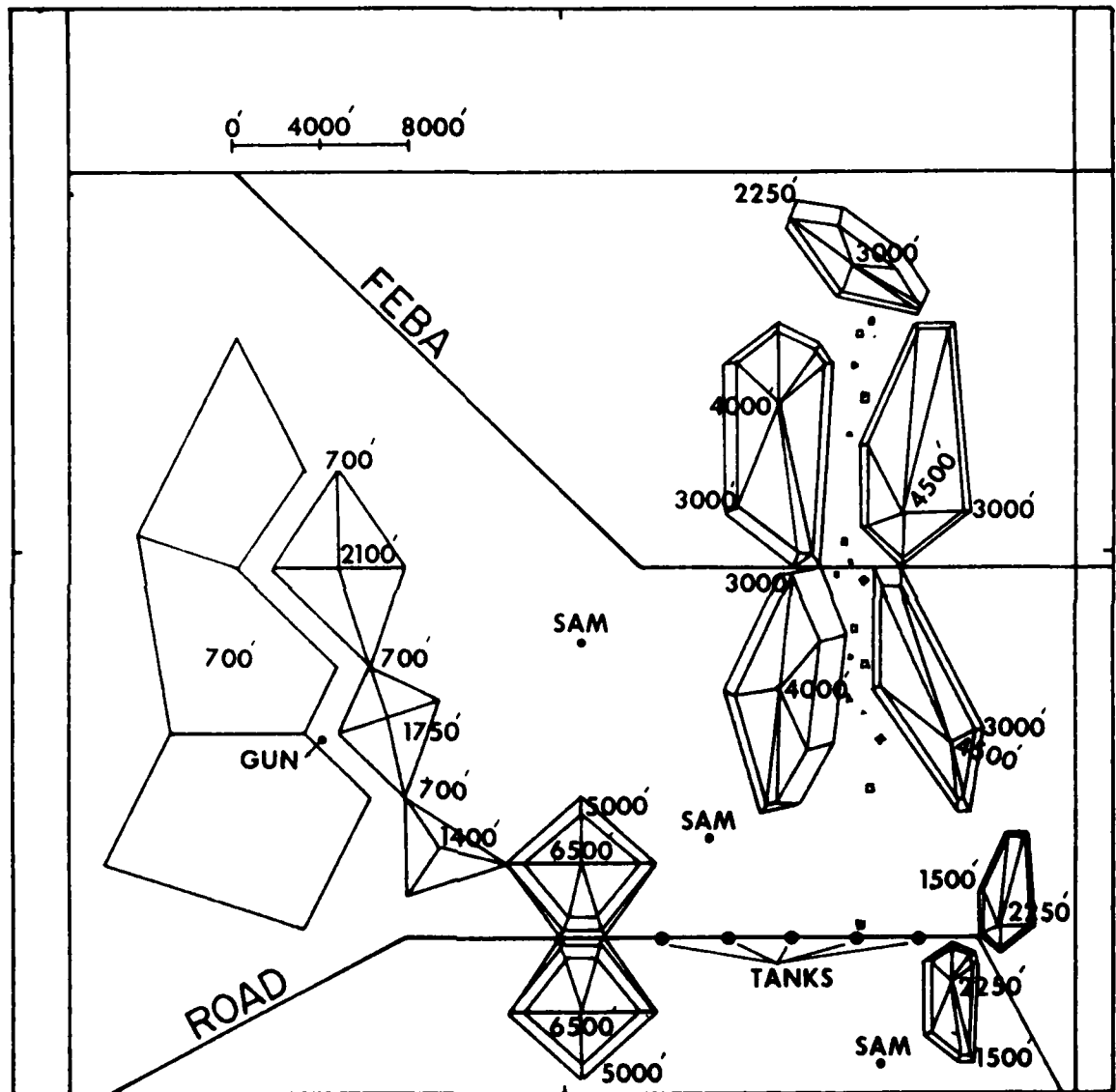


FIGURE 1

The AAA site began tracking when the aircraft flew within range. If the pilot took evasive action, which consisted of +3 G's or more, or -1.5 G's or less, for six consecutive seconds, the aircraft would evade AAA kill; if not, the aircraft would be hit and go out of control. Muzzle flashes were the only indication that the aircraft was being fired upon. The aircraft did not have the capacity of destroying the SAM or AAA batteries.

The enemy target in this environment was a tank which was located at one of six randomly selected positions on the road stretching between the two mountain ranges at the Southern end of the battle zone. The tank, once placed in one of the six positions, remained stationary. It showed muzzle flashes from its cannon, but did not have offensive capabilities. The A-10 aircraft had only the capability of firing its gun. The tank was considered destroyed when it was hit by one round during the first sequence of firing, in the two-dimensional space occupied by the tank.

In addition, a special feature was added to the environment which allowed the pilot to see his own shadow when his altitude was below 500' AGL.

Subject Population

The subjects for this study were combat ready A-10 pilots, as determined by Tactical Air Command Headquarters. They were all in Mission Qualification Training at Davis-Monthan AFB, AZ. They ranged in age from 26 to 35 years. Table 1 shows a breakdown of the seven subjects with respect to flying experience. Three of them had combat experience and all but two of them had participated in Red Flag exercises.

Experimental Runs

The experimental sequence for the subjects was as follows. Each subject was briefed individually by a research instructor pilot (IP) on the combat environment, including all the offensive and defensive characteristics. He was given a map of the environment which he was allowed to study before entering the simulator. He was allowed to take the map along during the simulator run. The pilot was initialized approximately ten miles north the forward edge of the battle area (FEBA) in IFR conditions at an altitude of 5500 feet. The pilot's only instructions were that he was on his own and that his mission was to ingress to the battle area, destroy the tank and egress safely across the FEBA. The experimental run was terminated when one of the following occurred:

- a. SAM kill
- b. AAA kill
- c. Terrain crash
- d. Over G
- e. Safely crossed FEBA

A-10 COMBAT ENVIRONMENT STUDY

<u>SUBJECT</u>	<u>RANK</u>	<u>AGE</u>	<u>FLYING TIME</u>	<u>A-10 TIME</u>	<u>FIGHTER TIME</u>	<u>COMBAT</u>	<u>RED FLAG</u>
#1	CAPT	28	1100	300	900	NONE	X3 2-A7; 1-A-10
#2	CAPT	29	1450	225	525	NONE	X1
#3	CAPT	32	2700	300	920	677	X1
#4	CAPT	33	2700	50	1000	680	X2 F-4
#5	MAJ	35	3700	50	2000	350	X3 F-105
#6	1LT	26	650	70	450	NONE	NO
#7	1LT	26	600	65	400	NONE	NO

TABLE 1

RAW SCORES

	H	M		H	M
S	11	12	S	28	16
D	8	32	D	15	9
	AM			PM	

H= HIT TANK
M= MISS TANK
S= SURVIVED
D= DESTROYED

TABLE 2

As soon as each run was terminated, the pilot was immediately reinitialized and another run began. Each subject flew a set of runs in the morning and a second set in the afternoon. Each set lasted between an hour to one hour and a half. Each subject was given feedback as to what happened at the termination point of each run: if he hit the tank, if he survived, and if he was shot down, the source of his demise. Between periods, the subjects were not allowed to discuss tactics among themselves so as not to bias their individual approaches to solving the tactical problems.

Analysis

On the basis of whether the pilot hit or missed the target, survived, or was destroyed, a chi square analysis was performed. The overall analysis with all data pooled showed statistical significance at the 0.05 level. This simply means that the pilot's offensive scores (hitting the tank) and defensive procedures (survival) are highly correlated. When the morning performance was compared with the afternoon performance, there was a significant increase in survival and offensive capabilities in the afternoon. Table 2 shows a comparison of A.M. vs P.M. scores.

A scoring system was developed in order to plot curves which were representative of individual performance with respect to offensive and defensive outcomes. Scores assigned were as follows:

Defensive:	
+2	No detection
+1	Detected/not killed
0	Killed by SAM, AAA, Crash, or over "G"
Offensive:	
+2	Fired/kill tank
+1	Fired/missed tank
0	No fire on tank

The combined (offensive plus defensive) scores of all subjects indicated an overall improvement after repeated training sessions. The mean total scores for the seven subjects across the 20 training trials are shown in Figure 2. The scores shown with a possible range of 0 to 4 indicate the combined offensive and defensive capability of the pilot.

An examination of the data from a separate consideration of offensive and defensive scores, shown in figure 3, provides some further insight into the apparent decline of performance trials 11 and 18. Scores for both offensive and defensive performance improved rapidly from trials 1-8, with offensive performance scores entering the acceptable range (greater than +1.0) from trials 5/6 on. The marked jump in average offensive scores from trials 7/8 to trials 9/10 indicate that, in general, the pilots had "solved" the offensive portion of the problem confronting them. However, at no time during this period (trials 1-10) did the average defensive score move into the acceptable range (greater than 1). That is, on the majority of the trials the average pilot was being detected and/or shot down - although by trials 9/10 most pilots were getting the target tank first. This is particularly significant in view of the fact that the scenario was

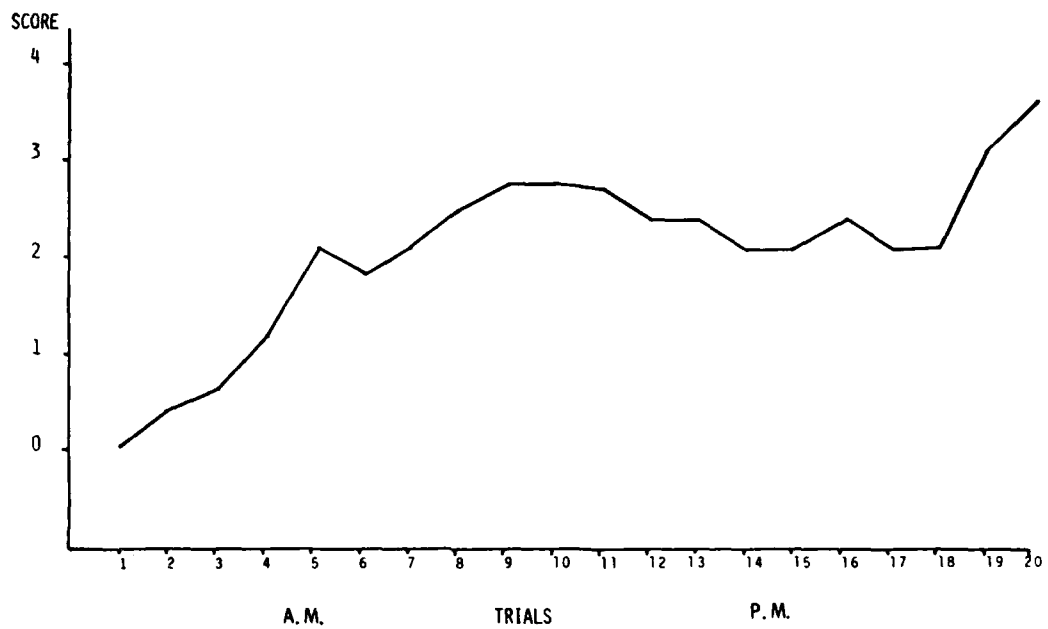


FIGURE 2

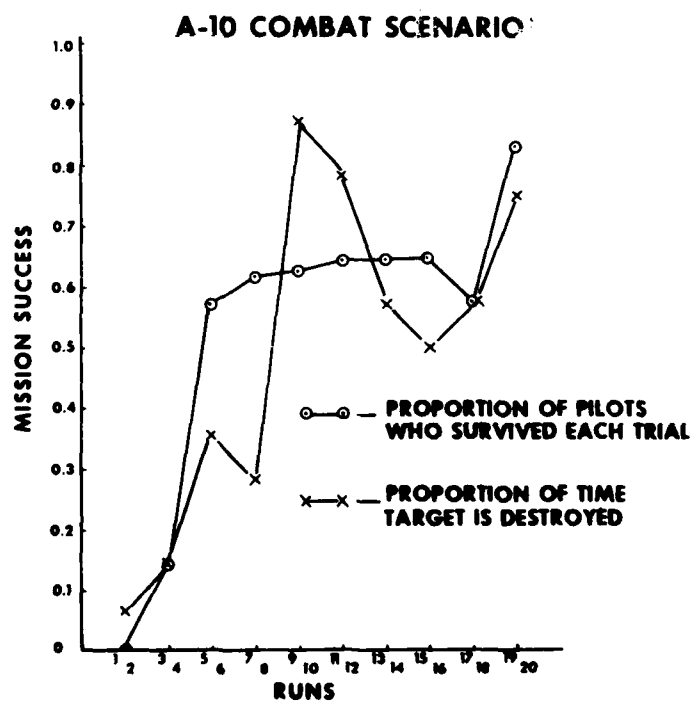


Figure 3

specifically set up so that the pilot could, in fact, acquire and destroy the tank and return without being detected or shot at by the enemy AAA or SAM batteries. Clearly, the pilots had not "solved" the defensive aspects of the problem by the end of the first ten sessions. The nature of the data in figure 3 in conjunction with that in table 2 suggests that the pilots began to attend more to the defensive aspects of the problem scenario in the afternoon sessions (trials 11-20).

The data clearly indicate that the pilots overall have learned to perform better offensive and defensive maneuvers after repeated trials in the simulator. However, the offensive problems are apparently solved much more rapidly than the defensive ones. Possibly because they are the most salient aspects of the problem and due to the nature of the pilots' previous training. The defensive problems are solved much more slowly and require greater practice.

Conclusions

This being the first attempt to use the ASPT (or any other simulator) for the production of a full combat scenario, the preliminary results are quite encouraging. The visual system was programmed to almost full capacity to produce the battle environment in which the pilot was free to fly and develop his own tactics in destroying the target and surviving the threat environment. In this sense, the pilot is operating in a completely open loop fashion, as he would largely operate in true combat, and as such, may be able to develop the flexibility and problem solving strategies he will be called upon to develop in actual combat. The learning curves indicate the pilots are acquiring and integrating appropriate information so as to improve their tactical performance.

The A-10 pilots' acceptance of this type simulation was remarkably positive. All of the combat ready pilots appeared very enthusiastic about the utility of this sort of simulation. They pointed out that they had never had an opportunity, except for real combat, to deal with the combat environment in a holistic way as it was presented to them in the simulator. The demand of dealing with the SAM and AAA weapons while conducting their offensive maneuvers, they felt, was particularly instructive. The "pop-up" maneuver, for example, which is part of their standard repertoire, has to be clearly modified when in range of either the SAM or AAA site. They were in unanimous agreement that the simulation was very compelling and believable. They noted that with the use of wide screen visual presentation, in conjunction with the G-seat and G-suit, the use of platform motion was not necessary to provide a highly realistic training environment.

In short, with the limited combined scenario presented, combat ready pilots exhibit:

- a. Clear learning of offensive and defensive tactics.
- b. Favorable responses to such training

Recommendations

It appears that the simulator may be able to supply an important training methodology for tactics development. With the development of greater computer capacity, the visual and other systems may be capable of producing dynamic changing combat environments which would allow the combat ready pilot to maintain his combat skills at a very high level. Flight simulation should fill the training void of those flying tasks which are impractical or impossible to practice in the real aircraft. It is, therefore recommended that continued development of combat environments be made with ever increasing variability and flexibility so the total concept of simulator tactics development can be more thoroughly tested and exercised. It is also recommended as a follow-on from such development, that comparisons be made between the performance scores in exercises such as Red Flag with pilots trained in simulation and with pilots who have not had such exposure. Such a program could very well determine what sort of transfer of training is taking place from the simulator to the tactical exercise field.

References

1. Future Views: Aircrew Training 1980-2000. Memo by Maj Jack Thorpe, Life Sciences Directorate, Bolling Air Force Base, D.C. 20332
2. DeLeon, Peter. "The Peacetime Evaluation of the Pilot Factor in Air-to-Air Combat. Rand Corporation Report R2070-PA. Santa Monica, CA, 1977

EFFECTS OF VISUAL AND MOTION CUES ON PILOT
EFFECTIVENESS DURING ENGINE-OUT TRAINING



George L. Cefoldo obtained his M.ED. in Guidance and Counseling and B.S.ED. in Secondary Education from Ohio University. After teaching psychology in the public schools he entered undergraduate pilot training in the USAF and was then assigned to the 4950th Test Wing, Wright Patterson AFB, Ohio as a C-135 research pilot. His responsibilities included support of missile and space activities for NASA, the Department of Defense and other government agencies; development projects in electronic countermeasures (ECM and ECCM), aircraft cockpit design, and component testing. In 1980 he joined the Boeing Military Airplane Company (BMAC) where he is an analyst in training device development.



Christopher J. Brady obtained his B.S. in Electrical Engineering from the University of Kansas. His three years of professional experience have been in industry. His work at Boeing included various systems engineering and hardware/software integration activities on the Weapon System Trainer. In addition, he spent nine months as an avionics analyst during the cruise missile competitive fly-off. He is presently a design analyst for new simulation products.



Robert K. Knapp (Ph.D. 1960, Michigan State) is Associate Professor of Psychology at Wichita State University, where he teaches courses in industrial, learning, and motivation psychology, and serves as Department Coordinator of Graduate Studies. In 1979 he became a Staff Consultant in Human Factors and Simulation at the Boeing Military Airplane Company, with responsibilities in Research and Development in the training system/simulation area.

EFFECTS OF VISUAL AND MOTION CUES
ON PILOT EFFECTIVENESS DURING ENGINE-OUT TRAINING

ABSTRACT

This study was designed to determine the need for visual and/or motion systems during engine out training in non-centerline thrust transport category aircraft. The KC-135A Flight Station portion of Boeing's Weapon System Trainer (WST) with a six degree-of-freedom motion system and three window daylight, dusk, and night visual system was used for this study. Qualified KC-135A air crews with 900 to 3000 hours experience were randomly presented normal and engine-out takeoffs with motion/no motion and varied visual conditions. Pilot Performance Data was recorded by the automatic data extraction system of the WST and six-channel strip chart recorder. Pilot recognition and response time was chosen for this analysis as the key to good performance during engine failure.

Fastest response time (and correspondingly lowest sideslip, bank angles, and roll rates) occurred in cue configurations involving motion and out-of-window visual displays. This configuration also produced the most efficient pilot management of engine loss. Subjective data suggested that although the subjects were committed to the need for motion cues in flight training devices, their error rates were very high when perceiving and describing actual motion cues.

INTRODUCTION

A major advantage of flight training devices is their ability to train pilots in situations which would be unsafe in true aircraft. Engine failure during takeoff is one such example. Here, it is critical for a pilot to recognize the emergency and initiate corrective action.

A multiple-engine, non-centerline thrust aircraft such as the KC-135 reacts to engine failure with an immediate yaw in the direction of the failed engine and sideslip in the opposite direction. If the emergency occurs during or after liftoff the additional problems of "Dutch Roll" must be countered. The frequency of the Dutch Roll is such that if a pilot takes two to three seconds to react to the engine loss he will excite or strengthen the roll and yaw tendencies. The KC-135A Flight Manual states that a "pilot reaction time of 3 to 4 seconds may allow a yaw angle of 9 to 12 degrees and bank angles of up to 15 degrees to develop prior to the initiation of corrective action". Further, the flight manual states in a WARNING that the pilot should "use extreme caution when bank angle is used, since the outboard engine pod will make contact at a bank angle of approximately 8 degrees" (Ref. 10). At the point of takeoff the outboard pods are 6.3 feet above the runway. Reaction time is thus critical to good performance during engine failure. The pilot who has had the opportunity to practice the engine failure emergency in a realistic training device should manage such an emergency better than one who encounters engine loss for the first time during the actual event.

The six degree-of-freedom flight training device with visual displays offers the opportunity to address nagging questions as to the comparative contributions of visual and vestibular motion cues in training tasks. Arguments for and against motion and visual system are familiar to researchers in training devices. (Caro, Ref. 1; Cohen, Ref. 2; Gundry, Ref. 4; Koonce, Ref. 5; Schwing, Ref. 8).

It can be argued that the dynamics of aircraft responses to sudden power asymmetry are first detected by the vestibular receptors, with visual stimulus sources used as consultant identifiers or as confirmers of senses felt (Cohen, Ref. 2). Alternatively, one can argue that body action occurs first in the case of learned reactions when the source of disturbance is previewed with the eyes as well as from a motion cue. This argument relies on the fact that the human vestibular apparatus tends to summate the various vectors of acceleration operating (e.g. yaw, sideslip, roll, pitch) and report them as a mean vector of motion, possibly contributing to vertigo (McCormick, Ref. 6). Thus, motion cues at times present a poor basis for corrective action during emergencies. On the other hand visual cues are useful only if the user happens to be looking in the area in which the cue is provided. In addition to representing the visual world a visual system can have a motion effect as investigated by Young, who states that a visual field can "trick" the human motion sensing apparatus into perceiving motion when none is occurring (Young, Ref. 12). This phenomenon is most evident in 360° or wide screen movie presentations such as those at Disneyland.

It appears that the issue of the relative importance of motion and visual cues will not easily be resolved and that cost may become the deciding factor in the purchase of visual or motion systems for training devices.

This study was conducted to determine the value of visual and motion cues on training effectiveness. From an informal study on motion requirements/needs, an emergency situation - outboard engine failure at takeoff - was chosen as a standard case. This allowed the study team to concentrate on the aspects of visual and motion cues contributing to pilot effectiveness in engine-out training.

METHODS

Subjects. Fifteen KC-135A aircraft commanders volunteered as subjects. Pilot experience level ranged from 900 flight hours to 3000 hours, with an average of 2,100 hours. Minimum flight time in the KC-135A was 500 hours; mean KC experience, 1,600 hours.

Equipment. The KC-135A Flight Station portion of Boeing's Weapon System Trainer (WST) was used for the study. This training device has a six degree-of-freedom motion system (Figures 1 and 2). The three window visual system has the capability of providing daylight, dusk, and night visual scenes projected onto the pilot's and copilot's front windows and pilot's side window.

Data Collection. Data was collected using three different and independent methods. The primary source of data came from the WST Automatic Data Extraction System (ADE). This system, which stores data in disc files, is



Figure 1 KC-135A WST at rest

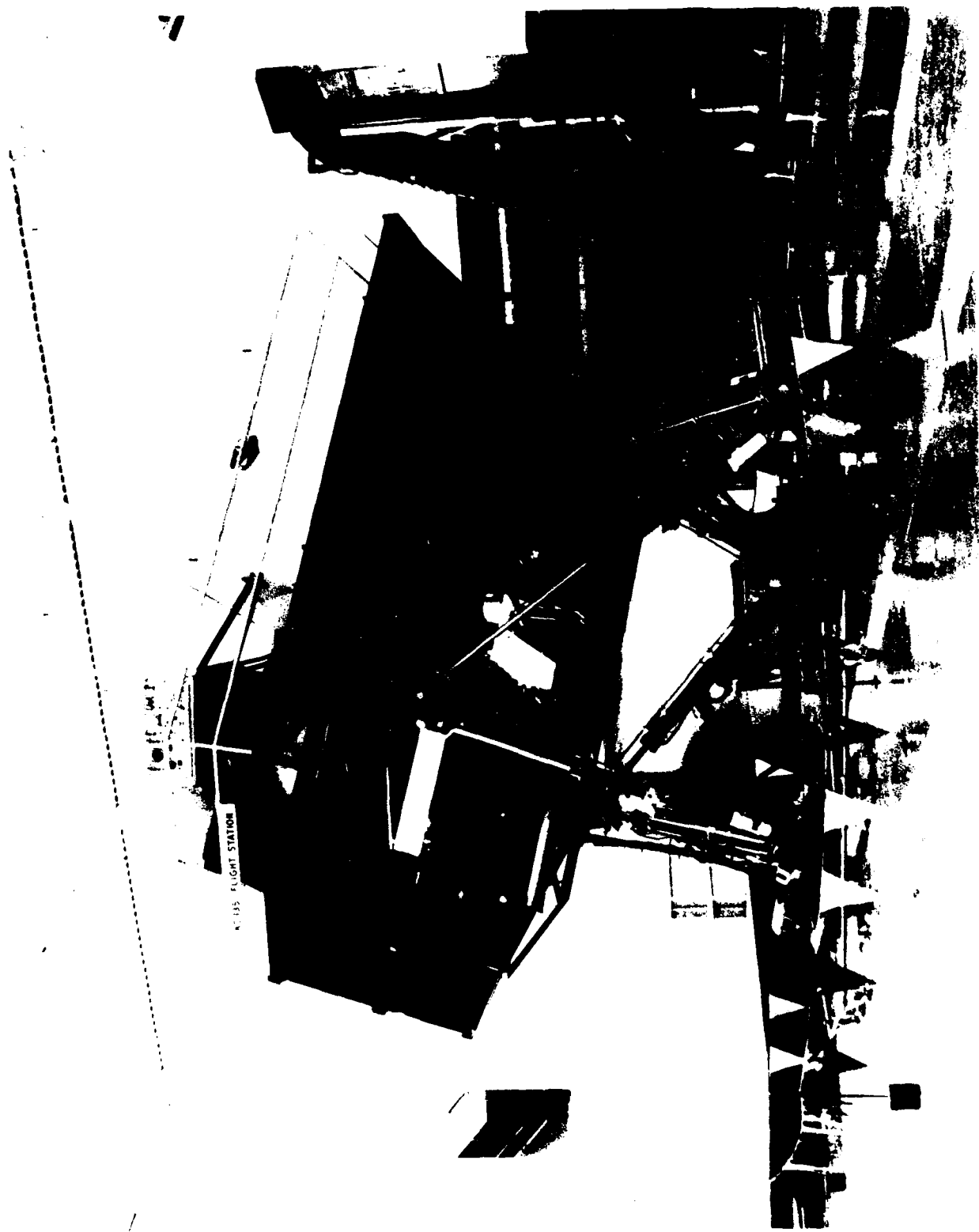


Figure 2 KC-135A WST with a number 4 engine failure (extreme case)

Alternatively, a small n approach was adopted for identifying effects of experimental variables and suggesting trends (Robinson and Foster, Ref. 7). This analysis, which must be considered tentative, utilized pooled motion cue combinations rather than separate analysis of the eight individual motion cues and interactions. Moreover, the dependent measure to be reported is pilot response time (elapsed time from engine failure to compensatory control input), which correlates positively with other dependent measures (bank angle, engine pod-to-ground clearance, yaw rate and angle, and sideslip angle (Example Figure 3). Means are reported due to their ease in graphing data and difficulty of presenting such large numbers of raw scores.

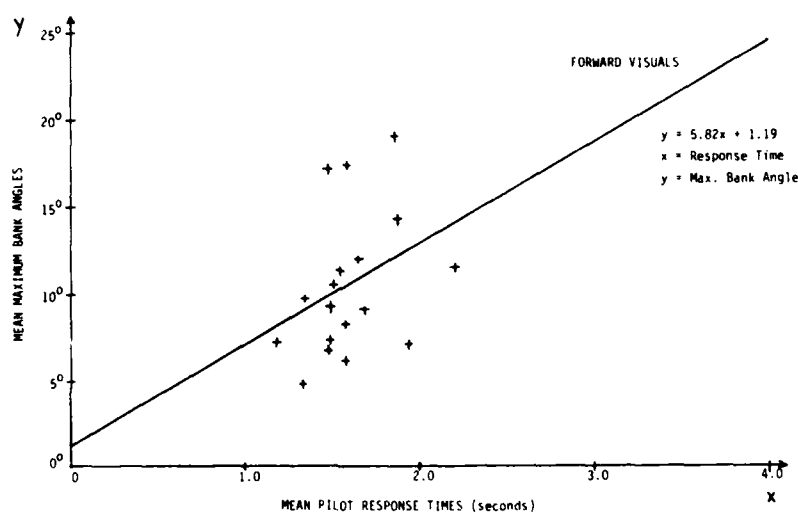


FIGURE 3. RESPONSE TIME vs. BANK ANGLE

The pilots who participated were all highly-trained, but had virtually no experience in simulators with motion systems. To both introduce the pilots to motion cues and assure them that the motion system was operable, we made no effort to damp or conceal the simulator's vertical excursions as it came up from rest or returned to rest. All test sessions began and ended with such an excursion; but on no-motion runs, the motion system was "clamped" off with the simulator in its raised "neutral" position, and no further motion cues were imparted. These preparatory simulator vertical excursions occurred at the beginning of each session, after twelve takeoffs when a stretch break was taken, and again after the 24th takeoff run. To alleviate boredom, after every fifth run, pilots were given a chance to fly an instrument approach and landing.

Following each takeoff run, pilots were asked to evaluate the adequacy of both motion and visual cueing systems for engine-out training. Questions about motion cues were asked following no-motion runs as well, to clarify whether the subjects could discriminate motion from no-motion conditions in the absence of verbal prompts and feedback from the experimenter. Of six possible motion cues imparted on motion runs, the subject had to identify at least two of the three primary motion axes (pitch, roll, and yaw) plus either the third primary axis or one of the secondary axes (surge, heave and sideslip) in order to be credited with correct motion cue identification.

RESULTS

Despite limitations in our data due to limited facility time, a case can be made for the reliability of the data by comparing pilot compensatory response to engine failure with and without motion cues where forward only vision was provided. Here, eight of sixteen subjects contributed data (167 takeoffs). Mean response time for the no-motion condition, forward vision only, was 1.71 seconds, which corresponds to the grand mean for all subjects for all takeoffs (1.83 seconds). With motion, these same subjects responded slightly quicker (mean = 1.56 seconds), a difference which is negligible (variance for all runs for all subjects = 0.22 seconds, standard deviation = 0.47 seconds).

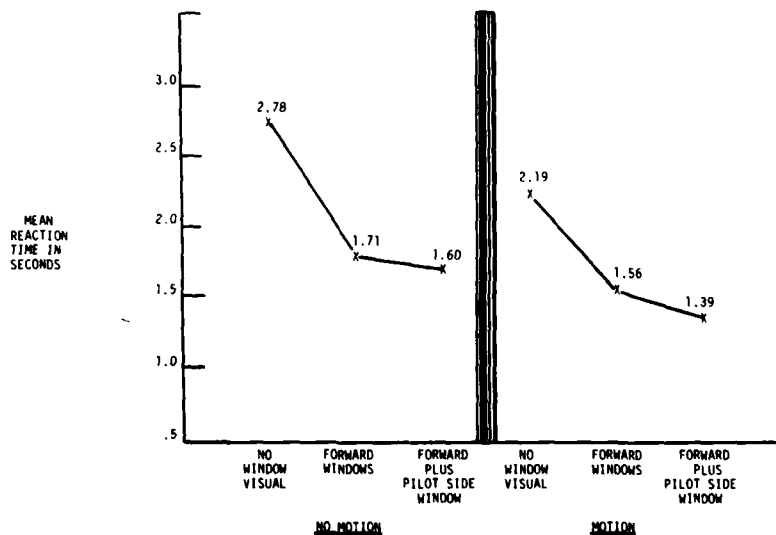


FIGURE 4. MEAN LATENCIES IN SECONDS BETWEEN ENGINE LOSS AND PILOT-INITIATED CORRECTIVE ACTION

Other comparisons in the data must be considered less reliable, due to fewer data points, but provide interesting results. For example, longest pilot response times are associated with absence of vision cues, regardless of presence of motion cues (2.19 seconds with motion vs 2.78 seconds without motion). Addition of a left peripheral window display to the forward display quickens pilot response. (No motion - 1.71 seconds, forward visual vs 1.60 seconds, forward-plus-side window. With motion - 1.56 seconds, forward vs 1.39 seconds, forward-plus-side window display.)

A disparity in pilot management of engine loss was apparent in all visualized data. Response to engine #1 (far left) was consistently more efficient than to engine #4. (Example: Forward-plus-pilot's left window, no motion, 1.40 -- 1.72 sec., respectively; with motion, 1.08 -- 1.60 sec., respectively). This implies a contribution to engine loss detection by the presence of peripheral cues in the event of left outboard engine failure whenever the pilot is looking out forward as the primary visual source. The data implies support for changes in aircraft cockpit design, and for the inclusion of side window visuals on training devices. Visual confirmation of engine-out conditions can occur and further quicken positive action if the pilot sees the failed engine's instruments. Without an out-of-window scene, time required to detect engine #1 or #4 failure is virtually the same (2.72 seconds, engine #4, -- 2.82 seconds, engine #1). Figure 5 is a representation of the KC-135 engine instrument panel. Further study needs to be undertaken to determine if the copilot has a similar problem with engine #1. More work with side window visuals should be done to prove that the side window displays contribute to increased training efficiency.

TABLE 2.
PILOT RESPONSE TIMES (SECONDS) TO LOSS OF #1 AND
#4 ENGINES WITH VARIED VISUAL AND MOTION CUES.

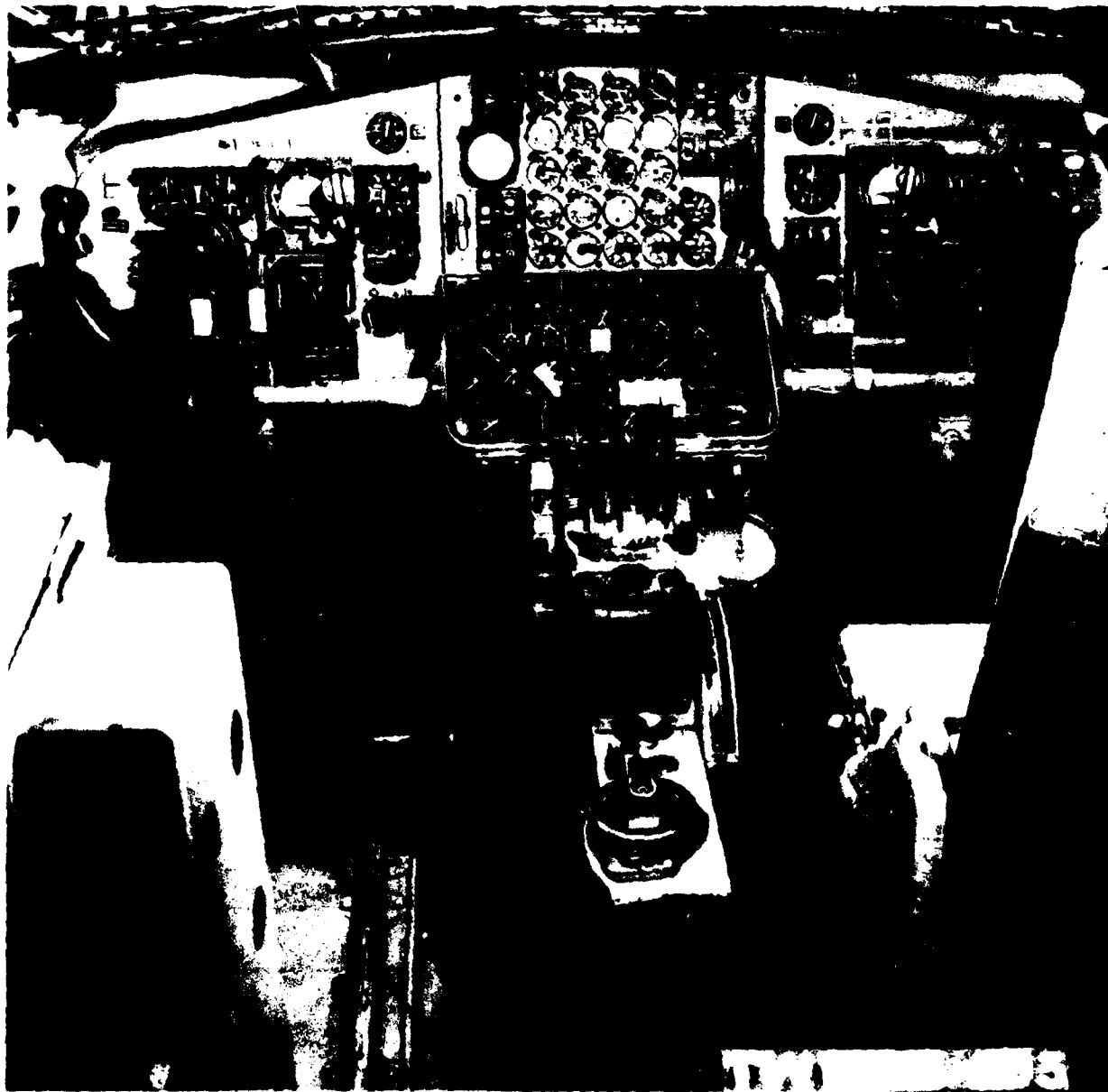
	NO ACTIVE WINDOWS		FORWARD WINDOWS ACTIVE		FORWARD AND LEFT SIDE WINDOWS		
AFFECTED ENGINE	NO MOTION	MOTION	MOTION	MOTION	MOTION	MOTION	MEANS
#1	2.82	1.84	1.57	1.52	1.42	1.08	1.71
#4	2.72	2.29	1.86	1.64	1.78	1.60	1.98

FIGURE 5. KC-135A INSTRUMENT PANEL

ENGINE INSTRUMENTS

1

#4



Specific Questions About Motion Cues. When neither motion nor visual cues were operating, judgments by pilots that "motion" cues were adequate occurred on 16% of takeoff runs (Figure 6, Line 1). Moreover, they erroneously specified the presence of motion cues on 84% of these minimal cue runs (Line 7). When visual cues were present (Figure 6, Lines 2 and 3), subjects' ratings of the adequacy of motion cues increased dramatically (79, 80%) while the level of confusion about the presence of motion increased to 93% (Line 8). In summary pilots were apparently convinced by the window displays that motion cues were operating when none were, and these "cues" were regarded as adequate for management of an engine loss emergency.

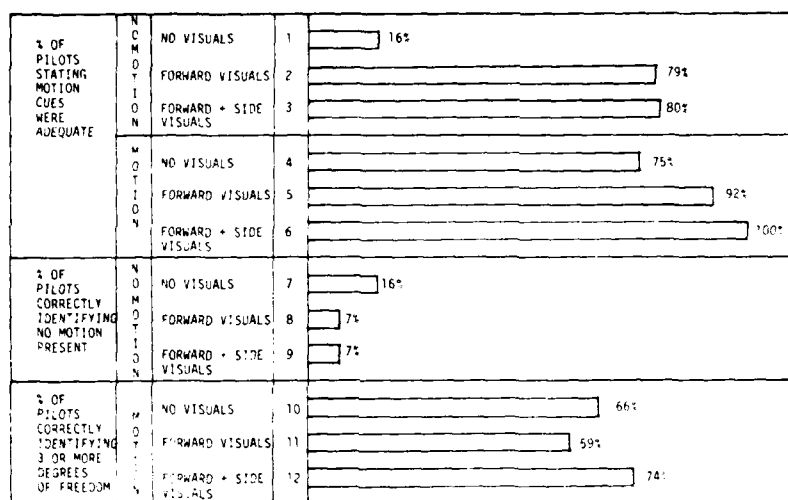


FIGURE 6. PILOT QUESTIONNAIRE RESULTS

The addition of motion cues (Lines 4, 5, and 6) led to judgments of increased adequacy but did not clear the perceptual confusion regarding the presence or nature of motion cues (Lines 10, 11, and 12). Pilots tended to be confused about the presence of motion or to deny in some cases that it was there. The most accurate identification of motion cues occurred on runs where motion and full visual cues were present (Line 12), but even here, 26% of the time incorrect judgments occurred.

An answer to the errors in motion perception caused by the inclusion of visual systems may come from the phenomenon of "self motion" as explained by Young (Ref. 12). Young presents data that suggests peripheral cues are required for self motion to occur and that subjects' mental set is very important. In the present case, the subject was "set" to perceive motion by the elaborate tour of the facilities and preparatory motion excursions described earlier in this paper. However, the peripheral cues provided in out-of-window forward visuals are minimal; and, thus, should not have encouraged the phenomenon of self motion. This fact may have been offset by the acceleration or change of visual field velocity during takeoff which can induce the sensations of pitch and roll so long as the velocity is, according to Young, "in order of the threshold of the semicircular canals (approximately $0.2^\circ/\text{sec.}$) and of the otoliths (.005 g's)."

Self motion, cannot account for the other side of the coin when motion is added to the visual presentation. In this case, false sensations of the body at rest must have been present. In summary, the subjective data imply that our pilots perceived motion when none was occurring and yet sometimes failed to perceive real simulator motion.

General Ratings of Visual/Motion System Contributions. In addition to post-takeoff interrogation, pilots were given general questionnaires about visual and motion systems in trainers at the conclusion of the study sessions. A summary of subjects' attitudes about visual/motion systems follows (percentage indicates agreement or strong agreement with the statement):

- o Is a motion system essential in an aircraft simulator? (70%)
- o I enjoy attending a simulator with motion more than one without. (100%)
- o A disturbance motion system is the most important factor in recognizing aircraft problems or emergencies. (80%)
- o A visual system is essential for training devices. (90%)
- o I enjoy attending a simulator with a visual system more than one without. (100%)
- o A motion system is not needed with expanded visuals. (30% agreed with this statement, 30% disagreed, and the remainder were undecided).

These attitude data, though tentative, suggest that pilots consider motion and visual systems about equally important, enjoy simulators with both, and are unsure whether visual cues can adequately supplant motion cues. They are more sure that motion cues are essential in aircraft training devices and that motion cues are most important in recognizing emergencies. The latter is in contrast to the pilots demonstrated inability to determine whether the motion system was on or off.

CONCLUSIONS

Pilot Performance. An intriguing finding in the present study was that pilots consistently responded more rapidly to loss of #1 engine (left outboard) than to loss of #4 (right outboard). Our considered opinion is that instruments associated with #1, being peripherally perceptible to the pilot, provide early cues to engine failure.

In the present study window displays led to improved pilot performance despite the disadvantaged visual presentation, where the horizon dropped out of view at the moment of engine failure. Improved performance with visual cues occurred in both the motion and no-motion conditions. The combination of forward plus left side vision and no-motion produced pilot reactions as timely as the combination of motion cues plus a forward-only window scene. These data conflict with those of DeBerg, McFarland, and Showalter whose subjects failed to show an advantage for visual displays in flight, (Ref. 3). In general, pilots performed better with an active visual system and an inactive motion system than they did when only the motion system was active.

Subjective Responses. The pilots reported strong beliefs in the importance of motion cues in managing engine loss and stated that disturbance motion cues are most important in that context. They also manifested a strong preference for simulators with visual and motion systems. Still, their post-trial attempts to identify the particular cues just experienced were characterized by excessive errors. The most dramatic of these occurred with both visual and motion systems active. Some pilots denied that motion had actually occurred (8% of the judgments). The opposite effect, where pilots reported the presence of motion when none had occurred, was substantially more frequent (93%) and suggests that a phenomenon such as visually-induced "motion" was operating.

Future Research. A full study of pilot performance based on the preliminary research outlined above should be undertaken. The failure management disparity between Engines One and Four needs to be resolved and possible action taken to improve instrument configuration so that response latencies are not degraded by cockpit instrument positioning.

The effect of side windows, i.e. peripheral cues, on performance should be further assessed and the training efficiency of this configuration explored.

1. Caro, P.W. The relationship between flight simulator motion and training requirements. Human Factors, Vol. 21, 1979.
2. Cohen, E. Is motion needed in flight simulation used for training? Human Factors, Vol. 12, 1970.
3. Deberg, O.H., McFarland, B.P., and Showalter, T.W. The effect of simulator fidelity on engine failure and training in the KC-aircraft. AIAA American Institute of Aeronautics and Astronautics Visual and Motion Simulation Conference. Dayton, Ohio, 1976.
4. Gundry, A.J. Thresholds to roll motion in a flight simulator. AIAA American Institute of Aeronautics and Astronautics Visual and Motion Simulation Conference. Dayton, Ohio, 1976.
5. Koonce, J.M. Predictive validity of flight simulators as a function of simulator motion. Human Factors, Vol 21, 1979.
6. McCormick, E.J. Human Factors Engineering, Third Edition. New York: MacGraw-Hill, 1979, p562.
7. Robinson, P.W., and Foster, D.F. Experimental Psychology; a small-n approach. New York: Harper & Row, 1979.
8. Schwing, R.L. The man-rating associated with AFFDL LAMARS system. AIAA American Institute of Aeronautics and Astronautics, Visual and Motion Simulation Conference. Dayton, Ohio, 1976.
9. Shirley, R.S., and Young, L.R. Motion cues in man-vehicle control. IEEE Transactions on Man-Machine Systems. Vol. MMS-9, No.4. December, 1968.
10. USAF Series KC-135A Aircraft Flight Manual, T.O. IC-135 (K) A-1. February 1966; Change 46, August 1980.
11. USAF Series KC-135A Aircraft Flight Manual, T.O. IC-135 (K) A-1-1. Appendix I, Performance Data, June 1966; Change 38, August, 1979.
12. Young, L.R. Visually induced motion in flight simulation. AGARD Conference Proceedings No. 249: Piloted Aircraft Environment Simulation Techniques. Brussels, Belgium: NATO Advisory Group for Aerospace Research and Development, 1978.

A REAL-TIME COMPUTER IMAGE GENERATION SYSTEM
USING TEXTURED CURVED SURFACES



Geoffrey Y. Gardner
Staff Scientist
Grumman Aerospace Corporation

Dr. Geoffrey Y. Gardner is a Staff Scientist and principal investigator of the Advanced Computer Image Generation project at Grumman Aerospace Corporation. He holds a BA from Harvard and a PhD (EE) from the Polytechnic Institute of New York. During his 20 years with Grumman he has performed research in advanced applications of computers including the analysis of stress electrocardiograms and the identification of bullets.



Edwin P. Berlin, Jr.,
Computer Design Engineer
Grumman Aerospace Corporation

Edwin P. Berlin, Jr., BSEE, Massachusetts Institute of Technology, designs high-throughput computers. He holds a patent on a three-dimensional display device and has another pending.



Bob M. Gelman
Engineer
Grumman Aerospace Corporation

Bob M. Gelman obtained his B.S. from Cooper Union in Mathematics. His 6 years of professional experience has been in industrial and military applications. He has developed software systems for flight test equipment and simulator installations. His hardware experience has included video and 35 mm film studio equipment design. He is currently developing software techniques for real-time computer image generation.

A REAL-TIME COMPUTER IMAGE GENERATION SYSTEM USING TEXTURED CURVED SURFACES

Dr. Geoffrey Y. Gardner, Edwin P. Berlin Jr., and Bob Gelman
Grumman Aerospace Corporation

ABSTRACT

This paper describes a next generation CIG system that produces a more faithful representation of the real world than current edge systems. Using textured curved surfaces to model scene features, the system produces realistic scene detail providing better flying cues in training simulators. Advanced techniques for scene modeling and imaging are implemented in a unique system architecture to achieve real-time image generation of superior quality.

INTRODUCTION

As computer image generation (CIG) has developed over the past two decades, the simulator community has come to rely on it as the best means of providing visual cues for training. To achieve the high data rates required by real-time displays, early CIG systems had to simplify the computation by reducing the world they modeled to a linear approximation defined by edges. Although edge systems have been greatly refined over the years, the basic limitations of the approach persist. Consequently, current CIG systems still produce a stylized representation of scene features that is characterized more by linear artifacts than by the true nature of the real world. In addition, current CIG systems are unable to provide adequate scene detail. As a result of these shortcomings, current CIG systems are severely limited in the quality of training that they can produce.

In an attempt to satisfy the stringent requirements of effective training current CIG manufacturers are striving to increase scene content by increasing the edge capacity of their systems. But serious cost barriers stand in the way. As the edge count goes up so do the costs of scene modeling, data management and image generation. CIG manufacturers are relying on a breakthrough in hardware or edge-handling techniques to surmount these barriers, but they ignore the basic problem. The simplistic straight edge is an inefficient and ineffective primitive with which to model the subtle, non-linear complexity of the real world.

To avoid the limitations inherent in edge systems, the Grumman Aerospace Corporation's Advanced Computer Image Generation project (ACIG) is pursuing a unique approach to develop a next-generation CIG system. To model a scene we use a geometric data base of curved surfaces to represent the non-linearity of the real world. A mathematically generated texturing, mapped onto the surfaces, produces essential scene detail unavailable in current systems. The total data base, composed of parameters of analytic functions instead of discrete vertex points, is much more compact than that required for edges, yet the scene content is far greater and represents the real world much more faithfully. Our goal is to develop techniques that take advantage of this streamlined data base to reduce the costs involved in scene modeling, data storage and transfer, and image generation, and to provide the essential flying cues required to assure effective training. Because we realize that

this effort will be meaningful only in its ultimate application, we have included as a major part of our project the development of a novel system architecture to implement our CIG techniques in cost-effective real-time hardware.

This paper will describe the research and development work performed in the ACIG project and work funded by the Air Force under the contract entitled Advanced Computer Image Generation Visual/ Sensor Simulation (AVSS).

PROGRESS ON ACIG

In order to avoid the limitations of edges in modeling the natural curvature of real-world features, we have chosen a scene data base that includes curved as well as planar surfaces. The simplest form of curved surface is the quadric, or second-order, surface (1). Although quadric surfaces have been studied extensively for non-real-time image generation applications, such as computer-aided design, they have been considered only for limited use in real-time CIG systems (2). This neglect of a very powerful modeling tool stems partly from the early success of edge systems and partly from real geometric limitations of the quadric surface.

Because the quadric surface is the simplest curved surface it is not as easily fitted to irregular terrain data as are higher-order surfaces. For this reason, more attention has been given to higher-order surfaces, in particular the bicubic surface. However, even though bicubic surfaces can model irregular terrain more easily and with greater slope continuity than quadrics can, they require prohibitive computation to determine silhouette boundaries, to produce intensity shading and texturing and to implement antialiasing (3). In addition, bicubic surfaces are best implemented as sets of surface patches. The number of patches involved and the complexity of the patch definition produce a cumbersome and costly data base. Modeling with bicubic patches, therefore, tends to be another, more sophisticated, brute force approach whose success depends on major breakthroughs in both software and hardware.

Our strategy has thus been to develop techniques that take advantage of the analytic simplicity and minimize the limitations of quadric surfaces to produce the most cost-effective visual display for simulation.

Implementation of Quadric Surfaces

Quadric surfaces can model a scene as the eye perceives it, as a set of individual features each defined by a small number of surfaces. We can model a significant scene feature such as a tree or a hill with one or two surfaces as opposed to the numerous planar patches required in edge systems. Although a great deal of flexibility in modeling complex features can be gained by using multiple intersecting quadric surfaces, this is not cost-effective. Surfaces of second order intersect to produce curves of fourth order which require too much computation for real-time feasibility. Therefore, our first step in implementing quadric surfaces has been to introduce a data base constraint to maintain computational efficiency. We compose our data base as a set of objects, each of which is defined by one quadric surface and a finite number of planes. We found it efficient to limit the number of planes to six,

although there is no theoretical limit. An object may include a quadric with no bounding planes or may be defined by planes only. Many scene features can be defined by a single object; complicated structures, such as aircraft, are defined by multiple objects.

The simplicity of this data base allows for efficient techniques to project all the boundary curves onto the image plane, since all boundary curves are second-order. The quadric silhouette is projected as the limb curve, and each curve of intersection between the quadric and a bounding plane is projected as an intersection curve. The nature of perspective geometry also allows a simple computation of the silhouette plane of the quadric surface. We have developed sophisticated visibility logic using the projection of the intersection between a bounding plane and the silhouette plane to define a visibility line on the image plane. The visibility lines are used to delete all portions of the limb and intersection curves which are invisible. Thus, we have greatly simplified the intraobject visibility determination, the removal of hidden surfaces on a single object, by using only the boundary information.

Interobject visibility, removal of hidden surfaces on one object occulted by another object is even simpler. A priority list of objects is established for each frame, initially containing only those objects defined in the data base to be adjacent (such as two mountain peaks or an aircraft wing and fuselage). The bounding plane between two adjacent objects is used to determine which object has priority relative to the current eyepoint. On a scan line basis, interobject visibility is tested if the boundary points of two objects overlap. The test first checks the priority list to resolve the visibility. If the two objects are not in the list, test of distance to the silhouette planes is used and the priority determination is added to the list.

In this manner, we have developed a unique and efficient solution to the hidden surface problem of curved surfaces. Because this technique operates on a scan line basis, using only boundary information, it reduces the problem to a simple level that can be handled in real-time.

Shading of Bounded Quadric Surfaces

Our technique for determining the visibility of quadric surfaces achieves its efficiency by using only the boundary points in the image. Surface shading must be computed for all surface points in the image. Since the number of these points is considerably greater than the number of boundary points, a brute force implementation would be costly. By taking advantage of surface coherence, we can significantly reduce the computation of smooth surface shading. We have developed a technique that uses the fact that the shading due to diffuse reflection from quadric surfaces varies smoothly along a scan line. To shade a quadric surface along each scan line we compute the shading at each boundary point and at a point midway between. Interpolation between these points produces an efficient and acceptable approximation to the exact shading. Figure 1 shows the effectiveness of this technique. The model of the KC-135 was constructed of 21 objects requiring a total of 532 data values to define the data base. To produce equivalent quality of smooth shading and feature definition, edge systems would require a data base an order of magnitude greater than ours.

Texturing of Bounded Quadric Surfaces

Although quadric surfaces such as hyperboloids provide an effective basis for modeling major terrain features, texturing must be overlaid to represent natural detail necessary to produce essential flying cues. To minimize the scene data base and still provide a variety of texture patterns representative of a mission gaming area, we have developed a texturing technique that uses a mathematical function to represent the statistical characteristics of surface detail with a limited number of parameters (4). The value of the function, computed at each pixel, is used to modulate the surface shading. Although this is the most computationally intensive technique in our system, we have determined that real-time implementation is feasible at an acceptable cost.

An important feature of any effective texturing technique is perspective validity, that is, the texture pattern must be fixed to the surface in the scene as it is viewed continuously from different eyepoints. We achieve perspective validity by defining our texturing function as a function of scene coordinates. To avoid computing the scene coordinates for each pixel we use an interpolation technique similar to that used for shading. Dynamic image testing has confirmed the perspective validity provided by this technique and has demonstrated the superior flying cues produced by the scene detail generated by the texturing. Figure 2 shows how effectively terrain can be modeled by quadric surfaces with scene content enhanced by texturing. The scene consists of four hyperboloids and a ground plane with texturing generated by a 23-parameter function.

The power of our functional approach to texturing is demonstrated further in Figures 3 and 4. Because we can control the function completely as we generate the texturing, we can add variable translucence to produce natural features with very irregular boundaries, such as clouds and trees. Control of the function can be implemented dynamically to produce frame-to-frame variations to simulate wind effects on the clouds or trees.

PROGRESS ON AVSS

To develop a next-generation CIG system free of the limitations of current edge systems, the Air Force has undertaken the three phase AVSS project. Phase I includes development of advanced CIG techniques and an overall system concept. Phase II will include software development, image testing, and hardware design. Phase III will involve construction of a real-time prototype system. Grumman's effort on Phase I has included the investigation of candidate techniques to provide the features listed in Table 1. Based on our investigation we chose the best technique for each feature and developed a system concept to incorporate all chosen techniques in a feasible real-time system. In the implementation of each feature, the technique we developed represents a significant advancement in CIG technology. We will describe the system concept and some of the most significant techniques.

System Concept

The standard system approach in current CIG systems is a large pipeline which implements all of the equations, tests, and flow of a particular set of techniques. This results in a massive special-purpose processor with many different types of modules. Typically, circuit boards must be wire-wrapped, and interconnection of boards is a problem. A change in the features requires changes or additions to the hardware. This type of large system has frequent failures and is extremely difficult to repair and maintain. Current systems use TTL and even ECL which dissipate large amounts of power.

Figure 5 shows a block diagram of our system architecture. The basic premise of this design is to partition the processing to be performed into tasks which can make effective use of parallelism. These tasks are then pipelined at the frame level. Tasks may be divided into subtasks which are performed by an array of processing elements operating in parallel. Tasks are chosen to minimize interprocessor communication.

There are two critical tasks which must be partitioned. The first is to transform, project and remove hidden curve segments for each object in the scene. This task is performed by a number of processors which we call object processors. This task partitions very efficiently - each object processor computes one object in the scene. Interprocessor communication within this task is not needed because all operations can be performed on a given object with no information about other objects in the scene.

Once the curve and surface information is determined for each object, the entire set of objects must be rendered with interobject visibility determined. This task is partitioned by dividing the frame into subframes, with each subframe computed by a separate processor. This is an appropriate partitioning because, while there are many objects in a scene, the number of objects overlapping a subframe can be limited to a small number. With only a little overhead for scan line intersection and antialiasing at the subframe border, interprocessor communication at this level is unnecessary.

Each object processor determines which subframes require its object information and routes object information over a bus connecting object and subframe processors.

Object information enters the object processors from a standard mainframe computer. This computer takes information from a simulator console or flight simulator computer and determines which objects are in the current scene. The scene is paged into memory from disk as a function of eyepoint and look angle. Object processors make use of frame coherence in that, if an object is present in two successive frames, it is processed by the same object processor. Thus, the mainframe computer needs only to transmit new objects to object processors as they appear and keep track of object processors which can be reclaimed. This limits the bandwidth between the mainframe and the object processors.

At the output of the subframe processors, the separate subframes are pieced together and converted into a raster format for an RGB display. The single output signal is the highest bandwidth channel in the system.

There are many advantages of the proposed system architecture. Because of efficient task partitioning, the problem has been defined in terms of many identical modules, each of which operates at a fraction of the total system throughput. Since the modules are identical, they can be implemented in a cost-effective manner using LSI technology. Each processor will be smaller, cheaper, and use less power when implemented in this way. Cost can be minimized by trading off the throughput of each processor as a function of technology, and the size, number and complexity of each processor. The system is flexible since system parameters such as number of objects or size of frame can be varied by changing the number of modules. Additionally, each processor is programmable, so that system features can be altered, extended or customized simply by updating the software. Such a system is much more resistant to obsolescence than hardware-oriented pipeline systems.

For prototype debugging, our risk is minimized since we can build and debug a single object and subframe processor. These processors can be driven by a general purpose computer to produce a full image for testing before the final design is committed. At that point, the processors can be replicated to build a real-time system.

Surface Visibility

We refined our intraobject visibility technique greatly by taking advantage of scan-line coherence. Our refined technique will be implemented in each object processor and will use the computed visibility lines of an object to determine all visible boundary portions and those scan lines on which each portion is visible. The object processor will pass this visibility information to the appropriate subframe processors which will then compute only the visible boundary points. This represents a significant increase in processing efficiency over our old technique, which required computation of all boundary points on a scan line, testing the visibility of each, and deleting those that were hidden. The effectiveness of our new technique is demonstrated by Figures 6 through 9. These figures also demonstrate the complexity of the objects that can be modeled using quadric and planar surfaces.

Tonal Computation

We refined our technique for diffuse shading by extending the scan line interpolation to interpolation across scan lines as well. An interpolation function will be computed for a surface in the object processor and passed to the appropriate subframe processors. The subframe processor computation will be limited to incremental calculation of the function along each scan line with incremental updating of interpolation function coefficients from scan line to scan line. A significant benefit of this refinement is that it eliminates the need for projecting into scene coordinates during scan line processing.

Specular reflection, which provides valuable cues for target detection, is much more complicated to model than diffuse reflection and is consequently not included as a feature of current systems. We extended our diffuse shading

interpolation technique to provide an efficient approximation to the physics of specular reflection. A good mathematical model for specular reflection involves an expression of three vector dot products, one of which is the dot product used for diffuse reflection. Our analysis has shown that the other two dot products vary across a surface almost as smoothly as the diffuse shading dot product. We will therefore approximate each dot product by interpolation and compute the expression. The model for specular reflection requires raising the expression to a power as high as 10, but this can be done efficiently by using an exponent that is a power of 2 or by using a look-up table. The added computation for this technique is acceptable and should provide an effective representation of the essence of glint from windows, still water and metallic surfaces.

Antialiasing

The ideal solution for antialiasing an image is to filter out all spatial frequencies higher than half the spatial sampling frequency. We developed a prefiltering technique that approximates the ideal solution very effectively by applying a non-uniform weighting to the image over a region covering two sampling periods in the horizontal and vertical directions (5). Current CIG systems use an area-weighted average for each pixel. This technique applies a uniform weighting over one sampling period and is therefore a poor approximation to the ideal solution. Figure 10 shows a test image of a set of annular surfaces of one-half-pixel width with severe aliasing. Figure 11 shows the result of antialiasing using the current area-weighted average technique. Figure 12 shows considerable improvement in antialiasing using our technique. Although our technique greatly outperforms that of current systems, it is much less costly to compute.

Scene Control

One of the significant problems for any CIG system is level of detail (LOD) management to avoid system overload. Our compact data base, using textured quadric surfaces, minimizes this problem by defining scene features as efficiently as possible. In addition, the nature of our object modeling allows us to implement LOD management effectively with only two levels of detail. The high level of detail will consist of features represented in full detail. The low level of detail will consist of a single object representing a cluster of these features. For example, a forest will be represented in high LOD as a large number of individual trees and in low LOD as a single textured, bounded quadric. At long distances, only the low LOD forest will be presented. At short distances, the high LOD trees will be shown. To transition smoothly as the viewpoint approaches a distant forest we will introduce a bounding plane to truncate the forest on the near end (Figure 13). The plane will be constructed at a fixed distance from the viewpoint and will continuously truncate the low LOD object as the eye approaches until the LOD object is completely eliminated. Meanwhile, the high LOD objects just beyond the plane (inside the low LOD object) will appear with diminishing translucence. As the high LOD objects emerge in front of the bounding plane, their translucence will be decreased till they are completely visible. The process would be reversed for viewpoint motion away from the forest. This

technique will introduce minimal data base overhead while providing effective scene control with smooth transitions to prevent overload.

DMA Elevation Modeling

The greatest problem involved in modeling with quadric surfaces is to model arbitrary topographical data, such as the Defense Mapping Agency (DMA) elevation data, with adequate surface continuity. However, modeling the DMA data base with edges has produced unacceptable representations characterized more by linear artifacts than by natural contouring. Our approach to this problem has been to model the significant terrain features with quadric surfaces and to represent the secondary terrain fluctuations with texturing. We have divided our approach into the following subtasks:

- o defining the significant features
- o isolating the DMA data samples for each feature
- o fitting a quadric surface to the data samples for each feature
- o adding bounding planes to each quadric to maximize surface continuity between features
- o determining texturing function parameters to represent secondary topographical variations in the DMA data.

In a limited empirical study using actual digitized elevation data, we developed a technique using low-pass filtering to reduce the data to its significant features, which can be predefined by the choice of filter bandwidth.

To isolate the significant features in the filtered data we developed a technique which applies the Laplacian operator to the data to detect points of extreme curvature at the feature boundaries. We also developed a technique analyzing the data profile by profile and using profile coherence within features.

Once the feature sample points are located, fitting a quadric surface by least squares minimization is straightforward. Computation time is acceptable in view of the fact that the modeling will be done off-line.

The equations of the quadrics fitted to the features provide the information necessary to fit bounding planes at the juncture of adjacent features. Our technique allows construction of layers of features, one on top of the other, to model complicated terrain.

The texture function parameters will be based on the frequency content of the original data above the low pass filter cutoff, i.e., those frequencies not included in the quadric surface determination.

In this manner, we will model the major topographical features of the DMA elevation data explicitly, and we will represent the minor topographical variations statistically. This approach has significant advantages over current edge techniques. First it will produce a far more compact data base. Second, it models the data as a set of features as the eye would perceive the scene and therefore provides an optimum representation for visual cues.

Third, the filtering and surface fitting operations suppress random errors which are known to be present in the DMA data. Finally, as shown in Figure 2, textured quadric surfaces produce a far more faithful representation of natural nonlinearity and detail than is possible using edges.

Other AVSS Features

Other system features are significantly enhanced by our ability to model with quadric surfaces. Scene modeling is simpler and more effective due to our ability to represent curvature so efficiently. This is true of cultural features as well as natural features, as shown in Figures 1 through 4. Implementation of moving models is simplified because there is less data to which transformation of coordinates must be applied. Greater capability for special effects is provided by textured quadrics, which can efficiently model clouds, puffs of smoke, and balls of fire. Our capability for dynamic texturing will enhance the realism of these effects to provide cues of wind and weapons effects. In addition, our ability to handle curved boundaries in the image will facilitate representing shadows as simply bounded regions on a surface and lights of finite size. Our antialiasing technique will produce an enhanced representation of point light sources free from distracting scintillation anomalies.

CONCLUSION

Textured quadric surfaces provide an efficient and effective means of scene modeling. They present greater scene content of higher quality than that produced by edge systems. The many fundamental advantages in this form of modeling allow cost-effective solutions to many of the problems that degrade current systems. At the same time, quadrics are far simpler and cheaper to implement than higher-order surfaces.

Our goal has been to find and exploit the most efficient means of providing essential cues to provide more valid training. We believe that quadric surfaces with texturing are the most efficient means, for they epitomize a fundamental truth stated by Einstein: "Everything should be as simple as possible, but no simpler."

ACKNOWLEDGMENT

The research described in this paper was sponsored in part by the Air Force Human Resources Laboratory (AFHRL) under contract F33615-79-C-0029.



Figure 1



Figure 2

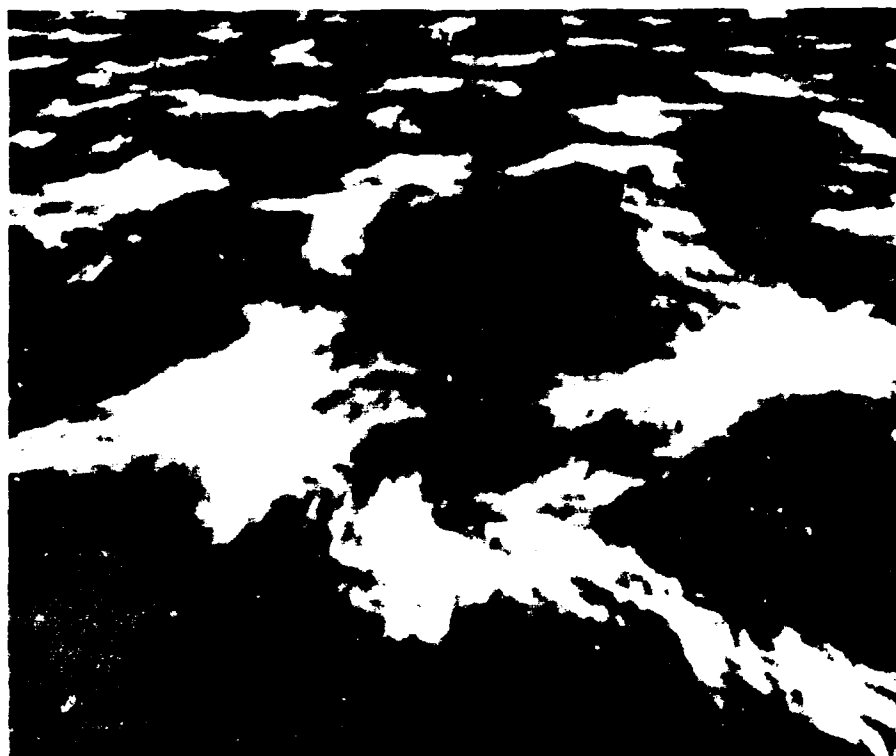


Figure 3



Figure 4

SURFACE VISIBILITY
TONAL COMPUTATION
ANTIALIASING
SCENE CONTROL
DMA ELEVATION MODELING
SCENE MODELING
MOVING MODELS
SPECIAL EFFECTS
SHADOWS
TEXTURING

Table 1

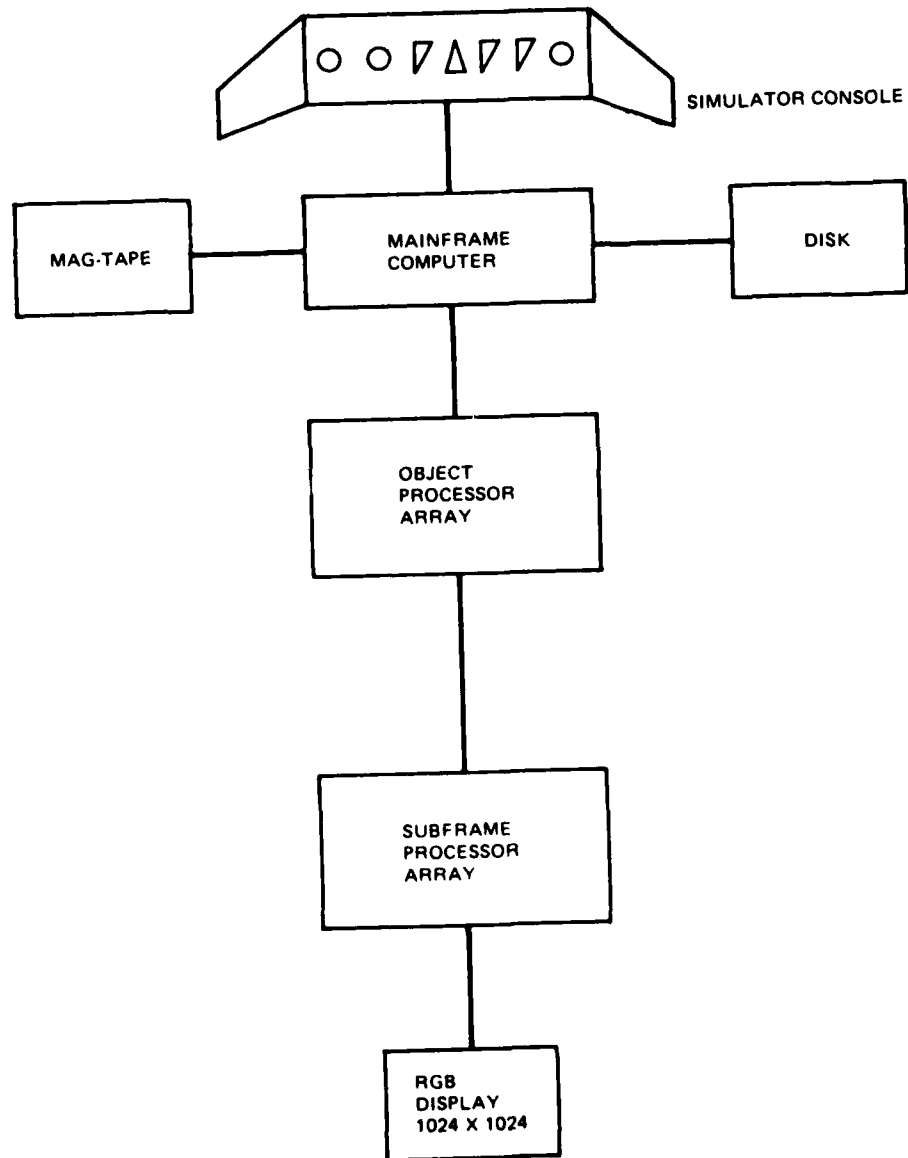


Figure 5

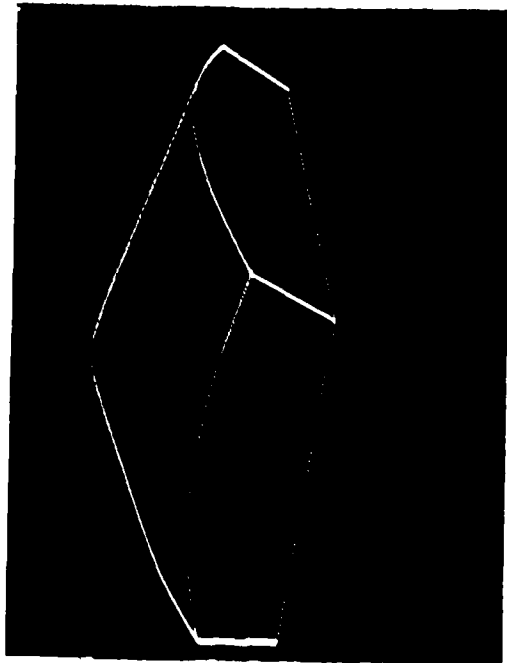


Figure 7

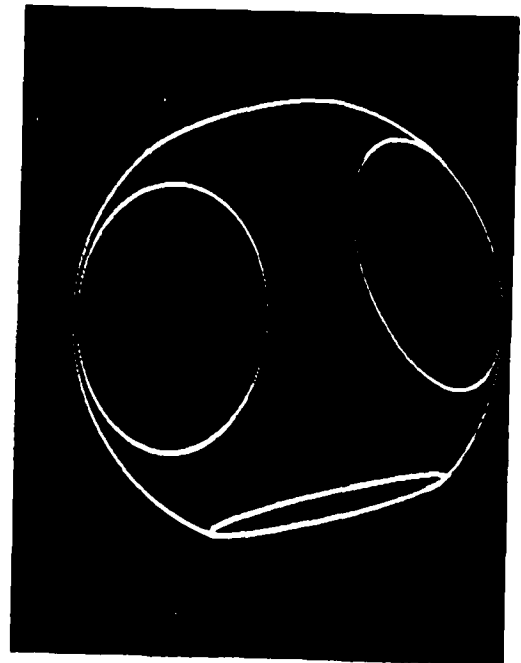


Figure 9

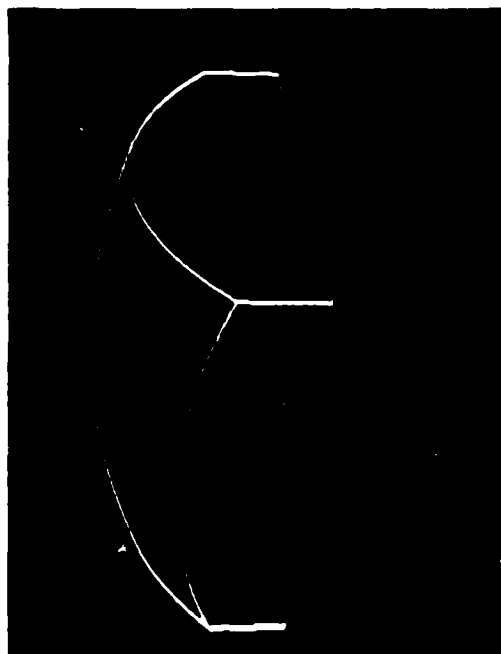


Figure 6

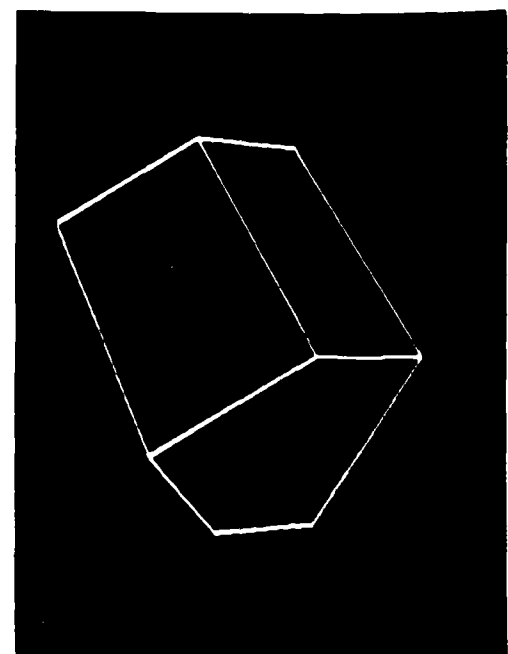


Figure 8

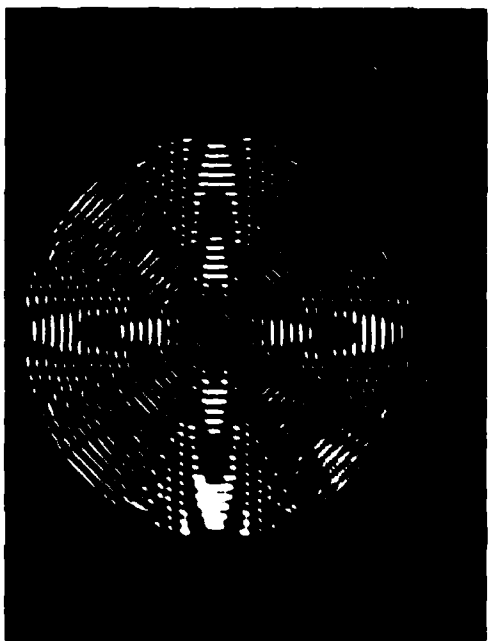


Figure 10



Figure 11

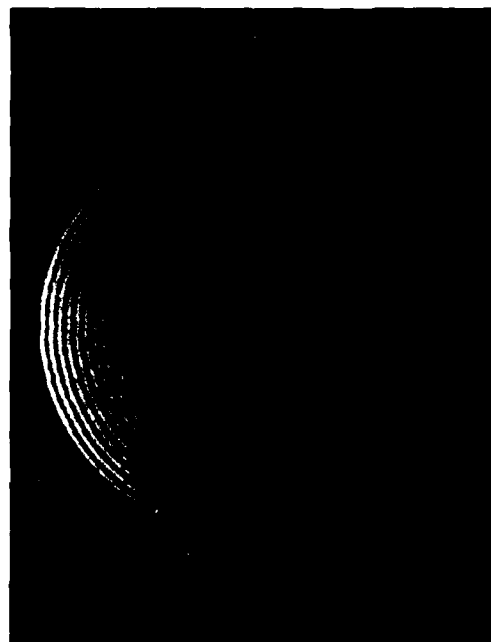


Figure 12

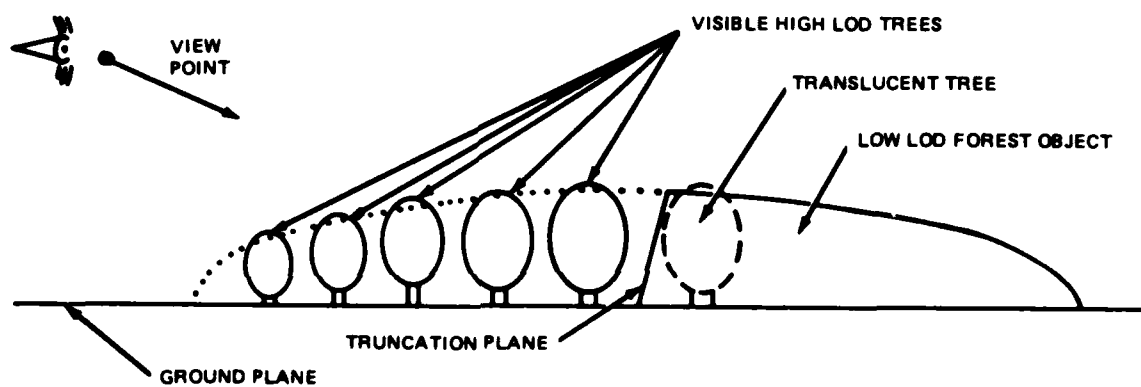


Figure 13

REFERENCES

1. Gardner, G.Y., "Computer Image Generation of Curved Objects for Simulator Displays," Eleventh NTEC-Industry Conference, Orlando, Florida, November 1978.
2. Yan, J.K., "Real-time Generation and Smooth Shading of Quadric Surfaces," First Interservice/Industry Training Equipment Conference, Orlando, Florida, November 1979.
3. Yan, J.K., "Computer Generation of Curvilinear Objects," Second Interservice/Industry Training Equipment Conference, Salt Lake City, Utah, November 1980.
4. Gardner, G.Y., "Computer-Generated Texturing to Model Real World Features," First Interservice/Industry Training Equipment Conference, Orlando, Florida, November 1979.
5. Gardner, G.Y., and Berlin, E.P. Jr., "Effective Antialiasing of Computer Generated Images," Second Interservice/Industry Training Equipment Conference, Salt Lake City, Utah, November 1980.

SESSION II

Chairman

Captain Thornwell F. Rush
Assistant Chief of Staff for Flight Training,
Chief of Naval Education and Training,
Pensacola, Florida



Captain Thornwell F. Rush, of Camden, South Carolina, entered the Navy as a midshipman at the U.S. Naval Academy in July 1947. He was commissioned an Ensign in June 1951 and was designated a Naval Aviator in November 1952.

Captain Rush served his first sea tour with Fighter Squadron 171 with deployments in the USS WASP and USS CORAL SEA between January 1953 and July 1955. Subsequently, he reported to the U.S. Naval Academy as a company officer in the Executive Department. In August 1959, Captain Rush joined Attack Squadron 86 where he served as Maintenance Officer until reporting to the Naval War College as a student in August 1962. Upon completion of his training at the Naval War College, Captain Rush was assigned to the USS FORRESTAL where he served as Flight Deck Officer and Assistant Air Operations Officer. Upon completion of his shipboard tour, he reported to Attack Squadron 36, USS ENTERPRISE, assuming command of that squadron in March 1966. He was relieved in May 1967 while deployed on the USS AMERICA.

In June 1967, Captain Rush reported to the Bureau of Naval Personnel and served as the aviation detailer for Lieutenant Commanders and below. He was transferred in June 1969 to the USS SHANGRI LA where he served as Operations Officer, Executive Officer and Commanding Officer for decommissioning the ship in July 1971.

Captain Rush returned to Washington, D.C. in August 1971 and attended the National War College. He returned to the Bureau of Naval Personnel in July 1972 as the Special Assistant to the Chief of Naval Personnel for POW/MIA matters. He served in this capacity until his detachment in April 1975. Captain Rush assumed command of USS LEXINGTON, CVT-16, on 9 July 1975 and detached in May 1977. From there he was ordered to Commander Cruiser Destroyer Group One as Chief of Staff, a position he filled from June 1977 until August 1979. In September 1979, Captain Rush reported to Chief of Naval Education and Training as Assistant Chief of Staff for Flight Training, the position in which he currently serves.

A 3D SYNTHETIC IMAGERY GENERATOR IN REAL TIME



Pascal Leray
Centre d' Electronique de l'Armement

Pascal Leray obtained the title of engineer in 1969 from Ecole Centrale de Paris. His 12 years of professional experience have been in industry and teaching (Mathematics, Automation, Numerical Analyses, Statistics). In AMX, he designed a simulation program for the missile PLUTON. He wrote and implemented a graphic subroutine package called "GRAFOR" (Graphic-Fortran) at the Centre d' Electronique de l'armement" (CELAR). In 1976 he simulated hidden surface algorithms on a SIGMA 7 computer. These studies were followed by the hardware and software conception and realization of the Synthetic Imagery Generator (GJI).

ABSTRACT

The recent needs in aircraft training, spatial flights have increased the studies of flight simulators, with realistic real-time picture animation.

These pictures may be :

- aircrafts, space-shuttle, vehicles, landscapes, airports,...

One of the missions of the CENTRE D'ELECTRONIQUE DE L'ARMEMENT is military systems assessment.

In order to evaluate military aircrafts it was build a dog flight simulator. One of the enhancement decided in 1977 for this simulator consists in a video synthetic image generator for the target projection.

KEY-WORDS

- 3 D graphics,
- raster-scan displays,
- computer aided design 3 D,
- simulation.

1 - INTRODUCTION

The objectives of the generator were :

- definition : 512 X 512,
- brightness levels : 256,
- regeneration time for each image : 40 mS,
- output : Red Green Blue coded via a look-up table of 256 words of 24 bits,
- complexity of the object : up to 400 polygons,
- objects : aircrafts, helicopters, vehicles,...

The goal of this paper is to describe :

- a/ The concepts of this CIG system, primarily used for representation of realistic objects in aircraft simulators.
- b/ The design and architecture of this system and its performances.
- c/ The different applications of this system.

2.1. - THE CONCEPTS OF THE CIG SYSTEM

In order to realize a system giving these possibilities in real time, it was necessary to find a performing algorithm of hidden faces elimination, able to be implemented in hardware.

In 1976, at the beginning of these studies the basic algorithms were those of :

- 1/ WATKINS
- 2/ WARNOCK
- 3/ SHUMACHER.

A simulation of algorithm 1 and the study of the second showed that it would be very difficult to wire them.

The third algorithm, however, brought the following idea :

It was possible to prepare before the real-time display a list of the polygons of the object, called PRIORITY LIST. This list is obtained by a sort among the polygons from the farthest to the nearest.

When the object is displayed in real-time it suffices to send the polygons on the screen in the same order, just as a painter which would paint first would paint first the farthest plans, and would superpose the nearer ones.

The difficulty lies in the case of complex objects. In this case, the priority list is not unique.

When a face 1 hides face 2, face 2 can hide face 1 when we turn around the object.

Scientifically speaking, the graph of the priorities

presents cycles, and we have no list of priority independently of the point of view.

In order to cut these cycles, we have 2 solutions :

- separate the object in clusters by planes, each cluster having a priority list without cycle,
- separate the space in viewport solid angles, so that in each solid angle no cycle can appear, when we change the point of view.

This method can be implemented :

- first by defining a list of solid angles,
- then by computing priority lists in each one.

The corresponding program operates in the following manner :

- the determination of solid angles is obtained by testing one by one all the polygons of the object : the program retains only those which minimize cycles in the priority list,
- after that, from a given list of solid angles the program computes priority list in each solid angle. If there are another cycles after this phase, the program introduces new solid angles, until no cycle appears.

In order to test the priority of a facet A with a facet B, we have determined a criterion by means of scalar products between the normal of facet A and the segments joining one vertex to the vertices of B.

The result of this program is a set of N priority lists corresponding to the N solid angles.

2.2. - SHADING AND SMOOTHING

The polygons of the objects must be :

- Planar,
- Convex.

Their color may be fixed (simple shadowing) or variable in light intensity (smoothing).

So, it is possible to display real edges with uniform shadowing and curved surfaces with smoothing. An interpretation of the algorithm of H. GOURAUD has been wired in the hardware of the system.

2.3. - ROTATE THE SCENE

The rotation of the scene is realized by a bit-slice microprocessor and a fast multiplier TRW.

REMARK : In this first version, we have implemented neither conic projection, nor clippings : it was, in fact no useful to generate aircrafts, vehicles or simplified scenes.

3 - DESIGN AND ARCHITECTURE OF THE SYSTEM

After the object has been digitized, we compute solid angles and priority lists. So it remains in real time to :

3.1. - CALCULATE SHADING

3.2. - SMOOTH FACETS

3.3. - ROTATE AND TRANSLATE THE SCENE

3.4. - DETERMINE THE GOOD PRIORITY LIST CORRESPONDING TO THE POSITION OF THE OBSERVER

3.5. - SUPERPOSE FACETS IN AN IMAGE MEMORY, FOLLOWING THE INCREASING ORDER OF PRIORITY (GIVEN BY THE PRIORITY LIST)

These tasks are realized by 2 hardware modules :

a/ MICROPROCESSOR MODULE :

Built with AMD 2900 series
with :

4 K of 64 bits words of microprogram memory,
16 K to 32 bits words of DATA memory.

The machine built contains only 1 microprocessor but the architecture and the bus for exchanges allows an extension to 2 microprocessors with their own memory.

The micro-instruction cycle time is about 200 nS,

The microprogram constitutes the program of the module (there is no program memory).

During an instruction, the microprocessor can execute :

- a logical or arithmetical test,
- or an arithmetic operation,
- or a branch (conditionnal or not).

Or the three operations in the same time.

The input of this module is :

- The data base of the scene, loaded in the DATA memory by a main frame-computer before real-time display,
 - coordinates of the vertices of the scene,
 - description of the facets (or polygons) of the scene,
 - list of normals of the polygons,
 - a set of priority list.
- The dynamic parameters of the scene :
 - rotation matrix of the scene,
 - the scale factor of the scene,
 - the direction of the light source.

These parameters are sent in real-time by a main-frame computer which knows the relative position of the objects in the space (for example : aircrafts, helicopters,...)

In real time the microprocessor computes first :

3.1. - SHADOWING

For the shadowing we use the following formula :

$$S = 255 \times (\cos (\text{TETA}) + 1)$$

Where TETA is the angle between light source and the normal of the facet.

3.2. - SMOOTHING FACETS

We compute at each vertice of the object :

$$(S1 + S2 + S3 + \dots S n)/N$$

Where S1 ... Sn represents the shadows of the facets containing this vertice.

3.3. - ROTATE AND TRANSLATE THE SCENE

The microprocessor computes :

$$V' = M \times V + T \text{ where :}$$

M is the rotation matrix of the object
v represents the coordinates of a vertex
T represents the translation vector.

3.4. - RESEARCH OF THE GOOD PRIORITY LIST

Corresponding to the solid angle containing the observer.

3.5. - FACETS LOADER

After tasks 1 to 4, the microprocessor sends to a FACET GENERATOR MODULE the description of each facet from the farthest to the nearest according to the order of the priority list.

Each facet is decomposed in trapezoidal blocks which are defined by :

- position XG, XD of the beginning of edges right and left,
- number of lines of the block,
- slopes of the edges right and left,
- shadows of the extremities left and right of the first segment,
- slopes of the shadows left and right,
- position Y of the first segment.

These datas are sent to the FACET GENERATOR MODULE which superposes the facets in an image memory.

b/ FACET GENERATOR MODULE :

This module is entirely in hardware.

The tasks accomplished by this module are :

- From a line to the following :
 - increment XLEFT and XRIGHT :
 $XLEFT = XLEFT + DXLEFT$
 $XRIGHT = XRIGHT + DXRIGHT$
 - increment SLEFT and SRIGHT :
 $SLEFT = SLEFT + DSLEFT$
 $SRIGHT = SRIGHT + DSRIGHT$
 - decrement DY :
 $DY = D - 1$
- Inside of a line :
 - computation of the slope of shadow :
 $DS = (SRIGHT - SLEFT) / (XRIGHT - XLEFT)$
 - computation of the current shadow :
 $S = S + DS.$

AD-A110 226

AIR FORCE HUMAN RESOURCES LAB BROOKS AFB TX
1981 IMAGE II CONFERENCE PROCEEDINGS.(U)

F/G 14/2

NOV 81 E G MONROE

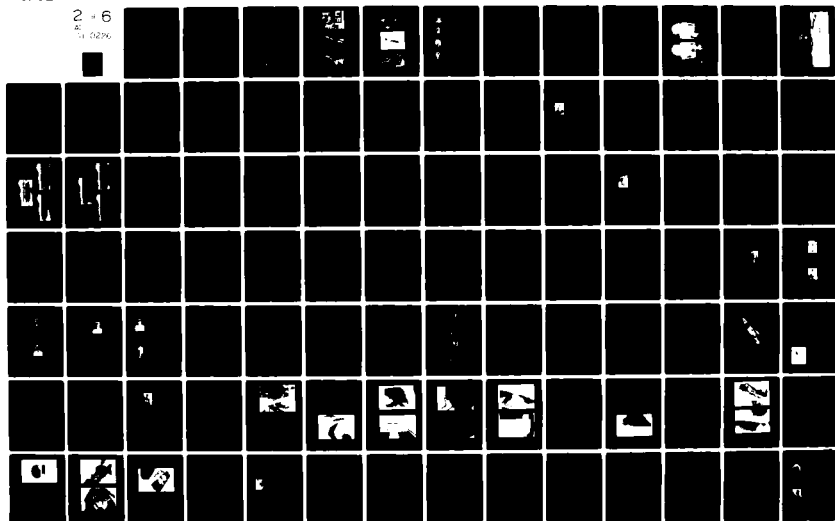
AFHRL-TR-81-48

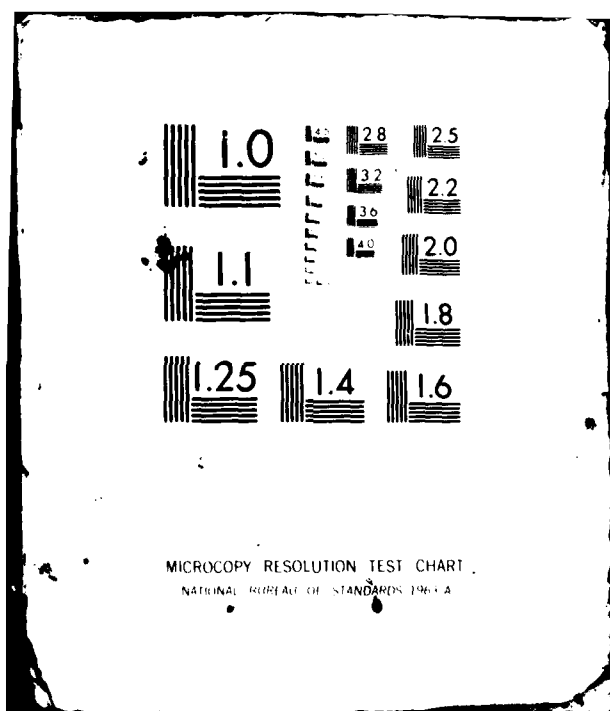
UNCLASSIFIED

NL

2 + 6

01 0296





The cycle time of the module is : 100 nS/pixel.

The facet generator module outputs pixels through an image memory whose size is :

512 X 512 X 8 bits.

There are 2 image memories which are filled in flip-flop.

The information (8 bits per pixel) is sent to the TV projector through D/A converters.

At the same time, the same information is sent to a pseudo-color table of 256 words, and via 3 D/A converters to a Red Green Blue monitor.

4 - PERFORMANCES OF THE CIG SYSTEM

- The CIG system can display in real time up to 400 facets of medium size with the microprocessor version.

- The medium time necessary to compute one pixel is about 100 nS.

- The performances in bi-processor version have not yet been tested, However we can hope a gain of about 100 % in facets.

- If POLYNUM is the number of polygons, the computation time of the object is given by :

$$\begin{aligned} T &= 0.200 \times 897 \times \text{POLYNUM} && \text{if the polygons are smoothed} \\ T &= 0.200 \times 585 \times \text{POLYNUM} && \text{if the polygons are not smoothed} \end{aligned}$$

(This time is given for an instruction cycle time of 200 nS).

5 - THE DIFFERENT APPLICATIONS OF THE CIG SYSTEM

The first generation of CIG system (GSI 1) was operational in 1980 may.

The applications of this system are numerous :

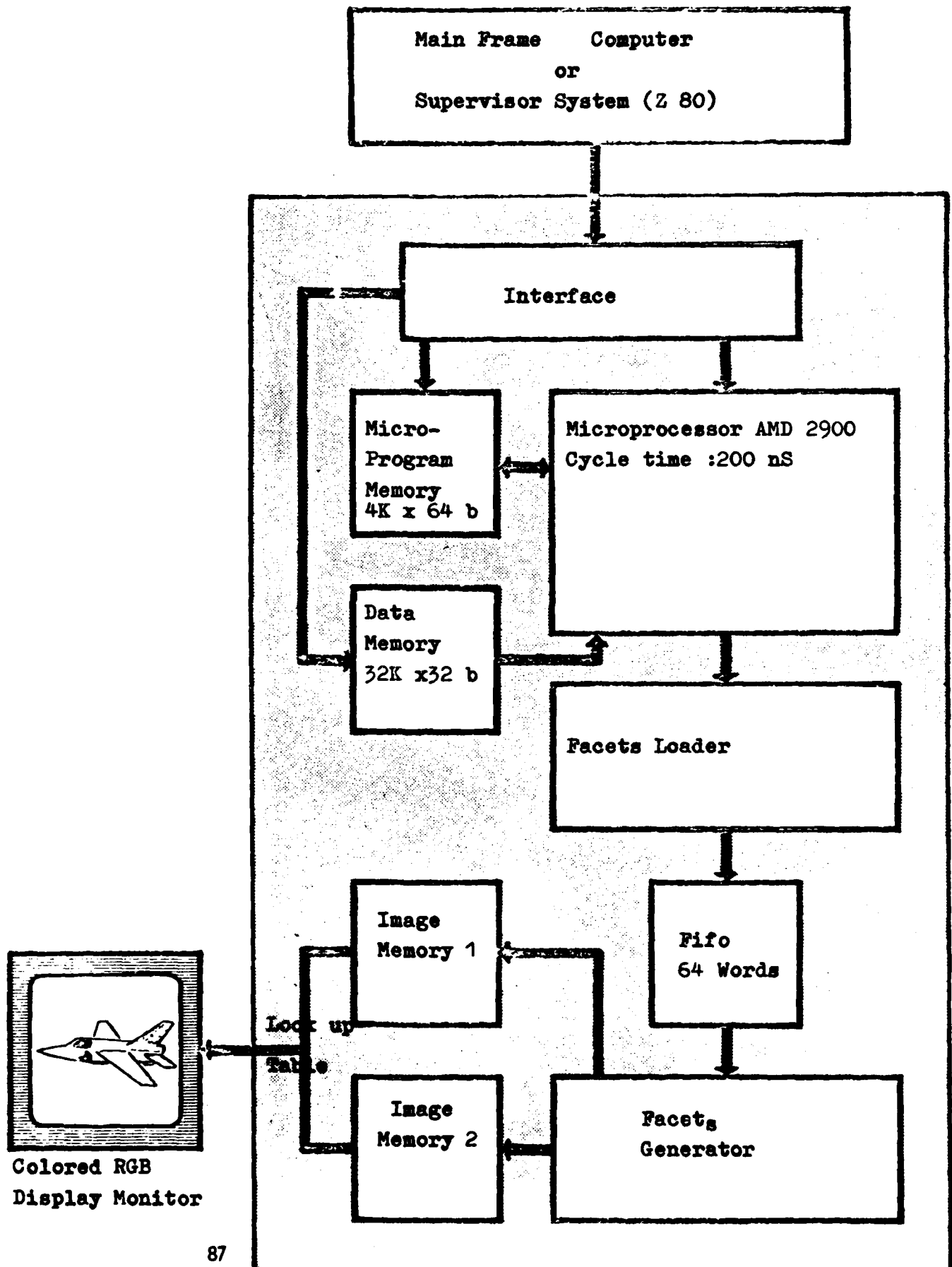
- generation of aircrafts, tanks, helicopters, images...,
- recognition of the attitude of an aircraft by comparison between a photography and a synthetic image,
- out of the simulation domain, we can mention :

- representation of forms in design engineering :
(architecture, urbanism, vehicles, aircraft design),
- medical and chemical application,
- movies
- TV and Audio Visual production,
- microinformatics.

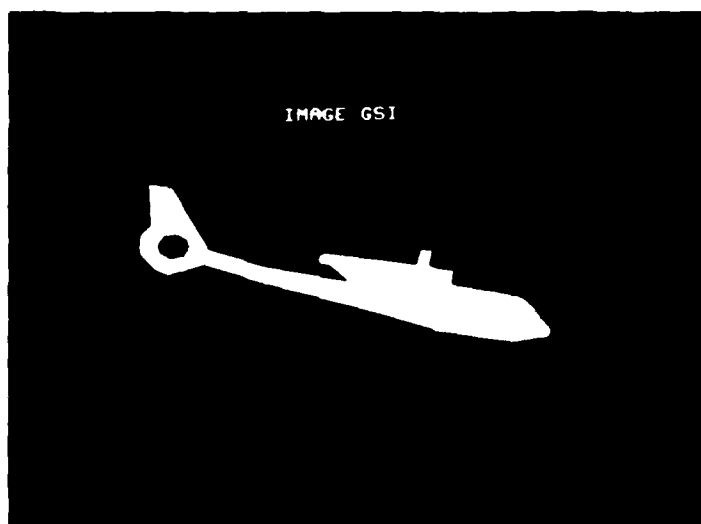
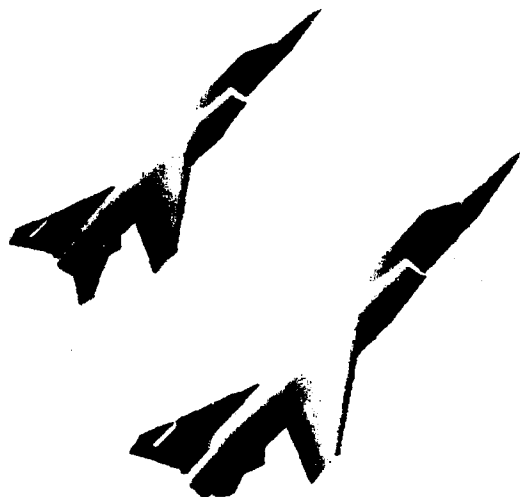
6 - BIBLIOGRAPHY

- 1/ GOURAND, H
"COMPUTER DISPLAY OF CURVED SURFACES" University of Utah
UTEC-CSc-71-113, JUNE 1971.
- 2/ WATKINS, G.S
"A REAL = TIME VISUBLE SURFACE ALGORITHM" Computer
Science Department, University of UTAH,
UTECH. csc-70-101 JUNE 1979.
- 3/ WARNOCK, J.E
"A HIDDEN-SURFACE ALGORITHM FOR COMPUTER-GENERATED
HALFTONE PICTURES"
TR4-15 COMPUTER-Science Department, University of UTAH
1969
- 4/ J.E. SUTHERLAND, RF SPROULL, R.A. SCHUMACKER
"A CHARACTERIZATION OF TEN HIDDEN SURFACE ALGORITHMS"
ACM computing surveys, vol 6. N 1, March 1974,p 1-55
- 5/ LERAY, P
"GENERATION EN TEMPS REEL D'IMAGES SYNTHETIQUES
TRI-DIMENSIONNELLES"
AFCET Conferences-April 78 - November 80-

SYSTEM GSI 1







LOW-COST AIR-TO-GROUND WEAPONS DELIVERY SIMULATION
USING MICROPROCESSOR-DRIVEN DISPLAYS



Dorwin L. Kilbourn
Research Physicist
US Army Missile Command



William R. Phillips
Electronics Engineer
US Army Missile Command



J. Earl Bailey
Professor of Aerospace Engineering
The University of Alabama



James E. Dudgeon
Professor of Electrical Engineering
The University of Alabama

Dorwin L. Kilbourn obtained his MS in Physics from Auburn University. His 27 years of professional experience has been in industry, military and academia. For the past twenty years, he has been involved in the Army's missile guidance development programs. From 1970-74 he was responsible for establishing requirements and overseeing development of the Electro-Optical Simulation System (EOSS) facility, for which he received the Civilian Meritorious Service Medal. During the past seven years, he has been responsible for development of new hardware-in-the-loop simulation equipment for evaluation of missile guidance equipment.

William R. Phillips received his BS in Electrical Engineering from the University of Alabama. His thirteen years of professional experience has been in industry and the military. His work at Sperry-Rand, 69-71, was involved with power system design on the NASA Skylab Program. For the past nine years he has been involved in the Army's missile guidance development program. During the past four years, he has been responsible for operation of the Electro-Optical Simulation System and the development of hardware-in-the-loop simulations.

Earl Bailey obtained his BS and MS degrees in aeronautical engineering from Mississippi State University in 1955 and 1958. His 25 years of professional experience include the USAF at Wright Field (1955-57), General Dynamics at Fort Worth (1958-62), and NSF Faculty Fellow at MIT (1966-69). He has been at the University of Alabama since 1962 and teaches courses in flight dynamics and flight control. He currently serves as Professor of Aerospace Engineering and Director of the Aerospace Engineering Flight Dynamics Laboratory, where he is involved in flight simulation and flight-control research.

James E. Dudgeon received his BSSE and MSEE from the University of Michigan in 1962 and 1963, respectively. He received his PhD in electrical engineering from the University of Alabama, Tuscaloosa, Alabama in 1968. He is currently Professor of Electrical Engineering and Director of the Microprocessor Laboratory at the University of Alabama. His research interests include electronics, digital hardware and software, microprocessors, radar, and electro-optical signal processing. He has been an NASA/ASEE Faculty Fellow and has worked for NASA and the US Bureau of Mines. Dr. Dudgeon is a member of IEEE, Eta Kappa Nu, Pi Mu Epsilon, and Sigma Xi.

Low-Cost Air-to-Ground Weapons Delivery Simulation
Using Microprocessor-Driven Displays

ABSTRACT

A low-cost flight simulation facility for helicopter gunship air-to-ground weapons system simulation has been developed under U. S. Army Missile Command contract DAAK40-79-C-0060 by The University of Alabama. The system encompasses interfacing the following features into the Electro-Optical Simulation System (EOSS) to constitute an Air-to-Ground Weapons Delivery Simulator:

1. Distributed microprocessor (host PDP11/34) color graphics system for video instrument panel and cockpit window graphics.
2. Surplus Apollo program optics adapted for high-resolution cockpit window displays.
3. Weapons special effects and trajectory software package.
4. Fully instrumented separate pilot and gunner cockpits.
5. General-purpose fire-control system console.

I. INTRODUCTION

In the spring of 1979, technical personnel of the Army Missile Command's EOSS (Electro-Optical Simulation System) facility were presented the problem of visually simulating a tracer trajectory for a high-velocity projectile. The solution of this problem led to the development of a Low-Cost Air-to-Ground Weapons Delivery Simulation (WDS) facility. The major portion of the work was performed under contract DAAK40-79-C-0060 by The University of Alabama. Due to austere funding, some of the major subsystems were fabricated from excess government property collected over the past several years, which kept the cost for the WDS development under two hundred thousand dollars.

The need for the development of the WDS was brought about by an exploratory development program for a high-velocity kinetic energy projectile to be launched from a helicopter gunship. The scenario involves a pilot bringing his aircraft up from cover, locating an enemy target (generally an armored vehicle), maneuvering his gunship in line with the target, firing a burst or volley of projectiles, observing points of impact and miss-distances, realigning his gunship and firing a second volley of projectiles. (This scenario can be repeated if necessary and if time permits before returning to cover.) Each projectile contains a tracer material so that the gunship pilot can observe the trajectory of the round and its impact point. The accuracy of the projectile's trajectory is affected not only by the aiming error of the pilot but by the "noisy" environment of the helicopter serving as a launch platform. This hostile launch environment led to the need to develop a capability for simulation of helicopter-pilot dynamics along with their resulting impact on the projectile trajectories.

The solution to the problem was to develop a microprocessor Video Display System (VDS) which would generate the tracer trajectories and through video techniques overlay the trajectories on television displays of the target scene provided by the EOSS terrain model. A functional block diagram of the Weapons Delivery Simulation (WDS) facility is shown in Figure 1. The basic subsystems are:

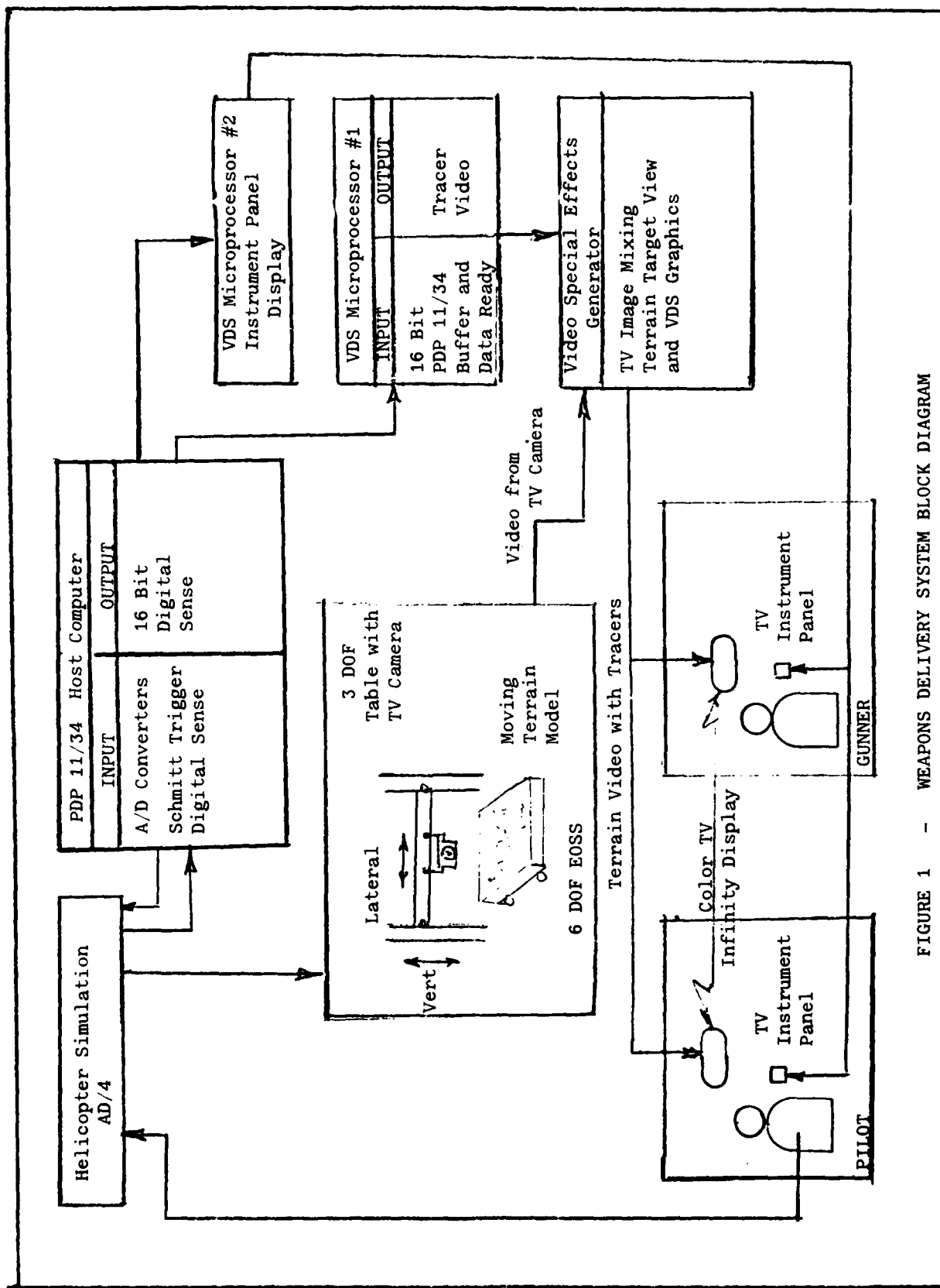


FIGURE 1 - WEAPONS DELIVERY SYSTEM BLOCK DIAGRAM

1. Helicopter cockpit mock-up with pilot and copilot-gunner stations including collimated out-the-windscreen display, color TV instrument panel and full flight controls for helicopter flight simulation.
2. EOSS 6-DOF motion simulation including a 3-DOF flight table with vertical and lateral motion capability and a scaled moving terrain model for range closure.
3. Helicopter dynamics simulation generated on an AD/4 analog computer.
4. PDP11/34 host computer for generating trajectory data and flight instrument panel data.
5. Two microprocessor video display systems (VDS): one (VDS #1) for generating tracer trajectories and other special effects for overlaying on the windscreen display, and the other (VDS #2) for generating the cockpit instrument panel displays.
6. A video special effects generator for mixing the output of VDS #1 with the video from the EOSS TV camera.

The EOSS facility, including the AD/4 analog computer and a PDP11/20 minicomputer, were the only hardware equipment on hand at the outset of the program. The PDP11/34 minicomputer and video special effects generator were purchased as off-the-shelf items. The two cockpit stations including the windscreen infinity displays, flight controls and instrument panel were fabricated from excess hardware, and the two VDS units were conceived, designed and fabricated by the contractor. All video display software for programming the PDP11/34 and the two VDS units had to be developed and checked out. The helicopter simulation software had to be adapted from a more complex simulation in order to fit the AD/4 computer.

The following sections describe the general concept of the Weapons Delivery Simulation concept and the subsystems which comprise the facility.

II. WEAPONS DELIVERY SYSTEM

Cockpits

The cockpits of the WDS were made from a wooden COBRA mock-up salvaged from a HELLFIRE contract. The normal tandem configuration was abandoned in favor of providing two side-by-side units with each having its own infinity windscreen displays, instrument panels and appropriate controls. In Figure 2, the unit on the left is the pilot's cockpit and contains flight controls salvaged from a wrecked UH-10. Potentiometers mounted on these flight controls provide helicopter control inputs to the helicopter simulation on the AD/4 analog computer. To provide aural realism, helicopter sound generators are provided in each cockpit.

Partial flight instrument data is displayed to both the pilot and the copilot/gunner stations on separate 12-inch color graphics television display monitors which have an eight-megahertz bandwidth for greater horizontal resolution capability. Typical flight data displayed includes velocity, altitude, percent throttle, pitch-roll attitude (artificial horizon) and side acceleration. Other data can be readily programmed and displayed through the host minicomputer and VDS microprocessor #1.

Each cockpit has its own color TV/mirror/beamsplitter infinity windscreen display. The infinity displays were considered mandatory for the

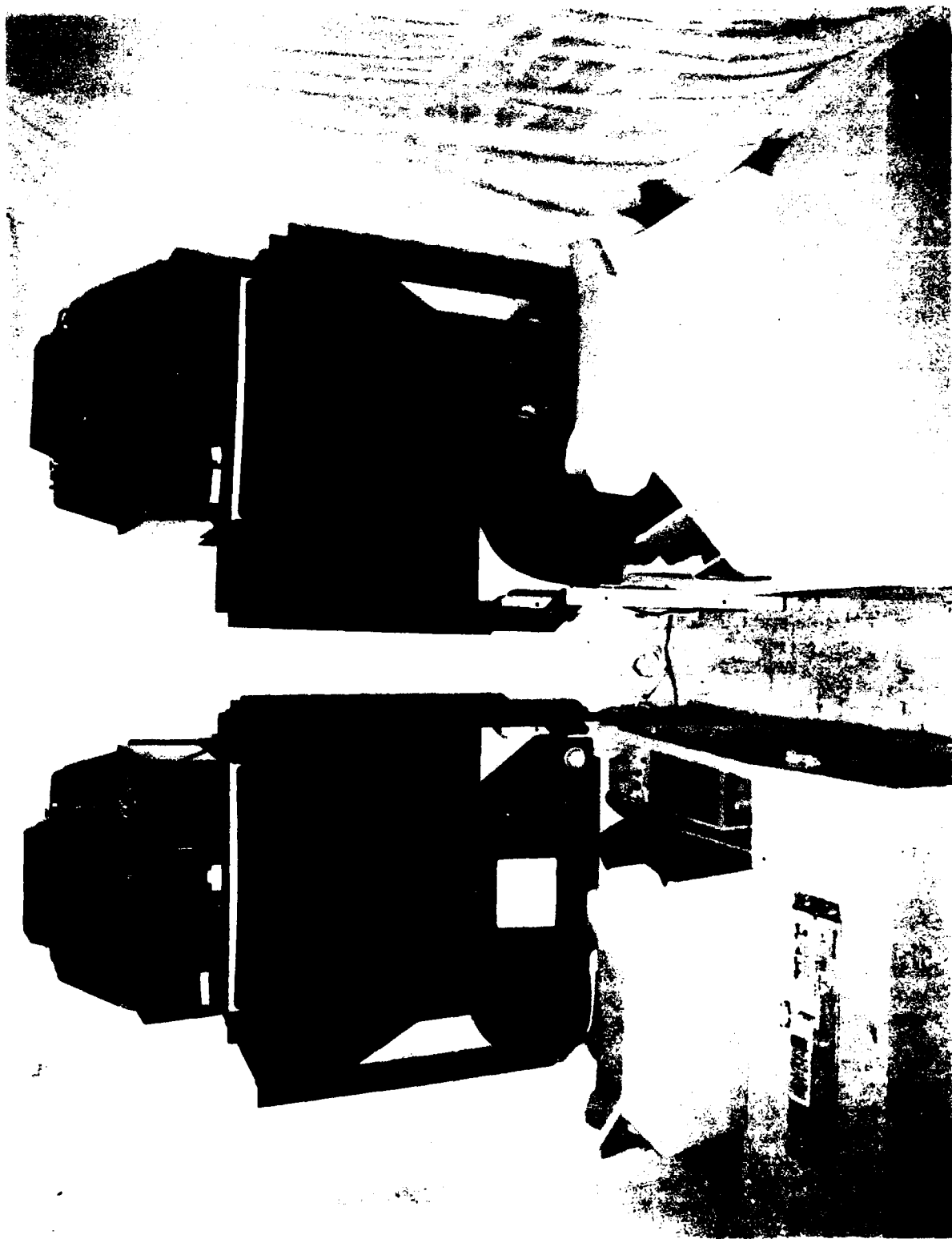


Figure 2. Pilot and Gunner WDS Cockpits

EOSS simulation so that look-angle independence from head motion could be achieved and inside-outside-the-cockpit pilot visual lags could be adequately simulated. The low development cost requirement dictated that a standard 525-line color-video monitor be used. This requirement in conjunction with the high resolution requirement of air-to-ground weapons delivery simulation limited the field of view of the windscreen displays to 25 degrees. This narrow windscreen field-of-view does not limit the range of research expected to be performed in the EOSS. Pilot handling qualities at moderate-to-slow forward speeds are adequate and the target detection/acquisition/engagement task at 2- to 4-kilometer ranges is not adversely affected by this display field-of-view. Image quality is excellent and vertical image resolution is approximately three arc minutes per TV line.

The cost for two infinity mirror/beamsplitter display systems would have been prohibitive for the funding allowed under the program. However, after the completion of the Apollo lunar program, EOSS personnel acquired several of the Farrand optical display systems used in the Apollo simulators. The optics were transferred to The University of Alabama and cut to form spherical mirrors and beamsplitters for the windscreen displays. Two new mounts for the mirrors, beamsplitters and 21-inch Sony color television systems were designed, built and assembled by the University's personnel.

The cockpits can be used in at least three modes of operation: (1) pilot flying gunship and handling fire-control of weapons-delivery with copilot/gunner merely serving as an observer; 2) pilot flying gunship and copilot/gunner operating fire-control units such as would be required in a man-in-the-loop missile flight; and 3) as a subject/experimenter system with the subject occupying the pilot's cockpit and the experimenter occupying the copilot cockpit.

EOSS

The 6-DOF EOSS described in Ref. 1 generates the realistic and precisely controlled spectral and dynamic environments required for the evaluation of optically guided systems. Five degrees of freedom (Figure 3) are provided by a vertical assembly system consisting of a three-axis gimbaled camera/seeker mount which can be moved laterally along a beam which in turn can be driven vertically between two columns. A large, moving three-dimensional terrain model (scaled 1/600) provides the sixth degree of freedom which simulates range closure. An AD/4 analog computer provides input commands for the position, rates and accelerations of each of the six motion drives and, in addition, completes the Euler angle transformation. The newly added cockpits, displays, and VDS units provide the EOSS with a man/machine/target interface and the capability for supplying a total weapons system simulation.

Helicopter Simulation

The requirements for the EOSS helicopter simulation model are as follows:

1. A simplified mathematical force and moment model of a generalized helicopter for piloted simulation. The simulation equations of motion must be implemented on the EOSS AD/4 analog computer.



Figure 3. EOSS Terrain Board and Television Camera - Flight Table

2. The helicopter model should provide good flight dynamics simulation fidelity over the 0- to 100-knot speed range.

3. The equations must be in a generalized form so that coefficients can be chosen to represent a broad range of vehicles with minimum modification.

4. The rotor model should be general enough to provide for implementation of various autopilot and HUD display concepts for air-to-ground weapons system simulation.

The helicopter model selected for the EOSS implementation was developed by NASA Ames Research Center personnel (Reference 2) for flight dynamics, terminal area guidance, and avionics systems studies. Developed primarily as a UH-1 simulation, the rotor equations are sufficiently general so that a wide range of helicopter configurations can be modeled. NASA Ames Research Center used an all-digital real-time implementation of the subject equations to support the broad range of user applications.

Considerable simplification was required to implement the NASA simulation on the EOSS AD/4. Simulation hardware verification and simplification was accomplished with the aid of a PDP11/34-based numerical integration of the equations of motion reported in Reference 2. Additionally the simplified equations implemented on the analog computer were numerically integrated for comparison with the reference case. Comparisons were made at 100 ft/sec, 50 ft/sec, and 20 ft/sec. Simplifications were accepted as valid if the dynamic response error for control inputs were small.

The nonlinear helicopter simulation uses approximately 40 multipliers and 120 amplifiers. Resolvers are used for Euler angle transformations.

Currently the EOSS helicopter model is being used to analyze helicopter-fired, unguided missile dispersion. Effects of helicopter flight dynamics on autopilot configurations for weapons pointing and HUD target displays are subjects of current research.

The model employs a "quasi-static main rotor representation, uniform inflow over the rotor disk, and simple expressions for the contribution of the tail rotor, fuselage, and empennage." Reference 2 presents a detailed validation of the model performance by comparison with UH-1 flight data. In Reference 2 conclusions are stated: "The model appears to be satisfactory for flying-qualities investigations at forward speeds and usable, but less realistic, for hover." The model appears to be quite acceptable for the general class of studies proposed for the WDS system.

VDS, Microprocessor Video Display Systems

Two VDS microprocessors (See Figure 4) are used to generate an out-the-cockpit display produced by a 21" raster scan color TV and mirror-beamsplitter optics and an instrument panel display that uses a 12" TV with separate red, green, and blue inputs. The out-the-cockpit imagery is formed by mixing video from a terrain-board-TV-camera-probe with VDS-generated special effects. The VDS uses dot-mapped graphics techniques to produce such effects as missile tracers, target designators, and firing and impact

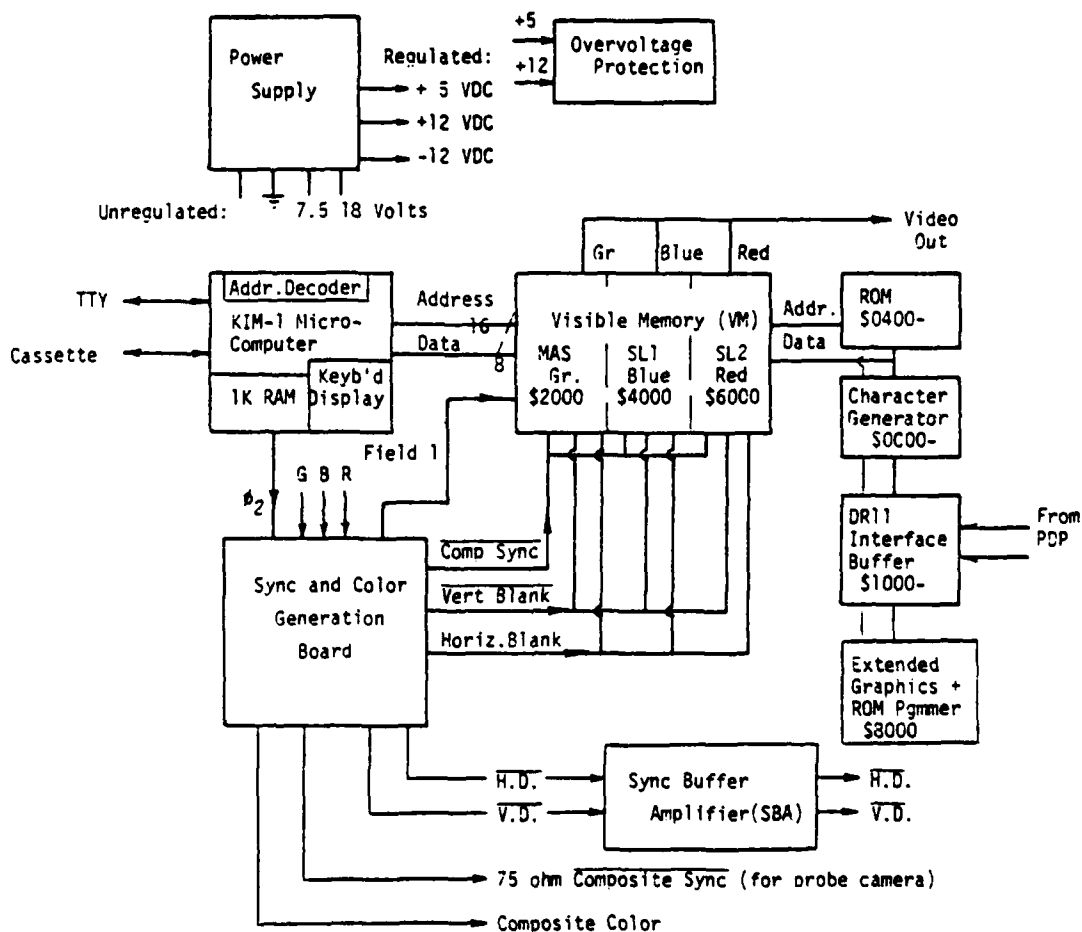


Figure 4. Video Display System Hardware

flashes and can produce color or black-and-white data displays that can be overlaid with standard RS170 video from a terrain board probe. Each VDS system can be controlled from its own terminal or operate in a slave mode to a host computer such as the PDP11/34 minicomputer. Much of the computational load for graphics and special effects is done by the VDS, freeing the host computer for tasks such as missile and aircraft simulation with rapid refresh rates.

Simulation

As the helicopter model runs on an AD/4 hybrid analog computer, the PDP11/34 monitors aircraft and missile parameters (A/D channels), transforms stored inertial coordinates to pilot's-eye perspective, and sends screen coordinates and instrument-panel data to the VDS microcomputer through a 16-bit parallel output port (DR 11). Weapons system projectile tracer trajectories are computed by the PDP11/34 and displayed through VDS #1 in a real-time overlay of the terrain board image. Target miss-distances are automatically computed and displayed by the host computer. Up to 16 missile trajectories can be simultaneously displayed to allow for rapid fire or missile volley operation.

The PDP11/34 and VDS can transform a 250-point, three-color night-landing runway scene to a pilot's-view perspective image and update a color instrument panel with seven digital readings plus an artificial horizon at a rate of approximately 15 times a second.

The VDS dot-mapped raster scan graphics resolutions of 320 dot x 400 line interlaced scan, black and white or 320 x 200 with 8 colors are hardware switch-selectable. The VDS uses a 6502 microprocessor whose addressing modes (especially indexed indirect and indirect indexed) and fast and efficient memory access cycle make it excellent for rapid data movement.

Three 8k x 8 visible memory boards with cycle stealing generated video are controlled by three bits for each pixel in a 320 dot by 200 line format. Stock Micro Technology Ltd. memory boards are modified to operate as slaves to a master video sync generation board.

Graphics Software

The VDS which is implemented on the PDP11/34 and which does the transformation to pilot's-eye perspective with fixed-point binary fraction arithmetic and sine, cosine lookup tables used for fast coordinate transformations. The PDP11/34 communicates with the VDS using a DR11 parallel 16-bit output port using two sequential 16-bit words. When 32 bits of data are received by the VDS, an interrupt is generated to initiate the graphics program stored in VDS read-only memory (ROM). Eight of the 32 bits are designated as a control byte through which the PDP passes operational commands to the VDS. The VDS graphics options are designed to download as much computation from the minicomputer as possible. The interrupt-service routine options contained in microprocessor ROM are as follows:

Instrument Panel
2 x 2 Tracer
17-Point Best Fit Line

Flash
Target Designator
Execute VDS Program Starting at VMA

B10 = 1	Fill Screen	Inverted (dark) ASCII Char. at VMA
B10 = 0	Erase 8K Block	ASCII Character at VMA
B9 = 1	Red VM	Erase dot at VMA
B8 = 1	Blue VM	Erase Word at VMA
B8 = B9 = 0	Green VM	Transfer Byte of Data to VMA
Display or erase two adjacent dots	(B10 = 1 erase, B10 = 0 write)	Display Single Dot
Vertical Block Fills 8 dots wide		Tracer zones with autoerase option (b7 = 1)
by no. of lines = (PORT+2)		

To obtain speed, a number of different interrupt-service routines are used, each written to efficiently handle a particular task. With an eight-bit control word, 256 options could be included in one interrupt-service routine, but the program overhead to test these options would make the average interrupt execution time prohibitively long. Therefore, interrupt service routines with a limited number of options were designed for each of the different simulation tasks (tracers, instrument panel, windscreen view, color graphics).

Air-to-Ground Weapons Delivery Scenario

A typical scenario simulated in the projectile display mode is a pilot-weapons-system-operator flying a helicopter missile-carrier. The analog simulation of the aircraft on the AD/4 analog computer receives pilot control inputs from the simulator cockpit and outputs aircraft inertial position and Euler attitude angles. These outputs are used to drive the EOSS 6-DOF drives such that the flight table TV camera which provides the terrain visual scene is at the proper position and attitude over the terrain model. The operator can fire a missile or projectile (also simulated on the analog or digital computer) at a target whose position on the terrain model is defined by a surveyed target data base. The relative missile-firing point inertial position and missile attitude angles are output from the simulation. The aircraft kinematics outputs are used to drive the flight table mounted TV camera viewing the terrain model and along with the missile kinematics provide graphics display information to the PDP11/34 analog-to-digital converters. The PDP11/34 samples the aircraft and missile kinematics inputs approximately 20 times per second and repetitively computes the pilot perspective view imagery of the missile tracer as seen by the pilot. The PDP11/34 computes the TV screen (pilot outside-the-window image plane) coordinates of the missile tracer at a particular instant of time and passes the data to the VDS approximately twenty times per second.

The VDS interprets the data received and writes into one bit of display memory to display a dot on the TV screen at the pilot image perspective view missile location for the current time. The VDS automatically remembers the dot location in memory and erases it when the next missile position becomes available. The net effect is to display a missile tracer or flare as a series intermittent of dots along the computed missile trajectory. The display is used to create the illusion (simulation) of a moving missile tail flare or projectile tracer, thus providing the operator with targeting information.

The VDS PDP11 digital software has the capability of trajectory-display generation for single missile tracers or multiple rapid-fire projectile tracers. Single-missile tracer trajectory information is generated

externally to the PDP11 via the analog computer solution and is monitored by the VDS software analog-to-digital routines. Rapid-fire tracer trajectory software for the PDP11 can handle computations for 8 projectiles simultaneously. Rapid-fire VDS software utilizes a trajectory lookup table for reference projectile-trajectory generation and internally performs all display perspective view computations necessary for display generation.

The missile-trajectory is viewed by the operator as a point relative to the aircraft windscreen (pilot field-of-view if the pilot is looking parallel to the aircraft longitudinal axis) or as a perspective point superimposed over a target image as seen by a TV camera viewing the target scene. Figure 5 illustrates the viewing geometry.

The geometry and reference frames used for single-projectile trajectory computation are illustrated in Figure 6. The $x_1 y_1 z_1$ axes are used as an earth-fixed reference for aircraft position or fixed-platform location. $x_A y_A z_A$ are aircraft body axes with Euler attitude angles defined by a ψ, θ, ϕ Euler angle sequence. The $x_A y_A z_A$ origin is located at the pilot's-eye point and x_A is parallel to the aircraft longitudinal axis. The missile is launched from an aircraft parallel to the x_A axis at time t_f and is aimed by the pilot maneuvering the aircraft to align the x_A axis so that its extension passes through the target. The missile wind-axis system $x_W y_W z_W$ is assumed to be initially (t_f) aligned with the aircraft $x_A y_A z_A$ body axes so that $\psi_A = \psi_W, \phi_A = \phi_W, \theta_A = \theta_W$.

During missile flight, the relative missile aircraft trajectory is computed referenced to $x_I y_I z_I$ (0) axes, transformed point by point into the $x_A y_A z_A$ axis system, and then normalized to create the perspective view coordinates seen by the pilot. The relative aircraft missile position is:

$$x_I = x_{EO} - x_A + x_E$$

$$y_I = y_{EO} - y_A + y_E$$

$$z_I = z_{EO} - z_A + z_E$$

where

x_E, y_E, z_E = relative missile/firing-point position

x_{EO}, y_{EO}, z_{EO} = firing-point position

x_A, y_A, z_A = aircraft position, etc.

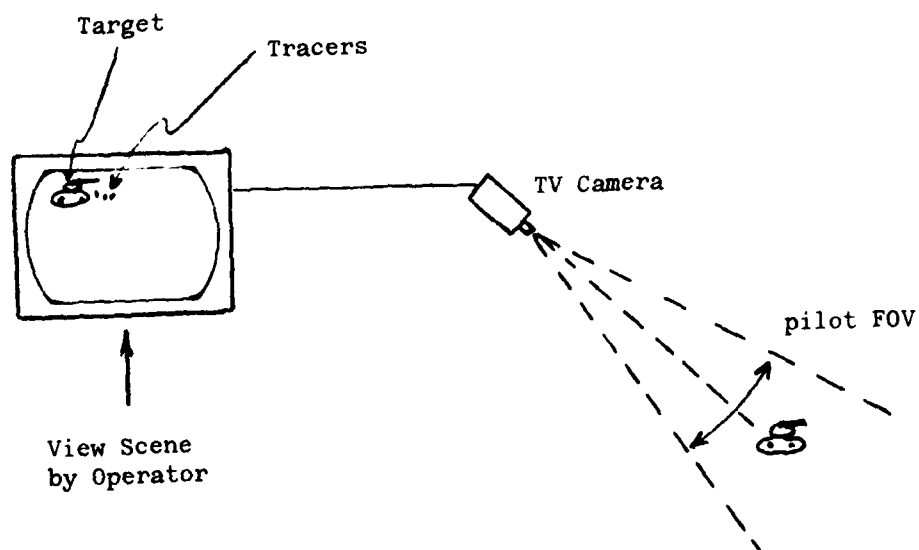
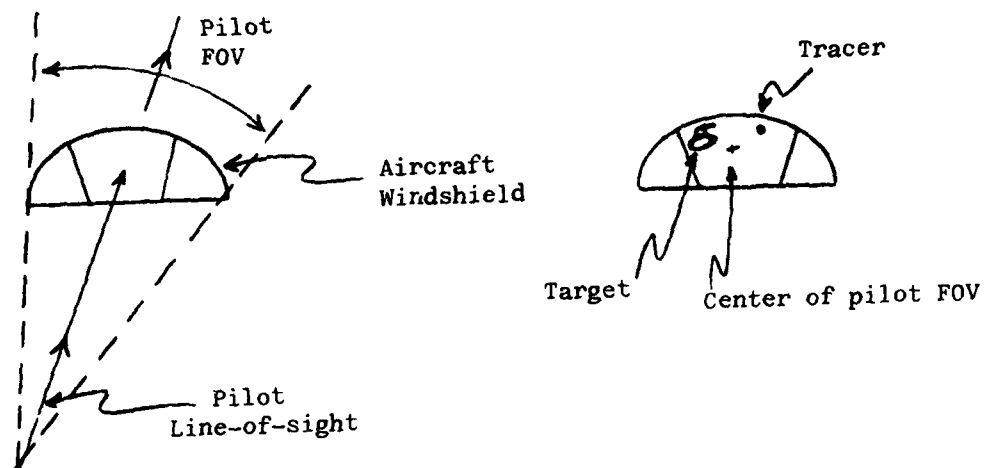
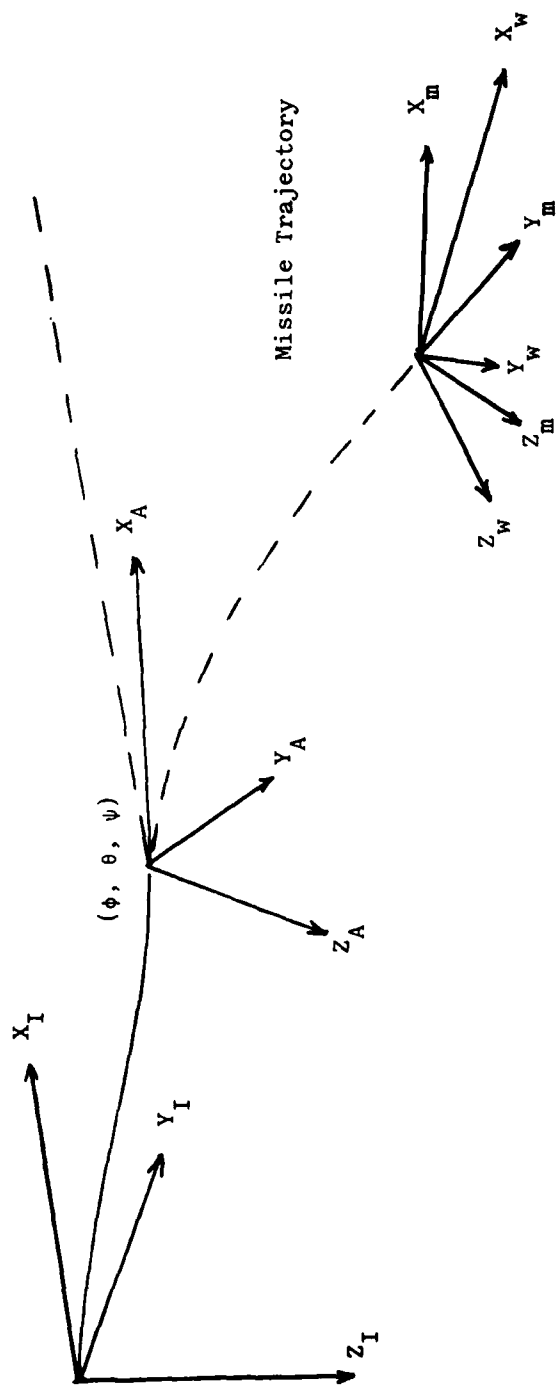


FIGURE 5 OPERATOR VIEWING GEOMETRY



X_I, Y_I, Z_I = Inertial Reference
 X_A, Y_A, Z_A = Position/inertial
 X_m, Y_m, Z_m = Missile position/firing position of aircraft
 ϕ, θ, ψ = Attitude angles
 ϕ_w, θ_w, ψ_w = Wind axis orientation angles
 Missile wind axes non-rolling ($\phi_w = \phi(t_f)$)

FIGURE 6
PROJECTILE TRAJECTORY

where 160 is the horizontal offset from the center of the TV screen and 100 is the vertical offset. K15 and K16 are scaling factors which are dependent on the TV camera FOV. VY and VZ are the TV screen dot matrix locations and VY ranges from 0 to 320 and VZ ranges from 0 - 200 as shown in Figure 7.

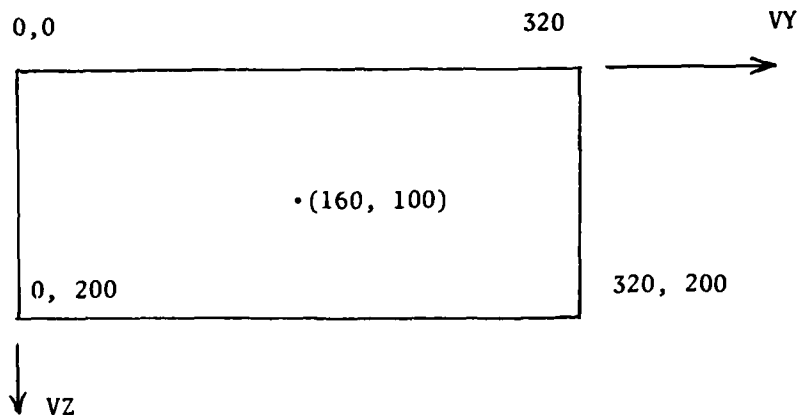


Figure 7. TV Screen, Graphics Overlay Coordinates

The computer graphics overlay uses the dot reference coordinates VY, VZ. The constants K15 and K16 effectively scale the display field-of-view.

III. SUMMARY AND CONCLUSIONS

Through the use of salvageable equipments from other government programs and the ingenious application of microprocessor technology, the Army Missile Command has been able to expand its utility of its hardware-in-the-loop EOSS facility to include man-in-the-loop capability. Experimental studies of the man/machine/missile interactions can now be performed which should greatly improve the Army's ability to resolve many problems in the laboratory which previously had to be done in the field or piecemeal in the laboratory.

The hardware has been installed and the software debugged. The system is being checked out preparatory to running the first experimental studies on an air-to-ground weapons delivery study. Although this low-cost VDS simulator has been developed primarily to study the problems of a gunship pilot launching high-velocity kinetic-energy unguided projectiles, the utility of the WDS is foreseen to be useful in many applications. Problems associated with launching and guiding systems such as TOW, HELLFIRE and conventional ammunition are typical applications. Human-factor studies of task-loading of pilot and copilot/gunner constitute another category of applications, and the adaptability of additional components such as HUDs and helmet-mounted sights will extend the range of this versatile simulation facility.

IV. REFERENCES

1. Haselwood, S., Gregory, P. C., and Kilbourn, D. L.; "EOSS: A Dynamic Six Degree of Freedom Environmental Simulator for Evaluation of Electro-Optical Guidance Systems," AIAA Guidance and Control Conference (Vol. I), Stanford, California, August 14-16, 1977.
2. Talbot, P. D. and Corliss, L. D.; "A Mathematical Force and Moment Model of a UH-1H Helicopter for Flight Dynamics Simulations," NASA Ames Research Center TM-73, 254, 1977.

THE INFLUENCE OF FIGURAL COMPLEXITY ON THE
DETECTION, RECOGNITION, AND IDENTIFICATION
OF TARGETS IN CGI DISPLAYS



Moira Lemay
Department of
Psychology
Montclair State
College

Moira Lemay obtained her Ph.D. in engineering psychology from the Pennsylvania State University. Her work experience has been in government, industry, and academia. She worked at the US Naval Research Laboratory and at IIT Federal Laboratories before going to Montclair, where she heads the graduate program in Industrial/Organizational psychology. She has done research in human performance, tracking behavior, vigilance, and visual perception in a three-dimensional display. Her most recent work has been in the area of complexity in CIG simulations, particularly of electro-optical sensors.

The Influence of Figural Complexity on the Detection, Recognition, and Identification of Targets in CGI Displays

Abstract

The aim of this study was to determine the minimum amount of complexity necessary in a computer generated scene for the detection, recognition, and identification of targets. Complexity was manipulated by modeling six targets in full detail and then removing detail until there was just enough to model a three-dimensional object. The targets were embedded in a computer-generated scene, photographed, and made into slides. The slides were shown to three groups of subjects in three experiments. In the first, subjects were asked to detect the presence of a target; in the second, they were asked to recognize which of six possible targets it was and in the third, they were asked to identify which of four possible targets of the same type this particular target was. Target complexity had no significant effect on detection or recognition. However, more complex targets were much easier to identify, especially when complexity was in the form of internal detail. Identification errors greatly exceeded errors in recognition, and errors in detection were relatively rare.

Introduction

Low level night flying of high performance aircraft depends for its success on the amount and interpretability of information about the terrain below and in front. Direct visual information may be severely limited and night sensing devices such as Low Level Television (L3TV) and Forward Looking Infra-Red (FLIR) are essential aids in many missions.

These electrooptical (E/O) displays, now installed in some aircraft, require training in their use and computer generated image (CGI) simulations have been developed for this purpose. The level of transfer of training in using such images has been assumed to be a function of realism which in turn is seen to be related to scene complexity. Complexity in this context is defined as the addition of features to the display, each of which increases the fidelity to the E/O sensor display by a small amount at an increasing cost (Bunker & Heeschen, 1975).

The question then arises as to the extent of complexity necessary to permit positive transfer of training to the task being simulated. The present study addresses itself to this problem.

CGI simulations normally have a "cartoon-like" quality which is quite different in appearance from the E/O sensor displays. Moreover, the CGI pictures are made up of a large number of elements or edges which go to depict each object in the scene. If every detail of an object is represented, an extremely large number of edges is required, with a commensurate cost increase. However, objects can be represented in a recognizable way using only a moderate number of edges. The necessary number of edges for the completion of several tasks is the subject of this report.

In a previous study (LeMay & Reed, 1980), the addition of visual noise and an edge transfer function to the scene was also investigated. The transfer function effect was not significant, but the effect of noise was, so only noise was included in the present study. Since the effect of number of edges in a scene and visual noise may be expected to depend on the task being performed, three

representative tasks were examined in the present study. They are the detection, recognition, and identification of objects in a simulated scene.

Detection is defined as the ability of an operator to discriminate between the presence and absence of a target; recognition is the assignment of a detected target to a class of possible targets; and identification is the selection of one individual target from a class of targets.

Detection

Studies on the detection of just barely visible (or audible) targets in a background of noise have been numerous since the inception of the work on the theory of signal detection (TSD) described by Green and Swets (1966). The general problem of visual search for complex targets was reviewed by Teighner and Mocharnuk (1979). They defined complexity in terms of stimulus dimensionality, i.e., the number of attributes such as form, direction, color, etc., which a stimulus may have. They reviewed the findings of nine earlier studies, and concluded that time to detect a target decreases as the number of stimulus dimensions (complexity) increases and that rate of stimulus processing increases (i.e., time per stimulus decreases) as number of stimulus dimensions increases. In other words, complex targets are more easily detected and processed (recognized?) than simpler targets.

Uttal and Tucker (1977) present a multi-stage model of perception in which each stage can be explored only if thresholds for previous stages have been exceeded. They measured performance in a detection task and found that complexity was a powerful determinant of susceptibility to masking by noise.

These and other studies offer somewhat contradictory, and not always relevant predictions for the present study. It seems that complexity sometimes aids and sometimes hinders detection performance. Most directly relevant is the study by Uttal and Tucker (1977), which found that complexity hindered detection, especially in the presence of noise. The present study uses simulations of real-life targets, and subjects them to a controlled analysis in the laboratory. It is expected that complexity will have little or no effect on detection performance, and that the presence of noise will hinder performance, perhaps interacting with complexity.

Recognition

The distinction between recognition and identification has not always been clearly made in the literature, and the term "discrimination," suggested by Gibson (1969) has sometimes been used for both tasks. For present purposes, a somewhat arbitrary division has been made between those studies which ask subjects to recognize one of a class of targets, such as letters of the alphabet, and those which ask subjects to identify a particular target which has usually been constructed by the experimenter.

Pasnak (1971) used a same-different recognition task with simple and complex random polygons. Overall errors were greater for simple than for complex figures, and subjects responded to the whole contour for simple shapes, and the distinctive parts of the outlines of more complex shapes.

Staller and Sekuler (1977) asked subjects to respond to

mirror-image and nonmirror-image stimulus pairs in a two-choice response, and complexity seemed to influence the quality of pattern processing, in that particular targets were responded to with significant differences in reaction time.

A number of studies (Frowein & Sanders, 1978; Nygard, et al., 1964; Berkhout & Philips, 1979; Guttman, Snyder, Farley & Evans, 1979) lead to the conclusion that recognition is more difficult than detection, that simpler patterns may be harder to recognize than complex ones, and that complexity influences the quality of pattern processing, so that there are differences among particular targets.

In the present study, the stimuli are constructed so that they are increasingly degraded by the subtraction of edges, both in outline and internal detail, and this is defined as decreasing target complexity. They are further degraded by the addition of visual noise and these conditions are applied to six different targets. It may be expected that noise will result in more errors of recognition, some targets should be harder to recognize than others, and the simpler, more degraded targets should be harder to recognize.

Identification

Studies of the identification of patterns have frequently made the distinction among detection, recognition and identification. Resell and Willson (1973) defined the three tasks as they are defined here and found that detection probability rises with the S/N ration of a video tube, i.e., noise lowers detection rate. Snyder (1973) reviewed a number of studies on detection, recognition, and identification, and elucidated several measures for use in studying them. Most relevant here is the percent or probability correct, which can be a measure of completeness (number of correct responses divided by the number of possible targets) or accuracy (number of correct responses divided by the total number of responses, correct and incorrect). The former is the measure used in the present study. Snyder also introduced the MTFA (mean transfer function area) as a measure of overall image quality, and found that it was related to judged quality and information extraction as measured by responses to a series of questions about a scene.

On the basis of these and other studies, as well as a consideration of the tasks in the present study, several expectations may be advanced. It would seem that more complex targets would be more easily identified, since this was an actual finding in earlier studies, and because better images led to easier identification in some studies. A variable in the present study which has not been isolated in previous research is that of the internal details of a target, as exemplified by the surface details of buildings, such as doors and windows. A previous study (LeMay and Reed, 1980) found these to be important determinants of judged complexity. Therefore, it might be expected that targets that are more complex in terms of internal detail will be more easily identified than targets with simplified or missing internal details.

It would also seem that the functions relating target complexity to detection, recognition, and identification should be independent of one another, based on Swets, Green, Getty, and Swets (1978), and that detection should result in the fewest errors, while identification

should result in the most errors.

Method

Subjects

The subjects for the detection experiment were 14 students in an experimental psychology class at Montclair State College. Thirteen of the same subjects also served in the recognition experiment. Both sets of data were collected in a group setting.

The subjects for the identification experiment served individually. They were eleven volunteers from classes at Montclair State.

Stimuli

The stimuli for all three studies were composed of 108 slides of various scenes generated on a computer according to the methods described by Bunker and Heeschen (1975). The scenes were of six targets at each of six levels of complexity and three levels of visual noise. They were used in a $6 \times 6 \times 3$ factorial design with repeated measures on the same subjects (Kirk, 1968).

The six targets were embedded in a scene as they would be likely to appear when viewed from an aircraft. The targets consisted of a (n): aircraft hangar; factory; water tower; single house; airstrip; single aircraft on the ground. Only one target appeared on each slide.

Each target was presented at each of six levels of complexity. Since a previous study (LeMay & Reed, 1980) had shown that the number of internal details was an important determinant of subjective complexity, the levels were chosen so that there were two levels of complexity of figure outline, and three of added internal detail. These are illustrated for one target (the factory) in Figures 1 and 2. The simple outline consisted of the barest minimum number of edges to outline two dimensions of an object, so that the basic building facade is a rectangle. The more complex outline consisted of the greatest detail in the outline of that particular building.

The three levels of internal edges consisted of, first, an outline with no internal detail at all. In the second level, the doors and windows were represented by blocks or rectangles. At the third level, windows and doors were articulated.

When the most complex level of internal and external edges were combined, the resulting stimulus was a fairly realistic picture of the object represented. The other levels of complexity should be thought of as degradations of the representation.

Since the FLIR and L3TV images are generally viewed in conjunction with a considerable amount of visual noise, each of the 36 combinations of target and complexity was subjected to two levels of noise, as well as being generated with a clear picture. This added a 3-factor variable, resulting in a 3 (noise level) \times 2 (internal edges) \times 3 (external edges) \times 6 (targets) factorial design with 108 conditions. This was presented to all subjects in a repeated-measures design.

The scenes were generated and shown on a TV screen, and still pictures were taken of them and made into slides and into still pictures so that the scenes could be presented to subjects easily.



Figure 1. Simple outline of the "factory" target at three levels of internal complexity.

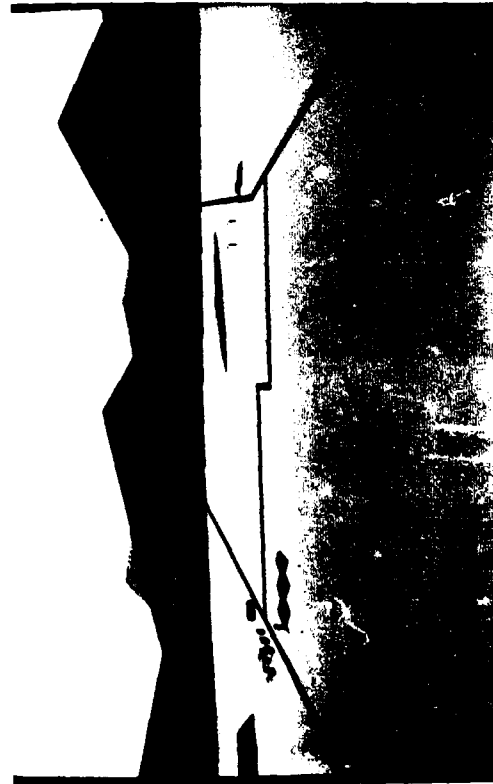
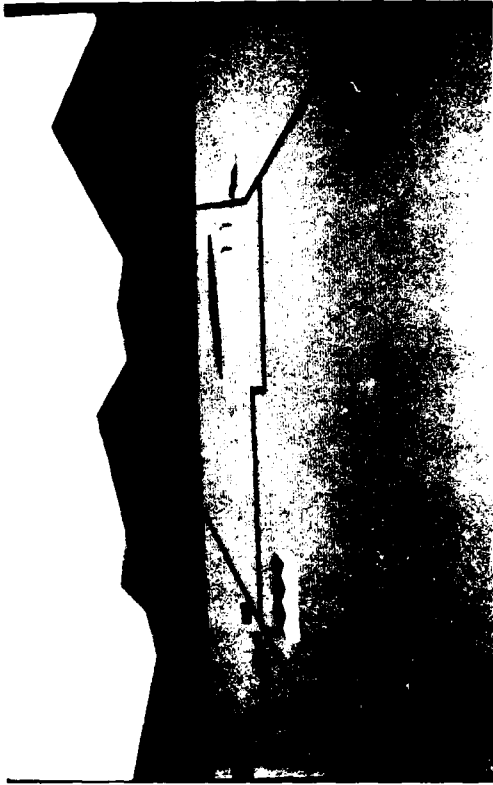


Figure 2. Complex outline of the "factory" target at three levels of internal complexity.

Procedure

For the detection experiment, three slides were taken of the basic scene with no targets in it, one for each noise level. These were interspersed with the slides on which there was a target and presented to the subjects for a very short period each in one random series of 216 slides on which there was a target 50% of the time.

Subjects were instructed to record on an answer sheet whether or not there was a target in the scene, regardless of which target it was. Subjects were not informed of target probability.

In the recognition experiment, the slides were presented in a random series of 108. This time, however, subjects were instructed to mark on an answer sheet which one of the six possible targets was on the slide just shown. They were first acquainted with all of the targets, using the scene with all six targets in it, in full detail, i.e., with the maximum number of edges.

Subjects were run individually in the identification experiment. First they were acquainted with the appearance of the targets using a set of drawings mounted on the wall in front of them. These consisted of four drawings of each target type, one of which was the target in the scene, and three of which were of other, similar targets. There were 24 drawings in all: four hangars, four water towers, four airstrips, etc. They were visible to the subjects at all times throughout the experiment.

Then, subjects were told they would be shown a set of slides in which one of the six pictured targets would appear. The slides were shown briefly, as before, and subjects informed the experimenter which target of the 24 pictured was in the slide. If the subject was uncertain, the slide could be shown again, as many times as the subject wished, although each time was of the same very short duration. Thus, two measures of subject performance were obtained: first, number of errors made in identifying the target and second, number of repetitions necessary for identification.

A short de-briefing session was held after each experiment. Subjects were informed of the target probability in the detection experiment, and had reached the conclusion that it was .50 before the experimenter so informed them. In the identification experiment, no subjects had been aware of the fact that there were only six possible targets; they all thought there had been more than one of each target type.

Results

The dependent variable for the detection and recognition experiments was whether or not the subject had made an error in each category. An error was scored as one and a correct response as two. This was also used for identification and, in addition, the number of repetitions of each stimulus slide was scored. These data were subjected to a treatments by subjects analysis of variance (Kirk, 1968) to determine the effects of noise, target complexity, and target type on errors and, for identification, number of repetitions.

Detection

For the detection experiment, the only significant main effect was that of target type. Significant interactions were

obtained between target type and noise, external edges and internal edges, and external edges and noise. The house, the water tower, and the factory were difficult to detect, and this was especially so when noise was added to the display. It should be noted that these are relatively small targets.

The interaction between noise and external edges is accounted for by a very slight increase in difficulty of detection at both higher complexity and higher noise levels. In other words, the more complex a target is under noisy conditions, the harder it is to detect.

It should be borne in mind that, despite some significant interactions, the ability of subjects to detect targets is not really affected by target complexity, or even much by noise. The actual overall error rate in the experiment was quite low. Subjects detected 91.88% of all the targets presented. This result is presented in Figure 3 where it can be compared with the data obtained for recognition and identification. The overall false alarm rate was 18.33%.

Recognition

The results of the recognition experiment were similar to those for the detection experiment, in that the only significant main effect was that for target type, and there was a significant interaction between target type and external edges. No other effects were significant. This seems to be the result of the data for the plane, where more external edges make it more difficult to recognize, and the factory, where the opposite is true. The reasons for this are mentioned later. The plane, the hangar and the factory were the most difficult targets to recognize.

The actual overall error rate for recognition was considerably higher than that for detection. Only 77.24% of all targets presented were recognized correctly. Although the number of errors declined as complexity increased, this result was not significant. It must therefore be concluded that increasing target complexity does not enhance recognizability.

Identification

The results for identification are quite different from those for detection and recognition. Here, all main effects except that of noise are significant, and there are no significant interactions.

The variable of most interest in the present study is that of complexity. Both internal and external edges had a significant effect on errors of identification (internal: $F=16.83; p<.001$; external: $F=6.13; p<.03$). These results are also presented in Figure 3 where it is clear that targets with more detailed, complex outlines are more easily identified than those in which the outline has been degraded by removal of some detail.

Degrading the target image by removal of internal detail has an even more drastic effect on identification. The complete absence of internal detail represented by the least complex targets results in an 80% error rate in identification. A Duncan multiple range test indicates a significant difference between the first and second level of complexity, but not between the second and third

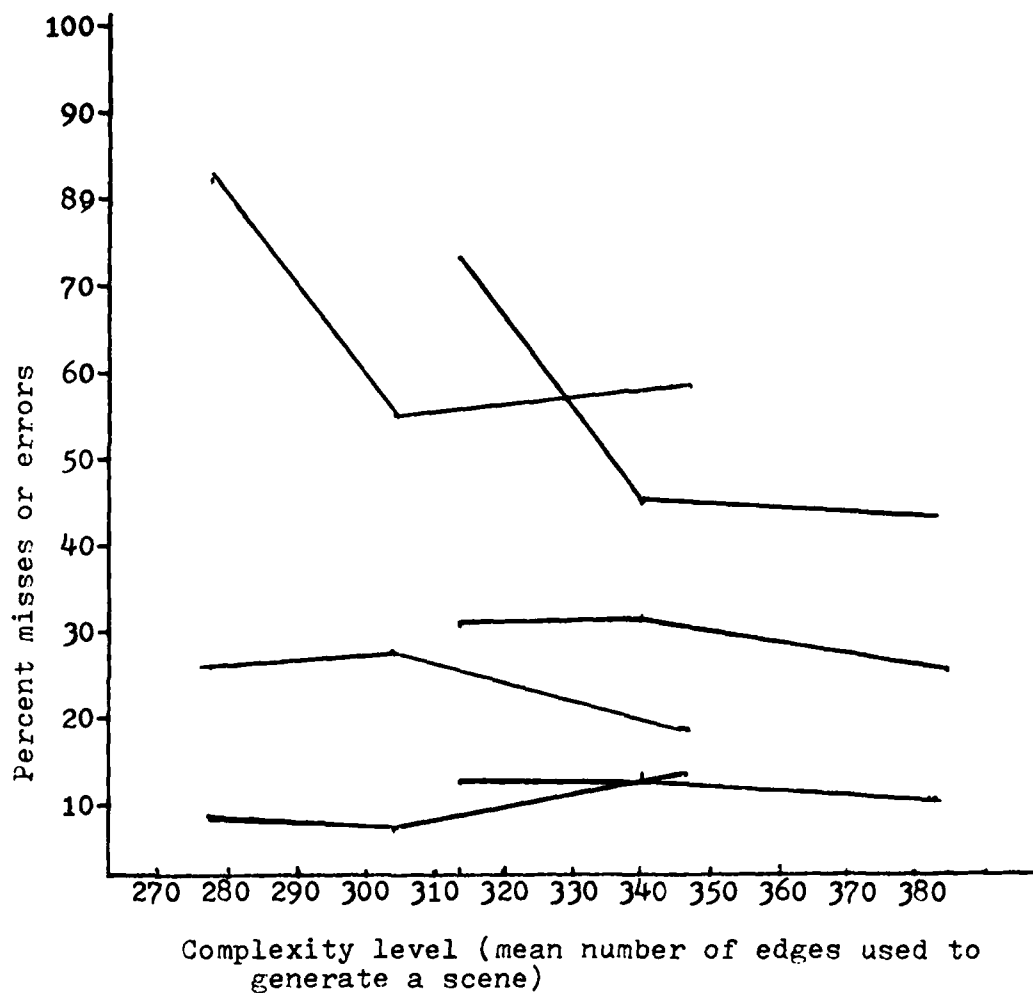


Figure 3. Percentage of errors in detection, recognition, and identification for six complexity levels.

levels, i.e., absence of internal detail makes a target difficult to identify, but simply presenting some internal detail decreases the error rate significantly. Further articulation of detail does not result in additional improvement.

The effect of target type on identification errors was also significant. This data is presented in Table 1. The factors which determine difficulty in particular target identification are not clear, and will bear further investigation. The overall error rate for target identification was 59%.

Table 1

Mean error score (an error was scored as 1, a correct identification was 2) for each target, and mean number of repetitions for each target as a function of noise level in the identification experiment.

Target Type	<u>Errors</u>	<u>Repetitions</u>		
		No Noise	Moderate Noise	Heavy Noise
House	1.78	2.83	2.71	3.45
Plane	1.73	2.26	2.12	2.28
Factory	1.61	2.27	2.04	2.82
Hangar	1.57	2.54	2.76	2.12
Airstrip	1.39	1.92	1.97	2.01
Watertower	1.38	2.08	2.16	2.74

The repeated presentations, constituted a second dependent variable which was subjected to the same type of analysis of variance. Noise and targets were the only significant main effects, and they interacted significantly with one another. There was also a significant interaction between external edges and targets.

Discussion

The most significant result of the present investigation from the point of view of the simulation of E/O displays is the finding that the complexity of a target, in terms of the number of external and internal edges which go to make it up, influences performance on an identification task but has no effect on the recognition and detection tasks used here. Thus, a high degree of complexity in simulation may be necessary only for training operators in the identification of particular targets and not for simply recognizing a class of possible targets or detecting the presence of a target.

Considering the similarity of the experimental situations, the tasks produced markedly dissimilar results in terms of the number of errors. The overall error rate was only 8% for the detection task. It jumps to 23% for the recognition task, and to 59% for the identification task. Where they are affected by degradation in target complexity, identification errors jump to 80%. Detection is a relatively easy task, and is not affected by complexity.

It is not surprising that complexity did not enhance target detectability. In fact, the addition of detail to a target may, in a sense, add to a visual noise factor and thereby make it harder to detect. Evidence for a phenomenon like this was suggested by Teichner

and Mocharnuk (1979) and Uttal and Tucker (1977). The surprising result here is that the addition of visual noise to the scene did not affect detectability. It is even more surprising that there was no interaction between noise and internal edges, since the addition of internal edges to a target in an already noisy scene would seem to make it more easily seen as part of the noisy background and thus harder to detect, as in the studies mentioned. Instead, however, there is an interaction between noise and external edges and noise and target type. This is probably because targets with some detail in their outlines (the house and the factory) were the most difficult to detect under noisy conditions. These results seem to indicate that target complexity may have a slight negative effect on detectability, but it is too small to have produced a main effect.

While it was to be expected that target complexity would not effect detectability, the lack of any main effects other than that of target type is surprising for the recognition experiment. In particular, it would seem that complexity of detail should affect the recognizability of a target, especially since several of the targets were chosen because of their rather unique shapes, such as the hangar, with the distinctively curved roof, or the airstrip with its rather characteristic projections in various directions. Both of these characteristics were missing in the simplified outlines. Yet neither target was particularly difficult to recognize, and the factory was actually easier to recognize without the high level of external detail. If, as Gibson (1969) suggests, pattern recognition depends on the presence of "critical features," it is not evident in the recognition part of these experiments. It would seem that there is enough variability in the shapes of the objects chosen so that a fairly large degree of departure from either the outline or the internal features of a particular target does not render it unrecognizable as a member of a certain class of targets.

While the absence of detail does not seem to affect target recognition, it has a very clear effect on the exact identification of a target as being one, and only one, of its general class. The application of Gibson's (1969) critical feature model would seem to be relevant here. Both external and internal edges had a significant effect on identification. Degrading a target image by subtracting either external or internal critical features makes it more difficult to identify.

This is perhaps most readily apparent in the case of internal edges. The total absence of any internal edges, as in the most simple targets, results in an extremely high error rate (over 70% even for targets with a complex outline). Adding any amount of internal detail immediately brings the error rate down near 50% for both simple and complex outlines. Internal details certainly seem to act like critical features for the identification of targets. This observation is borne out by the significance of the difference between the first and second levels of internal detail (the presence or absence of any detail) and the lack of a significant difference between the second and third levels.

The absence of an interaction between external and internal edges is reflected in the relationship shown in Figure 3. The effect of internal edges with a complex outline is repeated for the simple outline, but at a lower error rate. Thus, internal and external

detail act separately and additively to lower the error rate for target identification. There are no other significant interactions, either with noise or with target type, indicating that the main effects of complexity apply across the various types of targets and levels of noise. In other words, where complexity is an important variable, as in the identification task, it acts by itself in a simple fashion regardless of other variables. This should make it easier to deal with in an applied situation.

The measure of number of repetitions was not significantly affected by complexity, but only by target type and noise. It is not surprising that some targets require more time to identify, or that these targets should be the most difficult to identify in terms of errors. The effect of noise is also to be expected, since noise increases uncertainty. This would probably be true even if the error rate were not related to the number of repetitions, i.e., even if they had guessed correctly, subjects would still prefer more time to examine a target under high noise than under low noise conditions (Swets, Green, Getty & Swets, 1978).

It is interesting to note that, when subjects were questioned after participating in the identification experiment, none of them realized that there were only six targets, with six different versions of each. They all thought that there was more than one airstrip, factory, house, etc. This, of course, reflects the high error rate, but it also emphasizes the importance of the complexity of figures for the identification process.

Conclusions and Recommendations

1. Since hits and false alarms in detection, and errors in recognition, are not affected by complexity either in external or internal detail, a very low level of such detail is probably all that is necessary for the simulation of these tasks. Bare outline figures, such as those used at the simplest level in the present study, are probably sufficient in CIG simulation.

2. Errors in identification are drastically affected by complexity, and it is probably necessary to simulate considerable detail if unacceptable levels (70-80%) of error are to be avoided. The best combination for use in identification training is probably the higher level of outline complexity with the middle level of internal complexity, since the third level of internal complexity does not seem to lower the error rate.

3. Error rates for recognition and identification are high, and may be unacceptable for practical application. They may be improved, however, with training, and training may interact with complexity, so that subjects may be trained to recognize and identify simpler targets. More research is needed in this area.

4. Noise is an important variable which has significant effects on all three tasks, and interacts with target characteristics which are not covered by the manipulation of target edges, as is shown by

the interaction of noise with target type. The role of noise should be further investigated, (especially as it pertains to the simulation of E/O displays.)

References

- Berkhout, J. and Phillips, J. Visual target acquisition in the presence of complex backgrounds. In Bensel, C.K.(ed) Proceedings, Human Factors Society 23rd Annual Meeting, 1979, 394-396.
- Bunker, M. and Heeschen, R. Airborne Electro-Optical Sensor Simulation. AFHRL-TR-75-35, July, 1975.
- Frowein, H. and Sanders, A. Effects of visual stimulus degradation, S-R compatibility, and foreperiod duration on choice RT. Bulletin of the Psychonomic Society, 1978, 12, 106-108.
- Gibson, E.J. Principles of Perceptual Learning and Development. New York: Appleton-Century-Crofts, 1969.
- Green, D. and Swets, J.A. Signal Detection Theory and Psychophysics. New York: Wiley, 1966. (Reprinted by Krieger, Huntington, New York, 1974)
- Guttman, J., Snyder, H., Farley, W. and Evans, J. The effect of image quality on search for static and dynamic targets: MTFA-performance correlations. In Bensel, C.K. (ed) Proceedings, Human Factors Society 23rd Annual Meeting, 1979 339-343.
- Kirk, R. E. Experimental Design: Procedures for the Behavioral Sciences. Belmont, CA: Brooks/Cole, 1968.
- LeMay, M. and Reed, L. Complexity Judgements of Computer Generated Simulations of Electro-Optical Displays. In Press
- Nygard, J.E., Slocum, G.K., Thomas, J.J., Skeen, J.R. and Woodhull, J.G. The Measurement of Stimulus Complexity in High-Resolution Sensor Imagery. AMRL-TDR-64-29, 1964.
- Pasnak, R. Pattern complexity and response to distinctive features. American Journal of Psychology, 1971, 84, 235-245.

- Rosell, F.A. and Willson, H. Recent psychophysical experiments and the display S/N ratio concept. In Biberman, L. Perception of Displayed Information, New York: Plenum Press, 1973.
- Snyder, H.L. Image quality and observer performance. In Biberman, L. Perception of Displayed Information. New York: Plenum Press, 1973.
- Staller, J. and Sekuler, R. Stimulus and response factors in mirror-image discrimination. Perception and Psychophysics, 1977, 22, 592-598.
- Swets, J., Green, D., Getty, D. and Swets, J. Signal detection and identification at successive stages of observation. Perception and Psychophysics, 1978, 23, 275-289.
- Teichner, W. H. and Mocharnuk, J. B. Visual search for complex targets. Human Factors, 1979, 21, 259-275.
- Uttal, W.R. and Tucker, T.E. Complexity effects in form detection. Vision Research, 1977, 17, 359-365.

ALL NATURAL COLOR - COCKPIT BRIGHT/DAYLIGHT JAPANESE CGI SYSTEMS
(A Look at One Japanese Company)



John L. Westland
President, John Westland & Sons, Inc.
Aviation Consultants
Redondo Beach, CA

John Westland is a Naval Aviator and retired Captain in the Naval Reserve. He has a degree in International Marketing from the University of Southern California. Is a graduate of American Airlines Captains School and has been flying transport aircraft and flight simulators for more than 30 years. Less than 18 months after his graduation as an ensign and naval aviator, he was appointed Officer-in-charge of all Link Instrument Training at the Naval Air Station, Pensacola, Florida. He was responsible for the quality of instruction given to more than 1,500 Aviation Cadets, Enlisted and Officer flight students each month from the USA and many other countries in the free world.

Since June of 1980, he has been consulting with Hitachi Denshi concerning CGI visual display systems.

ALL NATURAL COLOR - COCKPIT BRIGHT/DAYLIGHT JAPANESE CGI-SYSTEMS

(A LOOK AT ONE JAPANESE COMPANY)

By

Capt. John L. Westland USNR (RET)

President
John Westland & Sons, Inc.

ABSTRACT

Hitachi Denshi Co., Ltd. has been manufacturing trainers, simulators and visual display systems for more than 20 years. All of their systems have been sold only in Japan, to the Japan Defense Agency, universities and domestic industry.

A short history of the company, a partial list of some of the visual systems, trainers and simulators has been included plus a general outline of the full color - daylight CGI display system Hitachi is marketing today.

INTRODUCTION

Hitachi Denshi Co., Ltd. has more than 20 years' experience in the research, development and manufacture of flight and other simulators and visual display systems for a variety of simulators and other training applications.

They are currently able to meet the visual display requirements of the new FAA Phase II, with their "Bestview series", and will shortly be able to deliver a Phase III CGI visual display system with their full natural color - cockpit bright/daylight pictures and their hybrid modelling techniques.

Over the last few years Hitachi Denshi has acquired world-wide recognition through highly developed systems technology in broadcasting systems, CCTV systems, radio communications systems, information processing systems, oscilloscopes, integrated circuits, image orthicons, image processing systems, photo-multiplier tubes, tri-electrode color videcon tubes and color freeze picture transmission systems, etc. They are looking forward to the time that industry and the defense services will recognize the quality and the uniqueness of their image systems.

Hitachi Denshi Co., Ltd. is a division of the Hitachi Ltd. group which was founded in 1910. Hitachi Ltd's net sales in 1979 was over 12 billion US Dollars. They employ about 150,000 people in 40 main companies and about 440 subsidiaries.

Bestview Major Specifications

<u>Item</u>	<u>Specifications</u>
Visual Display Capacities	Display Surfaces 350 *
Position Resolution	Display Light Points 4,000 *
	Vertical 483
	Horizontal 1,024
Available Hues	Red 6 bits
	Blue 6 "
	Green 6 "
	All natural colors are available by the above color element combinations.
Colors available	Surface 49 colors
	Light Point 15 "
	Total: 64 colors
Scene Update Rate	30 Hz, interlace television system
Occultation	10 levels
Edge Smoothing	Yes
Numbers of Channel and Display Units (windows)	1 channel and 2 windows to 4 channel and 6 windows
Brightness	More than 30 ft-lm reference white brightness on CRT surface
CRT Resolution	Vertical more than 350
	Horizontal " 500
	(measured by monoscope signal)
Deflection Distortion	Less than 7%
Raster Distortion	Less than 2% (BTS method)
Display Units	26" RGB shadow mask CRT - of very high brightness, sharp pictures.

* The 350 surfaces and the 4,000 light points are generated separately and can be displayed separately or together for more scene flexibility.

Bestview Field of View Options

	<u>Radius (mm)</u>	<u>Horizontal</u>	<u>Vertical</u>
Type 1	1,200	47 degrees or more	36 degrees or more
Type 2	1,300	44 degrees or more	33 degrees or more
Type 3	1,400	40 degrees or more	30 degrees or more

Actual field of view is determined by the dimensions of the cockpit.

GENERAL DESCRIPTION OF HITACHI'S BESTVIEW VISUAL DISPLAY SYSTEMS

The computer generated image system has been used by Hitachi in many fields of computer technology besides in their visual display system for simulators.

Hitachi has progressed by continuous research and development for more accurate scene generations and as a result of this expects to have even greater image realism very soon.

As early as in 1975, Hitachi Denshi's research and development of computer generated images were much further advanced than many of their competitors' visual systems are today.

The Bestview system is a CGI display system developed to provide full natural color daylight along with twilight, dusk and night scenes to give the pilots as much clarity and realism as possible.

The visual display system operates as follows:

- 1) Due to the raster scan operation as against the caligraphic operation, full natural daylight colors can be presented which meet the requirements today of the later phases of the new FAA regulations.
- 2) Hitachi's ability to produce full daylight in all natural colors including blue brings greater realism, not only to the airport scenes but also to enroute flying between airports. Simulator flying in adverse weather conditions, as is required, takes on new dimensions of reality when pilots use Hitachi's Bestview visual display systems.

Operational Capabilities:

The Bestview system simulates scene information and is guided by the movements of the aircraft by a computer generated image system and displays the scenes on one to four channels as required by the user.

Landscape and Landing Areas:

In the Bestview system, with full bright daylight colors, all objects can be displayed in their natural colors such as runways, markings, taxiways, ramp areas, natural vegetation, hills, mountains, blue rivers, blue lakes, blue oceans and vast city areas as well as realistically portraying small villages and towns.

Light Points and Surfaces

The simulation of ground scenes by use of light points and surfaces, airport lighting, city lighting, etc. can be independently displayed with 4,000 light points and/or 350 surfaces. This gives the greater flexibility in developing scenes using both the light points and surfaces or using the light points and surfaces independently.

Weather Conditions

The weather effects, such as clouds, fog and lightning can be realistically displayed in Bestview scenes. The visibility will be changed gradually from a far point to a close point in response to the flight path being flown.

Simulation Capability

Simulation of terrain, ground obstacles and markings:

Terrain, ground obstacles and markings are simulated by the following conditions due to the capabilities of Hitachi's advanced computer processing and hardware performances.

- 1) The surfaces are created by use of either 3 or 4 edges.
- 2) About 450 surfaces for one scene are in the data base. 450 surfaces are used so that a minimum of 350 surfaces can be displayed to reduce the overflow conditions of various surface distribution.
- 3) Natural terrain, cultivated terrain, buildings - with lighted windows - and other man made objects are represented by using approximately 100 surfaces of the available 450 surfaces. Current "Bestview" displays have a total of ten (10) occultations for one scene.
- 4) Markings - Bestview simulates markings in great detail to aid pilots in their approaches.
 - a) Indication markings - Center line, end, touchdown zone, edge, and runway markings are all represented in clear white colors in contrast to the dark colored runways or black on light colored runways.
 - b) Taxiways - Taxiway centerline and stop positions are represented in yellow colors.

Light Points (defined as light strings)

The light points are equally spaced and have the same defined color on a straight line. One independent light point is also defined as a light string.

There are 15 light point colors for fixed intensity to variable intensity. Five colors are used for the polyhedrons and make an occultation of light points.

Light strings can be selected for one scene using 600 strings or less. Each light string has 255 light spots maximum.

Landing Lights and Taxi Lights

- 1) The landing lights' brightness and illumination will vary according to the distance from the landing lights. If only one landing light is used, the illumination is reduced in half, but the range of illumination is not changed.
- 2) The taxi lights illuminate runways and taxiways with less brightness than landing lights.

Scene Mode

The simulation for scene mode of day/twilight/night is as follows:

- 1) Day - Day is displayed by the building up of surfaces bounding one scene.
- 2) Night - Night is represented by the light strings that have been stored in the computer to make light spots. Horizontal and seaside lines are also displayed.
- 3) Twilight - Twilight is displayed by a combination of surfaces and light spots.

Field of View

The pilots see the images outside the cockpit windows through display units. The display units consist of shadow mask 26" color CRT and optical components. Optical components consists of spherical mirror and beamsplitter. The image will be closed to infinity. The display channels can be varied from one to four along with from two to six display units (windows).

Data Base

50 scenes can be stored in magnetic disc storage system. Scene selection is achieved manually or automatically.

- 1) The manual selection is made by the scene select switch on the visual control panel.
- 2) In addition to the take off and landing at airports, when an aircraft flies a high altitude route (area), the following automatic selection is available:

High altitude scenes of 400 N.M. area are provided. When the aircraft is entering or departing the area defined as an airfield scene, the scene will be changed automatically to correspond with the flight route. About one second is required for scene changes. During the change, the scene become a gray color, as in clouds.

Instructor Operation Console

The visual display control panel controls all of the Bestview visual systems, including adjustment and changes to the environmental conditions. By use of a color monitor, the instructor observes the same scenes as being viewed by the pilot and the co-pilot.

Hardware System

The Bestview visual display system will produce computer generated images and displays the scenes on a raster scan type 26" color CRT with almost infinity image of scenes. The environmental conditions displayed can be selected from the visual display control panel.

The Image Generation Equipment: Consists of Display Processing Equipment, Display Image Generation and Control Equipment to change the scenes of Day/Twilight/Night by using a computer generated image and raster scan system.

The image generation equipment will process the data stored in the central processing unit corresponding to the position and posture of the aircraft giving this information on the display units for pilot, co-pilot and on instructor's visual display.

The display unit consists of a shadow mask color 26-inch CRT with collimating mirror and beamsplitter which provides the authentic scenes for both the pilot and co-pilot with almost infinity scenes.

Display Processing Unit

Display processing unit consists of a general purpose computer and peripherals. The general purpose computer provides flight parameters to the Display Image Generation and Control Equipment. The flight parameters are calculated by the aircraft's current position and attitude and included the selection of the window's view.

Display Processing Units hardware components are as follows:

- * CPU SEL 32/7780 or Perkin Elmer 3320
- * 10 M Byte Moving Head Disc. 10/32 or DMR CMD Processor Sub-system
- * MTU Tape Sub-system 800/1600 EPI or Perkin Elmer Model 456/32
- * Display Terminal Perkin Elmer Model 550 or CRT Operator Console

Display Image Generation and Control Equipment

The image generation and control equipment will receive the scene data (such as surface and light string data), parameters to make a coordinate conversion for the aircraft location, data for color of each figure, simulation data for the environmental conditions, from the display processing equipment and will provide the computer generated image signals corresponding to proper windows.

- 1) Interface - Interface will transmit necessary data to selector, surface generator, light spot generator and color control equipment from the display processing unit transmitting the following data:
 - a) Surface data
 - b) Light string data
 - c) Parameter for selector
 - d) Parameter for surface generation
 - e) Parameter for light spot generation
 - f) Data for color
 - g) Data for selecting the environmental condition
 - h) Parameters for various maintenance program.
- 2) Selector - Selector has two kinds of packages for the surface (selector 1) and light strings (selector 2), and receives the following data through the interface:

a) Parameter to select the figures which can be seen in each window, calculated by the display processing unit.

b) Data for surface or light strings defined as a scene.

Selector will select the surface which can be seen at each window in the surface data received by the parameter as shown in item a), and will transmit the surface data to surface generator.

Light strings: the selector will select the data similarly as surface data, and will transmit the data to the light spot generator.

3) Surface Generator

a) Receives the parameter to make a coordinate conversion through the surface data interface by the selector 1.

b) Surface data will be changed to the coordinate of aircraft axis based on the eye point of pilot by a parameter. The new coordinate is defined as a field-of-view coordinate.

c) Makes a perspective transformation in the scene coordinate (defined as a scene coordinate), and calculates perspective images of all surfaces.

d) Converts the data from item c) to the data to be displayed in the raster scan color CRT, and provides the output the same as the surface image. 350 surfaces are available.

4) Light Spot Generator

a) Receive the light string data from the selector 2 and parameter to make a coordinate conversion from the interface.

b) Generate individual light spots from light string data and transform the scene points into the field-of-view coordinate.

c) Make a perspective transformation of light points into the scene coordinate.

d) Synchronize the data from item c) to raster line of CRT. 4,000 light spots are generated by the light spot generator. Light strings have maximum of 255 light spots.

5) Color Control Equipment

Colors for surface images produced by the surface generator and light points produced by the light spot generator are generated by color data that has been already designated on each figures.

When surfaces or light spots hide more than two other surfaces or light spots the color of figure having the higher priority will be displayed.

The visibility, fog and landing lights are displayed with the control of brightness and frequency characteristics by the data that has been selected.

The color control equipment will provide natural colors by combining the red, green and blue colors.

Display Unit

Each display unit consists of high brightness 26" color CRT and highly accurate optical components.

Visual scenes are displayed on the CRT receiving the video signals and sync, corresponding to each window produced by image generation equipment. The optical components used present the pilots with an almost infinity image of the scenes displayed on the CRT.

High Brightness Color CRT - High brightness CRT display utilizes the 26-inch RGB Shadow Mask CRT, and provides bright and sharp picture.

High Accurate Optical Component - Highly accurate optical component consists of spherical mirror and beamsplitter installed in each visual display unit.

Visual Display Control Panel

Visual display control panel is installed in the instructor console of the flight simulator and controls all of the visual display system.

Color Monitor

Monitor is used for surveillance of the scenes and displays the front and side scenes of pilot and co-pilot.

Software System

The software of Bestview visual display system consists of image generation program, data base management program and test programs.

Scene Generation Program

The image generation program is an on-line process program to do processing in real time necessary for the generation of visual display scenes. The program consists of the following sub-programs.

- 1) Interrupt Process Program - The interrupt process program inputs the system mode of flight simulator to the display system and controls the program corresponding to each system mode, and also controls the sequence of conduct and computation cycle of each program.
- 2) Data Transfer Program
 - a) Input-output processing program - the program processes the input-output data to flight simulator, display image generation and control equipment and visual display control panel.
 - b) Visual display control panel process program - the program processes the the necessary selected conditions such as environmental conditions of visual display control panel.

3) Scene Control Program

The program calculated the changed conditions of scene due to location and altitude data of aircraft from flight simulator, and controls the change of scene for airfield and cloud display.

4) Surface Selection Process Program

The program will select the surface data and block of light strings which can be seen in each window corresponding to the location and azimuth of aircraft relative to the selected scene data base.

5) Parameter Process Program for Coordinate Conversion and Perspective Conversion

The program calculates the parameters for the coordinate conversion from the ground to the field-of-view and from the field-of-view to the perspective image on the display.

6) Polyhedron Process Program

The program process to make the hiding of surfaces of polyhedron due to the data for position, azimuth and altitude of aircraft relative to the map data selected. Will also conduct the occultation process between each polyhedron.

7) Horizon Line Process Program

The program calculates the position of horizon line for each window relative to the aircraft attitude.

8) Environmental Process Program

The program processes the environmental conditions such as lightning, clouds, visibility and fog selected by the visual display control panel.

9) Subroutine Programs

The programs are for the function processing such as trigonometric function and square root included in the equations used for visual display system software.

Data Base Management Program

1) Scene Data Base Input Process Program

The program process on-line, the input data of surfaces and light strings by using a card reader, and loads and stores them easily in memory system.

2) Scene Data Base Management Program

The program is used for the process of omitting, adding and re-editing parts of scene data base stored in auxiliary memory system according to the requirements.

Test Program

Test programs are used to test hardware of the visual display systems and consist of display processing equipment, display image generation and control equipment.

1) Test Program for Display Processing Equipment

The program will test and check the operation of main memory and digital components including peripheral equipment of computer.

2) Test Program for Display Image Generation and Control Equipment

The display processing equipment simulates the hardware structures of display image generation and control equipment on software base, and the test data is given to the display image generation and control equipment and the output data is fed back to the display processing equipment to compare with the result of software simulation and to provide diagnostic analysis of the display image generation and control equipment.

The Connection with Flight Simulator

We designed the connection of the visual display system with flight simulators to be very simple. The major items in hardware connections with the flight simulator are:

- 1) Installation of the display units in cockpit windows.
- 2) Installation of visual display control panel in the instructor console.
- 3) Installation of image display equipment in the computer room.
- 4) Installation of interfaces in the computer room.

The details of above items are determined when the hardware and software used for the flight simulator system are known.

Maintenance

The following items are provided to improve the maintenance of visual display system:

- 1) Maintenance - Sufficient space is available.
- 2) Tools - The visual system has been designed to eliminate the use of special tools.
- 3) Self Test Program - Self test program for each functional block is provided to improve the maintenance of display system.

SPECIAL FEATURES OF THE BESTVIEW VISUAL DISPLAY SYSTEMS

As image problems have appeared Hitachi Denshi has developed solutions for some of the problems as follows:

Edge Smoothing

The solution to the jaggedness of the edges, one of the weak points in raster scan type system is accomplished partially in vertical direction only in this economically priced system for the following reasons:

- a) In view of the effective resolution of the system i.e. 1,024 (H) x 483 (V) lines, it is necessary to obtain the balance between the horizontal and the vertical resolutions.
- b) Since the picture movement in the screen is more often vertical than horizontal, the compensation in vertical direction is more effective than horizontal.

In this system, the smoothing effect is obtained by producing one raster having the average value of two sampling lines. Thus, jaggies, stepping and scintillation etc. are reduced so as not to be readily apparent.

Runway Conditions

Following functions are provided in our Bestview visual systems to simulate varying runway conditions, such as patchy wet, patchy icy or wet on rubber residue in the touch down zone.

1) Indication on the Display

Colors such as light gray or white are used to distinguish one condition from the other i.e. dry, wet or icy etc. If the condition in same zone differs from the rest of the greater surrounding area, it is indicated in a different color from the rest by the data fed into the data base beforehand.

2) Output to the Simulator

A spare interface having the capacity of 48 words (16 bits) to feed the conditions as rubber residue, patchy condition etc. to the simulator is also provided.

Weather Representation

1) Variable Cloud Density and Gradual Breakout

The visibility is gradually reduced as the aircraft enters the clouds through the cloudtop or cloudbase as set by the switch on the control pane. Conversely, when the aircraft is emerging from the middle of the clouds, the visibility gradually improves from the initial state of clouds, emerging sight of the ground and to the final visibility level set by the visibility switch at an altitude below the cloud base.

The clouds density is indicated by the difference in the altitude of aircraft between the zero visibility point in the clouds and the point the aircraft enters the clouds. For instance, when the clouds are thick, zero visibility point comes just inside the clouds and when it is this, it is still visible at a point further inside the clouds.

The color of the clouds when the craft is totally in the cloud is either gray or black just like the totally invisible state under day/twilight/night flight.

2) The Effect of Fog on Airport Lighting

When fog reduces the visibility, the lights will be gradually dimmed or obscured setting used depending upon the fog.

3) Category II and III Weather

These conditions are produced by giving the date for the clouds and visibility as required.

Optional Facility

The Bestview Visual Systems are provided with optional capability to produce images at a predetermined position in the scene.

1) Moving Hazard

The images moving from a set position, consists of surfaces and light points representing a vehicle or an aircraft which are produced in the scene. The timing of the start of motion is given from the instructor operation console with a push button. Work is now in progress to add greater model realism with combinations of CGI and T.V. etc. - some excellent aircraft air to air work was prepared for the Japanese military program.

2) Partial Obscuration of Ground Scenes

This is produced in the scene during the approach and landing phase of the flight below 2,000 ft HAA and within the radius of 10 miles from the airport. This is defined separately from the clouds. The surfaces of light gray color and the predetermined size having the priority over any other surfaces or light points are placed at predetermined positions in the space, and the visibility around them is set to an adequate level with the visibility switch to soften the effect. These clouds are so positioned so that no two clouds overlap.

3) Patchy Fog

During the final approach and landing phase of flights below 2,000 ft. HAA and within the radius of 10 miles from the airport, vertical surfaces of predetermined sizes and having the priority over any other surfaces or light points are placed at predetermined positions on the ground. The visibility around them is set to an adequate level to soften the effect. These are so positioned so that no two fog scenes overlap.

A PARTIAL LIST OF THE SIMULATORS FOR TRAINING AND OTHER USES

MANUFACTURED BY HITACHI DENSHI CO., LTD., TOKYO, JAPAN

1. P-2J Operational Tactical Trainer
2. PS-1 Weapon System Trainer (Flight Trainer)
3. PS-1 Weapon System Trainer (Tactical Trainer)
4. T-3 Flight Simulator
5. C-1 Flight Simulator
6. Submarine Tactical Trainer (STT)
7. Mine Tactical Trainer (MTT)
8. Active Sonar Trainer (AST)
9. Surface Group Anti-Submarine Tactical Trainer (SATT)
10. General Purpose Flight Simulator
11. Flight Control System
12. Rocket Dynamic Characteristic
13. V/STOL Airplane with Visual System
14. Automatic Landing and Taking Off
15. Space Travel Simulator with Visual Display
16. Dynamic Characteristic of Airplane
17. Warning System of Airplane
18. N-Type Rocket
19. Tracking Tester with Visual Display System
20. Ship Operation and Control with Visual Display System
21. Atomic Power Reactor
22. Strong Earthquake Response Analyze Computer
23. Flood Forecasting
24. Cerebrum and Heart Simulation for Medical Use

A Brief explanation of some of the simulators with defense applications:

P-2J & PS-1 Operational Weapons System Flight Tactical Trainer

P-2J and PS-1 are anti-submarine attack airplanes whose mission is to search, detect, discriminate and then attack enemy submarines. It's training mission is to improve the probability of target location, using many kinds of sensors, and to identify, process and to evaluate the sum total of the data information received from the sensors.

P- J and PS-1 Operational Tactical Trainers provide a team training of crew (pilot and five operators) in the simulator to improve the tactical capability of anti-submarine warfare by P-2J and PS-1 airplanes.

Crew training, as a team, is one of the most important factors of the simulator training programs because of the complexity and high level of electronic sensor equipment and systems used for anti-submarine warfare.

The simulator instructors can set the tactical conditions and maneuvers of one or more targets and provide the data for evaluation of individuals and teams in the various training exercises.

PS-1 Operational Flight Trainer

PS-1 Seaplanes can take off and land in very rough seas. PS-1 flight simulator or had to create the required realism of rough seas, so that take-offs and landings on the waves could be accomplished in addition to the ordinary functions and performances of a conventional flight simulators.

The following operational training programs are available in the simulators just as they would be encountered in the actual seaplane training exercises at sea.

- a) Taxiing on smooth water
- b) Taking off and landing on smooth water
- c) Military requirements while airborne
- d) Taxiing on rough seas
- e) Taking off and landing on rough seas

T-3 Flight Simulator

T-3 flight simulator provides real and accurate simulation of all functions and characteristics of the T-3 elementary training aircraft used for ab initio pilot training.

C-1 Flight Simulator

The C-1, 2-engine jet flight simulator, with its Bestview CGI/TV full color and bright daylight, twilight and night scenes provides the simulation for all normal functions, performances, and characteristics of the C-1 in addition to its many military functions, such as, military equipment drops, paratroopers, enemy radar detection, etc.

The pilots, navigators and plane captains train as a crew to develop greater skills of coordination for the many highly technical military operations in the simulator costs.

Playback functions, storing operational data of the training progress for instant freeze, and/or later replays of the training exercises will show the dynamic variation of the instruments readings from the scheduled missions requirements etc. An evaluation function stores the quantitative data for training evaluation and types out the mission's results upon command.

Submarine Tactical Trainer

Hitachi Denshi's submarine tactical trainer programs provide intensive training for all crew members of submarines in the same operations as on board actual submarines on tactical training missions of search, detection, classification, discrimination, tracking, attack, evasion, etc..

Simulating other submarines and targets, such as destroyers, ships, aircrafts, helicopters, etc. in the tactical environment required by the various tactical training missions provides the evaluation of data of the training level of the various stations and crew members as well as the data developed during the training exercises.

Mine Tactical Trainer

A major advance in underwater mine detection training has been made by Hitachi Denshi with their mine tactical trainer that simulates all the tactical training to complete the various mine sweepers missions.

The tactical situations are controlled by the instructors according to the mission requirements.

The evaluation of the data of various levels of the training exercise is recorded and compared with the actual mission programs.

SUMMARY

The quality of the images, the full range of colors, the bright daylight, and the realism of moving models of the current CGI made by Japanese companies, or at least one Japanese company, may come as a surprise to many people.

And, according to several Hitachi Denshi engineers responsible for image production, they feel their present work, in general, is as good or better than the image systems they have viewed during their current visits to many airlines, aircraft/simulator manufactures in Japan, USA, Canada & Europe, where they have looked at the Vital III, IV, SP-1, SP-2, CT-4, DIG and Compuscene systems being displayed.

CONCLUSION

The Japanese have been very successful in marketing their 35mm cameras, TV sets, studio TV cameras, automobiles, etc. in many parts of the world.

However, they have been slow and patient in introducing new products, researching the potential markets to be sure their products would meet the high standards of quality that people have come to expect.

Given time, exposure and marketing experience, Hitachi Denshi, may do as well with their "Bestview" CGI and more advanced hybrid visual display systems in the future.

Thank you for your interest.

PANEL DISCUSSION

"What You Always Wanted to Know About CIG
But Were Afraid to Ask"

Chairman

Mr. Herbert A Cooles
Manager, Advanced Technology
American Airlines Training Corporation



Mr. Cooles is presently Manager Advanced Technology at American Airlines Training Corporation. He has been actively engaged in the development and application of simulation technologies for the past eighteen years. This experience has included almost all facets of the science and art of flight simulation. His most recent activities are concerned with the development of advanced visual simulation techniques for both commercial and military applications.

Mr. Cooles received his B.S. degree from Texas A & M University and graduate work at U.S.C. He is an Associate Fellow of the AIAA.

PANELISTS

Colonel John A Hall
USAF Tactical Air Warfare Center



Colonel John A. Hall was born 1 August 1928 in Smithville MS. He possesses a Bachelor of Arts from the University of Mississippi and a Master of Science from George Washington University.

Colonel Hall was assigned to USAFTAWC, Eglin, AFB, FL, on 23 August 1978 as the Asst DCS/Aircrew Training Devices. He became the DCS/Aircrew Training Devices on 22 January 1979.

Colonel Arlin "Art" Deel
USA NASA/Ames Research Center



Colonel Arlin "ART" Deel is the Development Project Officer and the Army/NASA Program Manager for the Rotorcraft Systems Integration Simulator (RSIS), an advanced R&D simulator to be used for rotorcraft handling qualities research and systems development. He is a Master Army Aviator rated in both fixed- and rotary-wing aircraft with over 4500 flight hours. He has completed three years in his present assignment.

PANELISTS

Commander William D. Jones, USN
Staff, Chief of Naval Air Training (CNATRA)
Corpus Christi, Texas



Commander William D. Jones, USN, has served in Naval Aviation for 24 years. In addition to four tours in Attack Squadrons he has served as training officer for the A7 Fleet Replacement Squadron and commanding officer of an advanced jet training squadron. Currently assigned to the staff of the Chief of Naval Air Training, he has been involved with the acquisition of the 2F129 and 2B37 flight simulators; he is the staff's program manager for VTXTS and is assigned as a member of the VTXTS Source Selection Evaluation Board.

Lieutenant Colonel Dennis L. Cole, USAF
Commander, Detachment 3, 4200 Test and Evaluation Squadron (SAC)
Plattsburgh AFB, New York



Lt Col Cole was commissioned through the Reserve Officer Training Corps in 1965 following graduation from Rensselaer Polytechnic Institute, where he earned a Bachelor of Aeronautical Engineering Degree. After an educational delay to acquire a Master of Science in Management Degree from the same university, he entered active duty in 1967. Upon completion of pilot training, he transitioned to the F-100 Super Sabre and flew 162 combat missions while stationed at Phan Rang AFB, Viet Nam.

In 1979 he assumed command of Det 3, 4200 TES, coordinating the unit's functions of on-site acquisition management of WST modifications, Development Engineering Prototype Site operations, Software Configuration Management, and training program support actions.

SESSION III

Chairman

Lieutenant Colonel Bobby R. Adams
Chief, Aviation Systems
Naval Training Center
Orlando, Florida



Colonel Adams was born on May 10, 1940 in Buford, Georgia, and was educated in the public schools in that city. He majored in Business Administration at North Georgia College and graduated in 1962 with a Bachelor of Science degree, and as a distinguished military graduate of the Reserve Officers Training Corps received a commission as a second lieutenant in the Regular Army.

In June 1962, he entered active military service and was assigned as platoon leader of Echo Company, First Airborne Battlegroup 503d Infantry at Fort Bragg, North Carolina. From June 1962 to February 1964, Colonel Adams attended the Infantry Officers Basic Course, Airborne and Ranger Schools and served as Battle Group S-1. He attended the Officers Fixed Wing Aviators Course in 1964 and was assigned to Darmstadt, Germany.

Colonel Adams returned to the United States in 1966 and attended the Rotary Wing Qualification Course at Fort Rucker, Alabama.

From April 1966 to April 1967, Colonel Adams served in the Republic of South Vietnam as a scout pilot, Rifle Company Commander, and Aide-de-Camp in the First Cavalry Division.

Colonel Adams attended the Project Managers Course at the Defense Systems Management College in 1979 and assumed his current duties in February 1980.

His military decorations include the Distinguished Flying Cross with one Oak Leaf Cluster, Bronze Star with two Oak Leaf Clusters, Meritorious Service Medal, Air Medal with nine Oak Leaf Clusters, Army Commendation Medal with two Oak Leaf Clusters, and Vietnamese Gallantry Cross with Silver Star.

TURNKEY CAD/CAM SYSTEMS
IN
CIG DATA BASE CREATION



John L. "Jack" Booker
Acquisition Director and
Principal Investigator
Naval Training Equipment Center
Computer Systems Laboratory
Orlando, Florida

John L. Booker is Acquisition Director and Principal Investigator on Tasks 8741, "Low Level CIG for Trainers" and 8743, "Area of Interest CIG" for the NAVTRAEQUIPCEN Computer Systems Laboratory, Code N-74, Orlando, Florida. He served as project engineer for the Aviation Wide Angle Visual System (AWAVS) CIG system procurement with General Electric Co. which was delivered in 1978. He has been active in computer graphics since 1967 and has served as project engineer on a number of other computer graphics system procurements in the laboratory including an IDIOM and E&S LDS-1. He received the Master of Engineering degree from the University of Florida in 1967, BSEE from N.C. State University in 1961 and AB degree in Journalism from the University of North Carolina in 1953. Mr. Booker is a member of Tau Beta Pi, Eta Kappa Nu, Sigma Xi, IEEE Computer Society, SIGGRAPH and the ACM.



Sam T. Giambarberee
Programmer/Analyst
Naval Training Equipment Center

Sam T. Giambarberee obtained his B.S. in Computer Science from the University of Central Florida and is currently working on his M.S. degree. His three years of experience in computer graphics involves data base creation techniques of various 3D models. His work requires use of the Applicon 3D graphics computer and the Movie BYU software package implemented on a VAX 11/780.

TURNKEY CAD/CAM SYSTEMS IN CIG DATA BASE CREATION

ABSTRACT

The Naval Training Equipment Center experience in use of a Turnkey Computer Aided Design/Computer Aided Manufacturing (CAD/CAM) System interfaced to a widely available 3-dimensional image rendering software package provides effective interactive graphics input, creation, modification and control of CIG visual data bases. The system in use provides many interactive features. It can produce calligraphic vector drawings and/or continuous tone raster images on TV video tape or photographic output devices.

INTRODUCTION

The Computer Aided Design/Computer Aided Manufacturing (CAD/CAM) segment of the computer graphics industry has seen continuous growth during the last 10 years. There are a large number of turnkey CAD/CAM systems commercially available which provide interactive features for creating two-dimensional (2D) and/or three dimensional (3D) drawings and data bases. One characteristic all of these systems have in common are highly developed man-machine interfaces which provide visual feedback tightly coupled to various interactive I/O devices. Most of the turnkey CAD/CAM software packages represent hundreds of manhours of graphic programming and human engineering design.

Another characteristic most of the turnkey systems share in common is that line drawings or vector drawings are supported rather than continuous tone polygons and polyhedra usually associated with computer generated imagery (CGI or CIG) systems. There are numerous 2D CAD/CAM systems commercially available which support applications in schematic drawings, circuit board design, and graphic arts. There are not so many which support 3D applications and these are considered top-of-the-line systems by many people.

During the early days of computer graphics development, several centers of excellence developed in the university community. One of these, which was responsible for numerous landmark publications, was the graphics group in the Computer Science Department of the University of Utah under Ivan Sutherland and David Evans. The graphics software developed at Utah represented the latest in rendering and hidden line algorithm development and was a significant resource for Utah graduates as they migrated to other Universities and set up other graphics groups.

Many of the good features of the graphics software developed at the University of Utah have been incorporated into a software package called Movie BYU distributed by Hank Christiansen of the Civil Engineering Department of Brigham Young University (BYU). During the years when the graphics software was being developed at the University of Utah, Dr. Christiansen was serving as a consultant at the University of Utah in structural engineering with the Computer Science graphics group. He originally developed Movie BYU as a finite element analysis system for structural design.

The Movie BYU software package is available from BYU for a distribution fee of \$300 and has been installed on a number of different computers. The development of Movie BYU has been sponsored by a number of government agencies and commercial sponsors.

During the summer of 1978, it occurred to members of the graphics group of the Naval Training Equipment Center (NAVTRAEQUIPCEN) Computer Systems Laboratory (Code N-74) that the power and flexibility of an existing CAD/CAM system in generating, manipulating and modifying 3D drawings and data combined with the power of the Movie BYU display and rendering software could provide an excellent starting point for developing an in-house, non-real-time Computer Image Generation (CIG) system capable of producing high detailed/high visual quality images for training simulation applications. Movie BYU was installed on the in-house computer system, a VAX 11/780, and an existing CAD/CAM system used to interactively create and modify 3D data. The body of this paper, then, describes the system which has evolved in the laboratory.

BODY

The Naval Training Equipment Center (NAVTRAEQUIPCEN) Computer Systems Laboratory (Code N-74) has had a turnkey CAD/CAM system in operation in-house since the summer of 1978 when an Applicon AGS 835 Graphics System was delivered by General Electric Company as part of the Aviation Wide Angle Visual System (AWAVS) Computer ImageGeneration (CIG) System as part of the Off-Line Data Base Creation Facility which was described in a paper presented at the 1977 Image Conference at Williams AFB.⁽¹⁾ This system has been used to develop and maintain 3D drawings of objects used in creation of the visual environments and 3D data bases used by the real-time CIG system.

The Applicon AGS 835 is shown schematically in Figure 1. It consists of a main processor cabinet containing a minicomputer and display processor, and a user terminal consisting of a storage scope and interactive I/O devices. The main processor cabinet contains a general purpose minicomputer (DEC PDP 11/04) which maintains the graphic data base, services interactive I/O device interrupts, and generates a list of graphic processor display generation instructions for the custom Applicon display processors. The user terminal consists of a local vector generator and Tektronix storage scope display terminal, alphanumeric keyboard, a small x, y digitizing tablet, a large 34x44 inch digitizing table for direct input from maps and large size drawings, and a set of 64 discrete programmable function button switches for graphic subroutining.

The standard Applicon 3D AGS 880 operating system is used to provide interactive display control, image manipulation, picture component additions/deletions, and modifications. Data is input via the terminal keyboard, programmable function buttons and/or the digitizer tablet. Not all of the AGS 880 features are required for our CIG application. Some of the capabilities in use are the image viewing transformations, working grid accuracy for inputs, the teach mode functions, macro capabilities, and standard I/O output format. Some of the Applicon AGS 880 features used by Code N-74 for manipulation and control of 3D images in CIG data base development are described in following paragraphs.

The large and small digitizer tablets provide input of point data to the graphic data base by use of working grids which provide accuracy in each axis to one part in 16,777,215. The terminal operator when working in 3D usually works in two orthogonal views either front-top or front-right side views. Front-right, for example, will allow x and y to be specified in the front view or z and y in the right hand view. A deep plane for z can be specified in the right hand view which will remain static until changed and allows multiple

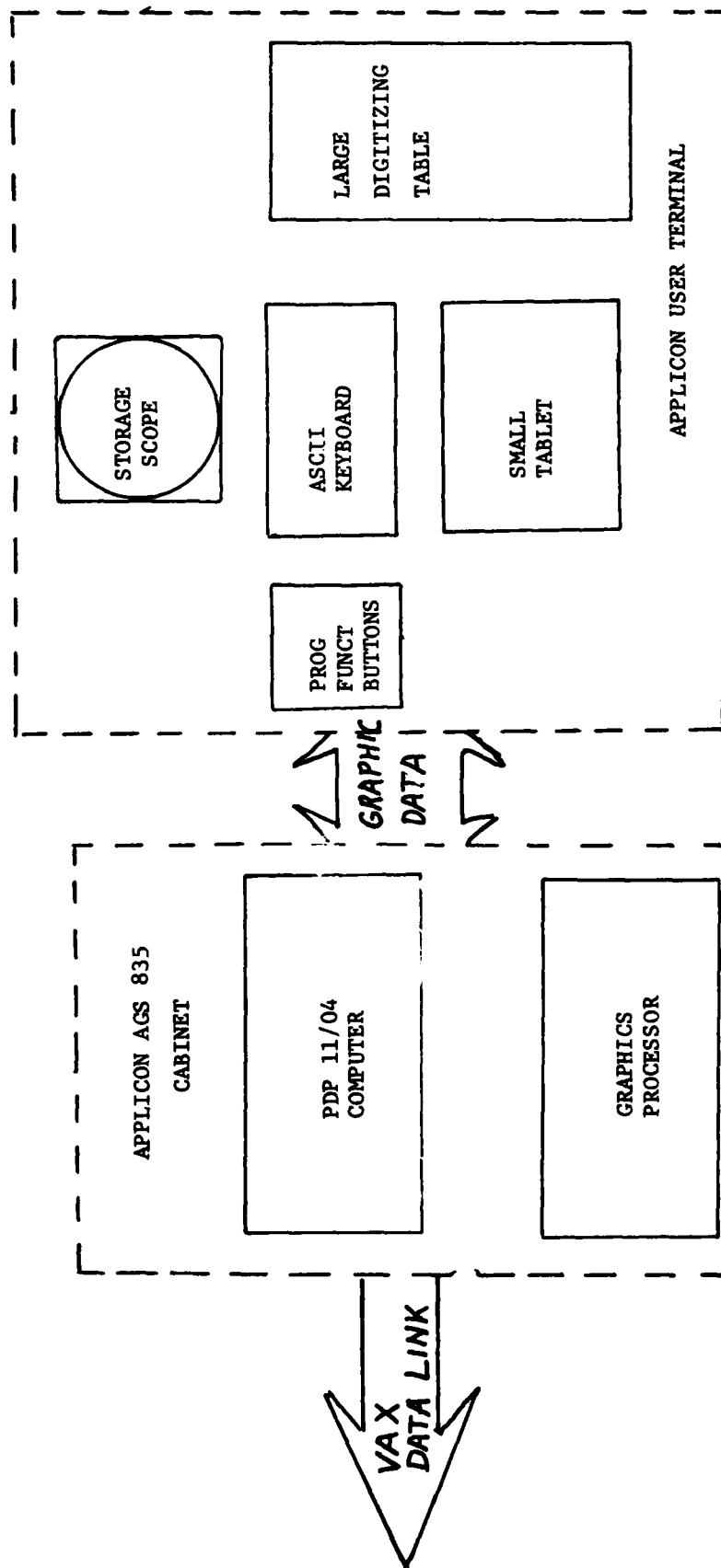


Figure 1

points to be input from the front view with the same z. Likewise, a deep plane in the front view provides a constant x value for y, z points entered in the right hand view.

Up to four views may be viewed simultaneously, with front, right, top and isometric views being a typical four window format. Isometric, dimetric, axiometric, and true perspective projections from any viewing location may be specified and generated in addition to standard orthogonal views. Most CIG applications require either two window or four window formats of the primary orthogonal views and/or isometric views. Drawings may be edited and modified in isometric as well as in front, top and side views.

An unusual feature of the Applicon system is use of character recognition software in conjunction with the digitizer input stylus. A teach mode is provided in which the operator may literally teach the software his individual handwriting. The teach mode allows customized symbols to be defined for each of the AGS 880 interactive graphic functions which are then entered into a custom dictionary for each operator. The teach mode also allows macro definition of sequences of AGS 880 commands to be defined symbolically for references by the keyboard or programmable function buttons and graphically for reference by the digitizer stylus.

One of the main NAVTRAEQUIPCEN Code N74 CIG data base applications has been to edit and modify 3D CIG data bases produced by GE for the Visual Technology Research Simulator (VTRS) and AWAVS CIG system. The GE data bases are entered into the Applicon from card format listings of vertexes, faces and object models using symbolic labels. A group of Applicon macros were developed which allow the GE data bases to be entered via the keyboard and yet retain the GE label information in the internal Applicon data base.

An Applicon drawing is put together from component libraries on disk memory of the computer. The library is a user-created collection of all the basic graphic components that will appear on the final drawing. A component can be any graphic entity, simple or complex, composed of arbitrary 3D lines and dimensions. In the CIG application the components are forced to be constructed in an orderly manner such that the end result is a closed polygon, or face, that can be manipulated in a desired fashion.

The Applicon provides 15 Save Bins that can be used to save any part of a drawing. In the CIG application, bins 1 and 2 are set aside for construction of the drawing (3D data base). Bin 1 contains the current composite object being constructed from multiple faces. Bin 2 contains the current composite drawing constructed from multiple objects.

When coordinate data is entered into the Applicon data base, heavy use is made of the Applicon's Setpoint facility which provides graphical calculations, graphical constructs and allows symbolic assignments to graphical entities. Vertexes may be referenced graphically and symbolically as V_1, V_2, \dots etc., faces FACE1, FACE2, FACE3,etc., where each face is made up of V_1 thru V_n in a connected sequence. In the GE data base, faces are composed of closed n vectors connected in clockwise order.

The Applicon macros allow easy input of the GE CIG data base entities, vertexes, edges, faces, objects, and models. Original data input is via the terminal keyboard and programmable function button invocation of the input

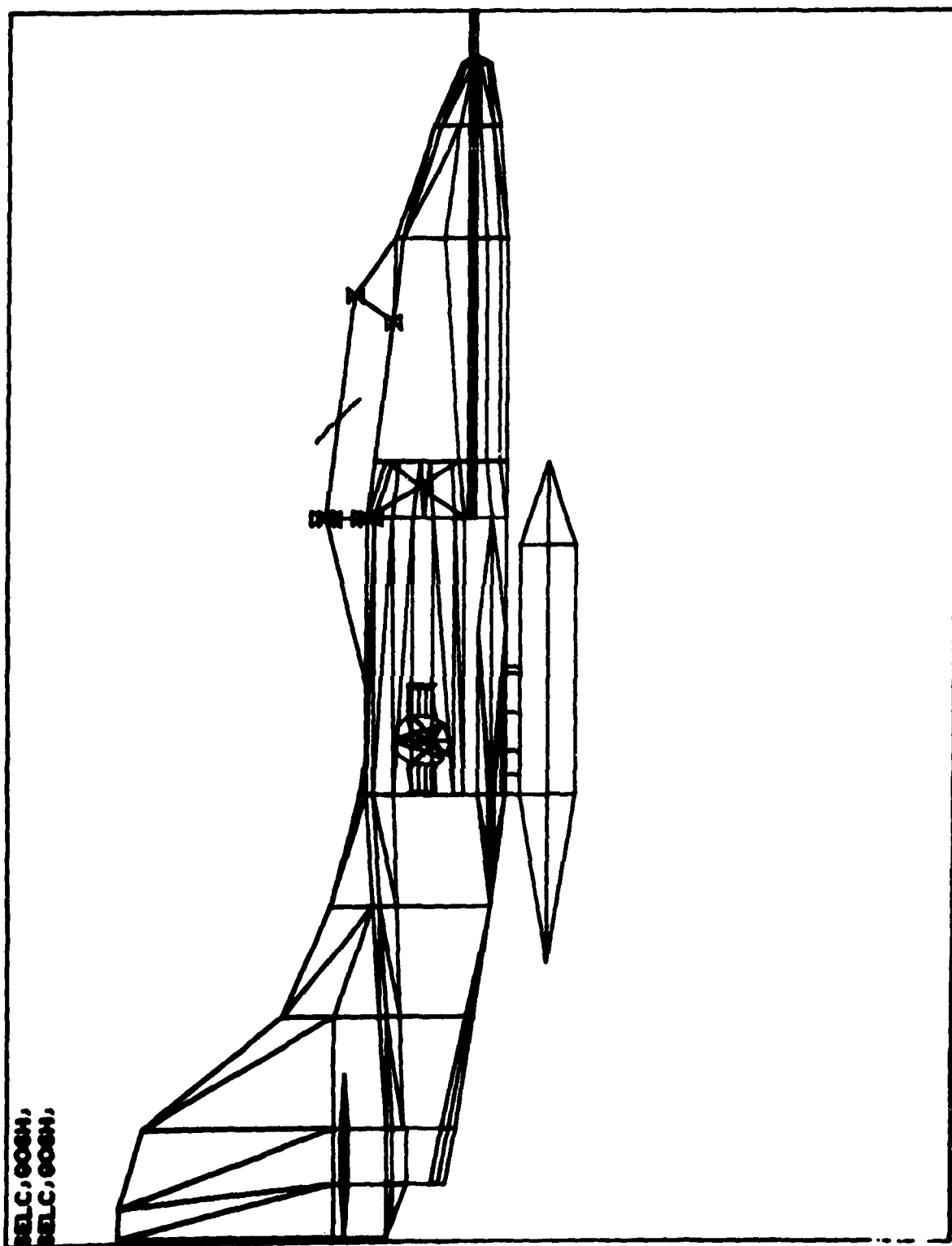


Figure 2

NO. OF SELECTED COMPONENTS: 6
 NAME: P1
 TYPE: POLYARC
 PATTERN SEGMENT SIZE: 0.001 NUMBER OF SEGMENTS: 1

PATTERN: ———

ARROWHEAD PLACEMENT: NEITHER END
 LINE HEIGHT: 1

LEVELS: 1			
VERTICES	X	Y	Z
1	8.000	-0.375	3.500
2	16.000	-0.375	2.500
DISTANCE: 8.062			
3	15.000	-1.125	1.125
4	8.000	-1.125	2.000
5	8.000	-0.375	3.500

DATA KEYWORD: 041000 - GRUP: TACR08

Figure 3

SELE TACHOS.GOSH,
SELE TACHOS.GOSH,

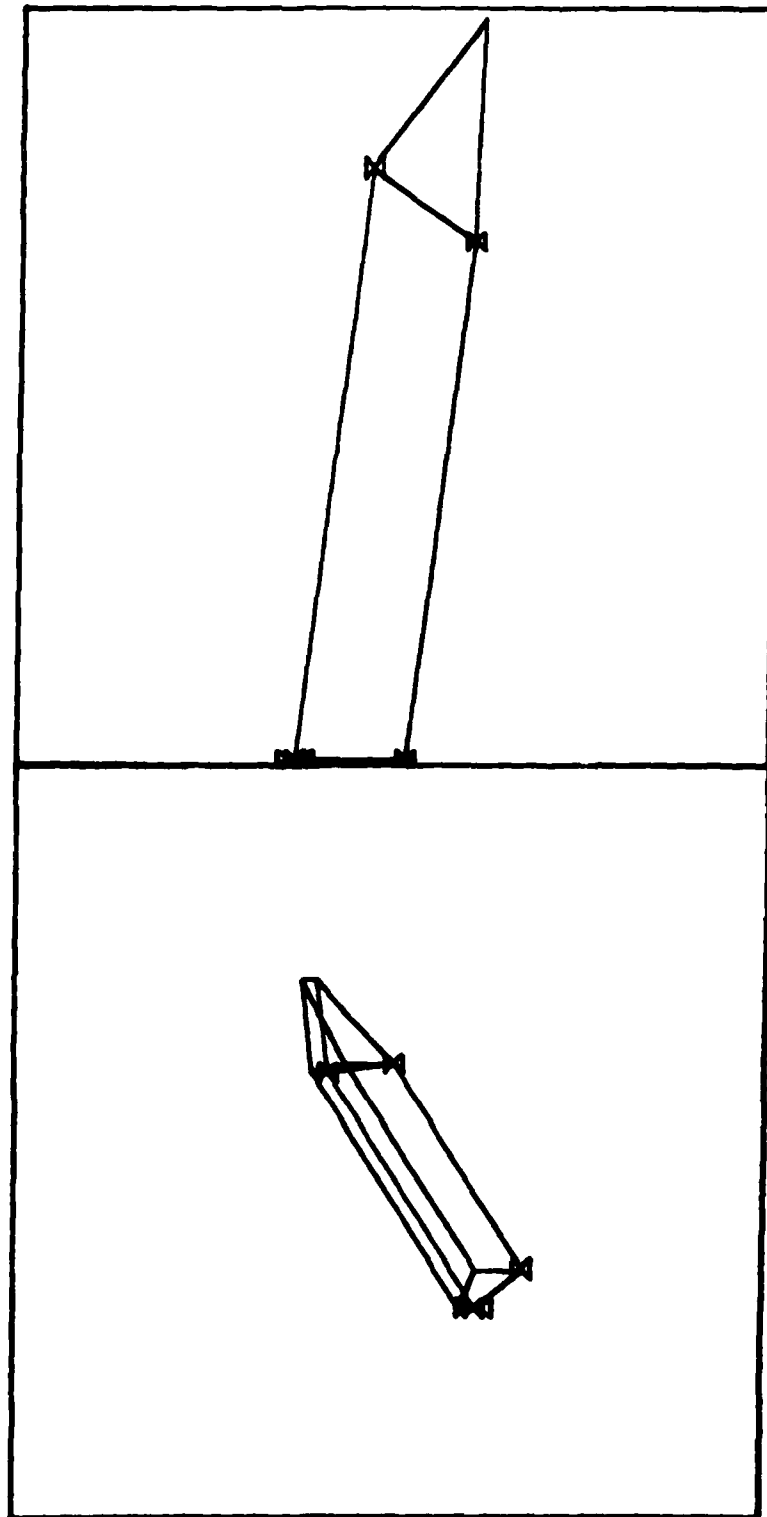


Figure 4

macros. Graphic image feedback is provided on the storage scope display and often shows up inconsistencies in operator input. The programmable function buttons provide flexible control of the input sequence.

Once a CIG data base has been entered into the Applicon data base as a drawing, any vertex, edge, face, or object may be selected by the stylus on the graphic tablet. Since the input procedure has retained the GE symbolic labels originally used on the GE card input format, a symbolic designation for each vertex along with x, y, z coordinate data for each point may be obtained in listing format on the display. This is shown in figures 2, 3 and 4 where a front view of a TA4J is shown in figure 2 with an edge selected. The edge relates to a face which is designated by select "butterflies" in figure 2. One face containing the edge is identified as TACA08 for which a listing of the vertexes making up the face is shown in figure 3. Once a single face is symbolically identified, each face in the group may be selected and the coordinate data of its vertexes listed. For instance, the faces of object TACA labeled TACA01 thru TACA08 may be individually listed on the display monitor. Objects such as object TACA may be isolated and displayed separately as in figure 4.

Once the object is selected, it can be changed and all of the new information displayed. Documentation can then be updated to the new values provided in the listing output. Automation of the update process is the next step and will be initiated this fiscal year in the laboratory.

Applicon drawings may be output in hard copy picture form on a Tektronix thermal printer or on a Calcomp Model 1060 high speed, 64 inch, multi-color, drum plotter. Another nice feature of Applicon data bases is that a standard digital I/O format specification IO 121 will convert an Applicon drawing into an ASCII disk file which can be run over a communication link or magnetic tape to the Code N-74 in-house VAX 11/780 computer.

Movie BYU was installed on the Code N-74 VAX 11/780 during the summer of 1978. The software package was well documented and contained a section describing interface procedures for various types of graphic peripheral devices called "Device." The Movie BYU package was installed on the VAX/VMS operating system and test pictures being generated on a Dicomed D47 image recorder within a month after receipt of the Movie BYU magnetic tape.

Movie BYU is a collection of FORTRAN programs which may be used for display and manipulation of data representing mathematical, architectural, and topological models whose geometry may be described in terms of panel (n-sided polygons) and solid elements, or contour lines. The program modules are entitled DISPLAY, UTILITY, SECTION, TITLE, MOSAIC and UPDATE. The six programs display the data as either line drawings or continuous-tone images, modify it, clip and cap it, generate title or geometric model files, convert contour definitions into polygonal element mosaics, or update old geometry files.

The DISPLAY module is the heart of the system and supplies most of the capabilities utilized in the CIG display application developed by Code N-74. DISPLAY is organized into three sub-modules, COMMAND, HIDDEN and DEVICE which supply interactive commands, hidden line or hidden surface algorithm options, and output display options.

The interactive command processor, COMMAND, provides some 36 commands. The number and type of output device, translation and rotation of both global and local rigid body axis systems, color and shading rules, uniform, linearly varying, matching at boundaries, highlights, hidden line, hidden surface algorithms ("poor man's" or Watkins'), vector or scalar function for displacements or stresses, contour generation, surface patches, and animation features are all options which are provided.

The HIDDEN processor provides hidden line algorithm options for line drawing or vector output formatted display devices or hidden surface options for continuous tone raster formatted photographic or TV video output. The "poor man's" hidden surface algorithm eliminates all back facing polygons and effectively cuts the problem size in half. The other option is the scanline hidden line/surface algorithm developed at the University of Utah by Gary Watkins or "Watkins'" algorithm. It is a completely rigorous scanline algorithm which takes advantage of line-to-line coherence of images.

The DEVICE module allows selection of the output format for which a display is to be generated. The Code N-74 configuration of I/O devices available on the VAX 11/780 consists of a Tektronix 4014 storage scope display which accepts vector format display, and a Dicomed D47 color image recorder high resolution raster format 4096 lines by 4096 pixels per line. The continuous tone raster format allows shading to be calculated by one of three rules. The shading may be uniform over the element, may vary linearly over the element or may vary linearly with shading matched at the element boundaries (i.e., smooth surface simulation).

During the spring of 1979, the use of the Applicon in CIG data base update and modification mode, and availability of ASCII files containing the Applicon data base drawing description, coupled with a working Movie BYU package with flexible I/O options begged for development of a translation program which would allow combining the power of both systems for use in CIG data base development. A translator program which accepted the Applicon "Apple I/O" ASCII drawing file as input and converted it to the input format for Movie BYU data bases. This program was installed and operational on the VAX 11/780 by early summer 1974 and pictures of a GE CIG data base installed on the Applicon were being converted and displayed on the Dicomed by the Movie BYU program.

An interesting capability provided by the combined Applicon data base and Movie BYU display options which is not provided by the turnkey CAD/CAM system is the ability to display vector drawings on the Tektronix 4014 storage scope with hidden lines removed. The Applicon alone cannot do this. Figure 5 shows an isometric drawing of the GE CIG data base of a TA4J aircraft without hidden lines removed. Figure 6 shows the same isometric drawing with hidden lines removed by the Movie BYU Watkins' hidden line algorithm. Finally, figure 7 shows a shaded image with uniform shading over each surface generated on the Dicomed D47 camera station.

SUMMARY AND CONCLUSIONS

The NAVTRAEQUIPCEN Computer Systems Lab has had a turnkey CAD/CAM system in operation since 1978 which has been used to develop and maintain 3D drawings (i.e., data bases) of objects used in creation of CIG data bases.

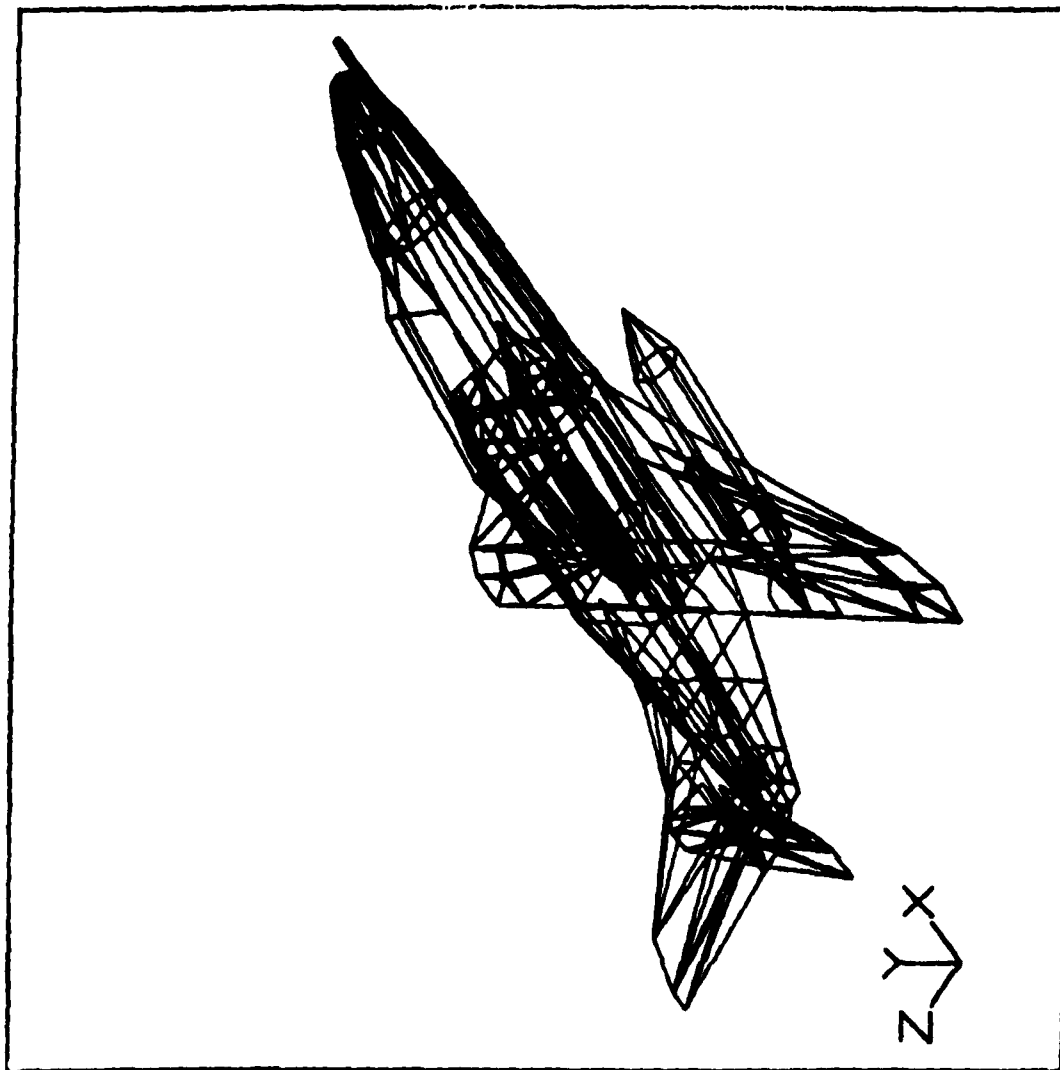


Figure 5

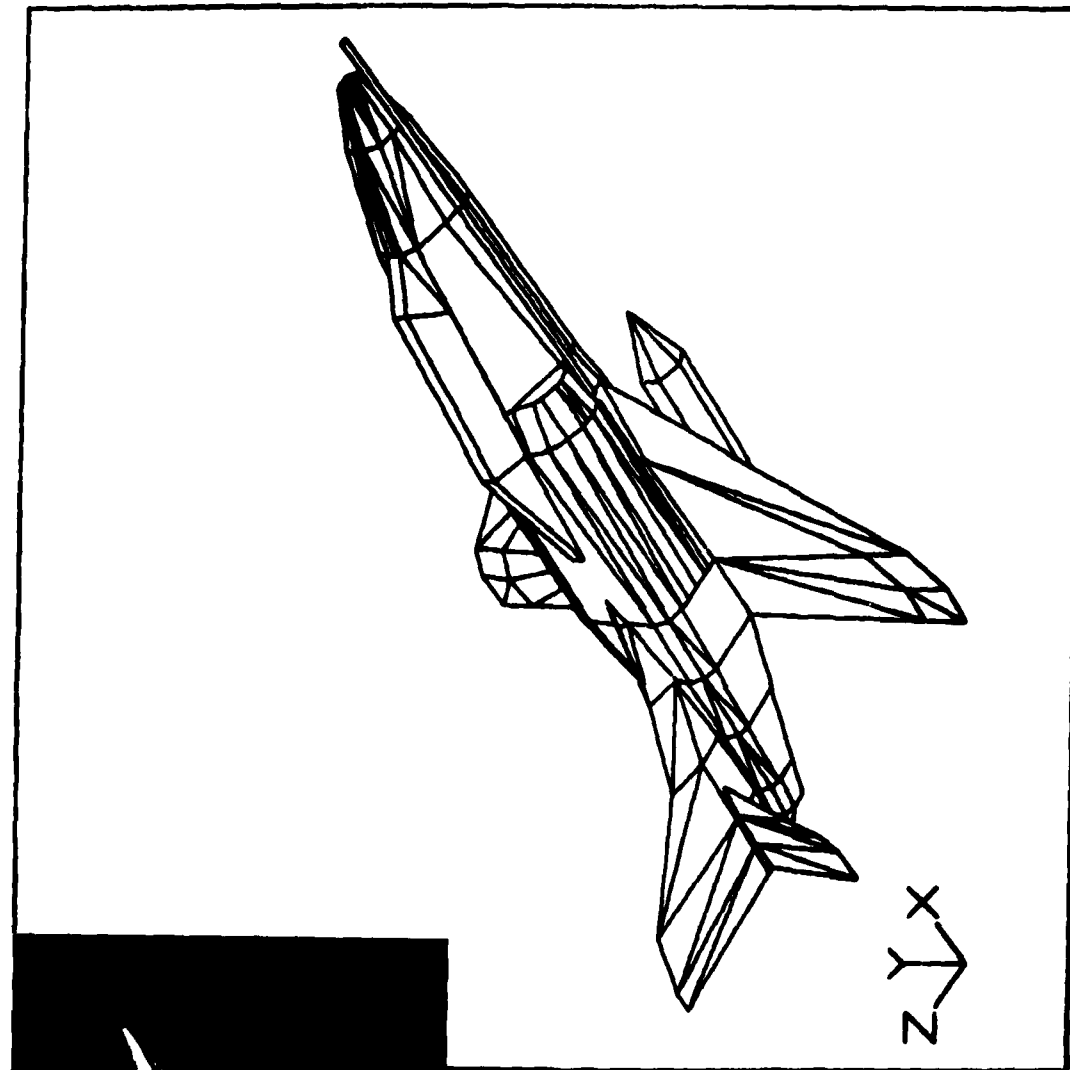


Figure 6



Figure 7

This turnkey CAD/CAM system is a minimal configuration Applicon AGS 835 Graphics System which was supplied as part of the AWAVS Off-line Data Base Development Facility Subsystem.

The standard Applicon 3D AGS 880 operating system is used to provide interactive display control, image manipulation and picture component additions, deletion and modifications. Data is input via a terminal keyboard, programmable function buttons and/or digitizer tablet. A group of Applicon macros were developed in-house to aid data input from standard CIG data base format. The symbols and mnemonics contained in the data base listings are maintained internally in the Applicon data base. These can then be interrogated and retrieved at any time on the Applicon display terminal.

Once a CIG data base has been input as a drawing on the Applicon system, it can be viewed on the storage scope display, manipulated, augmented or modified using the interactive features provided by the AGS 880 3D graphic operating system. Changes to an existing drawing may be listed and retrieved on the display in symbolic form. The x, y, z coordinates for any vertex may be retrieved with its associated symbolic tag. Changed coordinates are then entered into the CIG data base source file with the VAX/VMS editor software.

Output from the Applicon may be obtained in picture form from a Tektronix thermal printer or in "Apple I/O" format on a nine-track magnetic tape unit. All Applicon drawings are in 3D vector format with no hidden line removal. Other display formats may be obtained by transferring Apple I/O data on the magnetic tape to the VAX 11/780 for further processing.

A transformation program was developed to accept "Apple I/O" formatted data as input and produce outputs compatible with the input formats required by a 3D rendering software package on the VAX 11/780. This rendering package is part of a larger system of programs called Movie BYU which was installed on the Code N-74 VAX 11/780 during the summer of 1979. The current rendering software uses the January 1980 version of Movie BYU.

Movie BYU is available from Brigham Young University for a distribution fee of \$300 and has been installed on a number of different computers. The development of Movie BYU has been sponsored by a number of government agencies including ARPA, ONR, and NASA at the University of Utah, ERDA at Lawrence Livermore Labs and BYU and the Corps of Engineers at BYU. A number of commercial sponsors were responsible for the most recent January 1980 version.

Once the Applicon data has been transformed into Movie BYU input format, a large number of display options are available on the display equipment within the Computer Systems Laboratory. Output can be obtained on the display in vector form on a Tektronix 4014 storage scope display with hard copy output. Hidden line removal is available using either a "poor man's" hidden surface algorithm which removes back facing polygons or the more accurate, but computationally intensive, Watkins hidden surface algorithm. Continuous tone solid object images may be obtained on a Dicomed D-47 color image recorder in photographic form or in TV video format from an IKONAS Graphics Systems digital image frame buffer.

Our experience has shown that use of standard turnkey CAD/CAM graphics software for interactive control of data base creation and modification processes coupled with a rendering software package such as Movie BYU has

produced a powerful computer generated display facility at nominal development cost. The CAD/CAM software provides interactive features which have evolved through more than a decade of user experience, and represents more than a hundred manyears of software development. Movie BYU represents the distillation of the best of the University of Utah software developed by some of the "giants" of computer graphics during their graduate study years. It provides a powerful and very flexible display rendering capability. The only development effort required in our laboratory has been development of the "Apple I/O" to Movie BYU format translator and the effort to install Movie BYU on the VAX 11/780 computer. Use of existing software rather than custom development from scratch represents a tremendous leverage in the use of programming manpower. The power and flexibility of the resulting synergism probably exceeds what our in-house programming capability could have produced over any reasonable time period.

REFERENCES

- (1) "AVIATION WIDE ANGLE VISUAL SYSTEM (AWAVS) CGI SYSTEM," John L. Booker, Naval Training Equipment Center, Code N-214, in Proceedings of the 1977 Image Conference held at Williams Air Force Base, Arizona 85224, 17-18 May 1977
- (2) "AGS/880 Specification 3D Graphic Operating System," published 1977 by Applicon Incorporated, publication number ai-880-PS-B 77090.
- (3) "GRAPHICS UTAH STYLE - 80," notes for a workshop in Interactive Computer Graphics with Emphasis on the MOVIE System. Hilton Hotel Convention Center, Salt Lake City, Utah, July 28 - August 1, 1980. Presented by Hank Christiansen and Mike Stephenson, authors of MOVIE.

THE SHUTTLE MISSION SIMULATOR VISUAL DATABASES



Thomas H. Henderson is an Aerospace Technologist in the Flight Simulation Division of the NASA Johnson Space Center, Houston, Texas. His twenty-year career has included visual simulation assignments in all of the NASA manned spaceflight programs. Mr. Henderson acquired a BS in physics and a BA in mathematics from the University of Texas in 1961.

Thomas H. Henderson
The NASA Johnson Space Center
Project Engineering, Simulator Development Branch
Houston, Texas

THE SHUTTLE MISSION SIMULATOR VISUAL DATABASES

THOMAS H. HENDERSON
Project Engineering, Simulator Development Branch
The NASA Johnson Space Center
Houston, Texas 77058

ABSTRACT

Three visual databases in the Shuttle Mission Simulator (SMS) are described. These are used in four Digital Image Generation Systems (DIGS) to simulate the visual environment of all phases of the space shuttle mission. Solutions are described for various simulation tasks, including landing sites, visual landing aids, stars, sun glare and payloads.

BACKGROUND

The mission simulators at the NASA Johnson Space Center have been the primary simulators for flight crew training in the NASA manned space programs. The Mercury Procedures Trainer, Gemini Mission Simulator, Command and Lunar Module Simulators, Skylab Simulator, Orbiter Aeroflight Simulator, and now the Shuttle Mission Simulator have all contained high fidelity representations of spacecraft interiors, instruments, and window visual displays. Previous visual displays used starballs, films, and closed circuit television (CCTV) utilizing models or electronically generated images.

The demanding payload simulation requirements of the space shuttle missions precluded the use of models and required innovative new techniques. The SMS contractor, the Singer Company, satisfied these requirements by a company-developed Digital Image Generation System.

INTRODUCTION TO THE SHUTTLE MISSION SIMULATOR VISUAL SYSTEM

The SMS visual system includes four DIGS. The Motion Base Crew Station (MBCS) DIGS simultaneously generates three color real-time scenes. These three views are displayed in any four adjacent windows of the six SMS forward windows according to the SMS operator's selection. An identical DIGS supplies the forward window scenes for the Fixed Base Crew Station (FBCS) (Figure 1). These two forward window DIGS use identical visual databases. The database for each DIGS is stored in a 67 megabyte disc memory unit.

A third DIGS generates the FBCS black and white closed circuit television scenes from Orbiter payload bay and Remote Manipulator System (RMS) arm cameras. These are displayed on two Orbiter onboard TV monitors. Either of the monitors may contain a split-screen view showing the centers of two camera fields-of-views. The SMS does not permit simultaneous split-screen views on both CCTV monitors. Thus, up to three independent views may be generated by the CCTV DIGS. The CCTV database is very different from the forward windows database.

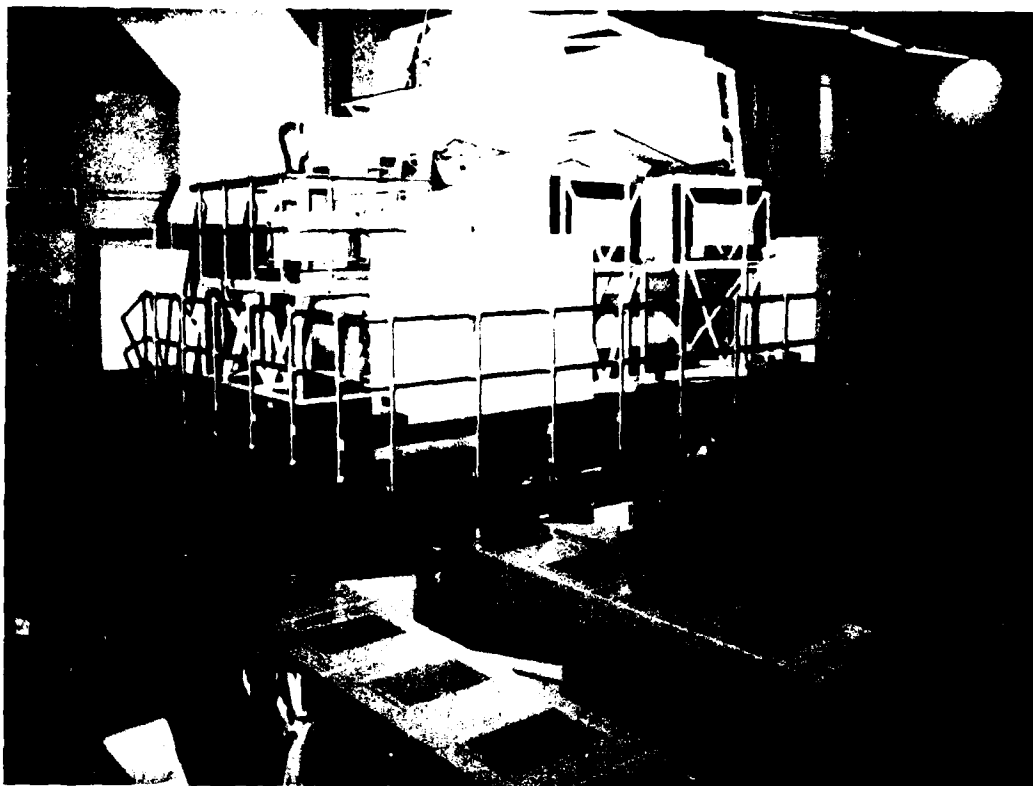


Figure 1. Fixed Base Crew Station, MBCS in background, DIGS in foreground

A fourth DIGS, using a database slightly simpler than that for the CCTV DIGS generates three black and white views for display in the two aft overhead and the two aft payload windows. Two independent views of the payload bay are used when attention is centered there. The third overhead view would then be shared and displayed identically on both overhead windows. But, for example, when the mission task is a rendezvous, the SMS operator would select the overhead windows for independently generated views with the aft windows shared.

This paper will describe the three visual simulation databases used in the forward and CCTV/aft DIGS rather than the SMS DIGS hardware, Interdata 8/32 support computers/peripherals, special visual effects generation hardware, or window display hardware. To give these database descriptions full meaning and to enable a better understanding of the space shuttle missions, some of the simulation requirements, techniques, capabilities, problems and solutions will be given emphasis.

FORWARD WINDOWS DATABASE - EARTH ORBIT SIMULATION

The earth was modeled as a 1620-sided spherical polyhedron in the SMS forward windows database. Each side or face approximates an equilateral triangle with edges averaging 460 nautical miles. DIGS hardware curved surface shading prevents visibility of the triangle edges except at the horizon. The 26 1:5,000,000 scale Global Navigation charts were used to model surface detail with 3,000 polygons (faces) and 19,000 polygon vertices (face boundaries).

Large land areas were modeled with fidelity sufficient for recognition. The level of detail modeled was consistent everywhere. Thus, smaller islands did not have enough detail for recognition. Later, some detail was added to enable identification of candidate contingency landing site terrain.

Limited success was achieved in meeting the goal of realistic presentation of vegetation and global color patterns. The earth's bright saturated colors are pleasing to the eye but appear somewhat cartoonish.

The earth's horizon provides an out-the-window visual pitch and roll attitude reference. Apparent motion of terrain features provide a visual yaw reference. Large cyclonic cloud patterns were modeled to provide a visual yaw reference over the oceans. Four earth databases were compiled differing in amounts of cloud cover:

1. Cloud-free earth
2. Approximately 10% cloud cover - only over oceans
3. Approximately 25% cloud cover - almost all in ocean areas
4. Approximately 50% cloud cover - mostly over the oceans

Configuration 4 (Figure 2) approximates the earth's 50%+ average cloud cover and has been the only configuration used during training sessions. For variety, any of the other earth databases could be assigned.



Figure 2. USA from 1800 nautical miles altitude. Few clouds over land. Extra detail near White Sands for Northrup Strip contingency landing site.

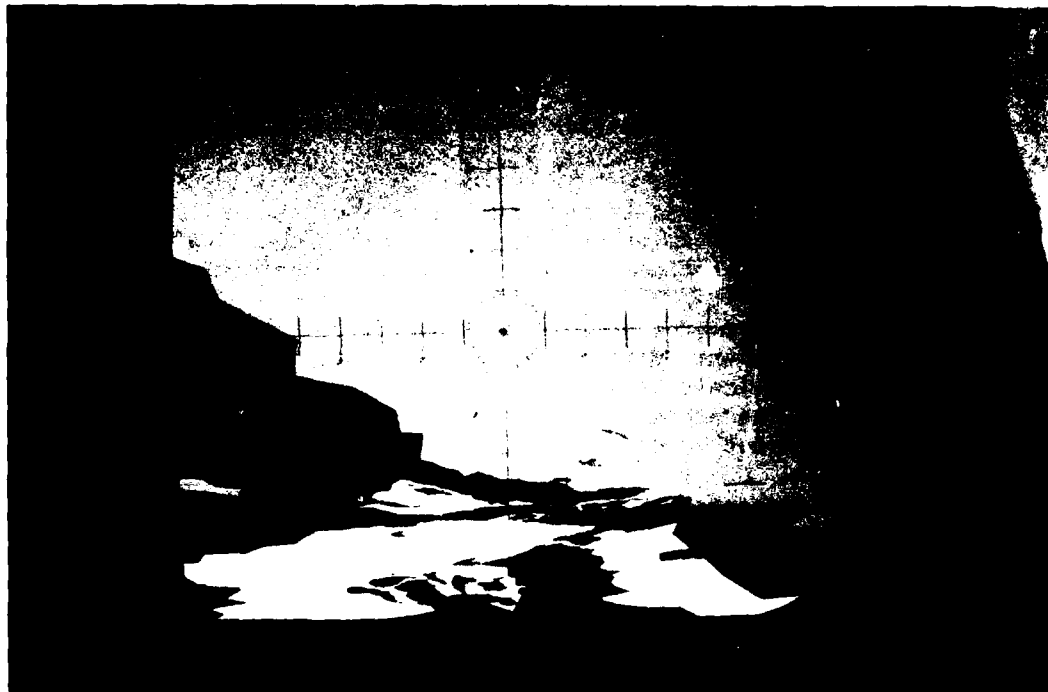


FIGURE 3. Detailed Edwards TAEM/Landing Scene overlies west coast earth scene.



FIGURE 4. Edwards AFB Runway 22

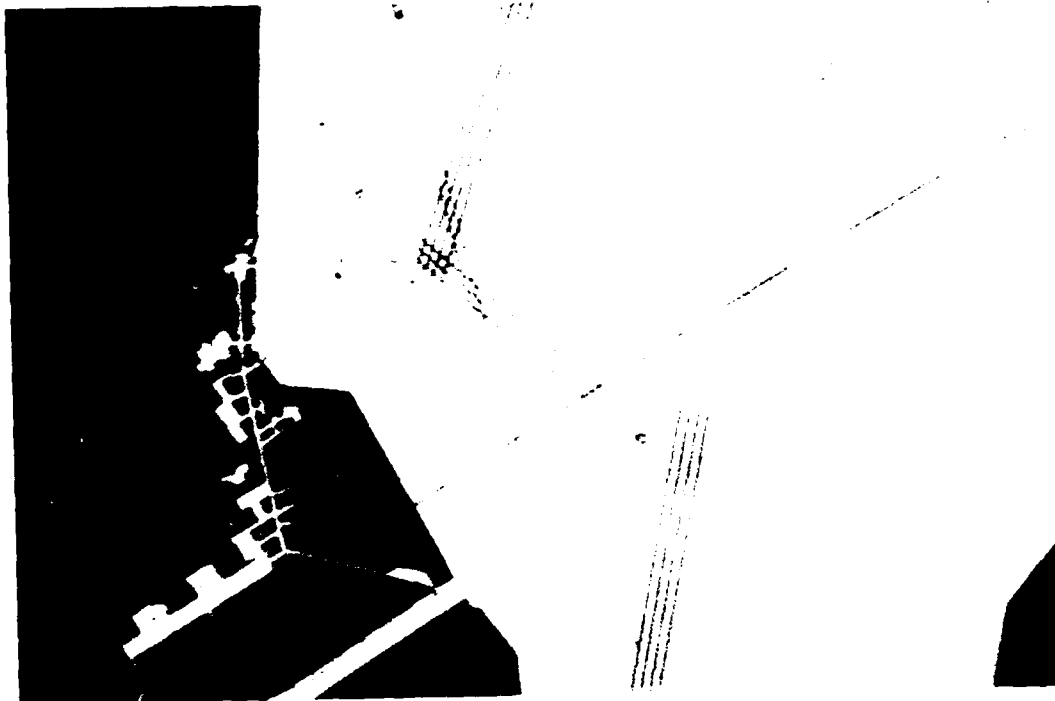


FIGURE 5. Edwards AFB/Rogers Dry Lake from 58,000 feet altitude.

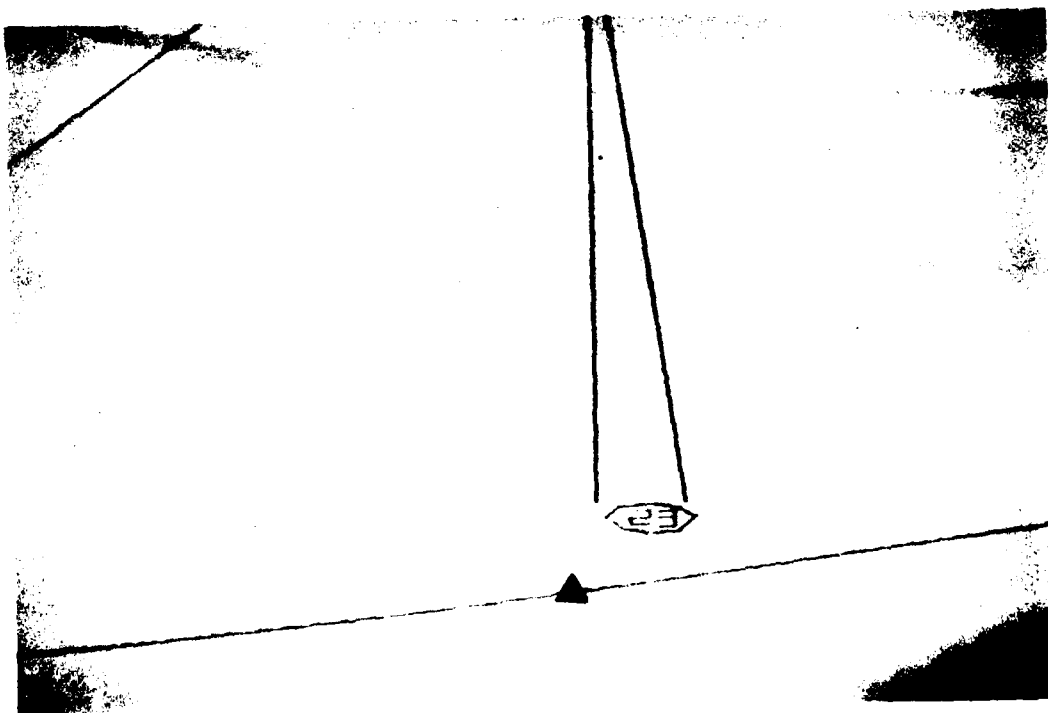


FIGURE 6. RW 23, Outer glide slope triangle. Threshold stripe and touchdown markers (barely resolved).



FIGURE 7. Approach to KSC following a launch abort. 45,000 feet altitude.



FIGURE 8. Launch tower for the Space Shuttle seen from the Orbiter.

FORWARD WINDOWS DATABASE - EDWARDS AIR FORCE BASE LANDING SITE

Edwards Terminal Area Energy Management (TAEM) and approach/landing areas are modeled from 1:250,000 scale maps for the TAEM area to 1:4800 scale maps in the landing area. This database lies on top of the earth model and is accessed under 150,000 feet altitude. The large TAEM area surrounding Edwards Air Force Base measures 276 statute miles north to south and 190 west to east (Figure 3). Experience has shown this to be somewhat larger than needed. The TAEM includes shoreline, lakes, metropolitan areas, major highways, and mountains modeled as a two-dimensional flat surface (2D).

Edwards 15,000 foot concrete runway 4-22 is modeled, (Figure 4) along with all of the Rogers Dry Lake runways (Figure 5). Hangers along the flight line were modeled with the added dimension of height (3D), but other main base and residential areas 2D. Several airports, mines, and other ground features were modeled to provide visual cues during the Orbiter's turn to final approach heading. Seven hills near Edwards Air Force Base were modeled 3D to provide a height cue for a lakebed runway 17 landing.

Centerline stripes, touchdown zone marker rectangles, the energy reference mark rectangle, and the outer glide slope aim point marker triangle are modeled for runway 23, the primary orbital flight test runway (Figure 6). Some of these features are also included on runways 17 and 4-22. Low altitude cues modeled for runway 23 include the microwave scanning beam landing system (MSBLS) vehicle, a fire truck, a NASA truck and tire marks. Runway 4-22 has a 107 face boundary B-52 on the taxiway and includes 3D distance markers for determining landing rollout. The Edwards TAEM/landing scene was modeled using 11,000 face boundaries.

FORWARD WINDOWS DATABASE - KENNEDY SPACE CENTER LANDING SITE

Following delivery of the SMS, a relatively high-fidelity 8800 face boundary DIG model of the Kennedy Space Center (KSC) area (Figure 7) was added by Singer Link SIMCOM, the SMS support contractor at the NASA JSC.

A similar modeling philosophy was used. All KSC landings will use runway 15-33, constructed for the space shuttle program. KSC landings are planned in the early flight test missions only in the event of Return of Launch Site (RTLS) aborts. In later operational space shuttle missions KSC will be a primary landing site. Two structures are modeled 3D, the 524 feet tall Vehicle Assembly Building (VAB) and the launch tower on KSC 39A (Figure 8).

FORWARD WINDOWS DATABASE - CONTINGENCY LANDING SITES

The space shuttle contingency landing sites simulation initially used the Edwards or KSC scene under 150,000 feet altitude. The Edwards or KSC scene was rotated in azimuth to align RW 4, 22, or 17 as appropriate with the heading of the selected contingency landing site runway. Later the transition altitude to the Edwards scene was reduced to 45,000 feet to allow use of approach cues modeled in the earth orbit scene. This simulation was still somewhat unsatisfactory. Flight operations

training personnel requested that the runway pattern be discernable above 45,000 feet to aid approach maneuvers. Also, the switchover to the Edwards scene, was somewhat disconcerting to the flight crewmen.

The solution chosen was to model a simple landing database for each of the four current contingency landing sites: Northrup Strip, New Mexico; Rota Naval Station, Spain; Kadina Air Base, Okinawa; and Hickam Air Force Base/Honolulu International Airport, Hawaii.

Detail is concentrated in the runway area. A minimum of detail is provided elsewhere - only enough to establish site recognition, runway identification, and approach cues. The first of these, Northrup Strip (Figure 9), required only 600 face boundaries to model the scene.

Northrup Strip would become the primary landing site if the Rogers Dry Lake were wet. Rota Naval Station, Spain, might be used following a launch abort initiated just prior to the planned orbital insertion.

FORWARD WINDOWS DATABASE - VISUAL LANDING AIDS

Precision Approach Path Indicator (PAPI) lights were approved in October 1980 for the space shuttle program. They provide a backup visual indication on the ground of the outer glide slope approach flight path angle. Following the Orbiter's turn to final approach heading this angle is nominally 20 degrees until the preflare pitchup maneuver to the 1.5 degree inner glide slope is begun at 1750 feet altitude.

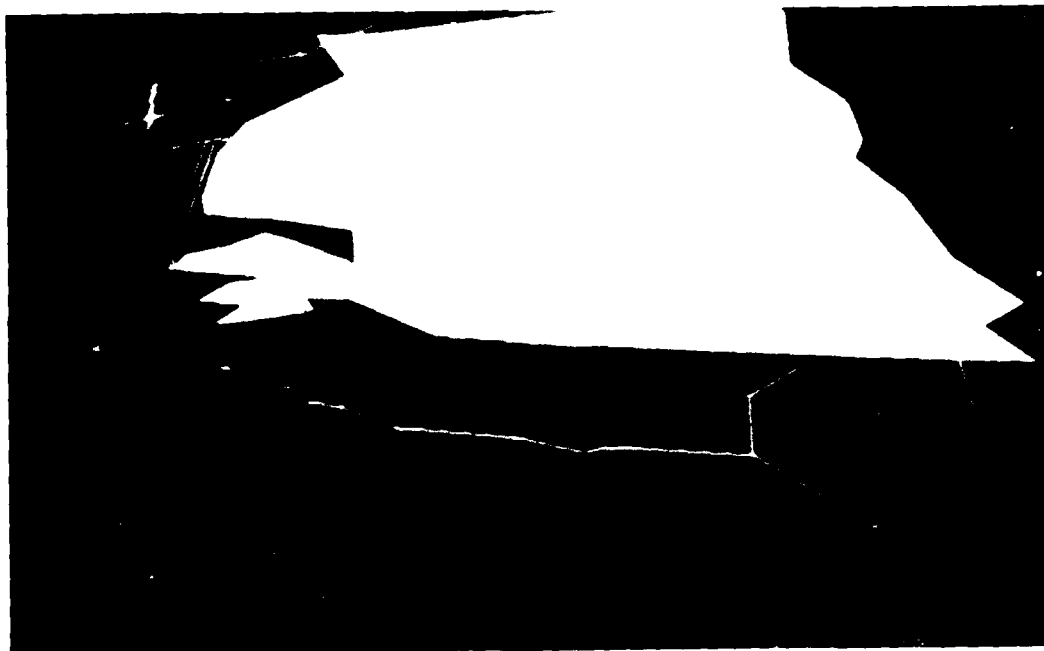


Figure 9. White Sands, Holloman AFB, (Northrup Strip runways unresolved)

PAPI's are similar to Visual Approach Slope Indicator (VASI) lights. Four PAPI lights, spaced 25 feet apart are placed 6500 feet short of the runway threshold at the outer glide slope aim point. These white over red lights give indications of 17, 19, 21, and 23 degree glide slope respectively. The nominal 20 degree glide slope can be kept accurate within one degree by maintaining the proper combination of two red and two white lights. Accurate control of glide slope is a necessity since the Orbiter's landing approach cannot be aborted. Nine PAPI systems are scheduled: two for KSC, four for Northrup Strip, and three for Edwards.

At this writing, preliminary work is being done to develop a PAPI light simulation approach.

SIMULATION OF SPACE VEHICLES IN THE FORWARD WINDOWS DATABASE

The forward window DIGS is capable of simultaneously showing any two other moving space vehicles. A simple 112 face boundary model of the Shuttle External Tank is the only vehicle modeled thus far that has been used in training sessions. The External Tank is not seen while attached to the Orbiter, nor during a normal tank release sequence. However, a roll maneuver could provide a side window view of the External Tank, to verify adequate separation.

Space vehicles that need to be seen from the forward windows will be modeled for the forward DIGS. It is a simple operation to convert aft database vehicles modeled in units of 1/32 inch to forward window database using units of 1/32 foot. Both the Inertial Upper Stage (IUS) and the Spinning Solid Upper Stage (SSUS) vehicles will need to be seen from the forward windows. The Remote Manipulator System (RMS) arms will not be simulated in the forward windows.

STAR SIMULATION

Stars are simulated in the forward windows and in the two overhead window displays. These enhance simulation realism, provide attitude motion cues and enable backup navigation training using a forward or an overhead window.

One thousand seventy-nine stars are included in the star database simulating 87 constellations. These include all but twelve stars listed in the American Ephemeris and Nautical Almanac, which range between - 1.6 to + 4.7 magnitude. Thirteen dimmer stars down to 5.6 magnitude were added to the constellations of Ursa Minor, Grus, Corona Australis, and Crater to make them more identifiable.

The SMS stars look very realistic and have received excellent crew acceptance. The constellations can easily be identified even though they fall short of the full stellar brightness range. The forward window stars are projected using only the green guns of the color

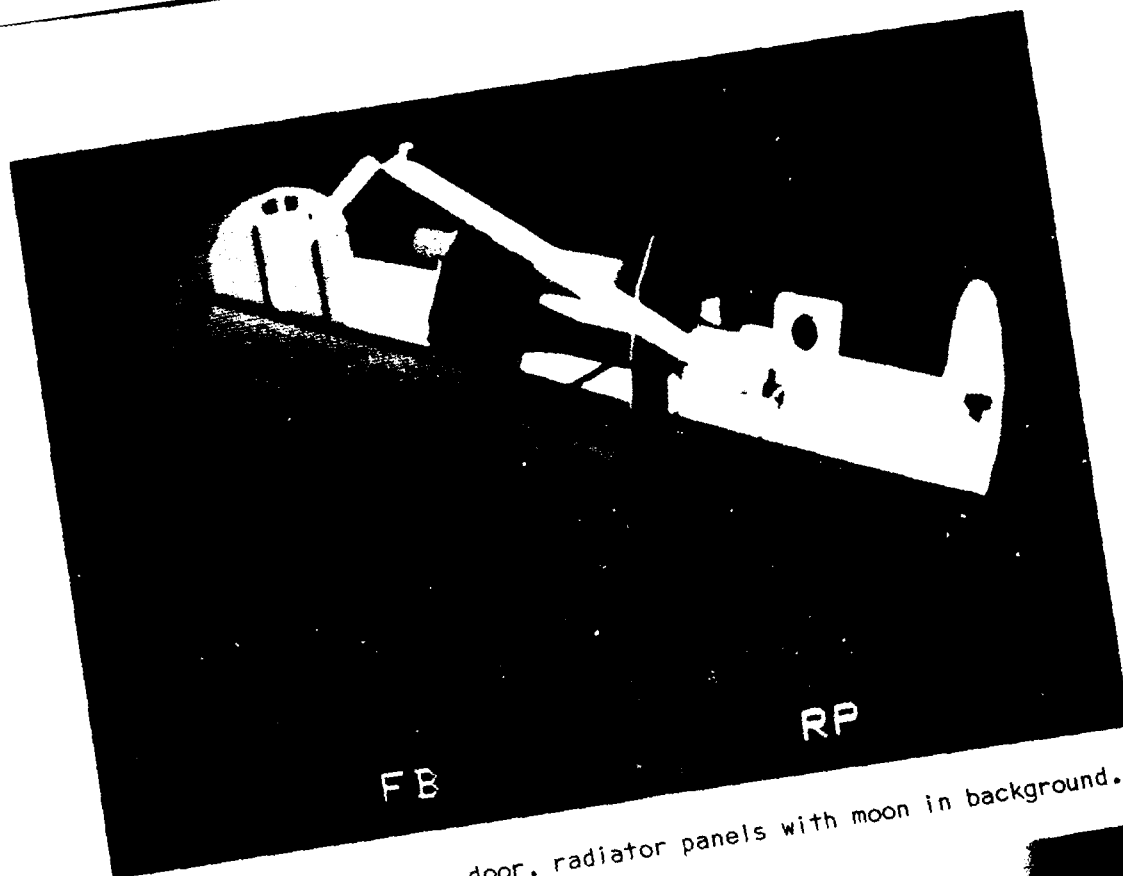


FIGURE 10. Payload bay, door, radiator panels with moon in background.

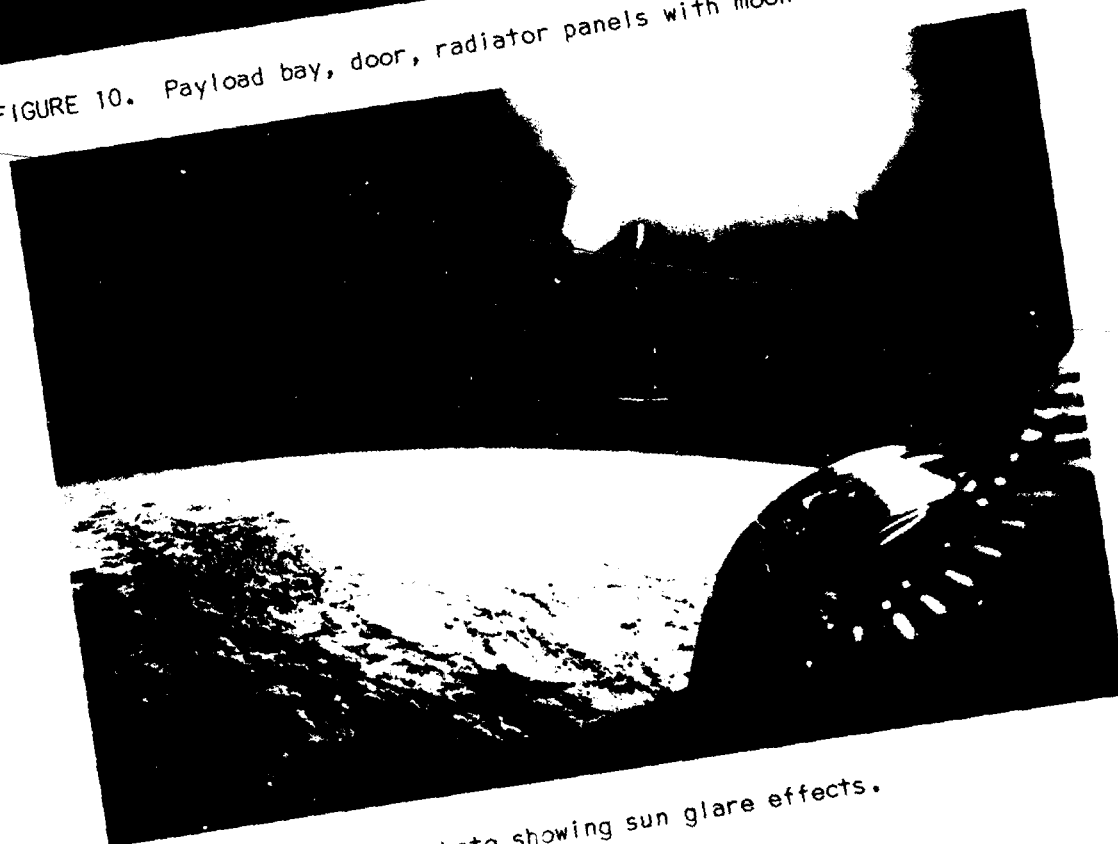


FIGURE 11. Gemini 10 photo showing sun glare effects.

CRT's. The stars do not appear green, however, because of their small size and low brightness.

A recurring problem in the forward window displays has been the variance of star brightness from one day to another. Often the dimmer stars cannot be seen. A workaround solution was to create three new star databases. In the first the dimmer stars are boosted one-half magnitude in brightness. In the second database the boost is one magnitude; in the third, two magnitudes. The brightest stars are kept at maximum TV brightness. Thus, in each of the three new databases the brightness range is compressed making the dimmer stars more visible. The appropriate database may be selected prior to each day's training session, or changed during a session, if needed.

The Hughes Light Valve projectors/Farrand pancake window displays made stars difficult to see in the overhead windows. The solution chosen was to use 2x2 picture element-sized stars. Even though the brighter stars look like marbles, constellations can still be readily identified. Stars are not simulated in the CCTV system or in the payload bay windows where payload bay lighting would wash out any stars. Also, no need exists to simulate planets.

SUN GLARE SIMULATION

Solar glare is important in space shuttle missions. The first space shuttle orbital flight test is scheduled to launch into an early morning sun which would prominently shine into the spacecraft commander's left quarter window.

Simulation of the sun and moon as one-half degree diameter discs proved unsatisfactory. Lunar maria and crater rays were initially modeled in the front window DIGS to distinguish the moon from the sun. These lunar features were too small to be unambiguously discerned. The sun remained virtually indistinguishable from the moon. Worst of all, its small dim television image appeared pitifully insignificant buried in the blackness of space (like the moon appears in Figure 10). In contrast, the photo image of the sun in Gemini 10 photo S-66-46111 (Figure 11) appears as a 10 degree diameter ball of light. Effects of sunlight are seen on the window 15 to 20 degrees from the sun.

The solution implemented was to provide a large sun glare model (Figure 12). A yellowish 1/2 degree diameter "real sun" (omitted in the CCTV-Aft black and white systems) is buried in a 10 degree diameter white solar glare circle. This is enclosed by a 13 degree diameter circle. The largest circle, 35 degrees in diameter, simulates sun glare effects 17.5 degrees from the solar center. Realism is further enhanced because the sun glare model usually washes out the stars elsewhere in the window. For atmospheric flight the dimmer two rings are eliminated.

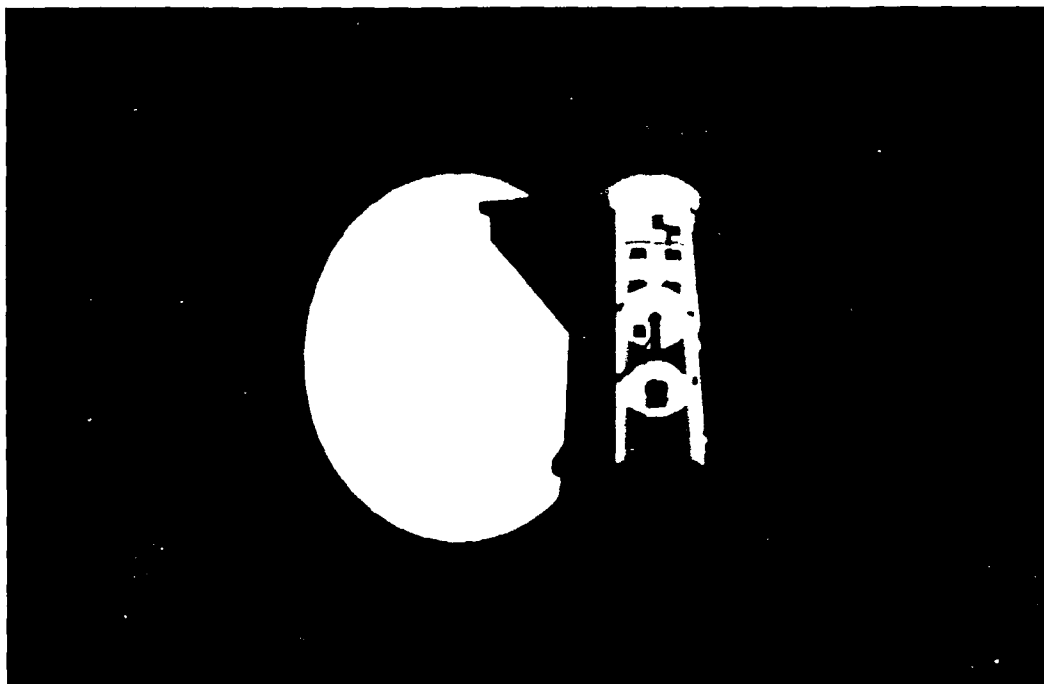


Figure 12. Space Shuttle Orbiter with sun glare model in background.

The sun glare model is also valuable to warn space shuttle trainees and SMS instructors when a CCTV camera is being pointed near the sun. Pointing at the sun in flight would probably damage a camera sun sensor. This sun glare simulation has received good flight crew acceptance.

DATABASES FOR THE CCTV AND AFT WINDOWS DIGS

The CCTV and aft window databases are similar. They differ greatly from the forward windows database. The detailed earth of the forward windows is simulated merely as a featureless white circle. A darker circle is accessed for the earth's nightside.

The CCTV and aft window databases focus on meeting payload operations requirements. The Orbiter exterior and payload bay are modeled. Operation of the payload bay doors and radiator panels are simulated. One or two RMS arms can be simulated. Three payload configurations have been simulated (Figures 13, 14, and 15), and include:

- Config. 1. Development Flight Instrumentation (DFI) containers and pallet. Induced Environmental Contaminators Monitor (IECM)
- Config. 2. DFI-IECM (800 face boundaries)
One RMS arm mounted on the port side. The RMS will deploy the IECM to measure thruster plume contamination.
Office of Science and Terrestrial Applications (OSTA-1)
Development pallet (1200 face boundaries).



FIGURE 13. Configuration 1: Three DFI containers with IECM on top.



FIGURE 14. Configuration 2: OSTA-1 viewed from port payload bay window.

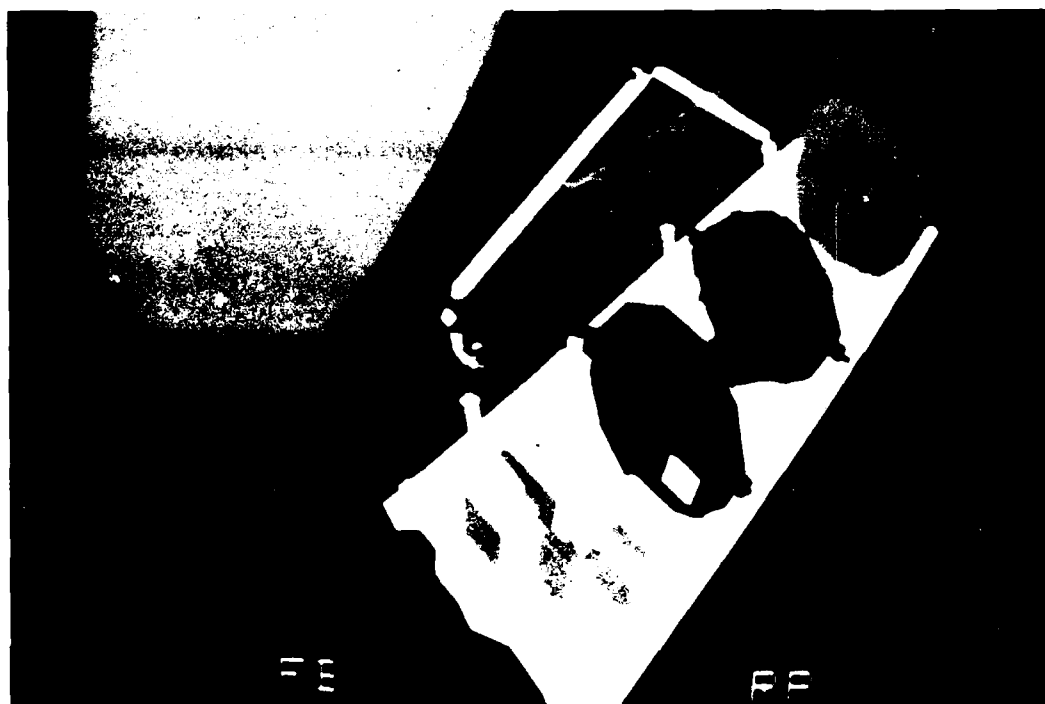


Figure 15. RMS, moving to grapple IECM behind PFTA. Earth in background.

Config. 3. DF1/IECM, RMS port arm (600 face boundaries)
Payload Flight Test Article (PFTA) (1500 face boundaries)

Deployment, retraction, and jettison of the RMS arm(s) is simulated. The RMS arm is modeled using seven independently-moving components: the Manipulator Positioning and Retention Mechanism (MPRM), the shoulder, the upper arm, lower arm, wrist pitch segment, wrist yaw segment, and the end effector. The RMS wrist and elbow cameras are simulated including the elbow camera pan/tilt unit motion.

Two forward and two aft payload bay bulkhead CCTV cameras are simulated including motion of their pan/tilt units. Separate SMS hardware is used for special camera effects and generation of alpha-numerics displayed on the CCTV monitors.

Simple models of the payload bay, RMS, and payloads are used in a hardware/software solution for solving real-time occlusion priorities. These occlusion models can be displayed for debug purposes instead of the normally visible models.

DIFFERENCES BETWEEN THE CCTV AND AFT DATABASES

It is physically possible for the RMS arm to see the nose of the Orbiter or even underneath, so these features are modeled for the CCTV database. This detail cannot be seen from the aft or overhead windows so it can be eliminated.

It was discovered that unseen detail modeled in the Orbiter's nose and tail sections place an additional load on the DIGS hardware. Thus, detailed payload scenes could cause scanline overflows in the CCTV DIGS, which is limited to 256 intersections per scanline. Orbiter exterior and payload bay database simplifications are planned to prevent such overflows.

DATABASE MODIFICATIONS

New databases are generated using a digitizing tablet/menu system similar to other computer generated image systems. Databases can also be altered in real-time using an on-line color modification (OLCM) program. Parameters that can be changed with the OLCM program include color, intensity, resolvability code and switching distance. Use of the OLCM program reduces database debug time by enabling rapid observation of database parameter changes.

Effort is underway for an IUS mission deploying the Transmission and Data Relay Satellite (TDRS) and for a demanding SSUS mission. The SSUS mission includes three SSUS vehicles with tilt mechanisms, spin tables, and sun shields. The SSUS mission requires twelve individually-moving components in the payload bay, three of which may move simultaneously.

Future effort will continue to be simulation of new space shuttle payloads to meet specific mission training requirements.

CONCLUDING REMARKS

The development of computer generated image technology to its present state has been rewarding. Computer generated imagery has proved indispensable in satisfying visual simulation requirements for the space shuttle missions. The SMS visual databases provide greater simulation capability than previous simulators; and they have the capacity to be easily expanded to meet future requirements.

NAP OF THE EARTH (NOE) MANEUVERING
WITH COMPUTER GENERATED IMAGERY (CGI)



Frank Lewandowski
Senior Scientist
Link Flight
Simulation Division
The Singer Company

Frank Lewandowski received Bachelor of Science degrees in Electrical Engineering and Mechanical Engineering from the University of Illinois and has had specialized training in the fields of photogrammetry and mathematics. His 29 years of experience has been in industry. During his 25 years at Singer he has participated in the initial design of new products including precision comparators, photographic image processing and image handling devices. In his current Link position he is investigating the possible range of visual effects in the digital image generation systems.

NAP OF THE EARTH (NOE) MANEUVERING WITH COMPUTER GENERATED IMAGERY (CGI)

INTRODUCTION

It has proven to be almost impossible to design theoretically a digital data base for a specific training task for Nap of the Earth (NOE) maneuvering. The eye is very particular about the data it processes and will use cues without consciously being aware of what data is being obtained from the scene. Many unusual perceptual effects become evident only when the scene is viewed on the display. It is through these observations that changes and improvements to the digital visual system are made. Some examples of these unforeseen perceptual effects are "floating" trees that required a shadow under them to fix them to the ground, rectangular object faces rather than triangular faces to give pilots the correct perceptual cues (1), rotor blades that "strobed" until modeled by switching 45° blade patterns each TV frame, and the addition of checkerboards to terrain faces to indicate changes of slope as we will demonstrate in the movie that follows. This paper serves to illustrate that the methodology employed to provide necessary flying cues was laborious and exhaustive, yet even in retrospect it appears there is no better method presently available.

Initial pilot reactions to helicopter NOE visual scenes were discouraging. Although the scenes contained what had originally been considered sufficient detail the pilots found it difficult to perform many of their requisite tasks. Low altitude maneuvering (4' to 50' skid height) was particularly substandard in that slight changes in terrain slope were extremely difficult to detect.

It is obvious that the maneuvering areas should be enhanced to provide more landing information for the pilot. However, simply adding scene detail to make the model more complex may not contribute any additional landing cues to the pilot. In fact, the addition of this detail may overload the computing capability of the image generator. It is necessary, therefore, to determine precisely what task-relevant information will increase the performance capabilities of the pilot.

The straightforward solution was to provide additional cues in the near field to aid the observer. When the decisions had to be made on the selection and/or elimination of objects it was realized that numerous compromises were necessary and there was almost no existing information to aid in making these decisions. Of paramount importance was determining the contribution that 2D and 3D objects made to low altitude maneuvering, the optimum spacing of these objects, and the relevance of the type of 2D or 3D objects (trees, logs, stumps, checkerboards, etc.). Geometric patterns, either checkerboards or light points, can be generated relatively easily and usually minimize CGI loading. Hence, an effort would be made to incorporate these elements if they proved useful.

EQUIPMENT USED

The problems of visual data base evaluation were compounded by the unavailability of the entire helicopter simulator for the long periods of time necessary for the lengthy scene debugging and subsequent tests. The decision was made to utilize the R&D CGI unit located at the LINK facility in Sunnyvale, California. This research CGI unit has a single infinite image display window and uses the same color CRT as production units. It can display 4000 edges with 256 intersections per scanline at 256 levels of occultation. More recent CGI improvements (anti-scintillation, detail faces, visibility, fading) have not been incorporated; however these factors were not the subject of this evaluation.

The research visual system has a control panel which was programmed to simulate a simple helicopter. This permits dynamic evaluation of the scene during actual maneuvering as opposed to remote static observation. The control panel was also used to modify object switching distances and to add or delete particular objects from the scene during maneuvering.

TEST PROCEDURE

A low relief section of terrain was selected from a production data base and digitized for use in the laboratory unit. This particular area was chosen because of its subtle peaks and valleys. The shade of green in this scene was that most prominently used in production data bases. The area digitized was approximately 6,000' X 4,000'. The maximum height of the terrain is 450'.

Each pilot was permitted sufficient time to become thoroughly acquainted with the performance of his "aircraft" before his position was initialized to a point just off the edge of the terrain. He then was asked to "fly" at varying heights above the terrain over a loosely prescribed course. Estimated heights were continuously compared to a computer readout of height above terrain. (Forward speed and several other factors were also available but were not used in these particular tests.)

Before each run (and in some cases during a run) the visual scene was modified in color, type and/or size of objects, and density of objects. In most cases this involved the substitution of an entirely new data base. Pilot performance was compared for all combinations of data base.

The actual eye height readings and the analysis of the height deviations in each case have not been made a part of this report because the tests were run in several different time periods and with different subjects. Instead we produced a short movie of most of the experimental data bases to indicate the extent of these tests and to show subjectively how the data base choices for a NOE visual scene must be made.

MOVIE PREPARATION

The movie recording of each of these tests was taken in real-time but in stop action. That is, all of the flight parameters for each TV frame were recorded on disc during a real-time flight over the data base. In movie mode the position data for each frame is read back, the scene generated in real-time, the movie camera shutter opened for approximately one second, the shutter closed, and the positions for the next TV frame read in. It takes almost two seconds to record each frame or about sixty times longer to record the movie than to replay it. Several of the data bases evaluated involving real-time moving arrays projected onto the terrain could not be movie recorded because the array and movie mode could not be calculated simultaneously in the research CGI control computer.

DATA BASES/SCENES EVALUATED

Various experiments were performed on the low relief terrain copied and modeled from a production data base. These experiments resulted in a composite data base which seemed to contribute most significantly to NOE maneuvering.

1. Random Intensity and Color Alterations: One of the first experiments was to randomly alter the intensity of each terrain face to break up the large homogeneous green areas. Some interesting visual effects were noted in that when maneuvering at low altitudes some of the hills would appear as valleys and vice-versa. Some of these same effects have been noted in stereo viewers and other photogrammetric equipment. These effects were not predictable and the film recording did not necessarily convey the same visual effect. Randomly altering the color of the terrain faces was also discarded because it destroyed the terrain cues obtained by the normal intensity computation.
2. Accentuating Sun Vector: In the original data base the break between terrain faces was almost indiscernible when small slopes were modeled. The pilot, unable to detect a significant color change, could not detect peaks and valleys. To accentuate the face intensity differences, the computation was altered to make the intensity a function of the square of the cosine of the angle between the face normal and the sun vector. The slope change has not been significantly accentuated in those slight slope change areas.

To further accentuate the intensity differences the cube of the cosine of the angle between sun and face normal was used. In the movie it can again be observed that in the area of little slope change, the face intensity differences did not change enough to aid peak and valley detection. In the area of large slope changes, the face intensity differences became so pronounced that the terrain became almost black and white. This approach did not seem to have sufficient merit for improving NOE maneuvering.

3. Cross-stitching: In the continuing effort to accentuate terrain slope changes for the pilot, several data bases were designed with narrow lines modeled transverse to the scene edges. These lines were quite effective for this purpose as can be seen in the movie. However, the lines were somewhat disconcerting to the pilot and expensive in terms of using available scene detail. (Light and dark contrasting lines were used in this experiment as well as in all others. The moderately dark lines were universally preferred).
4. Edge Outlining: In another experiment in accentuating slope, line features were placed at the boundaries of all terrain faces. As before, both light and dark contrasting lines were used. These lines proved quite effective in delineating slope changes but did not provide any cues when the pilot was at a low altitude within the terrain face. Since they were line features (two pixels wide at all ranges) they appeared overly dark and large at all reasonable ranges and faded when approached at very close range. Narrow faces rather than line features become larger as they approach the eyepoint but were objectionable because of the number of scene edges required and because of image breakup at longer ranges.
5. Point Feature Outlining: To make the scene more aesthetically pleasing while maintaining the advantage of line feature outlining, point lights were substituted for line features. As with line features, there was no noticeable improvement of the scene. The system expense in terms of edges required actually increased.
6. Face Patterns Light Points: Neither point nor line outlining of the terrain faces aided maneuvering when the eyepoint was within the borders of large terrain faces (600-800'/edge). To provide cues within these areas light points were randomly distributed over the faces (as always both light and dark contrast was evaluated). Many average spacings were modeled; 100' between light points is the spacing recorded on the film strip. Spacing greater than 100' put the light points too far apart to provide any cueing. All practical spacings were much too expensive in terms of system capacity.

Patterned light points were also evaluated (some in the form of a small cross in the center of the large faces). These provided additional position cues because of convergence cues but did not provide enough position data to warrant their inclusion in the data base. (Line features in the center of the larger faces were also evaluated with similar results.)

The constant pixel size (1 x 1 or 2 x 2) of point and line features causes them to fade in the near field almost to the point of being indiscernible.

7. Face Patterns - Checkerboards: There has always been some reluctance to use geometric patterns on terrain because they would appear "unnatural". These patterns are, however, the most practical to implement and lend themselves to automated

data base entry. Many combinations of checkerboard sizes and colors were modeled and evaluated. The largest checkerboard (500') was of little value since it was only slightly smaller than the average face size. Since the checkerboard size could be varied easily, all sizes down to 50' were modeled and displayed (500', 200' and 100' were filmed for this presentation). With the 50' checkerboard the terrain scene became so "busy" that it disconcerted the operator. At high yaw rates with the small squares one could easily become nauseous. Repeated flights over the checkerboards narrowed the optimum square size to between 100' and 200'. 130' was used in all further experiments.

The checkerboard appeared to provide sufficient distance and near field cues to aid maneuver close to the ground without flying through the terrain. However, they did not provide any cue as to the absolute height above the ground. Without previously being taught the absolute size of the checkerboards their size could have been estimated from 1000' to 10' depending on the size of the hills themselves.

8. Checkerboard with Stumps: Previous programs evaluating NOE objects had narrowed the choice of acceptable objects to trees, stumps, and posts. (Other objects such as rocks, shrubs, bushes, and groundcover were singularly unsuccessful). The checkered data base, was populated by stumps (dimensions approximately 2' x 2' x 3') at a density of 1 per 20,000 sq. ft. The stumps served the purpose of establishing an absolute size of each square but caused the pilots to search for and fly from stump to stump.
9. Checkerboard with Trees: Thirty-foot high trees (without trunks) were substituted for stumps to determine if the choice of objects were significant. The trees were easier to find and made the terrain more realistic, but they did not provide enough parallel lines at their tops and bottoms to give adequate height cues. As with stumps, the pilot tended to fly from tree to tree.
10. Composite Data Base (Checkerboard, trees, stumps, posts): A composite scene utilized those data base features which seemed to contribute most significantly to NOE maneuvering. In the composite data base:
 1. The checkerboard gives cues of terrain shape.
 2. The trees are relatively large objects which provide a scale for the checkerboard.
 3. The stumps established the ground surface.
 4. The posts give precise height cues by size and observation of their parallel top surfaces.
11. Rotor Shadow: The final composite was useful for maneuvering but sparse areas remained in the data base. Ideally the data base should be evenly and densely populated with objects, however, the number of edges necessary for this purpose would far exceed the computing capacity of any CGI system. In an

attempt to provide near field cues at all times a translucent rotor shadow was projected onto the terrain immediately below the aircraft (flat terrain was used for the initial experiments). As the eyepoint approached the ground the shadow would appear in the window. The pilot soon learned that he could use the image of the shadow in his window to maintain relative position. It was later determined that he was not actually obtaining visual cues from the ground but simply using the shadow images as a position indicator.

A number of other "shadow" patterns with different colors and sizes were evaluated on flat ground planes. All provided an excellent mechanism for maneuvering but lacked realism and authenticity.

12. Ground Pattern: It was evident that some kind of ground pattern immediately about the eyepoint could provide the cues necessary for extremely close maneuvering. An attempt was made to replace the moving object rotor shadow with a moving object radial pattern of light points. This pattern proved to be a little disconcerting at high yaw rates and several other patterns were modeled. The projection of the patterns onto the terrain slopes was also implemented. Treating the pattern as a moving object made the projection computation quite reasonable for a single slope but when many slopes intersected at a point the number of patterns involved made the computation difficult.

Our efforts to implement the computation became so lengthy that it was determined that an array of points or faces could be computed in real-time and ground mapped onto the terrain easier than treating the patterns as moving objects.

A computer program to generate and project checkerboards of 5, 10 and 20-foot spacing and two-element light points of 5, 10 and 20-foot spacings was written. Twenty elements were used in all directions from the eyepoint giving an array size of 200, 400 and 800 feet. These patterns were used in flights over the original terrain with all other combinations of the terrain and objects discussed previously.

All pilots were impressed with the additional near field detail and their ability to maneuver confidently. The terrain could be flown with only the projected array or with any of the features previously tested. There was disagreement on the "best" of the patterns. Some pilots felt that the small computed checkerboards were "busy" and tended to "swim". This was particularly true of the 5-foot checkerboard. Discussions resolved the "best" pattern to be the 10-foot spacing, two-element light points for the following reasons.

First, the light points do not obstruct the terrain; secondly, its extent was large enough that it did not give the same type of cue as the shadow pattern. Third, the light points provide a more subtle pattern that a pilot can accept as simulated rocks or gravel.

The work done above illustrates the methodology required to produce task-related data bases. It should be noted that usually it was not possible to predict the outcome of the experiments in terms of visual perception.

It is clear to all of us designing data bases that it will be a slow, thoughtful and laborious procedure to produce future digital data bases. Much has been learned by ourselves and by others working on the same task. One day this data and the wealth of observations may be codified, analyzed, and a methodology developed, but until then we continue to build, observe and build again.

REFERENCES

- (1) Dennis McCormick, "The Importance of Being Square," Image Generation/Display Conference II.

INCREASED SENSOR SIMULATION CAPABILITY AS A RESULT OF
IMPROVEMENTS TO THE DIGITAL LANDMASS SYSTEM (DLMS) DATA BASE



Dr. Marshall B. Faintich
Supervisory Cartographer
Aerospace Cartography Department
Defense Mapping Agency Aerospace Center
St. Louis AFS, MO 63118

Marshall B. Faintich is Chief of the Techniques Office in the Aerospace Cartography Department at the Defense Mapping Agency Aerospace Center (DMAAC) in St. Louis, Missouri. He received his B.S. degree in Applied Mathematics from the University of Missouri at Rolla, and his M.S. and Ph.D. in Astronomy from the University of Illinois at Urbana-Champaign. He was involved in satellite systems research at the Naval Weapons Laboratory (now NSWC), Dahlgren, Virginia from 1971 to 1974, and was detailed to the Engineer Topographic Laboratories for study in digital image processing. He has been involved in geodetic studies, sensor scene simulation, and digital image technology at the DMA Aerospace Center and was detailed to L'Institut Geographique National, Paris, France, on a technical exchange. He has authored numerous technical papers on astrodynamics, computerized simulation, and digital image technology.



Mr. John Gough
Physical Scientist
Scientific Data Department
Defense Mapping Agency Aerospace Center
St. Louis AFS, MO 63118

John B. Gough is a Physical Scientist in the Scientific Data Techniques Office at the Defense Mapping Agency Aerospace Center (DMAAC) in St. Louis, Missouri. He was involved with radar while in the U.S. Air Force. He received his B.S. degree in Geography from the University of South Florida, Tampa, Florida. He has been involved in digital culture data production, sensor scene simulation, and digital image processing at the DMA Aerospace Center.

F/G 14/2

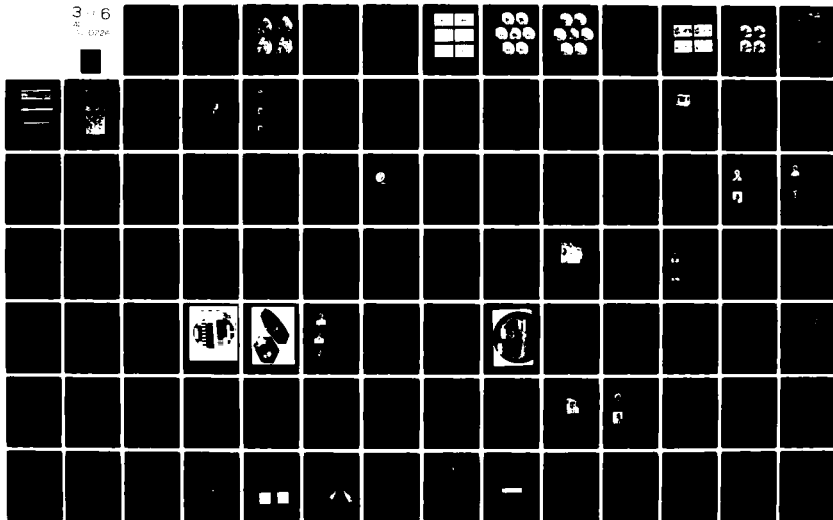
NOV 81 E G MONROE

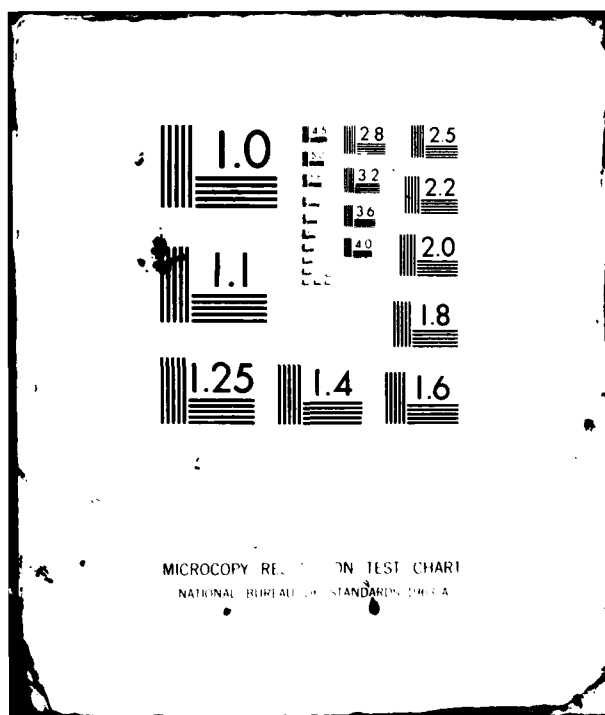
AFHRL-TR-81-48

NL

3 - 6

1122





INCREASED SENSOR SIMULATION CAPABILITY AS A RESULT OF IMPROVEMENTS
TO THE DIGITAL LANDMASS SYSTEM (DLMS) DATA BASE

ABSTRACT

The Defense Mapping Agency is producing digital culture and terrain elevation data bases to support advanced aircraft simulators. Data base analyses and sensor simulations have led to improvements in the specifications for these data bases, and have been used to define parameters to be included in a prototype data base designed to support visual and other high resolution sensors. These improvements and new parameters are discussed, and sensor simulations and data base displays are shown.

INTRODUCTION

In order to support advanced aircraft simulators by providing an improved low level radar training capability offered by digitally generated radar landmass images, the Defense Mapping Agency (DMA) is producing digital culture and terrain elevation data bases. The DMA has conducted extensive investigations in digital sensor simulation for the purpose of establishing an effective editing and analysis capability of these data bases (Faintich, 1979, 1980). The DMA is also pursuing advanced techniques for data base production through its research and development program. As a result of the technology developed for aircraft radar simulator support, multi-sensor scenes and data bases are being developed for both simulators and input to reference guidance systems. The primary purpose of this paper is to describe results obtained from improvements to the Digital Landmass System (DLMS) Data Base and compare these results with both actual and previously simulated sensor imagery. This paper does not necessarily represent DMA policy, nor is it a commitment to produce data in a particular manner.

CURRENT AND ANTICIPATED DATA BASE CONTENT

The current (July 1977 specification) DMA standard production data bases (Level I) contain large area cultural information, and digital terrain data sampled at a three second interval. The cultural data consists of point, linear, and areal features described by characteristics such as surface material category, generic identification, predominant height, structure density, and percentages of roof and tree cover. The cultural data is in lineal (planimetric boundary) format and although feature sizes may vary depending upon local circumstances, the data reflects a resolution on the order of 500 feet. Smaller features are aggregated into homogeneous features described by predominant characteristics. The current high resolution (Level II) data bases contain small area cultural information, and digital terrain elevation data sampled at a one second interval. This translates to a resolution of about 100 feet, with smaller features also aggregated. Detailed information is available in Reference 2, "Product Specifications for Digital Landmass System (DLMS) Data Base".

The terrain elevation data is produced by contour digitization from charts or directly from stereo pairs of photographs using advanced analytical stereoplotters. The cultural data is produced from both charts and photographs with a much higher level of manual effort required in order to perform the complex feature analysis. Because of the labor intensive nature of the task, the production of Level II cultural data ranges from 10 to 100 times the production cost of Level I data, depending on the area. The current Level I data base program covers roughly 20 million square nautical miles, with estimated data base completion dates in the 1985 to 1990 time period. Level II data is programmed only for small selected areas of interest.

The DLMS data bases have been shown to be adequate for support of long and medium range radar simulation (see Figure 1), and for short range radar simulation where Level II data is available. In addition, these data bases have shown some applicability for multi-sensor simulation. As integrated chip and microcomputer technology improves, however, on-board multi-spectral electro-optical navigation sensors continue to acquire and display terrain and cultural information with ever increasing resolution approaching that of a visual response. Training is required in the use of advanced aircraft displays, including forward looking infrared systems, low light level television, ultra-high resolution and real-time synthetic aperture radar, as well as an increased demand for visual training associated with low altitude mission profiles. Technology improvements will also allow greater realism in advanced simulators, and the demonstrated effectiveness of present simulators is driving requirements for simulators to support the new generation of navigation sensors.

In addition, the commitment of the DOD to the development of various types of weapon system guidance correlators is demanding new support data. Correlation may be made against pre-stored computer generated reference scenes for optical, infrared, microwave, conventional and synthetic aperture radar, and ultra-violet electro-optical sensors.

A crucial component in support of these new navigation/guidance systems is the ability to provide adequate digital data bases that describe a variety of global ground truth conditions. Both static and time-varying information such as texture, thermal and near-infrared properties, precise geometric properties, road patterns, population and traffic density patterns, and atmospheric weather data will be required in addition to current DLMS feature descriptors. Along with new types of feature descriptors, increased resolution and level of detail will be required.

Initially, much of the advanced data descriptors will not be cost effective or possible to collect and will have to be modeled from known parameters. As automated feature analysis and extraction techniques become developed, an increasing amount of these data types will be described more closely in agreement with their physical characteristics and will be included in the cultural data base. As an interim procedure, or for data base areas where higher resolution data is required only for increased data content and appearance, and not for reasons of precise ground truth, computer techniques such as texturization (Bunker, 1978) and synthetic feature break-up (Faintich, 1979) allow for the production of large data base coverage using existing techniques.



(a) Simulated



(b) Actual



(c) Simulated



(d) Actual

Figure 1. Level I DLMS Radar Simulations: Las Vegas, Nevada
(a) Long Range (85 n.m.) Simulation versus (b) Actual Radar;
(c) Medium Range (32 n.m.) Simulation versus (d) Actual Radar
Scope Photography

EVOLUTION OF DATA BASE PRODUCTION

The labor intensiveness of the present digital data base production process and the worldwide extent of DLMS requirements have led DMA to explore automation as a means of decreasing production costs. This is being accomplished within the technical base existing at DMA and via research and development programs through academic, industrial, and governmental institutions. Initial goals to increase production of current DLMS Level I and II data are being addressed by the implementation of specialized automated processing systems and computer assisted photo-interpretation stations. In order to establish the capability to produce anticipated data types and resolutions required by 1985, the DMA is expanding its Image Understanding program for the technology base required to support the development of an interactive, semi-automated feature analysis production system.

For purposes of quality control and data base applicability investigations, the DMA is developing the Sensor Image Simulator, a very high speed data base edit station and static scene simulator that allows for interactive query of individual features in the simulated sensor scene to determine the corresponding data base elements responsible for the simulated features.

In advance of the integration of future automated feature analysis techniques, the DMA has refined the DLMS data base specifications commensurate with current production capabilities to better support sensor simulation. The 1974 data base specifications were revised in July 1977, and the DMA is currently producing a prototype data base to support high resolution sensors.

1977 DLMS DATA BASE SPECIFICATION REVISION

As a result of an intense test and evaluation of the data produced for USAF Project 1183 (Robinson et. al, 1979), the DLMS data base specifications were changed to include the following major revisions:

- a. Standardization of feature descriptors where actual differences are insignificant;
- b. Decrease in the minimum size for strong reflectors;
- c. Decrease in the minimum size for building groupings with significant height differences;
- d. Increase in the minimum size for poor reflectors;
- e. Decrease in the minimum size for open areas with an urban area;
- f. Expansion and clarification of unique feature specifications;
- g. Reduction from six levels (IA, IB, IIA, IIB, IIIA, IIIB) to two (I, II);
- h. Standardization of percent roof cover descriptor;
- i. Portrayal of dense trees in urban areas;

- j. Increase of feature identification codes from 48 to 255;
- k. Portrayal of certain regional features apparent on low altitude radar;
- l. Description of seasonal and natural effects such as sea states;
- m. Portrayal of permanent snow and ice.

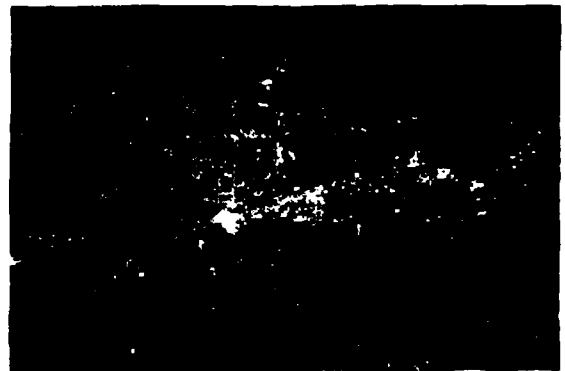
For comparison between the data bases, DLMS cultural and terrain data over Spokane, Washington, was chosen. This particular area was chosen because of existence of both 1974 and 1977 specification Level II data over a large area, availability of actual short range radarscope photography, and exclusion of this data in the test and evaluation study that resulted in the 1977 revisions. The comparisons between Levels I and II data may be somewhat biased, however, as the Level I data was produced using the Level II as a base. Although this is a standard technique, Level II data over a large area is usually unavailable to be used as a base, and the Level I data is compiled directly from feature analysis source materials. Figure 2 shows on-line 110 meter resolution data base displays of this area, wherein shaded relief of Level I terrain is shown, and gray levels represent radar reflectivity potentials. The synthetic break-up (SBU) data bases were produced by generation of random cultural, tree cover, and background features with descriptors normally distributed about original predominant values within homogeneous areal feature boundaries, based upon the percentages of tree and roof cover.

Inspection of these displays clearly shows the additional features portrayed due to decreased standards for strong and significant reflectors (Level I) and the reduction of features portrayed due to increased standards for poor reflectors (Level II). Also, the reflectivity potential for general residential/commercial areas is reduced, probably due to standardization of height descriptors. The SBU displays show the breakup of the areal features into background, trees, and brighter cultural reflectors due to elimination of adjustment for tree cover within a homogeneous area. Also of particular interest is that the differences between the 1977 Levels I and II displays at this resolution (for ≥ 15 n.m. radar scope displays) are much less than in the 1974 displays. This raises questions as to the need of Level II data at this resolution for short range simulation. For short/short range displays (< 10 n.m.), the differences are much more apparent.

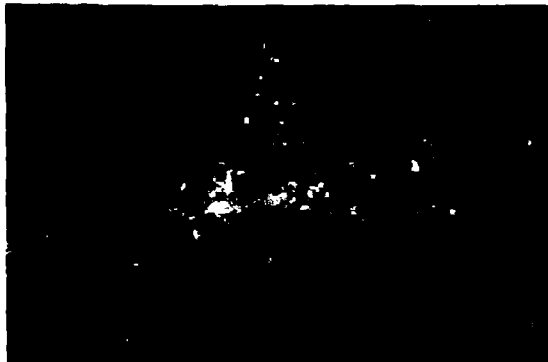
Now consider Figures 3 and 4. Radar simulations from the six data bases are compared with actual radar scope photography on 15 and 22 n.m. range displays. The gain settings for all six of the simulations in each figure are identical (except for Figures 4f and 4g) and were chosen for the best match between actual and the 1974 data base simulations. Note that the 1977 data bases provide for a better comparison with actual, especially better for Level I. In addition, for both Levels I and II, the general residential/commercial homogeneous returns are either missing under insufficient gain or appear as large homogeneous "blobs" without the benefit of SBU. The SBU simulations shown in Figures 4f and 4g have slightly lower gain settings to better match actual returns.



(a) 1974 Level I



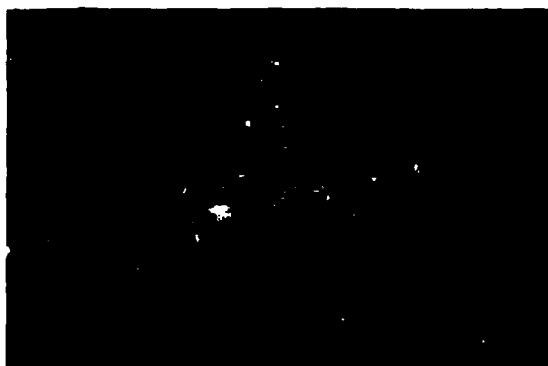
(b) 1974 Level II



(c) 1977 Level I



(d) 1977 Level II



(e) 1977 Level I SBU



(f) 1977 Level II SBU

Figure 2. On-Line Data Base Displays: Spokane, Washington

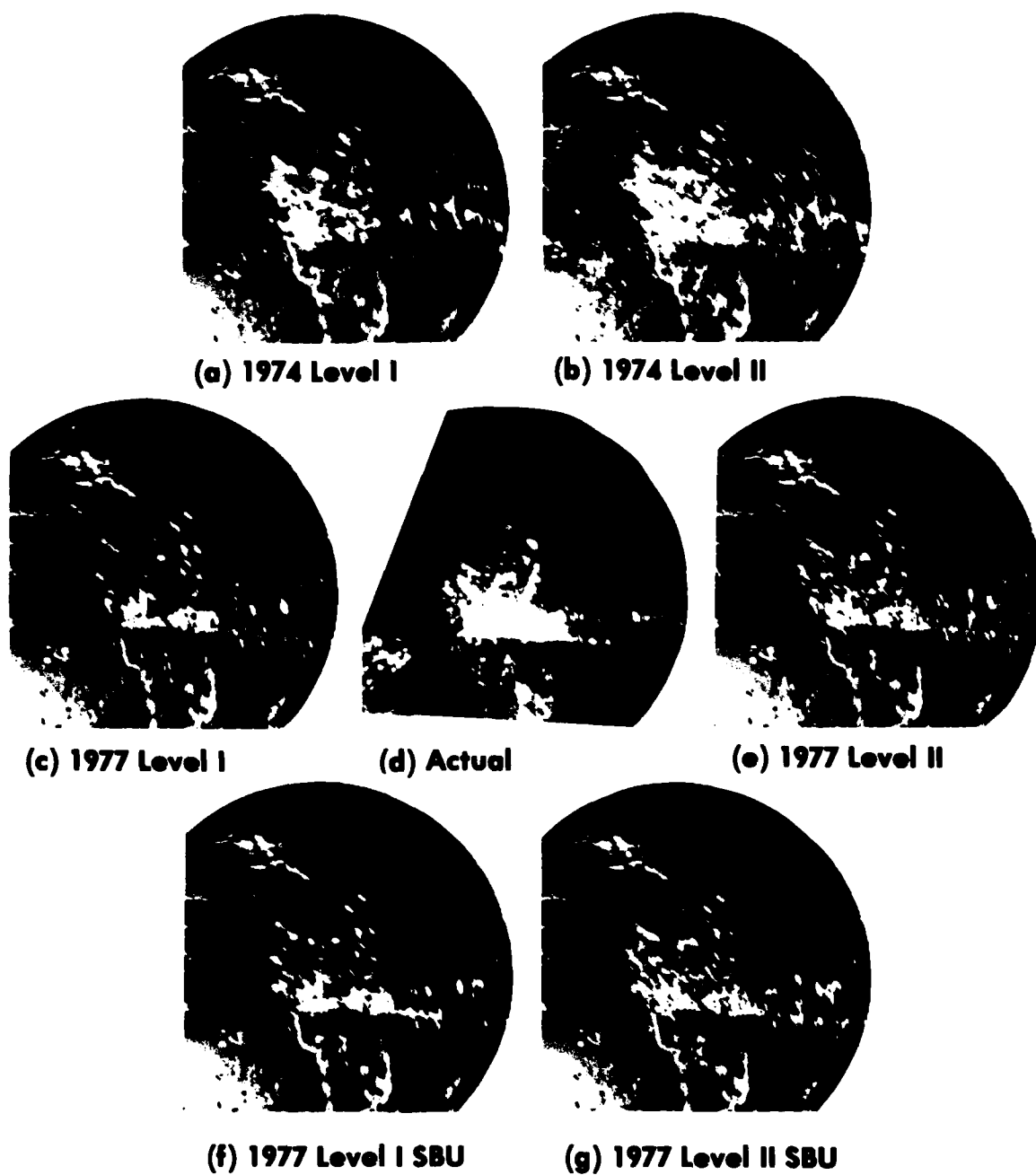


Figure 3. Short Range (22 n.m.) Radar: Simulations Using Various Data Bases versus Actual Radar Scope Photography

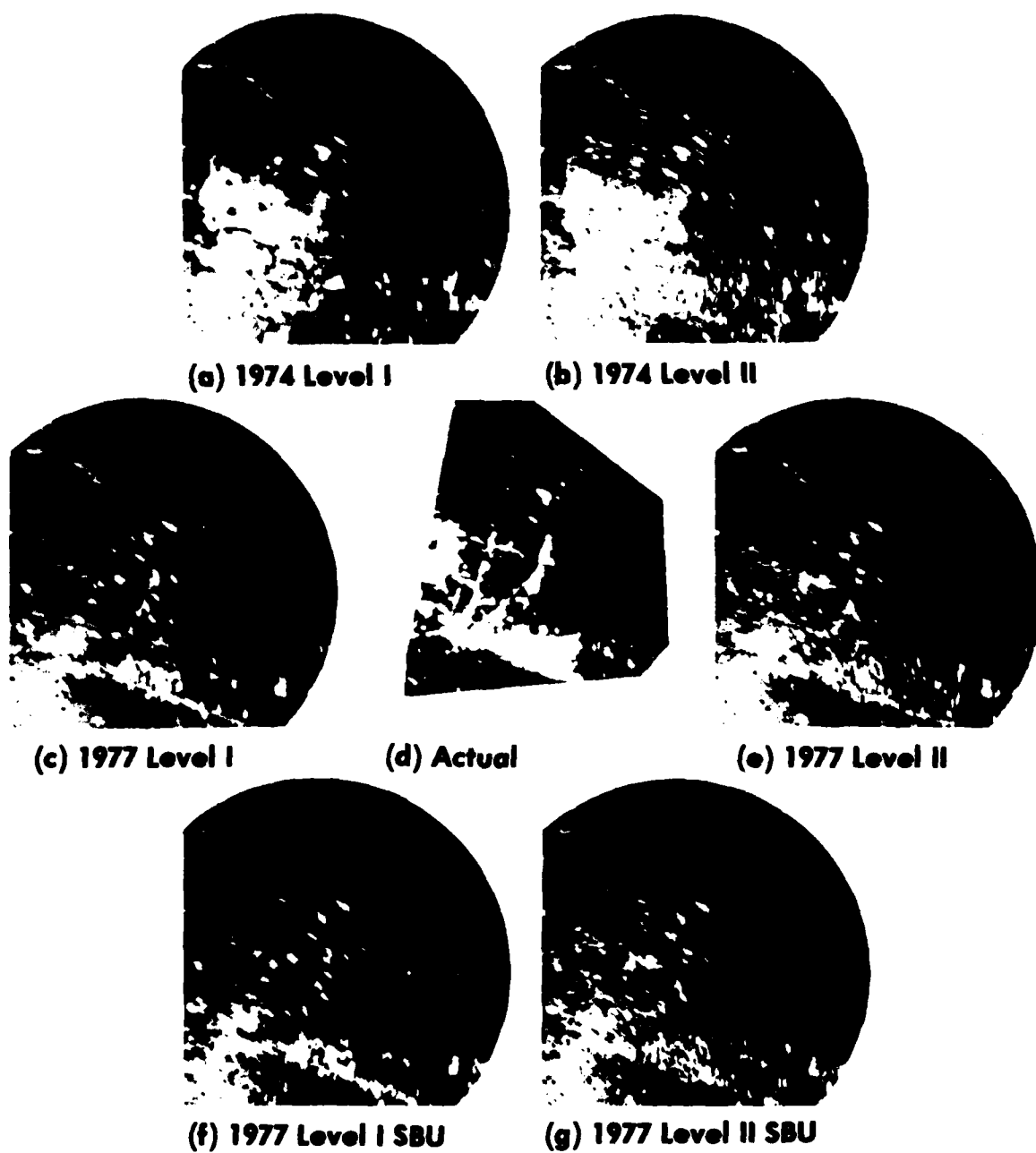


Figure 4. Short Range (15 n.m.) Radar: Simulations Using Various Data Bases versus Actual Radar Scope Photography

Figures 5 and 6 show data base displays and radar simulations, respectively, for the 1977 data bases with and without SBU at a resolution of 25 meters for 5 n.m. short/short range displays. Note that the differences between Levels I and II are quite apparent, and that the SBU technique continues to add to the effect of realistic simulation of the large areal features.

One may conclude from these studies that unless short/short range simulation is required for high precision conventional radar mission training, Level I DLMS data may be sufficient, and that the technique of synthetic break-up adds to the realism of the simulation. For areas surrounding high fidelity training data bases, synthetic break-up may be used to generate compatible frequency data for blending purposes.

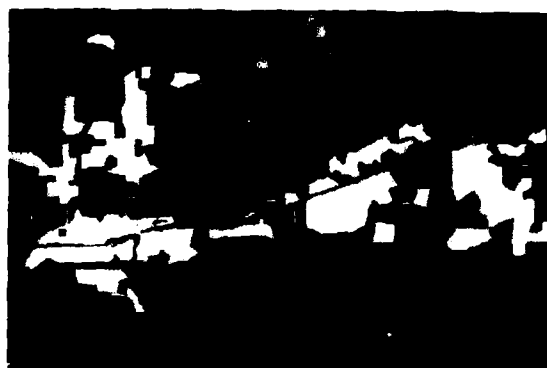
When considering non-conventional radars such as Synthetic Aperture Radar (SAR), the high precision of the Level II data may be required for much longer ranges. Figure 7 shows SAR simulations from the same 25 meter resolution data bases. Note that the effect of synthetic break-up adds greatly to the realism in the simulations.

PROTOTYPE HIGH RESOLUTION DATA BASE

The 1977 revision of the DLMS data base specifications includes descriptors that may not be needed for radar systems, but are certainly of value for simulation of other sensors. Figure 8a is a visual simulation of Port Angeles, Washington, and snow-capped Mt. Olympus from a 10,000 foot altitude, and Figures 8b and 8c compare shipboard visual simulation with actual photography. Figure 9 compares a black and white copy of a high altitude NASA photograph using color infrared (IR) film over Washington, D.C. Since a suitable IR model/data base has not yet been developed within DMA, this image is compared to a visual reflectance data base over the same area. Note the good agreement between the features. Note also the absence of major roads such as the Capitol Beltway about Washington.

In order to support high resolution sensor simulation, the DMA is producing a prototype data base (reference 3) for various sensors including visual, SAR, Low Light Level TV, and IR. This data base production is for evaluation of content requirements and production cost analyses. Large area (Level V) characteristics are currently specified, but small area (Level X) specifications for high detail portrayal are not. In general, Level V supplements Level I DLMS with additional feature descriptors, additional feature identification codes such as major transportation lines, and divides concrete/asphalt into separate surface material categories. The new feature descriptors are the roof descriptor, shape code, and microdescriptor.

The roof descriptor portrays ten roof types and four monitor types, yielding 40 different roofs. The shape codes are rectangular parallelepiped, (hemi-)spherical, pyramid, cone, cylinder, and other. The microdescriptor is a multi-purpose descriptor which describes some of the visual characteristics of a feature. This may be used to support synthetic break-up in a manner more realistic than by purely random means based on statistical percentages. The microdescriptors include vertical composition information such as height and location of a tower on a building, homogeneous area information such as the predominant dimensions of smaller features aggregated into larger areal features, and pattern definition where applicable such as road/street patterns.



(a) 1977 Level I



(b) 1977 Level II



(c) 1977 Level I SBU



(d) 1977 Level II SBU

**Figure 5. On-Line Data Base Displays: Spokane, Washington
High Resolution Grid (25 meter)**



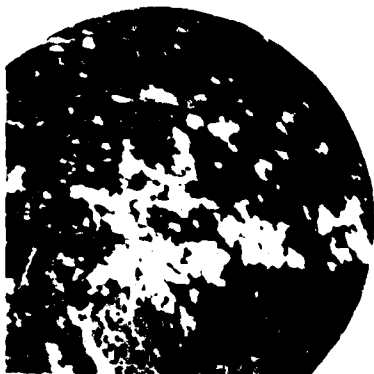
(a) 1977 Level I



(b) 1977 Level II



(c) 1977 Level I SBU



(d) 1977 Level II SBU

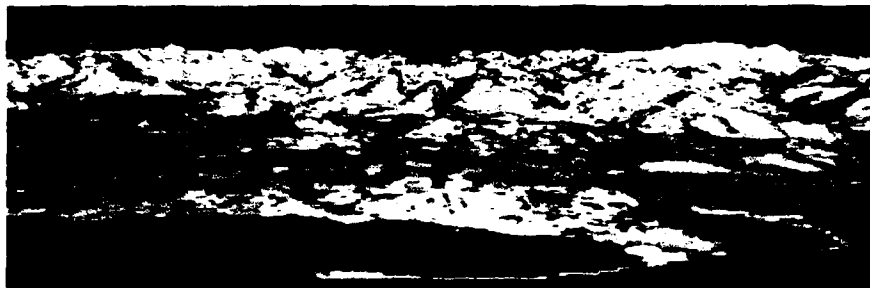
Figure 6. Short/Short Range (5 n.m.) Radar Simulations



(a) DLMS Level II SAR Simulation

(b) DLMS Level II SBU SAR Simulation

Figure 7. DLMS Synthetic Aperture Radar Simulations: Spokane, Washington



(a) Visual Simulation from 10,000 foot Altitude

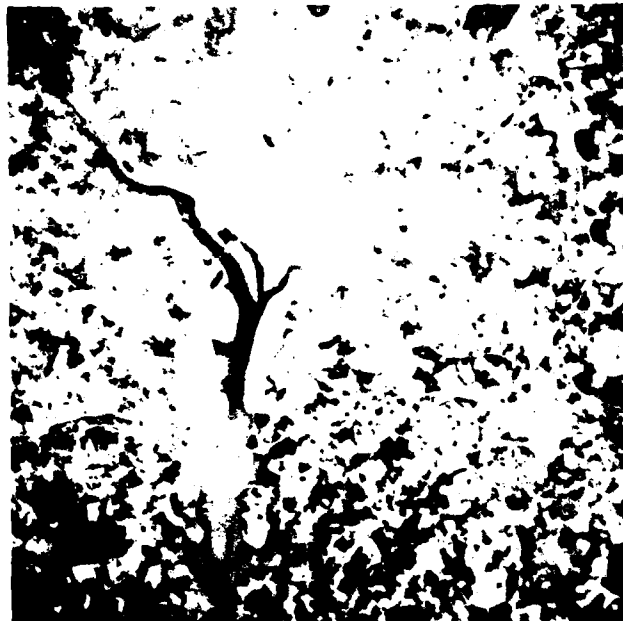


(b) Visual Simulation from Shipboard Level

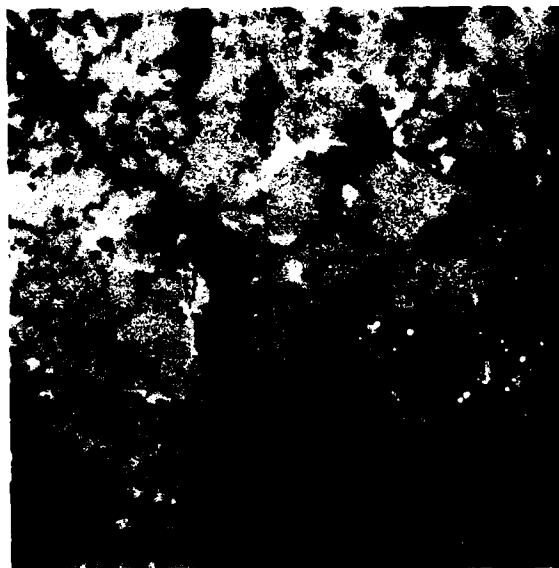


(c) Actual Photograph from Shipboard Level

Figure 8. Port Angeles, Washington and Mt. Olympus: Comparison Between Visual Simulations from DLMS Level I Data Bases and Actual Photography



(a) High Altitude Infra-red Photograph



(b) DLMS Level I Visual Reflectances

**Figure 9. DLMS Data versus Infra-red Photography:
Washington, D.C.**

After completion of the prototype Level V data bases, new sensor simulation investigations will begin. Previous investigations (Faintich, 1979) demonstrated the power of synthetic break-up in visual simulations using statistical percentages, and the new Level V data should provide for a much greater sense of realism and fidelity.

CONCLUSIONS

The DMA is continually striving within production constraints to improve the accuracy and level of detail in the DLMS data bases. Automated feature analysis techniques are being developed to aid in the collection of the data, and improved sensor simulations technology is helping to better utilize the information contained in the current DLMS data bases.

REFERENCES

1. Bunker, W. M.; 1978; "Training Effectiveness Versus Simulation Realism", Eleventh NTEC/Industry Conference Proceedings, Orlando, Florida, 14-16 November 1978, pp 291-298.
2. Defense Mapping Agency; 1977; "Product Specifications for Digital Landmass System (DLMS) Data Base", St. Louis AFS, Missouri.
3. Defense Mapping Agency; 1979; "Product Specifications for a Prototype Data Base to Support High Resolution Sensor Simulation", Washington, D.C.
4. Faintich, M. B.; 1979; "Digital Sensor Simulation at the Defense Mapping Agency Aerospace Center", Proceedings of the National Aerospace and Electronics Conference (NAECON), Dayton, Ohio, 15-17 May 1979; pp 1242-1246. (Reprinted in SPIE Proceedings, Volume 238, paper 238-49, 1980.)
5. Faintich, M. B.; 1980; "Digital Sensor Simulation: 1980-1985", Proceedings of the 13th Annual Simulation Symposium, Tampa, Florida; 19-21 March 1980; pp 181-190.
6. Robinson, R. et. al; 1979; "Test and Evaluation of USAF Project 1183 Digital Data Base", DMAAC TR 79-1, St. Louis AFS, Missouri.

SESSION IV

Chairman

John B. Sinacori
President, Sinacori Associates
Hollister, California



Mr. John B. Sinacori is an experienced aeronautical technologist operating as both an engineering consultant and contracted principal investigator. His experience in Aerospace firms includes flight dynamic and aerodynamic analyses, design of aircraft, rotorcraft and spacecraft, research on pilot-vehicle dynamics and all aspects of flight simulation including their conduct for training and vehicle development, simulator design and simulator research.

As the head of his own firm, he has been active in the design and development of advanced simulation equipment, research on simulator cueing and particularly the determination of motion and visual cueing needs for training and engineering development simulation and the design and development of advanced astronomical telescopes.

He holds a B.S. in Aeronautical Engineering from Rensselaer Polytechnic Institute and has performed numerous additional studies in electronics, optics, physics, mathematics, engineering and is a rated commercial pilot.

**PROJECT 2363:
LIQUID CRYSTAL LIGHT VALVE PROJECTOR**



Peter C. Baron obtained his M.S. in electrical engineering from Purdue University. His 26 years of experience at Hughes have included circuit engineering, advanced display development, air-defense system, display project engineering, and management of a variety of system engineering hardware development, study and proposal efforts. For the past 11 years he has headed the Hughes Ground Systems Group (Fullerton) display IR&D program covering hardware, device and software projects. Since 1976 he has had technical responsibility for a series of AFHRL programs (the latest being Project 2363) to apply the liquid crystal light valve technology to in-line infinity optics type simulator visuals.



Uzi Efron received his Ph. D. in Solid State Physics from Tel-Aviv University in 1976. His B.S. and M.S. degrees are also from Tel-Aviv University. Dr. Efron is currently the acting head of the Image Processing Devices Section of the Hughes Research Laboratories. He is responsible for the development of both the photo-activated and the electronically-addressed silicon light valves, as well as for the applications of these devices in image processing and display systems. From 1974 to 1977, Dr. Efron was with the Department of Non-Destructive Testing and Radiography at the Soreq Research Center, in which he served as Head of several projects dealing with Radiographic Image Processing.



Jan Grinberg received his Ph. D. in Physics from the Weizmann Institute of Science in 1970. He also has a B.S. and an M.S. in Electronics from the Technion-Israel Institute of Technology. Dr. Grinberg is currently the Acting Manager of the Exploratory Studies Department of HRL. The department conducts research in the areas of image analysis software and hardware, intelligent systems, image and signal processing devices, liquid crystal materials, e-beam and ion-beam resists, holographic gratings, and space batteries. He was previously responsible for exploring and developing novel liquid crystal light valve configurations using CdS and silicon photoconductors, and novel 3-D microelectronics structures for processing of image information.

PROJECT 2363: LIQUID CRYSTAL LIGHT VALVE PROJECTOR INVESTIGATIONS

PETER C. BARON, DR. UZI EFRON AND DR. JAN GRINBERG
Hughes Aircraft Company

ABSTRACT

The requirements of Project 2363 — for a full color noninterlace refreshed display with very high resolution for the background and the multiple targets — make extreme demands on the visual system. Results of a system definition study resulting in a compliant 3" light-valve-based liquid crystal light valve projector are briefly described. Accomplishments of the subsequent Component Development Phase (CDP) of the program, which was to develop the three high-risk components (very high resolution 3" fiber optic CRT, 3" polarizing prism, and 3" cadmium sulfide light valve) needed to implement this project, are summarized. The construction, operation and current performance capability of the silicon light valve — the key to fast response simulation applications — is then described, and the results of projector-level resolution tests conducted on the Project 2363 CDP breadboard projector are discussed. In summary, the project successfully demonstrated the feasibility — using interim cadmium sulfide and silicon photoconductor light valve configurations — of achieving the resolution needed to build a 2' of arc projector (at 20% MTF).

INTRODUCTION

The objective of Project 2363 was to make a major advance in the state of the art of simulation visual systems. Specifically, it was to develop the computer image generation (CIG) and visual system technology to provide the capability to present a full color, 60 hertz noninterlaced refreshed display using an In-Line Infinity Optical System (ILIOS) of the general type used on the Advanced Simulator for Pilot Training (ASPT) at Williams Air Force Base, Phoenix, Arizona. The system was intended to feature a background raster having a minimum required resolution of 4' of arc (at the pilot's eye point) and a design goal resolution of 3' of arc, and was planned to have a capability of displaying three small field of view (less than $30^\circ \times 30^\circ$) target rasters (located anywhere within the pilot's field of view) having a minimum required resolution of 2' of arc and a design goal resolution of 1' of arc. Figure 1 illustrates the requirements for this system. The visual system was to provide a minimum modulation of 20% at these resolutions and present an image having a brightness of 6 fL or greater as viewed through the ILIOS.

It should be noted that these requirements went far beyond the then current state of displays art. A window of a dodecahedron ILIOS cockpit represents a 90° field of view (if one provides for overscan to allow for 6 inches of pilot head-movement). A 4' of arc background raster then corresponds to 1330 scan lines, to be painted at a 60 hz rate — a significant challenge. A 2' of arc target resolution corresponds to approximately 2700 TV line resolution across the width of the pentagonal display used in ILIOS-type systems. Although the target raster field of view is very small, no known projection technique capable of real time television presentation had the resolving power to provide a modulation of 20% at this resolution.

SYSTEM DEFINITION STUDY

A prime contract was awarded to General Electric by AFHRL to implement the 2363 system in the fall of 1979. Hughes was awarded a subcontract by GE to participate in a "Phase I" system definition effort to define an additive-color liquid crystal light valve projector capable of meeting the minimum requirements of the program and of ultimately

meeting the design goal levels of performance (see Figure 2). Two candidate projector configurations were analyzed during the study. Both of them combined three liquid crystal light valve (LCLV) image channels in an additive color configuration; however, the LCLV image channels were implemented in different ways. In the first, a high resolution 5" CRT was used to drive a 2" LCLV through demagnifying optics (see Figure 3(a)). In the second, a larger 3" fiber optic LCLV was exposed by a fiber-optic faceplate CRT with which it was in direct contact. The former configuration can - with the demagnifying optics - provide a very small CRT line width to drive the LCLV. However, it was found during the study that it was not feasible to implement a dual-beam CRT (the dual beams were required to meet the high writing rate requirements at 60 Hz field rates) capable of simultaneously meeting the very high target raster resolution and the very high background brightness levels (needed because of the inefficiency of the demagnifying optics).

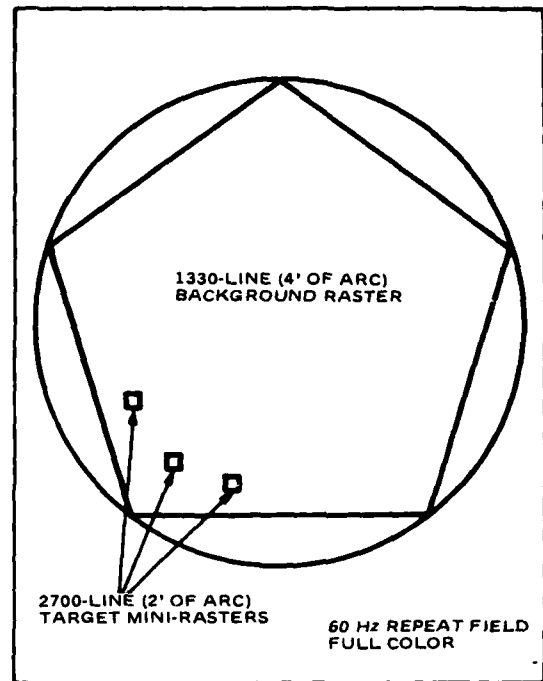


Figure 1. Baseline Requirements for Project 2363. The requirements shown represent a significant challenge to the Visual System.

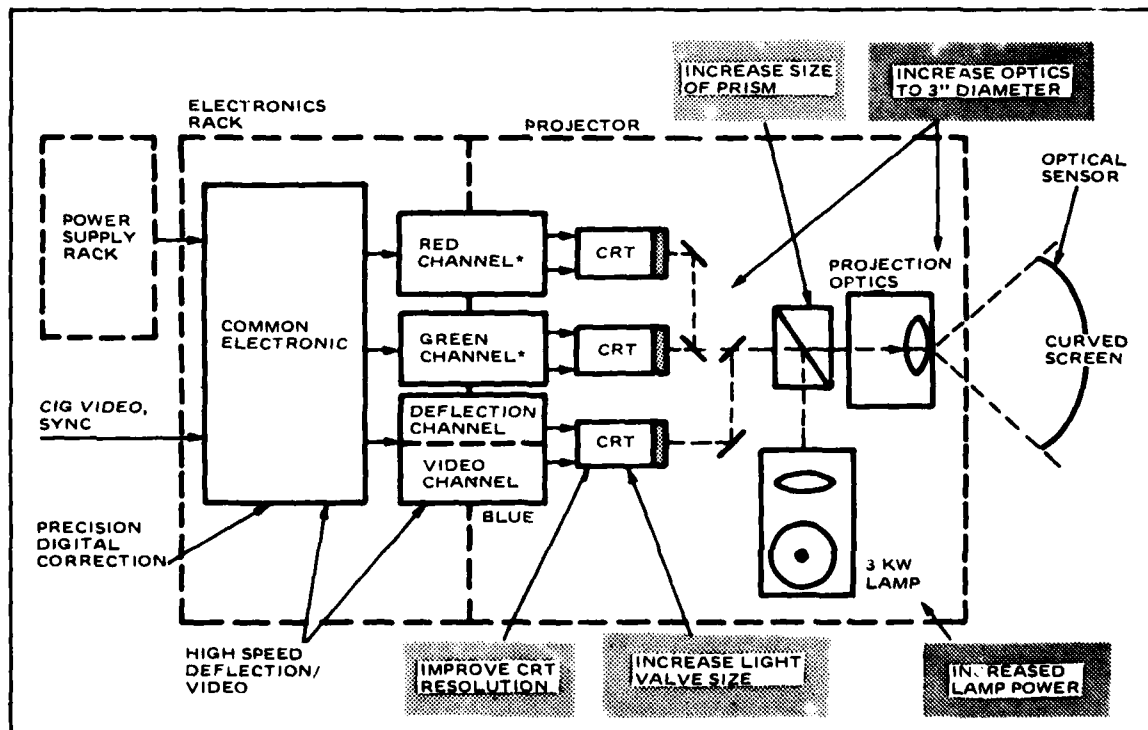


Figure 2. High Performance 2363 - Compliant Projector Configuration. The key to meeting target raster resolution, the critical parameter, is increasing the light valve prism and CRT size to 3 inches. High-speed CRT drive circuitry and sophisticated digital circuits, driven by stored correction values, ensure that high resolution and color convergence are maintained over the full displayable area.

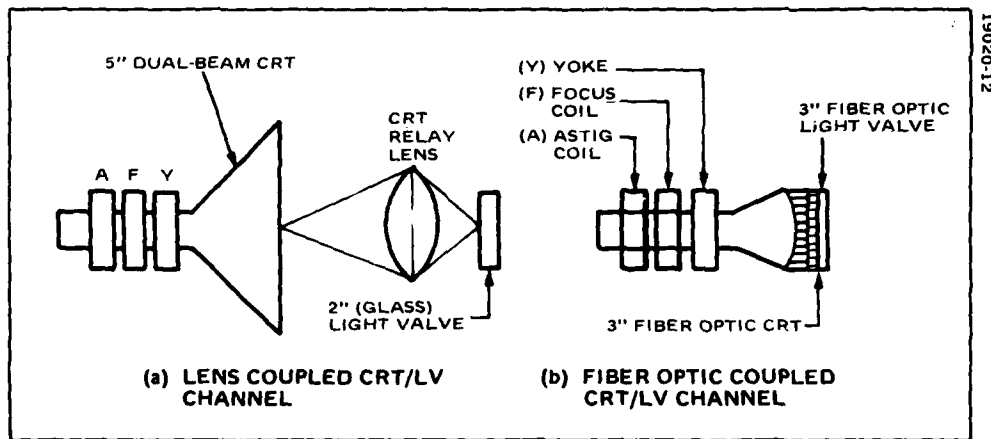


Figure 3. Comparison of Fiber-Optic and Lens-Coupled CRT/Light Valve Image Channels. The former is selected for the 2363 projector even though it requires a 3" light valve, because it is more compact, requires less brightness because of the higher optical coupling efficiency and does not require the development of a high risk dual beam CRT.

Furthermore, this approach demanded higher resolution from the light valve than was available and also resulted in a projector plate too large and heavy to be mounted on a dodecahedron structure. The second projector approach (Figure 3(b)), although limited in resolution by the CRT line width, was nevertheless found to have the requisite projection package – based on the assumption that increasing the size of the light valve, the polarizing prism, and the fiber optic CRT and increasing the resolution of the latter was indeed feasible. Although there was significant risk in developing these components, these risks were judged to be lower than for a dual beam CRT, and the lower weight and size were judged to be a considerable advantage. For these reasons, the second approach was selected as the baseline approach to meeting 2363 requirements.

An overview of the implementation of this 3" LCLV projector developed during the Phase I study is given in Figure 2. The figure highlights the differences between this projector and the full color projector developed under Project 1958. These differences are attributable to the need to meet the stringent requirements of resolution, color convergence (at the high resolution), raster inseting (without detecting raster outline) for three targets, noninterlaced 60 Hz operation and increased light output. Specific component features and hardware implementation techniques to meet these requirements are briefly summarized below.

- **Resolution.** Increase "usable diameter" of light valve and CRT by a factor of $3.0"/1.8" = 1.67$ (note: 2" light valve has usable diameter of only 1.8"). As a consequence, increase diameter of all appropriate illumination and projection optics components as required. Increase resolution of CRT by reducing the line-width from 1.1 mil to 0.6 mil. Match or exceed upper 20 percentile resolution of LCLV (50% square wave MTF at 20 cycles/mm). Curve inside

(phosphor) surface of CRT fiber optic faceplate, and provide digitally mapped focus and astigmatism programming to minimize loss of resolution across the field of view.

- **Color Convergence.** Provide novel color convergence technique based on digitally mapped and stored correction points. (Note; a variation of this technique has since been incorporated in a two-channel liquid crystal projector.) Use stable deflection circuits and provide optical feedback off screen to correct for residual position and gain drift. Provide microprocessors-aided interpolation to assist operator with rapid convergence alignment of the whole display area. Provide sufficient dynamic range on color convergence circuitry, so that the techniques implemented to achieve convergence can be used to linearize the display over the full field of view and to edge match with adjacent windows.
- **Inset Raster.** Provide precision linear deflection circuits to accurately position target rasters. Provide specially shielded magnetics on CRTs to minimize magnetic hysteresis effects which can cause target/background misregistration. Provide capability to dither background raster lines to eliminate line structures.
- **60 Hz Operation.** Shape raster to be pentagonal to eliminate wasted trace time. Use trace-trace (vs trace-retrace) mode of raster writing to minimize time required for retrace, and to provide the necessary compensation in the convergence circuitry to minimize misalignment of adjacent lines. Provide a 100 MHz pixel data rate capability, with digital gamma correction to avoid excessive degradation of the video signal due to gamma correction. Increase CRT anode voltage to 22 KV, and provide high beam current capability to provide the dithered highlight brightness to drive the light valve at the high background raster writing rates.
- **Increase Light Output.** Increase lamp power to 3.0 KW (note: with recent improvements in illumination system efficiency this should not be necessary). Coat all lens surfaces to minimize optical losses. Optimize dichroics to achieve best balance between efficiency and color range.

As shown, a number of sophisticated techniques must be employed to meet the specified requirements. Despite the apparent complexity, design analysis during the Phase I study showed that these techniques could be implemented with a reasonable number of circuits: 18 analog assemblies and 60 5" x 5" high density digital and analog circuit boards for the three channel projector. It was concluded that, assuming the three critical components could be developed, a 4' of arc background, 2' of arc target 60 Hz noninterlaced field full color visual system was entirely feasible.

2363 COMPONENT DEVELOPMENT PHASE (CDP)

To limit projector development risk, it was decided to first develop its three critical components. This component development phase (CDP) of the program was started in June, 1979 with the following stated objectives:

- To develop the three components critical to implementing a compliant projector: the 3", 0.6 mil fiber optic CRT, the 3" polarizer/analyzer prism, and the 3" light valve.

- To integrate these components into a working 3" monochrome breadboard projector and demonstrate operation with test patterns and television video.
- To confirm by testing that the projector has desired target and background resolution under conditions simulating those in the final projector.

3 Inch High Resolution 0.6 Mil CRT

The cathode ray tube is one of the important components in the system in terms of achieving the desired projector resolution. There are three major requirements that the CRT has to meet: 1) line width at the low writing rate of 10 Kips must be 0.6 mils or better for the target raster, 2) line width at the high writing rate of 300 Kips for the background raster must be less than 1.1 mils, and 3) the CRT useful screen size must be 3" or greater. The challenges in designing this tube were depositing the phosphor to yield the desired combination of resolution and efficiency for the target and background rasters respectively, building a gun capable of providing the desired line widths for the two widely different raster writing rate conditions, and building a 3" fiber optic CRT for which the fiber optic quality was acceptable over the full usable area.

The first two objectives were met with unqualified success. Development of the phosphor was the achievement of a major effort by the CRT supplier, Thomas Electronics. A number of phosphor types, weights (particle sizes) and layer thicknesses were tried before the final formula was found for meeting the resolution and efficiency requirements. It was concluded that P1 phosphor is the best, that line width as low as 0.5 mils is feasible, and that the resolution is primarily limited by phosphor particle size, as opposed to CRT gun limitations. In the design of the gun the challenge was to simultaneously obtain high resolution at low writing rates and a medium high resolution at very high writing rates, in high beam currents. These conflicting objectives were achieved: a 50% linewidth of 0.5 mils (20% better than required) was measured at 10 Kips, and a line width of 0.9 mils (~20% better than required) was measured at 300 Kips. Several iterations on tube design were required to achieve these results. Two deliverable assemblies were built by Thomas. The first one, with a 4" diameter faceplate, was delivered in July, the second, with a 2" diameter faceplate, was delivered in late October (see Figure 4). The latter exhibited the required performance. The two inch faceplate was selected for the second assembly in order to obtain the desired fiber optic faceplate quality. However, one can confidently extrapolate performance of this 2" CRT up to the 3" size. The magnetics (identical for the two tubes) on both CRTs were excellent, with both exhibiting a falloff in resolution of less than 15% over the usable area.

A problem was encountered with the fiber optic faceplate. The original supplier of quality fiber optic faceplates went out of business and was bought out by another fiber optic house. The latter company was unable to transfer the technology for making the very high quality, chicken-wire free numerical aperture 1.0 face plates, and consequently was unable to meet Hughes' requirements in the first CRT assembly. Thus, a 2" faceplate, available from a previous order, was used to assemble the second CRT, which is currently being used in the 2363 breadboard projector. The one remaining issue in the CRT development area then is to find a vendor capable of supplying the high quality fiber optic plates which do not exhibit chickenwire and can be supplied in the 3" size. Discussions with Galileo and Incom reveal this should be possible with some

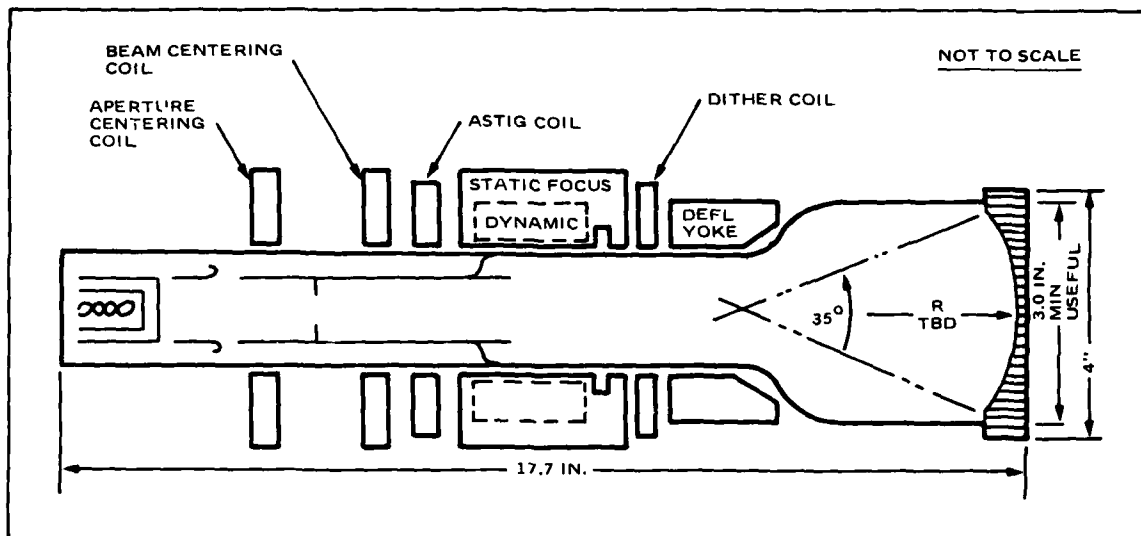


Figure 4. 2363 CRT and Magnetic Component Layout. The magnetics are potted in place around the CRT (the high permeability magnetic shield is not shown). A 2" version of this design has exceeded both target and background resolution goals and represents a significant advance in the state-of-the-art of light-valve driving CRTs.

development effort, assuming that the numerical aperture can be reduced from 1.0 to 0.66. Given the sensitivity of the SiLV, this is feasible. In fact, experimental MTF test results showed that a reduced numerical aperture is desirable, because it reduces the criticality of maintaining very close contact between the CRT and the light valve.

In summary, the final CRT meets or exceeds all requirements except for size. It has better than required resolution up to writing rates of 30 Kips (new IG requirement), good resolution uniformity, and provides the required brightness for all operating modes. It was also found that achieving this resolution is a low yield process, and it is felt that attempts to further improve linewidths are probably not cost effective. The one remaining problem - quality 3" fiber optic faceplates - appears to be tractable.

Index Oil Prism. Two parallel approaches to implementing a 3" prism were investigated: a fused silica prism and an "index oil" prism. Of the two, the latter emerged as the clear choice (see Figure 5). When used with a prepolarizer, it provides very high performance, whereas the fused silica prism is marginal at best. In addition, the index oil prism is not burdened with the single source procurement and delivery-time problems which plagued the fused silica prism.

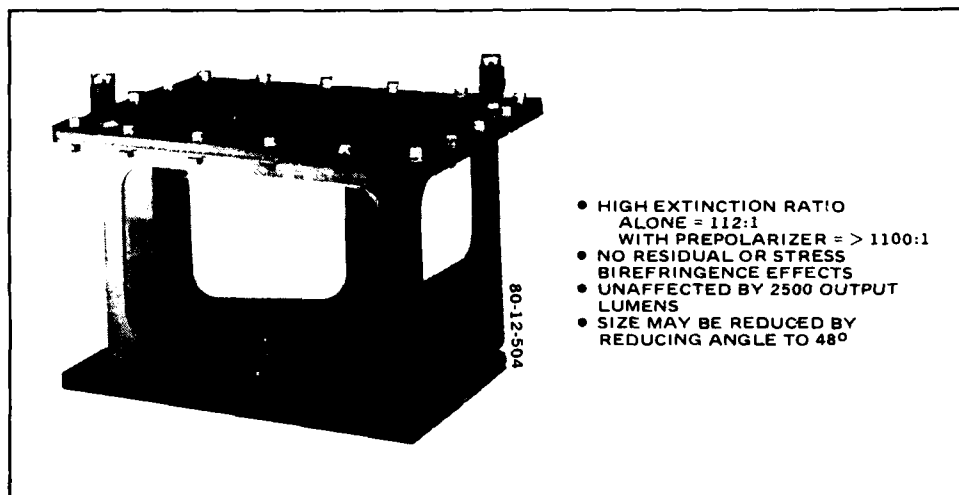


Figure 5. The 3-inch, 58° Oil Polarizer/Analyzer Prism. In conjunction with a prepolarizer of the same type, an extinction ratio of over 1100 was obtained. The index oil approach was selected over the solid glass fused silica prism because of its excellent performance, lower cost, and shorter procurement lead time.

Using two identical 58° index oil prisms in a prepolarizer – polarizer combination, a contrast ratio of >1100:1 was demonstrated. The prism seemed to be unaffected by the heat of the 2500 lumen (at the output) illuminating beam, and did not seem to be affected by vibration.

The two prisms in the 2363 breadboard occupy a considerable volume. This is attributable to three factors. First, a 58° angle was chosen to maximize contrast ratio and to permit comparison of the index oil prism's performance with that of the 2" fused silica prism, which had been built at 58°. Second, prism size was made large enough to accommodate any conceivable cone angle of the illuminant beam. Third, separate prepolarizer and polarizer prisms were used. In a productized design, prism angle will be reduced to 48°, which will reduce size but still yield a contrast ratio of greater than 500:1. Size will be tailored to a reasonable cone angle illumination system, and the prepolarizer and polarizer functions will be combined into a single prism assembly. Implementing these three changes should yield a volume reduction factor of greater than x 2.5.

3" CdS Light Valve. Before discussing the results of the 3" CdS component effort, it is appropriate to discuss a decision (later reversed) made at the start of the CDP effort which had a significant impact on this phase of the Hughes 2363 program. Determining the course of action on the CRT and the polarizing prism was straightforward. However, the light valve posed the following dilemma: The two major requirements imposed by the light valve are increasing size to 3" on the one hand and improving time response of the light valve on the other. It was clear that the Cadmium Sulfide Light Valve (CdSLV) in production at Hughes Carlsbad would not be able to meet the better than 20 ms response required to support a 60 Hz refresh system. The

silicon photoconductor light valve (SiLV) was the obvious candidate to solve this shortcoming. But at the start of this phase of the program in June, 1979, the SiLV was still very much an R&D device: it had not yet been built in the 3" size, it had demonstrated resolution only half as good as that required, it had exhibited severe edge breakdown problems, it had marginal contrast, and it had not yet been operated in a fiber-optic CRT driver mode with dynamic television imagery. For that matter, its response time — limited by the liquid crystal material — was only marginally adequate for 30 Hz and not good enough for 60 Hz operation. Consequently, it was decided to opt for developing a 3" CdS LV to prove the feasibility of a 3" size light valve on the one hand, and to provide a means of implementing a 3" breadboard system as a way of testing the other components on the other. A year later, when the program was reviewed, sufficient work had been done to establish feasibility of building a 3" CdSLV. Meanwhile the SiLV had made substantial progress during the previous year, so that it appeared close to being operable in a high light output projector. It was therefore decided to discontinue the 3" CdSLV effort and to devote the remaining funds to support the SiLV effort at the Hughes Malibu Research Laboratories (where an ongoing SiLV effort had been funded by AFHRL on a separate 2363-associated R&D contract).

In view of these facts, the subsequent discussion in this section will cover the 3" CdS LV and will describe the breadboard projector built to integrate it with the other two CDP-developed components. The following section will cover in detail the SiLV, the key element in applying liquid crystal projectors to simulation visuals.

The results of the 3" CdSLV effort were impressive, considering that only two 3" light valves were constructed (ten had been planned): the second of these light valves showed surprisingly good performance. Although it fell short of the specification on resolution and brightness uniformity, it did demonstrate that no fundamental problems arose in going to the 3" size. Relevant to the SiLV, it was found that the 0.5" f/o plate and the 0.5" glass counter electrode plate were sufficiently rigid to maintain a uniform 3.5 μ liquid crystal thickness across the 3" light valve. Equally relevant to the SiLV, much of the tooling developed for the 3" CdSLV is expected to be usable with the SiLV when its dimensions are increased to 3".

The 3" CdSLV was installed in the breadboard projector and driven by the 3" (useful screen) fiber optic CRT to demonstrate a full 3" system to AFHRL and General Electric at the August, 1980 engineering design review. Because of the poor quality of the CRT fiber optics and line width, only a limited number of measurements were taken using either limiting TV resolution or shrinking raster technique (<15%) over the usable area.

Breadboard Projector. The breadboard projector integrates the critical components developed on the Component Development Phase (CDP) with appropriate optics and electronics to demonstrate that system resolution goals have been attained for both the target and background rasters.

The breadboard projector was laid out on an optical plate to permit easy access to all components (see Figure 6). Part of the projector is the group of three critical components: fiber optic CRT, the light valve, and the prepolarizing and polarizing index oil prism. The CRT is driven by medium speed 1000-line electronics using linear amplifiers. Various raster modes selected at the control panel are provided to realistically simulate the target and background raster operating conditions of the final system. Power supplies are

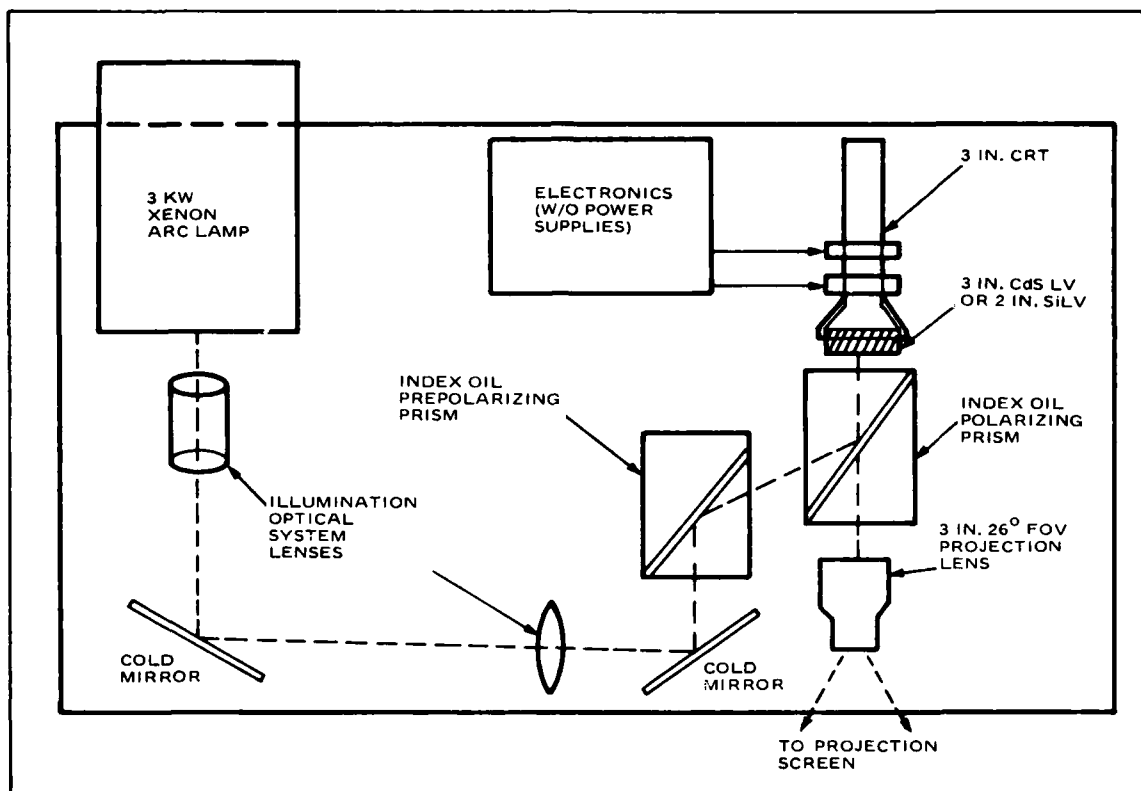


Figure 6. Optical Layout of Breadboard Projector. The projector combines the newly developed components to generate, using the 3 inch CdS light valve, a projected display having a limiting resolution of well over 3000 TV lines (extrapolating target resolution to width of projected pentagonal image).

mounted in a rack remote from the optical plate. Illumination is supplied by a 3.0 KW xenon arc lamp assembly featuring a nutated elliptical reflector which is housed in an off-the-shelf commercial lamp house, with the light collimated by the two lenses of an illuminating optical system. Cold mirrors remove the heat from the beam. The prepolarizing and the polarizing index oil prisms further filter the IR energy and yield a very high extinction ratio which eliminates the prism as a factor affecting the system contrast ratio. A custom designed 3" telecentric projection lens images the light valve generated polarized pattern on a 60" diameter round screen at a distance of 20 feet. The lens provides modulation in excess of 90% at the spatial frequency corresponding to two minutes of arc. These optical elements combine to project 2500 open gate lumens with a brightness non-uniformity of less than 15% over the quality circle.

To permit the use of off-the-shelf electronics in order to minimize the cost of building the breadboard projector, it was decided to measure the background raster (under realistic writing rate conditions) using the shrinking raster method. Vertical and horizontal rasters to measure either vertical or horizontal resolution are provided. The target raster is generated by a standard 525 line TV input, with the raster size variable to

change the effective resolution from approximately 0.5 min of arc to 3 min of arc, and with the raster positionable anywhere on the displayable area to verify resolution uniformity.

The breadboard projector was operated in two modes. Initially, the first delivered 4" CRT was used to drive a 3" CdSLV. As a result of the shift to the SiLV, and because the 3" fiber optic CRT faceplates were not available without chickenwire artifacts, the final projected configuration featured the very high quality 2" fiber optic CRT driving either a 2" SiLV or CdSLV.

This breadboard system was used to determine the projector resolution obtainable with a 3" liquid crystal light valve system, using either a CdS or a silicon light valve. The results of these tests are summarized in the section following the one below which describes the construction and performance of the SiLV.

DESCRIPTION OF THE SILICON PHOTOCONDUCTOR LIQUID CRYSTAL LIGHT VALVE

The key to the successful application of liquid crystal light valve technology to simulation is the Silicon Photoconductor Light Valve (SiLV). Although attempts to improve time-response characteristics of the Cadmium-Sulfide Photoconductor Light Valve (CdSLV), currently in production to support a growing line of graphic large screen display products, resulted in significant improvements, achieving the fast response time required to meet the needs of simulation does not appear practical with this light valve. For this and other reasons Hughes decided to investigate the feasibility of a silicon photoconductor-based light valve. Having established its feasibility in 1976, an IR&D program was initiated to develop a device which gives not only better time-response but also promises higher sensitivity, contrast ratio and resolution. With the Hughes IR&D program complemented by support from AFHRL under Projects 1958 and 2363 and additional support from NTEC, NAVSEA and PM-TRADE, development of the device has progressed rapidly over the past two years. To illustrate this progress, Figure 7 shows the improvement in the limiting resolution obtained with SiLVs over this span of time. Today the basic SiLV configuration is well established and, except for some device engineering issues to be resolved, the light valve can provide performance (although not cosmetic quality) comparable to that of the CdSLV, and with much better time response. Consistently good cosmetic quality will be achieved when the light valve is transferred into a production environment.

To gain historical perspective and an appreciation for its comparative advantages, it is helpful to view the SiLV as an evolution in the state of the liquid crystal light valve art. The generic advantages of a liquid light valve as a projection technique are numerous, with three of these particularly relevant to simulation visuals. First, the light valve modulates ("valves") an externally generated light beam with a liquid crystal layer which does not absorb light but simply changes its polarization. High light output levels are therefore achievable. Second, the technique is not constrained to a raster-only mode of operation, a feature which is very valuable in a variety of simulation applications. Finally, the light valve is photo-activated (as opposed to being modulated by an electrostatic charge as in most other light valves), which results in separating the light valve function from the image generating function and its complexities - the latter function typically being performed for the photo-activated light valve by a high resolution fiber optic faceplate CRT which can be designed and built independently of the light valve. This

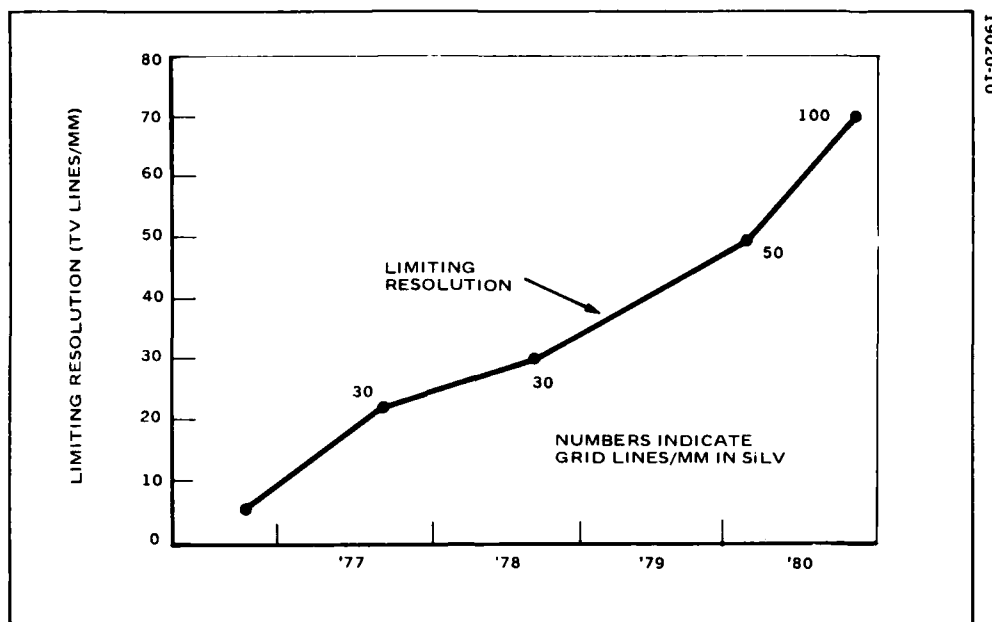


Figure 7. Progress in Limiting Resolution Obtained with the SiLV. Steady increase in resolution is attributable to increasing the grid spatial frequency, (see Figure 10 for details), and continued improvements in silicon processing and mirror deposition, respectively.

separation of the image generation and light valving functions is in turn beneficial for several reasons. Devices which combine these two functions are typically complex, hard to maintain and expensive. By comparison the LCLV is simple, easy to maintain, and should be lower in cost once in production. In addition, separation of the two functions allows each one to be optimized individually, thus providing a great deal of flexibility in adapting the technique to a variety of applications without costly re-engineering of a complex device. The accomplishments on the 2363 program attest to this flexibility.

To introduce and describe the SiLV, a brief description of the basic principles of operation of the liquid crystal light valve is given, followed by a comparison of the silicon and CdS light valves and a description of the theory of silicon light valve operation. Finally, the performance levels obtained with SiLVs built to date are summarized.

Description of the Generic Liquid Crystal Light Valve. A simplified explanation of the generic hybrid field effect (liquid crystal) light valve is given here for reference; more detailed description of the device and its operation can be found in the literature.⁽¹⁾ Figure 8 shows the construction of the device.

The principle of operation is best described by initially considering the cell simply as a photoconductive layer and a liquid crystal layer of small thickness sandwiched between two transparent conductive surfaces. With the photoconductor unexposed, a bias voltage applied to the two transparent conductive surfaces appears directly across the photoconductive layer, leaving the liquid crystal in its normal clear state. When the photoconductor

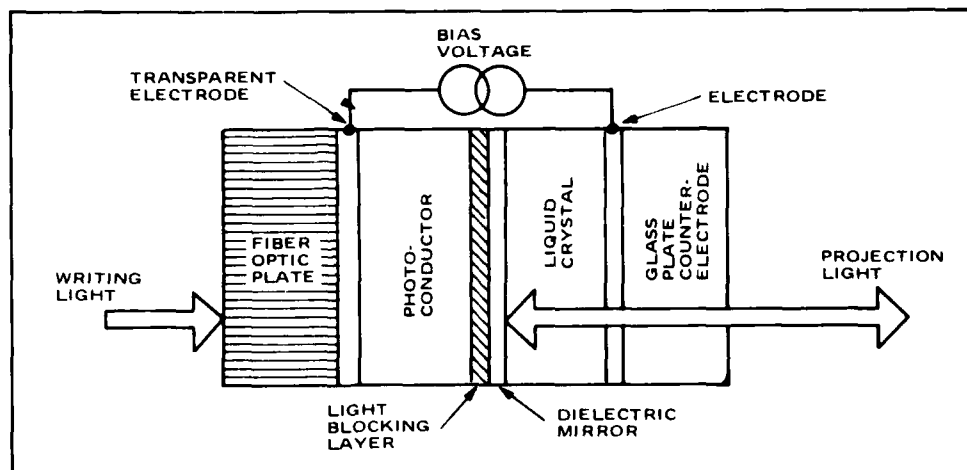


Figure 8. Construction of the Liquid Crystal Light Valve. Basic elements of the liquid crystal light valve are the same for the CdS and silicon photoconductor light valves. The two differ in the photoconductor material, thickness, the type of bias voltage, and the method of implementing the light function. Note that the figure is not drawn to scale; blocking the thickness of the fiber optic and glass counter-electrode plates is 0.5 inch (12.5 mm), whereas the active layers are approximately 1.5 to 5 mils (35 to 125 μ).

is activated by light, its impedance drops, and the bias voltage is applied across the liquid crystal layer causing the image exposing the photoconductor to be reproduced as a birefringent pattern in the liquid crystal light valve. To project this liquid crystal image, a dielectric mirror is inserted directly behind the liquid crystal layer. The cell is illuminated with near-collimated polarized light which travels through the liquid crystal layer, is then reflected by the dielectric mirror, and passes through liquid crystal a second time before being projected.

In the areas where the liquid crystal material has been activated by the voltage which varies with light input, the liquid crystal birefringence causes a rotation of the axis of polarization, which then permits the light to pass through a (prism) analyzer to the screen. To prevent the polarized projection light from exciting the photoconductive layer, an opaque, light-blocking layer may be inserted between the dielectric mirror and the photoconductive layer. This stack of thin film layers (i.e., the two transparent conductive layers, the photoconductor, the light blocking layer if required, the mirror and the liquid crystal layer) is sandwiched between a 12.5 mm thick glass plate on the projection side and a 12.5 mm glass or fiber optic plate on the input side.

Comparison of CdS and Silicon Light Valves. Figure 9 graphically illustrates the differences between the two light valves. The silicon photoconductor is a thin wafer (5 mil) as opposed to the CdS thin film layer; it is much thicker (by a factor of five) than the CdS. The lower capacitance and higher capacitive impedance associated with the increased thickness result in the ability to swing a wider range of voltages across the liquid crystal and therefore yield a higher contrast ratio. The silicon, instead of

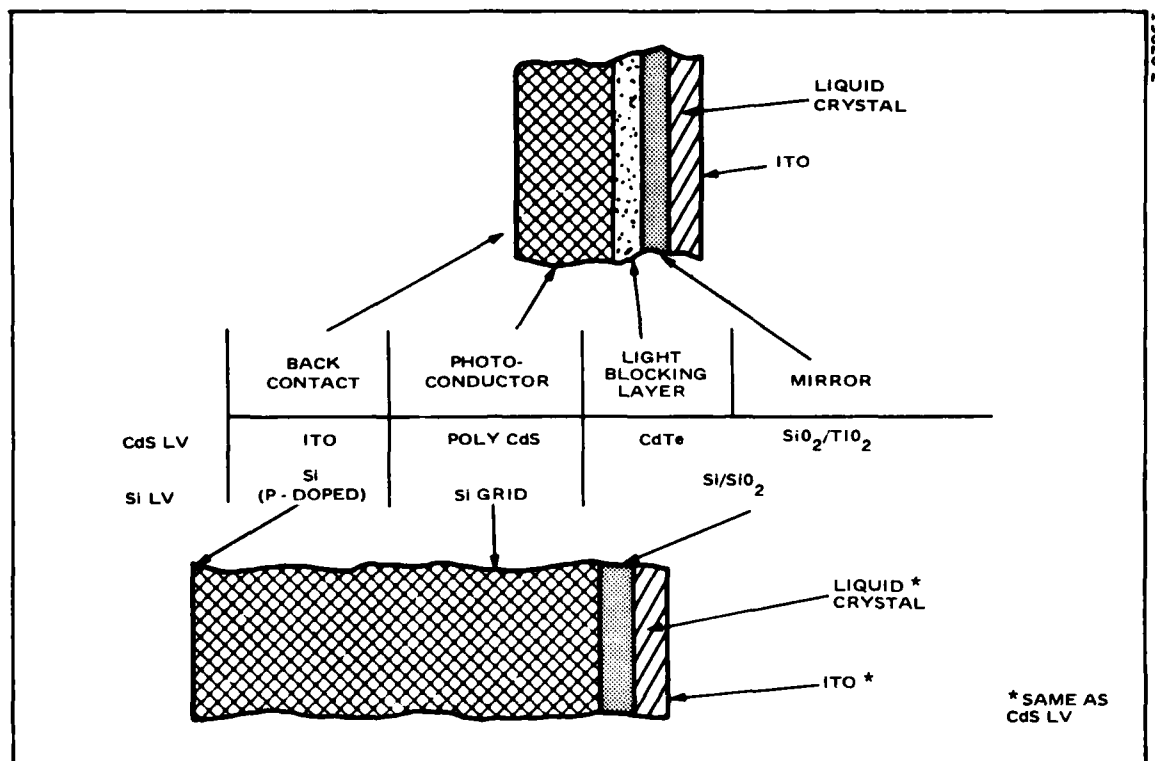


Figure 9. Comparison of Cadmium Sulfide (CdS) and Silicon Photoconductor Light Valves. The all-silicon construction of silicon light valve results in a simpler, more producible device with the potential for superior performance.

being sputtered down on the fiber optic plate as a thin film layer as the CdS is, is a thin wafer which must be attached to the plate and flattened to make the liquid crystal layer of uniform thickness. The silicon photoconductor is more sensitive, and sensitive over a wider range of the spectrum (approximately 0.4 to 1.1 micron), than the CdS. While this means that less imaging light is required to drive it (an advantage), it does demand of the light blocking layer a greater absorption over this wider spectral range. Fortunately, it appears feasible to combine the functions of light blocking and light reflection in a single Si/SiO₂ mirror which simplifies the overall device structure. A further difference between the two light valves is the back contact; this is an ITO thin film for the CdSLV and a heavily doped layer in the wafer for the SiLV.

In terms of overall device construction, the SiLV appears to be much simpler. Fewer layers are required and, perhaps more importantly, the number of materials used is drastically decreased. This, coupled with the use of a more mainstream material (silicon), should make the SiLV a much more producible device.

There is another significant difference between the two devices. While the CdS photoconductor is a continuous thin film which depends on its high lateral impedance to reduce image spreading and thus obtain good resolution, in the SiLV, the surface effects at the

MOS interface will cause the image to diffuse unless some precautions are taken. Thus, the SiLV requires a grid structure to confine the photo-generated charge pattern; this is illustrated in Figure 10(a). The left side shows the photoelectrons generated close to the back surface being driven across the depleted silicon toward the right hand surface where they are collected in heavily doped islands ("charge buckets") defined by the grid structure shown in Figure 10(b). If the field across the silicon wafer is maintained, the exposing image will generate a corresponding charge pattern at the right hand (mirror) side of the wafer, subject to some degradation because of the charge averaging action of the charge buckets. To keep the buckets from filling up and spilling over (thus causing the image generated charge pattern to wash out), the voltage is periodically briefly reversed (accumulation phase, see below) to empty out the buckets and start the image generation cycle over again. Because of the above, the SiLV requires a pulsed biasing voltage instead of the sinewave voltage used by the CdSLV.

In summary, the basic operation of the SiLV requires a grid structure which limits the resolution performance of the final device. Three grid structures of increasing resolutions have been implemented to date: 30, 50 and 100 grid lines/mm. The bucket sizes and spacings corresponding to these frequencies are shown in Figure 10(b). In theory, 150 grid lines/mm should be feasible; in practice, the best limiting resolution

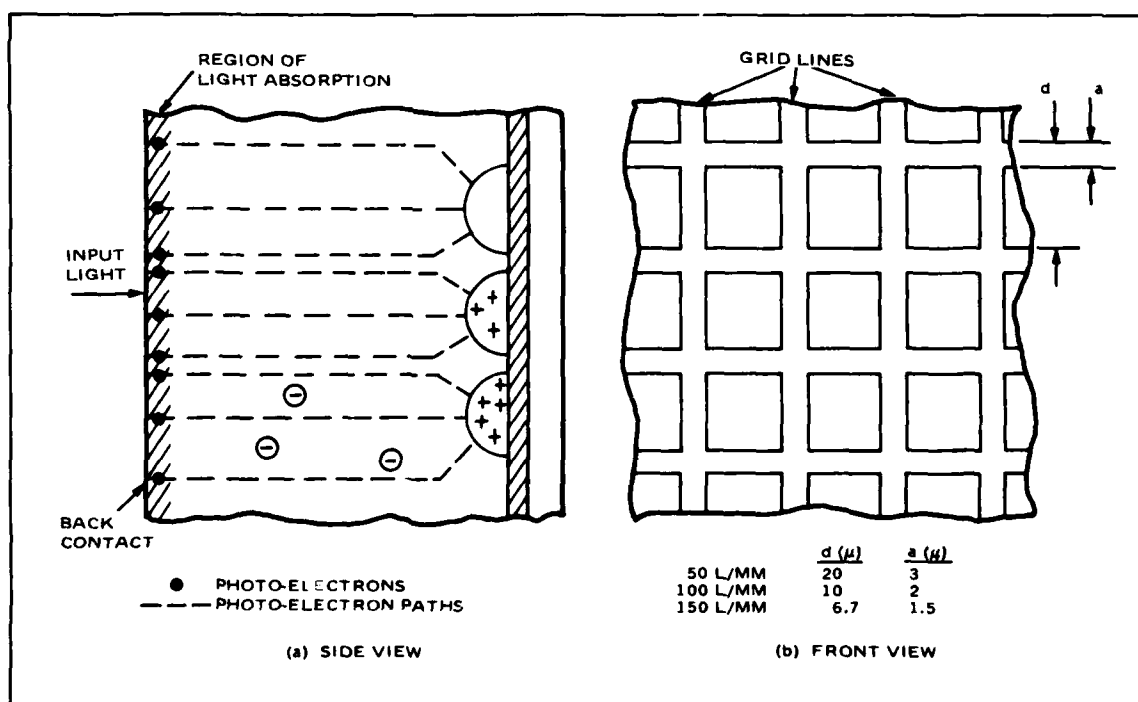


Figure 10. Illustration of Image Resolving Mechanism in the SiLV. Photoelectrons generated by light absorption near the back contact travel across the depleted silicon wafer and are collected in the heavily doped square regions which act as "charge buckets" to store the image temporarily. Spatial frequency of the grid lines which define the buckets is the primary factor in determining light valve resolution.

to date with the 100 grid lines/mm has been 70 lines/mm. For this case the grid pattern is no longer observable in the projected image (thus no aliasing occurs), indicating that a mechanism other than the grid structure limits device resolution.

Advantages of the SiLV over its CdS counterpart are briefly summarized as follows:

- Higher sensitivity due to silicon photoconductor.
- Faster response (limited by the liquid crystal) due to silicon photoconductor.
- Higher contrast ratio/brightness due to thicker photoconductor/higher switching value.
- Simpler device construction, with potential for better manufacturability.
- Potential for higher resolution – if theoretical limits are realized with improved processes.

SiLV Theory of Operation. The SiLV is based on a thin wafer of high resistivity, single crystal silicon as the photoconductor. The device consists of the silicon photoconductor coupled with an oxide layer to form a MOS structure. The readout beam is retro-reflected by means of a dielectric Si/SiO₂ mirror through the liquid crystal operating in the hybrid field effect mode. As mentioned above, this mirror also acts as a light blocking layer which serves to optically isolate the photoconductor from the high intensity readout beam. The MOS mode of operation consists of periodic depletion and accumulation phases. In the depletion (active) phase, the high resistivity π -silicon is depleted completely, and electron hole pairs generated by the input light are swept by the electric field, thereby producing the signal current that activates the liquid crystal. The signal electrons residing at the Si/SiO₂ interface are recombined by pulsing the MOS into a short accumulation phase. The spatial resolution of the input image across the silicon is retained by means of a boron-implanted p-grid at the π -Si/SiO₂ interface. The grid acts to focus the incoming electrons into the resolution cell defined by it, as well as to form charge "buckets" of the electrons already residing at the Si/SiO₂. This prevents lateral "spill-over" and consequent smearing of the charge pattern. A p⁺ (boron) ring is diffused at the silicon edge to prevent peripheral minority carrier injection into the active region. A thin layer of fast response, positive anisotropy, liquid crystal with a 45° twist angle is employed as the light modulator. The input electrode consists of a fiber-optic faceplate coated with indium tin oxide. A liquid crystal spacer as well as an indium tin oxide conductive layer are deposited on the front glass electrode. The whole structure is assembled within an air tight anodized aluminum holder as shown in Figure 11, which also shows a photograph of the finished light valve. The light valves produced feature a 1.6" clear aperture.

SiLV Performance. The table summarizes the significant performance levels of SiLVs built to date and compares them with the requirements of Project 2363. Figure 12 compares the MTFs for the highest MTF SiLVs with two CdSLVs, one of them a representative sample and the other one of the highest resolution CdSLVs built.

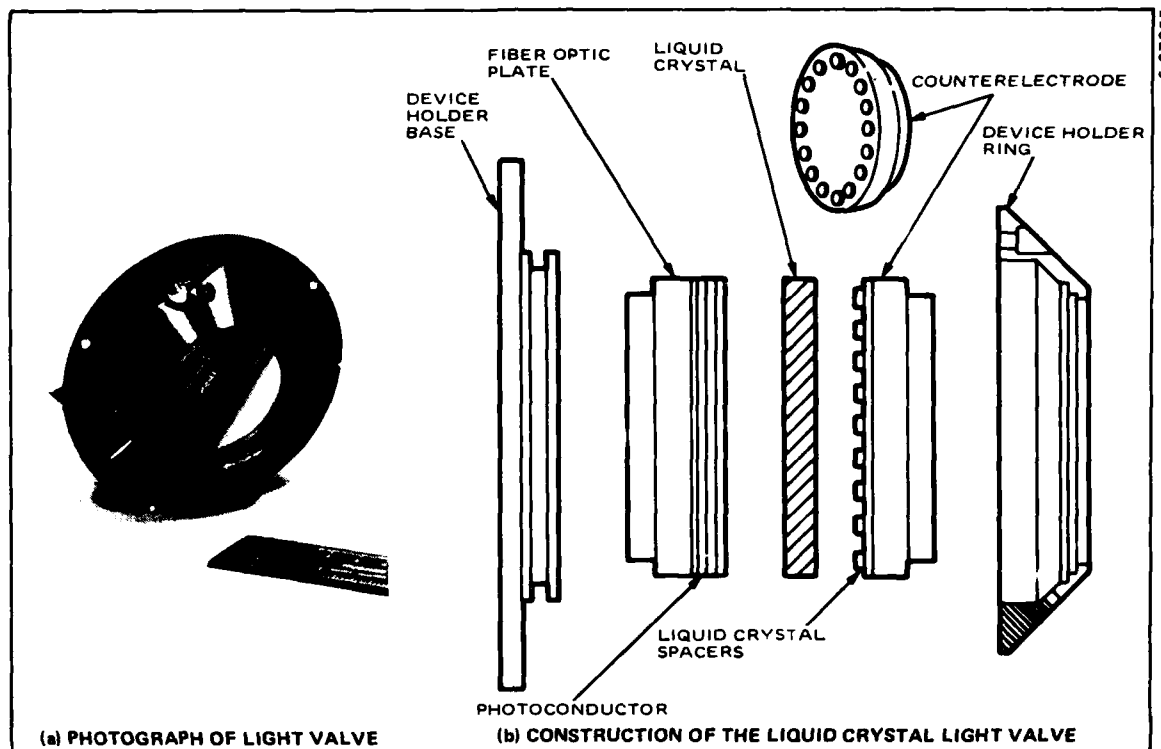


Figure 11. Hardware Characteristics of the Liquid Crystal Light Valve. The light valve is a compact (3.0" diameter, 1.5" thick), rugged device. In the CdS light valve, the CdS photoconductor is a thin film layer sputtered on the fiber optic plate; in the SiLV the photoconductor is a 5 mils thick silicon wafer which is independently processed and is then attached to the fiber optic plate.

As shown in the table, the ability to meet or exceed the required performance levels has been clearly demonstrated in the areas of contrast ratio (although at low light levels only), sensitivity and response time. Resolution to meet the requirements of a 2' of arc (2700 TVL/width at 20 percent MTF) has not been achieved; when the grid density was increased from 50 to 100 grid lines/mm, the light valve MTF did improve at the higher spatial frequencies (limiting resolution went from 50 to 70 TVL/mm) but did not improve modulation at the spatial frequency corresponding to 2' of arc (38 TV lines/mm). Further progress in exploiting the 100 grid lines/mm technology is expected to match the best CdSLV resolution (sufficient for 2' of arc) in the near term, and is also expected to approach the 1.5' of arc capability in the long run. Although performance falls short in three other areas (contrast ratio, switching ratio and maximum light-blocking level), these are degraded by a Si/SiO₂ mirror with inadequate light-blocking capability. This shortcoming can be corrected by an improved mirror design. A further shortcoming at the time of this writing is poor uniformity due to the fact that no effort had yet been made to attach the wafer to the fiber optic plate; the wafer was allowed to "float" freely. Implementation of a wafer attachment approach is expected to result in a uniformity of 30% or better in the near future. It should be noted that the best performance capabilities

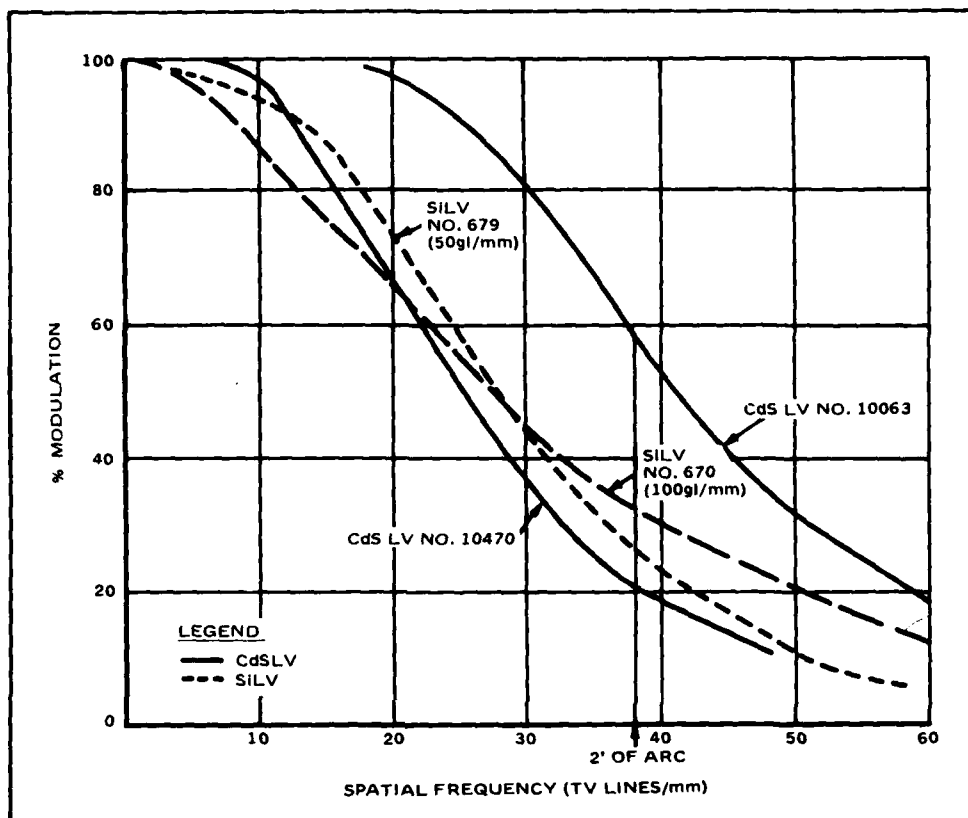


Figure 12. Comparison of the MTFs of the Best 50 and 100 Grid Lines/mm SiLVs with a medium and a high-resolution CdSLV. The silicon light valves exhibit resolution comparable to that of an average CdSLV, with the 100 grid lines/mm SiLV demonstrating better limiting resolution.

listed in the table have not been combined in a single device as yet, although this appears to be primarily a matter of yield rather than due to fundamental device limitations. Hughes is confident that the planned 1981 effort will meet all stated performance requirements. Further activity is expected to confirm the feasibility of increasing the light valve size to 3 inches.

RESULTS OF BREADBOARD RESOLUTION TESTS

Resolution tests were conducted for the breadboard projector using the two CdS light valves (Nos. 10063 and 10470), for which MTF curves are shown in Figure 12, and several of the 50 and 100 grid-line/mm SiLVs built. The projector MTF plots for these two CdSLVs and the SiLVs yielding the best projector-level response are shown in Figure 13. All of these tests were taken in a projector configuration in which both the CRT and the light valves were 2 inches in diameter for reasons previously discussed. First, for the CRT the final 2 inch assembly provided the best fiber optic quality and the best line width. Second, the SiLV was available only in the 2 inch size. Finally, although a 3" CdSLV was constructed, its resolution was not

TABLE OF CURRENT STATUS OF SiLV PERFORMANCE CAPABILITIES

Parameter	Achieved	Required by 2363
Size	1.6" usable	3.0"
Resolution: MTF @ 2' of arc	22% to 31%	55%
Contrast ratio	5:1 to 100:1 ⁽¹⁾⁽²⁾	50:1 (100:1 goal)
Sensitivity	10 to 30 uw/cm ²	40 uw/cm ²
Response time (decay to 10%)	10 to 40 ms	20 ms
Illumination level	2000 to 4000 fc ⁽²⁾	12,000 fc

- (1) High contrast ratios (10:1) and switching ratios obtainable only at low light levels.
 (2) Requires redesign of mirror in SiLV to optimize light blocking capability.

as high as required (i.e., as high as that of CdS LV No. 10063 Figure 12); projector MTF measurements were therefore made with both the No. 10063 CdS LV and a CdSLV (No. 10470) having MTF characteristics approximately those of the 3" CdSLV.

The square wave MTF measurements shown in Figures 12 and 13 were taken in the breadboard projector using one of the following techniques. To characterize the light valves (see Figure 12), a chromium-glass Sayce chart was placed in close optical contact with the fiber-optic plate of the light valve, and the test chart was back-illuminated by a bright unmodulated raster displayed on the CRT. The resulting aerial image in the plane of the screen was scanned by a 0.25 mil slit/photodiode assembly mounted on a motorized translation stage, with the amplified photodiode output recorded on an XY recorder driver horizontally in synchronism with the translation stage. The relative modulation was then derived by dividing the amplitude of the nearly sinusoidal output at a given frequency by the low frequency (2.5 lp/mm) output amplitude. For the projector-level MTF tests (Figure 13) the projector was driven by a Visual Information Inc. Model 216 Test Pattern generator with a series of vertical bar test patterns (corresponding to various spatial frequencies), and the resulting images were scanned by a slit-scanner and recorded as described above. The 525-line raster displayed on the CRT was sized to simulate the target raster writing rate conditions encountered in the ultimate full-color projector (10,000 inches/sec). It should be noted that SiLV MTF measurements were taken under low light level conditions.

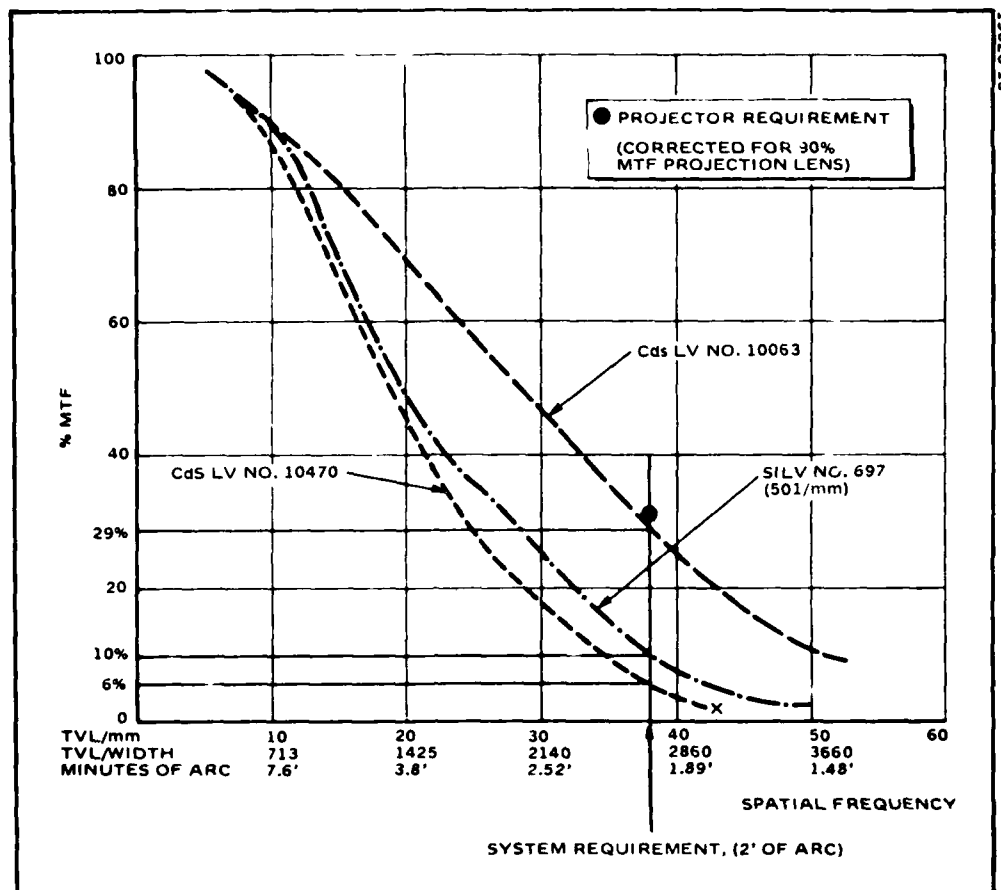


Figure 13. Comparison of Projector Performance Using Three Light Valves. System requirements (35% MTF at 38 TVL/mm) are nearly met with the No. 10063 CdS LV.

The resulting data is shown in Figure 13 with square wave modulation (MTF) plotted against TV lines/mm (spatial frequency). Also shown along the abscissa are the TV lines across the pentagon inscribed in a 3.0 inch diameter light valve, and the minutes of arc at the pilot's eye assuming the display covers a 90° field of view corresponding to these spatial frequency values. As shown, the projector modulation at 2' of arc (the required 2363 target resolution) is 29%, 10% and 6% for the No. 10063 CdSLV, the best (No. 697) SiLV, and the No. 10470 CdSLV, respectively.

The system requirement of 20% MTF at the pilot's eye translates into a requirement of 32% at the output of the breadboard projector, based on an educated estimate of the pancake window and (final) projection optics MTFs, and the known resolution of the breadboard projection lens. Thus, the breadboard projector with a high resolution CdSLV (No. 10063) extrapolated to 3 inches in diameter nearly meets the required MTF of 32%, and provides respectable MTF performance (10%) at 1.5' of arc. The silicon light valve does not measure up to performance, although it still provides good resolution performance (note that the SiLV performance measured corresponds to a 30% MTF for 1000 TV lines across a rectangular display). As stated before, it is

anticipated that exploiting the increased grid line frequency (from 50 to 100 grid lines/mm) will improve the silicon light valve MTF characteristics to match or exceed the MTF of the best CdSLV, with an attendant improvement in total projector resolution. With this improvement a system MTF of greater than 20% at 2' of arc, and an MTF greater than 6% at 1.5' of arc should be realized.

Although the primary test effort emphasis was on characterizing target raster MTF, a number of other tests were conducted, and are briefly summarized. Shrinking raster measurements of background raster resolution as a function of position showed that 2363 requirements were far exceeded at the high raster writing rates. Target resolution was estimated to drop off less than 15% as a function of display position on the 3 inch light valve. Finally, shrinking raster measurements of target raster resolution as a function of CRT writing rate--of interest because of the possible desirability of painting larger than 3° x 3° target rasters--showed a resolution loss of less than 10% when going from 10,000 to 50,000 inches per second on the CRT.

CONCLUSIONS

Significant progress has been made on Project 2363 toward implementing a very high resolution, multiple-target capable, full color liquid crystal light valve projector for in-line infinity optics-based wide field of view simulator visuals. The early phase of the program investigated alternative approaches to achieving the required target resolution and other demanding performance objectives, and selected a 3 inch, fiber-optic coupled CRT-light valve image generator as the basic building block for such a projector. The study further selected the analog and digital electronics techniques and hardware needed to achieve the 60 Hz frame rate operation, good resolution uniformity, color convergence at high resolution and target inseting capability required of the projector, and also defined a cost and platform-weight optimized implementation of a specification-compliant projector. It was concluded that such a projector is feasible, but only if the CRT, light valve and prism could be scaled up from 2 to 3 inches, and if the resolution of the CRT could be improved.

In the second (component development) phase of the program, Hughes developed these critical components. A 3 inch 0.7 mil fiber optic CRT was built; however the fiber optic quality of the fiber optic faceplate was not acceptable, and the second CRT was built in the 2 inch size to work around the unavailability of 3 inch high quality CRT faceplates. The linewidths of this second CRT--0.5 mils and 0.9 mils for the target and background rasters, respectively-- were significantly better than the required 0.6 mil and 1.1 mils, respectively. An index-oil prism technique, which immerses the thin film polarizer/analyzer beamsplitter plate in an index-matched oil, yields--when used in conjunction with a similarly constructed prepolarizer prism-- a prism free of residual, stress and thermal birefringence effects. 1000:1 (a factor of five higher than required). A partially completed effort proved the basic feasibility of increasing the size of the CdSLV from 2 to 3 inches. A breadboard projector constructed during this phase to integrate these components under conditions equivalent to those encountered in the ultimate 2363 projector demonstrated--using the 2 inch high resolution CRT and different light valves--that an MTF of 29% and 10% is achievable at 2' of arc resolution (across a 90° FOV), using a high resolution CdS light valve and a good silicon light valve, respectively.

As a result of a concurrently funded AFHRL research contract, Hughes internal R&D, and funding redirected within the 2363 project, major strides have been made in implementing a practical, operational silicon photoconductor light valve. From late 1979 through 1980, 2 inch fiber optic light valves were constructed and demonstrated in two types of operating projectors, driven by fiber optic CRTs to display dynamic television images. Liquid crystal response time was improved to permit operation at 60 Hz frame rates. Device construction was simplified by eliminating a separate light blocking layer. Silicon and mirror processing techniques were improved to yield better sensitivity and reduced operating voltages. High contrast was achieved at low brightness levels, and limiting resolution was improved to 70 TV lines/mm. Two improvements are required to make the device practical for simulation applications: improving the light blocking characteristics of the mirror to yield higher light output with good contrast ratio, and developing a technique for attaching the flat-polished wafer to the fiber optic substrate to yield the required brightness uniformity. Two further SiLV improvements are needed to meet the requirements of the 2363 projector: increasing the light valve size by a factor of 1.67 to 3 inches, and improving its resolution to equal that of a high resolution CdSLV. Except for the last item, all four of these improvements entail "device engineering"--as opposed to device R&D--and are expected to be achievable with a diligent effort. Further improvement of resolution is also expected when the inherent resolution capability of the 100 grid line/mm structure is more completely utilized, though with less certainty.

ACKNOWLEDGEMENTS

The work on this program was funded by the AF Human Resources Laboratory (AFHRL) under Contracts No. A36D813Y1Z3378 and F33615-79-C-0024 for the Project 2363 and Silicon Light Valve R&D programs, respectively. The Hughes Project 2363 effort was funded under a subcontract to General Electric, the prime contractor. The authors wish to acknowledge the key contributions of several individuals at Hughes toward accomplishing program objectives: Dr. Ralph Gagnon for his innovative work on the polarizing prism, Dave Eccles for his design and implementation of the breadboard projector electronics, Ron Gold for his design and implementation of the breadboard projector optics, Gary Best for his efforts on light valve and projector testing, and Peter Seats of Thomas for the technology advances required to implement the high resolution fiber optic CRT.

REFERENCES

1. W.P. Bleha, J. Grinberg, A.D. Jacobson, "AC-Driver Photoactivated Liquid Crystal Light Valve", 1973 SID International Symposium Digest of Technical Papers, Vol. IV, p. 42 (1973).
2. P.C. Baron, D.E. Sprottery, "Liquid Crystal Light Valve Projector for Simulation Applications" 1978 SPIE Conference, Visual Simulation Image Realism, Vol. 162, p. 138.
3. P.C. Baron, "A Color Liquid Crystal Light Valve Television Projector for the ATACS", 1978 AIAA Flight Simulation Technologies Conference (presented but not published).

LIGHT VALVE PROJECTION SYSTEMS
AS AN ALTERNATE
TO CRT DISPLAYS



Fernando B. Neves
Optical Systems Engineer
General Electric Company

Mr. Neves obtained his M.S. in Optics from The Institute of Optics at the University of Rochester. Prior to joining GE in 1980, he was involved in the design of Thermal Imaging Systems (FLIR). At GE he is the lead Optical Engineer involved in the Air Force ASPT program and the Navy VTRS programs, both utilizing light valve optical systems.



Jerome T. Carollo
Program Manager
General Electric Company

Mr. Carollo obtained his M.S. in Optics from The Institute of Optics at The University of Rochester. He has contributed to the development of a wide range of Visual Simulation Display Technologies. He is presently the Program Manager of the ASPT High Resolution Display Project for the Simulation and Control Department of General Electric.



Warren E. Richeson
Chief, Engineering Branch
AFHRL/OT

Mr. Richeson obtained his BS degree from West Virginia University and graduate degrees in mathematics from the University of South Carolina and the University of Notre Dame. He has worked in System Analysis and Design of Simulation Systems for the Air Force and NASA while employed by General Electric, TRW Systems, the University of Dayton Research Institute, and the U.S. Government Civil Service. He is presently the Chief of Engineering at AFHRL/OT at Williams AFB and is serving as Project Manager of the joint Air Force/Army project which is developing a dual color light valve projection system for the ASPT.



Joe A. Whisenhunt
Display System Engineer
General Electric Company

Mr. Whisenhunt obtained his B.S. and B.E.E. from North Carolina State University and his M.B.A. from Central State University. He has worked in Display System Design with GE in Syracuse, NY and Oklahoma City, and is presently the Project Engineer on the ASPT High Resolution Display System

INTRODUCTION

The Advanced Simulator for Undergraduate Pilot Training (ASUPT) was a project derived from a DOD directive to the three services requesting programs of advanced development in the area of training and education. The purpose was to insure that military training and education make the fullest use of recent technological advances. The ASUPT was a research device designed for investigating the role of simulation in the future Undergraduate Pilot Training (UPT) program. The development of the ASUPT system began in 1971 and was completed in 1975. In 1977 the A-10 cockpit was integrated into the ASUPT simulator. The usefulness of ASUPT, as a more general purpose research device, was recognized and the name was changed to Advanced Simulator for Pilot Training (ASPT). Since then a F-16 cockpit configuration has also been integrated into the system.

The visual system of the ASPT is an infinity image system that utilizes 7 facets of a dodecahedron structure to provide a wide field of view display. Each facet contains a Farrand Pancake Window[®] optical system and utilizes a large 36" diameter CRT as a display source.

In 1979, General Electric was contracted to develop an alternative functional replacement for the 36" ASPT CRT which made use of a standard production GE monochrome Light Valve TV Projector. The goals of this alternative display development are:

1. Investigate the use of the Light Valve TV Projector technology (with regard to resolution, light output capabilities, reliability, maintainability, and utility) as a feasible display imagery source in flight simulators and with flight simulator motion platforms.
2. Investigate the specific application and use of a lower cost, commercially available display device in the flight simulator and, specifically, in the ASPT system.
3. Develop an alternative image display source for the ASPT System which uses a 36" CRT that was specially designed and developed for the ASPT System.

This paper will describe this alternative display development. In addition, a rent program to develop a color alternative display using a dual GE color light valve based system, which provides a slewable High Resolution Area (HRA) within the background (BG) scene, will be described.

THE ALTERNATE DISPLAY SYSTEM DESCRIPTION

The concept of the alternate display system is to replace the large 36" CRT phosphor surface with a spherical rear projection screen. Imagery is projected upon this screen such that the observer views the CGI scenery through the Pancake Window[®] optical system.

The CIG scenery is generated by projecting upon a plane normal to the line of sight from the computed eye reference point position to points in the data base within the field of view. This two dimensional representation of the scene is converted into a video signal and fed to the display source. This view plane scene computation concept is shown in Figure 1. The scene must be displayed to the observer as though he were looking directly at this view plane to preserve the scene perspective.

The display source and optical system must have the appropriate mappings to prevent scene perspective changes and distortions. The Pancake Window[®] optical system may be functionally described as a monocentric optic that gives true angle imagery. That is, for an object point on the CRT or projection screen, the observed angle at the eye reference point is the same as the angle from the center of curvature of the CRT. This is shown in Figure 2.

The alternate display system configuration is shown in Figure 3. The alternate display system components are the light valve projector, projection lens, rear projection screen, and the mechanical mountings.

The display source is a General Electric model PJ 7155 monochrome light valve, which accepts electrical video signals. Properties of the light valve are given in Table 1. The light valve utilizes the video signal to velocity modulate an electron beam scanning in the horizontal direction, which results in a diffraction grating being formed on a transparent fluid surface. Light passing through an input bar plane, the fluid surface, and a Schlieren optical system produces light representation of the electrical video signal on the screen. The light source is an Xenon lamp. The projector is completely self-contained with all circuitry and power conditioning integrated into a single unit.

The projection lens projects the light valve raster upon the rear projection screen. Due to the mapping of the Pancake Window[®], the projection lens mapping must be defined so that the object height at the raster plane is related to the angle θ at the rear projection screen by the relation,

$$Y = f \tan (\theta)$$

Where, Y = raster object height
 f = effective focal length of the projection lens
 θ = the angle made by the screen image height as measured from the screen center

A lens with an $f \tan (\theta)$ mapping and no exit pupil motion versus field of view would meet this requirement if the pupil were placed at the projection screen center.

The projection lens of the alternate display is a folded 22 element design that includes a Pechan prism derotation device. The lens design was derived from previously designed wide field of view projection lenses designed for large

dome real image display applications. Optical performance parameters of the lens design are given in Table 2. The 90° circular field of view, of the lens, provides imagery for the so called overscan region of the display, that is, it permits the required 6" radius sphere of head motion from the reference eye point. The lens is designed to optically and mechanically interface with the light valve Schlieren objective. Translational and angular adjustments and a means for alignment were designed into the mechanical package to aid in this interface. The lens and light valve package are shown in the photograph of Figure 4.

The rear projection screen is an acrylic dome with the same radius as the CRT phosphor surface. This surface has been ground with a loose abrasive technique to achieve a gain of 8.0. A light shroud between the lens and the screen minimizes potential stray light problems.

Due to the requirements of the Air Force to place the display in any channel of the ASPT dodecahedron, a versatile mechanical mounting configuration was designed. The light valve axis must be positioned horizontal within 15° , although short term large angular excursions do not affect performance. The mechanical mounting is designed such that the light valve can be rotated about its axis and the light valve/lens assembly can be rotated to discrete positions about the axis of the Pancake Window. Utilizing rotations about these two orthogonal axes, the light valve axis can be positioned such that for the mean motion playform position the light valve axis is horizontal. The image rotation resulting from the particular installation facet is removed by rotation of an optical derotation.

PERFORMANCE OF THE ALTERNATE DISPLAY

The alternate display evaluation, although not complete, at the writing of this paper, is underway and qualitative comments on the display system are very positive. The reduced raster prominence appears to more than compensate for the slightly reduced resolution of the light valve versus CRT imagery. Alignments, edge matching and installation procedure of the display have received very favorable response as well.

Several areas of improvement to the current alternate display have been identified. These areas are:

- 1) the rear projection screen
- 2) Color matching to the CRT channels
- 3) minor mechanical modifications

The gain of the current rear projection screen is approximately 8.0. This achieved a 600 foot lambert screen luminance, however, the gain affected the luminance of the display versus head motion. A new screen candidate fabricated by using a flowing of a dispersive fluid appears very promising. It offers a much higher resolution, a more uniform appearance and a gain of 5.0 to improve the luminance versus head motion problem. The black and white light valve imagery does not match the black and green CRT imagery. A dichroic filter may be added to the light valve to match the light valve imagery to the CRT phosphor imagery. An added benefit of this modification is that it would permit an increase in the Xenon lamp output that would more than account for the lost luminance in going from a screen gain of 8.0 to 5.0. Several mechanical modifications could be made to make the alternate display even easier to align and maintain.

THE DUAL PROJECTOR DISPLAY

The resolution versus field of view trade-off in simulation has been approached in several display systems by adding a high resolution scene to a background scene. The dual projector display concept is to optically combine a 90° background scene with a servo slewable high resolution scene. The display system concept is shown in Figure 5. The system uses two GE model 5150 color light valves as sources. The background light valve imagery is projected via the background projection lens upon the rear projection screen to provide a 90° field of view to the observer. This projection lens path leads through a hole in a slewable mirror. Reflected from this mirror is the high resolution scene, which can be slewed to any point within the background scene or can be entirely outside the background scene.

Goals for the Dual Projector Display as a research vehicle require much flexibility of the system. The goals of the high resolution scene performances are given in Table 3.

The Optical Servo Subsystem (OSS) portion of the Dual Projector Display is currently in the late stages of design. The formidable optical design task is virtually complete and predicted performance for the system is close to meeting the goals of the program. Delivery of the OSS is expected by July 31, 1981.

This project was sponsored by the PMTRADE engineering R & D group under the direction of Dr. Ron Hofer as a joint Army/Air Force project. The Army has provided funding and GFE hardware for this effort and will participate in the planned testing and evaluation in October of 1981.

FUTURE LIGHT VALVE DISPLAYS

In addition to the GE light valve, there are several other light valves in various stages of development. Of the currently available configurations, the GE system appears to offer the best luminance to size/weight trade-off. The systems under development will offer potential improvements in resolution. Future improvements of the GE light valve are also being investigated.

SUMMARY

An alternate display system to replace the ASPT 36" CRT was described. This display system offers monochrome (black and white) imagery with the ability to be modified for color imagery. The imagery has a greatly reduced raster prominence and slightly reduced resolution. In addition, the maintenance of the alternate display offers advantages over the CRT display. The display is a viable option for the presently used CRT.

A current development program for a color dual projector display was also briefly described. The system expected to be demonstrated in October 1981 is versatile in providing a high resolution area which is slewable within the background.

TABLE 1
GENERAL ELECTRIC LIGHT VALVE PROJECTOR SPECIFICATIONS

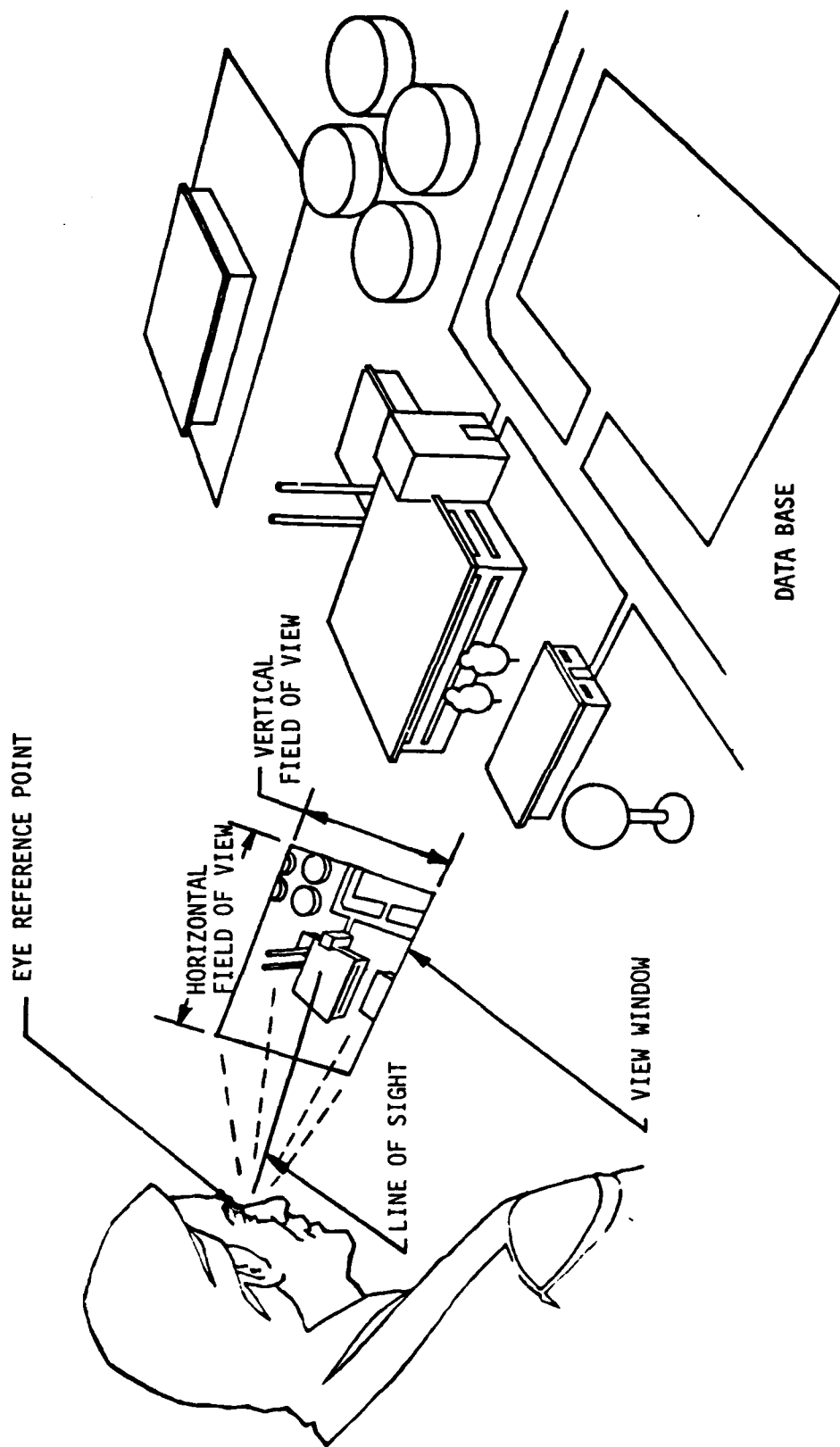
	PJ 7155 (Monochrome)	PJ 5150 (Color)
Output (lumens)		
Typical	2400	650
Minimum	2000	500
Limiting Resolution (TV lines per picture height)		
Horizontal	800	750
Vertical	750	650
Input Power		
Watts	1500	1600
Volt-amperes	2000	2150
Scan Standard		
Lines	1023	1023
Fields per second	60	60
Size	22" high, 17" wide, and 32" long	

TABLE 2
ALTERNATE DISPLAY, PROJECTION LENS DESCRIPTION

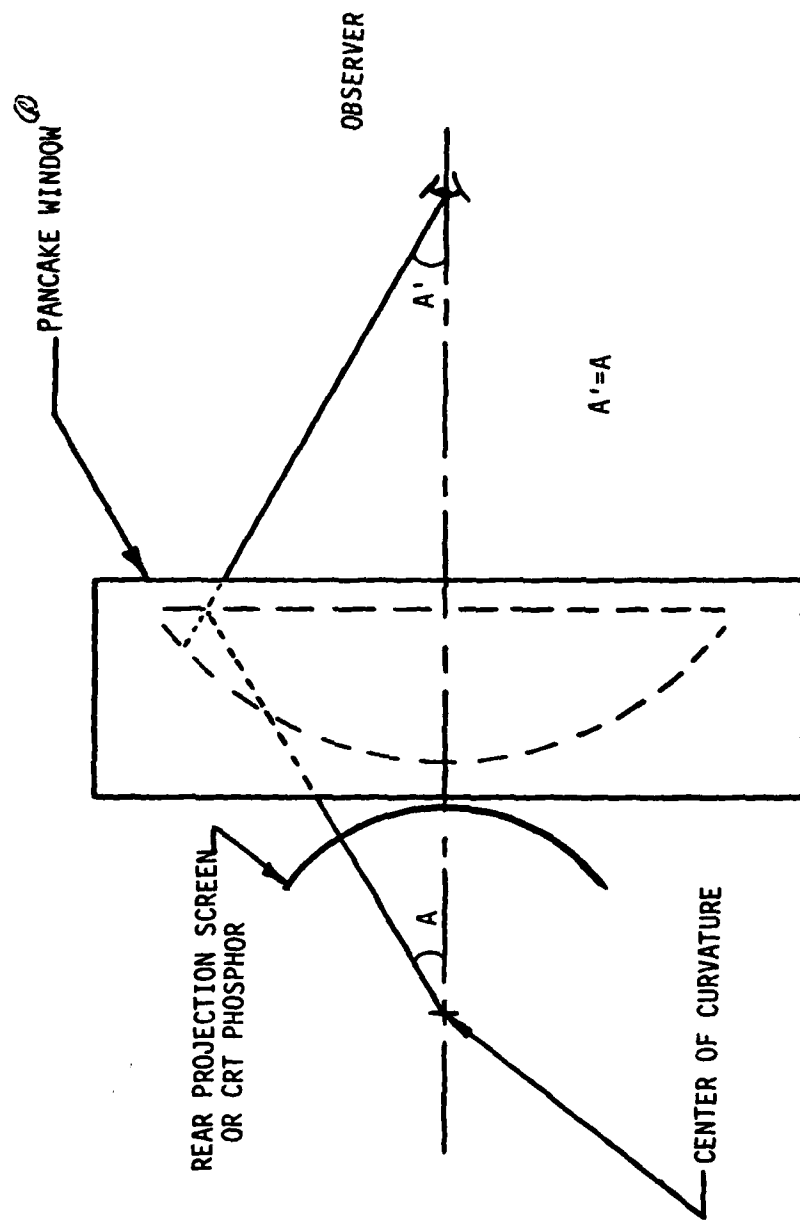
FIELD OF VIEW	90° TOTAL
F/NUMBER	3.0
OPTICAL DISTORTION	2.9% MAXIMUM
DEROTATION DEVICE	PECHAN PRISM
IMAGE RADIUS	609.6
RELATIVE ILLUMINATION	0.85
MISCELLANEOUS	1 INTERMEDIATE IMAGE FILTER CAPABILITY 1 FOLD MIRROR FOR USE IN ANY ASPT DISPLAY CHANNEL

TABLE 3
DUAL PROJECTOR DISPLAY SYSTEM GOALS

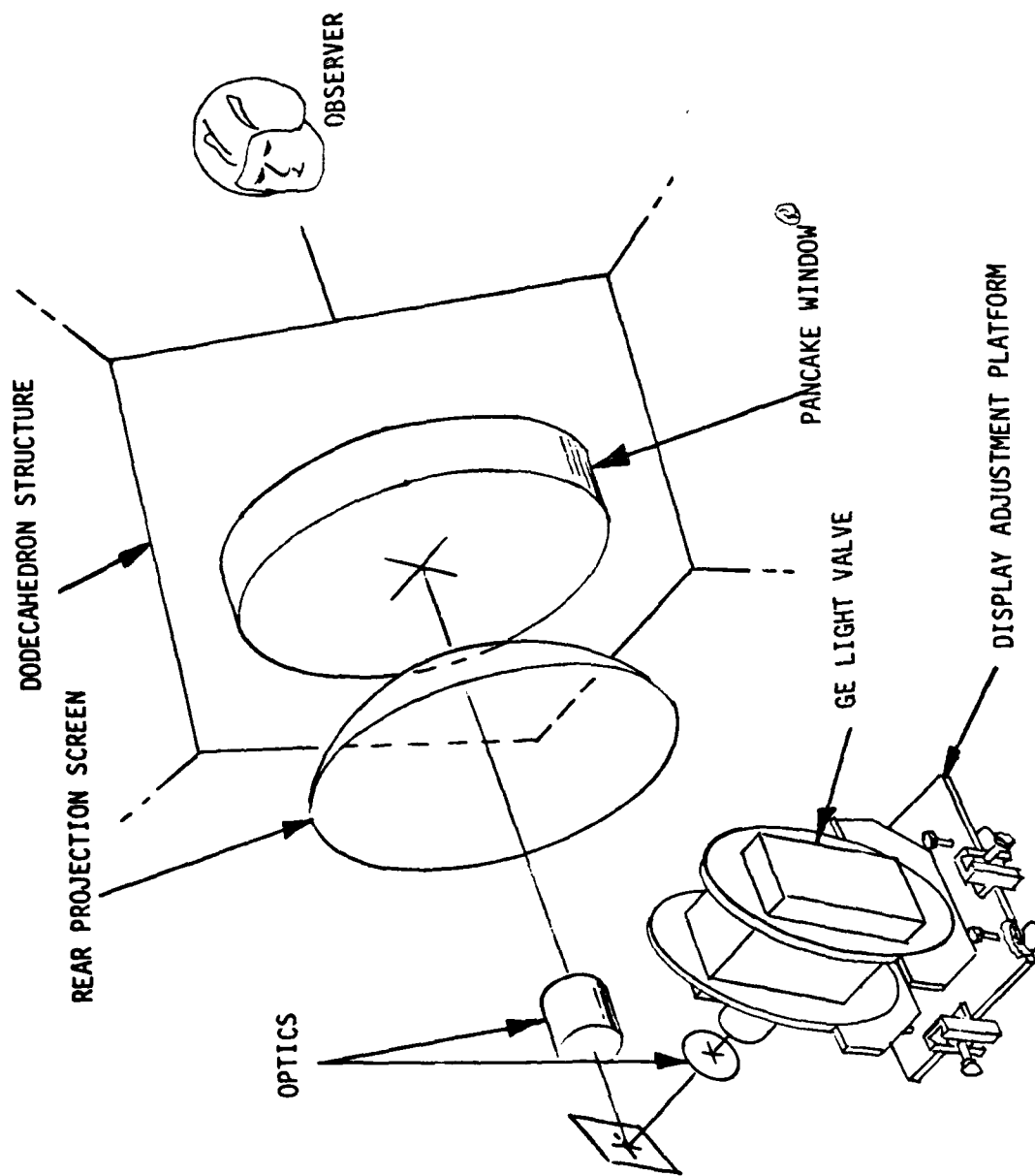
1. Provide a 1.0 arc minute average resolution scene that is slewable to any point in the lower resolution background scene.
2. High resolution slew rates of 300° per second that can be head or target tracked.
3. High Resolution display modes:
 - inset, abrupt transition
 - inset, gradual transition
 - superimposed
 - circular field of view
 - square field of view
4. Develop electronic inseting techniques.
5. Provide a modular design that is optically and mechanically interchangeable with any ASPT channel.



SCENE COMPUTATION GEOMETRY
FIGURE 1

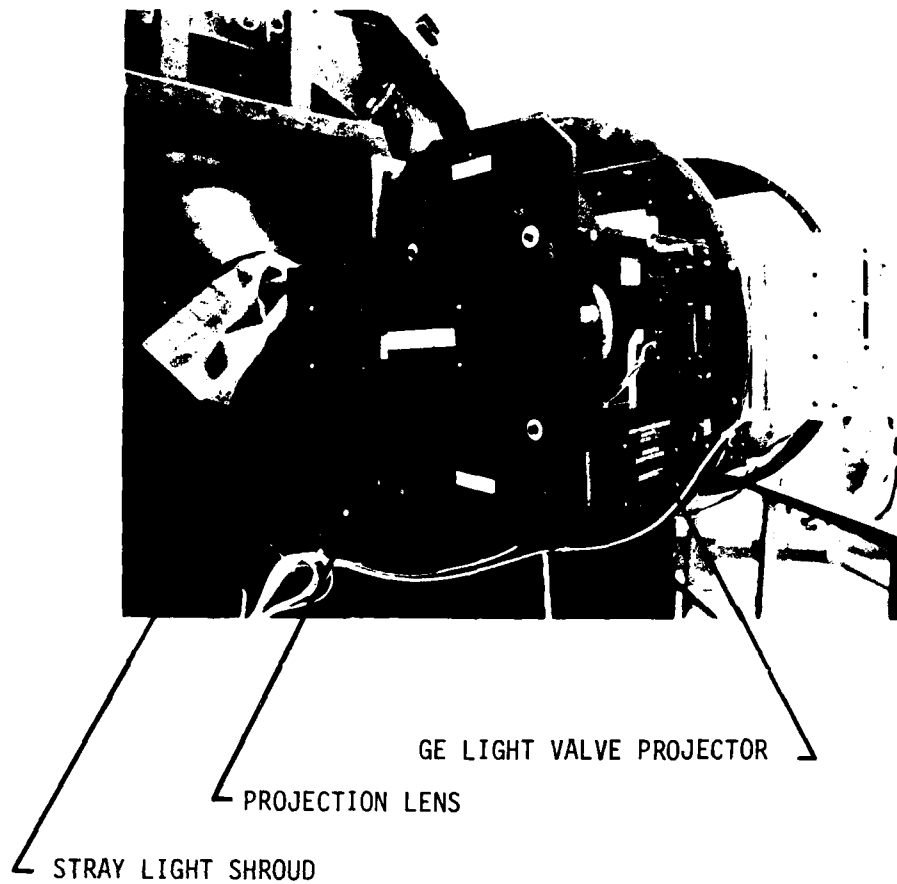


P
PACAKE WINDOW MAPPING CHARACTERISTIC
FIGURE 2

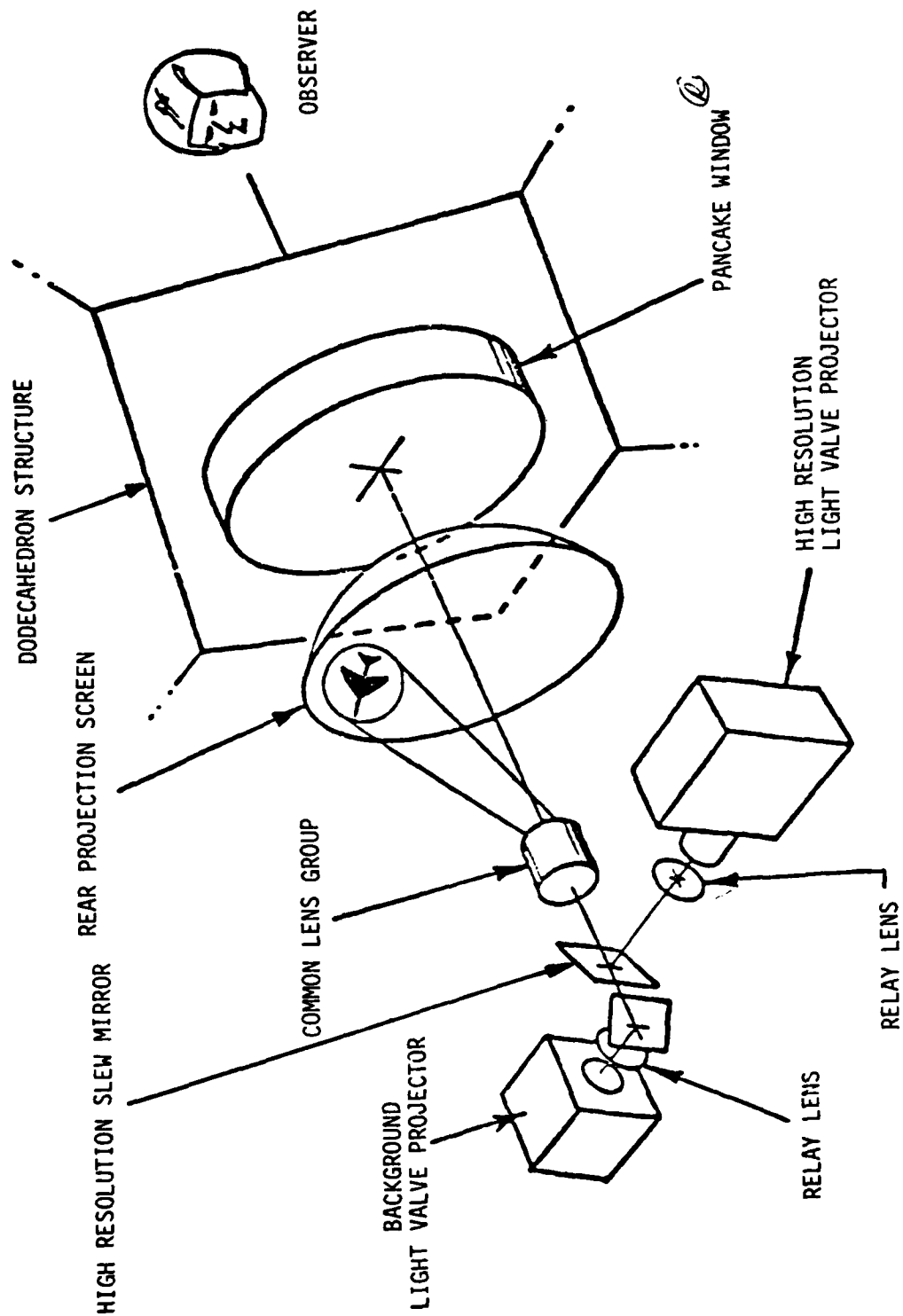


ALTERNATE DISPLAY CONCEPT

FIGURE 3



THE ALTERNATE DISPLAY SYSTEM
FIGURE 4



DUAL PROJECTOR DISPLAY CONCEPT

FIGURE 5

TITUS LIGHT VALVE PROJECTION SYSTEM



François Desvignes
Director
SODERN

François Desvignes was educated in physics at the CNAM Paris, 1947 with a specialization in optics (ESO Paris, 1945). His 35 years of professional life have been in Research, Industry and academia as Head of the Photometry Laboratory at the Institut d'Optique (Paris) since 1946 ; as Department Head of the Laboratoires d'Electronique et Physique appliquée in 1951 with activities on radiometry, solid state photoelectricity and infrared instrumentation ; at SODERN since 1971 where he is presently Director, to develop an electro-optical instrumentation activity (satellite attitude sensors, Earth resources, cameras, ...) which includes the video-image projection systems and as a Professor at the Ecole Supérieure d'Optique in the fields of photometry, radiometry, radiation detection and detectors (1962-78).



Jean R. Huriet
TITUS program manager
SODERN

Jean R. Huriet obtained his engineering diploma at the Institute for Optics in Paris and then he became doctor-engineer at the Paris University. His 20 years professional experience has been in research laboratory, satellite experiment management, before he came to Sodern in 1970 for the space projects management. He is in charge of the TITUS projection system program since 1978.

TITUS LIGHT VALVE PROJECTION SYSTEM

(TLVPS)

by F. DESVIGNES and J.R. HURIET - SODERN - LIMEIL - France

ABSTRACT :

The TLVPS has been developed for large screen TV display in 1976. Additional development work is running in the frame of the USAF 2363 program and for the Mirage 2000 simulation. The goal is to obtain high resolution areas (2 arcs minutes) inserted in a medium resolution (6 arcs minutes) background.

oOoOoOoOoOoOo

Five years ago, SODERN started the manufacturing of full colour projectors adapted to European live television standards, which provide an output greater than 2500 lumens, convenient for movie theatre screens up to 100 square meters (900 square feet). These laboratory models have been intensively used for demonstration purpose since 1977 and thus proven their reliability and low level of maintenance requirements.

The images produced by this type of projector have unique features in addition to the high luminous output :

- full colour capability (see figure 1),
- neither flicker nor lag,
- memory capability without smear,
- no apparent line structure with raster scan mode.

The resolution obtained with this first experimental projection system is considered of not sufficient for the military aircraft - air combat and ground attack - simulation needs : improvement programmes have been undertaken with the US Air Force and the French Delegation Generale pour l'Armement support*.

The performance can be expressed in terms of space and time resolution under the pixels rate figure of merit (number of resolved picture elements per unit of time).

* 2363 USAF project and Mirage 2000 simulation.

...

This projector figure of merit takes into account three terms :

- 1 - the light valve,
- 2 - the video electronics,
- 3 - the optics.

Presently the last one is not critical from the resolution point of view : the development effort for the resolution is put on the light valve and on the electronics.

The light valve uses the longitudinal Pockels effect, an electrically induced optical birefringence which is produced here in a thin slice of a synthetic crystal. An electrical image is written on the slice with a scanning electron beam. The light valve spatial resolution is mostly related to three parameters : the erasing-writing electron beam diameter, the crystal slice lateral dimensions, the spacing between the slice and a control grid which limits secondary electrons fallout.

The erasing-writing speed is related to the electron beam current, thus the pixels rate is controlled on the spatial and time resolution aspects by the electron beam characteristics.

The 1980 effort has been concentrated on the electron gun improvement which has produced an increase of the light valve resolution as shown by figure 2. A 30 % contrast transmittance (MTF) is obtained at 550 pixels per line with the new valve (TV2) against 5 % with the 1977 one (TV1), and a 5 % MTF is obtained at 100 pixels per line.

A new improvement of the electron gun is still possible.

An other way of investigation to increase the available number of pixels per image is to increase the size of the target of the light valve. The TV1 and TV2 light valves use a 28x38mm target. A SV1 light valve has been made and tested with a 38x38mm target.

The figure 3 is a picture of the display of a test pattern with the SV1 light valve. The observed MTF is the same as for the TV2, then the benefit in available pixels number is directly proportional to the area increasing : + 30 %. It can be used in two different ways either to fit with square shaped or pentagonal images or to increase the effective resolution in a rectangular image by use of anamorphosal optics.

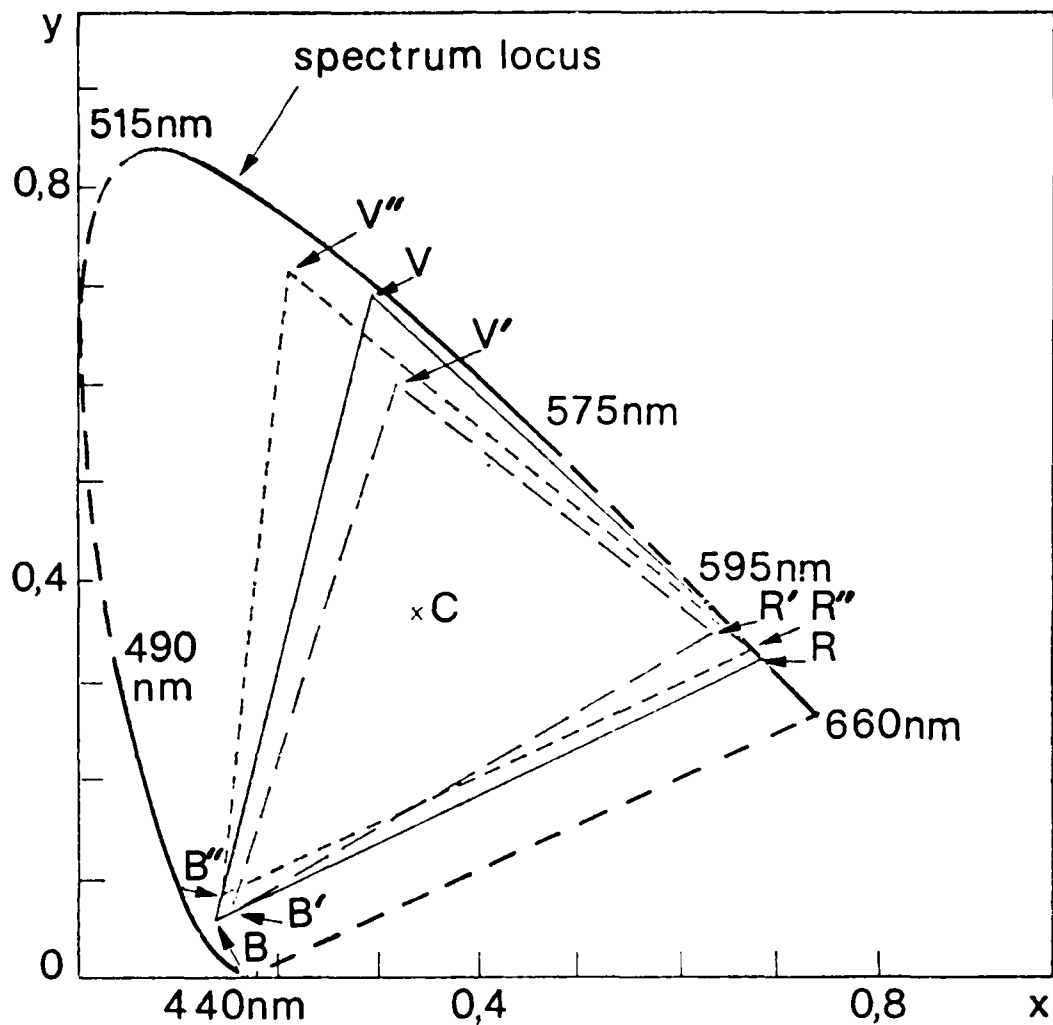
...

During the same time investigations have been made in order to grow larger crystals where the targets are cut. The DKDP crystals which allow to make the 38x38mm targets have a 50x50mm size. Bigger crystals have been grown up to 70x70mm which allow to cut 50x50mm targets (see figure 4). The electro-optical quality have been checked and sample targets made to check also the image quality after complete processing.

By the other hand a development work has been undertaken on the system aspect of the projector. That leads mostly to the improvement of the command circuitry of the light valves. The scanning capabilities will be extended to 1023 lines to take benefit of higher resolution and the video amplifier (140 V on 400 pF load) bandwidth is progressively extended from 5 to 7, 15 and possibly 30 MHz.

But it leads also to the repackaging of the projector in order to obtain suitable size and weight for simulation purpose, a prototype demonstrating the 1980 improvement will be available this year.

XY COLOR DIAGRAM



RVB TITUS protection system
 R'V'B' Typical shadow mask tube
 R''V''B'' NTSC reference diagram

figure - 1

IMPROVEMENT OF THE LIGHT VALVES TV2 VERSUS TV1 CHARACTERISTICS

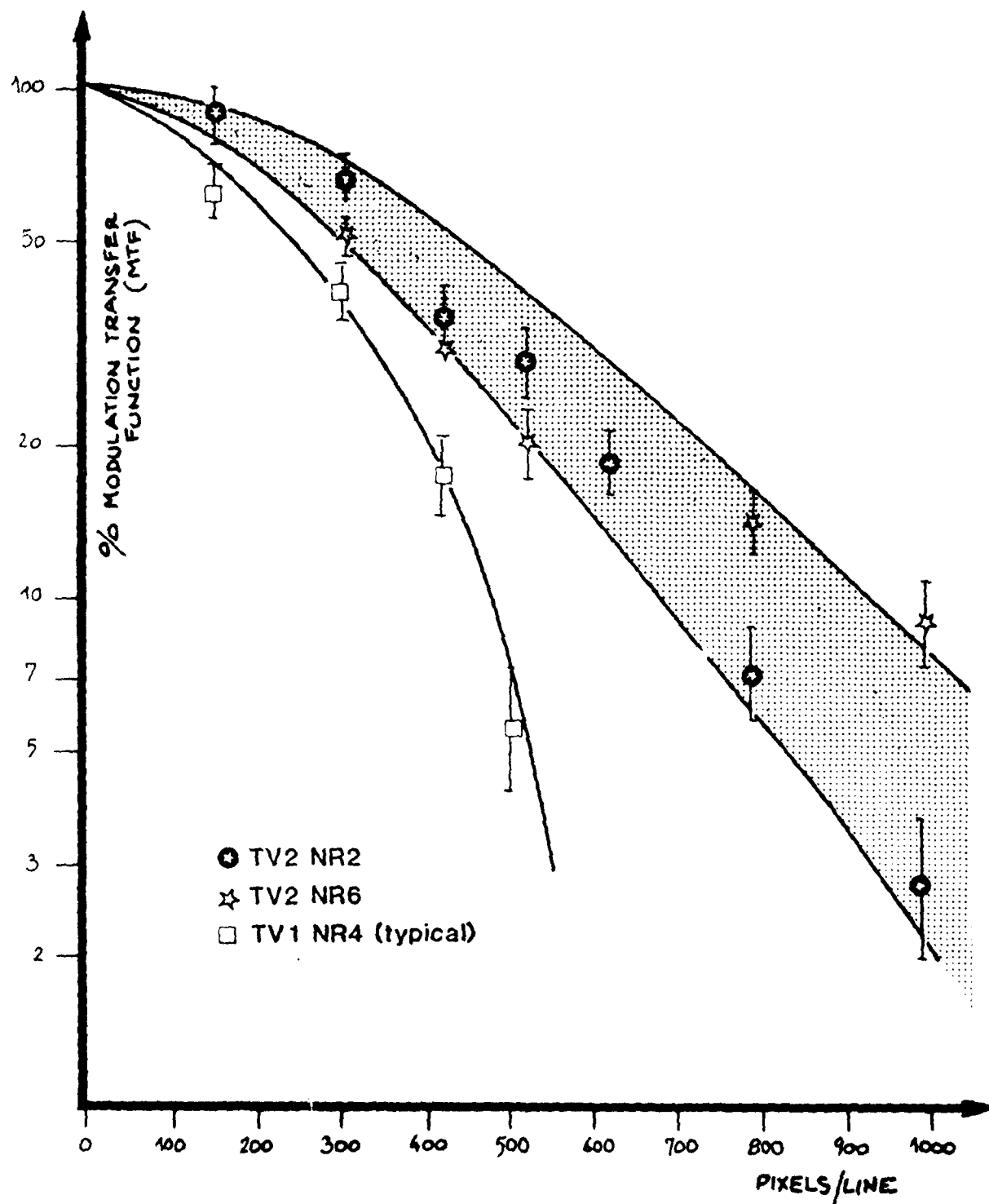


figure - 2

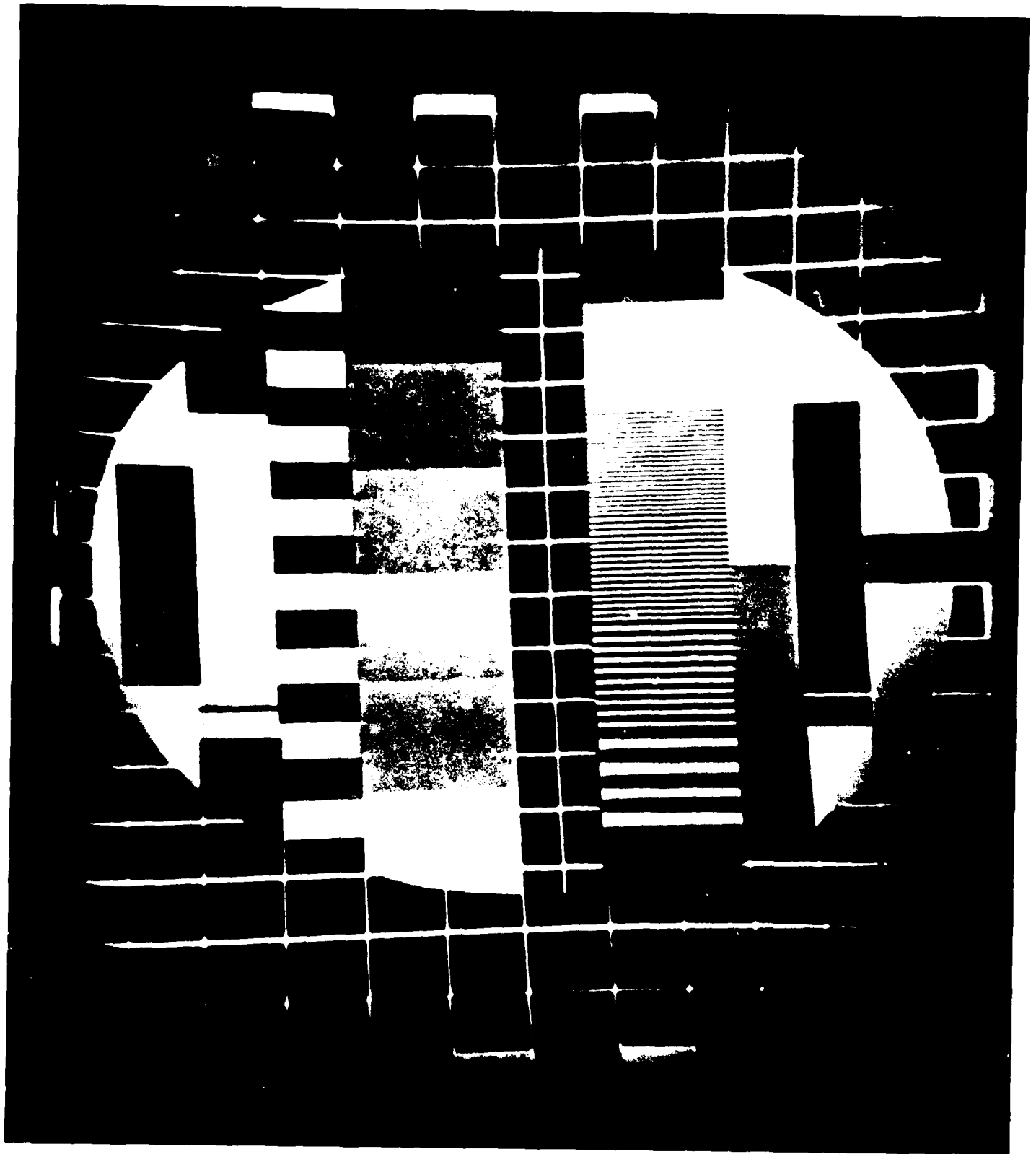


Figure 3



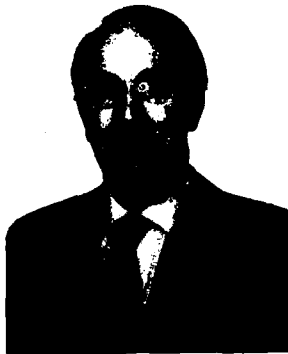
Figure 4

HELMET MOUNTED LASER PROJECTOR



Denis R. Breglia
Physicist
Naval Training Equipment Center

Denis R. Breglia obtained his M.S. in physics from St. John's University. His 15 years of professional experience has been with the Naval Training Equipment Center. His work has included exploratory development in the technology areas of laser weapon fire simulation, holography, computer graphics, and laser displays.



A. Michael Spooner
Head, Advanced Simulation Concepts Lab
Naval Training Equipment Center

A. Michael Spooner obtained his Ph.D. in electronic engineering from London University. His 39 years of professional experience have been mainly in industry. His contributions to research and development in flight simulation over the last twelve years have concentrated on the generation and display of visual scenes. He is Head of the Advanced Simulation Concepts Laboratory, Naval Training Equipment Center, Orlando, Florida. He is currently Chairman of the Simulation and Training Devices Technology Advisory/Coordination Group (SIMTAG) whose purpose is to coordinate R&D activity in simulation and training devices between the three services.



Dan Lobb
Optical Systems Consultant
University of Central Florida

Daniel R. Lobb studied Physics and Optics at Imperial College, London University, where he received his BS and DIC degrees. He has worked since 1962 for Sira Institute Ltd. on a variety of optical system design and development projects including automatic surface inspection, laser scanning devices, heads-up displays and star trackers. In recent years he has been involved in the development of display systems for flight simulation. He is currently on a one year leave of absence at the University of Central Florida.

Helmet Mounted Laser Projector

ABSTRACT

A display system for flight simulation is described. The system employs optics mounted on the pilot's helmet to project a scene onto a retro-reflecting screen. It is driven by two Computer Image Generation (CIG) channels, one providing a wide-angle display while the other provides a high-resolution, eye-directed inset. The concept uses both head tracking and eye tracking to provide an effectively unlimited field of view with high resolution at low cost.

1. INTRODUCTION

The Advanced Simulation Concepts Laboratory of the Naval Training Equipment Center is pursuing an exploratory development program to design a visual simulation system and analyze the feasibility of fabrication. The system will be designed for use in the Navy Visual Technology Research Simulator (VTRS) with new hardware intended to interface with existing VTRS equipment.

The system will have part of the display projection optics mounted on the pilot's helmet and be fully visually coupled, demanding use of both head-tracking and eye-tracking techniques. Optical design for the display system is currently well advanced and experiments have been carried out in both head- and eye-tracking. This paper describes and discusses the evolution of the basic approach taken, and outlines the present design and the results of experiments.

The system performance objectives include an effective total field of view which is limited only by cockpit structure and the pilot's normal freedom of movement within the cockpit. Associated with this large field of view, typically 8 steradians, the target resolution is 3.3 arc minutes per line pair. The scene is to be presented without noticeable seams or discontinuities, and is to be available, without distortion, to two or more subjects in the same simulated aircraft. The method proposed has potential for presenting a collimated picture and eventually a three-dimensional picture.

2. DESIGN CONCEPTS

a. Visual Coupling

The very demanding specification is achievable in principle by many different approaches. But generally, the cost of attaining the basic objectives - very wide field, high resolution and multiple-user operation - would be considered excessive using available display technology. In general, the wide angle and high resolution objectives together demand a powerful pixel generation capability, leading to multiple projectors and very broad electronic bandwidths, and to multiplied cost of computer image generation or other video generation systems. The requirement for multiple-user operation,

taken together with the very large field angles, would in general require very costly collimation optics, or else duplication of the entire simulation apparatus (with large actual separation of the users).

The approach taken is based on matching the display system performance, in terms of field of view and resolution, to the visual performance parameters of the observer's eyes. The observer's capability to perceive high detail at any instant is restricted to a relatively small area of interest corresponding to his foveal vision. The size of the instantaneous field in which he can perceive any visual information at all is less than the field available to the observer through head and body movements. By providing a display system which presents high detail imagery only where the observer is looking, with an instantaneous field which matches his instantaneous field, the observer will perceive the display as having high detail imagery throughout his total available field. But the total burden on the display system, in terms of computed and resolved pixels in each frame, is very usefully limited. For these reasons, there has been a strong thrust in recent years to visually coupled systems of different kinds, in which the projected scene or a high-detail insert follows the observer's head- or eye-direction.

b. NTEC System Goals

Figure 1 shows an artist's concept of the NTEC display looking over the observer's shoulder. The display has an eye directed area of interest (AOI) field which is a nominal 1000 television line (TVL) raster driven by a dedicated CIG channel and a head directed instantaneous field of view (IFOV) which is a second nominal 1000 TVL raster driven by a second CIG channel. The system is largely compatible with the existing VTRS computer image generator (Ref. 1). Table 1 lists the system performance goals chosen for the design.

The VTRS CIG has a capability of providing 2,000 potentially visible edges distributed between the two display rasters. If this capacity is shared equally between the displays, the scene complexity or edge density will be approximately twenty times higher in the AOI channel relative to the IFOV channel.

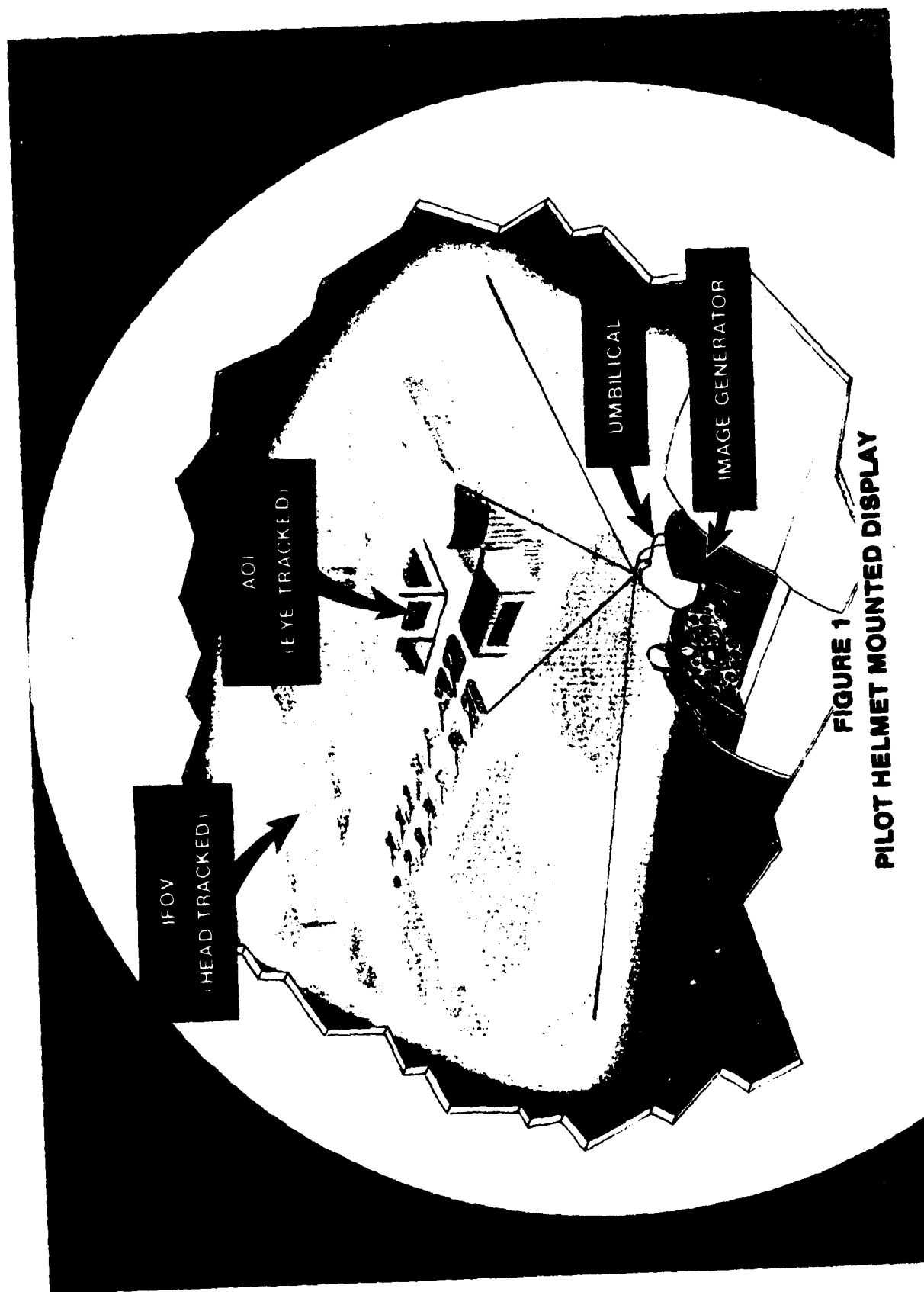


FIGURE 1
PILOT HELMET MOUNTED DISPLAY

TABLE 1. SYSTEM PERFORMANCE GOALS

Apparent Field of View	Restricted only by cockpit structure
Instantaneous Field of View	145° diagonal
Area of Interest	36° diagonal
Apparent Resolution	3.3 arc min/TV line pair
AOI Resolution	3.3 arc min/TV line pair - on axis
I FOV Resolution	13 arc min/TV line pair - on axis
Luminance	10 Foot Lamberts (Highlight)
Color	Full
Contrast	30:1

c. Helmet Mounted Projector

The display configuration was developed from a Helmet-Mounted Laser Projector concept described in a contract report (Ref. 2) delivered by American Airlines and Redifon Simulation Ltd. Helmet-mounted optical systems commonly have small CRTs on which an image is generated and the optics project light into one or both of the user's eyes via mirrors or beam splitters located in front of the user's eyes. In the Redifon proposal, the scene is projected outward from the helmet onto a dome screen from an exit pupil located above the user's eyes. The screen is given a strongly retro-reflective coating so that a relatively large proportion of the projected light is reflected to the user. In order to achieve high brightness in the display over a wide angle, without mounting excessively heavy optics on the helmet, Redifon proposed to use a laser display system and a coherent fiber optic link to carry light to the helmet. The use of lasers permits high brightness across a wide projected field without requiring wide-aperture projection optics. The flexible fiber link permits the more massive optical components, including the lasers, modulators and line scanner, to be mounted at a remote location, off the helmet. The fiber link to helmet mounted optics is not a concept unique to Redifon, but Redifon has made the fiber link itself more viable by proposing to put a light-weight frame scanner on the helmet. This means that the optical fibers are required to transmit line images, rather than full frame images; few fibers are required, with significant advantages in flexibility of the link and reduction of manufacturing difficulty.

The aspects of the Redifon concept described above have been retained in the NTEC development. In other respects the concept has been modified, mainly to reduce the likely cost and time required to build a working system.

Helmet mounting of projection optics generally has several advantages for visually coupled displays:

- (1) The display automatically rotates with the head-pointing direction.
- (2) There is no significant distortion due to rotation of the projector.
- (3) Good photometric efficiency is possible (with either direct projection into the eyes or outward projection onto a retro-reflecting screen).
- (4) Two or more subjects can use the same simulator cockpit without seeing distorted views of each other's head/eye directed scenes (cross-talk), and each can receive an undistorted scene image.
- (5) With binocular projection the technique has potential for effective collimation of the scene, and for 3-dimensional presentation (neither at present planned by NTEC).

d. Dome Screen

Projection outward from the helmet onto a screen, rather than projection directly into the pilot's eyes, was selected for these reasons:

- (1) It does not require beam splitters or any other hardware to be fixed immediately before the pilot's eyes thus obstructing a normal view of the cockpit interior.
- (2) It permits a very wide instantaneous field of view, comparable with the pilot's total field with head fixed, to be projected and viewed by both eyes.
- (3) It provides automatic and precise blanking of the projected outside-world scene at the cockpit outline, since the cockpit structure does not retro-reflect, without need for head position tracking or electronic raster blanking.

e. Head-Tracking Functions

Since the projected rasters rotate with the user's head, the view direction used to compute the scene must be updated at field rate to include head rotations. A tracking device, measuring pitch, roll and yaw of the helmet with respect to the cockpit, must therefore be included in the visual simulation system.

Errors in helmet attitude data transmitted to the CIG produce errors in location of the perceived scene. Inadequate precision can result in image jitter, low accuracy will produce image swimming, and inadequate response will cause the image to lag head movements.

Image lag due to CIG throughput delay can be compensated, since the error is known given fast head-tracker response, by offsetting the projected image rasters using optical deflectors.

f. Eye Direction Following Functions

The small AOI raster, with high resolution and high detail content, is required to be shifted, within the wide field of the helmet mounted projector, so that this area is always on the axis of the pilot's eyes.

Within the optical projection hardware, this requires provision of deflectors to shift the scene vertically and horizontally. Within the CIG system, it is necessary to provide corresponding shifts in computed locations of the AOI view window and raster. Data to determine the eye-following deflections must be provided by an eye attitude measuring system.

3. DISPLAY SYSTEM

Figure 2 shows a functional diagram of the display system.

Mounted off the helmet are lasers, intensity modulators and a line scanner. These components provide two intensity modulated line scan images, one for the AOI raster and one for the IFOV. The two line scan images are carried to the helmet-mounted components by two flexible coherent fiber optic bundles.

Mounted on top of the helmet are galvanometers driving flat mirrors. These provide frame scan and eye-following offsets of the projected rasters. The frame-scan and offsetting optics are followed by a compound projection lens system which relays the light to an exit pupil location in front of the user's forehead and projects the light outward toward the display screen providing the angular magnification required to fill a 145° instantaneous field.

The screen is a spherical dome surrounding the simulator cockpit giving the user a total field (with head and body movements) which is limited only by cockpit structure. The screen is coated with a retro-reflecting material.

The CIG system has inputs from head-tracking and eye-tracking devices, not indicated in Figure 2. These inputs determine rotations of the view direction to follow head orientation, and computed offsets of the view window and raster to follow eye attitude. In addition to providing video signals to modulators and controlling simple line and frame scan functions, the CIG system controls offsets in the projected rasters produced at helmet-mounted deflectors. These offsets are principally for eye following but also compensate for errors due to finite computational throughput time.

4. LASERS, MODULATORS AND LINE SCANNER

Figure 3 is a functional diagram of the optical system feeding the helmet-mounted projector.

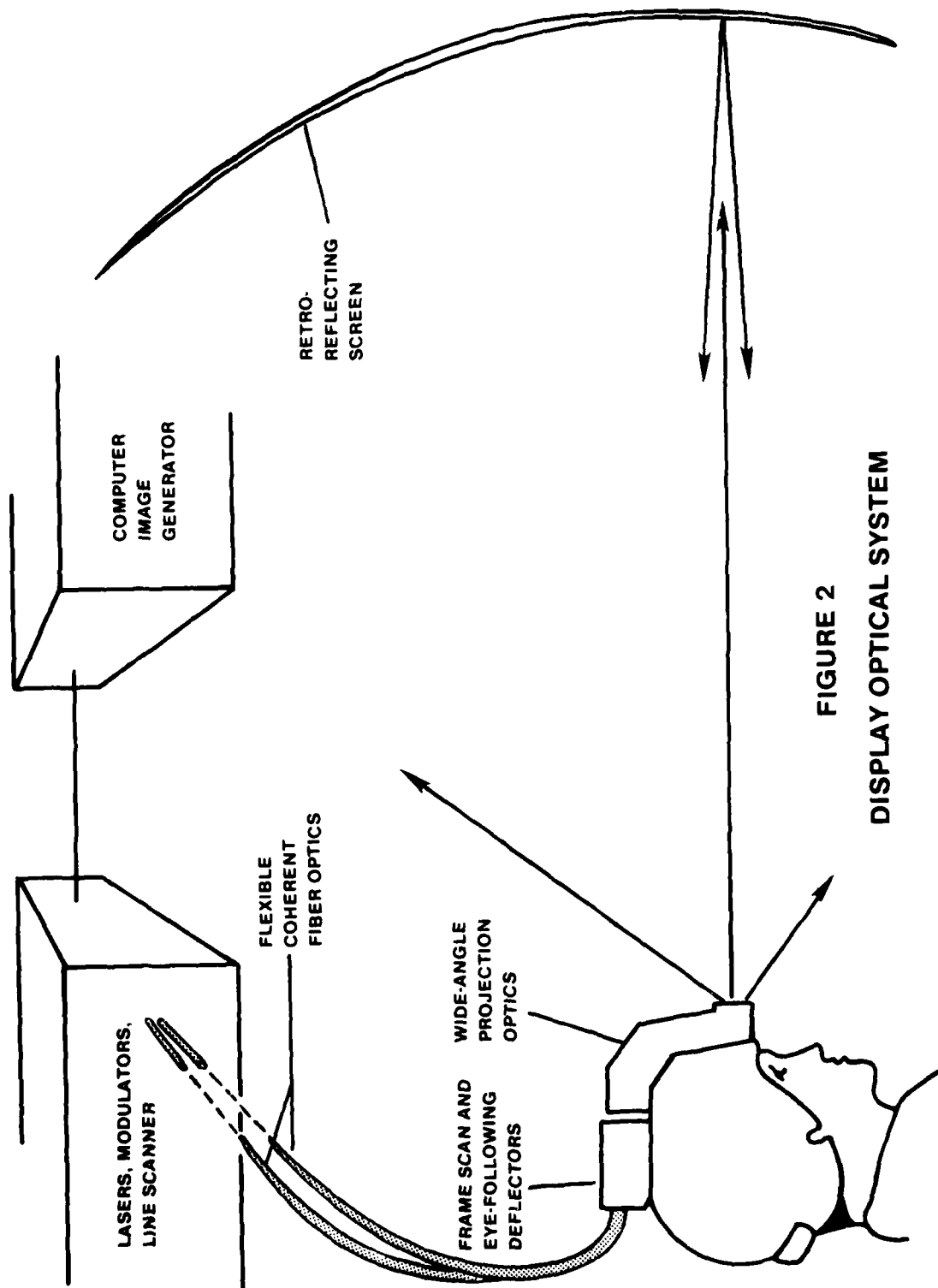


FIGURE 2
DISPLAY OPTICAL SYSTEM

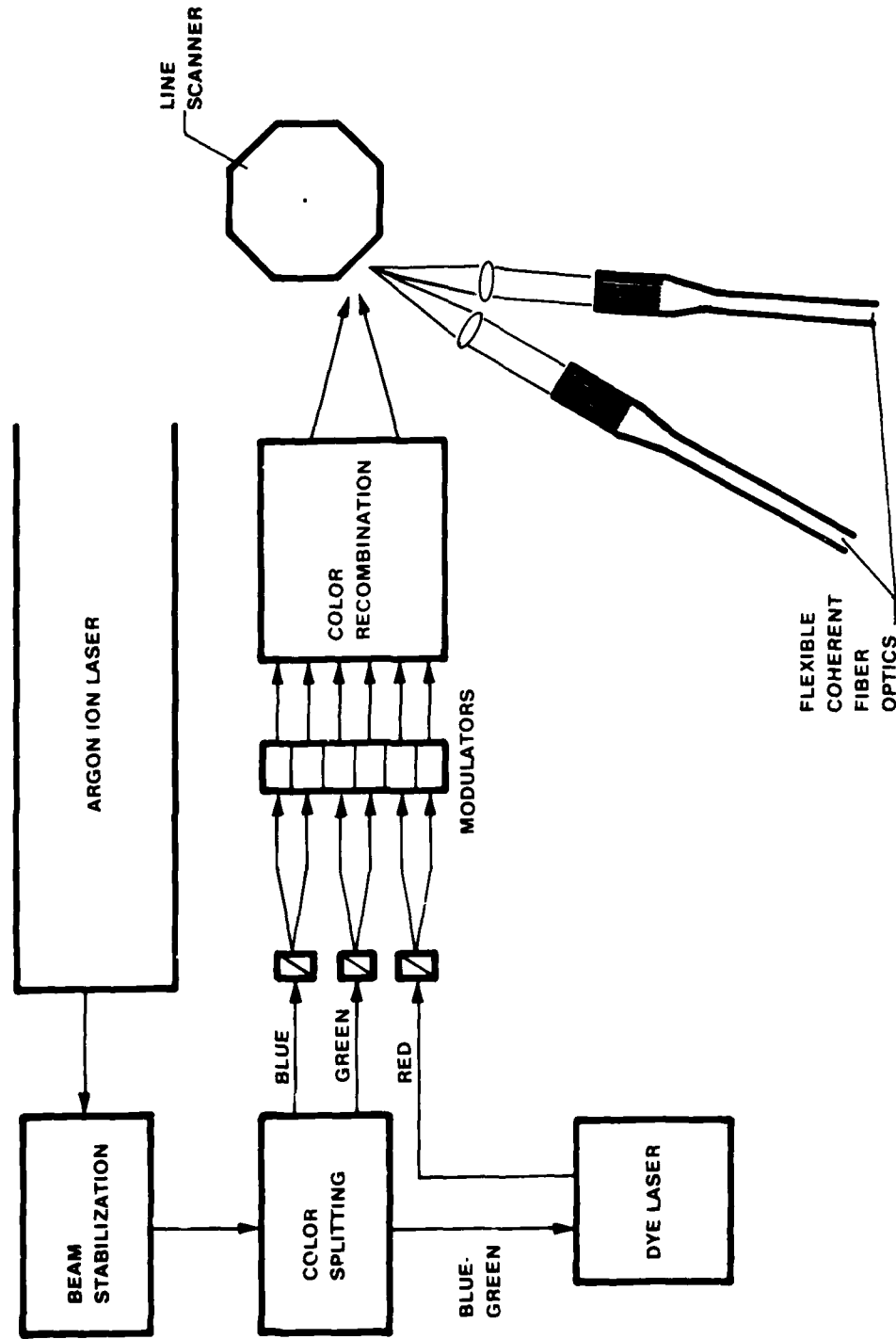


FIGURE 3
OFF - HELMET OPTICAL SYSTEM

The beam from an Argon ion laser, operated in all-lines output mode, is split into its separate wavelength components by a dispersive optical system. Part of the power at 514.5 nm is split off to provide a green beam, and power in a selected set of blue wavelengths is split off to provide a blue beam. Blue-green components, plus residual green power, are used to pump a Rhodamine 6G dye laser, which is tuned to output red light at wavelength 610 nm. Dispersive optics are used to recombine separate wavelengths assigned to the blue primary onto a single beam, and similarly to recombine the separate wavelengths assigned to pumping the dye. The Argon laser output power required to achieve a 10 f.l. display brightness is estimated, based on pessimistic assumptions, at 10W.

Red, green and blue beams are each split in two for AOI and IFOV rasters, and the six separate beams are intensity modulated at acousto-optic modulators. These beams are then combined to give two full-color beams, which are then scanned at a common line scanner and imaged, separately, onto two coherent fiber optic bundles.

The line scanner is a rotating polygon having 24 facets, rotating at 76,725 rpm to give a line rate of 30,690 lines/second to both modulated full-color beams. The line scan images will be 10 mm long by 10 microns wide. Each image will fall on a single row of 1000, 10 micron, optical fibers. (The fiber bundles may, for manufacturing convenience and to allow some selection, have many rows of 1000 fibers each.) The maximum expected laser power density on the input end of the IFOV fiber bundle is 20 W/mm², which is within a factor 2 of a measured damage threshold. Therefore, tolerance to incident power is an important part of the fiber optic procurement specification. The fiber optic bundles will be approximately 9' long, permitting the lasers, etc., to be remote from the simulator cockpit.

5. HELMET-MOUNTED OPTICS

The design for optics mounted on the user's helmet is shown in Figures 4, and 5.

The helmet-mounted optics include mirror scanners driven by galvanometers, and the final wide-angle projection lens which directs the light outward to the display screen. The mirror scanners are used to generate frame scan for the two projected rasters, AOI and IFOV. They also provide a capability for controlled offset of the two rasters with respect to the axis of the helmet mounted projector lens. Light from the two line scan images, input by fiber optics, is first passed through a scanner subsystem which permits the two line scans to be shifted along their own lengths. This produces a line-direction shift of the projected rasters, normally a horizontal shift, which is used primarily for following horizontal eye rotations. After passing through relay lenses, the two beams are reflected at separate scanner mirrors mounted on the shaft of a single galvanometer so that the line offset mechanism shifts the two rasters together.

In each beam, the light path is folded at a narrow strip of flat mirror on a window located at a line scan image. The light is then recollimated by a spherical mirror and relayed onto the frame scanners, passing through the window.

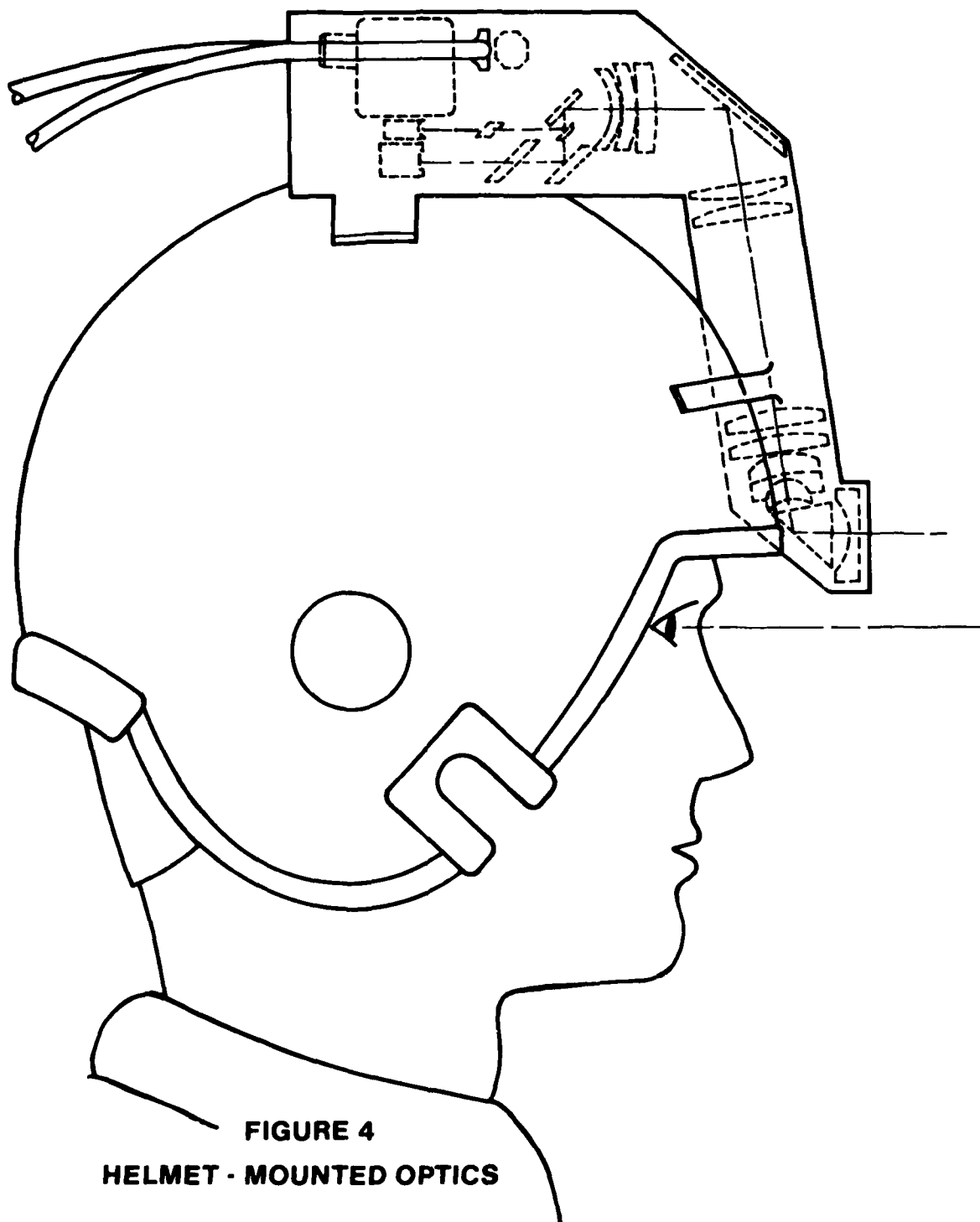
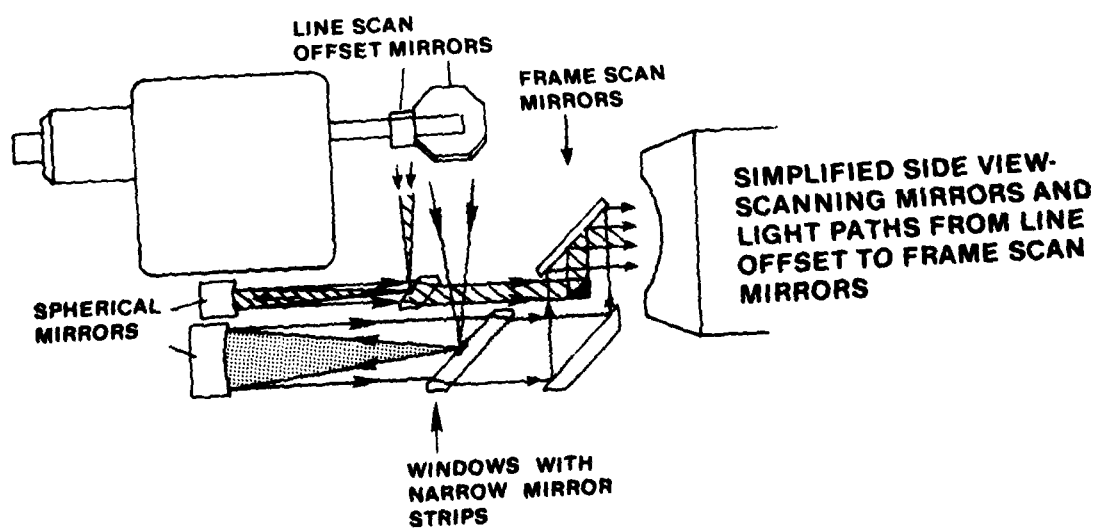
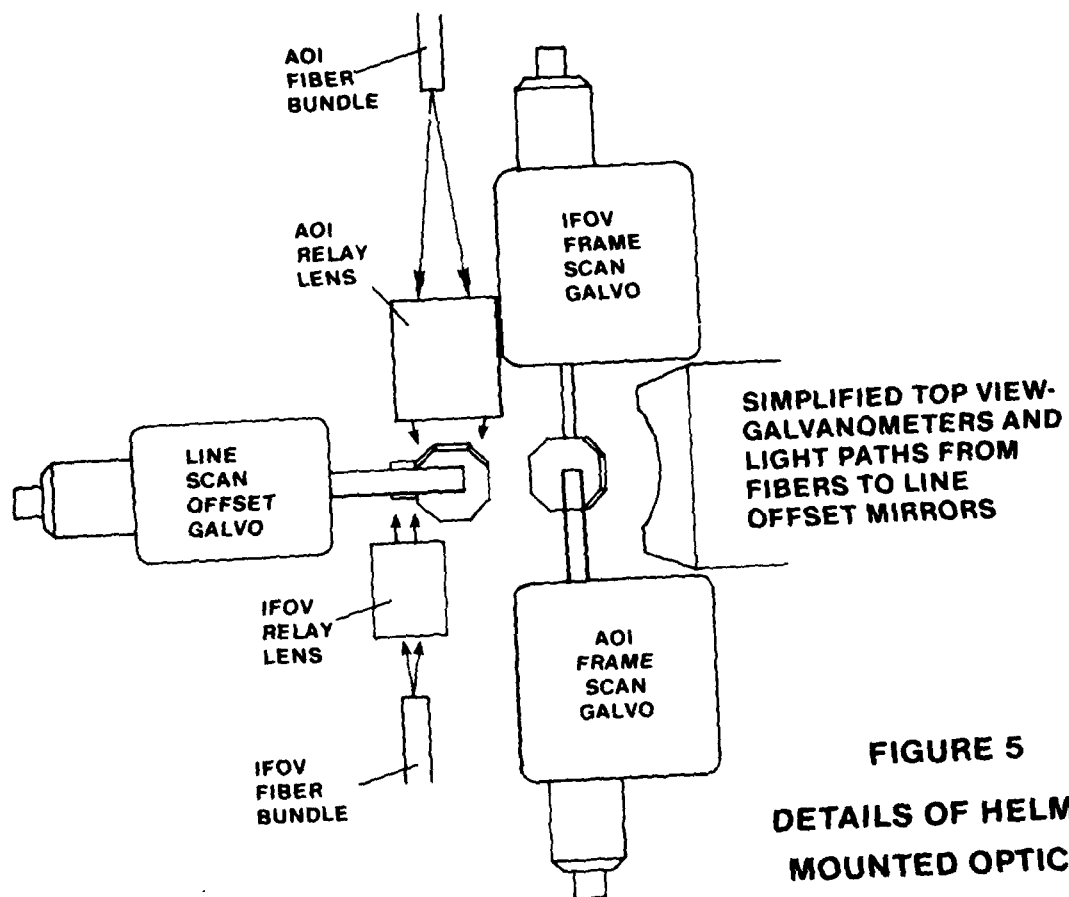


FIGURE 4
HELMET - MOUNTED OPTICS



Two flat mirrors, driven by separate galvanometers, provide frame scan and also combine the two beams on a common optical axis. The frame scanners provide controlled offset of the rasters in the frame scan direction, which is normally the vertical direction. The AOI beam is deflected at a single galvanometer-driven mirror, designated the AOI mirror, which produces the cyclic linear ramp scan required for the AOI raster. The IFOV beam is first deflected at a small galvanometer-driven mirror, designated the IFOV mirror, which generates cyclic linear ramp scan to produce 3/4 of the frame dimension for the IFOV raster. The IFOV beam then falls on the AOI mirror which adds frame scan to complete the IFOV raster.

The two beams are effectively combined at the small IFOV mirror. The IFOV beam is reflected from it, while the AOI beam, which has a larger diameter, passes around the mirror with partial obscuration by it.

Controlled offset of the rasters in the frame direction is provided by an offset only at the AOI mirror. Since both beams are deflected at this mirror, the two rasters are deflected together. The offset is used primarily to follow vertical eye rotations.

The frame-scan and raster offsetting optics will be located on top of the pilot's helmet. The raster images generated at this point will have moderate field angles, AOI and IFOV line lengths being respectively 11° and 44° . Light emerging from the frame-scan system is relayed by a complex lens and mirror system to an exit pupil which will be located in front of the pilot's forehead, approximately 30 mm above his eye level and 70 mm forward of his eyes. The system will provide angular magnification and direct the combined raster images outward onto the display screen.

The final lenses will produce substantial pincushion distortion, corrected in CIG, which is useful in distributing resolution optimally across the projected field.

6. COCKPIT AND DISPLAY SCREEN

The display screen will be a ten foot radius dome, already available in the VTRS facility, coated with retro-reflecting material. The separation of the user's eyes from the projector exit pupil will be approximately three inches so that the screen surface will be required to provide a reasonably uniform spread of light within 1.5° of the retro-reflective direction. A photometric gain in excess of 1000 is in theory possible, given this requirement on beam spread, but the target figure for screen gain is 100, which is considered likely to be achieved.

Commercially available retro-reflecting screen materials have characteristics similar to the required material, but none is close enough, and therefore a special product is required. This development is currently underway through a contract with the University of Arizona Optical Sciences Center.

The method of projection, from a point a few inches from the user's eye-point, produces potential problems due to light falling on the cockpit structure. Internal surfaces of the cockpit will reflect low-brightness images of the projected scene and it is necessary to ensure that these images

will not be noticeable. This is done essentially by arranging that the photometric gain of the screen is very much higher than the gain of cockpit surfaces - in fact by three to four orders of magnitude - so that the relative brightness of the screen image is two to three orders higher than that of ghosts within the cockpit. The dim ghost images on the cockpit structure will normally not be visible against a background of ordinary internal cockpit lighting.

The wide-angle scene projected onto the screen will have sharp boundaries due to shadowing by cockpit structures. Shadows produced by the lower edges of cockpit windows are not visible to the user, but shadows produced by window struts have been found, in simple experiments, to be very noticeable. The helmet-mounted projection technique is likely to be used only in simulator cockpits in which window struts are omitted.

Windows themselves will also be omitted to avoid possible specular reflection of projected light by the windows directly to the user, and care will be taken to avoid specular reflections to the pilot from cockpit instrument surfaces.

Use of the helmet mounted display will require some relatively minor alterations to the simulator heads-up display. The heads-up display beam combiner will be made as thin as possible, and its reflection coefficient reduced, so that it will not produce an objectionable displacement or shadow in the forward area of the projected scene. The brightness of display light reflected to the pilot from the heads-up display lens and CRT will be low compared with the brightness of the screen image. The CRT location will be shifted so that its virtual image falls at the screen distance.

7. SOME DEVELOPMENT PROBLEMS

In general, the approach taken in design of the display system has been chosen to reduce procurement problems to a minimum so that a visually coupled system, using helmet mounting, can be assessed as soon as possible and at relatively low cost.

Given the basic idea proposed by American Airlines and Redifon, potentially severe development problem areas include: the fiber optic link, the helmet-mounted frame scanner and the retro-reflective screen. The specification on the fiber optics is relaxed considerably by allowing the helmet-mounted system to be relatively complex. In particular, the length of the AOI line image to be carried by the fibers is minimized by locating the line scan offsetting system on the helmet; and the output end configuration of the fiber bundles is simplified by use of a relatively complex flat-field lens system on the helmet. The complex lens system, by providing angular magnification, also reduces the specification on frame scanners so that existing galvanometers can be used. The complexity of the helmet-mounted projection system which is evolved on these lines might make a binocular system, with separate optics for each of the user's eyes, prohibitively bulky. Therefore, a decision was made not to attempt a binocular arrangement, and to forego effective binocular collimation and immediate potential for three-dimensional projection. This greatly eases the specification on the display screen, since there is no immediate requirement to provide retro-reflection selectively to each of the user's eyes.

Some potentially severe electro-optics problems are avoided by electing to design the scanning system to project two rasters, although this requires two separate galvanometers on the helmet and separate relay optics up to the frame scanners. The alternative approach is generation of a single raster which must fill the IFOV field and be capable of the resolution required for the AOI. This implies a need to generate resolved pixels at rates in excess of 200 MHz. Components at or beyond current state-of-the-art are required (a) to provide pixel speed-up for the CIG signal assigned to the AOI channel, (b) to intensity modulate, and (c) to provide line scan. The fiber optic link for the single raster must have approximately 4000 fibers in the row used compared with 1000 per bundle given the present NTEC approach. If two separate rasters are projected, the signal bandwidths implied are easily handled by conventional electronics, modulators and line scanners.

Thus, within the CIG and display components, development problems are reduced mainly at the expense of bulk on the user's helmet. The current estimate of weight for the helmet, based on weight of existing galvanometers, some detailed optical design and outline design of mounting structure, is 2.5 lbs.

Some CIG development will be required. A contract has been awarded to General Electric, Daytona to recommend modifications to the VTRS-CIG to allow it to interface to the display system. These modifications include: capability for two channels to select and process different levels of detail simultaneously from the same active environment; capability to interface simultaneously to the host computer, the head tracking system and the eye tracking system; capability to provide distortion correction in both channels; capability to synchronize output video with a roughly synchronized line scanner; capability to blank and blend inset AOI with surrounding IFOV; and capability to provide offset signals to the line scan offset and frame scan galvanometers to follow eye movements and compensate for errors due to rapid head attitude rates. As of this writing, the CIG modifications are considered low risk developments.

The most severe residual development problems are considered likely to be found in the areas of head tracking and eye tracking. Fast, precise head tracking is vital to any helmet-mounted system for stability of the projected image. While eye-tracking need not be precise, a method must be identified which has high reliability, which can be set up rapidly, and which is acceptable to pilots - probably ruling out most of the current clinical techniques.

The present status of the NTEC investigations of head- and eye-tracking are described below.

8. HEAD TRACKING

The head tracking system is required to measure yaw, pitch and roll of the observer's head relative to the simulated cockpit structure. In order to determine performance requirements on the head tracking system a helmet mounted sight (Polhemus Spasyn Helmet Mounted Sight Model IIIA) has been procured. This system was interfaced to the VTRS CIG system which, in turn, supplied video to a miniature projection CRT mounted on a helmet.

This equipment was then utilized to perform a subjective evaluation experiment. The experiment consisted of having the CIG fly along a canned flight path over an environment consisting of an airfield and surrounding terrain. The observer's head direction determined the viewing direction used by the CIG to compute the scene.

The observed defects in image stability were:

a. A noticeable angular displacement of objects in the scene while the observer's head is rotating.

b. An occasional jitter of the displayed imagery even when the head tracking system sensor was fixed relative to the transmitter and cockpit.

The angular displacement with observer's head rotation was found to be directly related to the known throughput delay of the head-tracking and CIG system. The total delay is 0.1 sec, so that a $30^\circ/\text{sec}$ head rotation rate produces a 3° image displacement. This effect was judged to be objectionable and an effort is underway to correct the defect by dynamically displacing the raster. The amount of angular displacement is made equal to the difference between current (or most recent) measured head attitude and the head attitude utilized to compute the current scene. This approach causes the instantaneous field of view to be reduced by the amount of the motion compensating displacement during head motion. As of this writing, the hardware has been fabricated using a microprocessor and the software program completed. However, the evaluation was not yet underway. This technique should eliminate the effect of CIG throughput delay at the expense of reduced instantaneous field of view during head motions. The effect of head tracking system throughput delay cannot be eliminated but may be reduced utilizing linear extrapolation. The capability to perform linear extrapolation is included in the microprocessor and will be evaluated concurrently with the CIG throughput delay compensation scheme outlined above.

The magnitude of the display jitter, using the current head-tracking device, was approximately 15 milliradians. Measurement of signals indicated that a large part of this system noise originated in the internal components of the head tracking system. As of this writing, the manufacturer has agreed to evaluate the system.

An in-house analysis of alternative electro-optic techniques for head attitude sensing is being pursued. For use in a simulator, it should be feasible to improve on existing head-trackers which were designed for use in a real cockpit environment, since the simulator environment permits much greater flexibility in design.

9. EYE ATTITUDE MEASUREMENT SYSTEM

The eye attitude measurement system provides the CIG with the viewing direction needed to place the high detail area of interest in that part of the projected field corresponding to the observer's central vision. The eye direction information is not used to stabilize the resultant display but merely to select the area within which high detail and resolution appear, so that the measuring device may have relatively poor precision, accuracy and response. Some of the design goals for the eye tracking system are: (a) to

be visually unobtrusive, (b) a precision of $\pm 2^\circ$, (c) an accuracy (relative to head pointing direction) of $\pm 2^\circ$ and, (d) a response time of less than 16 milliseconds. Experiments utilizing a one-axis (azimuth only) limbus tracker indicate that these requirements will suffice provided that the width of the AOI is 25° or more, and the response time (sum of eye tracker and CIG response times) is less than 100 milliseconds. (The experiments were carried out using photographic imagery, with variable resolution but not variable detail, so that applicability to CIG imagery is somewhat questionable.)

If the total throughput delay is too large, a technique utilizing saccadic prediction may be required. Such a system is currently being developed under a contract with Carnegie-Mellon University (Dr. Terry Bahill - Principal Investigator). Dr. Bahill is also investigating the use of electro-oculography (EOG).

Reference 3 provides an excellent survey of eye attitude measurement techniques and limitations. Ideally, the selected method for eye tracking will require no attachments to the subject's head. Although remote oculometers exist, they are not capable of measuring eye attitude for a large range of head rotations, and the use of multiple remote oculometers to cover all likely head attitudes does not seem practical. The least obtrusive head-mounted technique for eye tracking is EOG. This method requires electrodes to be taped to the subject's face, but the electrodes are not found seriously objectionable and they do not have significant weight or obstruct the subject's vision in any way.

For these reasons, EOG is considered a promising method for use in eye-coupled flight simulation displays. EOG techniques are notorious for drifting but drift can be corrected in theory by automatic recalibration utilizing a single remote oculometer which will provide a reading whenever the observer is looking within 10° of it. Thus a combination of two unobtrusive techniques may prove feasible.

The eye-attitude measuring system remains a high risk area. However, a system which has no eye tracking, in which the AOI remains in the center of the head-tracked IFOV, is considered a viable alternative. In this case, the area of the AOI would be increased, with some loss of resolution, to encompass most normal eye rotations with respect to the head.

10. SUMMARY AND CONCLUSIONS

A visual simulation system has been described which takes advantage of human visual system limitations to provide a display which will be perceived as having both high resolution and very wide angle, utilizing only two display/image generator channels. The system design appears feasible utilizing available technology with the exception of two high risk areas namely: head attitude and eye attitude measurement systems.

REFERENCES

1. Morland, D. "System Description - Aviation Wide-Angle Visual System (AWAVS) Computer Image Generator (CIG) System Report", NAVTRAEQUIPCEN 76-C-0048-1, February 1979.
2. Redifon Simulation Ltd., "Scanned Laser Final Report Specification and Modification Supplement", American Airlines Contract with NAVTRAEQUIPCEN, N61339-77-C-0001, December 1979.
3. Young, L. and Shenna, D. "Survey of Eye Movement Recording Methods" Behavior Research Methods and Instrumentation Vol 7 (5), 397-429, 1975.

SESSION V

Chairman

Dr. Conrad L. Kraft
Chief Scientist, Crew Systems
Boeing Aerospace Company
Seattle, Washington



Conrad L. Kraft, Chief Scientist, Crew Systems and Simulation, Boeing Aerospace Company. His Ph.D. is from Ohio State University in Engineering Psychology and his M.A. and B.S. are from the University of Wyoming in Experimental Psychology. His 37 years of professional experience has been in industry, academia and the military. He was the scientific liaison between O.S.U. Research Foundation and the Aero-Medical Laboratory, Wright-Patterson Air Force Base, Ohio (1952-59) before going to Boeing in Seattle. With Boeing he has been particularly interested in aviation safety and most recently chaired the committee which developed the specifications for Boeing's Flight Crew Training Simulator's Computer-Generated Visual system, the Compuscene built by General Electric.

SOME PSYCHOPHYSICAL ASPECTS OF VISUAL PROCESSING OF
DISPLAYED INFORMATION



Yehoshua Y. Zeevi
Visiting Professor
Man-Vehicle Laboratory
Massachusetts Institute of
Technology

Yehoshua Y. Zeevi obtained his Ph.D., M.S. and B.S.E.E. from the University of California at Berkeley, the University of Rochester and the Technion - Israel Institute of Technology, respectively. His professional experience has been in the academia, mostly with the Technion, Harvard University, Lawrence Berkeley Lab., and M.I.T. He has worked extensively with display systems studying signal detection, eye movement characteristics and visual information processing. He is presently a visiting Professor at the Man-Vehicle Lab., Department of Aeronautics and Astronautics, M.I.T., working on visual aspects of flight simulators.



John G. Daugman
Resident Tutor, Physics
and Psychology, Winthrop
House; Graduate Student,
Harvard University

John Daugman obtained his B.A. from Harvard University in Physics and is currently a Ph.D. candidate at Harvard in Psychology. He has worked on mathematical models of physiological filters and two-dimensional frequency characterization of psychophysical channels. He also has been developing an electronic system for real-time Fourier image analysis and synthesis. The first generation of this system known as the Picasso is already used in several research laboratories.

SOME PSYCHOPHYSICAL ASPECTS OF VISUAL PROCESSING OF
DISPLAYED INFORMATION

Y.Y. Zeevi and J.G. Daugman

Man-Vehicle Laboratory
Dept. of Aeronautics and Astronautics
Massachusetts Institute of Technology
Cambridge, Massachusetts

and

Department of Psychology
Harvard University
Cambridge, Massachusetts

ABSTRACT

Design of visual simulators calls for consideration of behavioral components so that one may better match display and visual system characteristics in order to optimize bandwidth and data base allocation. In this paper we consider some of the well documented and better understood aspects of visual psychophysical capabilities, with special emphasis on spatio-temporal frequency analysis. It is concluded that one should attempt, and it may at this stage be feasible, to design display systems employing an exponential spiral raster which matches the information density in the display to the information handling capabilities of the visual system.

SOME PSYCHOPHYSICAL ASPECTS OF VISUAL PROCESSING OF DISPLAYED INFORMATION

As one strives to generate more realistic imagery in advanced simulators for pilot training (ASPT), scene complexity and requirements for bandwidth and data base increase tremendously (Schachter and Ahuja, 1980). Since practical limitations impose constraints on the attainable scene complexity, it becomes crucial to attempt an optimal design of computer generated imagery (CGI). Although it is not immediately clear exactly what the criteria for design optimality ought to be, certainly such criteria will depend in part on the information processing properties of the human visual system. It is therefore relevant, regardless of the approach employed in visual simulation and the technology implemented, to consider physiological and psychophysical characteristics so as to match the CGI resources to the inherent signal detecting abilities of human observers. In this paper we present an overview of some aspects of these capabilities of the visual system, with special emphasis on the dynamics of visual signals, spatio-temporal modulation transfer functions for target detection, and some considerations of signal-to-noise ratio.

It is important to observe that the visual world is mapped by the retina onto dynamic patterns, even during visual fixation because of the constant involuntary movement of the eye. During fixation the visual-occulomotor system still generates slow drifts lasting a few hundred milliseconds, separated by rapid jumps known as microsaccades having high velocities and amplitudes of a few minutes of arc (Boyce, 1967). It is believed that there is an elevation of visual threshold and a suppression of pattern information processing during these microsaccades, as during larger saccades such as those which subserve foveation in visual space and position correction during tracking movements. Thus in the natural mode of visual information processing, the world is necessarily sampled into temporal frames of a few hundred milliseconds. Various studies indicate that some kind of weighted response integration takes place over such frames (Koenderink & van Doorn, 1978; Legge, 1978). If in fact drift duration coincides with the duration of the processing frame, then there should be a dependency of the drift on the stimulus temporal structure, determined by the time-frequency uncertainty principle $\Delta f \Delta t = \text{const}$ (Gabor, 1946). One of us (YYZ) is presently investigating possible adaptive characteristics of intersaccadic frame duration. Considering the signal detection problem, integration of visual signals over such finite frames is essential in order to achieve an acceptable signal-to-noise ratio, since the visual system is exposed to a variety of sources of noise that contaminate the image quality. Even the quantal nature of light imposed some constraints in the course of evolution on visual system design (Rose, 1974). The evolution of photoreceptors achieved the theoretical limit of signal detection, since retinal rods can respond to single photons.

As a consequence of this optimal design, however, photon noise induces signal variability. Secondly, since the energy of a single photon is far less than that of any appreciable bioelectric signal, an intermediate process of amplification is necessarily incorporated into photoreceptor design. This process introduces an internal source of noise. Consequently, about 5-15 photons are required for a photic stimulus to be detected reliably. In addition, there are in the visual system various other sources of neural noise. The interplay of all of these sources of noise determines, for example, the psychophysical increment intensity thresholds. Theoretical analysis indicates that due to photoreceptor nonlinearity, quantal noise is the main limiting factor of incremental intensity sensitivity only over an intermediate (mesopic) range of light intensities. At low and high intensities, receptor and neural noise determine the bound on sensitivity (Zeevi & Mangoubi, 1978). The noise characteristics of the human visual system are relevant for CGI both in terms of an observer's ability to resolve "barely visible" contrast in space/time, and in terms of how noise-free a display system must be in order to be perceptually realistic.

Although image blurring would be an expected consequence of eye movements during integration time, visual acuity experiments actually indicate that artificial image stabilization does not improve acuity whereas increasing the signal duration up to about 300 msec does (Keessy, 1960). Thus, such experiments indicate that at some stage in the processing hierarchy there should exist a mechanism for separation of spatial and temporal information. One model assumes that this operation takes place in the frequency domain, arguing that in the early stages of preprocessing, visual signals are decomposed into spatio-temporal harmonic frequency components and that subsequently these are grouped and summed in the frequency domain to provide a "frozen picture" (Fig. 1) or for the extraction of temporal or velocity information (Gafni & Zeevi, 1977, 1979; Zeevi & Gafni, 1980). In short, if we consider an idealized expansion

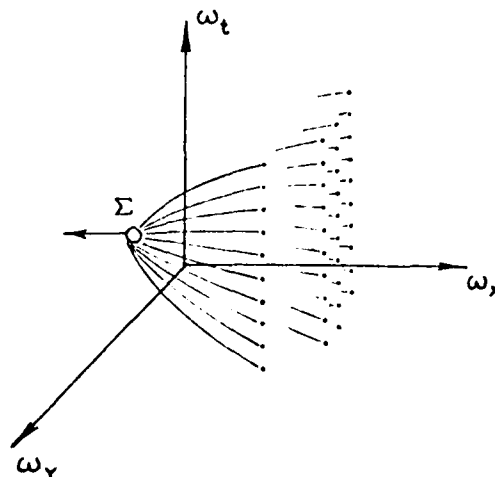


Fig. 1. Grouping and summation of spatio-temporal harmonic components to provide a "frozen picture". Segregation of components is by spatial frequency; summation operates across temporal frequencies.

into three-dimensional harmonic components, the extraction of spatial information from a dynamic pattern can be formally presented by

$$f(x,y,0) = F^{-2}\{F^3[f(x,y,t)]d\omega_t\}$$

where F^3 represents the three-dimensional Fourier transform and F^{-2} the inverse two-dimensional transform. This model brings us to an important and somewhat controversial facet of vision research.

In engineering we often prefer to characterize systems in the frequency domain employing transfer functions. This approach was found to be useful also in optics and subsequently in vision research where spatial and temporal frequencies have been widely used by various investigators (e.g. Campbell & Robson, 1964; Kelly, 1961). The global envelope of human visual system sensitivity, represented in Fig. 2, specifies the total range of spatio-temporal modulation

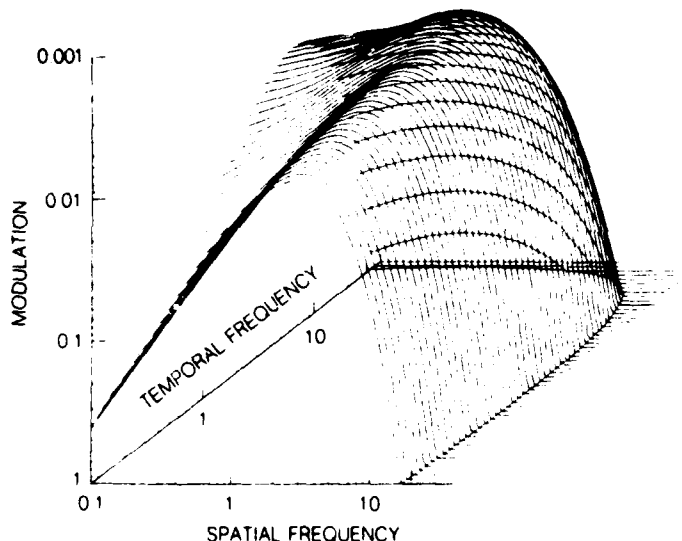


Fig. 2. Global envelope of spatio-temporal sensitivity of human visual system. (From Kelly, 1977.)

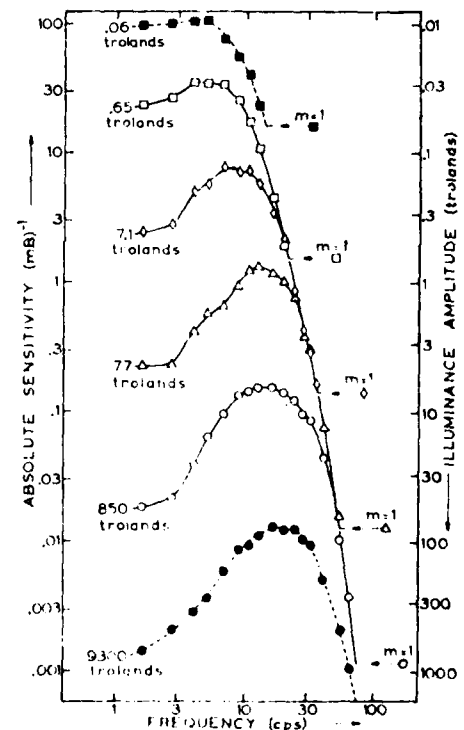


Fig. 3. Human sensitivity to uniform flicker. Peak sensitivity shifts to higher frequencies at higher levels of mean luminance. (From Kelly, 1961.)

that can convey visual information. Any image information involving modulation outside of this spatio-temporal envelope, or on low points on the surface, in general may not be detectable. A number of gross constraints for CGI present themselves immediately from Fig. 2: First, CGI displays based on television techniques employing raster scans must have frame rates exceeding roughly 50 Hz in order for the frame flicker to be imperceptible. The critical flicker fusion frequency depends, however, on many variables. (i) As may be clearly seen in Fig. 2, for the lower spatial frequencies the temporal sensitivity extends to higher flicker frequencies than is the case for higher spatial frequencies. (ii) The spatio-temporal detection envelope changes in shape considerably as a function of eccentricity, the distance on the retina away from the fovea. The surface shown in Fig. 2 applies only for foveal vision (roughly the central two degrees). Eccentric vision is worse in detecting all spatial frequencies than foveal vision, but temporal modulation of peripheral information significantly enhances its detectability. (iii) The mean luminance level at which image contrast is viewed also has a considerable effect on the shape of the spatio-temporal envelope and the locations of its maxima; Fig. 3 shows flicker sensitivity curves at a range of luminance levels spanning five log units. The higher the mean luminance, the higher the flicker frequency that can still be resolved without fusion. (iv) The mean luminance level also affects the peak of the purely spatial modulation transfer function, as in the temporal case: the higher the mean luminance, the higher the spatial frequency of maximum sensitivity. At low (scotopic) luminance levels, non-foveal regions of visual space are in fact the most sensitive areas for low and intermediate spatial frequencies. These four characteristics are readily recognizable in the common experience of viewing ordinary television in one's visual periphery, with a perceptible flicker that is not noticeable in foveal viewing; and in the well-known loss in visual acuity with eccentric viewing or with reduced ambient luminance.

In order to make optimal use of bandwidth resources in CGI, its allocation to spatio-temporal modulation should not exceed the detection limits of the human visual system as functions of eccentricity, mean luminance, and the limiting tradeoffs between spatial sensitivity and temporal sensitivity. The economies resulting from these considerations can be very large, since the psychophysical magnitudes of the dependencies mentioned above typically exceed a ten-fold range. Particularly significant is the dependence of resolution on eccentricity, since pixel density requirements translate directly into CGI bandwidth requirements. As seen in Fig. 2, the disappearance of spatial frequency contrast sensitivity above roughly 20 cycles per degree (cpd) for foveal vision implies that pixel densities in central viewing need not exceed 1.5 minutes of arc, which corresponds to a pixel size of 0.5 millimeter when viewed from a distance of one meter in order for the discreteness of the image to be unresolvable even when

adjacent pixels are at maximum contrast. (In this estimate we do not consider the phenomenon of hyperacuity, in which vernier separations as small as 4 seconds of arc may be resolved, because this capability arises from the detection of phase information independent of spatial frequency (Westheimer, 1979).) The fall-off in visual acuity with increasing eccentricity from the fovea is dramatic: for spatial frequencies in the range of 0.25 to 2 cycles per degree, the contrast thresholds increase by a factor of two for every 12 degrees in eccentricity (Koenderink, Bouman, de Mesquita, & Slappendel, 1978), and for any given spatial frequency the visual field is blind beyond a certain critical eccentricity. The critical eccentricity decreases monotonically as a function of spatial frequency; thus, for example, a spatial frequency of 2 cpd becomes invisible at an eccentricity of 30°; 5 cpd becomes invisible at 20°; 10 cpd becomes invisible at 15°; and 16 cpd becomes invisible at 6° (Koenderink *et al.*, 1978). Thus if one were to generate a pixel-based display system in such a way as to have pixel size be specified by the maximum detectable spatial frequency for each eccentricity, then at a viewing distance of one meter the pixel size should vary monotonically with eccentricity from 0.5 mm in the fovea to 2 mm at an eccentricity of 20° and 0.5 centimeter at an eccentricity of 30°. This ten-fold reduction in required pixel density over the first 30° in eccentricity implies likewise a ten-fold reduction in CGI bandwidth allocation as a function of eccentricity. The potential bandwidth reduction is very substantial: a one-degree wide "ring" centered on the fovea with a radius of 50 degrees in a conventional constant-pixel-density display consumes 300 times as much bandwidth as does a one-degree patch in the critical fovea, but 94 % of the bandwidth is wasted since such an image is indistinguishable for human observers from one whose pixel width at this eccentricity is 16 times greater.

Because the function relating the required pixel size to the eccentricity is a radial function, it may be most efficient to design CGI displays with spiral rather than Cartesian raster systems. Current rapid advances in unobtrusive eye-position-tracking technologies (e.g. IR beam, magnetic coil, CCD camera) make it possible in principle to track the location of foveal viewing and to use this real-time information to define the origin-of-coordinates in CGI displays for parameters such as pixel density that depend on eccentricity. Generating images in polar rather than rectangular coordinates is technically easy to do, since the required X- and Y-axis deflection signals for CRT plates require only a quadrature phase-split pair of sinusoids and an exponential ramp function to produce the log spiral wave forms:

$$\begin{aligned} V_x(t) &= (e^t - 1) \cos(\omega t) \\ V_y(t) &= (e^t - 1) \sin(\omega t) \end{aligned}$$

(The exponential ramp would also have to multiply the beam current in order to maintain a constant phosphor writing speed independent of radius to keep luminance constant; and it might be necessary to add raster noise proportional to radius to smear out the separation of raster lines at large eccentricities.) A constant rate of informa-

tion flow into a spiral raster display produces effectively a "polar pixel" whose solid angular subtense is proportional to eccentricity (since the rotary velocity of the beam is proportional to eccentricity and raster density is inversely so), and this property automatically matches the fall-off in resolution of the visual system reciprocally with eccentricity. (One of us (JGD) has designed and used such spiral raster displays for psychophysical purposes.) Thus a log spiral raster automatically converts a constant rate of information flow from CGI hardware into a display whose information density more-or-less matches the decline in visual acuity with radius. The desired distribution of information density would be roughly as represented in Fig. 4, as adapted from Koenderink et al.'s (1978) model for the size distribution of retino-cortical units. Their careful measurements of spatial frequency sensitivities as function of eccentricity suggest that when a single scaling factor compensates for eccentricity by multiplying both the spatial frequency content of a target and its extent, then the spatio-temporal contrast thresholds are identical across the entire visual field.

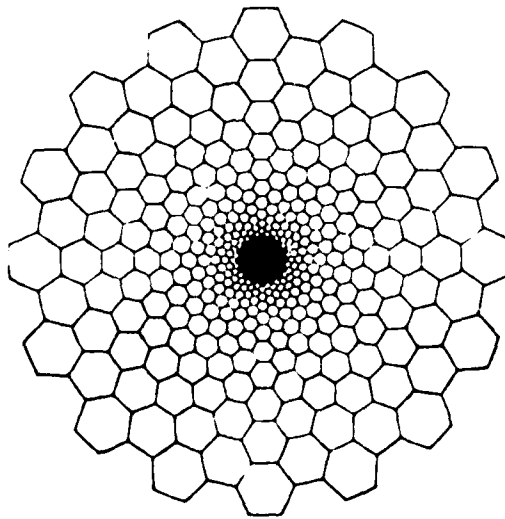


Fig. 4. Proposed spatial distribution of information density in CGI displays to match human visual resolution for optimizing CGI bandwidth allocation. (From Koenderink et al., 1978.)

It is generally believed today that the global modulation transfer functions discussed so far (at various eccentricities and luminance levels) are in fact just "envelopes" of more sharply defined underlying mechanisms. This so-called "channels" hypothesis has been especially articulated with regard to spatial frequency mechanisms. In part the model is supported by physiological measure-

ments of the response properties of single neurons in the visual cortex of cat and monkey. Many investigators have reported that neurons in cortical Area 17 respond to the visual world in a way that is localized both in space and in spatial frequency, in the sense that the "best" stimulus for evoking large responses from single neurons in terms of nerve impulse frequency is a stimulus that exists in a certain well-defined region of visual space (the "receptive field" of the cell in question) and is also localized in spatial frequency by a certain periodicity of luminance modulation. Thus a stimulus becomes "irrelevant" to a given cell either by its being in the wrong location in visual space or by its having the wrong spatial frequency of contrast modulation. These joint characteristics, of retinotopic mapping of visual space and spatial frequency tuning, necessarily require a trade-off in localizability in the two domains (just as the time-frequency tradeoff mentioned earlier). The response characteristics of cortical neurons are conveniently described in terms of a receptive field profile, which is a function over visual space specifying the excitatory or inhibitory influence that light has on a cell. Typically such measured profiles have the appearance shown in Fig. 5 : one or two regions in which light excites the firing rate of the cell, interleaved by one or two regions in which light inhibits the cell, and beyond these regions light has no influence on the cell. It is obvious that trying to increase the spatial resolution of such mechanisms by making them smaller would destroy their spatial frequency tuning, since the limiting case of an infinitesimal detector would respond equally well to all spatial frequencies. Likewise it is obvious that increasing their spatial frequency tuning by adding more periods of excitatory/inhibitory regions would occupy a large region of visual space and thus destroy spatial resolution. The particular

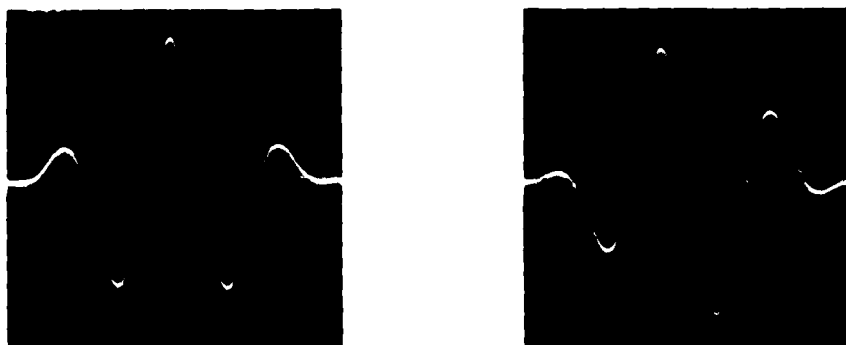


Fig. 5. Gabor elementary signals possessing localization in both the space domain and the spatial frequency domain. The product of the "spread" in these two domains is minimal for the functions shown, which are sine and cosine multiplied by a Gaussian. The functions form a complete basis set.

functions shown are the product of a sinusoid or cosinusoid and a Gaussian; Gabor(1946) proved that such functions minimize the product of their "spread" in the space domain and the spatial frequency domain. With both the even and odd members (sine and cosine) included, the functions form a basis. Mathematically, they are described by

$$f(x) = e^{-(x/\lambda)^2} e^{-i\omega'x} e^{i\theta}$$

for spatial frequency ω' , spatial extent λ , and spatial phase θ which is 0 for even symmetry and $\pi/2$ for odd symmetry. The description of these waveforms in the spatial frequency domain may be obtained by the Fourier transform of $f(x)$, which is

$$F(\omega) = e^{-(\omega-\omega')^2 \lambda^2} e^{i\theta}$$

from the Modulation Theorem. It is seen that the "spread" in the space domain is λ while the "spread" in the spatial frequency domain is $1/\lambda$, so sharpening up the resolution in one domain bears a proportionate price in the other domain. The fact that the visual system neurons evidently balance this trade-off by possessing relative spatial retinotopic localization and at the same time a spatial frequency bandwidth of about one octave with matched sine and cosine (phase quadrature) cell pairs (Pollen & Ronner, in press) is suggestive that important kinds of visual processing are going on in both domains.

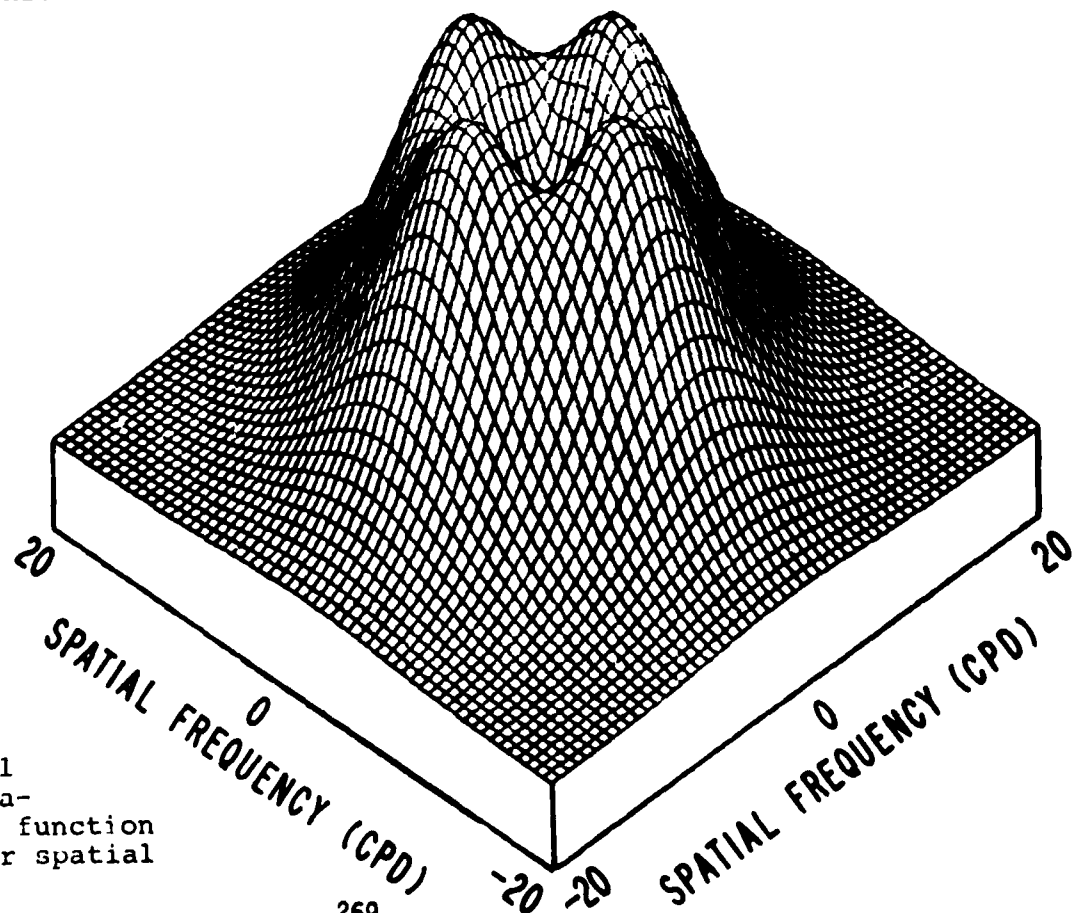


Fig. 6. Global spatial modulation transfer function in the Fourier spatial plane.

Psychophysical evidence for visual processing in the spatial (and temporal) frequency domains arises from the observation that a high contrast image containing only a "singletone" of spatio-temporal contrast modulation is capable of significantly lowering the sensitivity to similar "test" images presented either simultaneously (masking) or subsequently (adaptation). When the masking or adapting stimulus has a spectral content which differs from that of the test stimulus, it is possible to estimate a "bandwidth" of the threshold elevation effect in a parametric way. An excellent review of this broad literature is found in Sekuler (1974). The results of such experiments generally yield estimates of approximately one octave for the spatial frequency bandwidths of the underlying "channels," as well as an orientation bandwidth of approximately 15 degrees. If we consider for the moment just the spatial aspects of vision apart from the temporal, it becomes clear that the two-dimensional manifold of visual space has a 2D (not just a 1D) spatial frequency characteristic. It is useful to parse this spatial Fourier plane in polar coordinates, so that the radial coordinate is spatial frequency and the angular coordinate is orientation. Then the global modulation transfer function of the human visual system is found empirically to be roughly as shown in Fig. 6. The overall bandpass character of spatial contrast modulation sensitivity is reflected in the depressed center, indicating both low and high spatial frequency attenuations in sensitivity. The volcano's anisotropy reflects the well-known "oblique effect", by virtue of which the vertical and horizontal orientations are more readily detected than the oblique orientations. This effect is far more pronounced at higher spatial frequencies than at low; at around 10 cycles per degree, the anisotropy may amount to a three-fold difference in sensitivity at vertical versus oblique orientations. The global surface shown in Fig. 6 can be broken down into component 2D spatial frequency channels by studying masking interference effects. The resulting threshold elevation surface shown in Fig. 7 reveals the kind of spatial frequency / orientation mechanism that a "channel" is thought to be, namely a spectral filter with roughly a one octave spatial frequency bandwidth and about 15 degrees orientation bandwidth. The spectral shape shown can serve as a sort of guideline for the conditions under which two different spatial targets can mask each other or in other ways interfere as a result of being processed by the same frequency/orientation channel. As a rule, the spatial frequency bandwidth is proportional to the channel's center frequency, falling generally within an octave on either side. A channel's orientation bandwidth appears to be independent of what its preferred spatial frequency is. Within any particular channel, however, the orientation tuning and spatial frequency tuning are not separable variables, and the band of orientations over which a channel responds may shrink in size by a factor of two when driven at non-optimal frequencies (Daugman, 1980a). The polar spectral nonseparability of visual channels is predictable from considerations of neural receptive field profiles (Daugman, 1980b & 1981a).

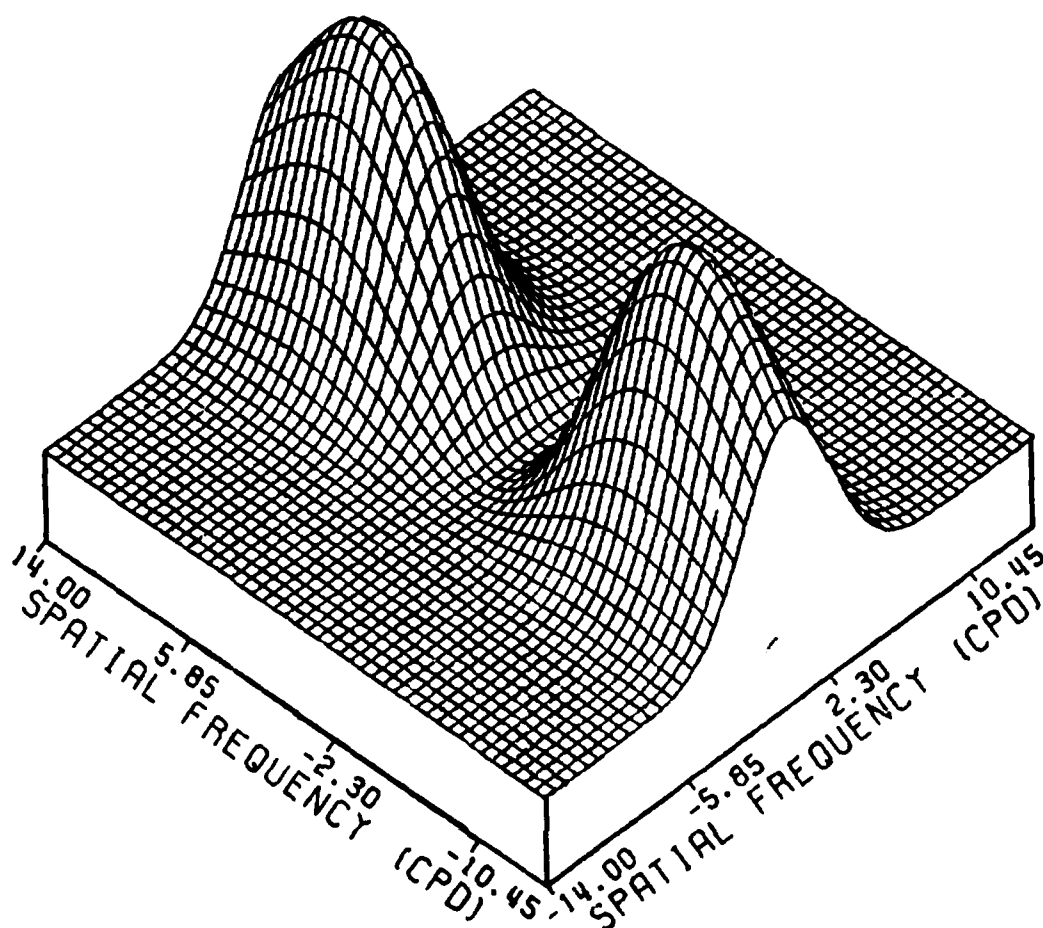


Fig. 7. The spectral shape of a two-dimensional spatial frequency channel in the human visual system, as inferred from spread-of-masking threshold elevation experiments.

The finite bandwidths of underlying spatial frequency channels makes it possible for information presented in closely adjacent frequency bands to interfere or mask mutually. This subject has been carefully explored by Julesz & colleagues (1980) regarding the masking effects of digital quantization of images. When an image is discretized into a coarse density of grey areas, it becomes very difficult to recognize when the density is only about 10×10 . By selectively filtering out the spectral components introduced by the discretization, Julesz (1980) showed that the recognition problem results from spatial frequency masking of the low frequency components by the intermediate frequencies arising from discretization. The high frequencies were not responsible for the masking effect, presumably because their spectral remoteness ensures that they would be processed by separate mechanisms in the visual system. As a general rule, it should be born in mind in CGI design that spatial information presented in spectral bands that are separated

by more than one octave in frequency or more than about 15 degrees in orientation will be processed independently by the visual system, while information bands spreading within a channel may be vulnerable to mutual masking. The relevance of such masking may be gauged by the principle emerging from Ginsburg's extensive studies (1978) of form vision with filtered images, that primarily the low spatial frequencies in an image are used for form identification and object recognition.

Until recently it was less known what the temporal structure of channels is. The assumption was that there exists only a bimodal partition, into "sustained" and "transient" mechanisms (Tolhurst, 1975). Recent experiments employing a broad repertoire of psychophysical techniques indicate however that there exist at least several temporal frequency tuned mechanisms (Gafni & Zeevi 1980a,b; Tyler, 1980; Zeevi & Gafni 1980). Experiments on masking with noise indicate a bandwidth of about one octave for the entire range of central frequencies 1-40 Hz studied with this technique (Tyler, 1980), whereas results of experiments based on subthreshold summation indicate a somewhat narrower bandwidth of 2 to 3 Hz for the range of central frequencies explored, 5 to 10 Hz (Gafni & Zeevi, 1980a). In these experiments, stimuli consisted of signals which match in spatial frequency (0.5 or 1.0 cpd) but differ in temporal frequency. The temporal frequency of one of the signals, f_1 , was either 5, 7.5, or 10 Hz and its contrast was adjusted to 75 % of its threshold value. The frequency of the second signal was $f_2 = f_1 + \Delta f$, where Δf is a variable quantity selected to yield a constant phase relationship between the flicker and its beating envelope (Fig. 8).

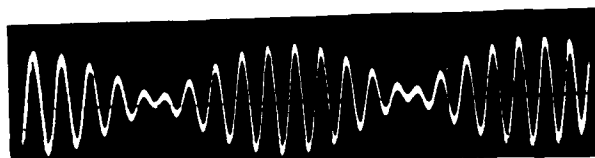


Fig. 8. The sum of two temporal frequencies with flicker and beating envelope being in phase.

The results of these subthreshold summation estimates are in Fig 9. It is interesting that whatever frequency is selected as f_1 ,

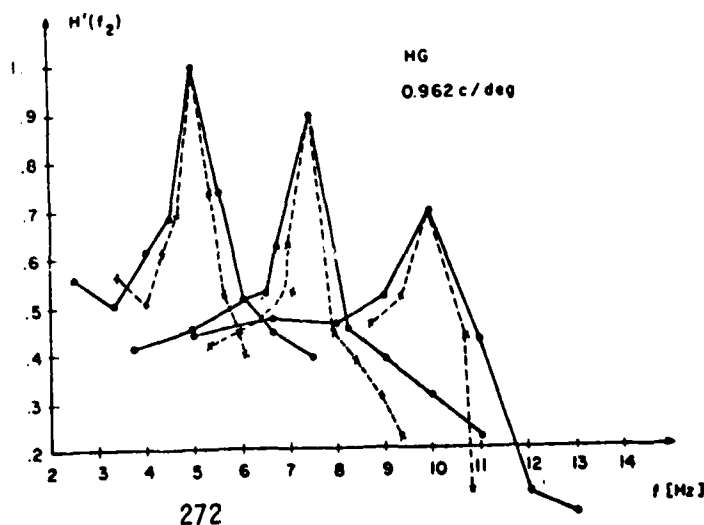


Fig. 9. Subthreshold summation data for the waveforms in Fig. 8, demonstrating the existence of narrow-band temporal channels.

a channel is found to be centered there. One possible explanation could be that the density of channels is very high, as in audition, with extensive overlap, but this was ruled out by frequency discrimination experiments. Thus it appears as though there are only a few channels with adaptive characteristics. If in fact there exists an adaptive mechanism which maximizes response sensitivity, a channel would adjust its central frequency so as to maximize its output for a given input signal combination. Correcting, accordingly, the raw data, one obtains even narrower bandwidths as shown by the dashed lines in Fig. 9.

Preliminary experiments were conducted at the Human Resources Laboratory of Williams Air Force Base, to determine and compare the masking effects of static and dynamic noise on target detection and tracking as assessed by probability of correct responses and their reaction time (Zeevi, 1980). Data such as those shown in Fig. 10 demonstrate that as target luminance and the corresponding contrast decrease, reaction time measured as saccadic latency increases. This is consistent with previous findings (Wheless et al., 1967) and should be taken into consideration in the design of display systems for ASPT. The effect of target luminance on saccadic latency is further substantiated once masking noise is introduced. This too is consistent with previous results demonstrating that noise masking is more effective than coherent masking at the same contrast level (Stromeyer and Julesz, 1972; Kronauer and Stromeyer, 1980). More interesting though are the findings indicating that dynamic noise has a significantly more detrimental effect on target detection performance than static noise of the same spatial spectral content. These findings further support our argument that dynamic signals are preprocessed in the visual system as a whole before being separated into spatial and temporal information.

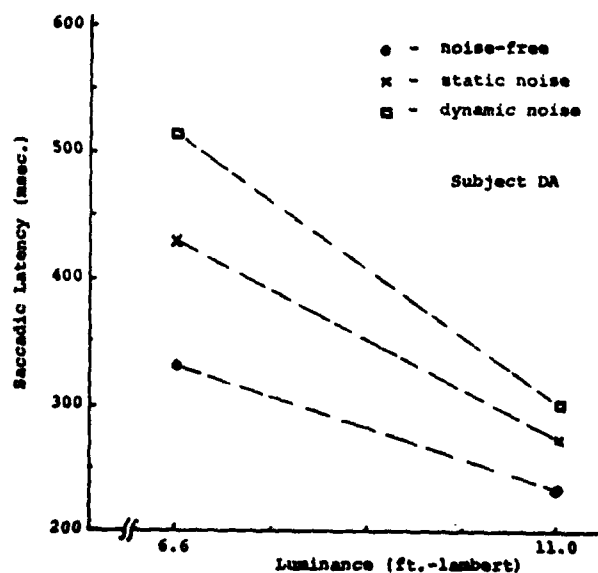


Fig. 10. Examples of saccadic latencies in detection and tracking of aperiodic point target subtending about 0.4° visual angle.

To sum up, we have discussed a few aspects of visual psychophysics relevant to the perception of displayed information. We examined signal-to-noise ratio, considering both internal and external forms of noise and its masking effects. The consequences of constant eye movements were discussed in terms of a temporal "framing" of the visual world, which is a crucial part of cortical information processing. The inherent trade-off between time and frequency resolution in such a scheme was a recurring theme throughout the paper. A convenient approach was to employ spatio-temporal frequency domain analysis, which is complementary to more traditional space-time analysis, but which captures more powerfully the visual characteristics that are relevant to engineering considerations. Both domains are really necessary for a complete representation of visual system characteristics. We discussed the global envelope of spatio-temporal sensitivity and the evidence that this envelope is comprised really of many relatively more narrowly tuned mechanisms. As reviewed from the literature, these spatio-temporal characteristics depend dramatically on eccentricity and mean luminance. For reasons of optimal bandwidth allocation these considerations should be taken into account in display design. Although for these reasons it appears to be attractive to generate displays using exponential spiral rasters, rather than Cartesian raster scans, it should be born in mind that there remain problems in superimposing the display origin of coordinates on the visual axis. Achieving this will require high precision measurement, computation, and prediction of eye position end point during the time course of saccades. Such instrumentation and algorithms are now beginning to appear feasible.

References

- 1) Boyce, P.R. (1967), Monocular Fixation in Human Eye Movement, Proc. Roy. Soc. B 167, 293.
- 2) Campbell, F.W. and Robson, J.G. (1969), Application of Fourier Analysis to the Modulation Response of the Eye, J. Opt. Soc. Am. 54, 581.
- 3) Daugman, J.G. (1980a), Two-Dimensional Fourier Analysis of Visual Channels and Cortical Receptive Fields, Optical Society of America, Sarasota, April 1980.
- 4) Daugman, J.G. (1980b), Two-Dimensional Spectral Analysis of Cortical Receptive Field Profiles, Vision Research 20, 847.
- 5) Daugman, J.G. (1981a), Formal Properties of Anisotropic Linear Cortical Mechanisms, in press, Vision Research.
- 6) Daugman, J.G. (1981b), Spatial Channels in the Fourier Plane, in preparation.
- 7) Gabcr, D. (1946), Theory of Communication, U. Inst. Elect. Eng's, 93, 429.
- 8) Gafni, H. and Zeevi, Y.Y. (1977), A model for Separation of Spatial and Temporal Information, Biol. Cybernetics 28, 73.
- 9) Gafni, H. and Zeevi, Y.Y. (1979), A Model for Processing of Movement in the Visual System, Biol. Cybernetics 32, 165.
- 10) Gafni, H. and Zeevi, Y.Y. (1980a), Temporal Frequency Channels in the Visual System, Technion, EE Publication No. 394.
- 11) Gafni, H. and Zeevi, Y.Y. (1980b), Temporal Channels in Vision, Annual Meeting Optical Society Am., Chicago.
- 12) Ginsberg, A.P. (1978), Visual Information Processing based on Spatial Filters Constrained by Biological Data, Ph.D. Thesis, Cambridge University.
- 13) Julesz, B. (1980), Spatial Frequency Channels in One-, Two-, and Three-Dimensional Vision: Variations on a Theme by Békésy, in Visual Coding and Adaptability (C. Harris, ed.), Erlbaum.
- 14) Keesy, V.T. (1960), Effects of Involuntary Eye Movements on Visual Acuity, J. Opt. Soc. Am. 50, 769.
- 15) Kelly, D.H. (1961), Visual Responses to Time Dependent Stimuli: I. Amplitude Sensitivity Measurements, J. Opt. Soc. Am. 51, 422.
- 16) Kelly, D.H. (1977), Visual Contrast Sensitivity, Optica Acta, 24, 107.

- 17) Koenderink, J.J. and Van Doorn, A.J. (1978), Detectability of Power Fluctuations of Temporal Visual Noise, Vision Res 18, 191.
- 18) Koenderink, J.J., Bouman, M.A., Bueno de Mesquita, A.E. and Slappendel, S. (1978), Perimetry of Contrast Detection Thresholds of Moving Spatial Sine Wave Patterns. II. The Far Peripheral Visual Field (eccentricity $0^\circ - 50^\circ$) J. Opt. Soc. 68, 850.
- 19) Koenderink, J.J., Bouman, M.A., Bueno de Mesquita, A.E. and Slappendel, S. (1978), Perimetry of Contrast Detection Thresholds of Moving Spatial Sine Wave Patterns. I. The Near Periphery Visual Field (eccentricity $0^\circ - 8^\circ$), J. Opt. Soc. Am. 68, 845.
- 20) Kronauer, R.E. and Stromeyer, C.F. (1980), Comparison of Masking with Noise and Coherent Signals (Personal Communication).
- 21) Legge, G. (1978), Sustained and Transient Mechanisms in Human Vision: Temporal and Spatial Properties, Vision Res., 18, 69.
- 22) Pollen, D.A. Ronner, C.F. (1981), Personal Communication, Paper submitted to Science.
- 23) Rose, A. (1974), Vision: Human and Electronics, Plenum Press, N.Y.
- 24) Schacter, B and Ahuja, N. (1980) "A History of Visual Flight Simulators, Computer Graphics World, 3, 16.
- 25) Sekular, R. (1974), Spatial Vision, Am. Rev. Psycho., 25, 195.
- 26) Stromeyer, C.F. and Julesz, B. (1972), Spatial Frequency Masking in Vision - Critical Band and Spread of Masking, J. Opt. Soc. Am., G2, 12.
- 27) Tolhurst, D.J. (1975), Sustained and Temporal Channels in Human Vision, Vision Res., 15, 1151.
- 28) Tyler, C.W. (1980), Narrowband Flicker Channels Revealed by Temporal Frequency Masking, Annual Meeting Opt. Soc. Am., Chicago.
- 29) Westheimer, G.W. (1979), The Spatial Sense of the Eye, Invest. Opthal. and Visual Sci., 19.
- 30) Wheelless, L.L., Cohen, G.H. and Boynton, R.M. (1967), Luminance as a Parameter of the Eye-Movement Control System, J. Opt. Soc. Am., 57, 394.

- 31) Zeevi, Y.Y. and Mangoubi, S.S. (1978), Noise Suppression in Photoreceptors and its Relevance to Incremental Intensity Threshold, J. Opt. Soc. Am., 68, 1772.
- 32) Zeevi, Y.Y. (180), Analysis of Eye Movements in Target Tracking and Detection Tasks, U.S. Air Force, OSR-SCEE Report No. F49620-80-C-0038.
- 33) Zeevi, Y.Y. and Gafni, H. (1980), Some aspects of Motion Perception, Proc. IEEE International Conference on Cybernetics, Cambridge, Mass.

AD-A110 226

AIR FORCE HUMAN RESOURCES LAB BROOKS AFB TX
1981 IMAGE II CONFERENCE PROCEEDINGS.(U)

F/G 14/2

NOV 81 E G MONROE

AFHRL-TR-81-48

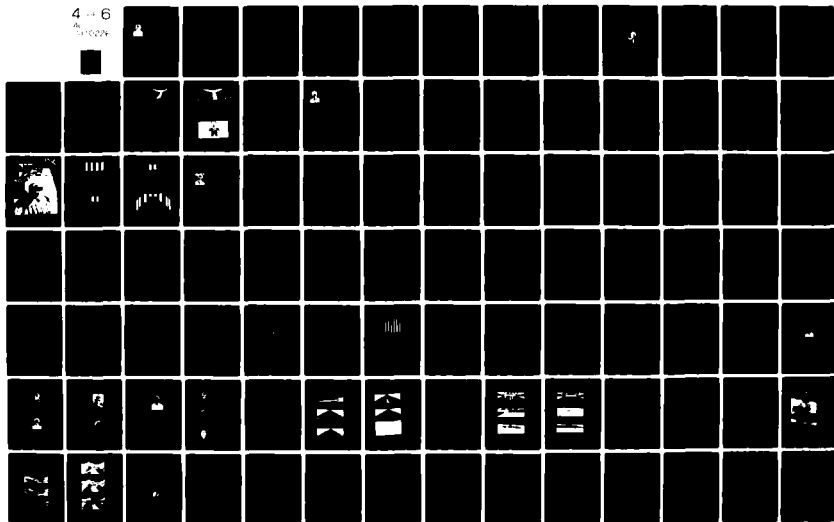
UNCLASSIFIED

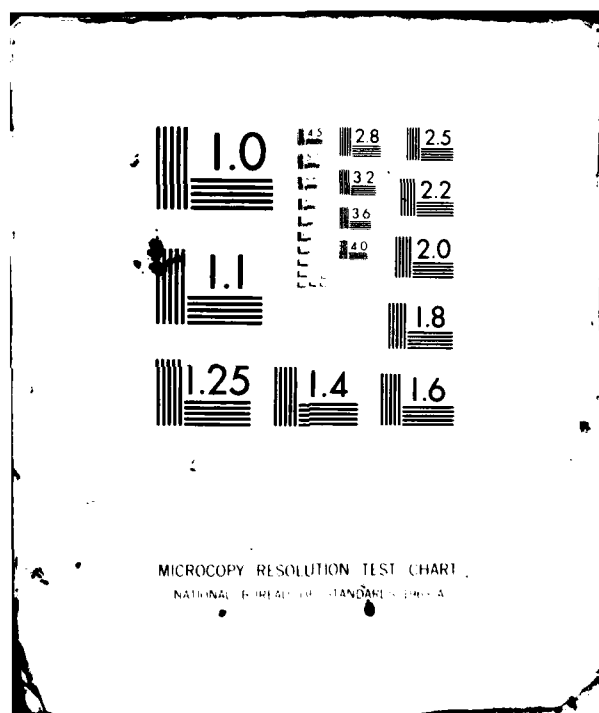
NL

4 - 6

As
101024

1





VISUAL ILLUSIONS
AND
VISUAL SIMULATION



Duncan L. Dieterly
Chief, AFHRL Technology Office
NASA-Ames Research Center

Duncan L. Dieterly obtained his Ph.D. from the University of Maryland in Industrial/Organizational Psychology in 1975. His 19 years of experience in the USAF span a spectrum of research and management areas. His research in human factors, costing, systems management and problem solving is well known.

VISUAL ILLUSIONS AND VISUAL SIMULATION

INTRODUCTION

Visual illusions are occurrences which have fascinated mankind for centuries. The artist and magician have adjusted to the phenomena of illusions and have capitalized upon their application. The artist to perpetuate an emotional feeling of depth, the magician to amaze with the intent of having the audience believe in their powers. In both cases, the phenomena is accepted and integrated to the advantage of the craftsman's objectives. The illusion is perpetuated as reality frequently even after it is discovered. Why then have we who are concerned with visual simulation not also learned to use illusion rather than avoiding it at all costs in our attempts to mirror the reality of the visual world?

The answer probably lies somewhere in the technicians dedication to engineering fidelity and lack of understanding the importance of psychological fidelity. Although psychological fidelity is recognized as a concept, it is hardly a term found in a contract specification for a visual display system. We must assume a less parochial presence and explore the psychological fidelity of visual displays to a greater extent. It is time to realize, in spite of all the sophisticated technology associated with computer image generation (CIG), we are still trying to capture a three-dimensional world on a two-dimensional surface. We, therefore, must search for the most functional ways to expand the psychological fidelity of a CIG system as well as routinely seeking the advanced technology of the future which will provide the magic number of edges to allow us the luxury of complete engineering fidelity.

The focus of this paper is upon some of the possible applications of illusions in enhancing visual simulation. The objective is to suggest ideas or directions which should be explored in future developments of computer image generation systems. The ideas are not completely crystalized into concrete applications, but are presented to tease, taunt, and intrigue the scientist and technician attempting to force greater visual psychological fidelity from existing systems.

In this paper, the technological limits of CIG simulation are accepted and alternative approaches to increase the psychological fidelity of CIG visual systems are suggested. An emphasis on the type of clues needed focuses on the application of the knowledge available about visual illusions. Visual illusions have been employed for centuries to obtain a psychological fidelity as opposed to reproduction of a scene.

ILLUSIONS

An illusion is an effect of psychological importance and is only labeled as an illusion by the illusionist who knows what is actually transpiring. For the individual experiencing the illusion it is the reality of their perception. When an individual looks at an ambiguous figure which reverses from an attractive woman to an old hag, the phenomena may be titillating; but what is actually occurring? How can these lines be made to convey only one or the other figure? Admittedly, perhaps no more than an interesting parlor trick, we must recognize the significance of this occurrence and be prepared for it. In this instance the illusion should alert us to a possible error situation in a visual simulation presentation. We must have a series of discrete dimensions which do not have another figure or context embedded in them to adequately provide the required visual display. By deleting several lines, either a hag or woman remains. It is your choice, but the reversal is ended by reducing the ambiguous lines.

However, other illusions may provide a simple way of generating reality while utilizing their characteristics. The Phi Phenomena may be adapted to make moving lines or other aspects of a display rather than actually generating a moving line. The after-image effect could be the basis of presenting a series of dashed figures with overlapping dashes that when presented in a rapid sequence would appear as a solid figure.

I am specifically addressing the use of illusions to a CIG approach, although many of the ideas would apply equally to any visual simulation system. It would be important for us always to realize that the visual systems that are used in all simulation capitalize on one of man's greatest illusions. That is the illusion of movement by synchronized presentation of a series of static pictures. We might also wish to consider alternative ways to further our application rather than forcing more edges for increased reality. What if we speeded up the presentation rate and introduced partial figures that overlap? Would they be perceived as a total entity? If so, can the speed be manipulated to escape edge dependency?

In addition to these ideas relative to the technology associated with a CIG system, should we develop a research unit which could use animation and film to establish the approaches that are of interest, thereby saving the computer programming effort for actual scenes generation until after initial testing verification in a filmed mode. The current complaint that CIG scenes are cartoonish may be an indication as to where we need to get assistance. Who has better used the concept of minimal cues to show us reality than the animator? The potential for cost savings as well as the introduction of a new series of technicians might increase the probability of further success in psychological fidelity as well as apparent engineering fidelity.

The psychologist and puzzle aficionados have identified a series of two-dimensional illusions such as the Pogendorf Illusion that are simple line drawings. These were generally considered as atypical phenomena

which must be explained away through elaborations of perceptual theories. Although a large body of data have been generated about these, the more interesting aspect is how far can we take them rather than dissipate them through analysis. What is the outer limit of line and pattern illusions and how long does it remain an illusion even after the individual has become educated about the occurrence? Again looking to the art world, the illusions created there are not only lasting, but quite impressive. The use of perspective is the basic ingredient and that is but a manipulation of the penned line to produce not what the artist sees, but what he wants us to see. He essentially distorts his learned perception back to the actual perception of the scene. The Mueller-Lyer illusions, the Ponzo illusion, and the vertical-horizontal illusion are all examples of the artist's stock and trade.

Learned perception is the intellectual perception which over-rides the perceived stimuli. This produces the intriguing phenomena that is experienced when you turn a coin between your fingers and perceive a round object of a specified value rather than a set of changing ellipses. This is due to a familiarity and learned perception which disregards the actual information and elaborates upon it from the individual's memory store. It is the individual's learned perception which is so critical in understanding psychological fidelity. For highly repetitious situations the perceptual stimuli trigger learned perceptions and anticipated actions. In the example of the coin, the illusion is unimportant, but in other situations it could be dangerous.

The more sophisticated artistic displays of "anamorphosis" and "trompe l'oeil" are elegant examples of an extremely complex application of perspective, shadow and light, and hue variation. Anamorphosis was the production of a distorted image which looked normal when viewed from an unusual direction or through a distorting mirror. Perhaps only an entertainment for 16th and 17th Century aristocrats, but certainly a triumph in the technique of two-dimensional perceptual illusions. "Triumph L' Oeil," or the "deceit of the eye" is adequately demonstrated on the elegant ceiling paintings of the 15th Century with, of course, the Sistine Chapel as the ultimate application. Although the artist uses their skill to generate these illusions, they have learned to adjust to the individual's perceptual limits and learned perception.

A cadre of artists have, therefore, succeeded in grasping the limits of human vision and utilized all the illusions that they could develop to produce the reality that learned perception demands. As Blackmore states, "But even perception cannot proceed without expectations, built into the brain in the form of experiences with which it is familiar." (p. 91). It is therefore critical for simulation technology to review these artistic triumphs in an attempt to apply the principals to CIG displays. It should also serve as a warning in that as we seek reality through technological advancement, we may inadvertently introduce distortion.

TYPES OF ILLUSIONS

What are the causes of illusions? There would appear to be four categories of illusions. These are: (1) Outside the capability of individual, (2) on the borderline of capability, (3) contrary to learned perception, and (4) unusual or unknown phenomena. In the first case, the individual's perceptual limits are used to deceive or confuse the individual. The prestidigitator's illusion of suspending a beautiful young lady is based on the low luminosity of the background and the use of apparently invisible wires. The reproduction of a video picture is based upon the limit of size perception of the human eye since it is actually comprised of a series of dots. By establishing the limits of the human's perceptual system, the technicians may produce an illusion of reality.

An example of borderline illusions are the set of imbended figures and after image illusions that are well known. The Necker cube is a representative example. These illusions function at the borderline of perception in the sense they provide ambiguous cues which allow for reversed perceptions of the figure. They are not designed for a single perception but multiple perceptions. They occur at the limits of our perceptual capacity.

Those illusions which are contrary to our learned perception are the type that artists use as mentioned earlier or the well-known Ames trapezoidal room illusion with its unusual effects. The individual's learned perception about rooms and the limitation of only monocular viewing produced the perceived size effects obtained. The fourth category of illusion may be only a matter of experience. For example, the illusion of a location of a fish in water caused by the refraction of the water may be overcome through experience, but when first encountered, is definitely deceiving. In encountering unknown perceptual patterns, the individual matches to their experience base. An individual who sees a rhinoceros for the first time may perceive it as a horse with a horn and call it a unicorn.

NECESSARY CUES

The perpetual demand to understand or determine the necessary cues associated with a training mode is still being articulated (Wang, 1980). The cue issue is too closely emmeshed with a demand for total reality. Individuals use cues and learn to depend on a cue hierarchy in a repetitious environment. It allows them to make choices when only a few cues are available and provides them with a priority system for excluding less credible cues during system overload. What these cues are specifically, eludes us in the real world. However, in the laboratory, research is showing some interesting results. For example, in a study of pattern recognition the authors contend (Hsu and Burright, 1980) that: "The still very exciting, promising and eclectically supported idea...that a few (perhaps about three) dimensions are basic and critical to the pattern recognition problem for man or machine

clearly remains viable." (p. 41). This finding supports the use of minimal cues in learning situations and emphasizes the importance of understanding these cues in any given context.

Although major research projects have attempted to determine cue requirements, none have provided data that is appropriate. In the STRES report, a major research effort, the author could only passively state: "However, available scientific and operational information provides little useful guidance on how to design ATD visual systems to maximize training effectiveness." (Semple, 1981; p. 13). The difficulty is that we continue to search for answers in the available literature when the problem has never really been addressed in the research context except in some indirect social psychological studies of feature identification. The question needed to be answered is "what perceptual cues does an individual need to respond correctly?" Obviously a question which becomes more complex as task complexity increases. Eye scanning studies of cockpit instruments during flight segments have shown patterns, but not linked them to performance.

It would appear reasonable to assume that individuals disregard extensive amounts of perceptual information in familiar situations and in fact have a propensity for completing the perception with anticipated and learned data. The fact that you can recognize a loved one with almost no detailed perceptual data and while an acquaintance requires far more data to make the same identification supports this contention. The demand for a cue-enriched environment, therefore, diminishes as familiarity increases. The cue-enriched environment may be reduced to a basic minimum if the minimum were known. In "Nap of the earth" flying, for example, users would ideally like to have trees with leaves, however, the cue necessary presumably has nothing to do with leaves, but the color density of the green object. Therefore, by taking a solid green object and varying intensity toward a speckling pattern, the necessary cue may be adequately simulated. So, rather than more detail, what is required is a perception changing from solid to less dense, different-hued figures which simulate the rapid articulation toward the object.

Le Master and Longridge (1978) found that increased detail did not aid in air-to-ground target acquisition. A study reporting the application of pseudo random noise codes to generate surface texturing of infrared and low-light-level television systems may be generalized to the Nap-of-the-earth situation. (de Spautz, et al, 1980). They developed a technique of the use of cyclic codes for providing surface detail that provides different levels of detail for different ranges. If this technique could be linked to the actual cues required for a simulation, a powerful approach would be available now. Many illusions are dependent upon low-light availability and limited texture perception.

As Semple, et al (1981), concludes: "...presumably there is no objective way of relating details of the visual scene (e.g., field of view, resolution, color, texture, and scene interest) to the process of

human information extraction and use." (p. 29). The dilemma only becomes more complex. The psychological fidelity of a simulation cannot be considered directly unless the cue information is available. General knowledge of how individuals process cues does provide the detail necessary to establish psychological fidelity.

The phenomena of subjective contour figures as reported by Kanizsa (1955), Schumann (1904) as reviewed by Coren (1972) are highly dependent on minimum cues and the individual's inclination to fill in the missing cues is a case in point. The cue issue will follow us into the new century but we must attempt to mediate between total reality and actual need in terms of visual technology. If we could establish the appropriate cues, it would seem ideal to train in a reduced cue environment and then build towards a cue enriched environment rather than the reverse. Currently we are trying to provide total cue environments and asking the trainee to magically pick out the correct cues for the task -- an interesting exercise in exploration, but not effect in training.

CONCLUSION

In this brief presentation I have tried to reverse the trends of technology by suggesting alternative ways of increasing psychological fidelity. The job in question is accurate visual simulation with an emphasis on the current merits of CIG. The possible use of information about illusions to reduce cue requirements has been suggested. In addition, the study of minimum cues for success has been indicated as a possible method for establishing the necessary information for training. Also drawing upon animation and artists techniques greater psychological fidelity may be obtained in future CIG applications. The search for increased fidelity must be considered as a culmination of increase psychological and engineering fidelity.

REFERENCES

- Blackmore, C.: Mechanics of the Mind. Cambridge University Press, London, 1977.
- Coren, S.: "Subjective Contours and Apparent Depth", Psychological Review, Vol 79, No. 4, pp 359-367, 1972.
- de Spautz, J.F., Bender, M.B., and McNamara, V.M.: Flight Training Simulator: Surface Texture via Pseudo Random Noise Cues, AFHRL Text Report, AFHRL-TR-80-13, Brooks AFB, Texas, 1980.
- Hsu, S. and Burright, R.G.: Comparative Evaluations of RADC/HSU Texture Measurement System with Perceptual Analysis, Sequehana Resources & Environment, Inc., Oct 1980.
- LeMaster, D.W. and Longridge, T.M., Jr.: Area of Interest/Field of View Research using ASPT, AFHRL Technical Report, AFHRL-TR-78-11, (AD A055 692), Williams AFB, Arizona, May 1978
- Semple, C.A.: Simulator Training Requirments and Effectiveness Study (STRES): Executive Summary, AFHRL Technical Report, AFHRL-TR-80-63, Wright-Patterson AFB, Ohio, Jan 1981.
- Semple, C.A., Hennessy, R.T., Sanders, M.S., Cross, B.K. and McCaulley, M.E.: Aircrew Training Devices: Fidelity Features, AFHRL Technical Report, AFHRL-TR-80-36, Wright-Patterson AFB, Ohio, Jan 1981.

THE IMPORTANCE OF BEING SQUARE



Dennis C. McCormick
Applications and Training Analyst
Singer Company, Link Flight Simulation Division

Dennis McCormick is an Applications and Training Analyst in the Advanced Products Operation at Link Flight Simulation Division of the Singer Company. He has been involved in the human factors of simulator visual systems during his two years with Link. Prior to this, he was a pilot in the U.S. Navy flying both land and carrier aircraft and managing air traffic control systems.

He holds a B.S. Degree in Electrical Engineering from the University of Idaho and an M.S. Degree in Electrical Engineering from the Naval Postgraduate School. He is currently pursuing a degree in Industrial Psychology at San Jose State University.

THE IMPORTANCE OF BEING SQUARE

Abstract

The performance of a pilot controlling a simulator equipped with a CIG visual system improves significantly when flying over a data base primarily composed of rectangular surfaces. This is because of an acuity to the orientation of rectangular shapes and because the pilot makes valid unconscious perceptual assumptions that the data base surfaces are rectangles. The powerful force of erroneous perceptual assumptions due to the same mechanism is illustrated by a CIG illusion where the engine pylons of a KC-135 tanker appear to lean inward from their normal position. The knowledge gained from determining the cause of the pylon illusion and correcting the pylon's appearance can be applied to data base design. This will improve the transfer of data base spatial information to the pilot and increase the training effectiveness of the simulator system.

Introduction

Increased costs and safety restrictions associated with pilot training in actual aircraft has produced a growing demand for aircraft simulators and trainers equipped with Computer Image Generation (CIG) visual systems. These CIG systems construct a replica of real world out-the-window scenes through the use of visible surfaces. Early CIG systems displayed few scene elements, but the number of visible surfaces that the visual systems can process and display has increased greatly over the past few years. The number of displayed surfaces is still not sufficient to provide task essential spatial information without careful data base design. Therefore, to attain high levels of system effectiveness, it is important to extract the maximum spatial information possible from the data base surfaces. If more were known about the perceptual transfer of information, the scene could be designed to make more efficient use of the processing capacity of the CIG visual system. Improving the efficiency of information transfer to the pilot and therefore increasing the effective utilization of CIG capacity is the subject of this paper.

The surfaces of the visual world surrounding a pilot in flight normally display a characteristic texture. This, and other features aid the pilot to determine the orientation, or slant and tilt of the surface. Perspective information conveyed by the texture is a primary factor contributing to the judgement of surface orientation. A surface that does not display texture, does not provide information defining its slant or tilt (Carel). The orientation of a terrain surface is essential information for the control of low altitude flight. Thus, the surfaces displayed by CIG visual systems presently used for pilot training pose a perceptual

problem because they do not provide a perceptually complete texture to support slant or tilt judgements. Since the surfaces displayed by present CIG systems do not possess texture, the orientation of these surfaces is, by necessity, judged by the shape of the surface as defined by data base edges.

The shape of CIG surfaces have a significant effect upon the performance of a pilot during simulated low altitude maneuvers. It has been observed that pilot performance improves when the CIG terrain surface is described by a rectangular checkerboard pattern (Buckland), or when scene content rectangularity is emphasized (Bunker). It appears that a significant factor causing the improved performance is man's sensitivity to the orientation of rectangles and its special case, the square. This sensitivity is often attributed to the constant exposure of a carpentered world (Coren). The vast amount of experience attained from determining the orientation of real world rectangles carries over to the rectangles of the CIG world.

Pilot judgement with respect to rectangles is good, however there is another significant factor which causes improved pilot performance over a rectangular data base. The image displayed by a CIG visual system lacks many of the perceptual cues a pilot would receive in the real world. For example, even though he sees the image with both eyes, he does not receive real world binocular information such as retinal disparity from the CIG display. When the visual information describing an object in the field of view is not sufficient to support an unambiguous identification of the object, the observer makes perceptual assumptions which provide the necessary information to complete a mental concept of the object. These assumptions are based upon anticipations (from scene content, events, experience and other factors) of what should be present. The mental concept of the object is then transformed in position, size, and orientation until it matches the sketchy information provided by the actual object (Pinker). The assumptions can be developed through conscious thought such as when a pilot attempts to recognize another aircraft after he has detected it, or the assumptions can be generated unconsciously, when the pilot is not aware of the perceptual assumptions being made. It is an unconscious assumption that appears to cause an interesting illusion when viewing a CIG data base model of a tanker aircraft from the refueling eyepoint position.

When viewing a KC-135 tanker model from the refueling position the engine pylons of the tanker, which should appear perpendicular to the wings, appear to lean inward as much as 30 degrees. The apparently inward leaning pylons can be seen in Figure 1. An observer's initial reaction to the illusion is that the CIG processing or the mapping of the display is in error, especially since the amount of leaning increases as the tanker is approached. Engineering investigations did not reveal any possible source of the distortion in the tanker.

Then it was suspected that the engine and pylon rotation was caused by the pilot's visual system responding to inadequate cues. This was confirmed by viewing a plastic scale model of the aircraft from the refueling eyepoint. When looking at the engine pylons with both eyes they appeared to be in their correct orientation. However, when one eye was closed the pylons leaned inward similar to the view of the CIG tanker. In this case the visual information describing the scale model aircraft pylons was reduced by the elimination of binocular cues. Insufficient pylon information apparently causes the observer to make unconscious perceptual assumptions which produces the leaning pylon illusion.

The major cue defining the orientation of the pylon is its shape which approximates a parallelogram. Since there is insufficient information to unambiguously define the orientation of the pylon, some perceptual assumptions must be made by the pilot. It appears that the observer unconsciously assumes that the shape of the pylon is a rectangle and then mentally orients the rectangle in space to fit the image seen on the CIG display. This perceptual process is similar to that used when viewing a perspective drawing of a house (Figure 2). The roof is assumed to be a rectangle and its parallelogram shape defines its orientation in 3D space. (1) If the true shape of the roof was not a rectangle and there was no information to reveal its unusual shape, the roof would appear slanted differently than it actually is. This is the situation that occurs with the tanker pylons.

For some pilots, the leaning pylon illusion was more than a curiosity. The variable amount of leaning, which was a function of eyepoint position relative to the tanker, also had a destabilizing effect upon the apparent position of the wing. For some observers, the wing appeared to move slightly fore and aft, and up and down. The pilot who was susceptible to this illusion and used the wing and pylons as secondary cues to maintain his refueling position was faced with the difficult task of flying relative to a rubber airplane. To increase the training effectiveness of the tanker model for all pilots, it was necessary to discover the reason for this effect and minimize the appearance of the leaning pylon.

In order to destroy the illusion that the pylon and engine are leaning, it was necessary to provide additional spatial information to control the perceptual assumptions being made by the pilot. This requires an additional cue, or cues to provide information that the actual shape of the pylon can't be a rectangle. It was thought that if a square was placed

(1) It has been observed (Stevens), that intersecting lines appear to cross at right angles in space and define a plane. Also, the perceptual default assumption of a quadrilateral figure is a rectangle (Minsky).

on the inside surface of the pylon it would be perceived correctly which would provide additional information describing the orientation of the pylon surface and destroy the illusion. This was done but the resulting appearance of the pylon was unexpected. The pylon remained in its leaning position, however, the square appeared to be a vertical strut between the wing and the pylon. The proper orientation of the pylon was perceived by approximating its shape with a series of narrow rectangular parallelopipeds, however, this was unacceptable because of its unrealistic appearance and the high number of surfaces required to model it. Eventually it was discovered that the illusion can be destroyed by adding the shadow of the wing generated by an overhead sun across the pylon and engine. This adds perceptual information that makes it difficult to assume that the pylon is a rectangle. The more accurate perception of the pylon's orientation could be the result of two different strategies. Since the pylon can't be a rectangle due to the information provided by the shadow, then the next reasonable assumption that could be made is that the pylon is perpendicular to the wing. Or, as stated by Lawson and Gulick, "Instead of contours giving rise to depth it is depth that gives rise to contours." The unshadowed portion of the pylon provides information that it extends in depth forward of the wing which adds depth information and produces a more accurate perception of the pylon's shape or contour.

The exact mechanisms that eliminate the illusion is a subject for further study but the effect on the appearance of the pylon by adding a simple shadow is dramatic. A model of the tanker was modified such that two of the pylons had shadows and the other two (on the other side of the aircraft) did not have shadows (Figure 3). When people see the tanker via a CIG display, they perceive a tanker that has normal pylons on one side and abnormal pylons that are leaning inward on the other side. It is convincing evidence that the leaning pylon is not a CIG error but a human perceptual error.

The perceptual assumption that causes the pylon illusion can easily occur in other areas of a CIG data base. If other data base features such as terrain surfaces are not rectangles but could be perceptually assumed to be rectangles then the perceived orientation of the surfaces would be in error. This explains why a data base with an emphasis on rectangularity is more effective than one that reproduces the irregular features of the real world. If the majority of surfaces in a data base are rectangles then most of the perceptual assumptions made by the pilot are valid. When viewing a data base where the emphasis is placed on realism, many erroneous perceptual assumptions can be unconsciously made by the pilot which distorts the actual spatial relationships of the data base. This can occur even when a simple form of texture is displayed. Increased efforts to produce a realistic (and usually more complex) data base could foster more illusions, which reduces the perceptual fidelity of the data base. Without the capability to

generate a perceptual real world equivalent surface texture on all surfaces, emphasis should be placed on rectangular data base design to insure perceptual fidelity.

Emphasis on rectangular features and scene realism are not necessarily incompatible. It is possible to design a data base that appears both fairly realistic and has a high level of perceptual fidelity. This is done by identifying task relevant rectangular features that are present in the real world. These features are then given priority in the design, generation, and display of the data base. The result is a data base that appears realistic because there are few artificial rectangular shapes. The data base also maintains a high level of perceptual fidelity because most of the visible features are in fact, rectangles.

This design approach has been incorporated in airport data bases for some commercial and government simulators. A runway (Figure 4) appears realistic even though a great number of rectangular shapes are displayed because rectangular shapes present in the real world runway are given priority during data base design. For example, concrete and asphalt patterns are rectangular and describe the orientation of the runway surface with a low probability of generating perceptual errors. Tire skid marks are essentially rectangular and therefore, they are modeled as rectangles to avoid perceptual errors. With the runway surface described by features that resist perceptual errors the efficiency of spatial information transfer to the pilot is high. Because of a greater quantity and quality of spatial information the landing performance of a pilot is improved.

Summary

The primary purpose of flight simulator visual systems is to convey to the pilot information that is equivalent to essential task relevant information presented by the real world. CIG visual systems which must provide this information are limited by the number of surfaces they can process and display. Therefore, it is important to display surfaces that convey the necessary information efficiently to maximize the effective use of the CIG system processing capacity. This can be accomplished by emphasizing the presence of rectangular surfaces within the data base. It should also be recognized where non-rectangular, four-sided surfaces can't be avoided, additional surfaces may be required to destroy an adverse illusion. This data base design approach which can be applied to both present and future CIG systems, will increase CIG system information transfer efficiency, perceptual fidelity, and training effectiveness.

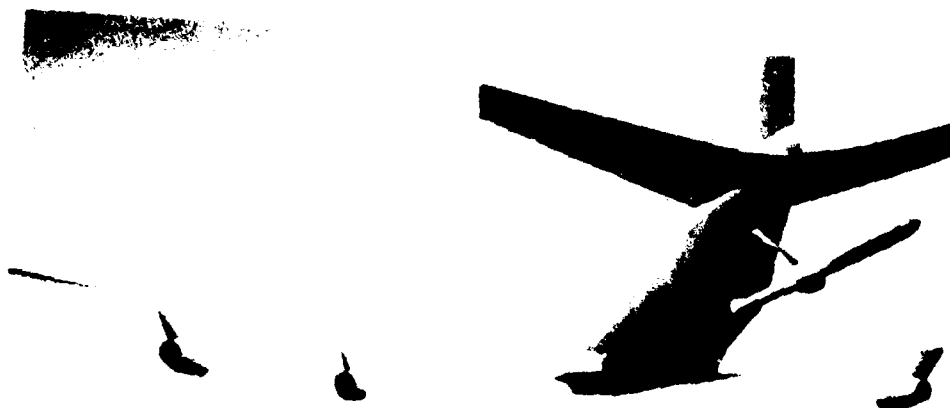


FIGURE 1



FIGURE 2

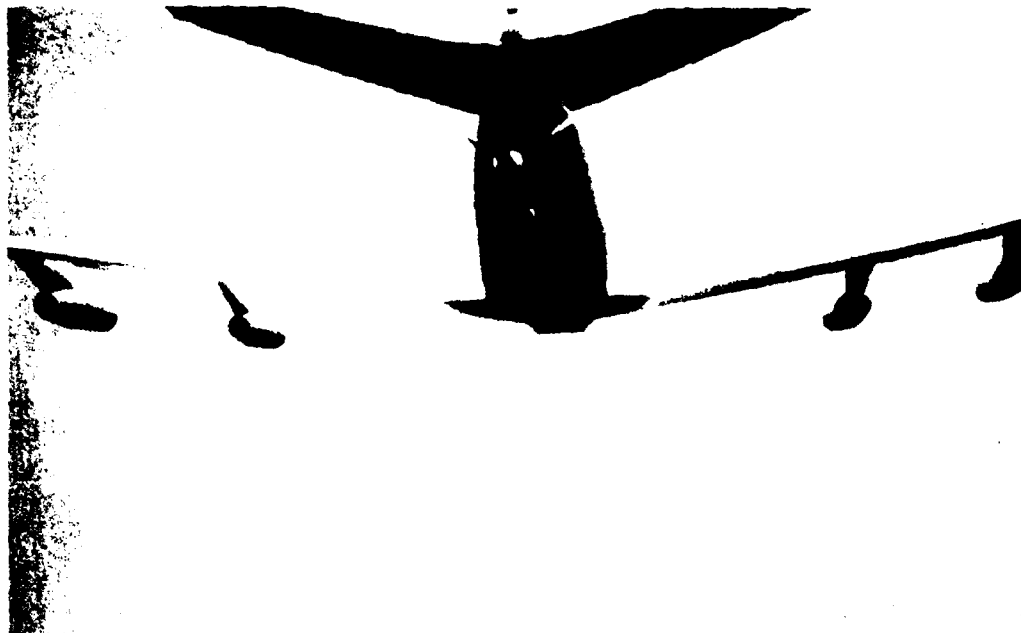


FIGURE 3



FIGURE 4

References

- Buckland, G.H., "Visual Cue Requirements for Terrain Flight Simulation," in Proceedings, Interservice/Industry Training Equipment Conference and Exhibition, 2d, Salt Lake City, 1980 (Washington: National Security Industrial Association, 1980), pp. 92, 93.
- Bunker, W.M., "Training Effectiveness Verses Simulation Realism," SPIE Vol. 162, Visual Simulation and Image Realism (1978) (Bellingham, Washington: SPIE, 1978), pp. 76-82.
- Carel, Walter, L., Visual Factors in the Contact Analog, R61ELC60 (Ithaca, New York: General Electric, 1961).
- Coren, S. and Grigus, J.S., Seeing is Deceiving: The Psychology of Visual Illusions. (New Jersey: Lawrence Erlbaum Associates, 1978).
- Lawson, R.B., and Gulick, W.L., "Stereopsis and Anomalous Contour", Vision Research 7 (1967): pp. 271-297.
- Perkins, D.N., "Visual Discrimination Between Rectangular and Non-Rectangular Parallelopipeds", Perception and Psycho-Physics 12 (1972): pp. 396-400.
- Pinker, Steven, Mental Imagery and the Visual World (Cambridge: MIT Center for Cognitive Science, 1980).
- Stevens, K.A., Surface Perception from Local Analysis of Texture and Contour, Phd Dissertation (Cambridge: MIT, 1979).
- Minsky, M. "A Framework for Representing Knowledge" in The Psychology of Computer Vision, Edited by P.H. Winston. (New York: McGraw-Hill, 1975).

VISUALLY INDUCED SELF-MOTION SENSATION ADAPTS
RAPIDLY TO LEFT-RIGHT REVERSAL OF VISION



Charles M. Oman
Principal Research Scientist
Man Vehicle Laboratory
Massachusetts Institute of
Technology

(photo not available)

Charles M. Oman received his BSE degree from Princeton University and SM and PhD degrees from Massachusetts Institute of Technology, where he served on the Aeronautics and Astronautics faculty from 1972-1979, teaching subjects in control engineering and physiology. His research has focussed on the physiology of the vestibular organs, spatial orientation perception, sensory motor adaptation, eye movements, postural reflexes, and motion sickness. Currently, Principal Research Scientist, he is responsible for two vestibular experiments selected for flight on Spacelab-1, an international NASA-ESA shuttle mission (1983).

Otmar L. Bock received his MD degree in 1978 from the University of Hamburg, where he conducted research on vestibular function and completed a thesis on a mathematical model for caloric nystagmus. Dr. Bock was a Research Fellow in the Man Vehicle Laboratory at MIT from 1979-1980, and is now working in the Laboratory of Dr. O. Grusser at the Physiological Institute in Berlin, West Germany.

VISUALLY INDUCED SELF-MOTION SENSATION ADAPTS RAPIDLY TO LEFT-RIGHT REVERSAL OF VISION

ABSTRACT

After one to three hours of active movement while wearing prism goggles which left-right reverse the field of view, 10 of 15 (stationary) human subjects viewing a moving stripe display (back projected onto the windows of a flight simulator) experienced a self-rotation illusion (circularvection) in the same direction as seen stripe motion, rather than in the opposite (normal) direction, thus demonstrating that the central neural pathways which process visual self-rotation cues can undergo rapid adaptive modification. Exposure to visual reversal apparently reversed the perceptual interpretation of visual information only from the portion of the subject's field of view conditioned by the goggles. Reversal of circularvection was not accompanied by a reversal of the slow phase of the vestibulo-ocular reflex. Implications of these findings will be discussed in the context of flight simulation.

INTRODUCTION

Both visual and vestibular motion cues are known to contribute self-motion perception in a complementary fashion¹. In everyday life, head rotation results in an equal and oppositely directed angular motion of the visual scene relative to the head. This association between normal active head rotation and relative scene motion is believed to account for the phenomenon of "circularvection"² (CV): A pattern of stripes rotating around a stationary observer soon elicits a compelling sensation of self-rotation in the opposite direction³.

Because of the growing appreciation of the interplay between visual and vestibular self-motion cues in spatial orientation perception and control of body movement, visually induced self-motion (vection) has become the focus of considerable research interest¹. The understanding gained thus far has been exploited in applications as diverse as neurological diagnosis and flight simulation. In the latter application, for example, cockpit display systems which produce "vection" are now routinely used to alleviate the need for large magnitude motions of the simulator cabin. Many practical applications in which vection is exploited involve situations in which the normal relationship between visual and vestibular cues is disturbed, the visual scene distorted, or the field of view limited. Unless taken into account, adaptation to these factors would complicate the interpretation of experiments on vection, and should be considered in evaluating the design of flight simulator display systems and training strategies. Unfortunately, the adaptive capabilities of the neural pathways which mediate the sensation of vection have not been systematically studied. The objective of the present experiments was to document the character and time course of the vection adaptation associated with one particular type of visual "rearrangement"⁴.

When human subjects wear optics which either left-right ("mirror") reverse or invert (rotate by 180°) vision, the normal relationship between left-right head rotation and relative visual scene motion is reversed. For example, head rotation to the right is then accompanied by relative scene motion to the right with respect to the head, with the result that the seen world is no longer perceived as stationary⁵. Spatial orientation is severely impaired. However, after an extended period of vision reversal (days to weeks), the seen world appears more stable⁵, and subjective visual "normalcy" and coordinated movement are gradually restored⁶. Active movement by the subject is thought to play a vital role in the adaptation process⁴. The slow phase component of the horizontal vestibulo-ocular reflex (VOR), which contributes to perceptual stabilization under normal vision, has been shown⁷ to reverse after a week of vision reversal. The neural pathways believed to mediate adaptive changes in the VOR have recently been explored in animals⁸. One might also expect that under visual reversal the neural interpretation of visual self-rotation cues would eventually adaptively reverse, and be manifest perceptually in a reversal of the CV phenomenon. We have demonstrated such a reversal, accompanied by only a modest reduction in vestibulo-ocular reflex gain, in 10 of 15 subjects within a brief (1 to 3 hour) period of exposure. Reversed CV was only demonstrated when the size of the moving stripe display we used to elicit CV was limited to the field of view conditioned by exposure. A preliminary report has appeared⁹.

METHODS

Three experiments, which differed somewhat in protocol details, were conducted using 15 adult volunteers with no overt oculomotor or vestibular disorders. As symptoms of motion sickness often occur under visual reversal, drugs (scopolamine, 0.5 mg, or scopolamine, 0.4 mg/dexedrine, 5.0 mg) were orally administered prior to Experiments I and II. In all experiments, left-right vision reversal was achieved using the prism goggles shown in Figure 1, which permitted a binocular field of vision subtending approximately 45 degrees horizontally and 28 degrees vertically¹⁰. Two Dove prisms, mounted base to base, were held in front of each eye (with bases in a sagittal plane) by a plexiglass frame, fixed to the head by an adjustable band. A black shield closely fitted to the face and the prisms excluded all non-reversed visual information.

In all experiments, CV was tested before and immediately after a period of exposure to reversed vision ("preliminary" and "final" tests). For all subjects in Experiment II, and for one subject in Experiment III, CV was also tested at intervals during the exposure period. Subjects were seated in the closed, motionless cabin of a flight simulator (Link GAT-1). Equal width (6.4°) vertical light and dark stripes, moving left or right at $8^\circ/\text{sec}$ were back projected onto the translucent front window, about 70 cm from the subject. During testing without the goggles before and after exposure, the shape of the moving display could be varied using appropriate masks applied to the window, whereas in tests made during exposure, the shape corresponded to the field of view

of the goggles. Subjects were asked to verbally report the onset and disappearance of any CV. Because of the transposition of the visual location of the hands with goggles on, subjects were asked to report their perceived direction of self-motion with respect to the direction of seen stripe motion, with respect to their left and right eyes, or both. Motion reports made using these two different methods were always consistent.

The gain and phase of the horizontal VOR were tested in the dark before and after exposure using sinusoidal simulator angular velocity (0.2 Hz, 30°/sec peak velocity, 6-8 cycles). Eye movement was measured in the dark using conventional DC electrooculography. Subjects performed mental arithmetic to maintain alertness. (In the case of certain subjects, we also performed one or more additional brief tests during the preliminary and final test sessions. These included acceleration threshold measurements, an evaluation of gaze stabilization during active head movement, an oculogyral illusion test, and a pseudorandom cabin motion nulling test. Results of these additional tests will be reported elsewhere.) The present paper will focus on circularvection and VOR test results.

When not participating in the brief pre-exposure tests, our subjects explored their reversed visual environment by walking through the laboratory buildings in the company of an observer. Head and body movements in the horizontal plane were encouraged. When they occurred, motion sickness symptoms were maintained at an acceptable level by intervals of eye closure and/or head immobilization.

RESULTS

Experiment I

In this experiment (5 subjects), we first confirmed that pre-exposure CV direction was opposite to seen stripe motion ("normal CV") using the 63° (horizontal) by 28° rectangular stripe display shown in Figure 2a. Latency of CV onset ranged from 8 to 47 sec. Then, after the prism goggles were fitted, the subjects exposed themselves to vision reversal for 180 to 230 minutes.

After the exposure period, the prism goggles were removed, and CV was tested using a 30° (horizontal) by 19° display, shown in Figure 2b, which stimulated only the field of view previously exposed to the goggles. After a latency of between 10 and 42 seconds, all five subjects reported an unequivocal sensation of motion in the same direction as the seen stripe motion. Subjects usually likened the sensation to being "pulled along with the stripes". We refer to this perception as "reversed circularvection" (RCV). Four of the five subjects in Experiment I experienced compelling sustained RCV until, some 30 to 60 seconds later, we suddenly increased the display size to 63° (horizontal) by 28°. Subjects then reported that RCV immediately ceased, and after several seconds, that normal (unreversed) CV appeared. Changing back to the narrow field abolished normal CV, and RCV was reestablished after several seconds. This sequence could be demonstrated repeatedly over several minutes. Active head movements (eyes open in light) appeared to abolish RCV. Our fifth subject experienced an initial 17 second period of compelling RCV, followed

by periods of normal CV and RCV, even though the display area remained narrow.

Experiment II

To more systematically define the time course of CV adaptation, seven additional subjects participated in a second experiment in which CV was systematically tested every 30 to 40 minutes during a 190 minute exposure period. To more clearly demonstrate the dependency of CV direction on the region of the visual field stimulated, CV was measured before and after exposure using a rectangular "central visual field" display (CVF, 29° horizontal by 17°) shown in Figure 3b, and also using a "peripheral visual field" display (PVF, 180° horizontal by 23°, with a dark mask of the CVF display area), Figure 3a. Before exposure, the CVF test was preceded by a PVF test. After exposure, two CVF tests (both directions of stripe movement) were followed by a PVF test, and the head was immobilized in an effort to avoid readaptation. Subjects were asked to verbally report the first appearance of CV, its direction, and their sensation of self-rotation in 45° increments. For purposes of comparison between subjects, we converted these reports to a four bin velocity scale, described in Table 1. When vection could not be demonstrated using the display alone, we attempted to trigger it with a brief rotation of the simulator cab, thus providing a transient semicircular canal motion cue (present during normal head rotation, but absent using conventional CV test procedures). As shown in Table 1, four subjects demonstrated RCV. The first RCV episode occurred after 95 to 190 minutes of exposure.

Experiment III

Three additional subjects underwent an exposure period (which ranged from 150 to 220 minutes), but used no anti-motion sickness drugs. Symptoms were controlled only by eye closure and head movement limitation. Two of the subjects were tested in as in Experiment I, but using only the 63° by 28° front window display. RCV was not found after the exposure, perhaps because we failed to test with the narrow 30° by 19° display. The third subject underwent a protocol similar to Experiment II, and demonstrated RCV after 80 minutes of exposure with goggles on, and with the CVF display in final testing with goggles removed.

Vestibulo-Ocular Reflex Tests

VOR slow phase velocity gain and phase re: trainer velocity were measured in all experiments before the first pre-exposure CV test, and after the exposure, just before the goggles were removed. Data from two subjects in Experiment I could not be analyzed due to technical problems. In the remaining ten subjects in Experiments I and II, VOR gain decreased from 0.72 (S.E. = 0.35) to 0.55 (S.E. = 0.29) after exposure. This change was significant (Paired Sample T Test, $P < 0.001$). Among those seven subjects in Experiments I and II, who experienced RCV, again decreased from 0.80 (S.E. = 0.39) to 0.64 (S.E. = 0.31), also a significant change ($P < 0.005$). Slow phase eye velocity of the ten subjects lagged trainer velocity by 180° (S.E. = 7°) prior to exposure and lagged

by 176° (S.E. = 11°) after exposure. The slow phase VOR gain of the three Experiment III subjects who did not use drugs decreased from 0.74 (S.E. = 0.30) to 0.47 (S.E. = 0.17). We were unable to demonstrate significant differences between the drug and non-drug groups in terms of VOR gain decrease. As confirmed by direct inspection of the eye movement records, none of our subjects showed any evidence of reversal of the VOR slow phase component. (Apparently systematic changes in the occurrence of the fast component of nystagmus were, however, observed. These will be reported in detail elsewhere.)

DISCUSSION

Our subjects showed approximately a 20 percent reduction in VOR slow phase gain over their brief exposure period. This short term gain reduction could be due to uncontrolled changes in alertness caused by motion sickness or fatigue. Scopolamine is known to depress oculomotor responses¹¹, but the gain reduction in our drug and non-drug groups appeared similar. Alternatively, the gain reduction we observed may represent the early stages of the adaptive VOR change described by Gonshor and Jones⁷. Their subjects, who did not use drugs, showed similar gain changes during the first day of exposure.

Our results imply that vision reversal soon produces a corresponding reversal of the interpretation of visual self-rotation cues from that portion of the field of view (referred to the head) which has been conditioned by the exposure. This change is adaptive, in that it appears directed towards the goal of veridical self-motion perception. The reversal of circularvection is presumably mediated by a central mechanism which establishes a new association between the direction of motion of the visual input relative to the head and self-rotation direction information provided by non-visual (e.g. vestibular) sensory modalities during body movement. Non-visual self-rotation information is not available at the retinal level. It therefore can be argued that the adaptive process is central in origin, and not a retinal phenomenon.

RCV could only be demonstrated when the field of view was limited to or less than the field of view of the goggles. With a wide field stimulus (as in Experiment I), RCV appeared to be overwhelmed by normalvection. In Experiment II, normal CV response to PVF stripe motion was, if anything, enhanced by exposure of the central field to vision reversal. Our findings suggest that visual information from the exposed central field of view is transmitted centrally along pathways which are separate from those carrying information from the peripheral visual field, and that each of these pathways may be separately modified as a result of sensory experience. The occasional presence of alternating normal CV and RCV during early per-exposure tests indicates that RCV may not develop gradually. Instead, it is as if a second, competitive mechanism develops.

It is important to point out that RCV cannot simply be explained as a "negative after-effect"¹², since RCV was demonstrated without preceding unreversed CV. Similarly, RCV is distinctly different from the brief episodes of "inverted self-motion perception" reported¹³ to occur during prolonged (4 to 12 minutes)

optokinetic stimulation: RCV could be demonstrated after distinctly shorter latencies (order of seconds), with no preceding normal vection, was sustained for periods greater than 5 seconds (usually 20 seconds to more than a minute) and could be quickly and consistently manipulated by altering the display size.

It is not surprising that the RCV velocity magnitudes reported were modest, given the narrow field of view of the goggles, as normal CV can be more effectively elicited if peripheral retinal areas are exposed to the moving display¹⁴. In this regard, we note that whether or not a subject demonstrated RCV within the allowed exposure period appeared to be correlated with CV strength produced with a narrow field stimulus. In Experiment II, subjects B1-B4 showed strong, normal CV at least once, either in CVF pre-exposure tests or during the first four per-exposure sessions, and they were the only subjects in this experiment to show RCV. Test scheduling constraints limited exposure to 190 minutes in Experiment II. Had the exposure for subjects B5-B7 been extended, it is conceivable that they, too, would have shown RCV. The exposure duration in Experiment I was not so constrained. All five subjects in Experiment I experienced RCV.

In animals, convergence of visual and vestibular head rotation information is known to occur in vestibular nucleus neurons¹⁵, which are thought to determine the slow phase velocity of vestibular and optokinetic nystagmus under many conditions. The extent to which vestibular nucleus neurons contribute to rotation perception is unknown, although there appears to be a close relationship between the time course of normal CV in man¹⁶ and the response pattern of some vestibular nucleus neurons in animals^{15,17}. It would be interesting to know if a reversal in visual sensitivity of vestibular nucleus neurons can be demonstrated in animals after several hours of active exposure to vision reversal.

CONCLUSIONS

1. Reversed circularvection (RCV) was demonstrated in 10 of 15 subjects after 1 to 4 hours of active head movement while wearing left-right vision reversing goggles.
2. Exposure to left-right visual reversal apparently reversed the perceptual interpretation of visual information only from the conditioned portion of the subject's field of view.
3. Development of RCV appears adaptive, i.e. directed toward the goal of veridical self-motion perception and is probably of central, rather than retinal origin.
4. RCV is quickly abolished when active head movements are made eyes open in the light with goggles off.
5. RCV cannot be explained as a negative after-effect artifact or as an inverted self-motion perception resulting from prolonged stimulation. RCV was demonstrated in one subject without the use of anti-motion sickness drugs.
6. Horizontal VOR slow phase gain decreased similarly in both the drug and non-drug groups. No evidence of VOR slow phase reversal was found.

NOTES AND REFERENCES

1. J. Dichgans and Th. Brandt, in Perception, Handbook of Sensory Physiology, Vol. VIII, R. Held, H. Leibowitz, and H.L. Teuber, Eds., (Springer, Berlin, 1978), Chapter 25.
2. M. Fisher and A. Kornmuller, J. Psychol. Neurol. (Lpz.) 41: 273-308 (1930).
3. E. Mach, Grundlinien der Lehre von den Bewegungsempfindungen, (Englemann, Leipzig, 1875).
4. R. Held, J. Nervous and Mental Disease 132, 26-32 (1962).
5. G. Stratton, Psych. Rev. 4, 341-360; 5, 611-617 (1896).
6. P. Ewert, Genet. Psychol. Monog. 7, 177-363, (1930); T. Erisman, Proc. Congr. German Psychol. Assn. Bonn, 54, (1947); H. Kottenhoff, Acta Psychologica, 13, 79-97, 151-161, (1957); I. Kohler, Psychol. Issues 3, 1-72, (1964), C. Harris, Psychol. Rev. 72, 419-444, (1965).
7. A. Gonshor and G. Melvill Jones, J. Physiol., 256, 381-414, (1976).
8. E. Keller and W. Precht, J. Neurophysiol. 42, 896-911 (1979), G. Haddad, J. Demer, and D. Robinson, Brain Res. 185, 265-275, (1980).
9. C. Oman, O. Bock, and J-K. Huang, Science 209, 706-708, (1980).
10. Prism axes were adjusted to eliminate diplopia at a distance of 3 meters. The monocular field of view through each eye was 28° by 28°.
11. A. Benson and J. Brand, Quart. J. Exptl. Physiol. 53, 296-311, (1968).
12. W. Thalman, Amer. J. Psychol., 32, 429-441 (1921).
13. Th. Brandt, J. Dichgans and W. Buchele, Exp. Brain Res. 21, 337-352, (1974).
14. Th. Brandt, J. Dichgans and E. Koenig, Exp. Brain Res. 16, 476-491 (1973).
15. J. Dichgans, C. Schmidt, and W. Graf, Exp. Brain Res. 18, 319-322, (1973); V. Henn, L. Young and C. Finley, Brain Res. 71, 144-149 (1974).
16. L. Young, in Posture and Movement, R. Talbott and D. Humphrey, Eds. (Raven Press, New York, 1979), 177-187.
17. J. Allum, W. Graf, J. Dichgans, and C. Schmidt, Exp. Brain Res. 26, 463-485, (1976); W. Waespe, B. Waespe and V. Henn, Pflug. Arch. ges. Physiol. 373, Suppl. R87 (1978).
18. This work was supported by NASA Grant NSG-2032 and NASA Contract NAS9-15343. Dr. Bock was supported by a NATO Science Fellowship. We thank J.-K. Huang, our subjects, and also Professors R. Sivan, L. Young, R. Held, Dr. O. Garriott, M. Pankratov, and E. Boughan.

PRELIMINARY TESTING			GOGGLES ON TESTING DURING EXPOSURE PERIOD					FINAL TESTING	
SUBJ	PVF	CVF	1	2	3	4	5	CVF	PVF
B1	4 (+++)	- (/)	4 (+++)	7 (+++)	7.5 (++)	3 (++)	5.5 (+++)	1.5 (+++) 1.5 (+++)	2 (+++)
B2	7 (+++)	5.5 (+++)	5 (+++)	11 (+++)	19.5 (++)	4 (+++)	5 (++)	23.5 (+++) 21 (+++)	19 (+++)
B3	11.5(+++)	8 (++)	5 (+++)	21 (++)	- (+)	14 (++)	16.5 (+++)	15 (++) 9 (++)	9 (+++)
B4	9 (++)	- (/)	- (/)	- (/)	18 (+++)	121 (++)	5 (++)	- (+) 3 (+++)	3 (+++)
B5	- (+)	- (+)	23 (++)	18 (++)	12.5 (++)	63 (++)	8 (++)	- (/) - (+)	3.5(+++)
B6	10 (+++)	- (+)	12 (++)	- (+)	12 (++)	10 (+++)	60 (++)	- (+) - (+)	20.5(+++)
B7	- (+)	- (/)	- (/)	- (+)	- (/)	- (/)	- (/)	- (/) - (/)	35 (+++)

TABLE 1. EXPERIMENT II CV TEST RESULTS. Shaded areas designate occurrence of reversed circularvection.

For each test, latency is given in seconds, followed by magnitude on a 4 bin scale: (+++) is strong vection greater than 25% of stripe velocity; (++) is vection present. (+) indicates sustained vection present after triggering simulator rotation stopped. (/) denotes no vection, even with triggering rotation. "-" indicates CV latency not measured.



Figure 1: Subject wearing prism goggles and ECG electrodes

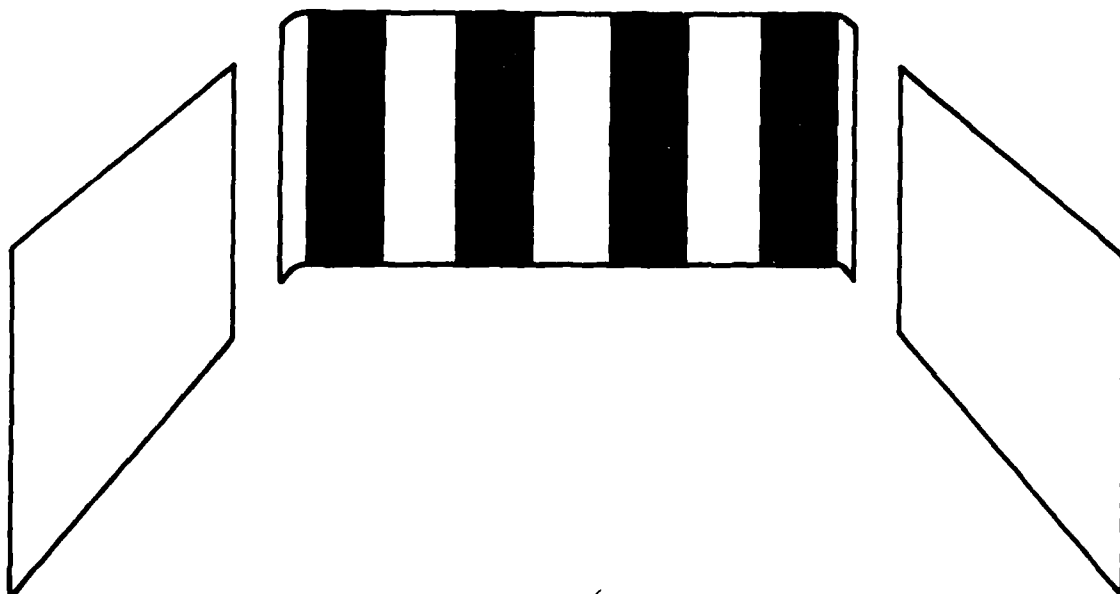


Figure 2a: 63 deg. by 28 deg. moving stripe display used in Experiment I. Schematic of display as seen from a position inside the GAT - 1 simulator cabin, above and behind the head of the seated subject.

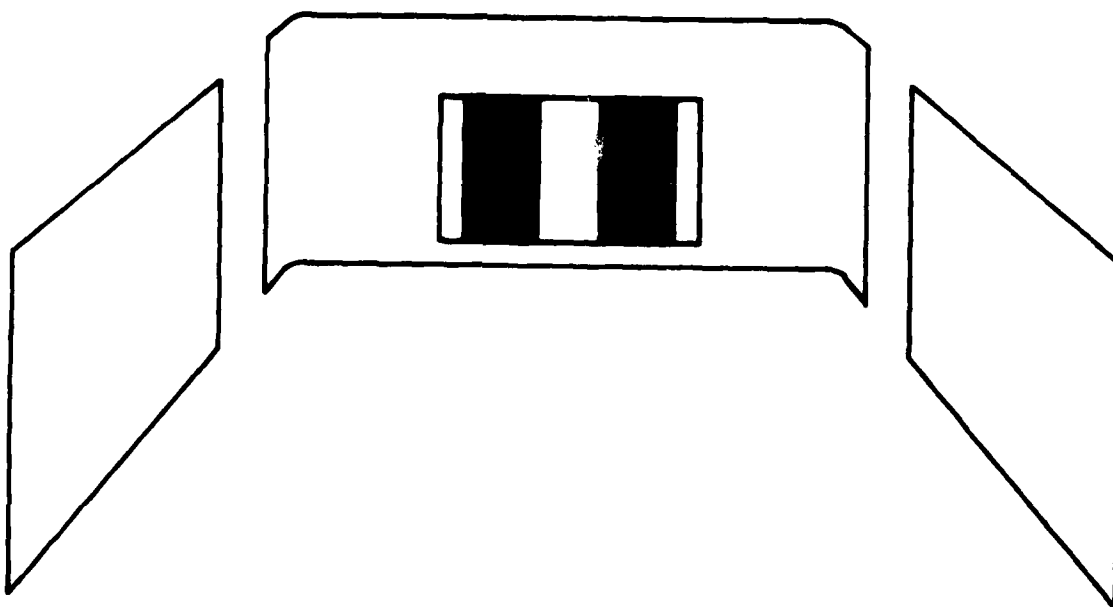


Figure 2b: 30 deg. by 19 deg. moving stripe display used in Experiment I.

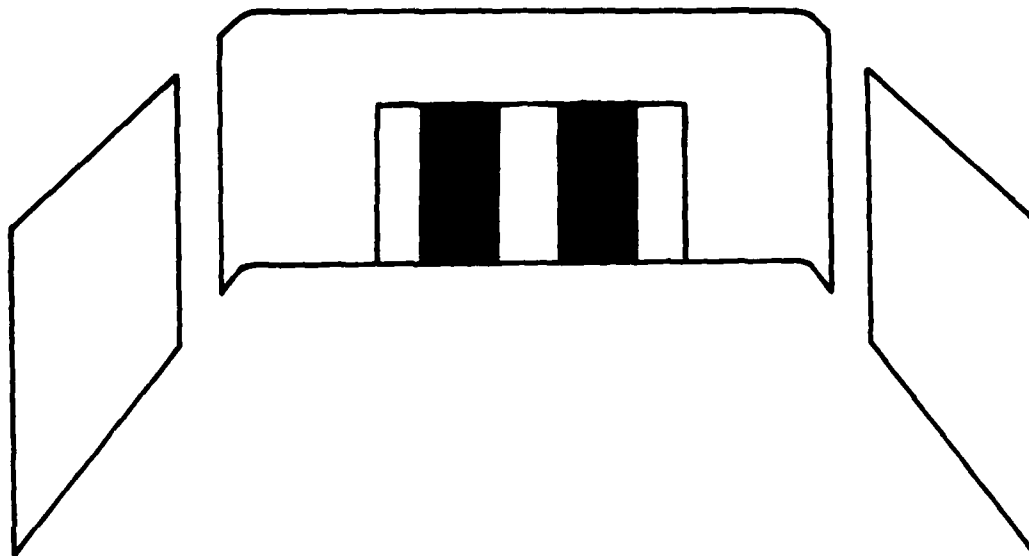


Figure 3a: Central Visual Field (CVF) moving stripe display used in Experiment II (29 deg. by 17 deg.)

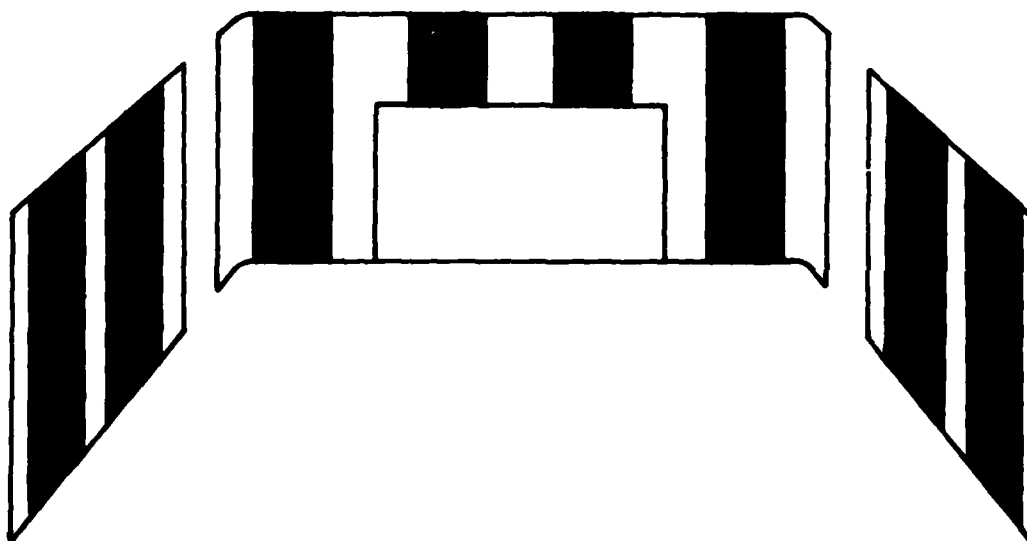


Figure 3b: Peripheral Visual Field (PVF) moving stripe display used in Experiment II (180 deg. by 23 deg.)

THE RELEVANCE OF CHANNEL THEORY
FOR THE DESIGN OF SIMULATOR IMAGERY



David M. Regan
J. W. Killam Research Professor in
Physiology and Biophysics.
Professor of Ophthalmology and
Otolaryngology, Dalhousie University

David Regan obtained his Ph.D., M.Sc. and ARCS from Imperial College, University of London, all in physics. His D.Sc. was subsequently awarded by the University of London. After lecturing in physics at London he spent 11 years in the research Department of Communication and Neuroscience, Keele University before moving to Dalhousie University, Canada in 1975. His interests cover psychophysical evoked potential and single-cell studies of normal and disordered vision and hearing. Most recently he has worked on depth and motion perception, visual sensitivity to expanding flow patterns, visual factors in aviation, contrast vision in multiple sclerosis, amblyopia in children, and disorders of auditory FM sensitivity.

No
Photo
Available

Ronald Kruk
Graduate Student, Department of
Psychology, Dalhousie University

Ronald Kruk received his B.A., M.A. in psychology from the University of Manitoba. From 1968 to 1975 he served as a pilot with the Canadian Forces. He is currently a graduate student of David Regan at Dalhousie University. His principal research activities have been in the area of visual psychophysics, and computer software to support experimentation.

No
Photo
Available

Kenneth Ian Beverley
Assistant Professor, Department
of Physiology and Biophysics,
Dalhousie University

Kenneth I. Beverly received his B.A. in Physics and Psychology, and his Ph.D. in Communications and Neuroscience from Keele University, England. He spent three years in post doctorate research on electronic imaging systems at Nottingham University in 1976, where he has continued his work on electronic imagery and biophysical research.

No
Photo
Available

Thomas M. Longridge
Research Psychologist, Operations
Training Division, Air Force
Human Resources Laboratory

Thomas M. Longridge received his B.A. from UCLA in experimental psychology. He obtained his M.A. and Ph.D. in sensation and perception from the University of Arizona. From 1972-1975 he served as a research psychologist at the USAF School of Applied Aerospace Sciences. He was an Associate Professor of Behavioral Science at the USAF Academy from 1975-1977. He joined AFHRL in 1977, working principally in the area of visual simulation research.

THE RELEVANCE OF CHANNEL THEORY FOR THE DESIGN OF SIMULATOR IMAGERY

ABSTRACT

There is a body of experimental evidence supporting the hypothesis that an early stage of visual processing consists of analyzing retinal image information into a number of abstract categories or features, called channels. This paper briefly reviews the channel hypothesis and cites potential implications for flight simulator visual display design. The results of a preliminary study designed to investigate the relationships between channel sensitivity and flight simulator landing performance are presented.

1 INTRODUCTION

1.1 THE CHANNEL HYPOTHESIS

It may well be true that, in most flying situations, the limits to a pilot's performance are set by his cognitive skills developed by prior training and experience. Nevertheless, flying situations may exist for which his flying performance comes up against the limited sensitivity or discrimination of his visual sensory system. For example, the importance of seeing one's adversary before he saw you was already a byword among military pilots when the airplane's major role was as an army scout. In more recent times the importance of visual sensory factors is implied by the insistence that both military and airline pilots should have excellent visual acuity, colour vision and stereoscopic depth perception.

If we assume that, in some situations, flying performance is limited by visual sensory factors, then we might expect that flying tasks could be found for which a pilot's performance could be predicted on the basis of visual tests. However, this expectation has not yet been fulfilled. Reports of strong correlations between flying performance and visual test results have so far been sparse (Semple, Hennessy, Sanders, Cross and McCauley, 1980).

During the last 10 years we have adopted the following rationale in seeking visual tests that will predict flying performance. There is a body of experimental evidence supporting the hypothesis that an early stage of visual processing consists of analyzing retinal image information into a number of abstract categories or features. In psychophysical jargon this is accomplished by passing the retinal image through a few sets of information-processing "channels" (Braddick, Campbell and Atkinson, 1978; Regan, 1981). The essential property of these sets of channels is that, to a

first approximation, they have nonoverlapping sensitivities so that they analyze the visual world into independent categories. The individual channels within a set may have overlapping sensitivities. The essential property of an individual channel within a set is that it operates independently of all other channels. The outputs of individual channels may be subtracted or otherwise reorganized so as to enhance discrimination (e.g., as in opponent color process). We suppose that, reorganized or not, the outputs of these channels feed into later stages of visual processing at which cognitive and learned factors are important, and that to a first approximation, the properties of channels are not affected by cognitive factors.

For our present purpose, the significance of the channel hypothesis is that channel processing would be important in visually-guided flying tasks, and channel processing could be largely described and understood in ways that are familiar in physics and electrical engineering. Thus, the early "channel" stage of visual processing could be more easily understood in quantitative terms than the later cognitive stages, and the two levels of processing could be separated (Regan, 1981). Channels that have so far been identified include sets of channels for colour (Young, 1802a, b; Wright, 1946), spatial frequency (Campbell and Robson, 1968; Blakemore and Campbell, 1969), stereoscopic position in depth (Richards, 1970, 1971), stereoscopic motion in depth (Beverley and Regan, 1973, 1975; Regan, Beverley and Cynader, 1979a, b), changing-size (Regan and Beverley, 1978), and sideways motion (i.e., motion parallel to the frontoparallel plane (Sekuler, Pancel and Levinson, 1978).

In principle, an initial channel analysis of visual information could offer a considerable advantage in acquiring skills of eye-hand coordination. If, for example, learning how to catch a ball can be regarded as a process of establishing one or more "hard wired" ways of processing the outputs of certain visual channels, then the skill would transfer from a simple visual environment to a complex visual environment because the absence of overlap between sets of channels and of "cross talk" between channels would render the initial channel analysis more or less indifferent to scene complexity (Regan, 1981; Regan and Beverley, 1980).

Conversely, either too much "cross talk" between channels or too much overlap between sets of channels might cause flying performance in complex visual situations to fall below flying performance in a simple visual situation. In order to test this suggestion we designed a tracking device that measures a subject's ability to track a test square whose size changes (as though moving in depth) while at the same time the square executes side-to-side movements (Regan and Beverley, 1980). This test assesses a subject's ability to use his changing-size channels in conditions where appreciable cross talk is possible.

1.2 RELEVANCE OF CHANNEL THEORY FOR DESIGN OF SIMULATOR IMAGERY

If the channel hypothesis proves to be valid to any substantial extent, there are several possible implications for aviation research and these are discussed in detail elsewhere (Regan, 1981). In brief, some flying tasks might depend on only one, or at any rate very few sets of channels (Regan,

1981). Furthermore, different flying tasks might depend on different sets of channels. If this is the case, then visual test results on one set of channels might predict performance in one flying task, while test results on other sets of channel might predict performance in a second flying task, and this is currently under experimental investigation.

If the only visual information available for later cognitive processing is the outputs of the various sets of channels, then the task of simulator imagery reduces to effectively driving the relevant sets of channels. If a particular set of channels is not involved in the visual tasks being learned, then that set of channels need not be driven by a visual display used in training for this task. Finally, the minimum dynamic and spatial (e.g., resolution) performance of a visual display could be defined by reference to the dynamic and spatial frequency properties of the channels involved in the visual tasks to be learned. It would be unnecessary for the visual display to have a wider temporal or spatial frequency bandwidth than the widest bandwidth of the relevant channels.

All this depends on the validity of the channel hypothesis, but the channel hypothesis as set out in Section 1.1 above is subject to experimental test and experimental refutation. In particular, the following points are open to experimental refutation: (a) non-overlapping sensitivities of sets of channels; (b) independent operation of different channels; (c) lack of cognitive effect upon channel properties.

2 BACKGROUND

2.1 STEREOSCOPIC PERCEPTION OF POSITION-IN-DEPTH AND OF MOTION-IN-DEPTH

The designers of flight simulators have generally reduced costs by not including a stereo visual display on the grounds that, since classical stereo vision is almost ineffective at distances over 10 metres or so, it is unlikely to be important in flying. The purpose of Section 2.1 is to suggest that, even when cost and complexity prevent the inclusion of a stereo display, the simulator designer should note that the human visual pathway contains a stereo motion system that may be important out to longer viewing distances than classical stereo vision. This stereo motion system might be involved not only in landing helicopters on oil rigs or ships and in nap-of-the-earth operations, but also in some tasks with fixed-wing aircraft. It is therefore possible that unexpected transfer of training difficulties might be experienced as a result of omitting a stereo display.

Psychophysical evidence that motion in depth and position in depth are processed separately.

Recent evidence supports the idea that there are separate stereoscopic channels for position in depth and for motion in depth. Beverley and Regan (1973) pointed out that the relative velocities of the left and right retinal

images provide a precise cue to the direction of motion in depth (Figure 1). Their evidence that the human visual pathway uses this cue was obtained psychophysically. They found that, after inspecting an image oscillating in depth, visual sensitivity to motion in depth was depressed. The important point was that only a narrow range of directions of motion in depth was affected. They proposed that there are several stereoscopic motion-in-depth channels, tuned to four different directions in depth. Figure 2B shows the directional tuning of these channels for one human subject.

Richards and Regan (1973) reported a different sort of evidence that binocular disparity is processed separately from the relative velocities of the left and right retinal images. They found subjects whose visual field contained regions that were "blind" to disparity, yet were sensitive to motion in depth, while other regions of the visual field were blind to motion in depth, yet sensitive to disparity.

In brief, the newly-discovered stereo system for motion is quite distinct and different from the classical stereo system for position in depth. Testing a subject's classical stereo vision does not necessarily tell us about his stereo vision for motion. In view of the failure of classical stereo vision at distances over 10-20 metres it might seem surprising that the ratio between stereo and monocular sensitivities for motion in depth does not depend on viewing distance.

A further distinction between the stereo motion channels and the classical stereo position channels is that their dynamics are very different (Regan and Beverley, 1963a). Figure 3 illustrates this point; Panel A shows how visual sensitivity to sideways oscillations depends on oscillation frequency. Visual sensitivity is best i.e., threshold is lowest) for oscillation frequencies between about 1 and 5 Hz, but oscillations can still be seen up to 25 Hz at least. In contrast, panel B is a similar plot for the stereo motion channels. Visual sensitivity for oscillations in depth falls off from the lowest frequency tested (about 0.8 Hz), and oscillations in depth cannot be seen at all above about 3-5 Hz. Putting this another way, the stereo motion channels are far more sluggish than the sideways motion channels.*

* The stereo motion data of panel B was obtained as follows. The subject's left eye viewed a bar or dot pattern oscillating from side to side at a frequency F Hz while the right eye viewed a similar pattern oscillating at $(F + \Delta F)$ Hz. In binocular fusion the target appeared to change periodically in depth at a frequency ΔF Hz, but though this frequency ΔF was available in binocular view, it was not available to either left or right eye alone. Panel B shows how visual sensitivity to the ΔF Hz movements in depth were affected by the value of ΔF (Regan and Beverley, 1973a).

The ability to discriminate between different directions of motion in depth

Figure 2A shows a subject's ability to discriminate between different directions of motion in depth (Beverley and Regan, 1975). This ability is remarkably acute, a difference of as little as 0.1° to 0.2° in direction being detectable. Figure 2A might help to explain the well-recognized ability of tennis and baseball players, automobile drivers and pilots to make very acute judgements of the direction of motion in depth. This high acuity cannot be entirely explained in terms of the directionally-selective channels of Figure 2B, since they would predict an acuity of only about 1° to 2° . Beverley and Regan proposed, therefore, that the outputs of the channels of Figure 2A are subtracted at a later stage so as to give the acute discrimination of Figure 2A, much as the outputs of red, green and blue cones pass through an opponent colour process and thus mediate our acute colour discrimination.

Brain cells sharply tuned to the direction of motion in depth and brain cells sharply tuned to position in depth

Recording from areas 18 and from the 17/18 border in cat visual cortex, Cynader and Regan (1978, 1981) found single neurons that were selectively sensitive to the ratio between left and right retinal image velocities. In other words, these neurons were tuned to the direction of motion in depth.* All the psychophysical motion-in-depth channels in man shown in Figure 2 had their equivalent neurons in cat visual cortex. Some of the most sharply-tuned neurons fired best when the retinal images moved in opposite directions, and thus responded to a range of directions spanning no more than 1° to 2° . Many of these neurons maintained their directional tuning over at least a four-fold range of speeds (Figure 4A). A second class of neurons fired best for trajectories that missed the head. These were tuned to a broader range of directions than the "hitting the head" class of neurons. Similar "motion in depth" neurons have recently been found in visual cortex of unanaesthetized, behaving monkey (Poggio and Talbot, 1981), so that it seems likely that equivalent neurons exist in human visual cortex.

Cynader and Regan (1978) also found a class of neuron that had been previously described. These neurons showed strong interocular facilitation (up to 100-fold) when motion was accurately parallel to the frontoparallel plane (Figure 4B). This class of neuron also can be regarded as being very selective to the direction of motion in depth.

* Note that these motion-in-depth neurons cannot be described as being selectively sensitive to the rate of change of disparity, i.e., to the difference between the left and right image velocities since many directions of motion correspond to a single rate of change of disparity (Regan and Cynader, 1981).

This third class of neuron was comparatively sharply tuned to disparity, i.e., to position in depth. In this they differed from many neurons in the first two classes, some of which maintained their tuning to motion in depth over a range of disparities as large as 12° . Other neurons of this type systematically changed their tuning as a function of disparity, for example, favouring motion towards the frontoparallel plane both for objects located nearer than the frontoparallel plane and for objects located beyond the frontoparallel plane.

Evoked potentials

Evoked potential studies bridging the inter-species gap between our psychophysical studies in man and animal single-unit experiments were carried out before these other studies were started. Regan and Spekreijse (1970) used Julesz patterns to obtain evoked potentials to stereoscopic motion in depth. Regan and Beverley (1973b) later found that different evoked potentials were produced by different directions of motion in depth, anticipating the conclusions of subsequent psychophysical and single-unit studies.

2.2 VISUAL PROCESSING OF CHANGING-SIZE AND SIDEWAYS MOTION

Psychophysical evidence that changing-size and sideways motion are processed separately

Since the channels described above are sensitive to the relative velocity of the retinal images, they can only be driven monocularly. A second stimulus for motion in depth is, however, effective monocularly as well as binocularly. This is the stimulus of changing size.

Figure 5 shows experimental evidence that the processing of changing-size information cannot be explained in terms of responses to motion. Subjects viewed a pair of bright squares on a dimmer background. We used the following two stimulus oscillations: inphase oscillations, in which opposite edges of a square moved in the same direction at any instant; antiphase oscillations, in which opposite edges of a square moved in opposite directions at any instant. Subjects first measured the smallest oscillation amplitude that could just be detected for an inphase test oscillation and for an antiphase test oscillation. Then they inspected a strong antiphase oscillation for 20 min and measured the two thresholds again. The antiphase threshold was much elevated, but the inphase threshold was comparatively little affected. When the experiment was repeated with an inphase adapting oscillation, threshold elevations were small for both test stimuli (Regan and Beverley, 1978).

This differential effect was still observed when the adapting stimulus was a bright square on a dark ground and the test stimulus was a dark square on a bright ground.

A weakness of these early experiments is that they were limited to two directions of motion, namely motion parallel to the frontoparallel plane (i.e., inphase oscillations), and motion along a line through the eye (i.e., antiphase oscillations). A more recent experiment extended the conclusions to a range of adapting trajectories. The rationale of this later experiment is illustrated in Figure 6A. On separate days, subjects adapted to 11 different trajectories. Each adapting oscillation had the same velocity along a line through the eye, i.e., the same antiphase component, but each adapting oscillation had a different velocity parallel to the frontoparallel plane (i.e., a different inphase component of oscillation). If the changing-size channel responded to the antiphase component and was unaffected by the inphase component, then all 11 adapting oscillations should produce the same threshold elevation for the antiphase test stimulus.

Figure 6B shows that this prediction was upheld to an accuracy of about +30% over a very wide span of trajectories. (The abscissa in Figure 6B plots Inphase components ranging from zero to +8 times the amplitude of the antiphase component.) Further evidence suggested that, in everyday vision, the prediction probably holds to considerably better than +30% due to the effect of eye movement. The experiment of Figure 6B was repeated with a rapid "jitter" oscillation added to the adapting stimulus. As shown in Figure 6C, the effect of this "jitter" was to reduce the influence of an inphase component upon the antiphase threshold elevation so that the influence was less than measurement errors (+5%) (Regan and Beverley, 1980). "Jitter" was most effective when it approximated the natural retinal image "jitter" that occurs in everyday life when the head is not artificially supported.

In order to explain these findings we proposed that the visual system contain a set of channels that operate as illustrated in Figure 7. The accuracy with which the computations $(x-y)$ and $(x+y)$ are carried out (better than 5%) may seem astonishing, especially since the accuracy is almost independent of the absolute values of x and y . It may seem less surprising when we reflect how casually we rely on such computations when judging the motion of speeding cars on busy roads.

In brief, these findings suggest that the set of changing-size channels allow the visual system to directly compute the line-of-sight component of an object's velocity, that is the velocity component along a line through the eye (V_{LOS} in Figure 8) even when both object and head are moving along arbitrary trajectories.

Brain neurons sensitive to changing size

All 101 neurons studied by Regan and Cynader (1979) in area 18 of cat visual cortex responded to changing-size. However, control experiments eliminated most of these neurons by showing that they were responding to changes in light flux or to motion of a single edge rather than to changing size. Nevertheless, a very few neurons in area 18 did satisfy the criteria for changing-size responses. In addition, there was evidence that a

considerable proportion of neurons slightly, but systematically emphasized changing-size even though no systematic preference was evident in simple spike counts.

2.3 TWO STIMULI FOR MOTION-IN-DEPTH: COMPARATIVE EFFECTIVENESS OF CHANGING-DISPARITY AND CHANGING-SIZE

Figure 9 illustrates that when an object moves directly toward the head, the two retinal images move away from each other and also grow larger. As discussed above, either of these two visual inputs by itself is capable of causing a sensation of motion in depth. In the real visual world the situation is almost always as shown in Figure 9, but in order to measure the relative effectiveness of the two inputs, we created artificial stimuli in which the two inputs of Figure 9 were antagonistic (for example, as an object came closer it grew smaller).

Subjects viewed a square whose size changed at a fixed rate, so that the square appeared to move in depth. The rate of change of binocular disparity was then adjusted by the subject so as to exactly cancel the impression of motion in depth produced by the fixed rate of change of size (Regan and Beverley, 1979a). It is possible to use Figure 10 to read off a subject's relative sensitivity to monocular and stereoscopic stimuli for motion in depth, given the inspection duration and speed.

In a number of flight tests, the focus of discussion has been whether the absence of binocular vision affects pilot performance. Three flight studies have found that the landing performance of pilots in daylight was not degraded by occluding one eye during landing (Pfaffman, 1948; Lewis, Blakeley, Swaroop, Masters and McMurty, 1973; Grosslight, Fletcher, Masterton and Hagen, 1978) and one study reported that landing performance could even be improved by loss of binocular vision (Lewis and Kriers, 1969) though this finding has been challenged by researchers who, nevertheless, found that monocular performance was no worse than binocular performance (Grosslight, Fletcher, Masterton and Hagen, 1978). In one of these studies the suspicion that pilots might try harder when one eye was occluded was addressed by repeating the flight tests with low-time pilots rather than experienced military pilots. Even though the low-time pilots were presumably stretched when landing normally with full binocular vision, monocular occlusions produced no reduction in landing performance (Lewis and Kriers, 1969).

The results of these flight tests are consistent with the notion that static binocular depth perception is unimportant at a range in excess of about 10 yards when other depth cues are available (Howard and Templeton, 1966).

However, judgements of motion-in-depth are a quite different matter from judgements of position in depth. Our laboratory experiments suggest that the flight tests discussed above may have confounded several factors, so that the results of these flight tests may apply to only a narrow range of visual situations. Consider the perception of the motion in depth of ground objects

during landing. If binocular vision is lost, the consequence for motion-in-depth sensitivity would depend on the following five factors (Regan and Beverley, 1979a).

(1) Inspection duration. A loss of binocular vision would be less important for short inspection times.

(2) The target's velocity in depth. Visual sensitivity to low velocities would be less affected by losing binocular vision.

(3) The absolute width of the object. Visual sensitivity to the motion-in-depth of wider objects would be less affected by the loss of binocular vision. (Except at very short distances, this would be independent of distance; see Regan and Beverley, 1979a, Appendix).

(4) The difference between binocular and monocular threshold for motion-in-depth sensation produced by changing-size stimulation. For our subjects and stimulus conditions, binocular thresholds were up to about 1.4 times lower than monocular thresholds (depending on the individual subject).

(5) Individual differences. These are large. Even over our small sample of five subjects we found a greater than 80:1 intersubject difference in the relative effectiveness of changing-size and changing-disparity in producing a sensation of motion-in-depth.

The following calculation is intended to illustrate this point. An airplane travelling at 140 mph is supposed to be 2000 ft from a runway measuring 100 ft wide. To anticipate, if the pilot (subject T.W. in Figure 10) looked at the runway for 1.0 sec, the monocularly-available cue of changing-size would be 76 times more effective than changing-disparity as a stimulus for motion-in-depth.

At 2000 ft the angular width of the runway is 2.72° . After 1 sec approaching at 140 mph, the angular width increases to 3.02° . Hence the mean rate of change of angular width $\dot{\theta}_S = 0.295^\circ/\text{sec} = 17.7 \text{ min arc sec}^{-1}$ (i.e., $8.86 \text{ min arc sec}^{-1}$ for each edge).

For subject T.W. the rate of change of disparity ($\dot{\theta}_D$) equivalent to $\dot{\theta}_S = 17.7 \text{ min arc sec}^{-1}$, for an inspection time of 1 sec is $\dot{\theta}_D = 1.4 \text{ min arc sec}^{-1}$ (from Figure 10), hence $\dot{\theta}_D/\dot{\theta}_S = 0.16$.

From the geometrical considerations outlined in Appendix 1, we would expect that $\dot{\theta}_D/\dot{\theta}_S = I/S$. In this case $S = 100 \text{ ft}$ and $I = 2.5 \text{ in.}$, as the geometrically predicted ratio $\dot{\theta}_D/\dot{\theta}_S$ is 0.0021.

Hence, allowing for geometric factors, changing-size would be 76 times more effective than changing-disparity as a stimulus for motion in depth, for subject T. W.

2.4 DYNAMIC PROPERTIES OF THE CHANGING-SIZE AND STEREOSCOPIC MOTION CHANNELS

Figure 11 plots thresholds for just-detectable motion in depth produced by two different visual inputs, namely changing-size (continuous line), and changing-disparity (bold broken line). The two plots are clearly different. In particular, changing-size grows relatively less effective at oscillation frequencies below about 1 Hz.

Figure 11 also plots thresholds for two different sensations produced by a single input. The input is changing-size, and the two sensations are changing-size (fine dotted line), and motion in depth (continuous line). The chief difference between the two curves is that changing-size is ineffective as a stimulus for motion in depth for a range of frequencies above about 3 Hz although at these high frequencies it is still effective in producing a sensation of changing-size.

2.5 MOTION OF THE SUBJECT THROUGH A FIXED EXTERNAL WORLD

Gibson (1950) discussed how a visual flow pattern can produce the impression that one is moving through the external world towards the focus of the flow pattern. He pointed out that this is an important visual cue for automobile drivers and pilots.

Testing the suggestion that changing-size channels might be involved in visual sensitivity to flow patterns, Regan and Beverley (1979b) measured elevations of changing-size thresholds caused by adapting to a flow pattern. Their finding that changing-size thresholds were indeed elevated, but only for locations near the focus of the flow pattern, gave some support to those suggestions (Regan, Beverley and Cynader, 1979b). This experiment indicates that visual sensitivity to expanding flow patterns is not necessarily a large-field phenomenon. A small-field mechanism may also be involved, though we should emphasize that our proposal is intended only as a partial explanation for visual localization of a flow pattern's focus.

2.6 SPATIAL FREQUENCY CHANNELS

Mathematical discoveries published by Fourier as long ago as 1807 (Herivel, 1975) led to the realization that any picture or scene can be broken down into many superposed sinewave gratings and conversely that, by superposing the appropriate sinewave gratings, any picture can be synthesized. By the 1950's, this fact was the basis of a standard technique for assessing the performance of lenses for aerial photography (Hopkins, 1957).

It was a considerable further step beyond the mathematical facts to propose that the human visual system analyzes the retinal image into spatial frequency bands. Campbell and Robson (1968) proposed that the human visual system contains "functionally separate mechanisms . . . each responding maximally at some particular spatial frequency and hardly at all at

frequencies differing by a factor of two. The frequency selectivity of these mechanisms must be determined by integrative processes in the nervous system, and they appear to a first approximation to operate linearly."

It is not yet clear what these spatial frequency channels correspond to physiologically. Some neurophysiologists have found neurons in the visual pathway of animals that have wave-like receptive fields so that they respond best to sinewave grating stimuli, and could act as physical Fourier analyzers (Pollen and Feldon, 1979). Other vision scientists favour quite different explanations, for example that every location on the retina has only four classes of receptive field size, and that the action of four classes is equivalent to analyzing the retinal image into four spatial frequency bands (Wilson and Bergen, 1979).

But whatever the physiological basis of spatial frequency channels may be, for our present purpose the main point is that human visual sensitivity for fine detail (i.e. high spatial frequencies) does not necessarily tell us about human vision for coarse and intermediate detail (i.e. low and intermediate spatial frequencies). A clear illustration of this point is given by the finding that many multiple sclerosis patients with normal Snellen acuity have severely impaired vision for coarse or intermediate detail (Regan, Silver and Murray, 1977; Ginsburg, 1978; Zimmern, Campbell and Wilkinson, 1979). Figure 12 illustrates the sinewave gratings used to test vision at different spatial frequencies, and defines "contrast" and "spatial frequency".*

Multiple sclerosis patients illustrate, in exaggerated form, visual differences that also exist between control subjects. In studies of 40 control subjects we found that those with 20/20 vision showed considerable intersubject variability at a lower spatial frequency of 5 cycles/degree (Regan, Silver and Murray, 1977; Regan, Whitlock, Murray and Beverley, 1980), so that a control subject's ability to see a low contrast object of moderate size would not be accurately predicted by his Snellen acuity, a point recently emphasized and put into a military context by Ginsburg (1980).

* Figure 12 also illustrates a common procedure for testing vision at a given spatial frequency. This is to adjust grating contrast until the subject can just tell the difference between the grating and a blank field of similar brightness. This contrast is his "contrast threshold" for that spatial frequency. Then contrast threshold is measured for several other spatial frequencies.

2.7 CONTRAST THRESHOLDS

The smallest contrast for which the subject can distinguish between a grating and a blank screen has been much studied. However, this is not the only type of contrast threshold. For example, there is a minimum contrast for which a changing-size channel can operate, and this contrast threshold may be somewhat higher than the contrast required to see the target (Petersik, Beverley and Regan, 1981). In other words, the fact that a subject can just see a target does not necessarily mean that he can use all his various visual channels (e.g., changing-size, motion, motion in depth channels): there may be a gap between the contrast threshold to just detect a target and the contrast threshold to activate a particular channel. For this reason we included measurements of contrast thresholds for changing-size and motion channels in the study on pilots' flying performance described below.

3 VISUAL TESTS AND FLYING PERFORMANCE

3.1 METHODS

Psychophysical tests: Procedure for measuring psychophysical thresholds

We used a staircase procedure (Wetherill and Levitt, 1965) to make all our threshold measurements. Four staircases were interleaved to prevent the subject from deducing the staircase strategy. Consequently, each run provided four estimates of threshold, one for each of the four interleaved staircases. Some estimate of reliability could be obtained by comparing these two estimates. Stimulus delivery was controlled by a computer (Commodore PET 2001) that also received the subject's response ("stimulus present"/"stimulus not present"), then computed and printed thresholds and standard deviation, according to the method described by Wetherill and Levitt (1965). A full account of methods is given elsewhere (Kruk, Regan, Beverley and Longridge, 1981).

Changing size and motion thresholds. Two 10×10 solid bright squares of luminance 6 cd/m^2 were presented on a Tektronix model 608 CRT. In one psychophysical test the subject fixated the centre of the square while the square's size oscillated at a frequency of 2 Hz (opposite edges oscillated sinusoidally in antiphase). In a second test the square's opposite edges oscillated sinusoidally inphase so that the square as a whole oscillated in position along a diagonal.

Contrast thresholds for motion perception. This test resembled the motion threshold tests described above except that the amplitude of oscillation was held constant at 6 min arc peak-to-peak and the contrast of the square was varied in successive presentations according to the staircase procedure. The subject was instructed that his task was not to detect the presence of the square. Instead his task was to detect the square's oscillation.

Contrast threshold for sinewave grating detection. All gratings presented were of mean luminance 6 cd/m^2 and spatial frequency 5 c/deg and occupied an area $4^\circ \times 5^\circ$. The subject was instructed to press buttons according to whether he detected or did not detect the grating. Gratings were presented according to the staircase procedure.

Tracking tests. The device used to carry out this test has been described previously (Regan and Beverley, 1980). In brief, a $0.5^\circ \times 0.5^\circ$ bright solid square was presented on a Tektronix model 608 CRT. The square's luminance was 6 cd/m^2 and it was superimposed on a background of luminance 24 cd/m^2 that subtended $10^\circ \times 10^\circ$. Thus, the contrast of the square was 25%. Contrast was checked directly by placing a strip of 0.6 log unit neutral density filter over the square.

In the antiphase tracking test the square started to expand at a constant rate ($13 \text{ min arc per sec per edge}$), and after a pseudo-random interval t it started to contract at the same rate, and after a second pseudo-random interval t it started to expand again at the same rate, and so on. The mean value of t was 3.0 sec.

The perturbed antiphase tracking task was similar to the antiphase tracking task described above except that the position of the test square was continuously moved about the screen by a noise waveform of bandwidth d.c.-0.7 Hz and RMS amplitude 22.5 min arc . Thus, this positional perturbation was quite severe, and the maximum sideways excursion during any test run could be several times the width of the square.

About 20 min were required to complete all the tracking tests.

In Table 1 the following abbreviations have been used to designate the 13 psychophysical measures.

- TI 1 - Inphase tracking, errors 0 - 0.25 Hz
- TI 2 - Inphase tracking, errors above 0.25 Hz
- TA 1 - Antiphase tracking, errors 0 - 0.25 Hz
- TA 2 - Antiphase tracking, errors above 0.25 Hz
- TP 1 - Perturbed antiphase tracking, errors 0 - 0.25 Hz
- TP 2 - Perturbed antiphase tracking, errors above 0.25 Hz
- SI - Inphase oscillation threshold
- SA - Antiphase oscillation threshold
- G - 5 c/deg grating contrast detection threshold

CPI - Inphase oscillation contrast threshold for peripherally-viewed square
CPA - Antiphase oscillation contrast threshold for peripherally-viewed square
CDI - Inphase oscillation contrast threshold for centrally-viewed square
CDA - Antiphase oscillation contrast threshold for centrally-viewed square

3.2 FLYING TESTS

ASPT simulator at Williams AFB

Pilots used the A-10 cockpit to make 12 restricted visibility landings in the ASPT simulator. Visibility was nominally 6000 ft (1829 m), 3000 ft (915 m) or 1500 ft (460 m), but pilots generally agreed that these nominal figures corresponded to considerably lower visibilities in real flying conditions. The 6000-ft visibility condition was included as a relatively easy task so that the experiment as a whole would not seem unreasonably difficult. In any event, there were very few crashes in either the 6000-ft or 3000-ft visibility condition, so the only data we report here are for the 1500-ft condition.

Pilots were instructed to land on each approach. The ground could not be seen at the start of each approach. Pilots were instructed that their initial air speed was 120 kts and glide slope 2.5° , but that their trajectory was incorrect in both centerline alignment (by +200 ft, i.e., +61 m), and range (by +1000 ft, i.e., +305 m). About 20 min practice was allowed before the test, comprising 10 min free flying then four visual approaches to landing and two landing approaches in each of three visibility conditions.

The simulator indicated a crash in any condition that would have resulted in a crash with an A-10 aircraft.

We defined the first visual flight correction as the first correction towards the runway which exceeded the mean of the previous maximum angles of bank by 50% or more. Typically, the ratio was considerably greater. For example, a pilot who used 5° - 10° angles of bank during instrument approach commonly used up to 30° - 40° of bank when he first saw the runway.

Flying grades

During the course of their regular training, Group 2 students had been assessed into four grades in the following aspects of flying performance in T37 and T38 jet trainers: General flying performance (FLY), formation performance (FORM), instrument flying performance (IF), and landing performance (LAND). The grades were as follows: U (unsatisfactory), F (fair), G (good), and E (excellent). We converted these letter grades to a four point numerical scale (U = 1, F = 2, G = 3, E = 4).

3.3 SUBJECT GROUPS

There were 12 subjects in each group. Group 1 comprised Air Force primary student jet pilots training on the T37 aircraft. The age range was 22-28 years, mean 23.6 years. Group 2 comprised Air Force graduating student jet pilots training on the T38 aircraft. Their age range was 23-29 years, mean 24.8 years. Group 3 comprised experienced pilot instructors. Their range was 26-37 years, mean 30.3 years, and their flying hours ranged from 1340-4940, with a mean of 2430. Group 4 was made up of experienced weapons officers who had a great deal of nonpilot flying experience. Some members (5) of this group had private pilot flying experience. Their ages ranged from 27-39 years with a mean of 32.9 years, and their flying (pilot) hours ranged from 0 to 180 with a mean of 36. Group 5 comprised nonflying control subjects taken from a University population. All had corrected vision of 20/20 or better and none had a history of ophthalmological disorder. Their ages ranged from 19-34 years with a mean of 23.4 years.

3.4 VISUAL TESTS AND FLYING PERFORMANCE: RESULTS

Correlations between the 13 psychophysical measures and landing performance on the ASPT simulator

For Group 2 (i.e., advanced students), good predictions of low-visibility landing performance, as assessed by the number of crashes, could be made on the basis of the antiphase tracking task (Table 1). By way of illustration, Figure 13 plots the relationship between antiphase tracking performance (ordinate) and the number of crashes (abscissa). There was a clear correlation ($r = 0.68$, $p = 0.008$).

The distance from the runway threshold at which the pilot made the first flight correction correlated most strongly with the results of the inphase tracking test. In particular, the better the pilot performed on these tests, the further he was from the runway when he made his first flight correction. By way of illustration, Figure 14 plots the relationship between the inphase tracking performance (ordinates) and the distance from the runway threshold at which Group 2 pilots made their first flight correction. The relationship can be seen to be remarkably close.

In addition we found that contrast thresholds for motion perception and changing-size perception correlated with landing performance (CPI and CPA, Table 1). Somewhat surprisingly, grating contrast threshold did not correlate significantly with the number of crashes nor even with the distance from the runway at which the first flight correction was made.

For Group 3 (pilot instructors) correlations were generally at much lower levels of significance than for Group 2 so that no firm conclusions could be drawn. These low significance levels might well have been due to intersubject

differences in several test and performance measures being considerably smaller in Group 3 than in Group 2.

Correlations between the 13 psychophysical measures and flying grades on T37 and T38 jet aircraft

Flying grades were available for Group 2 (advanced students) only. There were significant correlations between flying grades and several of the threshold contrasts for motion perception and these are reported elsewhere (Kruk, Regan, Beverley and Longridge, 1981). However, they should be treated with caution as flying performance was graded by subjective evaluation for purposes other than this study.

Which psychophysical tests distinguished between the various groups of subjects?

The tracking measures were far more successful than any of the threshold measures in distinguishing between the various groups of subjects.

The inphase tracking task (TI 1, d.c. - 0.25 Hz errors) distinguished between the different groups of flying personnel, in particular groups 2 and 3; 2 and 4; and (less clearly) 1 and 2. This task did not distinguish between the nonflying group and the flying groups, largely because the individual differences were very large in the nonflying group.

On the other hand, errors in the frequency range above 0.25 Hz distinguished between the nonflying control group (Group 5) and all groups of flying personnel at very high levels of significance.

As a whole, threshold measures were not at all effective in distinguishing between different groups of subjects. The sole exception was that the grating contrast threshold test distinguished ($p = 0.02$) between Groups 3 (pilot instructors) and 5 (nonflying control subjects).

3.5 VISUAL TESTS AND FLYING PERFORMANCE: PRELIMINARY CONCLUSIONS

Prediction of simulator landing performance on the basis of psychophysical tests

Of our 13 psychophysical measures, tracking performance related most closely to low-visibility landing performance on the simulator. In particular, landing performance, as assessed by the number of crashes, correlated most strongly with the student pilot's ability to track a target that appeared to move in depth. In addition, the greater the student pilot's ability to track a target that moved from side-to-side, the greater the

distance from the runway threshold that he made his first flight correction, and presumably the greater the available time to adjust his approach.*

Contrast threshold for a 5 cycle/deg grating relates to a subject's ability to see a low-contrast object of moderate size. One might therefore expect that, in a low-visibility landing, a pilot with a low grating contrast threshold would see ground features earlier than a pilot with a high grating contrast threshold, and therefore would make the first flight adjustment somewhat earlier. Surprisingly, this expectation was not fulfilled by our data. Furthermore, grating contrast threshold correlated only weakly with the number of crashes and with flying grades.

Although our findings are preliminary and await verification, perhaps it is not premature to speculate that a test involving superthreshold vision and eye-hand coordination (such as a tracking task) might be intrinsically a more effective predictor of landing performance than a threshold detection test.

* We should make the reservation that our protocol may have compelled pilots to fly in a way that ran to some extent counter to their training and experience of real flying situations. For example, pilots were instructed to land on every approach, and were not allowed the option to make one or more passes before landing. Our aim here was to bring out purely visual limitations to landing performance. However, this may have put very experienced pilots at a disadvantage, as suggested by the negative correlations between experience and number of crashes in the instructor pilot group (Group 3). We should also note that artificialities of the simulator environment may have penalized experienced pilots.

ACKNOWLEDGEMENTS

We thank the student pilots and pilot instructors (82 and 97 FTS, Williams AFB), weapons systems officers (58TTS, Luke AFB) and other experimental subjects for their cooperation in the flying study reviewed above. We are also grateful to the staff of the Air Force Human Resources Laboratory at Williams AFB, Arizona whose expert aid and advice made a major contribution to that flying study. From 1968-1975 this research was supported by the Medical Research Council and NRC of Great Britain, and from 1975 by the NSERC of Canada. R.K. was supported by the NSERC of Canada. K.I.B. was supported by the NSERC (Grant A-0323 to D.R.). From 1978 this research was sponsored by the Air Force Office of Scientific Research, Air Force Systems Command USAF under Grant AFOSR-78-3711

CAPTIONS TO FIGURES

Figure 1

The ratio between the velocities of the left (V_L) and right (V_R) retinal images provides an unambiguous cue to the direction of motion in depth. Positive values of V_L/V_R mean that the retinal images move in the same direction, while negative values indicate opposed motion.

Figure 2

A - Visual discrimination between different direction of motion in depth. Ordinates plot the smallest difference in directions that can be detected for different trajectories (abscissae). The best discrimination (about 0.2°) is for an object moving directly towards the nose.

B - Sensitivity curves for stereoscopic motion channels in the human visual system. These channels are selectively tuned to the ratio V_L/V_R (see Fig. 1). Values of V_L/V_R are plotted as abscissae, with corresponding directions in space indicated. Note that the narrow cone of directions passing between the eyes is exaggerated in this plot, so that the two centre channels are very sharply selective to the direction of motion in depth.

Figure 3

Channels for motion in depth are much more sluggish than channels for sideways motion. A - Visual sensitivity to sideways oscillations of a target plotted versus oscillation frequency. B - Visual sensitivity to oscillations in depth plotted versus oscillation frequency.

Figure 4

Spikes recorded from single neurons in cat visual cortex (plotted radially) as a function of the direction of motion in depth (plotted as azimuthal angle). A - This unit maintains its very selective tuning to the direction of motion in depth over a 4:1 speed range. Note that firing is almost restricted to a range of directions little wider than 1° . This directional tuning is achieved by interocular inhibition as shown by the arrows. B - This unit fired appreciably only when the target moved closely parallel to the frontoparallel plane in a left-right direction and when vision was binocular. Closed circles show firing when the two eyes were stimulated separately and open circles show firing when binocular vision was used. The dotted area indicates the very strong interocular facilitation observed for binocular vision.

Figure 5

Experimental evidence for the existence of changing-size channels.

This figure shows selective threshold elevations for changing size. The two test stimuli are shown at the top. Ordinates plot loss of visual sensitivity

to oscillation caused by inspecting a strong 2-Hz oscillation of size. Changing-size sensitivity fell considerably, but sensitivity to oscillating position was little affected. Note that the only difference between the two test stimuli was in the relationship between the motion of opposite edges of the square.

Figure 6

Experimental evidence that the changing-size channel extracts the velocity component along the line of sight. A - Experimental rationale. All trajectories had the same inphase oscillation component of 6 min arc pk-pk, but different amplitudes of antiphase component were added. B - Threshold elevations produced by adapting to the 11 trajectories in A. Antiphase test oscillations are dotted, while the continuous line plots inphase test oscillations. C - An 8-Hz "jitter" oscillation was added to the 2-Hz adapting oscillation of B.

Figure 7

Model of changing-size channel.

Figure 8

The changing-size channel computes the component of an object's velocity along the line of sight (V_{LOS}) even when both object and observer are moving along arbitrary trajectories. In the figure $V_{LOS} = V_T \cos a + V_0$ cosine B.

Figure 9

When a real-world nonrotating object moves closer, the retinal images grow larger and move apart.

Figure 10

Cancellation of motion-in-depth sensation by opposing changing-size and changing-disparity stimuli: effect of velocity. The subject viewed a square, each of whose edges moved outwards at constant speed for either 0.25, 1.0 or 3.3 sec (as marked on figure). The square then disappeared for 0.25 sec and the cycle repeated. Abscissae $\dot{\theta}_S$, the speed of outward motion of outward motion of each edge in min arc sec $^{-1}$ (where $2 \dot{\theta}_S$ is the rate of increase of a square's side length). Ordinates plot the rate of change of binocular disparity ($\dot{\theta}_D$ min arc sec $^{-1}$) required to cancel the sensation of motion in depth produced by the fixed rate of change of size $\dot{\theta}_S$.

Figure 11

Threshold versus oscillation frequency curves for changing-size stimulation producing motion-in-depth sensation (continuous line), changing-size stimulation producing changing-size sensation (fine dotted line) and changing-disparity stimulation producing motion-in-depth sensation (bold broken line).

Figure 12

A and B illustrate the sinewave gratings used to test visual contrast sensitivity. A is a high contrast grating (about 50%) and B is a fairly low contrast grating (about 10%). C shows the variation of light intensity across the screen for a grating of almost 100% contrast (continuous line) and for one of about 20% contrast (broken line). Percentage contrast is defined as 100 a/b. Contrast threshold is the percent contrast for which the subject can just see the grating.

Figure 13

Relation between tracking performance and the number of crashes.

Ordinates plot error in tracking a test square whose size continuously and unpredictably changed as though moving in depth. Errors in the frequency range below 0.25 Hz only are shown. Abscissae plot the number of crashes made in four low-visibility landings on the ASPT simulator (A-10 cockpit). Data for 12 graduating student pilots are shown.

Figure 14

Relation between tracking performance and the distance from the runway threshold at which pilots made the first flight correction. Ordinates plot errors in tracking a test square that moved unpredictably in the frontoparallel plane. Errors in the frequency range below 0.25 Hz only are shown. Abscissae plot the distance from runway threshold at which the first flight correction was made. Negative distances mean that the pilot had passed over the threshold before his first correction. Results are the mean for four low-visibility landings.

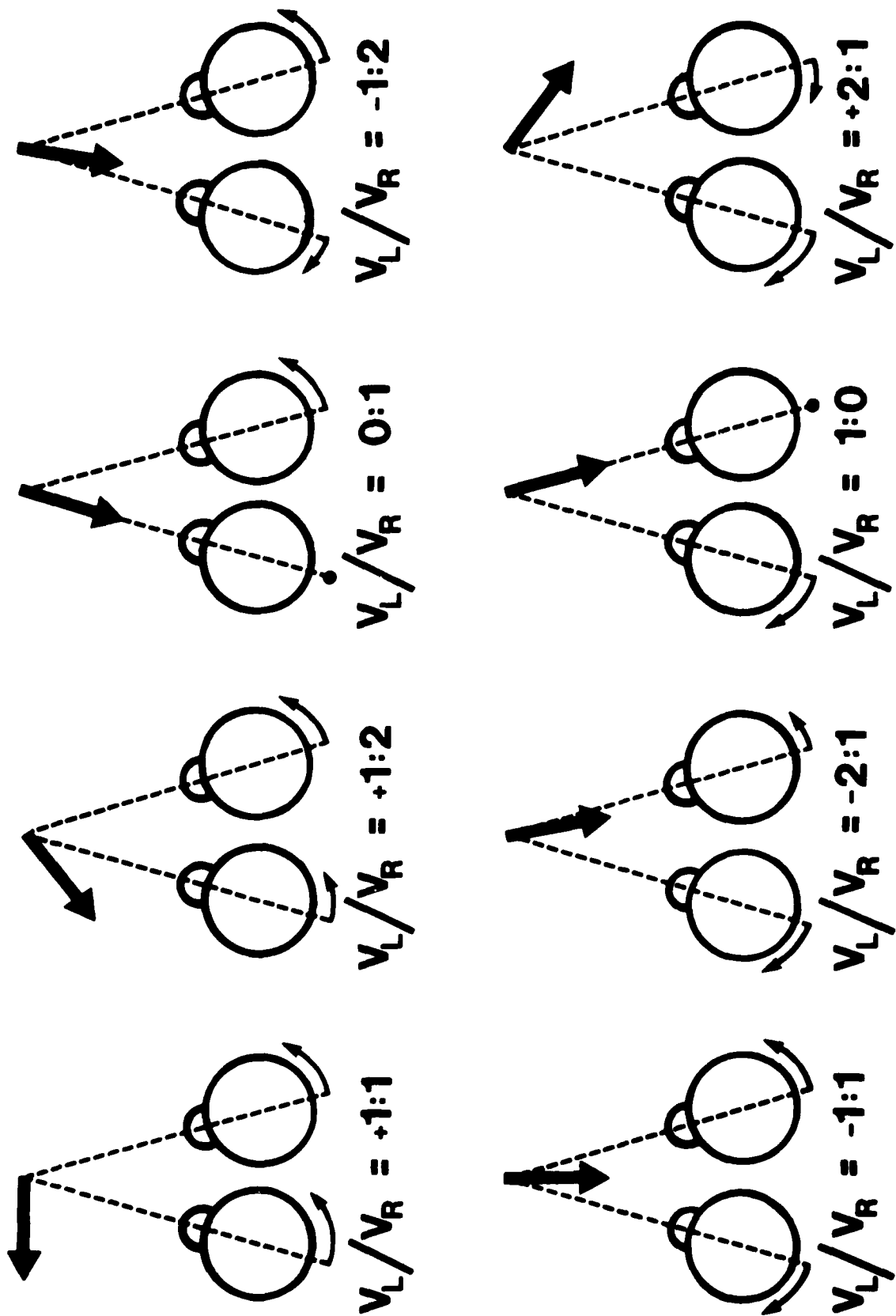


Figure 1.

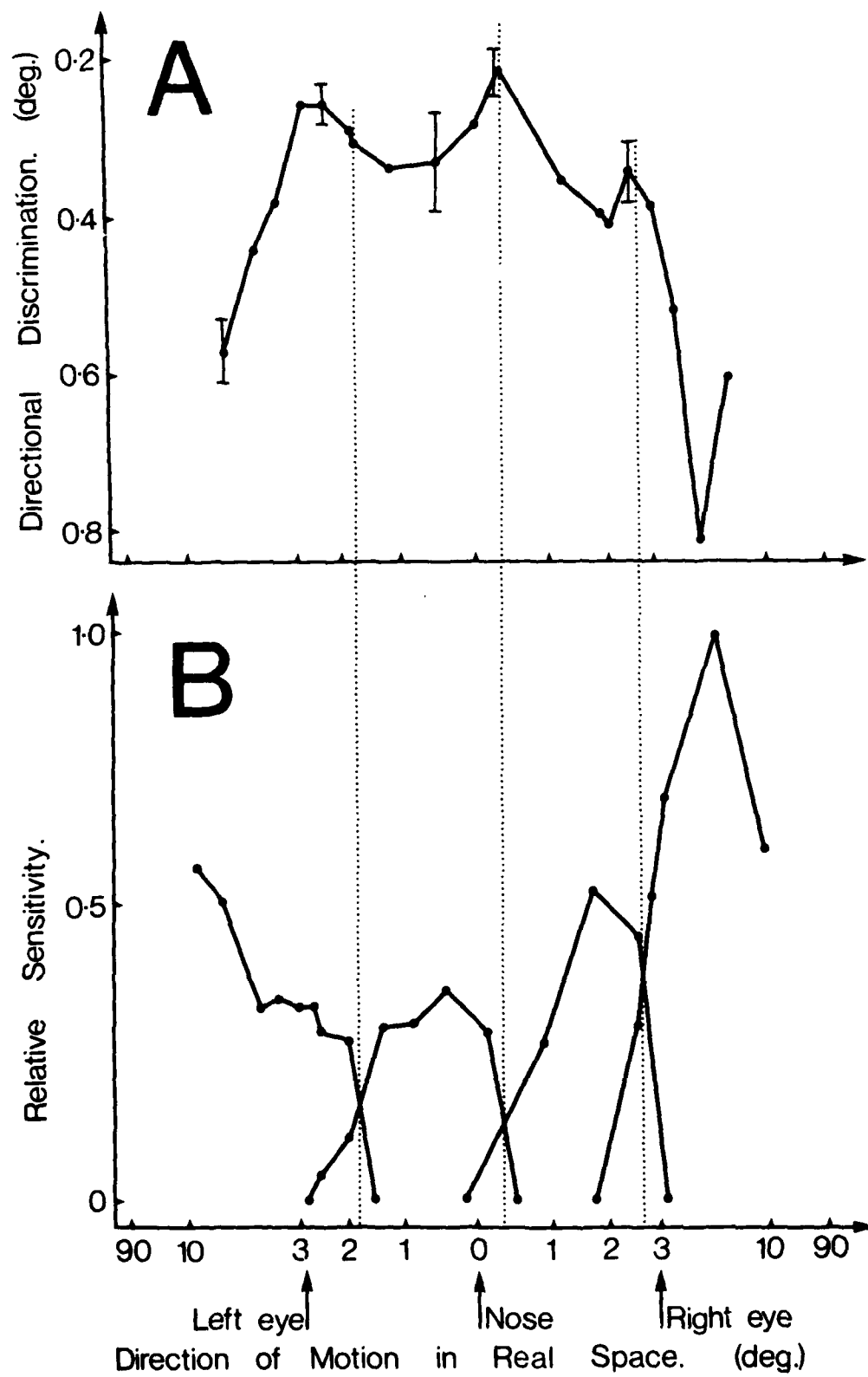


Figure 2.

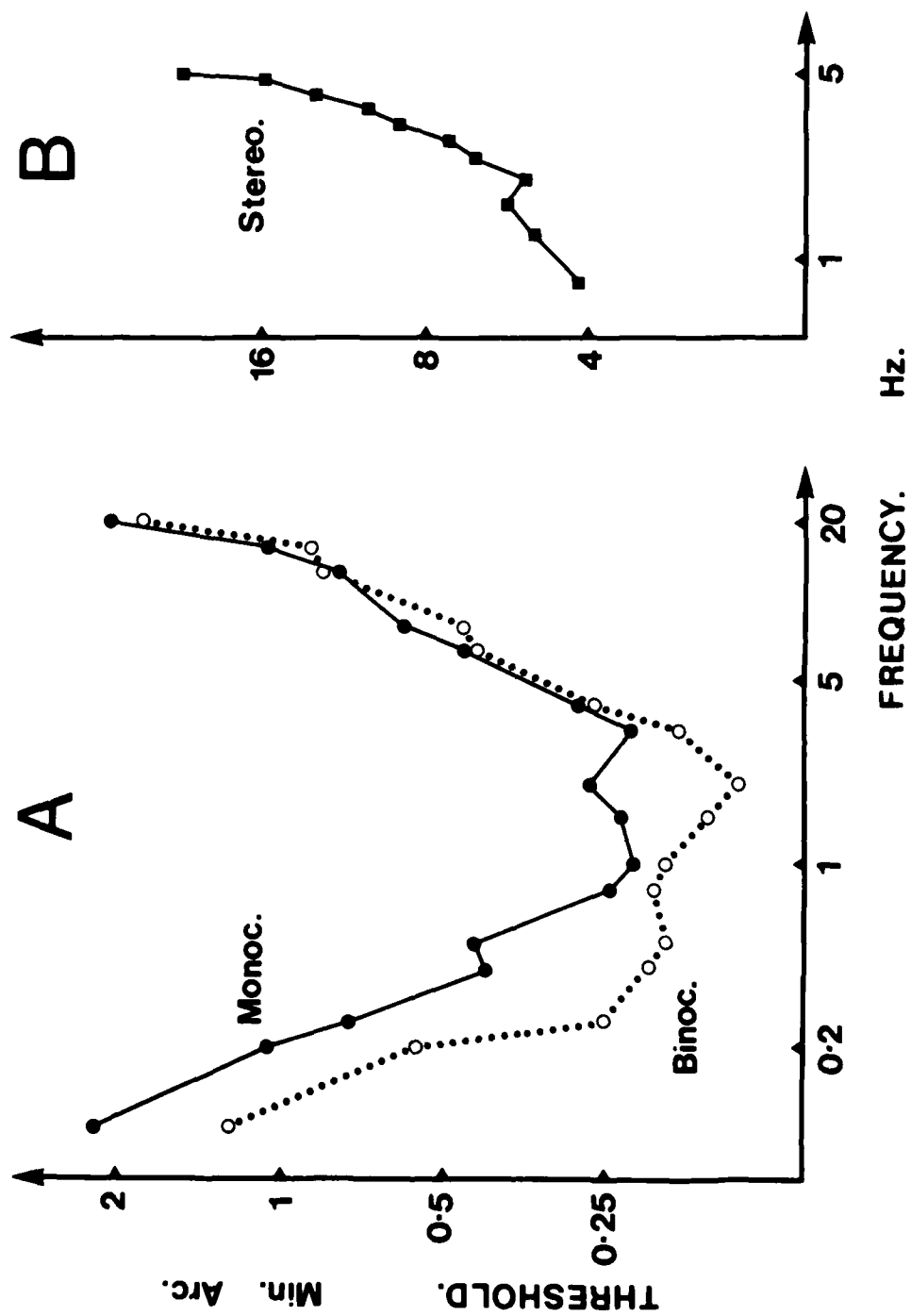


Figure 3.

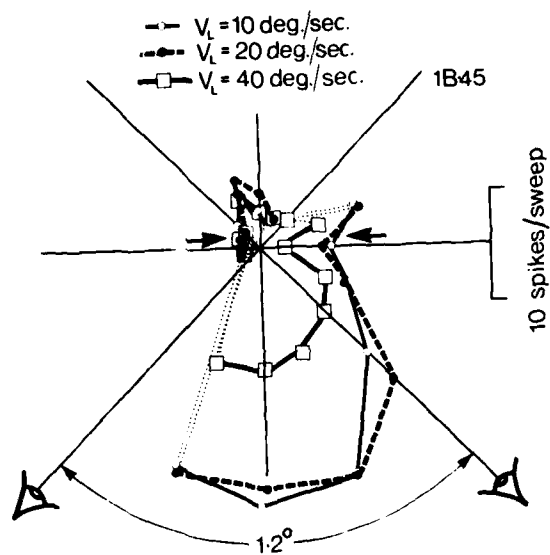


Figure 4a.

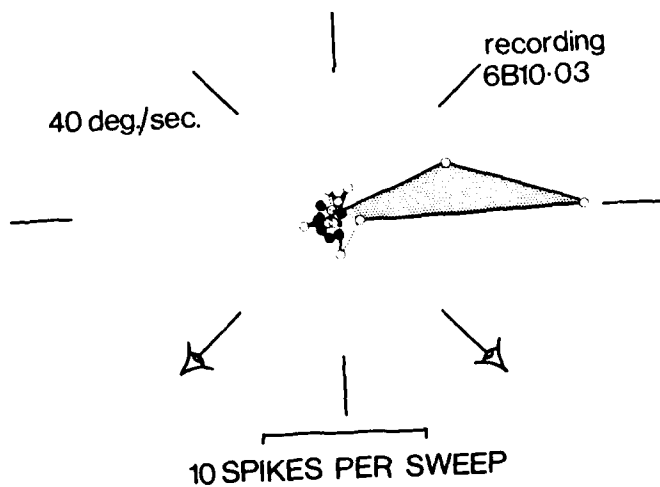


Figure 4b.

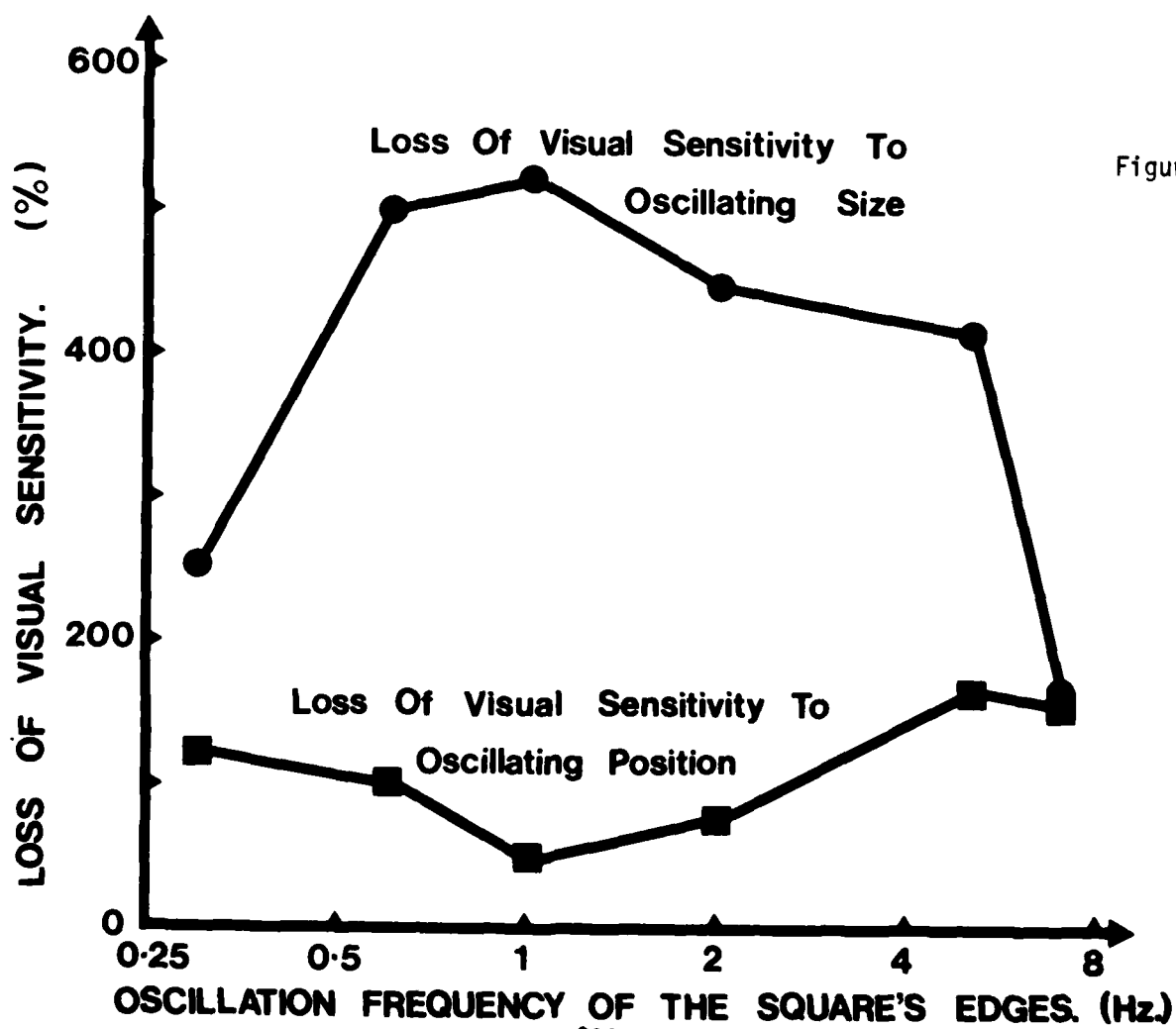
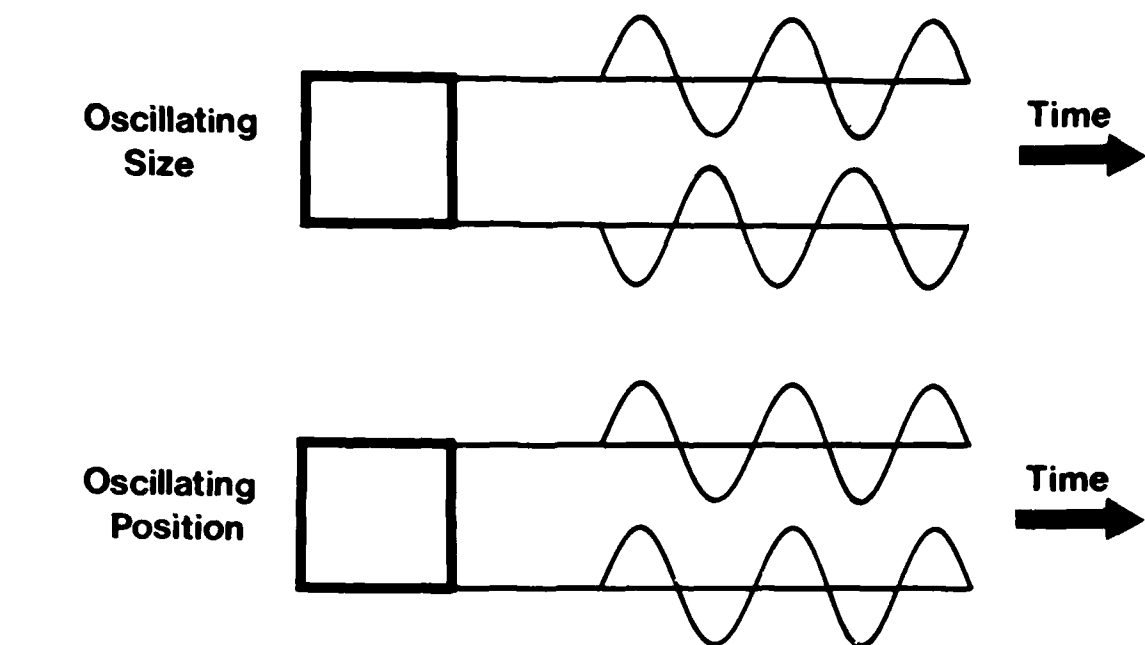


Figure 5.

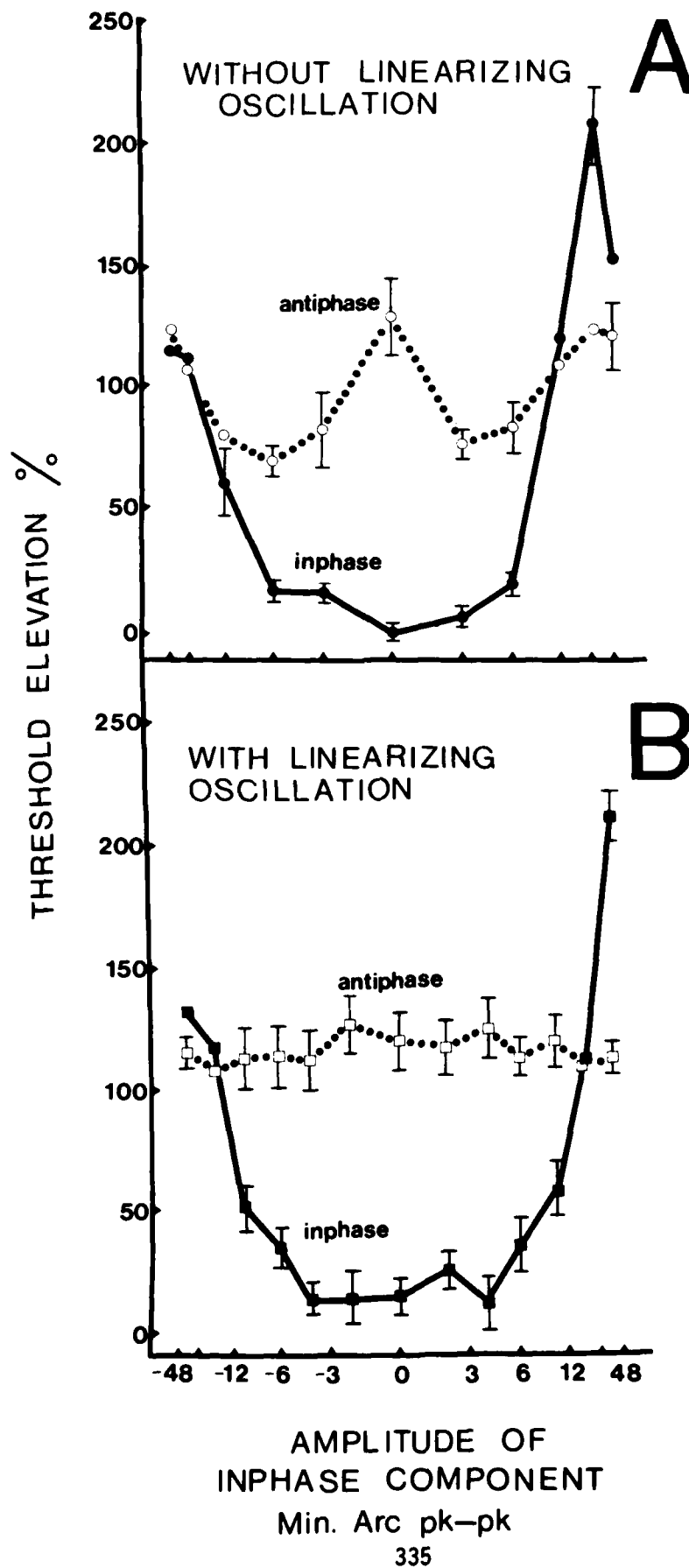


Figure 6.

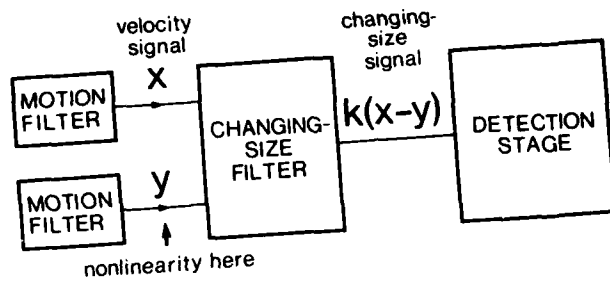


Figure 7.

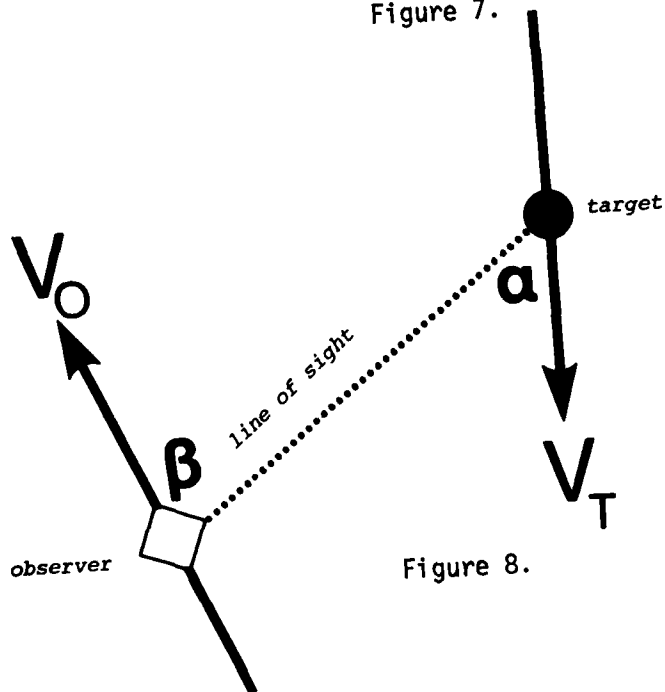


Figure 8.

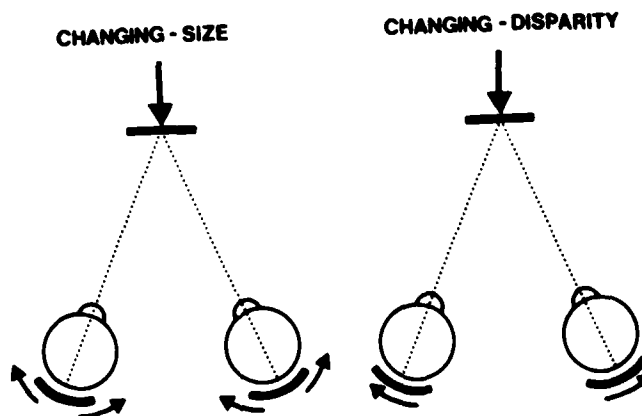


Figure 9.

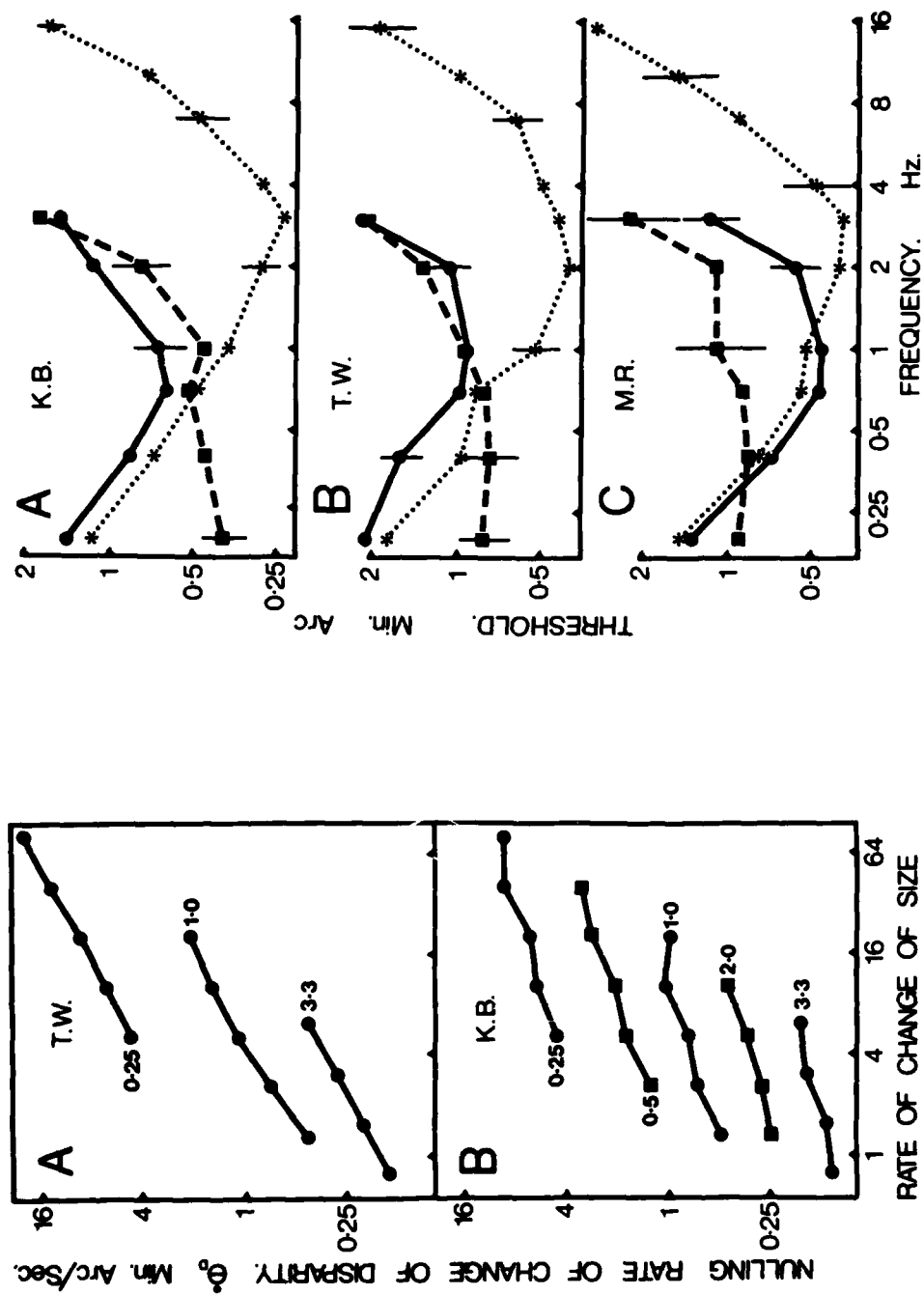


Figure 11.

Figure 10.

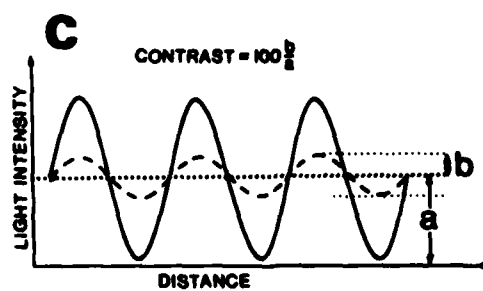
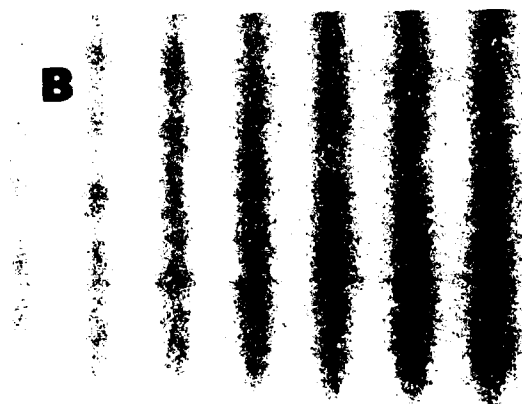
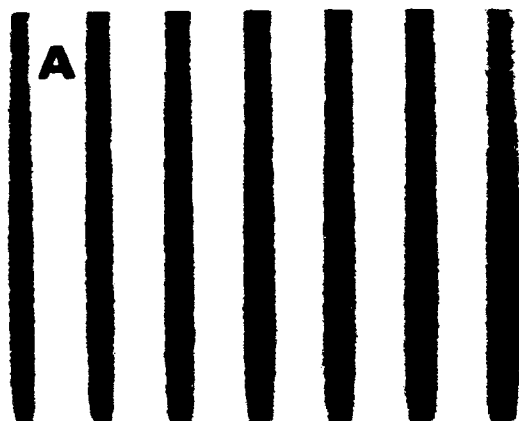


Figure 12.

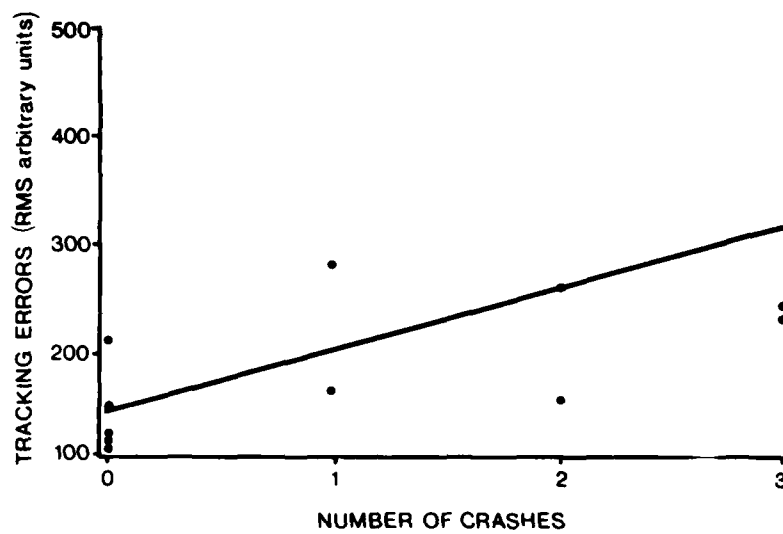


Figure 13.

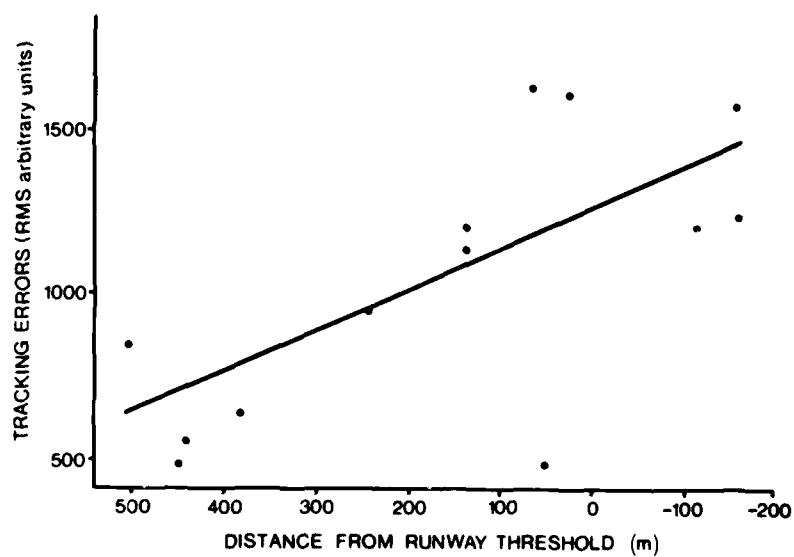


Figure 14.

Table 1

SIMULATOR PERFORMANCE AND VISUAL TESTS

Subject Groups	Correlations Between		r	p
2+3	crashes	& TA 1	0.43	0.02
2+3	crashes	& TP 1	0.49	0.008
2+3	crashes	& G	-.24	.13
2+3	correction	& TI 1	0.43	0.02
2+3	correction	& G	-.02	.46
3	crashes	& hours	-.35	.13
3	crashes	& age	-.43	.08
3	crashes	& IF	-.16	.30
1	TA2	& hours	-.56	.03
2	correction	& TI 1	0.7	0.006
2	crashes	& TA 1	0.68	0.008
2	crashes	& TP 1	0.53	0.04
2	crashes	& SA	0.68	0.008
2	crashes	& CPI	0.61	0.02
2	crashes	& CPA	0.51	0.05

FLYING PERFORMANCE AND VISUAL TESTS

2	TA 1	& FIF	0.56	0.03
2	SA	& FLY	0.50	0.05
2	CPI	& FLY	0.56	0.03
2	CPI	& FORM	0.58	0.02
2	CPA	& FLY	0.55	0.03
2	CPA	& FORM	0.59	0.02
2	CDI	& FLY	0.63	0.01
2	CDI	& LAND	0.57	0.03

FLYING GRADE AND FLYING GRADE

2	FLY	& FORM	0.64	0.01
2	FLY	& LAND	0.61	0.02
2	FORM	& LAND	0.82	0.0005

Correlation between visual test results and simulator performance.

All p values not shown were less than 0.05. The abbreviations are explained on page 19. "Hours" is total number of flying hours, and IF is total number of instrument flying hours.

REFERENCES

- Beverley, K.I. and Regan, D. (1973) Evidence for the existence of neural mechanisms selectively sensitive to the direction of movement in space. J. Physiol., 235, 17-29.
- Beverley, K.I. and Regan, D. (1975) The relation between discrimination and sensitivity in the perception of motion in depth. J. Physiol., 249, 387-398.
- Blakemore, C. and Campbell, F.W. (1969) The existence of neurons in the human visual system selectively sensitive to the orientation and size of retinal images. J. Physiol., 203, 237-260.
- Braddick, O., Campbell, F.W. and Atkinson, J. (1978) Channels in vision: Basic aspects. In Handbook of Sensory Physiology, Vol. 8 (ed. R. Held, H.W. Leibowitz and H.-L. Teuber). New York: Springer, pp. 3-38.
- Campbell, F.W. and Robson, J.G. (1968) Application of Fourier analysis to the visibility of gratings. J. Physiol., 197, 551-566.
- Cynader, M. and Regan, D. (1978) Neurons in cat parastriate cortex sensitive to the direction of motion in three-dimensional space. J. Physiol., 274, 549-569.
- Cynader, M. and Regan, D. (1981) Neurons in cat visual area 18 tuned to the direction of motion in depth: effect of positional disparity. Submitted.
- Gibson, J.J. (1950) The Perception of the Visual World. Baltimore: Houghton Mifflin.
- Ginsburg, A. (1978) Visual information processing based on spatial filters constrained by biological data. Thesis, Cambridge University. Published as AMRL-TR-78-129.
- Ginsburg, A. (1980) The measurement, interpretation and improvement of spatial vision for target acquisition. Abstracts AFOSR Review Flight & Tech. Training, A.F. Academy, Colorado.
- Grosslight, J.H., Fletcher, H.J., Masterton, R.B. and Hagen, R. (1978) Monocular vision and landing performance in general aviator pilots: cyclops revisited. Human Factors, 20, 127-133.
- Herivel, J. (1975) Joseph Fourier. Oxford: Clarendon Press, pp. 350.

- Hopkins, H.H. (1957) Optical Image Assessment using Frequency Response Techniques. Proc. Annual Summer School, Imperial College, London. London: Imperial College Press.
- Howard, I.P. and Templeton, W.B. (1966) Human Spatial Orientation. New York: Wiley.
- Kruk, R., Regan, D., Beverley, K.I. and Longridge, T. (1981) Correlations between visual test results and flying performance on the ASPT simulator. Aviat. Space Envir. Med., submitted.
- Lewis, C.E., Jr. and Kriers, G.E. (1969) Flight research programme: XIV. Landing performance in jet aircraft after the loss of binocular vision. Aerospace Med., 40, 957-963.
- Lewis, C.E., Jr., Blakeley, W.R., Swaroop, R., Masters, R.L. and McMurty, T.C. (1973) Landing performance by low-time private pilots after the sudden loss of binocular vision - Cyclops II. Aerospace Med., 44, 1241-1245.
- Petersik, J.T., Beverley, K.I. and Regan, D. (1981) Insensitivity of changing-size channels to spatial contrast. Vision Res., in press.
- Pfaffman, C. (1948) Aircraft landings without binocular cues: a study based upon observations made in flight. Am. J. Psychol., 61, 323-335.
- Poggio, G.F. and Talbot, W.H. (1981) Mechanisms of static and dynamic stereopsis. J. Physiol., in press.
- Pollen, D.A. and Feldon, S.E. (1979) Spatial periodicities of complex cells at one half octave intervals. Invest. Ophthalmol. Vis. Sci., 18, 329-434.
- Regan, D. (1981) The concept of visual channels: Its relevance to ophthalmology and to the performance of skilled tasks involving eye-limb coordination. In preparation.
- Regan, D. and Beverley, K.I. (1973a) The dissociation of sideways movements from movements in depth: psychophysics. Vision Res., 13, 2403-2415.
- Regan, D. and Beverley, K.I. (1973b) Electrophysiological evidence for the existence of neurones sensitive to direction of depth movement. Nature, 246, 504-506.
- Regan, D. and Beverley, K.I. (1978) Looming detectors in the human visual pathway. Vision Res., 18, 415-421.
- Regan, D. and Beverley, K.I. (1979a) Binocular and monocular stimuli for motion-in-depth: changing-disparity and changing-size inputs feed the same motion-in-depth stage. Vision Res., 19, 1331-1342.

- Regan, D. and Beverley, K.I. (1979b) Visually guided locomotion: psychophysical evidence for a neural mechanism sensitive to flow patterns. Science, 205, 311-313.
- Regan, D. and Beverley, K.I. (1980) Device for measuring the precision of eye-hand coordination while tracking changing size. Aviat. Space Environ. Med., 51, 688-693.
- Regan, D. and Beverley, K.I. (1980) Visual responses to changing size and to sideways motion for different directions of motion in depth: Linearization of visual responses. J. opt. Soc. Am., 70, 1289-1296.
- Regan, D., Beverley, K.I. and Cynader, M. (1979a) Stereoscopic subsystems for position in depth and for motion in depth. Proc. R. Soc., 204, 485-501.
- Regan, D., Beverley, K.I. and Cynader, M. (1979b) The visual perception of motion in depth. Sci. Am., 241, 136-151.
- Regan, D. and Cynader, M. (1979) Neurons in area 18 of cat visual cortex selectively sensitive to changing size: nonlinear interactions between the responses to two edges. Vision Res., 19, 699-711.
- Regan, D. and Cynader, M. (1981) Neurons in cat visual area 18 tuned to the direction of motion in depth: effect of stimulus speed. Submitted.
- Regan, D., Silver, R. and Murray, T.J. (1977) Visual acuity and contrast sensitivity in multiple sclerosis: hidden visual loss. Brain, 100, 563-579.
- Regan, D. and Spekreijse, H. (1970) Electrophysiological correlate of binocular depth perception in man. Nature, 255, 92-94.
- Regan, D., Whitlock, J.A., Murray, T.J. and Beverley, K.I. (1980) Orientation-specific losses of contrast sensitivity in multiple sclerosis. Invest. Ophthalmol. Vis. Sci., 19, 324-328.
- Richards, W. (1970) Stereopsis and stereoblindness. Exp. Brain Res., 10, 380-388.
- Richards, W. (1971) Anomalous stereoscopic depth perception. J. opt. Soc. Am., 61, 410-414.
- Richards, W. and Regan, D. (1973) A stereo field map with implications for disparity processing. Invest. Ophthalmol., 12, 904-909.
- Sekuler, R., Pantle, A. and Levinson, E. (1978) Physiological basis of motion perception. In Handbook of Sensory Physiology, Vol. 8. New York: Springer, pp. 67-96.

- Semple, C.A., Hennessy, R.T., Sanders, M.S., Cross, B.K. and McCauley, M.E.
(1980) Aircrew training device fidelity features (final report).
Canyon Research Group Inc. CRG-TR-3041 B, ASD/AFHRL Wright-Patterson AFB.
- Wetherill, G.B. and Levitt, H. (1965) Sequential estimates of points on a
psychometric function. Brit. J. Math. Stat. Psychol., 18, 1-10.
- Wilson, H. and Bergen, J.R. (1979) A four mechanism model for spatial vision.
Vision Res., 19, 19-32.
- Wright, W.D. (1946) Researches on Normal and Defective Colour Vision.
London: Kimpton.
- Young, T. (1802a) On the theory of light and colours. Phil. Trans. R. Soc.,
12-48.
- Young, T. (1802b) An account of some cases of the production of colours,
not hitherto described. Phil. Trans. R. Soc., 387-397.
- Zimmern, R.L., Campbell, F.W. and Wilkinson, I.M.S. (1979) Subtle distur-
bances of vision after optic neuritis elicited by studying contrast
sensitivity. J. Neurol. Neurosurg. Psychiat., 42, 407-412.

DEBATE

"Is the Eye Sufficient to See"

Moderator

Dr. Harry L. Snyder
Department of Industrial Engineering
Virginia Polytechnic Institute
Blacksburg, Virginia



Dr. Snyder received his Bachelor's degree from Brown University (1958), and his Master's (1960) and Ph.D. (1961) degrees from the Johns Hopkins University. He has approximately nine years of industrial experience in display design, evaluation, and human factors, as well as eleven years in teaching and research within a university setting. He served as Head of the Department of Industrial Engineering and Operations Research at Virginia Polytechnic Institute and State University for four years, and is currently a Professor in that department. He has written over 50 publications and reports dealing with human factors and displays, and is currently under contract to write two textbooks in this field. He has served as a consultant to numerous governmental, industrial, and university organizations, and has presented over 30 papers at technical meetings. He is a Fellow of the Optical Society of America, the Human Factors Society, and the Society of Engineering Psychologists, and is a member of the American Institute of Industrial Engineers, the Ergonomics Society, and the Society of Photo-Optical Instrumentation Engineers.

DEBATERS, PRO

Dr. Ralph N. Haber (Debate Organizer)
Department of Psychology
University of Illinois at Chicago Circle



Dr. Haber received his B.A. in Philosophy from the University of Michigan in 1953, an M.A. in Psychology from Wesleyan University in 1954 and Ph.D. from Stanford University in 1957. He taught at Yale University from 1958-1964 and was Chairman of the Psychology Dept. at the University of Rochester from 1967-1970 as well as Staff member at the Center for Visual Science from 1968-1979. He is presently Professor of Psychology at the University of Illinois at Chicago Circle.

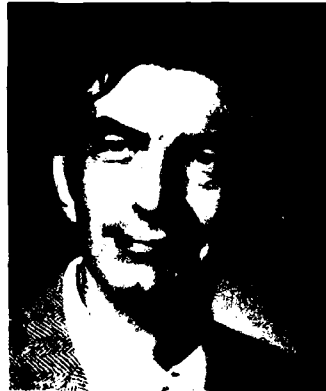
Dr. Kent Stevens
Artificial Intelligence Laboratory
Massachusetts Institute of Technology, Cambridge, MA



Kent A. Stevens obtained his Ph.D. from the Massachusetts Institute of Technology in Artificial Intelligence, and his M.S. and B.A. are from the University of California, Los Angeles in Computer Science and in Engineering. His 12 years of experience has involved computer graphics at Hughes Aircraft Company and the National Institutes of Health, followed with academic involvement in robotics at California Institute of Technology, and for the past six years, research into human vision at the M.I.T. Artificial Intelligence Laboratory. His interests are primarily in surface perception and the detection and encoding of texture and contour information.

DEBATERS, CON

Dr. Herschel W. Leibowitz
Evan Pugh Professor of Psychology
The Pennsylvania State University



Dr. Leibowitz received his Ph.D. degree in Psychology under the guidance of Professor C. H. Graham. He has published in the field of vision and holds numerous positions of high scientific stature. He is presently Evan Pugh Professor of Psychology at Pennsylvania State University.

Dr. Josh Y. Zeevi
Man-Vehicle Laboratories
Massachusetts Institute of Technology
Cambridge, MA



Yehoshua Y. Zeevi obtained his Ph.D., M.S., and B.S.E.E. from the University of California at Berkeley, the University of Rochester and the Technion-Israel Institute of Technology respectively. His professional experience has been in the academia, mostly with the Technion, Harvard University, Lawrence Berkeley Lab., and M.I.T. He has worked extensively with display systems studying signal detection, eye movement characteristics and visual information processing. He is presently a visiting Professor at the Man-Vehicle Lab., Department of Aeronautics and Astronautics, M.I.T., working on visual aspects of flight simulators.

SESSION VI

Chairman

Colonel Robert F. Lopina
Deputy for Engineering
Headquarters, Aeronautical Systems Division
Wright-Patterson Air Force Base, Ohio



Colonel Lopina was born on May 13, 1936 in Jamestown, New York. In 1957, he received a Bachelor of Science degree in Mechanical Engineering from Purdue University and was commissioned and entered the Air Force as a distinguished graduate from ROTC. Upon completion of the Communications Officer Course at Keesler AFB, Colonel Lopina was assigned to the Los Angeles Air Defense Sector at Norton AFB, California until 1963, followed by a one year tour as communications and radar maintenance officer at the 931st AC&W Squadron in Thule, Greenland. He attended the Massachusetts Institute of Technology from 1964 to 1967 and received the Master of Science, Mechanical Engineer, and Doctor of Philosophy degrees. He is also a graduate of the Air Force Squadron Officer School, the Armed Forces Staff College and the Air War College.

Colonel Robert F. Lopina is currently the Deputy for Engineering, Aeronautical Systems Division, Wright-Patterson AFB, Ohio. Previously, he was the Director of the Avionics Laboratory, Air Force Wright Aeronautical Laboratories, Wright-Patterson AFB. As Deputy for Engineering, he is responsible for providing system engineering management and technical direction to over 400 weapon systems and equipment developments and acquisitions assigned to the Aeronautical Systems Division and other government organizations. He supervises approximately 1600 military and civilian personnel in this capacity.

Colonel Lopina has had several articles published in technical journals in the fields of heat transfer and aerodynamics and co-authored a text on Introduction to Aeronautics. He is a member of the Air Force Association, American Institute of Aeronautics and Astronautics, American Society of Mechanical Engineering and the Society of Sigma Xi. His decorations include the Vietnam Service Medal and the Meritorious Service Medal with one Oak Leaf Cluster.

FLIGHT SIMULATOR VISUAL DEVELOPMENT
AND INSTRUCTIONAL FEATURES
FOR TERRAIN FLIGHT SIMULATION



George H. Buckland

George H. Buckland is a behavioral scientist at the Operations Training Division of the Air Force Human Resources Laboratory located at Williams AFB, Arizona. His current primary research efforts include the conduct and management of research in the area of visual displays systems requirements for USAF flight simulators. He received his PhD in Psychology from the University of Rochester in 1976, and he is currently serving as a Major in the U.S. Air Force.



Bernell J. Edwards

Bernell J. Edwards is a task scientist in instructional systems applications at the Air Force Human Resources Laboratory, Operations Training Division. His background includes 17 years experience in the design development, and management of instructional media programs in academic and military settings. He is currently investigating the application of instructional design principles within computerized visual environments for pilot training. Dr. Edwards received his PhD in Educational Technology from Arizona State University in 1974.



Steve Stephens

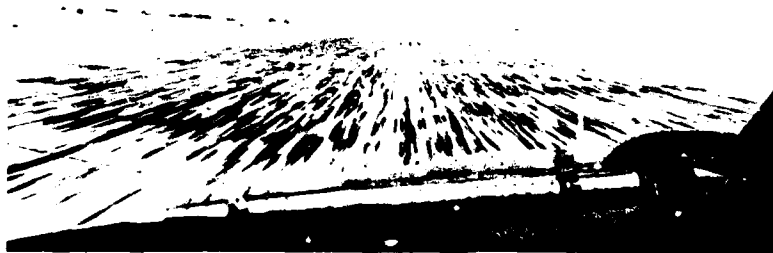
Clarence W. (Steve) Stephens is a computer specialist at the Air Force Human Resources Laboratory, Operations Training Division. As the primary data base modeler for the Advanced Simulator for Pilot Training, he has developed a number of unique computerized visual environments for both A-10 and F-16 simulations. Current projects include development of advanced data bases for low level flight and for enemy high threat environments. He is also modeling a complete data base library for Russian military weaponry and hardware. Mr. Stephens is now completing a degree in Computer Systems Engineering at Arizona State University.

FLIGHT SIMULATOR VISUAL AND
INSTRUCTIONAL FEATURES
FOR TERRAIN FLIGHT SIMULATION

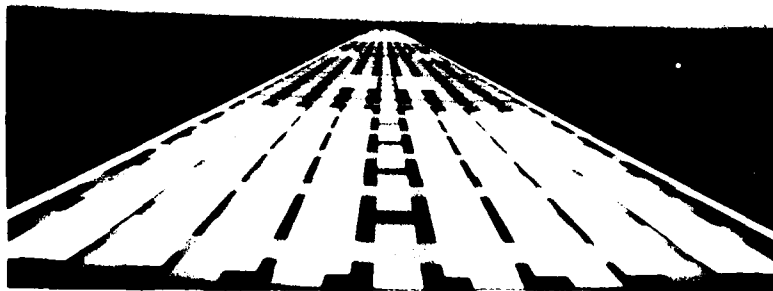
George H. Buckland, Bernell J. Edwards, and Clarence W. Stephens
Air Force Human Resources Laboratory
Operations Training Division
Williams AFB, Arizona

Lack of adequate visual scene detail is a serious limitation in the use of computer generated imagery for training low altitude terrain flight. Terrain flight profiles involve both low level contour flight which closely follows the profile of the ground and nap-of-the-earth (NOE) flight which includes maneuvering between and around vertical obstructions. Both ground textural pattern cues and vertical object cues appear to be important for pilots to judge aircraft height above the ground. AFHRL/OT has conducted research studies on both of these types of visual cues and is currently developing an optimal ASPT (Advanced Simulator for Pilot Training) visual environment for instructing terrain flight maneuvers.

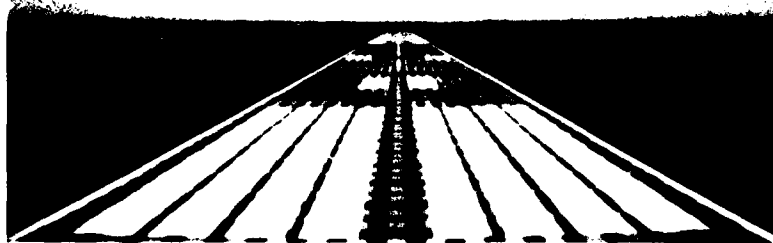
The initial research study of visual information cues for pilot depth perception investigated T-37 pilot landing performance in response to four different checkerboard-like texture patterns superimposed upon the simulated runway touchdown zone area. The check sizes used were 4, 8, 16, or 25 feet on a side (Figure 1). Two additional daytime runways also were used consisting of a simulated Air Force runway with standard markings and a completely bare runway with no markings except for the dashed centerline. A night runway scene was also used bringing the total number of runways tested to seven. In this study the average vertical velocities at touchdown ranged from 195 feet/minute for the night scene to 147 feet/minute for the four-foot texture pattern. Although the simulated aircraft vertical velocities at touchdown were much higher than those recorded during actual aircraft landing (32 ft/minute), the textured runway patterns did significantly reduce simulated aircraft vertical velocities at touchdown. Interestingly, this reduction in touchdown vertical velocity occurred in a near linear progression as a function of increasing texture detail (Table 1).



Williams AFB
Runway at
Touchdown

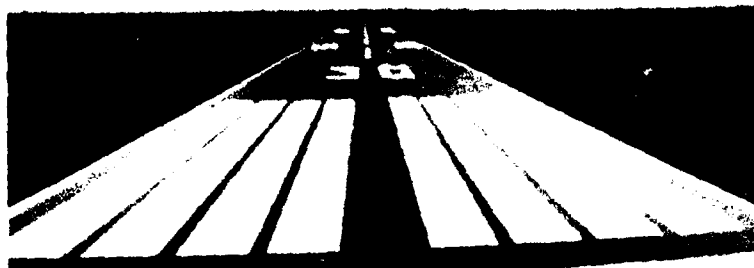


Four-Foot
Texture Pattern
Runway



Eight-Foot
Texture Pattern
Runway

Figure 1



Willy Runway



"Bare Bones"
Runway



Night Runway
with Touchdown
Zone Landing
Lights

Figure 1 (continued)

Table 1

T-37 AIRCRAFT VERTICAL VELOCITY AT TOUCHDOWN

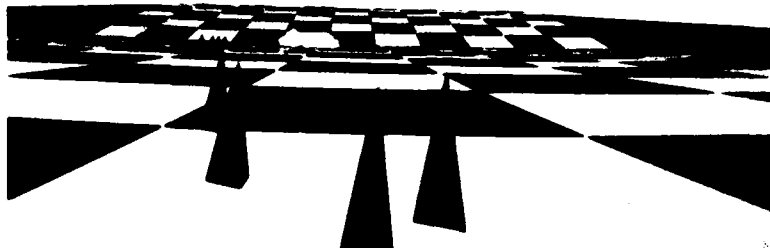
<u>Simulated Visual Scene</u>	<u>Without Overrun</u>	<u>With Overrun</u>	(Ft/Min) <u>Average</u>
Night	201	190	195
Bare Bones	195	171	183
Willy	172	179	175
25 Ft Texture	168	168	168
16 Ft Texture	158	173	165
8 Ft Texture	151	170	161
4 Ft Texture	136	158	147

Edwards Flight Test Center Cine-Theodolite
Tracking of T-37 Landings

32 Ft/Min

In a subsequent study AFHRL/OT investigated the effects of three types of visual cues, texture patterns (checkerboards, 220, 440 or 880 feet on a side), vertical objects (present or absent) and aircraft shadow (present or absent), upon pilot performance during NOE flight in a simulated A-10 aircraft (Figure 2). In this study pilots were instructed to fly at 50 feet above the ground on a ten mile course which consisted of eight valleys which were separated by low rolling hills that were either 100 or 300 feet high. The pilots were scored on their ability to maintain aircraft altitude at 50 feet plus or minus 30 feet in the flat valleys. Actual aircraft values were also collected at the crest of each hill. The pilots flew the course at 300 knots indicated airspeed plus or minus 15 knots.

In general the pilots reported that all three types of visual cues were useful, however, the vertical object cues and texture patterns were of greater help than the aircraft shadow. Some pilots reported that the aircraft shadow was particularly useful in signalling impending contact with the ground. The vertical object cues, especially the tree shaped cones of known height, were subjectively very useful in gauging height above ground. The texture patterns were also reported as desirable, but to a lesser extent than vertical object cues. Pilots reported a definite preference for the smallest texture pattern (220 foot square size) over the two larger size patterns. They especially disliked flying over the largest texture pattern without vertical object cues. Pilots would have also preferred more irregular "natural" patterns rather than the highly regular checkerboard features. Both the texture patterns and the vertical object cues produced statistically significant differences in pilot performance. However, only the texture pattern cues produced a significant effect on the time within tolerance scoring for altitude in the valleys, and the average minimum altitude values in the valleys (Tables 2 & 3). The vertical object cues did have a significant effect on the average aircraft altitude at the top of the hills (Table 4). Both the vertical object cues and the texture patterns significantly influenced the average minimum altitude values that occurred over each hill (Table 5).



220-Feet
Squares with
Vertical
Objects



440-Feet
Squares with
Vertical
Objects



880-Feet
Squares with
Vertical
Objects



220-Feet
Squares without
Vertical
Objects



440-Feet
Squares without
Vertical
Objects



880-Feet
Squares without
Vertical
Objects

Figure 2 (continued)
NOE I Visual Environment

Table 2

% Time Within Tolerance Scoring
for
Aircraft Altitude in Valleys (50 \pm 30 Ft.)

* Texture Patterns (Ft)			Vertical Objects		Aircraft Shadow	
220	440	880	With	Without	With	Without
77.4	72.6	64.7	72.2	70.9	71.1	72.0

* P .001

Table 3

Avg. Min. Altitude Values in Valleys

* Texture Patterns (Ft)			Vertical Objects		Aircraft Shadow	
220	440	880	With	Without	With	Without
43.0	45.5	47.0	44.8	45.5	45.7	44.6

* P .003

Table 4

Avg. Aircraft Altitude (Ft) at Hill Tops

* Texture Patterns (Ft)			Vertical * Objects		Aircraft Shadow	
220	440	880	With	Without	With	Without
67.8	67.6	69.2	63.6	72.7	69.3	67.1

* P .001

Table 5

Avg. Aircraft Min. Altitude (Ft) Over Hills

Texture * Patterns (Ft)			Vertical * Objects		Aircraft Shadow	
220	440	880	With	Without	With	Without
40.6	45.9	47.9	41.4	48.2	45.3	44.3

* P .001

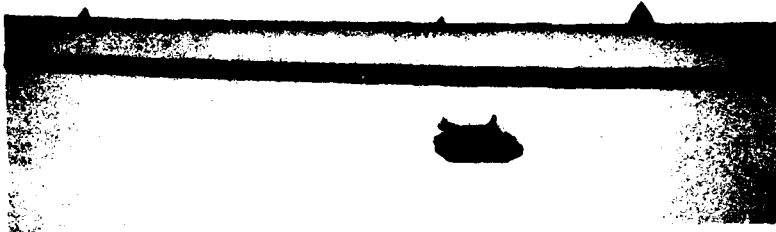
The presence or absence of the aircraft shadow did not produce any significant effects. The amount of time (cumulative total) in a "crashed" condition (in contact with ground) was low, with some pilots crashing into simulated terrain more frequently than others. No significant differences were found for this performance parameter due to visual cue variables. Overall, in this study, the terrain textural cues appeared to have a stronger effect on pilot performance than did the vertical object cues.

Since the development of the original NOE I environment researchers at AFHRL/OT have found that cone (actually tetrahedron) shaped "trees" appear to provide improved visual cueing when turned upside down so that the broader base is more directly visible to the pilots. This technique provides a very edge-efficient (6 edges total) visual cue which has effectively reduced terrain crash frequency during low level flight in our hostile threat simulation environments (Figure 3).

Our most recent terrain flight environment, named NOE II, uses both inverted cones and random ground texture patterns. Pilots subjectively report that this is the best ASPT visual environment yet for terrain flight. NOE II is modeled to approach as nearly as CIG capacity permits, the irregular natural features likely to be seen in actual terrain flight (Figure 4). The available edges are concentrated within and adjacent to the intended flight path in order to maximize available cues to the pilot. The flight path is bordered by hills which slope away from the path at realistic rise angles.

The NOE II environment will be used to study the combination of instructional techniques with display content variations to produce optimal training effects for terrain flight. With regard to vertical objects, inverted cones of several heights will be represented with the shape of the cone proportioned to the expected shape of a similar tree. Three tree heights (25, 40, and 55 feet) will be used with the 25 foot tree rather short and squat, the 55 footer tall and thin, and the 40 foot tree of medium proportion so that height can be easily distinguished using proportion as a cue. The placement and density of vertical objects will also be investigated with regard to effective altitude cueing and navigational check points along the route.

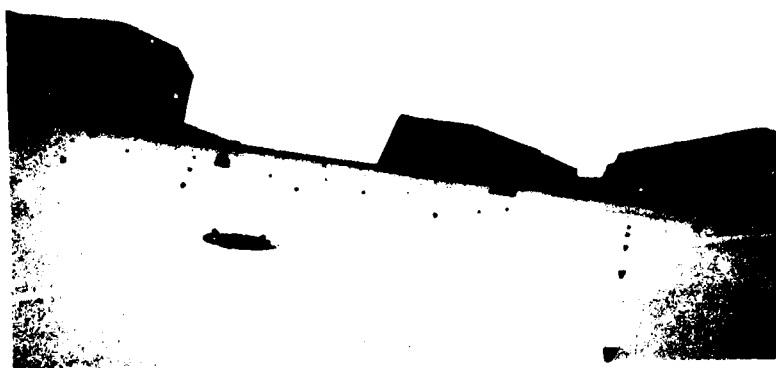
With regard to instructional variables, in one study various combinations visual and auditory cues will be provided to the pilot to test their effects on the acquisition of terrain following skills. These ancillary cues will be faded out as desired student pilot responses are established. In another study, variations of feedback associated with terrain strikes will be investigated to determine the content and timing of feedback as a means of reducing terrain impact and increasing low level skills. "Training down" sequences will also be tested in which pilots inexperienced in low altitude flight will be presented with successively more difficult altitude ceilings as they progress toward NOE flight proficiency. Other instructional variables are also under consideration, including the use of slow flight during early trials, concomitant



ZSU-23-4
Firing



Inverted Cone
Pattern



Anti-Aircraft
Artillery Site

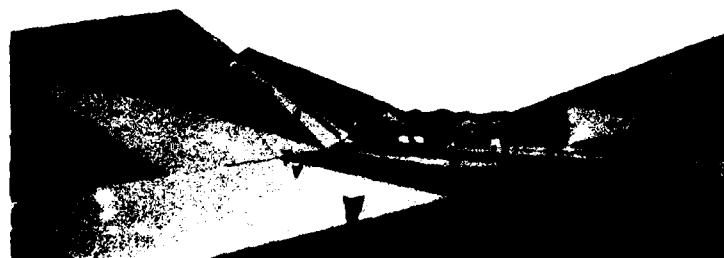
Figure 3
Hostile Environment with Inverted Cones

secondary information loading to vary task difficulty, and pretraining of environmental features and flight techniques in order to establish perceptual set/expectancies.

Several dependent measures of pilot performance will be used for the NOE II studies, including relevant aircraft state parameters sampled during selected portions of flight, time within tolerance scoring for altitude and airspeed, and terrain strike frequency, duration, and aircraft position. Initial data collections for NOE II studies are planned for the Spring and Summer of 1981. We expect to report preliminary results by the Fall of 1981.



NOE II From
About 100 feet
AGL - 100%
"Trees"

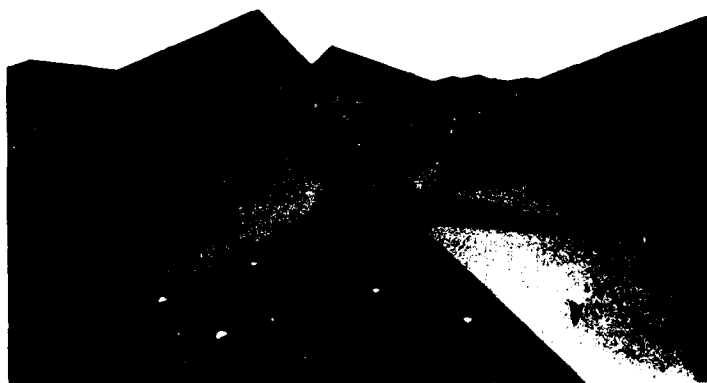


60% "Trees"

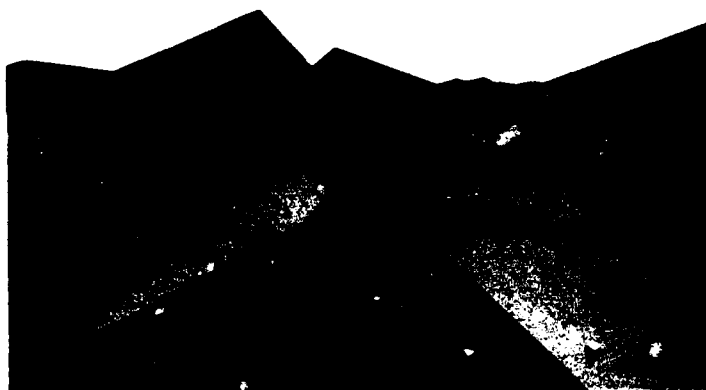


No "Trees" in
Ground Path

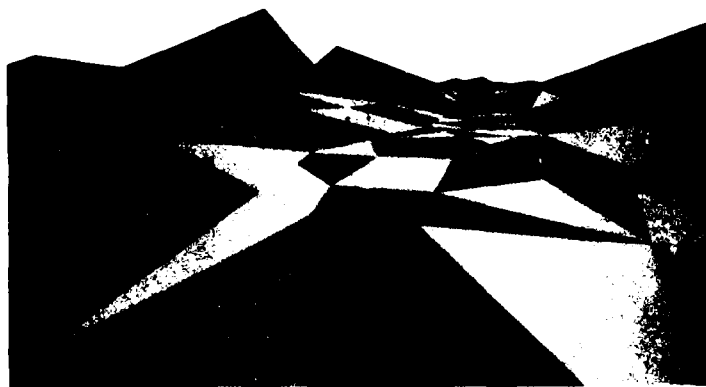
Figure 4
NOE II Environment
361



NOE II From
About
300 Feet AGL
100% "Trees"



60% "Trees"



No "Trees" in
Ground Path

Figure 4 (continued)
NOE II Environment

A Model-Based Procedure for Determining Visual Cue Requirements

GREG L. ZACHARIAS obtained his B.S., M.S., and Ph.D degrees from the Massachusetts Institute of Technology in 1967, 1974, and 1977, all from the Aeronautics and Astronautics Department.

Dr. Zacharias' professional background includes engineering systems analysis of navigation and control systems, and experimental/analytical studies of human perception and performance. At the Measurement Systems Laboratory of M.I.T., and at Astronautical Research, Inc., he analyzed the performance of radionavigation systems. While in the Air Force and attached to NASA-JSC, he was responsible for the preliminary design definition of the reentry autopilot for the Space Shuttle, and continued the design development after leaving the Air Force and joining the C.S. Draper Laboratory.

Since 1977, Dr. Zacharias has been with Bolt Beranek and Newman Inc., involved in applying modern control and estimation theory to the problems of measuring and modelling human control and decision-making. He has been engaged in studies of human motion perception, and its impact on flight control performance, and is currently engaged in modelling multi-operator performance and workload, in both flight crew and anti-aircraft artillery tasks.



William H. Levison

WILLIAM H. LEVISON was born in Cincinnati, Ohio, on March 21, 1936. He received the S.B., S.M., and Sc.D. degrees, all in electrical engineering, from the Massachusetts Institute of Technology, Cambridge, in 1958, 1960, and 1964, respectively.

From 1958 to 1964 he was with the M.I.T. Research Laboratory of Electronics, Cambridge, Massachusetts, where he conducted research concerned with the analysis of the cardiovascular system. He has been a Senior Scientist at Bolt Beranek and Newman Inc., Cambridge, Massachusetts, since 1964, and is presently engaged in studies of manual control experiments, and he has participated in the development of models for human control and information processing. His major interests are in further development of human operator models and in application of these models to areas such as aircraft display and control requirements, simulation requirements, and human performance in situations of environmental stress.

Dr. Levison is a member of Sigma Xi, Tau Beta Pi, Eta Kappa Nu, Institute for Electrical and Electronics Engineers, and the American Institute of Aeronautics and Astronautics.

A Model-Based Procedure for Determining Visual Cue Requirements

by

Greg L. Zacharias and William H. Levison

ABSTRACT

This paper outlines a model-based procedure for determining visual cue requirements for flight simulators. Issues addressed by the procedure include: (1) determination of task-relevant cues available from the visual scene; (2) the quality of the information available from such cues; (3) the cue set that the pilot should use in performing a specific mission; and (4) the degree of fidelity with which the various cues must be simulated. The optimal-control model (OCM) for pilot/vehicle systems provides the framework for the proposed methodology. As this model incorporates both the state-estimation and the control-response characteristics of the pilot, the procedure may be applied to monitoring as well as to continuous control tasks.

Introduction

Recent advances in digital computing technology have increased the capabilities of aircraft simulators for providing realistic presentations of extra-cockpit visual scenes. But with this increase in capability has come an increase in cost and complexity, and thus, as in the past, designers of simulators are still confronted with difficult choices between simulation fidelity and the need for cost-effective methods of simulation.

The specification of fidelity requirements for cueing systems is very difficult, however, for several reasons. The requirements are governed by the purpose of the simulation: training simulators have different needs than those of research simulators. They are also problem dependent (e.g., the need for motion cues for aircraft control in a gusty environment will depend on the gust response of the aircraft). Finally, the specification involves complex psychophysical as well as engineering factors. Not only is there a need to understand and account for the perceptual capabilities and limitations of a human pilot, but also one must account for the fact that the adaptive pilot may be able to compensate for simulator shortcomings, while maintaining system performance at the expense of workload.

These problems point to the need for understanding how the pilot utilizes the cues available to him, for effective execution of the given simulated flight task. Recognizing this need, and anticipating the eventual widespread use of sophisticated visual scene simulations, we have chosen to demonstrate how this understanding might be achieved through the use of human operator modelling technology, which focusses on visual cueing issues. This paper thus outlines an analytic and experimental effort aimed at developing and validating a quantitative model of the pilot's use of extra-cockpit visual cues.

Our analytic effort is centered on the Optimal Control Model (OCM) of the pilot, which provides the overall framework for relating cue integration to task performance. Our complementary experimental effort is chosen to satisfy two objectives: a) quantifying the independent parameters of the OCM that define the pilot's ability to utilize extra-cockpit visual cues; and b) validating the ability of the OCM in predicting pilot/vehicle performance in tasks involving multiple real-world visual cues. This report summarizes our analytic modelling effort, and outlines an experimental program for model development and validation.

Optimal Control Model

The OCM is a model of the man-machine system, based on the assumption that the well-trained, highly-motivated operator will adopt an optimal response strategy, subject to task requirements and subject to the operator's inherent information-processing limitations. Inputs to this model include system dynamics, task requirements (in terms of a quadratic "cost functional" to be minimized), and human-controller limitations. Model outputs include performance metrics such as means and variances for task variables, operator response strategy, and operator "noise" characteristics.

The reader is referred to the literature (e.g., Kleinman et al, 1971; Levison et al, 1969; Baron et al, 1970) for a full description of the mathematical development and validation of the model. Here, those aspects of the model that are most relevant to display analysis, as shown in Figure 1, are discussed.

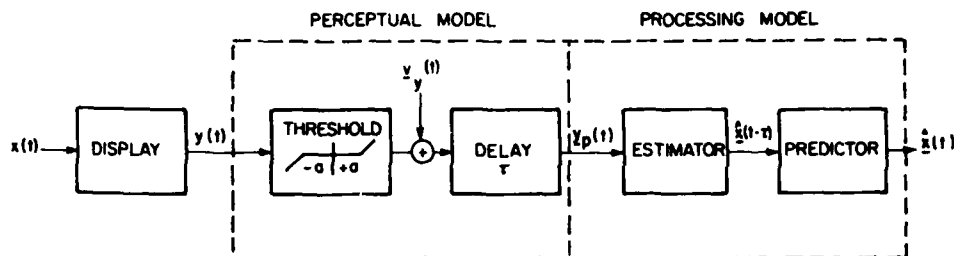


Figure 1. Information Processing Model

Display Variables

Let the "state" of the controlled element be represented by a set of state variables $x_i(t)$, $i=1, \dots, n$. In the OCM, it is assumed that the operator is "displayed" outputs y_1, \dots, y_m where each output is a linear combination of the state variables:

$$y_i(t) = \sum_{j=1}^n c_{ij}(t) x_j(t) \quad , \quad i=1, \dots, m \quad (1)$$

or, in vector-matrix notation,

$$\underline{y}(t) = C(t)\underline{x}(t). \quad (2)$$

If a quantity is displayed explicitly to the operator (say, by an indicator displacement), it is assumed that the human also perceives the rate of change of the quantity. Typically, it is assumed that higher derivative information is not available.

Equation 2 is very general with respect to representing display variables. Basic status information can be included, for example, by letting output variables be selected state variables. Display quickening is easily modelled by letting an output be a linear combination of error and error-rate state variables (Hess and Wheat, 1976). Flight director signals can also be expressed as linear combinations of appropriately defined state variables (Baron and Levison, 1973). Note, too, that the coefficients c_{ij} can be functions of time so that programmed scale changes or variable changes may be included in the problem formulation.

Treatment of these types of explicit "instrument" displays is fairly direct, but additional modelling work is required to define the informational

base provided by an extra-cockpit visual scene. We will discuss this shortly after reviewing the additional information-processing components of the OCM.

Perceptual Model

Limitations on the pilot's ability to process information "displayed" to him are accounted for in an "equivalent" perceptual model. This model translates the displayed variables y into delayed, "noisy" perceived variables y_p via the relation

$$y_p(t) = y(t-\tau) + v_y(t-\tau) \quad (3)$$

where τ is an "equivalent" perceptual delay and v_y is an "equivalent" observation noise vector.*

The various internal time delays associated with visual, vestibular, central processing and neuro-motor pathways are combined and conveniently represented by this lumped equivalent perceptual time delay τ . Typical values for this delay are 0.2 ± 0.05 sec. (Kleinman et al 1971).

The zero-mean, white, Gaussian observation noise vector v_y is included to account for the pilot's inherent randomness, due to random perturbations in human response characteristics, errors in observing displayed variables, and attention-sharing effects which limit the pilot's ability to accurately process all the cues simultaneously available to him. In combination with the OCM's motor noise model (see Kleinman et al, 1971), the observation noise model provides a convenient and accurate means of modelling pilot remnant and thus accounting for random control actions.

For manual control situations in which the displayed signal is large enough so that visual resolution ("threshold") limitations are negligible, the autocovariance of each observation noise component appears to vary proportionally with mean-squared signal level. In this situation, the autocovariance of the noise associated with the i th display component may be represented as

$$V_i = \pi P_i \sigma_i^2 \quad (4)$$

where σ_i^2 is the variance of the i th display variable, and P_i is the "noise/signal ratio" for the i th display variable, which has units of normalized power per rad/sec. Numerical values for P_i of 0.01 (i.e., -20 dB) have been found to be typical of single-variable control situations (Levison et al, 1969; Kleinman et al, 1971).

The perceptual model defined by (3) and (4) applies to "ideal" display conditions, in which the signal levels are large with respect to both system-imposed and pilot-associated thresholds. To account for threshold effects we let the autocovariance for each observation noise process be

* The use of the word equivalent in this context is to emphasize that the parameters may be lumped representations of a variety of limitations that cannot be "identified" separately by existing measurement techniques.

$$V_1 = \pi P_1 \left[\left(\frac{\sigma_1^2}{K_1^2(\sigma_1, a_1)} \right) + \sigma_{o1}^2 \right] \quad (5)$$

where the subscript i refers to the i th display variable. The quantity $K(\sigma_1, a_1)$ is the describing function gain associated with a threshold device

$$K(\sigma, a) = \frac{2}{\sqrt{\pi}} \int_{-\infty}^{-\frac{a}{\sigma\sqrt{2}}} e^{-x^2} dx \quad (6)$$

where " a " is the threshold and σ is the standard deviation of the "input" to the threshold device.* The net result of this type of describing function model is to increase the observation noise covariance as the display signal variance becomes smaller relative to the threshold. The quantity σ_{o1}^2 is a "residual" noise term which is introduced to account for performance degradation that arises when an explicit zero-error reference is lacking (Levison, 1971).

The sources of these threshold effects depend on the particular task being modelled. They may be associated with the system display implementation, for example, due to resolution limitations on a display screen. Or, they may be associated with the pilot's sensory limitations, such as one might identify with visual acuity thresholds.

One additional factor which tends to increase the observation noise (present on any given display variable) is the pilot's attention-sharing limitations. Because the numerical value associated with the pilot's noise/signal ratio (P_o) has been found to be relatively invariant with respect to system dynamics and display characteristics in single display situations, we associate this parameter with limitations in the pilot's overall information-processing capability. This forms the basis for a model for pilot attention-sharing where the amount of attention paid to a particular display is reflected in the noise/signal ratio associated with information obtained from that display (Levison et al, 1971; Baron and Levison, 1973). Specifically, the effects of attention-sharing are represented as

$$P_i = P_o / f_i \quad (7)$$

where P_i is the noise/signal ratio associated with the i th display. When attention is shared among two or more displays, f_i is the fraction of attention allocated to the i th display, and P_o is the noise/signal ratio associated with full attention to the task.

* For non-zero-mean signals this expression must be modified (see Baron and Levison, 1973).

Processing Model

The processing model shown in Figure 1 consists of a tandem estimator/predictor. The estimator acts on the perceived display vector $y_p(t)$ to generate a delayed estimate of system state $\hat{x}(t-\tau)$, where τ is the delay introduced by the perceptual portion of the model; the predictor then compensates for the delay to provide an up-to-date estimate $\hat{x}(t)$. The general expressions for these model elements are determined by system dynamics and task objective according to well-defined mathematical rules that are derived in Kleinman et al, 1971. The result is a minimum variance estimate of the system state, \hat{x} , which can then be used for either closed loop control actions (e.g., fight control), or open-loop decision-making (e.g., failure detection).

Visual Scene Analysis Methodology

With this brief overview of the OCM, we can now consider how extra-cockpit visual cueing can be treated within the model context.

Relevant Visual Cues

In contrast to the relatively well-defined set of visual cues provided by within-cockpit instrumentation, the extra-cockpit visual scene can provide the pilot with an exceptionally rich stimulus environment, even for a relatively simple scene. Attempting to describe and quantify this stimulus environment has been the object of many studies. For example, Brown (1973) discussed five "dimensions" of the visual world: field-of-view, range of luminance, color, spectral resolution, and visual motion. Staples (1970) listed fifteen factors that are present in the visual scene which can be of importance to the pilot, and noted that this list was incomplete. Gibson (1950,1955) concentrated on geometric and textural cues, but also noted the potential utility of the "traditional" cues for depth perception (i.e., lens accommodation, binocular convergence, and retinal disparity).

The literature on scene attributes is extensive, and some narrowing of focus is called for, if a successful attempt is to be made in the area of modelling this type of cue processing.

Matheny et al (1971) present a taxonomy of cues that is helpful in structuring and limiting the problem. They define relevant cues as cues which are directly useful for controlling the aircraft or for making decisions. The non-relevant cues are those that are not essential to the successful operation of the aircraft, but which may add realism or face-validity to the task.

It seems clear that in extending the optimal control model to account for perception of the visual scene, our first concern should be the relevant cues. Thus, for example, color can be neglected, since adequate foreground-background separation can be provided by a sufficiently large contrast differential. Similarly, range of luminance might be neglected if adequate surface definition is provided by the display hardware. Other "non-geometric" visual cue factors can be similarly neglected, at least for an initial analysis, so that modeling can concentrate on the basic geometric characteristics of the visual scene. These were identified by Gibson (1950) in his analysis of visual scene processing: Table 1 lists these "geometric" cues and the corresponding type of information they provide to a pilot concerning the state of his vehicle.

Table 1 Geometric Visual Cues

Cue	Information
Field Orientation	Attitude, Attitude Rate
Linear Perspective	Position
Motion Parallax	Linear Velocity
Apparent Size/Range (Looming)	Position
Occultation	Position

Field orientation provides the pilot with attitude cues: assuming that the visual world is inertially fixed, then any rotation of the scene elements, measured with respect to the vehicle (or pilot) frame of reference, must be due to self-rotation of the vehicle (and pilot). Linear perspective changes with the location of the vehicle; thus, these cues provide the pilot with positional information. Motion parallax is effectively a rate of change of linear perspective, and thus provides the pilot with cues for inferring linear self-velocity. The apparent size of an object (combined with the pilot's perceptual set which ensures size constancy) provides a "looming" or range cue which can be used to infer relative distances, and hence position. Finally, occultation of one object by another provides an angular "line-of-position" cue similar to one component of a navigation "fix", and, hence, also provides a means of inferring position.

The cues listed in Table 1 are essentially monocular cues, and do not depend on binocular processing capabilities. In addition, these cues can be provided by a fairly abstract display: a perspective line drawing of the scene, with "hidden" lines not drawn. Since the basic element of such an idealized display is a line segment (associated with an edge of solid object), it seems appropriate to consider in more detail just how such line elements can provide cues as to one's own attitude and position.

Recent OCM-Based Cueing Analyses

To see how these cues can be incorporated within the structure provided by the OCM, it is appropriate to briefly discuss two earlier approaches.

Wewerinke (1978) concentrated on the pilot's use of perspective geometry and motion parallax cues during a VFR landing-approach. By use of elementary perspective geometry, it was shown that rotational and translational vehicle movements can be related to changes in orientation and location of line segments comprising the extra-cockpit visual scene. For example, the perturbations in the perceived orientation of the runway center line, with respect to the aircraft's longitudinal plane of symmetry, can be expressed as:

$$w = C_h h + C_y y + \phi$$

where w is the center line orientation, C_h and C_y are trajectory dependent

constants and h, y , and ϕ are small perturbations in altitude, localizer error, and roll attitude, respectively. Similar expressions can be derived for orientational changes in other line elements comprising the visual scene, with corresponding expressions for their rates of change.

To model pilot processing of these cues, Wewerinke (1978) used the OCM and its "display vector" capability: each w_i associated with a scene line element was linearly related to the vehicle state vector \underline{x} so that

$$w_i = \underline{C}_i^T \underline{x} \quad (8)$$

where \underline{C}_i is the vector "display gain" associated with the i th line element.

If the pilot's display vector \underline{y} is composed of N extra-cockpit geometric cues, then

$$\underline{y} = \underline{C} \underline{x} \quad (9a)$$

where

$$\underline{C} = [\underline{C}_1, \underline{C}_2, \dots, \underline{C}_N]^T \quad (9b)$$

so that the display matrix \underline{C} , introduced earlier in (2), is completely defined for the purposes of model analysis.

To test this hypothesis of visual cue processing, Wewerinke conducted a model analysis of experimental data obtained from a simulated VFR approach and found that the data could be closely matched by assuming: a) approximately "nominal" pilot-related model parameters; b) optimal attention allocation between display vector elements; and c) individual display thresholds which were consistent with visual perception thresholds found in related psychophysical experiments. In short, this initial modeling approach toward visual cue processing was well-supported by the experimental data.

A simpler approach was utilized by Levison and Baron (1976) in their study of cockpit display designs for a terminal configured vehicle. One of the displays analyzed included a perspective drawing of the runway. The OCM-based model analysis incorporated this information by assuming that runway centerline orientation was an element of the pilot's display vector, thus providing a direct means for amalgamating perspective information with more conventional "instrument" information in a logically consistent manner.

These studies demonstrate that the OCM can be used to analyze extra-cockpit cueing, if two basic components of the model can be specified: the \underline{C} matrix of the "display" equation (2), which relates the vehicle state to the cue environment; and the observation noise vector \underline{v} of the "perceptual" equation (3), which specifies the fidelity of the extra-cockpit cues. In the following sections we outline a general approach for this specification.

Specification of Display Matrix

General Approach

Our basic objective is to specify how linear perturbations in vehicle state \underline{x} give rise to corresponding perturbations in the extra-cockpit cue set \underline{y} . To do this, we first define an appropriate "total" state vector \underline{X} , where

$$\underline{X} \equiv \begin{bmatrix} \underline{r} \\ \underline{\alpha} \end{bmatrix} \quad (10a)$$

where \underline{r} and $\underline{\alpha}$ specify the vehicle's position and attitude, in some specified earth-fixed coordinate system.* For example, if we choose the standard north-east-down Cartesian frame, then \underline{r} and $\underline{\alpha}$ may be given by:

$$\underline{r} \equiv (x, y, z)^T ; \quad \underline{\alpha} \equiv (\psi, \theta, \phi)^T \quad (10b)$$

where \underline{r} is defined by the vehicle's Cartesian coordinates, and $\underline{\alpha}$ by the corresponding Euler angles.

We then assume that we can define a functional relationship between this total state vector \underline{X} and a given extra-cockpit cue Y_i , of the following form:

$$Y_i = f_i(\underline{X}) \quad (11)$$

where f_i specifies the functional relationship. If N such cues comprise a cue set, we can then define a cue vector according to

$$\underline{Y} \equiv (Y_1, Y_2, \dots, Y_N)^T \quad (12)$$

so that

$$\underline{Y} = \underline{f}(\underline{X}) \quad (13)$$

where components of \underline{f} are the individual f_i . In general this will be a non-linear vector function, but the corresponding linear relationship can be found rather directly:

$$\delta \underline{Y} = \begin{bmatrix} \partial f / \partial \underline{x} \end{bmatrix} \delta \underline{X} \quad (14)$$

Here, $\delta \underline{X}$ and $\delta \underline{Y}$ are first-order perturbations in the state and cue vectors, and the bracketed term is the sensitivity matrix, whose (i, j) component is given by $(\partial f_i / \partial X_j)$.

This expression is simply another form of the "display" equation (2), if we let

$$C \equiv \begin{bmatrix} \partial f / \partial \underline{x} \end{bmatrix} ; \underline{y} \equiv \delta \underline{Y} ; \underline{x} \equiv \delta \underline{X} \quad (15)$$

Thus, equation sequence (10)-(15) provides us with a general means for specifying the appropriate C matrix, once the cue set \underline{Y} is identified, and the functional relationships \underline{f} specified. In effect, it is a generalization of the approaches cited earlier (Wewerinke, 1978; Levison and Baron, 1976), and allows for a unified treatment of the many cues available from an extra-cockpit scene.

Line Element Cueing

We will not go into detail here concerning specific visual cue set definitions, but it is appropriate to illustrate the approach by considering the cues available from a single line element in the visual scene.

* In general, the total state vector would also include higher derivatives associated with vehicle dynamics, etc., but for simplicity of discussion, we neglect them here.

Each segment is defined by two end points, and each such endpoint, as viewed by the observer, has a unit length line-of-sight (LOS) vector associated with it, pointing from the observer to the endpoint. With two three-dimensional LOS vectors, and with the constraint that each LOS vector is unit length, it then follows that a visual scene element has associated with it four independent parameters which specify it, relative to the observer.

Any four-dimensional cue set which contains the information in the LOS vectors will suffice for a display analysis. However, from a perceptual modeling standpoint, it is clearly more appropriate to work with informational quantities (cues) whose utility can be justified on psychophysical grounds. An appropriate set would appear to be the four basic stimulus attributes associated with a visual scene line segment: length, orientation, and location in the visual field, with location reflecting two attributes because the associated unit-length LOS vector is specified by two independent parameters (e.g., azimuth and elevation in the observer's frame).

Figure 2 illustrates how a visual scene line segment $\overline{P_i P_j}$ might be projected on an observer-centered unit sphere. The two LOS vectors \underline{u}_i and \underline{u}_j define the projection endpoints P'_i and P'_j , and also serve to define the "length" of the element, ξ_{ij} , in angular units subtended at the observer's location:

$$\xi_{ij} = \cos^{-1}(\underline{u}_i \cdot \underline{u}_j) \quad (16a)$$

The "location" of the element can be defined via the LOS vector pointing to the visual midpoint, which is given simply by:

$$\underline{u}_{ij}^M = (\underline{u}_i + \underline{u}_j) / |\underline{u}_i + \underline{u}_j| \quad (16b)$$

Note that this is a coordinate-free specification of location; observer-referenced "location" coordinates can be determined once an appropriate reference system is chosen. For example, direction cosines specifying the midpoint vector can be obtained by taking the dot product of \underline{u}_{ij}^M with the observer's three reference axes; alternatively, observer-referenced azimuth and elevation coordinates, specifying midpoint location, can be obtained by the appropriate geometric transformation.

Finally, the "orientation" of the element, measured with respect to the midpoint meridian and identified by v_{ij} in the figure, can be specified as follows:

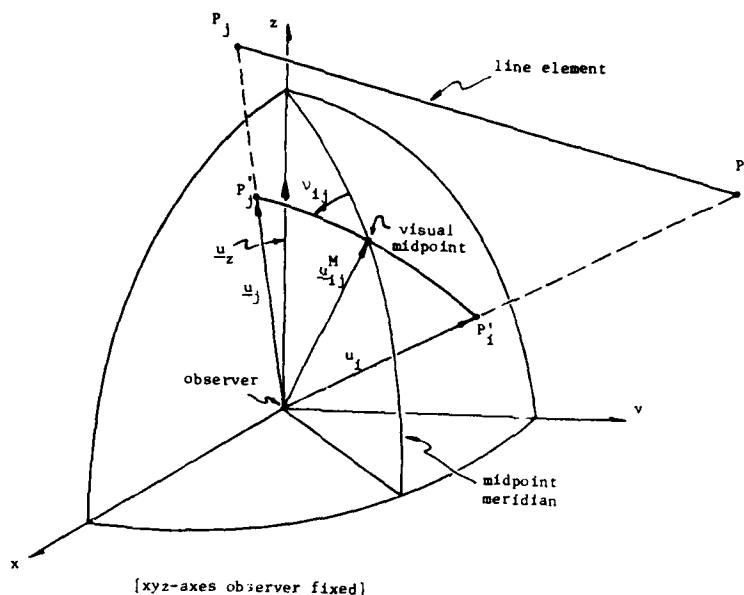
$$v_{ij} = \tan^{-1} [(-\underline{u}_z \cdot \underline{u}_{ij}^\perp) / (\underline{u}_z \cdot \underline{u}_{ij}^L)] \quad (16c)$$

where \underline{u}_z is an observer-fixed reference vector, and \underline{u}_{ij}^\perp and \underline{u}_{ij}^L are determined by the endpoint LOS vectors according to:

$$\underline{u}_{ij}^\perp = (\underline{u}_i \times \underline{u}_j) / |\underline{u}_i \times \underline{u}_j| \quad (17a)$$

$$\underline{u}_{ij}^L = (\underline{u}_j - \underline{u}_i) / |\underline{u}_j - \underline{u}_i| \quad (17b)$$

Figure 2. Spherical Projection of a Line Segment



This functional specification of the line element cues, given by (16a,b,c), corresponds directly to the general relationship given by (13) once we specify the dependence of the LOS vectors \underline{u}_i and \underline{u}_j , and the reference vector \underline{u}_z , on vehicle state \underline{X} . This is done directly by recognizing that if vehicle (observer) location is given by \underline{r} , while the location of endpoint P_i is given by \underline{r}_i , then the relative location of P_i with respect to the observer will be given by

$$\underline{\rho}_i = \underline{r}_i - \underline{r} \quad (18a)$$

so that

$$\underline{u}_i = \underline{\rho}_i / |\underline{\rho}_i| \quad (18b)$$

where a corresponding relation holds for \underline{u}_j . For \underline{u}_z , it can be shown that if we specify the observer's orientation vector $\underline{\alpha}$ (comprised of the three Euler angles), then \underline{u}_z can be expressed as an explicit vector function of the following form:

$$\underline{u}_z = \underline{g}(\underline{\alpha}) \quad (19)$$

With \underline{r} and $\underline{\alpha}$ specifying the vehicle state, it then follows that (16) through (19) specify the desired non-linear cueing relationship summarized earlier by (13).

With this cueing relationship so specified, it is now a direct matter of perturbation analysis to derive the corresponding linear display equations summarized by (14). We will not do this for the entire cue set just described, but simply illustrate the approach for the "length" cue ξ_{ij} .

From (16a) it can be shown that the change in length $\delta\xi_{ij}$ can be expressed by

$$\delta\xi_{ij} = [\underline{u}_{ij}^L \cdot (\delta\underline{u}_i - \delta\underline{u}_j)] / \cos(\xi_{ij}/2) \quad (20)$$

AD-A110 226

AIR FORCE HUMAN RESOURCES LAB BROOKS AFB TX
1981 IMAGE II CONFERENCE PROCEEDINGS.(U)

F/G 14/2

1981 IMAGE II CONFERENCE PROCEEDINGS. (U)

NOV 81 E G MONROE

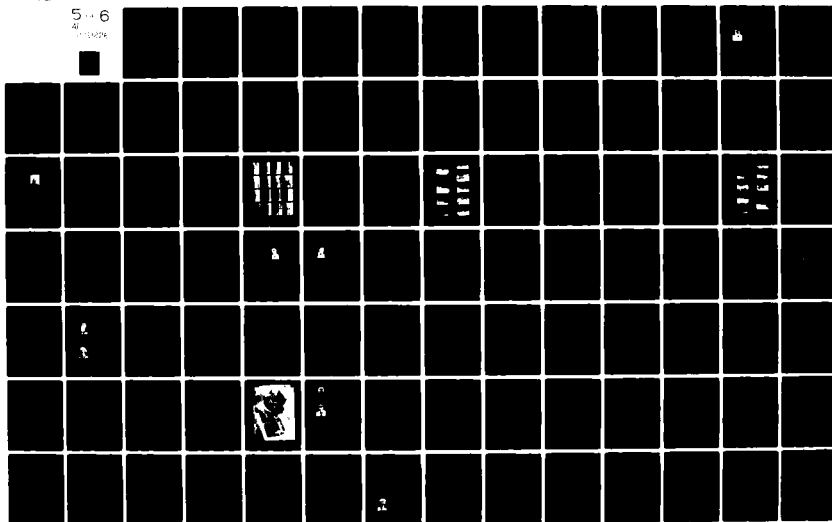
AFHRL-TR-81-48

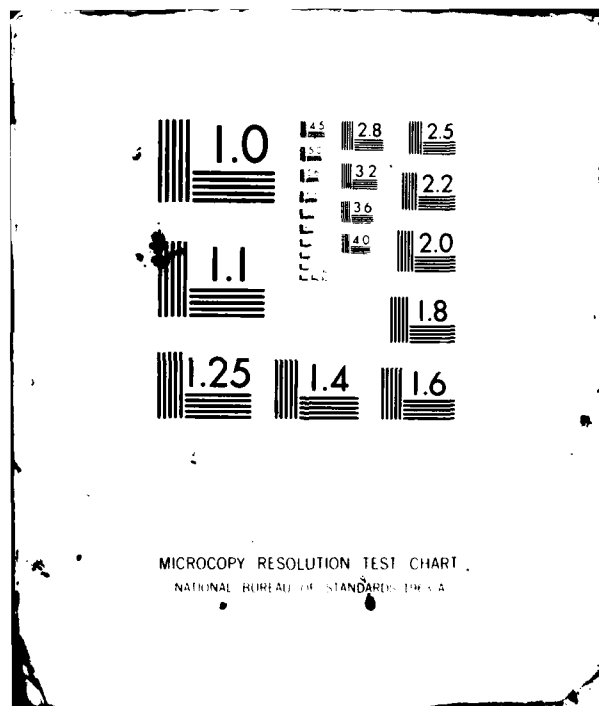
UNCLASSIFIED

NL

5.. 6

4. $\frac{1}{2} \times 10^3$





where \underline{u}_{ij}^L was defined earlier by (17b) and $\delta \underline{u}_i$ and $\delta \underline{u}_j$ are perturbations in the two endpoint LOS vectors. These, however, can be obtained from (18), assuming that the vehicle (observer) undergoes a perturbation in position $\delta \underline{r}$, while the endpoint locations of the (physical) line element remain fixed in space. The resulting expression for $\delta \underline{u}_i$ is then given by:

$$\delta \underline{u}_i = U_i \delta \underline{r} \quad (21a)$$

where

$$U_i = -[I - \underline{u}_i \underline{u}_i^T] / |\underline{u}_i| \quad (21b)$$

where I is the identity matrix and \underline{u}_i is defined by (18a). A corresponding relation holds for $\delta \underline{u}_j$.

These expressions for $\delta \xi_{ij}$ and $\delta \underline{u}_i$, taken in tandem, constitute a single scalar relation between the perturbation in the length cue, and the positional change in vehicle state. Similar expressions can be found for perturbations in cue orientation and position, although, because of their functional dependence, they involve not only perturbations in vehicle position \underline{r} , but also orientation $\underline{\alpha}$. The resulting set of four linear cueing relations can thus be expressed in the matrix-vector format of (14), or, equivalently, in the display equation format of (2).

It should be clear that this type of analysis, which has concentrated on single-element cueing, can be extended to multi-element cueing to account for additional cues arising from geometric relationships between different elements (e.g., the apparent included angle between two line segments sharing a common visual endpoint). In addition, semi-infinite segments can be treated as a special case, to allow for scene elements which "disappear" at the visual horizon (e.g., parallel infinite lines).

Specification of Observation Noise

The second component of the perceptual model needing specification is the observation noise vector \underline{v} , associated with the "perceptual" equation (3). As noted earlier in the OCM description, this implies a specification of the thresholds associated with each cue, and the allocation of attention among members of the entire visual cue set.

Visual Thresholds

Thresholds can be specified in one of two ways: *a priori* on the basis of related psychophysical measures, or *a posteriori* on the basis of "calibration" tracking experiments.

A priori specification can provide a first approximation to the relevant pilot-related thresholds, if an appropriate data base exists. Thus, for example, acuity estimates can be used to specify a "minimum" threshold for line segment orientation (Levison, 1976). If data is lacking, static discrimination experiments can be designed to identify thresholds relevant to the specific elements comprising the extra-cockpit scene (Wewerinke, 1978). In either case, such estimates usually suffer from the static nature of the

discrimination task being used to identify the threshold, and the lack of correspondence between such a task, and the task for which the cues are being used (e.g., flying an airplane).

These shortcomings provide the motivation for performing "calibration" experiments, from which relevant thresholds can be inferred. To illustrate the approach, we briefly describe an experimental study of closed-loop compensatory tracking, using for a display an electronically driven error bar, which moved with respect to a stationary reference bar (Levison, 1971). Rate (K/s) dynamics were used, four levels of display gain were explored, and both foveal and parafoveal ("peripheral") viewing conditions were considered. Model analysis via the OCM yielded estimates of observation noise for both displacement and rate perception for each experimental condition.

Figure 3 shows the experimentally-derived relationship between displacement (rate) observation noise and mean-squared display deflection (velocity). Results are shown for both foveal and peripheral viewing, and are repeated in Figure 4 on an expanded scale to better describe the relationships at the low end of the scale. In general, noise variance varied linearly with respect to signal variance, in accordance with the noise model specified earlier by (4).

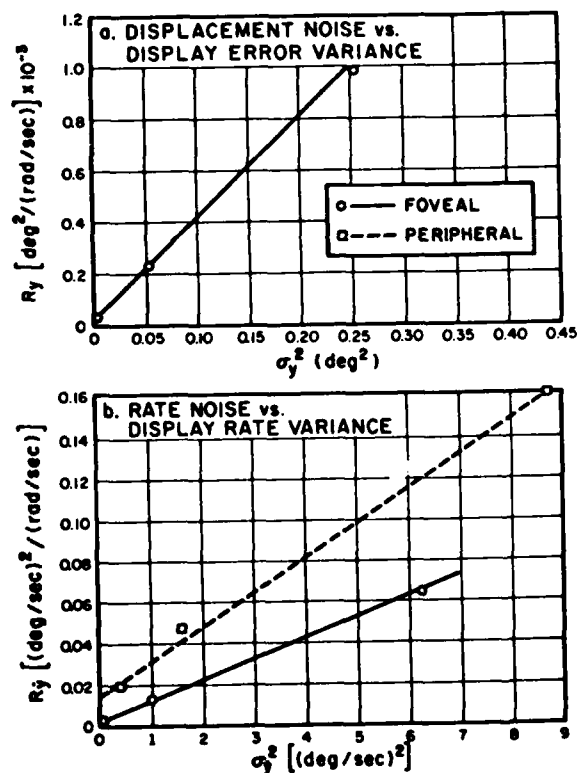


Figure 3. Observation Noise Power Density vs. Signal Variance (data/model comparison; expanded scale)

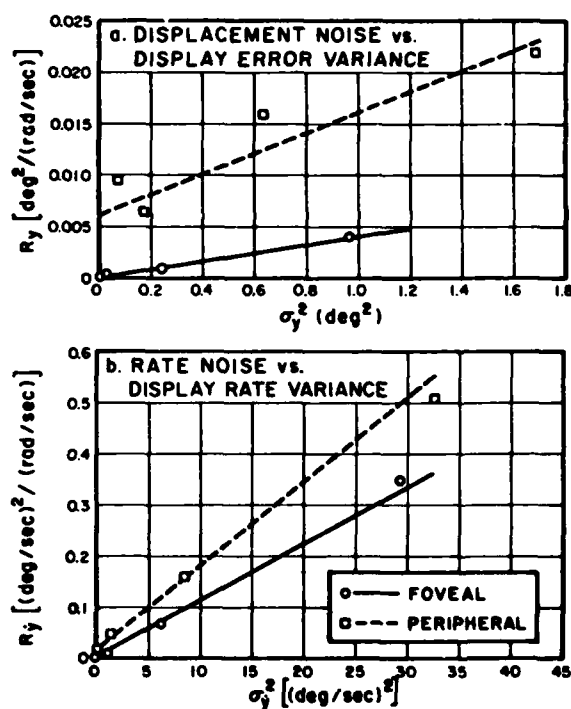


Figure 4. Observation Noise Power Density vs. Signal Variance (data/model comparison)

The results shown in the figures also agree both qualitatively and quantitatively with other results found in the literature relating to perceptual thresholds. Specifically:

1. Extrapolation of the curves to zero display variance reveals a positive intercept on the observation noise axis -- a condition that must hold if these results are to reflect a physically realizable threshold-like phenomenon.
2. Threshold values derived on the basis of the zero intercepts are of the same order of magnitude as threshold values reported elsewhere in the literature.
3. Zero intercepts for peripherally-viewed quantities are greater than intercepts for corresponding quantities viewed foveally, a finding which is consistent with the observation that higher visual thresholds are associated with peripheral viewing.
4. Peripheral-foveal differences are proportionately less for rate perception than for displacement perception, a result consistent with the most widely-held belief that moving objects in the visual periphery are "seen better" than stationary objects.

Because of the reasonableness of these results (and the lack of contradictory evidence), the inferred thresholds have been used in subsequent studies involving model predictions of pilot/vehicle performance in realistic flight control tasks, with considerable success.

A similar approach to threshold determination can be applied to the extra-cockpit cueing environment. What is required is a simplified pictorial display, which deliberately limits the pilot's information base, combined with a well-defined closed-loop piloting task. OCM-based model analysis of the resulting data can then be used to infer appropriate thresholds (for example, for line element length, orientation, and location in the visual field), which can then be used to extrapolate to situations involving richer cue environments.

To illustrate, Figure 5 shows a perspective display of an idealized roadway, which might be used to study lateral path regulation of an aircraft flying at constant altitude over flat terrain. The display can provide cues for inferring both position and attitude. Position cues are provided by: the apparent angles between the roadway and the horizon (a_1 and a_2), which reflect lateral displacement from the road centerline; and the apparent path angle (b), which reflects altitude above the road. Attitude cues are provided by: the horizon line, which reflects the aircraft's roll attitude; and the vanishing point location, which reflects the aircraft's heading with respect to the road centerline.

The control task of minimizing lateral deviations corresponds to the perceptual task of determining when the angles a_1 and a_2 appear to be equal. Likewise, the control task of maintaining wings level corresponds to the perceptual task of determining when the horizon line is parallel to the upper and lower frame lines. Thus, corresponding perceptual thresholds can be determined on the basis of data obtained from an appropriately-designed control task, and with the use of the OCM to infer equivalent perceptual

thresholds from the measured response data. Clearly, perceptual thresholds associated with other scene elements and scene element attributes can be determined in a similar fashion.

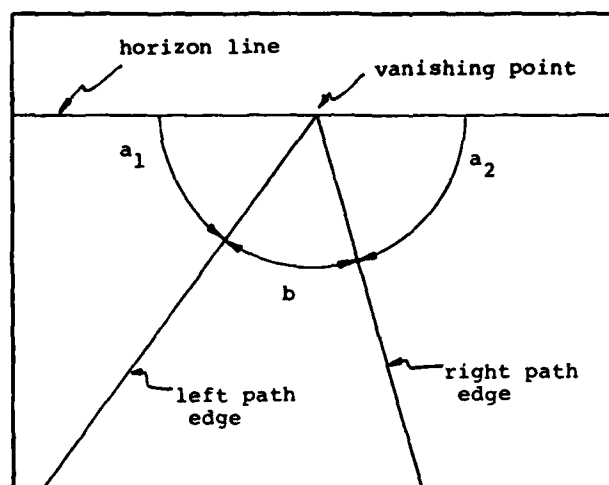


Figure 5. Perspective Display of Path

Attentional Allocation

The specification of the observation noise vector also requires a determination of the attentional allocation among members of the total visual cue set. Reference to (7) shows that this reduces to a specification of the individual fraction of attention, f_i , associated with the i th cue, for all cues presented to the pilot.

This may be accomplished simply by hypothesizing a "reasonable" allocation strategy, based on a knowledge of the informational requirements imposed by the control/monitoring task. This has been fairly successful in past applications, mainly because task performance is often insensitive to variations in attentional allocation. Alternatively, one may build upon the basic optimality assumption of the OCM, and postulate that the attention-sharing strategy be determined so as to optimize performance (Kleinman, 1976). Solving this optimization problem can be accomplished in a straightforward (although expensive) manner by simply adding an "outer" optimization loop to the OCM, which iteratively adjusts individual attention levels until task performance can no longer be significantly improved. The resulting attention levels then effectively comprise a prescriptive specification of attentional allocation, for "best" task performance with a given cue set.

Program for Experimental Validation

To validate this model of extra-cockpit visual cueing requires a well-defined experimental program, focussed on the identification of critical pilot-related model parameters. In this section we briefly outline a three-phase program which should be capable of providing the type of validation data deemed necessary.

The task of lateral path regulation at constant altitude provides a convenient compromise between a highly realistic task (which introduces modelling uncertainties due to task complexity) and a highly idealized task (which is quite tractable but has little face validity). A display similar to the one sketched earlier in Figure 5 could be used to provide the pilot with the needed position and attitude cues: position from the apparent inclination of the roadway, and attitude from the horizon line orientation and vanishing point location.

By artificially constraining the task dynamics, a series of single axis sub-experiments could be performed to quantify the pilot's ability to utilize these individual cues. For example, vehicle position could remain fixed and centered over the roadway, and the pilot given the task of single-axis roll control. By varying the effective display gain (the ratio of scene rotation angle to vehicle roll angle), the roll axis threshold could be determined, in a manner analogous to that discussed earlier and illustrated in Figures 3 and 4. In a similar fashion, roll attitude and heading could be constrained, and the pilot given the task of simple lateral path control. As noted earlier, this would provide a means of inferring the effective threshold associated with the (imaginary) roadway centerline orientation, again assuming that display gain variation is used as an experimental variable. Thresholds associated with other scene elements could be determined in a similar fashion.

Once these thresholds had been determined, the full multi-axis experiment could be conducted, with the aim of verifying the attention-sharing predictions generated by the OCM. Various hypotheses could be investigated via pre-experimental model simulations (e.g., attentional optimization, full cue interference due to scanning requirements, minimal cue interference due to the "integrated" nature of the display, etc.), and the corresponding model predictions of pilot performance compared to the measured data. The "best" match between model and data would then identify the model of perceptual processing most likely used by the pilot.

A second phase of the validation program could concentrate on the pilot's capabilities for altitude control, using the same display as in the first phase. Here, the primary height cue would be the apparent central angle defined by the roadway edges, while the primary flight path angle cue would be provided by the depression angle of the horizon line. Again, sub-experiments could be used to identify individual cue thresholds (via display gain variations), and a combined multi-axis experiment could be conducted to validate model predictions of attentional allocation among cues providing vertical path control information.

The third and final phase of the validation program could combine both lateral and vertical tasks, in a full five degree-of-freedom flight control task (at constant airspeed). The primary objective of this phase would be the validation of model predictions of attention allocation, between lateral and vertical axes, and among cues associated with each axis.

Determination of Simulator Visual Cueing Requirements

The discussion to this point has been concerned primarily with the perceptual limitations associated with the pilot, their impact on overall task performance, and their efficient representation within the structure provided by the OCM. However, it should be pointed out that the model, as defined, makes no explicit distinction between pilot-related perceptual limitations and simulator-related cueing limitations. Thus, the model is as applicable to a study of simulator cueing requirements, and their impact on closed-loop pilot performance, as it is to the above-discussed studies of inherent human perceptual limitations.

To use the model in this manner requires an initial translation step, from the basic simulator cueing characteristics (actual or proposed), to the underlying model parameters which characterize the perceptual "front-end" of the OCM. An illustration of this mapping process is given in Figure 6, which is taken from an analytic study of simulator cueing requirements for helicopter hover (Baron et al, 1980). Parameters associated with the computer-generated imaging (CGI) system were "mapped" into equivalent OCM parameters (e.g., the CGI display delay value was used to adjust the perceptual delay associated with the OCM's visual channel), so that the resulting OCM parameters reflected not only the basic human limitations, but also the non-ideal characteristics of the simulator.

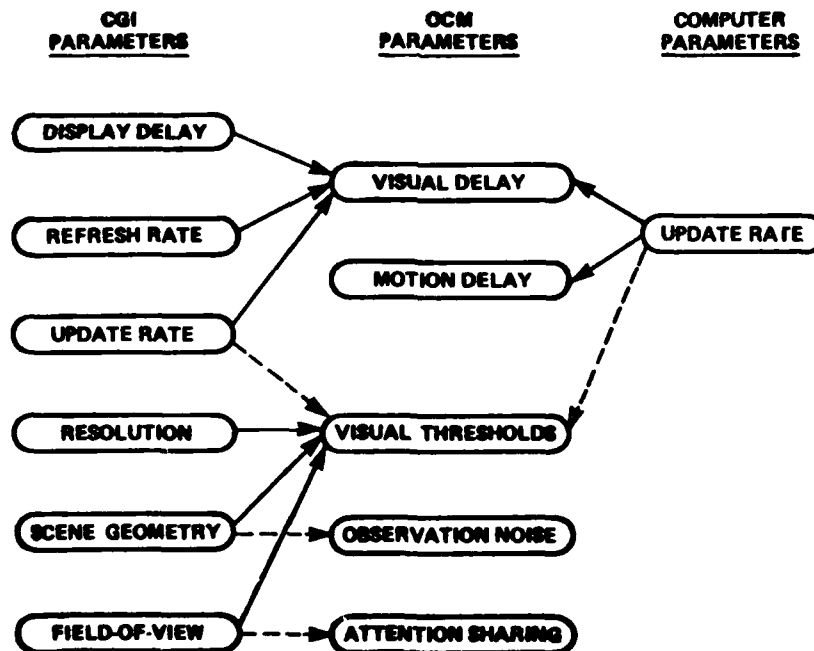


Figure 6. Simulator Mappings for OCM Analysis

Once this mapping is accomplished, the OCM may then be used to generate performance predictions, for the human pilot operating in the specified simulator cueing environment. If this mapping is done for a variety of configurations, and over a reasonable range of simulator-associated parametric values, corresponding performance predictions can then be "swept-out", by repeated use of the OCM.

This was done in the cited study (Baron et al, 1980), and Figure 7 illustrates the type of closed-loop sensitivity predictions which can be generated by this approach. The ordinate represents the relative hover performance decrement in percent: J is a composite scalar metric reflecting overall hover accuracy in the simulator, and J_{FLT} is the corresponding metric associated with the actual flight situation.* Since the ordinate is the normalized difference between these two metrics, it is, in effect, a fidelity metric for comparing in-simulator performance to in-flight performance, with a zero value indicating perfect simulator fidelity. The abscissa represents time delay in the CGI computer, and the curves (which are parameterized against mainframe computer cycle time) show how rapidly performance fidelity degrades with increasing delay.

Similar fidelity curves can be generated for other simulator cueing characteristics (e.g., CGI resolution, field-of-view, etc.), to support an extensive specification of the relationship between cueing deficiencies and expected simulator/aircraft performance mismatches. One can readily envision how such an information base could be used in a rational specification of task-specific simulator cueing requirements. Starting with a desired fidelity level to be met by the simulator, one could refer to the curves to identify preliminary parameter ranges which ensure that this level will be met or exceeded. Engineering and cost trade-offs could then be made within these ranges (e.g., balancing the increase in simulator fidelity achieved by increasing the CGI resolution, against the longer development times and higher costs associated with better quality hardware), to arrive at a reasonable choice of simulator specifications which will ensure meeting the desired fidelity level.

More sophisticated procedures can also be envisioned, which take into account cross-coupling effects between simulator parameters, to provide the designer with a "hyper-ellipse" of acceptable simulator parameter choices, given a desired fidelity level. It is not our intent to speculate on possible advanced design algorithms, however, but rather to point out potential applications of model-based fidelity metrics. It would seem that this general approach holds considerable promise for the rational and successful specification of simulator cueing requirements.

* The latter was calculated simply by assuming an ideal simulator having no cueing deficiencies, so that it replicated the flight environment perfectly.

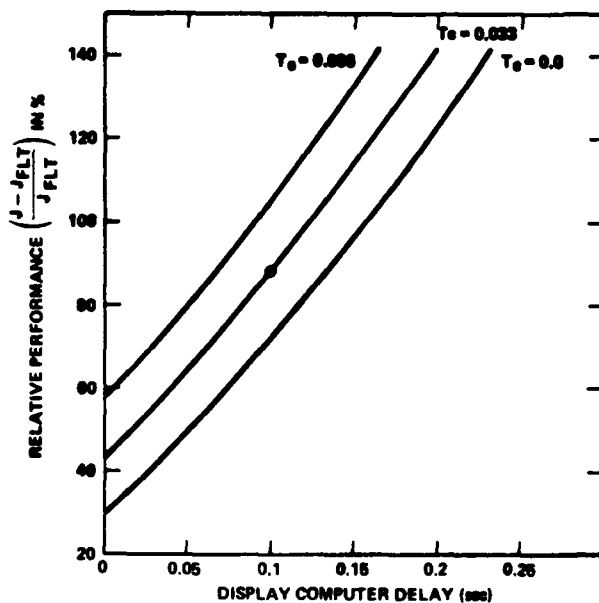


Figure 7a. Relative Performance Vs. Time Delay (Longitudinal Axis - Fixed Base).

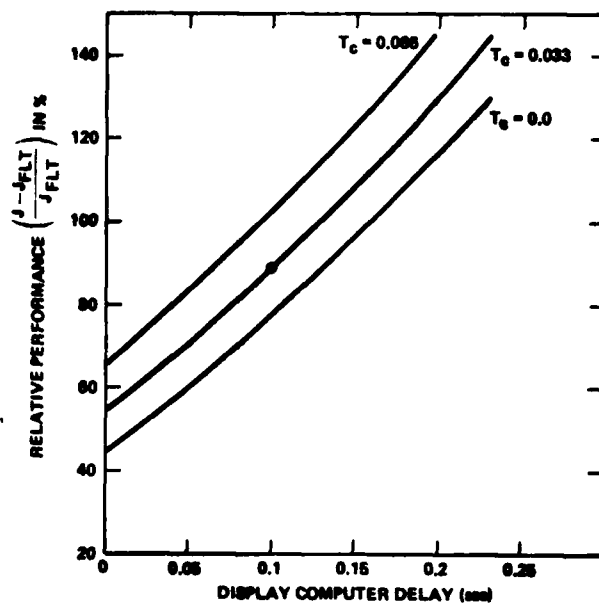


Figure 7b. Relative Performance Vs. Time Delay (Lateral Axis - Fixed Base).

Summary

In this paper we have outlined an analytic and experimental effort aimed at developing and validating a quantitative model of extra-cockpit visual cueing. The analytic approach uses the basic "perceptual" sub-model of the OCM, and concentrates on how such cues relate to the basic aircraft flight control variables of interest to the pilot. The analysis was limited to those cues provided by perspective geometric scenes of the extra-cockpit world, and a general geometric and perturbation analysis of the simulator environment was discussed. Its use in identifying the appropriate OCM-related "display equation" was illustrated by concentrating on single line element cues, and their informational content.

The experimental approach concentrates on identifying pilot-associated perceptual limitations in processing the available visual cues. A general flight task and extra-cockpit display was proposed for use both in the identification of relevant visual thresholds, and in the determination of human attention allocation strategies. Thresholds are determined by the use of appropriate sub-tasks combined with variations in display sensitivity, while attention allocation strategies are identified by hypothesis testing and model matching.

Finally, a general approach for the rational specification of simulator cueing requirements was outlined. It is predicated on a validated OCM-based model of extra-cockpit cueing, and introduces the notion of a model-based simulation fidelity metric. The approach provides a means of specifying desired fidelity levels, and identifying appropriate simulator configurations and parameter ranges, as a starting point for further engineering and cost trade-off studies in the simulator specification design cycle.

REFERENCES

- Baron, S., Kleinman, D.L. et al, "Application of Optimal Control Theory to the Prediction of Human Performance in a complex task," WPAFB, Ohio: Air Force Flight Dynamics Laboratory, AFFDL-TR-69-81, March 1970.
- Baron, S. and Levison, W.H., "A Manual Control Theory Analysis of Vertical Situation Displays for STOL Aircraft," NASA CR-114620, April 1973.
- Baron, S., Lancraft, R., and Zacharias, G., "Pilot/Vehicle Model Analysis of Visual and Motion Cue Requirements in Flight Simulation," NASA CR-3312, October 1980.
- Brown, J.L., "Visual Elements in Flight Simulation," University of Rochester, TR-63-2, December 1973.
- Gibson, J.J., The Perception of the Visual World, Riverside Press, Cambridge, MA, 1950.
- Gibson, J.J., et al, "Parallax and Perspective During Aircraft Landings," American J. of Psych., 68, 1955.
- Hess, R.A., and Wheat, W.L., "A Model-Based Analysis of a Display for Helicopter Landing Approach," IEEE Trans. on Syst., Man & Cybern., 1976, SMC-6(7).
- Kleinman, D.L., "Solving the Optimal Attention Allocation Problem in Manual Control," IEEE Trans. on Auto. Control, AC-21, 1976.
- Kleinman, D.L., Baron, S., and Levison, W.H., "A Control Theoretic Approach to Manned-Vehicle Systems Analysis," IEEE Trans. on Auto. Control, 1971, AC-16, 824-832.
- Levison, W.H., "The Effects of Display Gain and Signal Bandwidth on Human Controller Remnant," WPAFB, Ohio: Aerospace Medical Research Laboratory, AMRL-TR-70-93, March 1971.
- Levison, W.H., and Baron, S., "Analytical and Experimental Evaluation of Display and Control Concepts for a Terminal Configured Vehicle," BBN Report No. 3270, July 1976.

Levison, W.H., Baron, S., and Junker, A.M., "Modeling the Effects of Environmental Factors on Human Control and Information Processing," WPAFB, Ohio: Aerospace Medical Research Laboratory, AMRL-TR-76-74, August 1976.

Levison, W.H., Baron, S., and Kleinman, D.L., "A Model for Human Controller Remnant," IEEE Trans. on Man-Machine Syst., 1969, MMS-10, 101-108.

Levison, W.H., Elkind, J.I., and Ward, J.L., "Studies of Multi-Variable Manual Control Systems: A Model for Task Interference," NASA CR-1746, May 1971.

Matheny, W.G., et al, "An Investigation of Visual, Aural, Motion and Control Movement Cues," Naval Training Device Center, Technical Report NAVTRADEVCE 69-C-0304-1, April 1971.

Staples, K.J., "Motion, Visual, and Aural Cues in Piloted Flight Simulation," AGARD Conference Proc. No. 79 on Simulation, AGARD CP-79-70, March 1970.

Wewerinke, P.H., "A Theoretical and Experimental Analysis of the Outside World Perception Process," Proc. of the Fourteenth Annual Conf. on Manual Control, NASA Conf. Pub. 2060, November 1978.

Wewerinke, P.H., "The Effect of Visual Information on the Manual Approach and Landing," presented at the Sixteenth Annual Conference on Manual Control, MIT, May 5-8, 1980.

TRANSFORMATION REALISM:
AN INTERACTIVE EVALUATION OF OPTICAL INFORMATION
NECESSARY FOR THE VISUAL SIMULATION OF FLIGHT

Dean H. Owen

Rik Warren

Richard Jensen

Susan J. Mangold

Gregory Alexander

Lawrence Hettinger



Dean H. Owen obtained his Ph.D. from Purdue University and his M.S. from Iowa State University, both in Experimental Psychology. His 15 years of professional experience has been at Ohio State University, with specialization in perception. His research has included the study of form discrimination, perceptual set and learning, adaptation to visual distortion, and face recognition. Current work is involved with optical information for the perception of self motion in flight simulation.

Dean H. Owen
Associate Professor
Department of Psychology
Ohio State University

TRANSFORMATION REALISM:
AN INTERACTIVE EVALUATION OF OPTICAL INFORMATION
NECESSARY FOR THE VISUAL SIMULATION OF FLIGHT

Our research is an attempt to (1) isolate optical variables and invariants useful in the perception of self motion, and (2) use performance measures to determine the information used in guiding flight. Initial studies have been concerned with the role of optical flow and density parameters in sensitivity to change in speed and altitude.

Advances in hardware and graphics technique continuously result in more realistically detailed visual simulation of environmental surfaces. The goal of surface detail realism (e.g., trees, buildings, mountains) is pursued with little regard for either its necessity or the possibility that attention to irrelevant information might impede learning. Our approach addresses the problem of determining the optimal information in kind, quality, and magnitude that must be made available in order to produce time- and cost-efficient transfer from simulation to actual flight. The programmatic phases will be described, including underlying theoretical assumptions and their relation to the developing methodology. With fairly firm grounding on the principle of visual capture or dominance, initially only visual contact sources of information will be considered, with the realization that integration and contrast with vestibular, haptic, somatic, and coded information must eventually be considered.

Our approach follows Gibson (e.g., 1966, 1979) in distinguishing between the visual information specifying environmental surfaces and that specifying the relation of the perceiving individual to the surfaces. We are testing the assumption that schematic surface detail is sufficient for learning, if ecologically valid optical transformations are available to specify self motion. The initial phase of our program has been concerned with the identification of potential sources of optical information, including ways to specify the sources mathematically and isolate them empirically. The primary focus has been on variables of optical flow and optical texture, and their usefulness in the detection of change in altitude and speed.

An important concept for exploring the relationship between environmental variables (e.g., surface texture size, shape, and color; altitude and descent rate; forward speed and deceleration rate) and optical variables is that of the functional invariant. It is hypothesized that when optical conditions are the same, regardless of the environmental variable ratios which produced them, performance will be the same. The hypothesis is based on the assumption that the perceptual system only has access to optical information, and that adequate knowledge of the relation between self and environmental surfaces is available to guide one's own locomotion.

The first experimental step was concerned with understanding the relation between environmental variables and both optical variables and invariants. Two studies, to be described subsequently, were conducted to assess sensitivity to constant rates of loss in altitude and forward speed. The results converged on a common kind of functional invariant; fractional increase or decrease in optical rates of change. The second step consists of factorially

crossing optical variables while letting environmental variables take on any values necessary to simulate a desired event. This step, currently under way, allows exploration of two problems: (1) determining the appropriate metric for scaling optical invariants, and (2) separating speed-relevant variables from altitude-relevant variables. The metric issue is under study with two alternative candidates, in ground scaled units (e.g., texture block size) versus body scaled units (e.g., eyeheights). The criterion for choice of metric is whether one of the two alternatives results in functional invariance when they are factorially crossed, whereas the other does not. Solution of this problem is critical in determining what an individual needs to know in order to perceive distance (including altitude) and change in distance veridically (see Harker & Jones, 1980, pp. 25-31).

Change in speed is potentially specified by increase or decrease in optical flow rate (Warren, 1981a). Loss in altitude is potentially specified by several optical variables, including optical flow acceleration, decrease in optical density, and increase in optical "splay" rate (Warren, 1981b). (Splay indexes optical discontinuities along lines projecting to the vanishing point.) By controlling environmental variables, various kinds of optical information can be eliminated in order to assess the salience of those remaining. For example, optical acceleration can be eliminated during descent by decelerating path speed exponentially at the rate required to hold optical flow rate constant. A preliminary experiment indicates that descent is easily detected on the basis of optical density and splay-rate changes. Splay rate can, in turn, be eliminated as a source of information by using surface texture strips with edges perpendicular to the direction of travel (i.e., parallel to the horizon). Optical magnification remains as a source of information for descent, although preliminary tests suggest that observers are not as sensitive to it alone as to combined splay and density changes. In addition to those examples of information deletion and accretion, sources of information can be made irrelevant in contrasts with constant velocity or constant altitude trials, or held constant in factorial designs. All these types of control should prove useful in isolating the optical information necessary for simulation of a given flight maneuver. Further work will be concerned with optimizing these variables during training.

Given that tests of accuracy and efficiency in detecting change and non-change isolate optical invariants in passive judgment experiments, the next phase casts the problem in a research framework which mimics the interactive nature of actual flight. The experimenter is in control of the environmental variables studied in the first phase, namely surface texture size, shape, and color, and the variables used to initiate a trial, e.g., forward velocity, altitude, descent rate, and/or deceleration rate. A trial is initiated by requiring the pilot to take over the controls and, with all instruments covered, assess via visual contact whether there is a deviation from the desired flight path. If so, a compensatory control adjustment is made. Efficiency and accuracy of the control actions are related to initial optical values, the state of optical stimulation at the time the adjustment was made, and a ratio of the change in stimulation to the initial optical information values. The goal of this analysis is to determine the optical conditions which result in the initiation of adjustments, lead to their modification, and ultimately are achieved as a desired situation by the pilot.

The interactive paradigm thus turns control over changes in stimulation to the pilot as occurs outside the laboratory. The control actions become perceptual reports, and the x, y, z position of the aircraft over time can be used to compute optical variables. The researcher's task is to perform retrospective analyses of the optical information available to determine what the pilot used to guide his locomotion. This evidence can then be used to optimally allocate available detail (edges and/or points) in order to best simulate any given maneuver.

Success of this phase will lead to the study of complete flight subtasks, such as approach and landing or the avoidance of obstacles, and eventually to the study of transfer of training from simulator to aircraft.

Optical Information for Detecting Loss in One's Own Forward Speed

Warren (1981a) has systematized and mathematically isolated candidates for optical information specifying relative change in speed during self motion (see Appendix A). The experimental effort described here is an initial attempt to explore the efficacy of this approach. Loss in speed was chosen because it occurs in every case of locomotion, and appropriate sensitivity is necessary to guide approach to surfaces. When separated from change in altitude and direction, loss in speed provides an optically simpler point of departure for psychophysical study than would such changes in the path of locomotion itself.

Given a constant eyeheight (altitude), optical deceleration is specific to deceleration in the velocity of movement of the eye above the ground surface. For conditions having the same deceleration in rate of movement over the same surface texture at different altitudes, optical deceleration will differ since optical flow varies with eyeheight. Lastly, given constant deceleration, initial forward velocity should affect sensitivity to deceleration because a given loss in optical flow rate should be easier to detect relative to a lower than to a higher optical flow rate.

Accordingly, levels of deceleration rate, altitude, and initial forward velocity were chosen to explore the ability of observers to distinguish loss in forward speed from constant, level, forward locomotion. Levels of these three environmental independent variables were chosen so as to produce matrices with five levels of the optical flow variables. All adjacent environmental variable levels have the same ratio, so that the negative diagonals of the two-factor matrices have invariant optical flow values. The design simultaneously allows assessment of the effect of the optical variable and determination of whether an optical invariant is a functional invariant.

Method. A special purpose visual scene generator was used to produce 10-sec sequences representing self motion over a flat surface covered with rectilinear texture blocks. The center strip extending toward the horizon was fixed at 10 m in width, with two adjacent strips also of 10 m. This 30 m-wide area was flanked on each side by two strips of 30 m, for a total of 90 m. Successive adjacent strips on each side were 90 m and then 270 m, so that the multiplier of three was used throughout. The edges perpendicular to the direction of travel and within the three 10 m-wide strips were chosen to produce texture blocks from 5 to 20 m in length. Lengths were sampled

randomly from a rectangular distribution having lengths in all 5 m steps between these extremes. The texture blocks were filled in four earth colors: light green, dark green, tan, and a darker brown. Colors were randomly assigned to the blocks, resulting in various rectilinear shapes and sizes.

An analog computer was programmed to control the scene generator in order to vary altitude, initial forward velocity, and deceleration rate. The 10-sec trial sequences were videotaped and displayed on a Sony video projection screen 150 cm wide and 112.5 cm high, resulting in a field of view of 34 deg by 26 deg. The observer sat in a Link General Aviation Trainer-1 flight simulator with the motion base off. His point of observation was 3.2 m perpendicular to the center of the screen at a height of 1.67 m which matched the fixed position horizon on the screen. All sequences represented forward level movement over the center of the surface as shown in Figure 1.

A 3^3 full-factorial combination of deceleration rate (2, 3.5, 6.125 m/sec/sec), altitude (18, 31.5, 55.125 m), and initial forward velocity (18, 31.5, 55.125 m/sec) produced 27 different deceleration sequences. The three optical-variable matrices produced by these combinations are shown in Table 1. Figure 2 shows how combinations of environmental variable levels produce optical flow invariants, in this case for optical flow damping. Combinations of altitude and forward velocity levels produced nine different sequences representing forward movement at constant velocity and altitude. To equal the number of deceleration trials, each constant-velocity sequence was presented three times. Each observer was tested with three different orders of the 54 sequences.

The observer was instructed to indicate whether the event displayed represented movement at a constant speed or loss in speed by pressing one of two appropriately designated buttons. A 1000 Hertz tone initiated .5 sec before the onset of the trial served as a ready signal. Simultaneously with the beginning of the trial, a millisecond timer was started. Timing terminated when either button was pressed. The observer was unaware that time to respond was being recorded. Following the button press, the observer rated his confidence in the choice made on a three-point scale. "Three" represented very certain; "two," fairly certain; and "one," guessing.

Forty-two male volunteers participated in partial fulfillment of an introductory psychology course requirement. Each answered a request for non-pilots with no experience in flight simulators.

Results. Analysis of the errors (from reporting "constant speed" on deceleration trials) revealed no significant effect for sessions. Mean reaction time dropped significantly between the first and second sessions, but the effect was small ($\eta^2 = 3\%$). Proportion errors decreased with an increase in deceleration rate ($\eta^2 = 12\%$) and increased with an increase in forward velocity ($\eta^2 = 7.8\%$). The interaction of these two variables accounted for 3.6% of the variance. These effects are shown by the broken lines in Figure 3A. Figure 3B reveals the mean error-free reaction time decreased with increase in deceleration rate ($\eta^2 = 21.5$) and increased with increase in forward velocity ($\eta^2 = 10.2\%$).

Performance was next evaluated as a function of the three global optical variables computed as ratios of the three environmental variables. In order

Table 1

Combinations of Environmental Variables to
Produce Optical Variables and Invariants

A. Initial Global Optical Flow Rate (eyeheights/sec)

Altitude (m)	Initial Forward Velocity (m/sec)		
	18	31.5	55.125
20	.900	1.575	2.756
35	.514	.900	1.575
61.25	.294	.514	.900

B. Global Optical Flow Deceleration (eyeheights/sec/sec)

Altitude (m)	Deceleration Rate (m/sec/sec)		
	2	3.5	6.125
20	.100	.175	.306
35	.057	.100	.175
61.25	.033	.057	.100

C. Global Optical Flow Damping (% eyeheight/sec)

Initial Forward	Deceleration Rate (m/sec/sec)		
Velocity (m/sec)	2	3.5	6.125
18	11.1	19.4	34.0
31.5	06.3	11.1	19.4
55.125	03.6	06.3	11.1

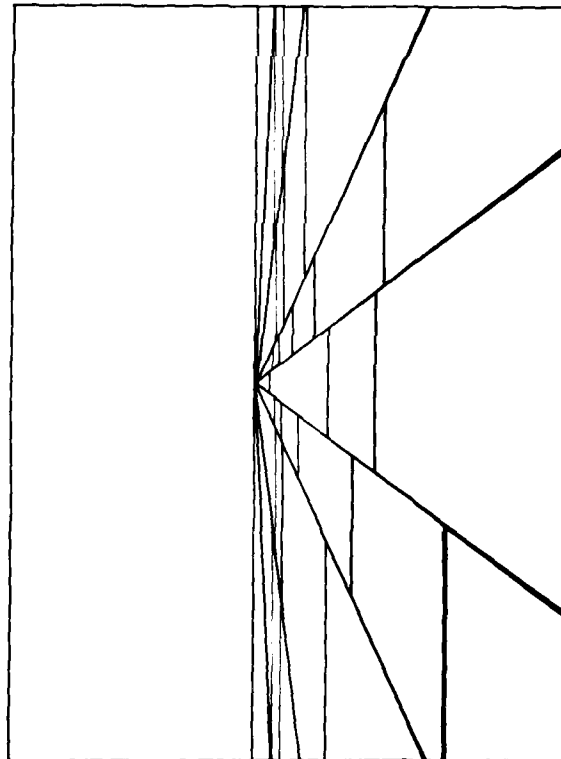


Figure 1. View of ground surface appropriate to an altitude of 20 m. The lines to the vanishing point are exactly as simulated; those parallel to the horizon are more sparse than actually used. See text for details.

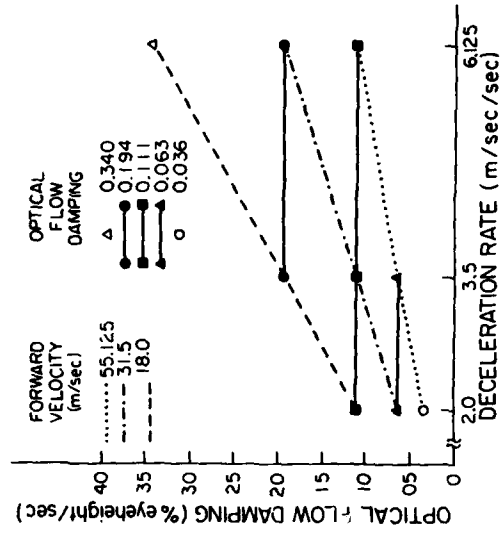


Figure 2. Global optical flow damping values at the initiation of a trial. Solid lines show optical invariants; broken lines are for different forward velocities.

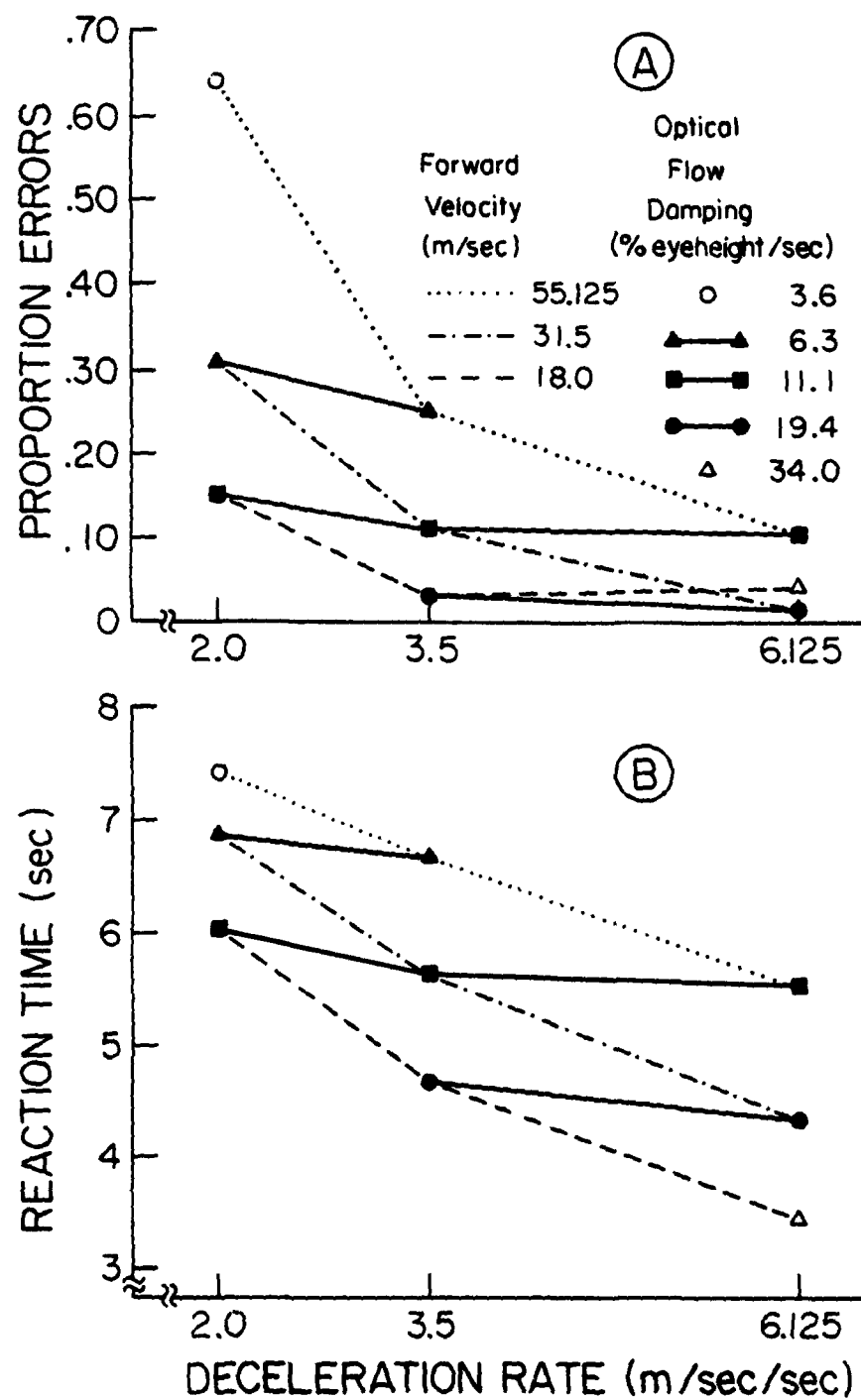


Figure 3. Mean proportion errors (A) and mean error-free reaction time (B) as a function of deceleration rate, forward velocity, and their ratio (global optical flow damping).

for an optical invariant to be considered a functional invariant, two criteria must be met: (1) Performance must be invariant even though the environmental variables producing the optical invariant vary over a broad range. (2) Performance must vary in an orderly fashion when the optical invariant has different values. The latter criterion is necessary to eliminate cases in which performance is invariant because detection is too easy (ceiling effects), too difficult (floor effects), or the optical variable is unrelated to the particular task used.

Using these two criteria to identify a functional invariant indicated that optical flow damping was the best candidate for invariant information underlying sensitivity to loss in forward speed of locomotion. The solid lines in Figures 3A and 3B reveal the extent to which optical damping invariants resulted in constant levels of performance.

Optical Information for Detecting Loss in One's Own Altitude

Any change in orientation, direction, or speed during locomotion may result in an increase or a decrease in an optical variable and may also leave some optical variables unchanged. Warren (1981b) has systematized and mathematically isolated candidates for global optical information specifying relative change altitude during rectilinear self motion (see Appendix A). The second experiment applied the paradigm used for deceleration to the optically more complex analysis of potential functional invariants for sensitivity to loss in altitude. Accordingly, levels of descent rate, forward velocity, and initial altitude were chosen to test the ability of observers to distinguish loss in altitude from level, forward locomotion. Except where noted, all conditions were the same as for the first experiment.

Method. Environmental variable levels chosen were initial altitudes of 20, 40, and 80 m; forward velocities of 18, 36, and 72 m/sec; and descent rates of 1.25, 2.50, and 5.00 m/sec. A full-factorial combination of these levels produced 27 different descent sequences and nine different sequences representing forward locomotion at a constant altitude that were repeated three times.

Table 2 shows two higher-order environmental variables that specify the change in optical locus over time: glide path in degrees and descent rate as a percent of initial altitude per second. Table 3 shows two optical flow variables: optical flow rate and optical flow acceleration. Figure 4 shows how combinations of environmental variable levels produce optical flow invariants, in this case for variables specifying initial fractional loss in altitude.

The observer was instructed to indicate whether the event displayed represented descent or level movement over the surface by pressing one of two appropriately designated buttons. The 54 trials of the single session were randomized individually for each observer with the constraint that no more than four level or four descent trials would occur sequentially. Twenty male volunteers participated in partial fulfillment of an introductory psychology course requirement.

Table 2
Higher-Order Environmental Variables and Invariants

A. Glide Angle (deg)

Descent Rate (m/sec)	Forward Velocity (m/sec)		
	18	36	72
1.25	3.97	1.99	1.00
2.50	7.91	3.97	1.99
5.00	15.52	7.91	3.97

B. Descent Rate as Percent of Initial Altitude (% eyeheight/sec)

Initial Altitude (m)	Descent Rate (m/sec)		
	1.25	2.50	5.00
20	6.25	12.50	25.00
40	3.13	6.25	12.50
80	1.56	3.13	6.25

Table 3

Global Optical Variables and Invariants

A. Initial Global Optical Flow Rate (eyeheights/sec)

Initial Altitude (m)	Forward Velocity (m/sec)		
	18	36	72
20	.900	1.800	3.600
40	.450	.900	1.800
80	.225	.450	.900

B. Initial Global Optical Flow Acceleration (% eyeheight/sec/sec)

Forward Velocity (eyeheights/sec)	Descent Rate (% eyeheight/sec)				
	1.56	3.13	6.25	12.50	25.00
.225	.35	.70	1.41	*	*
.450	.70	1.41	2.81	5.63	*
.900	1.41	2.81	5.63	11.25	22.50
1.800	*	5.63	11.25	22.50	45.00
3.600	*	*	22.50	45.00	90.00

* These cells were not used in the experiment.

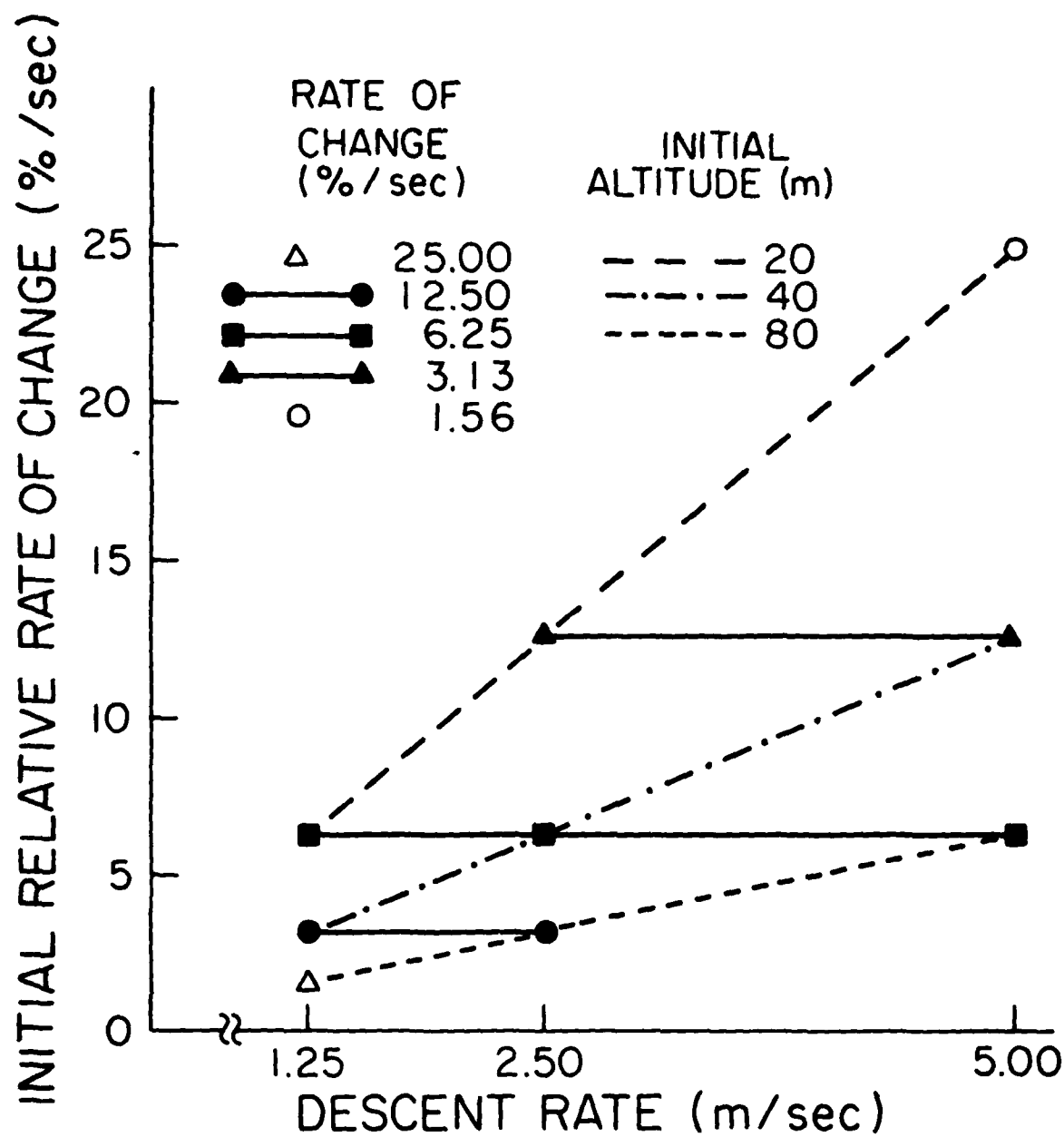


Figure 4. Relative rate of optical change at the initiation of a trial. Solid lines show optical invariants; broken lines are for different initial altitudes.

Results. For errors, significant effects included altitude ($\eta^2 = 2.2\%$), descent rate ($\eta^2 = 3.9\%$), and altitude by descent rate ($\eta^2 = 1.8\%$). For reaction times significant effects included altitude ($\eta^2 = 13.1\%$), forward velocity ($\eta^2 = .3\%$), and the three-way interaction ($\eta^2 = 1.6\%$). Figures 5 and 6 show effects for initial altitude and descent rate (broken lines), as well as for fractional rate of change in altitude (solid lines). Optical parameters specific to fractional change are functionally invariant for all reaction times, but only for low error rates.

Discussion

Of the candidates considered in the two experiments, relative or fractional rates of change best meet the criteria defining a functional invariant for detecting change in one's own motion. Simple rates of optical change (optical flow deceleration and acceleration, increase in optical density, or change in splay angle) have their effects perceptually with regard to their contribution to relative rates of change.

A phase analysis of the relation between perception and the environmental event under study will explicate the relationship among these variables. Three phases relevant to egomotion stimulation will be considered here: (1) the relation between the eye and the ground surface, (2) the information in the light, and (3) retinal transformations.

The first phase requires a description of the environmental event. Change in forward speed expressed as a percent of initial forward velocity describes relative displacement of the eye parallel to the ground surface. This relative rate of environmental change is specified as:

$$100(\ddot{x}/\dot{x}) \text{ (expressed in \% of initial altitude/sec/sec) (1)}$$

Change in altitude expressed as a percent of initial altitude describes relative displacement of the eye perpendicular to the ground surface. This environmental change is specified as:

$$100(\dot{z}/z) \text{ (expressed in \% of initial altitude/sec) (2)}$$

Velocity, change in velocity, and rate of change in velocity are not visible, however. Nor are altitude, change in altitude, and rate of change in altitude. Differences, increases, and decreases are equally specifiable under conditions of no emitted or reflected illumination, i.e., in the dark. What, then, is visible?

The second phase requires a description of what takes place in the medium between the eye and an illuminated, textured ground surface during an event. Four global optical variables have been isolated, all capturing higher-order relations among relations. All have rates of change identical to the rate of loss in speed or altitude. For the case of movement along a level path, \dot{x}/z specifies flow rate and \ddot{x}/z specifies flow deceleration. Global optical flow damping captures a higher-order relation between optical flow deceleration and optical flow rate:

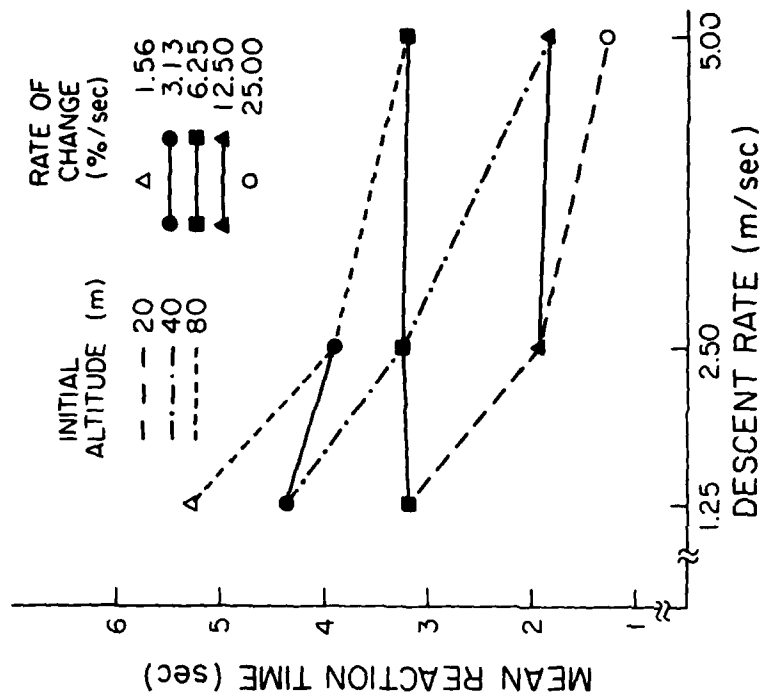


Figure 6. Mean reaction time for the nine combinations of descent rate and initial altitude. Each point represents 60 observations (20 observers \times 3 forward velocities). Solid lines show error rates for invariant values of initial relative rate of optical change; broken lines are for different initial altitudes.

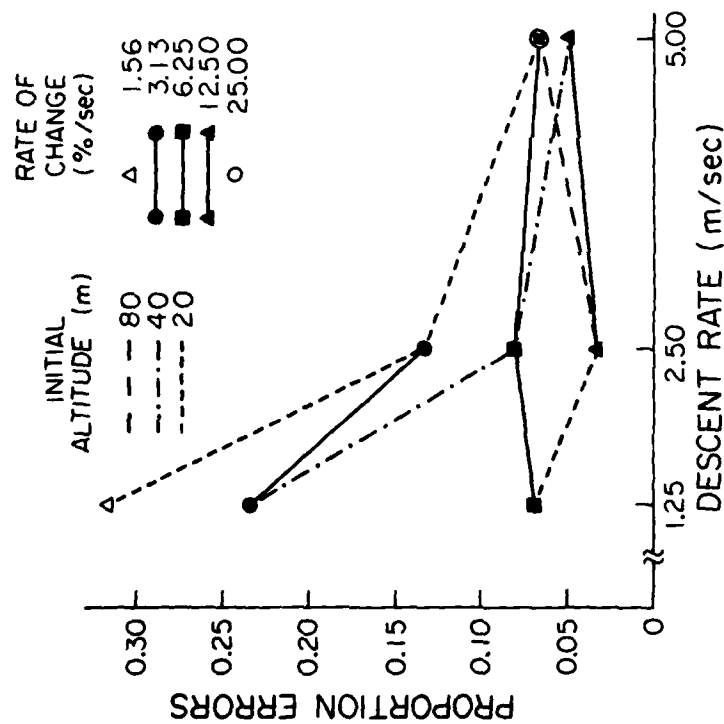


Figure 5. Proportion errors for the nine combinations of descent rate and initial altitude. Each point represents 60 observations (20 observers \times 3 forward velocities). Solid lines show error rates for invariant values of initial relative rate of optical change; broken lines are for different initial altitudes.

$$100(\ddot{x}/z)/(\dot{x}/z) = 100(\ddot{x}/\dot{x}) \quad (\text{expressed in percent of initial forward velocity/sec}) \quad (3)$$

Thus, damping specifies a rate of optical change that is identical to the rate of change in forward displacement of the eye relative to the ground surface. Percent decrease in forward velocity describes the relative change in rate of displacement of the eye at any instant. Percent decrease in optical flow rate describes the optical rate of change occurring in the ambient array along a potential path of observation. The rates of change are identical because optical flow rate change is (lawfully, mathematically) specific to change in rate of displacement of the eye.

For the case of constant rate of descent, three optical variables have been isolated: Global optical flow acceleration relative to initial optical flow rate is specified as:

$$100(\ddot{z}/z^2)/(\dot{z}/z) = 100(\ddot{z}/\dot{z}) \quad (\text{expressed in \% of initial eyeheight/sec}) \quad (4)$$

The same holds for change in global optical texture density relative to initial optical density:

$$100(\dot{z}/g)/(z/g) = 100(\dot{z}/z) \quad (\text{expressed in \% of initial eyeheight/sec}) \quad (5)$$

Warren (1981b) has shown that percent change in global optical splay rate is also identical to percent change in altitude (see Appendix A). Thus when descent rate is constant, all three of the optical variables isolated change at the same relative rate as that for displacement of the eye relative to the ground surface.

These relational identities also hold throughout the duration of the event even though optical variables may change at different rates. For example, with a constant descent rate global optical flow acceleration accelerates over time, while global optical texture density decreases at a constant rate. Since the same is true for global optical splay angle, the relative rates of change of all three optical variables will be the same at reaction time, i.e., equal to the relative rate of change in altitude at that time. Therefore, under these conditions the three candidates for functional optical invariants are indistinguishable in terms of relative rate of change. This is a good object lesson in the redundancy of optical information specifying any given event.

The third phase is a consideration of the proximal transformation as the retina moves forward along the path of observation sampling continuously the change in optical flow. As the eye loses velocity, while moving through the stable optic array, the relative rate of change of optical discontinuities focussed on the retina will be identical to the environmental rate of change. Change in eyeheight will produce a continuous proximal transformation as the retina moves downward along the path of observation sampling continuously the change in optical flow rate, density, and splay angle. The rate of change of positions on the retina past the optical discontinuities focussed on the retina will be identical to the optical and environmental rates of change. This last step completes the chain of specificities for stimulation from

environment, through medium, to retinal variables, and allows perception to be specific to the relation between the eye and the ground surface. The demonstration of functional invariants shows, in turn, that the perceptual system is sensitive to information specifying relative rates of displacement.

The results thus support the concept of transformational realism, i.e., when changes in stimulation appropriately specify the nature of an environmental event, there can be a correspondence between perception and the event. When adequate transformational information is made available, the chain of specificities will hold regardless of the level of detail realism, as long as a minimal density of optical discontinuities is available. Exactly what these limits are, as well as how optical invariants are used in guiding locomotion, pose problems for future study.

References

- Gibson, J. J. The senses considered as perceptual systems. Boston: Houghton Mifflin, 1966.
- Gibson, J. J. The ecological approach to visual perception. Boston: Houghton Mifflin, 1979.
- Harker, G. S., & Jones, P. D. Depth perception in visual simulation (Tech. Rep. AFHRL-TR-80-19). Williams Air Force Base, Arizona: U. S. Air Force Human Resources Laboratory, Operations Training Division, August, 1980.
- Owen, D. H., Warren, R., Jensen, R. S., Mangold, S. J., & Hettinger, L. L. Optical information for detecting loss in one's own forward speed. Acta Psychologica, in press.
- Owen, D. H., Warren, R., Jensen, R. S., & Mangold, S. J. Optical information for detecting loss in one's own altitude. Submitted for publication.
- Warren, R. Global optical bases for the perception of egospeed. Submitted for publication.
- Warren P. Global optical bases for the perception of change in altitude during egomotion. In preparation.

Appendix A

The environmental and optical variables are defined below following the systematization by Warren (1981a,b). A dot over a symbol indicates that the variable's value changes as a function of time.

Environmental variables.

Altitude = z (in m).

Forward velocity = \dot{x} (in m/sec).

Deceleration rate = \ddot{x} (in m/sec/sec).

Descent rate = \dot{z} (in m/sec).

Path velocity = $\dot{S} = \sqrt{\dot{x}^2 + \dot{z}^2}$ (in m/sec).

Ground unit (surface texture element) size = g (in m).

Lateral ground distance of a surface edge from the optical locus
= y (in m).

Glide angle = $\arctan(\dot{z}/\dot{x})$ (in deg).

Optical variables.

Global optical flow rate for level path = \dot{x}/z (in eyeheights/sec).

Global optical flow deceleration = \ddot{x}/z (in eyeheights/sec/sec).

Global optical flow damping = $100(\ddot{x}/\dot{x})$ (in % of an eyeheight/sec).

Global optical flow rate for glide path = \dot{S}/z (in eyeheights/sec).

Global optical flow acceleration (for the special case of constant path speed) = $100(\dot{S}\ddot{x}/z^2)$ (in % eyeheight/sec/sec).

Global optical texture density = z/g (in ground units/eyeheight).

Global optical splay rate: Consider a set of surface texture edges parallel to each other and parallel to the direction of rectilinear locomotion. The optical projections of the parallel edges intersect at a common vanishing point on the horizon. The optical splay of an edge line is defined to be the angular separation of the optical projection of the line from a line perpendicular to the horizon and passing through the common vanishing point. The latter line specifies the direction of locomotion, which may or may not coincide with surface texture edges. In addition to the presence of surface texture, optical splay depends only on height of the optical locus above the ground surface and lateral ground distance of the edge line under consideration from the optical locus.

Splay angle is given by

$SP = \arctan(y/z)$.

For vertical change in rectilinear locomotion with no lateral velocity, the rate of change of splay angle is given by

$SP = (\dot{z}/z) \cos SP \sin SP$.

Optical splay rate, then, depends only on the relative rate of change in altitude and the splay angle of a particular projection line. It is independent of forward velocity. For a given change in altitude, the more a projection line is splayed from the line specifying the direction of locomotion, the smaller the change in splay angle. The relative rate of change in altitude is a scaling factor which applies equally to all splay lines within an optic array, and is therefore an index of global optical splay rate:

$GSP = \dot{z}/z$ (in eyeheights/sec).

SCALED SUBJECTIVE COMPLEXITY OF LOW LIGHT LEVEL TELEVISION AND FORWARD LOOKING
INFRA RED DISPLAYS APPLIED TO COMPUTER IMAGE GENERATED SIMULATION.

Sybil de Groot



Sybil de Groot, Professor
Department of Industrial Systems
The School of Technology
Florida International University
Miami, Florida 33199

Sybil de Groot obtained her Ph.D. in Engineering Psychology from Ohio State University. Her 25+ years of experience in industry, academia, and for the military include a Master's in Experimental Psychology at Ohio State followed by early Human Factors research at John Hopkins and basic visual research at the USN's New London Submarine Base. Following the birth of her children, she joined Dunlap and Associates as a Staff Experimental Psychologist (1958-1962). Returning to graduate school at Ohio State, she worked as a Research Associate (Vision, Human Information Processing) until becoming a NSF Fellow (1967-68). As an Assistant Professor at Montana State University, Dr. de Groot helped develop the Master's Program in Human Factors Psychology, then became an Associate Professor at Florida International University in Miami, and recently, Professor of Industrial Systems.

SCALED SUBJECTIVE COMPLEXITY OF LOW LIGHT LEVEL TELEVISION AND FORWARD LOOKING INFRARED SENSOR DISPLAYS APPLIED TO COMPUTER IMAGE GENERATED SIMULATION¹

ABSTRACT

Nine subjects psychometrically scaled photographic sets of Low Light Level Television (L3TV) and Forward Looking Infrared (FLIR) displays of the same target-areas at pre-sunset along an equal interval continuum of scene-complexity. After each complexity scaling, subjects were debriefed as to their scaling criteria. Subjects also matched both sets of sensor display photographs with wider-angle, color photographs. Analyses included significance tests of different levels of scene complexity, correlations between scales, and content analyses in which scaling criteria were combined into descriptor sets from which visual parameters and physical measures amenable to CIG simulation were derived. While complexity scaling of FLIR displays was reported to be a different and more difficult task, subjects matched FLIR displays with color photographs faster and with fewer errors. Findings support a CIG simulation of L3TV sensor displays using an optical array of edges and surfaces with the degree of realism determined empirically using trade-off parameters. While moderate correspondence was found between L3TV and FLIR display complexity, with FLIR displays subjects revealed different expectancies, were more mission oriented, less certain of scaling criteria, and appeared to use target signatures as cues. Hence, realistic simulation of FLIR displays using the same CIG data base is uncertain unless restricted to time-envelopes when the two sensors present visually equivalent displays.

INTRODUCTION

Background. More is demanded today of Electro-Optical (E/O) sensor display technology than ever before including enhancement of damage assessment missions, flight control reconnaissance, and navigation tasks as terrain avoidance/following. (1,2) A dynamic, functionally interactive Sensor Simulator to present Low Light Television (L3TV) and Forward Looking Infrared (FLIR) views during very low, very fast flights by means of computer image generation (CIG) is under development at the Air Force Human Resources Laboratory at WPAFB.

A fundamental issue in all simulator development is determining what is required for positive transfer-of-training to operational environments on a cost effective basis. Despite plans for extensive use of simulators and ground trainers, there is a serious lack of "hard" human performance data (3) while little empirical data exists about E/O display characteristics and operator performance, especially at altitudes under 1000 feet and speeds in excess of 400 mph. (4) Although diverse opinions exist about what E/O sensor simulation should include, Brig. Gen. B.K. Partin zeroed in on the fact that the effect on operator performance of varying degrees of realism must be established. (5) Thus an assessment of human responses to L3TV and FLIR scenes is a purpose of this research. Since Rosell and Willson cited several display degrading factors beyond the control of sensor designers and, possibly, beyond deciphering by an operator (4), a second purpose was to establish a method to identify visual parameters which should be included in a FLIR/L3TV Sensor Simulator.

Bunker and Heeschen asserted that with computer generated imagery, realism is a function of the complexity of the scene that can be shown. (6) CIG techniques represent real world features by storing 3D information of edges and surfaces to produce a dynamic display on a 2D screen by transformation of the stored data. Although the state-of-CIG-art includes over 5000 edges, the level of instrumentation available at the ASM Branch of AFHRL permitted 2000 visible edges. This is the same as in the Advanced Simulator for Pilot Training with which operators were reported to experience difficulty detecting heights at low altitudes. (4) To improve the perception of distance in simulated displays of open space, Gibson suggested the use of texture gradients. (7) The application of texturing in simulated L3TV/FLIR displays would

¹ Research was initiated while the author was an ASEE-USAF Summer Research Fellow at AFHRL, WPAFB, Oh. and finished at Florida International University, Miami, Fl. under migrant #77-3242 from The Air Force Office of Scientific Research, AFSD, Bolling AFB, D.C.

increase the required number of CIG edges and surfaces as would other features associated frequently with complexity.(8)

Because programming time and hardware costs increase considerably as the number of scene edges increase, scene complexity, held to be a major determiner of realism, is also a major determiner of costs. Hence, trade-offs must be sought which coincide with visual parameters least important for positive transfer-of-training. CIG parameters available for trade-off consideration include edge smoothing, contouring, curvature, the addition of noise, number of grey levels, foliage masking, and weather algorithms.

Objectives. If differences in scene-complexity can be established, computer hardware and programming trade-offs could be determined empirically by simulating a scene of known subjective complexity, varying CIG parameters, and measuring performance. Thus, specific research objectives were:

- to scale the complexity of still L3TV and FLIR scenes.
- to identify scenes at significantly different levels of complexity.
- to determine major perceptual factors associated with complexity of L3TV FLIR displays.

- to relate perceptual with physical factors amenable to CIG simulation.

Assumptions. Subjects are assumed to be replicas of each other and able to produce unidimensional scene-complexity scales with the variability in their judgements distributed randomly. For a given stimulus scene the best value of scene-complexity is mean scale value, thus significant differences can be computed (9) and a scale of scene-complexity developed for a set of L3TV or FLIR displays producing a monotonic relationship with physical dimensions of the stimulus materials.(10)

THE METHOD

Stimulus Materials. The E/O Sensor Lab of the Air Force Avionics Laboratory began recording on to video tape FLIR and L3TV sensor displays of 16 local target-areas taken from atop the AFAL Tower at Wright Patterson Air Force Base in late winter, 1976. Although the FLIR system was a prototype model, the L3TV system was in standard production and use. Stimulus materials for the present research consisted of two sets of sixteen 8"x10" glossy photographs of still video displays of 16 target-areas recorded on 5/11/76 during one video taping between 1915 and 1922 o'clock in the time envelope classified as Pre-Sunset. One set consisted of L3TV displays, the other FLIR displays. The photographs of still video tapes, displayed on a CONRAC QQA 21" monitor, were made with a Hasselblad camera and tripod. Atmospheric and weather conditions at the time of the taping were: Temperature-65.6° F.; Relative Humidity-32%; Visibility-10 miles; Cloud Cover-Clear; Type of day-Hazy.

Both L3TV and FLIR sensor systems can present either a wide or narrow field of view, dimensions depending upon the particular system, model, and operating conditions. Since the sensor systems at the AFAL Tower present a narrow field, the stimulus photographs captured views of the environment subtending 6°20" - 7°40' of horizontal arc and 4°40' - 5°40' of vertical arc at the lens.

At some time-envelopes during daylight hours under good weather conditions, L3TV and FLIR sensors can present displays which are nearly equivalent, visually. Both displays can also look much like the normal, real world visual scene and, at times, present even an enhanced view. At other time-envelopes, however, L3TV and particularly FLIR sensors yield displays with predictably different characteristics, unlike daylight visual scenes. For example, FLIR sensors are noticeably responsive to relative temperature changes which occur around sunset as the heating property of the sun is withdrawn. A period of thermal transition is regularly displayed. This transition period could be fairly brief, depending upon climate and other factors, but it is not necessarily nor is it of constant duration. Some environmental features which have been reflecting heat from the sun cool down and their natural pattern of heat emissivity begins to register. Among environmental features which generate no heat of their own, some cool quickly while others dissipate heat stored during the day quite slowly over a period of hours. Similarly, in a night environment

standard L3TV sensors can be over-sensitive to small light sources. The phenomenon of "blooming", in which a light may become considerably enlarged, may occur. If corrections are not made, a light can bloom to flood the entire display.

Since the displays used in this research were recorded during the time-envelope of Pre-Sunset in late spring, of the two sensors the L3TV display most closely approximated a pre-dusk visual scene with some typical real world optical features such as elongated shadows and rounded, opaque foliage; no lights were blooming. The FLIR display revealed the beginning of a thermal transition period. Concrete objects appeared slightly warmer than the earth, while close foreground trees began to show a natural heat emission pattern with lightish trunks and branches. Some heat emitters, undetectable during the day, appeared as whitish blobs or smears when seen through foliage. At times, the level of water was faintly discernable within a nearby water tower.

The original stimulus materials are classified and cannot be presented. To give a rough impression of the content of the FLIR and L3TV displays, Figure 1 contains reproductions of daylight color photographs of each target-area, numbered and titled as during taping. While each picture has been cropped to the approximate narrow field of view, photographs of FLIR and L3TV sensor displays are not visual equivalents of these surrogates.

Procedure: Experiment 1. In separate sessions nine subjects scaled the two sets of photographs along a metathetic continuum of scene complexity divided into 7 equal intervals. (11) The subject sat before a table across which seven equally spaced, numbered categories were indicated with #1 labeled "Least Complex," #4 "Average Complexity," and #7 "Most Complex." The subject was informed that the stack of photographs immediately in front of him were taken from L3TV (or later, FLIR) video tapes of 16 local target-areas recorded at Pre-Sunset in late spring. He was asked to sort the photographs into one of the 7 categories of complexity, making the steps between categories as equal as possible with at least 1 photograph assigned to each category. Subjects could perform the scaling task in any manner they chose and take as long as they wished until they were satisfied with their scaling. All subjects scaled photographs of L3TV sensor displays first and were then debriefed. Later, the process was repeated with photographs of FLIR sensor displays.

Debriefings. After a subject indicated he was satisfied with his scaling, photographs in all categories were spread out vertically for maximum visibility. Comments were elicited from the subject by asking a series of questions such as: "What were you thinking about as you arranged the pictures in these categories? How did you decide which picture should go where? What made you decide this picture, say, belonged here instead of there (pointing)? Can you describe the difference you found between pictures you placed in lower categories with those in the middle or higher?" Since a pause was taken between each question, subjects usually started reporting about their scaling criteria by the second question. Observations and a verbatim transcript of comments made during scaling and debriefing were recorded.

Procedure: Experiment 2. Subjects matched both sets of FLIR and L3TV display photographs previously scaled for complexity with sixteen 3"x5½" color photographs containing within them target-areas. Subjects, handed the stack of small color photographs, confronted a covered table on which 16 FLIR (or L3TV) photographs were arranged in a 4x4 display. The arrangements of FLIR and L3TV photographs and the sequence of color photographs were randomized for all presentations. A subject's task was to match the sensor display photos as quickly as possible by placing a small color photo containing the scene on top of each. At a given signal, the cover was removed and a stop watch started which was stopped when the subject finished. While the subject stepped out of the room, the Experimenter noted any errors, set up the second arrangement, covered it, and rearranged the color photographs. Matching order was counterbalanced among subjects.

Subjects. Time and cost precluded subject groups of users and trainees reported to be the best judges of training requirements. (12,13) The group of 9 subjects was a sample of convenience selected on the basis of availability combined with knowledge

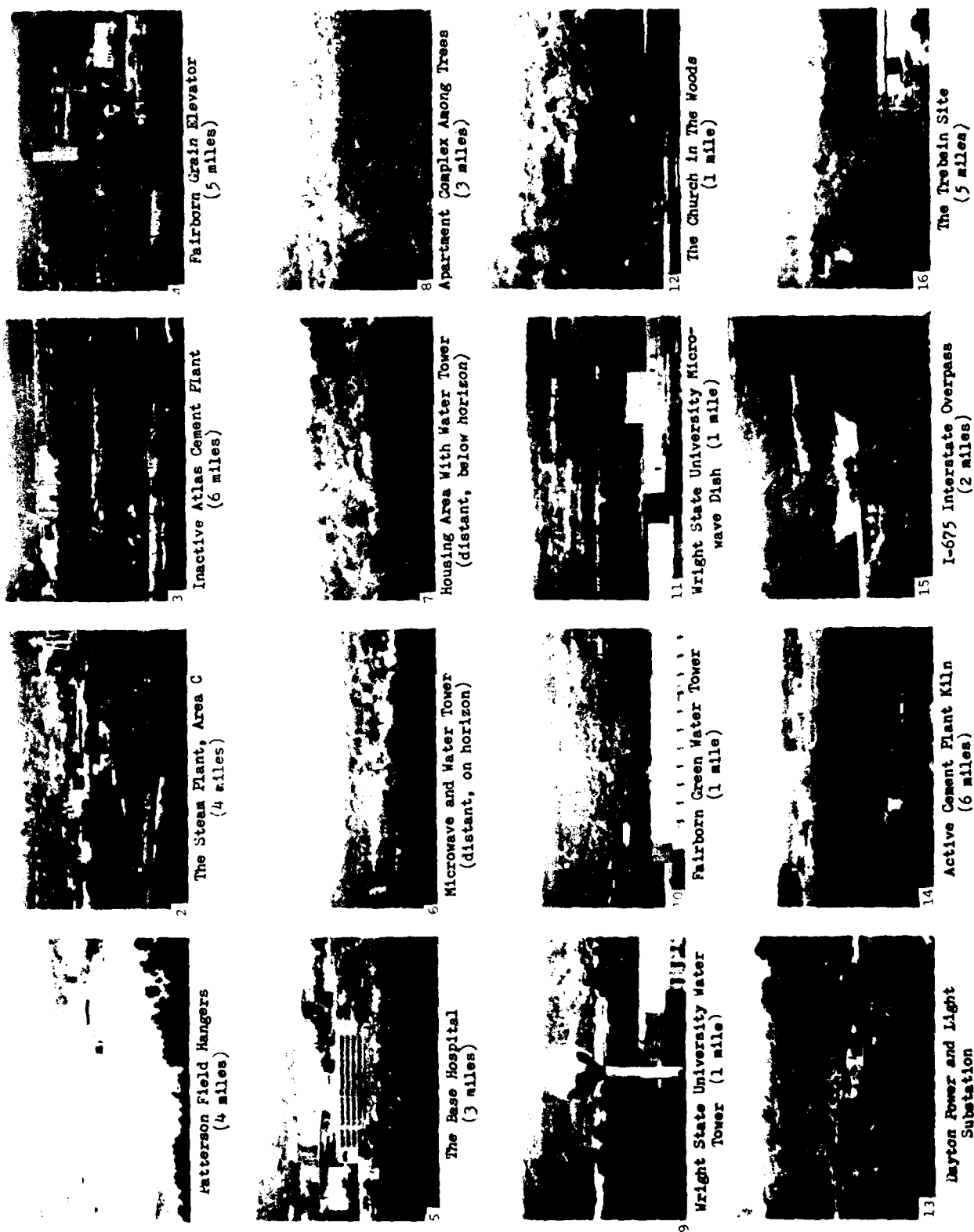


Figure 1. Number, Title, Distance, and Surrogate Daylight Photograph of Approximate Target Area for Each of the Sixteen FLIR/L3TV Displays.

and experience with E/O sensors. It included 2 Human Factors Psychologists, 4 Computer Engineers, and 3 E/O Sensor Experts. Although visually representative of user groups, the subjects' representativeness in terms of expectancies, cognitive associations, and use of perceptual cues is indeterminant.

Content Analyses. To determine major factors associated with subjective complexity of L3TV and FLIR displays, transcripts of each subject's comments during scaling and debriefing were subjected to a content analysis. Primary scaling criteria were defined as descriptors or key words used by a subject to describe the overall continuum, or to discuss the major differences between end points of the scale. Secondary criteria were defined as descriptors mentioned secondarily, or used to distinguish between intermediate scaling categories. Concepts used as criteria in describing the scaling task by a majority of subjects were included in the analysis. The two content analyses consisted of the following general steps:

- 1) Examination of the verbatim comments and debriefing responses with preliminary classification into primary and secondary descriptors stressed by each subject.
- 2) Enumeration of primary and secondary scaling criteria adduced by combining similar descriptors from all subjects.
- 3) An attempt to synthesize content analysis descriptors into physical parameters and derive physical measures useful in CIG applications.

RESULTS AND DISCUSSION

L3TV Complexity Scaling. Frequency distributions of the subjects' categorizations of each L3TV scene with the mean complexity value, \bar{X} , and standard deviation, s , are presented in Table 1. The scenes are ordered according to their mean complexity from low scale values indicating less complexity to greater complexity represented by higher scale values. The non-overlapping distributions enclosed in boxes identify scenes satisfying the Guttman-like steps required in Scalogram Analysis of L3TV

Table 1. Ordered Frequency Distributions of L3TV Complexity, N = 9.

#	Scenes	Scale Values		Complexity Categories						
		\bar{X}_9	s_9	least			most			
	Abbreviated Title			1	2	3	4	5	6	7
7	Housing Area (landscape)	1.1	0.3	8	1	0	0	0	0	0
16	Trebein Site (landscape)	1.7	0.9	5	2	2	0	0	0	0
8	Apartment Complex, Trees	1.9	0.8	3	4	2	0	0	0	0
12	Church in Woods	2.2	0.8	1	6	1	1	0	0	0
6	Microwave & Water Towers	2.3	1.2	2	4	2	0	1	0	0
15	I-675 Overpass	3.0	0.7	0	2	5	2	0	0	0
9	W.S.U. Water Tower	3.4	0.7	0	1	3	5	0	0	0
11	W.S.U. Microwave Dish	3.4	0.7	0	1	3	5	0	0	0
13	D.P.&L. Sub-station	3.8	1.3	0	1	4	1	2	1	0
14	Active Cement Plant	4.1	0.8	0	0	2	4	3	0	0
10	Fairborn Water Tower	4.4	0.9	0	0	1	4	3	1	0
4	Fairborn Grain Elevator	5.4	0.5	0	0	0	0	5	4	0
3	Inactive Cement Plant	5.4	1.0	0	0	0	2	2	4	1
2	Steam Plant	5.6	0.9	0	0	0	1	3	4	1
1	Patterson Field Hangars	6.6	0.5	0	0	0	0	0	4	5
5	Base Hospital	6.9	0.3	0	0	0	0	0	1	8

display complexity. (14) Figure 2 graphically presents scaled L3TV displays and the results of two-tailed t-tests of differences between the means. (15,16) Four significantly different levels of L3TV display complexity at the 99% level of confidence ($p < .01$) are identified by scene numbers enclosed in solid lines. Six significantly different levels of L3TV display complexity at the 95% level of confidence ($p < .05$) are established by the inclusion of 3 additional scenes enclosed in dashed lines. To permit a rough appraisal of changes in scene content-areas across six levels of complexity, scaled representative photographs of the target-areas at the 6 levels identified in Figure 2 are presented in Figure 3. Despite the loss of resolution in the surrogate photographs, the pre-sunset L3TV sensor displays also had diminished resolution but with different shadows, figure-ground relationships, less freedom

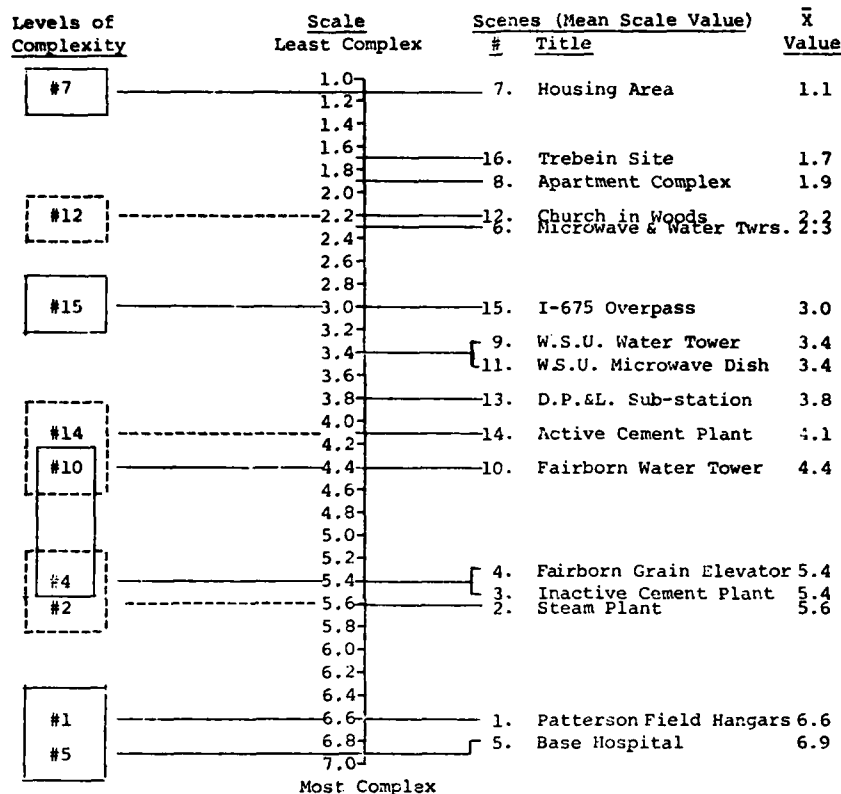


Figure 2. Scene Complexity Scaling of L3TV Scenes With Significantly Different Levels of Complexity Identified

from noise, and some edge distortion.

L3TV Content Analysis and Conversion to Derived Measures. Although few subjects made comments while scaling L3TV displays, descriptors elicited during debriefings were enumerated from transcripts. Table 2 presents similar descriptors combined into seven sets with the number of subjects using the descriptors of each set as primary or secondary scaling criteria, their combined total, and the percent of the subject group.

While one subject thought he might have gotten a different ordering if asked to scale on "clarity", the assumed unidimensionality of L3TV scene-complexity appeared to be dubious for only one subject who discovered that he must have used some conflicting criteria which might not be on the same scale. Most subjects immediately focused on specific features emerging from the figure-ground relationship with 100% discussing "objects."

An unmet expectation derived from the literature was that brightness, the "luminous output pattern," and contrast would be mentioned frequently. (17) Instead, only one subject spoke of "broken light uniformity." However, the light pattern may have been related to the way in which the background was regarded. To the 7 subjects who mentioned it, the background (terrain, landscape, foliage) appeared relatively unimportant. Only one subject implied a possible masking function. Unbroken lightish areas were merely trees to one subject while two described the vegetation background as non-informational and pretty much the same across all scenes. Three subjects clearly saw scenes comprised mostly of terrain or landscape as least complex while another referred to the "garbage of these surrounds." Two subjects mentioned "clutter", one referring to targets lost in the "clutter" of less complex scenes, while the

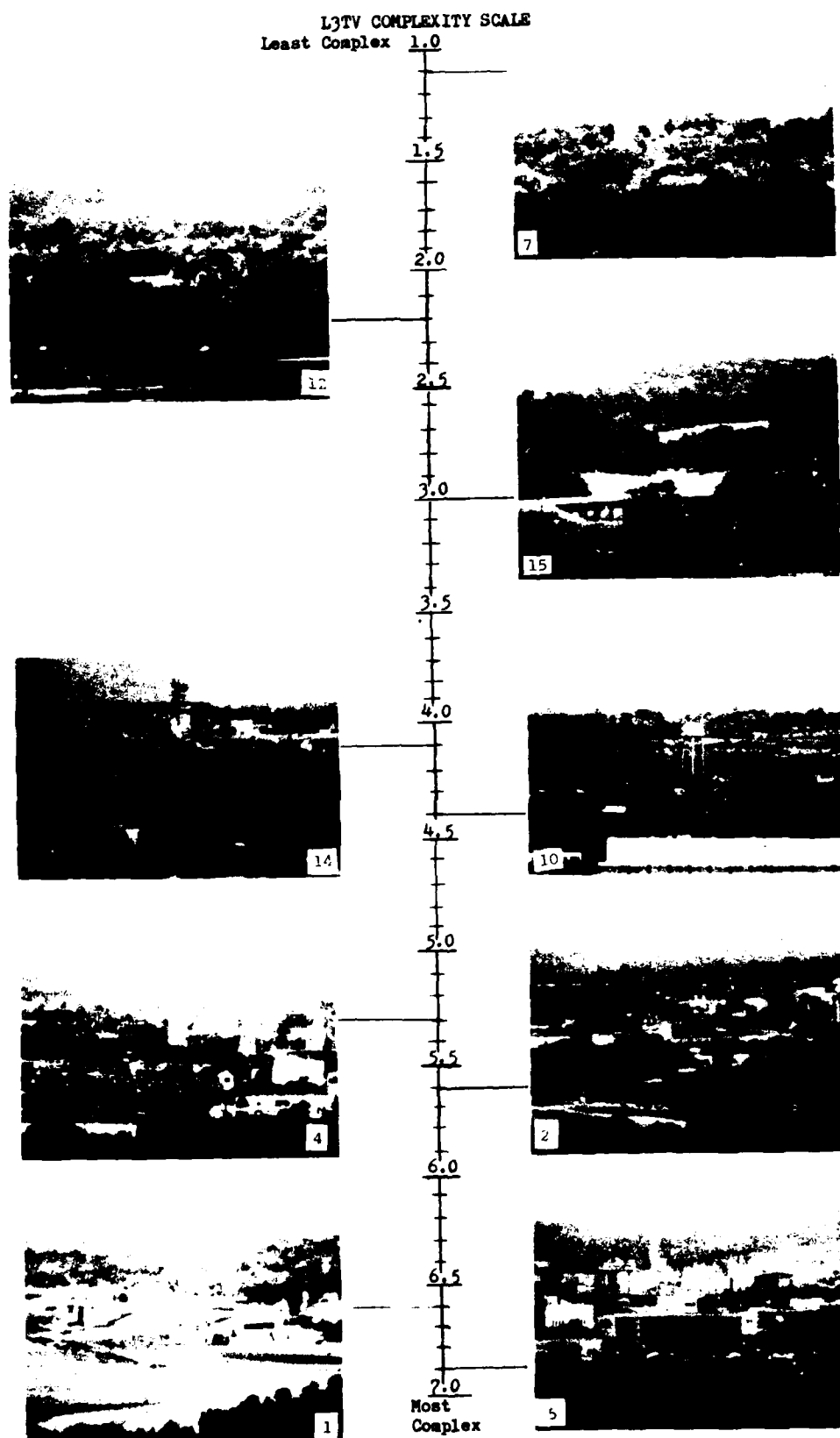


Figure 3. Surrogate Daylight Photographs of L3TV Target-Areas at Six Significantly Different Levels of Scene Complexity.

Table 2. Content Analysis of L3TV Scene Complexity With Synthesized Parameters and Derived Measures.

CHI- TNR1A				SET	DESCRIPTORS & KEY WORDS	PARAMETERS	DERIVED MEASURES
1st	2nd	N	%				
7	2	9	100%	1.	Number/more/frequency of man-made objects; cultural detail/information.	I. The number of man-made objects or object-areas in a scene.	(1) The number of separate, single entities ignoring substructural aspects, attachments, or features.
6	1	7	78%	2.	Vegetation, foliage, landscape, terrain, surrounds, ground, light uniformity.		(2) The number of single entities including substructural aspects provided the smaller feature can be recognized as a completed feature of the larger.
6	0	6	67%	3.	Simple/complex/outstanding geometric patterns/forms; distinctive/variety of shapes; complexity of man-made/discriminable objects.	II.a. The ratio of the area of man-made objects to the combined areas of foliage/terrain & sky. <u>or</u> b. The percentages of total scene area composed of man-made objects/ foliage & terrain/ sky.	
4	2	6	67%	4.	Area/size/percent/amount of man-made structures; cultural details relative to ground.		(3) Area of man-made objects.
1	5	6	67%	5.	Detailed/fine-type structures; lines of objects; detectable details; supporting/complex substructures in primary structures; sub-objects.		(4) Area of foliage/terrain. (5) Area of sky.
3	2	5	56%	6.	Black to white changes; clarity; clearest scenes; sharp edges; crispness/resolution; vague/distinct objects/targets.	III. The number of straight and curved lines which make up visible internal and external portions of man-made objects.	(6) The number of straight, curved, and total external lines. (7) The number of straight, curved, and total internal lines.
1	4	5	56%	7.	Number/direction/different directions of lines; straight/curved lines; detectable detail edges.	IV. Scene quality as reflected in resolvable detail.	(8) a. The shorter dimension of the smallest object in a scene during (2) <u>or</u> b. The length of the shortest line included in (6) or (7) above.

other described a profusion of objects in the most complex as "clutter."

The author's privately held notions that subjects would verbally relate informational content with scene complexity, and that most subjects would show a mission or task orientation, received little support. "Information" was used by 3 subjects, but in different contexts. Although all subjects were or had been associated in some way with the development of a Sensor Simulator, during L3TV debriefings only a total of 4 subjects mentioned any mission-oriented or task-performance words as "Target," "Recognition," "Identification," or "Detection."

Before attending to physical parameters and measures evolved from the content analysis in Table 2, a major limitation of the present study must be clearly stated: this research, restricted by the nature of the particular stimulus sets and subject group used, is best regarded as a heuristic, feasibility study. For example, in the entire stimulus set there were no natural geographical features or foliated objects which stood out as "figures." In addition, with the exception of patches of an interstate highway or part of a runway, there were few visible man-made alterations of terrain such as cultivated fields, orchards, local roads, or even fences. To satisfy simulator requirements for training in a variety of flight missions under varying circumstances, a larger data base would be required for definite conversions.

As illustrated in Table 2, the first physical parameter is based on Set 1 containing responses from 100% of the subjects. This parameter involves merely a counting process following an explicit definition of what constitutes a man-made object. Gestalt principles on the properties of figures plus grouping factors for partially concealed patterns should suffice. (19) Each separate figure, no matter the size or partial obscuration, could be counted as one. (20) Because figures are not necessarily the same as "man-made objects" (21), measures (1) and (2) were derived.

Set 4 (area of man-made objects) is related to Set 2 (terrain, foliage, etc.) but not necessarily inversely because the amount of sky visible varied with the scene. Since the sky was never cited as a scaling determiner, subjects probably lumped sky area in with foliage/terrain as background in this stimulus set. Yet it is also probable that in a terrain avoidance task the amount of visible sky would achieve greater significance. Sets 2 and 4, combining the responses of 89% of the subjects, were synthesized into Parameter II. Two aspects of this parameter are suggested with the second expected to be more applicable with a greater data base. The three measures, (3), (4), and (5), necessary to compute Parameter II could be achieved by placing an appropriately fine grid over a display photograph and counting area units.

Set 3 combines concepts of shape or outline complexity while Set 5 is focused on interior structures or patterns. Since both sets deal with aspects of object detail, they are related to Set 7 (number, kind, and direction of lines) not only because visual detail is graphically displayed by the presence of detectable lines or quick gradient changes but also because edge, slit, and line detectors are held to monitor specific regions of the retina. (22) Hence Parameter III incorporates the responses of 100% of the subjects and can be enumerated directly in the two measures (6) and (7), most meaningful to CIG programmers.

The common thread running through the descriptors in Set 6, incorporating responses of 56% of the subjects, is an apparent reference to image or scene quality. Subjectively, image quality of real-life scenes is influenced by many factors such as scene content, overall brightness, contrast levels, texture gradients, assigned task, noise, etc. A similarly extensive list of physical parameters has been identified as determiners. (10) Yet the traditional psychophysical approach tends to put first emphasis on resolution, as do many current optical, photographic, and electronic display approaches. (23,24) The human ability to resolve video targets appears to vary as a function of the geometry of the test pattern while varying system resolution appears to be a function of the number and length of lines and geometries of test charts. (10) Thus, attempting the simplest first, Parameter IV relates scene quality with resolvable detail. Since the visual acuity of the subjects exceeded system resolution revealed in the set of stimulus photographs, a logical initial approach to scene or image quality would be to measure the smallest extent of line or objects in each scene which can be recognized as such in measures (2), (6), and (7). Toward an L3TV/CIG Property List. Rather than taking the physical parameters synthesized from the content analysis and their constituent measures presented in Table 2 at face value, each measure should be validated by pairing the value found for each scene on the 8 derived measures with that scene's mean L3TV scene complexity score and applying any one of several correlational techniques. (25,26) In general, only measures found to have moderate to high positive correlation coefficients or good predictive ability should be retained. By such a culling an initial L3TV/CIG "Property List" could be established indicating which CIG parameters are most important for simulation and hence, must be included in a Sensor Simulator to maximize transfer-of-training.

Scaling FLIR Complexity. Two outstanding features distinguished the FLIR experimental sessions from L3TV scaling. The first was initial subject response to the scaling task; many started talking early in the process of scaling. The following excerpts from comments of six subjects demonstrate that despite their knowledge and familiarity with FLIR sensor displays, a majority seemed ill prepared: "Things are quite different...considerably harder!" "Holy Cow! This is a different ball game." "This is much harder...not the same job!" "This brightness is too high!" "...more difficult... than earlier...(some) overexposed." "...just isn't the same task."

The second feature, discovered at the end of a debriefing, was that the one subject who had been a pilot scaled the FLIR photographs as if he were on the "tactical mission of reconnaissance strike utility." Since the subject volunteered to rescale the set, it was so arranged. Subsequent debriefing revealed that in his second scaling the subject had assumed "the strategic mission of low level ingress." While this

subject had displayed a slight mission orientation in L3TV scaling, scaling FLIR scene-complexity became inextricably related to specific mission performance. Because none of the other subjects had demonstrated similar behavior, whether to include or exclude this subject's data in the scaling analysis became an issue. Examination of the subject's initial FLIR scaling (assumed tactical mission) revealed disparate categorization relative to the response distribution of the other 8 subjects on 56% of the scenes. Examination of his second scaling (assumed strategic mission) revealed an even greater disparity on 69% of the scenes. Inclusion of either scaling affected some means and standard deviations markedly. Hence, this subject was declared a non-replicate and his data excluded from the scaling analysis.

Ordered frequency distributions of the remaining 8 subjects' complexity scalings for 16 FLIR sensor display photographs are presented in Table 3 with their mean complexity scale value, \bar{X}_g , and standard deviation, s_g . As in earlier analysis, non-overlapping distributions encased in boxes reveal 3 Guttman steps of scene complexity. However, 7 FLIR scenes are encompassed in these steps in contrast to only 4 L3TV scenes earlier. Another comparison with Table 1 reveals that the frequency distribution for FLIR photographs, although based on one less subject, are a bit more spread-out than those for L3TV, particularly as scene complexity increases.

Table 3. Ordered Frequency Distributions of FLIR Complexity, N=8

Scenes		Scale Values		Complexity Categories							
#	Abbreviated Title	\bar{x}_g	s_g	least				most			
				1	2	3	4	5	6	7	
7	Housing Area (landscape)	1.0	.0	8	0 ¹	0	0	0	0	0	0 ²
8	Apartment Complex, Trees	1.6	.7	4	3	1	0	0	0	0	0 ²
12	Church in Woods	2.5	.8	0	5	2	1	0	0	0	0 ²
16	Trebein Site (landscape)	2.9	.8	0	3	3	2	0	0	0	0
6	Microwave & Water Towers	2.9	1.0	1	1	4	2	0	1	2	0
10	Fairborn Water Tower	3.0	.8	0	2	4	2	0	0	0	0
9	W.S.U. Water Tower	3.4	.7	0	1	3	4	0	0	0	0
15	I-675 Overpass	3.8	1.3	0	2	1	2	3	2	0	0
11	W.S.U. Microwave Dish	4.1	1.0	0	0	2	4	1	1	1	0
13	D.P.&L. Sub-station	5.1	1.4	0	0	2	1	2	1	3	2
3	Inactive Cement Plant	5.5	1.3	0	0 ²	1	0	3	2	2	1
2	Steam Plant	5.6	1.2	0	0	0	2	1	3	2	2
14	Active Cement Plant	5.9	.8	0	0	0	0	3	3	2	2
4	Fairborn Grain Elevator	6.0	.8	0	0	0	1	2	4	2	2
1	Patterson Field Hangars	6.1	1.1	0	0	0	1	1	2	4	2
5	Base Hospital	6.1	1.1	0	0	0	2	1	3	2	2

The excluded ninth subject's responses are illustrated in Table 3 by supranumerals. The superscript 1 indicates the subject's response assuming "the tactical mission of reconnaissance strike utility," the superscript 2 that for "the strategic mission of low level ingress." Had the ninth subject's first scaling been included, two Guttman steps would have resulted; had his second been included, none.

As in the earlier treatment of L3TV scenes, two-tailed t-tests of the difference between means were performed revealing four significantly different levels of FLIR scene complexity at the 99% level of confidence. These are illustrated in Figure 4 by scenes whose numbers are enclosed in solid lines. The inclusion of FLIR scenes differing in complexity at the 95% level of confidence ($p .05$) did not increase the numbers of complexity levels: it merely provided a few alternative scenes, enclosed in dashed lines, at the four levels of FLIR scene complexity already established. (16)

Although FLIR sensor displays are not their visual equivalent, surrogate daylight photographs illustrate 4 levels of FLIR scene-complexity in Figure 5. FLIR Content Analysis. Most subjects found complexity scaling of FLIR displays not only more difficult than L3TV scaling, but also a different kind of task. Although two subjects reported that they used the same criteria as earlier, one expressed dissatisfaction with his scaling. Others appeared less certain than before about what

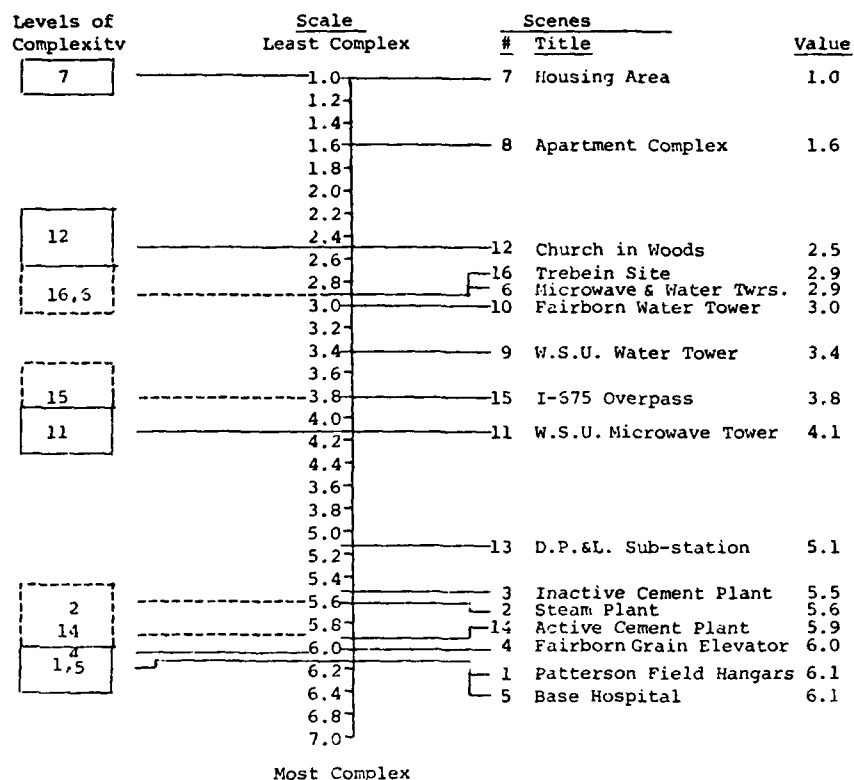


Figure 4. Complexity Scaling of FLIR Scenes Based on N = 8
With Significantly Different Levels of Complexity.

criteria they had actually used. Two reported that criteria appeared to change as they moved up the scale; another reported using conflicting criteria. Due to the above and to evidence of increased mission orientation, the ninth subject's comments during his first FLIR debriefing were included in the content analysis.

Perhaps because subjects sometimes had difficulty determining where the background left off and objects began, the background in FLIR displays was not treated as unimportant. Several subjects mentioned masking or smearing of objects into the background. Others chose to treat whited-out portions of buildings in the immediate foreground as ground. One subject specifically noted the area taken up by the sky.

The assumed unidimensionality of a scene-complexity continuum appears questionable with FLIR displays because many subjects showed increased uncertainty about their scaling criteria. Several spoke of flipping over or folding over the scale or parts of the scale. While a mission orientation was fully manifested by the ninth subject, a similar association with FLIR displays appears to influence other subjects because the use of mission-oriented and task-performance words occurred with greater frequency than in L3TV debriefings. For example, "Target" was used by twice as many subjects as before. "Recognition," previously cited by one, was referred to by five. "Identification" was mentioned by only one of the two using it earlier, but here with reference to "check-points" and "centers of man-made somethings." "Detection" was not used by any subject after scaling FLIR photographs---but neither were there references to sub-objects, sub-structures, or sub-patterns. "Information" was used more frequently with FLIR than with L3TV displays. Two subjects used it synonymously with object detail. Three referred to more global concepts of display/terrain/or cultural information.

The luminous output pattern or scenic pattern of contrast levels (17), while not cited directly, appeared to give many subjects difficulty. Although intellectually prepared to scale the heat patterns of FLIR displays, several subjects failed initially to recognize the whiteness/brightness of some display areas as information cues of relative heat or fuzzy edges of objects as heat emissivity. A couple of

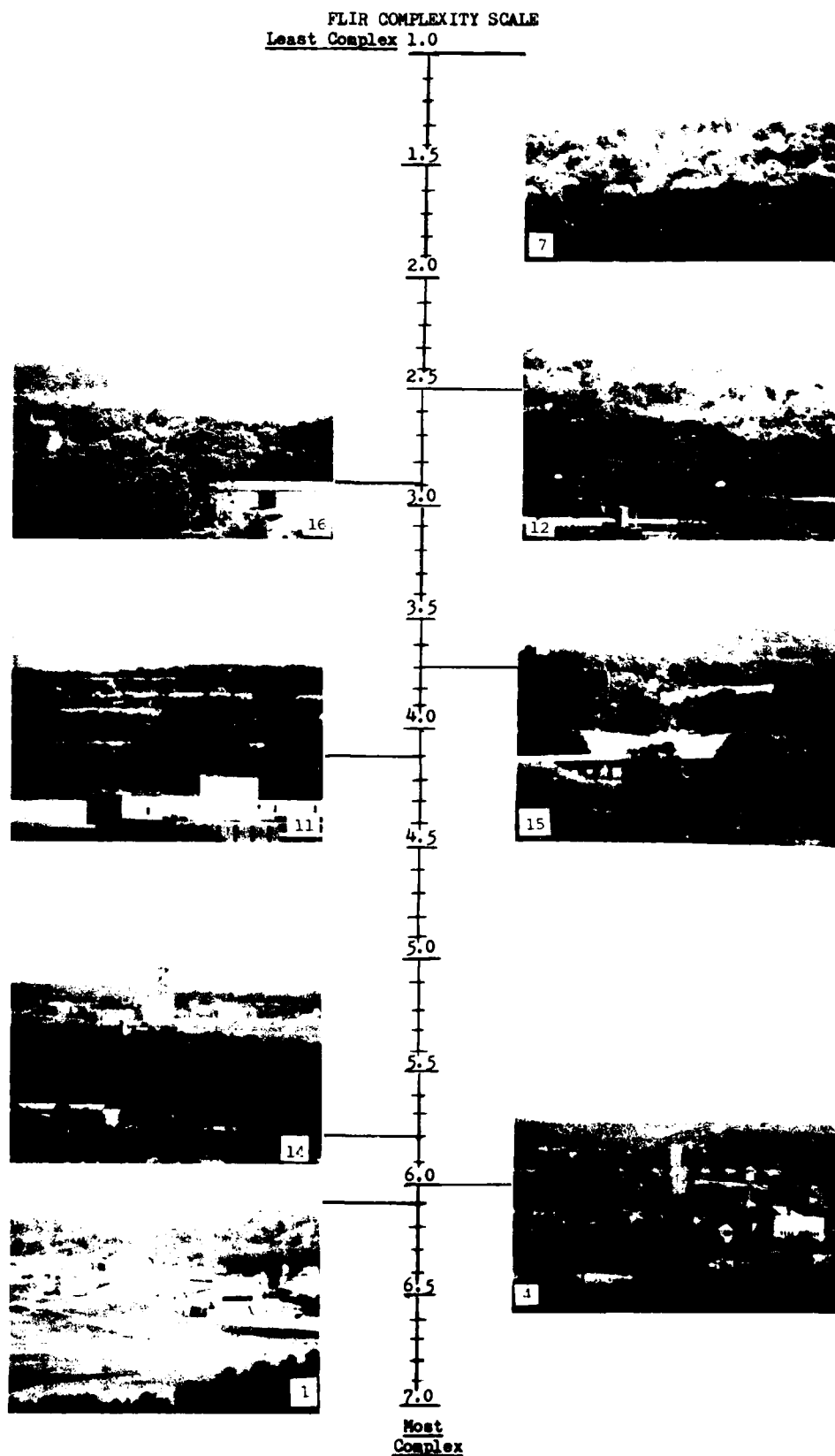


Figure 5. Surrogate Daylight Photographs of FLIR Target-Areas at Four Significantly Different Levels of Scene Complexity. (N=8)

subjects had to remind themselves what light areas meant. Some subjects complained about the washing-out, smearing, or obliteration of figural detail by brightness or being "over-exposed." In short, infrared information was often treated as noise. Despite prior experience, the predominant "gut level" response of the subject group was as if they had expected a display of a normal visual scene where brightness meant light and not heat.

Following the same procedure as earlier, a content analysis was performed on the transcribed comments and the results are presented in Table 4. Descriptors in parentheses are those of the ninth subject. With the exception of Set 8, descriptor sets are presented in Table 4 which contain comments of a majority of subjects.

Table 4. Content Analysis of FLIR Scene Complexity and Comparison of FLIR and L3TV Analyses.

CRI- TERIA TOTAL				DESCRIPTORS & KEY WORDS	FLIR Analysis	L3TV Analysis		
1st	2nd	N	SET		Topic or Subject	SET	Topic or Subject	%
8	0	8	89%	1. Number of recognizable/separate/man-made objects/targets; white/heat-producing spots (number of target-like things)	Number of man-made objects	1.	Number of man-made objects	100%
3	4	7	78%	2. Standout/distinct/clearer/more saturated than ground; contrast less blending/smeared/blue/red; (threat, false alarm)	Contour/edge gradient descriptors	2.	Background	78%
2	5	7	78%	3. Dociles/density of white/blobs; bright/light/heat emitting man-made objects (targets, defenses)	White-hot=man-made	3.	Object detail: pattern, shape, outline complexity	67%
5	1	6	67%	4. Percent area/size/amount of man-made objects/targets; amount white to surrounds/sky; density of man-made per unit area.	Proportion of object area to surrounds	4.	Proportion of object area to surrounds	67%
6	0	6	67%	5. Washed out/obliterated information; masked detail; too white/high brightness; poor quality, over-exposed (time consuming).	Detail; Masked or washed out	5.	Object detail: interior complexity	67%
2	4	6	67%	6. Defined/cultural detail; different/distinguishable things; specific/complex objects/shapes (differentiated targets).	Cultural detail, object shape	6.	Scene or image quality (resolution)	56%
1	4	5	56%	7. Homogenous/darker background; lighter trees/scene/foliage; surrounds; distribution of light; (masking=foliage, clutter)	Nature of background	7.	Lines and edges	56%
2	1	3	33%	8. Recognizable patterns; reverse recognition, (man-made geometry & patterns or unique shapes)	Patterns			

Comparison of FLIR and L3TV Content Analyses. Table 4 also presents a summarization for sets in both content analyses with solid lines connecting equivalent sets. Similarities can be noted in contrasting the FLIR content analysis of Table 4 with that of L3TV's Table 2 in that three sets of descriptors appear directly comparable. In both analyses Set 1, mentioned by the greatest number of subjects, refers to an increasing number of objects in a scene as complexity increases. Similarly, both Sets 4 refer to the proportion of object area as contributing to complexity. Set 7 in the FLIR analysis contains descriptors of the nature or appearance of the background, similar to Set 2 in the L3TV analysis. While 5 of the 8 sets in the FLIR analysis have no single equivalency, Set 2 of the FLIR analysis appears to be partially covered by Sets 6 and 7 of the L3TV analysis (dashed lines). Conversely, Set 3 of the L3TV analysis appears partly included in Sets 6 and 8 of the FLIR analysis.

From the preceding discussion and Table 4, it appears that the visual parameters and measures derived to quantify L3TV displays which can be most appropriately applied to FLIR displays are those based on L3TV descriptor sets 1, 2, and 4, namely:

Parameters I and II a or b with derived measures (1) (since sub-structural objects were not mentioned), (3), (4), and (5) (since sky was mentioned).

Evidence presented thus far indicates that while there is some correspondence between the visual parameters of FLIR and L3TV displays, that correspondence is far from total. One way to evaluate the degree of correspondence is by correlation. The complexity categories assigned the same target-area when scaling L3TV and FLIR photographs were correlated for each subject. the resulting coefficients, r , are presented in Table 5 with an estimate of the amount of variance in one scale common with or due to the variance in the other, r^2 . (27) The ninth subject's correlation using his first FLIR scaling assuming the tactical mission of reconnaissance strike utility is presented in parentheses. The average correlation, \bar{r}_9 , and common variance, \bar{r}_9^2 , include the ninth subject's data while the subscript 8's do not.

Table 5. Correlations and Common Variances Between Complexity Scales.

<u>Correlation Coefficients</u> <u>for Each Subject, r</u>		<u>Common Variance Between</u> <u>Each Subject's Scales, r^2</u>	
+.75		56%	
+.72		52%	
+.48		23%	
+.92	$\bar{r}_8 = .77^{**}$	85%	$\bar{r}_8^2 = 61.3\%$
+.70		49%	
+.82	$\bar{r}_9 = .72^{**}$	67%	$\bar{r}_9^2 = 55.6\%$
(+.31)		(10%)	
+.89		79%	
+.89	(** $p < .01$)	79%	

Inspection of Table 5 shows both average correlations to be significantly different from 0 at the 99% level of confidence and the common variance found between the two complexity scales are about 55% and 61%. Thus a moderate linear relation is found to exist between the L3TV and FLIR complexity scales. These statistics attach an added importance to the first two parameters and 4 of their 5 measures derived earlier:

I. The number of man-made objects or object area in a scene: (1) The number of separate, single entities, ignoring sub-structural aspects. (2) (not applicable).

II. The ratio or percent of the area of man-made objects to the combined or separate areas of foliage/terrain and sky. (3) The area of man-made objects. (4) The area of terrain/foliage. (5) Area of visible sky.

However, the individual who showed the greatest mission-orientation during FLIR complexity scaling also revealed the lowest correlation (+.31) and the lowest common variance (10%). That ninth subject's performance plus the increased mission-orientation of the other subjects while scaling FLIR scene complexity is an indication that task assignment has the ability to modify visual parameters and perceptual cues. This is brought more clearly into focus when the ninth subject's two complexity scalings of FLIR display photographs are correlated. FLIR complexity values assigned assuming a reconnaissance strike utility mission correlated with those assuming low level ingress at $r = -.13$, not significantly different from 0. When scale values from the same subject's second FLIR complexity scaling, the assumed low level ingress mission, are correlated with his original L3TV complexity values, a correlation coefficient of $r = -.68$ results, significantly different from 0 at $p < .01$.

Thus although the 50% correspondence found between the two complexity scales is moderately good, not only the content of FLIR displays but subjects' responses to that content differed from those to simultaneously recorded L3TV displays. Comments made during FLIR debriefings reveal issues contributing to the non-correspondence between FLIR and L3TV scene complexity. Those comments involve: a) different classifications of figures of interest vs. man-made objects, b) changing definition of clutter and noise, c) increased task/mission orientation, d) target cues or target signatures vs. shapes, patterns, and graphic detail, and e) differing perceptual sets and expectancies.

The above indicates that now pilots actually use sensor displays, most particul-

arly FLIR displays under specific flight assignments, must be taken into account when designing a simulator incorporating computer generated imagery for Sensor Operator Training if maximal transfer-of-training is to be achieved.

Experiment 2: The Matching Study. Because subjects' responses indicated that scaling FLIR scene complexity was a more difficult task, the matching study was performed somewhat as an empirical check-up. Had a formal hypothesis been expressed at the time of data collection, it would have been that matching daylight photographs would be faster and more accurate with photographs of L3TV displays than FLIR displays since L3TV displays seemed to have more in common with daylight views. As depicted in Table 6, performance was measured both in terms of the number of errors and the number of seconds to complete 16 matches.

Table 6. Time in Seconds and Numbers of Errors Matching Color Photographs.

FLIR DISPLAY SCENES		L3TV DISPLAY SCENES	
Times (sec.)	# of Errors	Times (sec.)	# of Errors
102	0	147	0
262	3	384	4
155 $\bar{X} = 160.0$	0 $\bar{X} = 1.22$	276 $\bar{X} = 227.1$	3 $\bar{X} = 2.00$
125	4	195	2
199 $s = 65.8$	2 $s = 1.56$	165 $s = 119.2$	3 $s = 2.19$
188	2	438	6
237 $s_{\bar{X}} = 23.3$	0 $s_{\bar{X}} = .55$	227 $s_{\bar{X}} = 35.1$	0 $s_{\bar{X}} = .77$
72	0	134	0
100	0	78	0

On the average, matches of color daylight photographs with L3TV display photographs occasioned more errors and required longer times than those with FLIR photographs. Because of high within-group variance, t-tests of differences between the means of both measures failed to reach significance. Nevertheless, since the direction of difference was opposite to that which had been expected, the implied hypothesis must be rejected. Despite the fact that scaling FLIR scene complexity had been cited as a more difficult and different task, the matching study revealed greater average accuracy (92.4% vs. 85%) with a shorter average matching time of about 10 seconds vs. 14.2 seconds per picture with FLIR than with L3TV.

The only way to account for this unexpected reversal is to observe that during the process of complexity scaling FLIR displays, a majority of subjects learned a visually efficient way to capitalize on unique FLIR informational cues. In fact, at the end of his FLIR debriefing one subject summarized, "One very valid thing I have learned from this is you have to treat FLIR as very different from L3TV."

CONCLUSIONS AND RECOMMENDATIONS

Conclusions.

1. Complexity scaling of either L3TV or FLIR displays can identify 3 to 6 significantly different levels of complexity for computer modeling to permit cost-effective Sensor Simulator design decisions based on empirical comparisons of performance with varying CIG parameters.

2. For L3TV displays, content analysis revealed: a) Scene complexity was unidimensional. b) Subjects focused on real-world man-made objects with the ground unimportant. c) A mission orientation was not elicited. d) Geometries of the visual array dominated most subjects' descriptors. e) Quantification can be achieved using 8 derived measures. f) "Realism" will be a function of these measures. g) A L3TV/CIG Property List is possible.

3. For FLIR displays content analysis revealed: a) Despite intellectual mastery, initial responses of most subjects regressed toward expecting a normal visual scene. b) The scene-complexity continuum is probably not unidimensional. c) Increased mission orientation is elicited. d) Perception of the background is more difficult due to blurring, blurring, and whiting-out. e) Some objects become redefined. f) Scaling FLIR complexity was more difficult, a different task, and a learning experience.

4. Although a fair to moderate linear relation exists between L3TV and FLIR scene-complexity, there was no correspondence between specific sets unique to each sensor: Set 3 from the FLIR content analysis (white-hot-man-made) and Set 5 from the L3TV content analysis (object detail: interior complexity).

5. Results of the matching study indicate that: a) Most mismatches occur with less complex scenes. b) Perceptual cues displayed by FLIR sensors are comparable to or better than graphic details displayed by L3TV sensors.

6. Additional evidence indicates that visual parameters associated with FLIR displays are modified by perceptual set, cognitive factors, and mission assignment.

7. In general, findings support a cost-effective CIG simulation of an L3TV display which stresses the optical array of surfaces, edges, and lines. Similar simulation of FLIR displays of a flight over land is questionable due to the nature of the sensor and influence of task and atmospheric variables upon performance and training. Findings suggest target acquisition models assuming a hierarchical ordering of target detection, recognition, and identification, may be adequate for L3TV but not FLIR.

Recommendations.

1. Because of built-in limitations of the present research, conclusions are tentative and replication is recommended with broader subject and display sampling.

2. Target-areas found to be significantly different in complexity for both sensors should be modeled. The perception of CIG simulated imagery in the Sensor Simulator under development was defined by size, shape, gray shade, contrast, noise, and curved surface shading. These should be systematically varied and evaluated with other CIG trade-off parameters as: texture, detail level, foliage masking, weather algorithm, kind of noise, and air speed smearing algorithm.

3. The measures derived to quantify L3TV displays should be tested with the recommended procedures to establish a L3TV/CIG Properties List on the original or new stimulus materials. The means to derive a FLIR/CIG Properties List is not recommended on the basis of the present data.

4. L3TV and FLIR sensors are said to be influenced by some 18 atmospheric variables of which sun angle (time of day) is only one. To improve simulation of displays for a variety of flight missions, those atmospheric variables need to be identified and assessed which: a) have essentially the same or similar visual effects on sensor displays and could reduce CIG costs without sacrificing transfer-of-training by similar programs, and b) have important and differing effects upon sensor displays and which, therefore, must be included in ground-based training involving sensor simulation.

5. Prior to implementation of a Sensor Simulator, intermediate briefing and training materials should be developed which address Airmen's expectancies and perceptual sets due to the influence of cognitive factors and mission orientation with FLIR displays. Such materials should include descriptions and illustrations of FLIR scenes for a variety of flight missions under regularly occurring transition periods and infrequent conditions which can disrupt operations. A separate topographical taxonomy may need to be developed with categorization of variables known or found to affect sensor displays.

REFERENCES

1. "Electro-Optical Navigation System Planned for B-52 G/H", Aviation Week and Space Technology, May 10, 1976, pp. 130-131.
2. "Human Resources Lab Accelerates Research", Aviation Week and Space Technology, July 19, 1976, p. 225.
3. Rosell, F. & Willson, R. Performance Synthesis of Electro-Optical Sensors. Tech. Rep. AFAL-TR-74-104, WPAFB, Oh., April 1974, pp. 50-56; 127-142; 175-194.
4. Reynolds, P. "76 AIAA Visual and Motion Simulation Conference", Astronautics and Aeronautics, July/August 1976, pp. 68-70.
5. Stein, K.L. "AFSC Stresses Increased Simulator Use," Aviation Week and Space Technology, July 19, 1976, pp. 101; 105-109.
6. Bunker, M. & Messchen, R. Airborne Electro-Optical Sensor Simulation. Tech. Rep. AFHRL-TR-75-35, AFSC, Brooks AFB, Tx., 1975, p. 89.
7. Gibson, J. Perception of Distance and Space in the Open Air, in Beardslee & Wertheimer (eds.) Readings in Perception. Princeton: Van Nostrand, 1958, 415-431.
8. Gibson, J. Optical motions and transformations as stimuli for perception, Psychological Review, 1957, 64, 288-295.
9. Munnally, J. Psychometric Theory. New York: McGraw-Hill Co., 1967, 31-56.
10. Biberman, L. (ed.) Perception of Displayed Information. New York: Plenum Press, 1973, pp. 13, 21, 35, 43, 76-84, 313-322.
11. Stevens, S. Rating Scales of Opinion, in Whittle, D. (ed.) Handbook of Measurement and Assessment in Behavioral Sciences. Menlo Park: Addison-Wesley, 1968, pp. 171-199.
12. Cream, B. & Woodruff, K. Functional Integrated Systems Trainer: Vol. I. Description and Evaluation. Tech. Rep. AFHRL-TR-75-6, WPAFB, Oh., Dec. 1975.
13. Smode, A. & Hall, E. Translating Informational Requirements Into Training Device Fidelity Requirements. Proceedings of The Human Factors Society 19th Annual Meeting, Dallas, Tx., Oct. 1975, pp. 33-36.
14. Edwards, A. Techniques of Attitude Scale Construction. New York: Appleton-Century-Crofts, 1957, pp. 5-9, 121-149, 172-198.
15. Peters, C & Van Vochria, W. Statistical Procedures and Their Mathematical Bases. New York: McGraw Hill, 1940, pp. 171-176.
16. McNemar, Q. Psychological Statistics. New York: John Wiley, 1949, pp. 116, 216-225, 352.
17. Snyder, H. Image Quality and Observer Performance, in Biberman (ed.) Perception of Displayed Information. New York: Plenum Press, 1973, 87-118.
18. Reed, S. Psychological Processes in Pattern Recognition. New York: Academic Press, 1973, pp. 11-53; 223-226.
19. Graham, C. (ed.) Vision and Visual Perception. New York: Wiley, 1965, pp. 548-567.
20. Braustein, M. Depth Perception Through Motion. New York: Academic Press, 1976, pp. 13-30, 41-56, 154-186.
21. Posner, M. Coordination of Internal Codes, in Chase (ed.) Visual Information Processing. New York: Academic Press, 1973, pp. 35-74.
22. Lindsay, P. & Norman, D. Human Information Processing. New York: Academic Press, 1972, pp. 1-10, 94-113.
23. Rosell, F. & Willson, R. Recent Psychological Experiments and Display Signal to Noise Concept, in Biberman (ed), op. cit., pp. 167-231.
24. McCormick, E. Human Factors in Engineering and Design. New York: McGraw Hill, 1976, 63-65.
25. Winer, B. Statistical Principles in Experimental Design. New York: McGraw Hill, 1962, pp. 576-621.
26. Hays, W. Statistics for Psychologists. New York: Holt Rinehart & Winston, 1963, 490-538.
27. Edwards, A. Statistical Analysis. New York: Rinehart, 1949, p. 331.

SESSION VII

Chairman

Dr. Robert M. Howe
Department of Aerospace Engineering
University of Michigan



Educational Background: B.S., Electrical Engineering, Cal Tech., 1945; AB, Physics, Oberlin College, 1947; MS, Physics, University of Michigan, 1948; Ph.D, Physics, M.I.T., 1950.

Career Highlights: U.S. Navy, 1943-46; 1950 to present, faculty member, Department of Aerospace Engineering, The University of Michigan, 1950-51, Instructor; 1951-54, Assistant Professor; 1954-57, Associate Professor; 1957 to present, Professor; 1963-68, Chairman, Information and Control Engineering Program, 1968 to present, Chairman, Department of Aerospace Engineering. Teaching and research in analog and hybrid computers, automatic control, flight simulation. Served as first national chairman of Simulation Councils, Inc. In 1957 was a "founder" of Applied Dynamics, Inc., now Applied Dynamics International, manufacturer of hybrid computers. Consultant to numerous companies. Member, USAF Scientific Advisory Board (Guidance and Control Panel); Science and Technology Advisory Group, USAF Systems Command; NASA Research and Technology Panel on Space Vehicles.

Memberships: Tau Beta Pi, Phi Beta Kappa, Sigma Xi, IEEE, AIAA, Simulation Councils, Inc., Biomedical Eng. Soc.

Publications: Over 30 articles in scientific and engineering journals; one book on analog computation.

COMPUTROL - A New Technique in Computer Image Generation

Jerry T. Lewis; Advanced Technology Systems



Jerry T. Lewis obtained his MBA from New York University where 15 years before he received his BSEE. His 25 years of experience has spanned various applications of the visual image. From closed circuit television to Graphic Sciences at Stanford Research Institute, he worked on security printing of U.S. Banknote and then to computer graphics at Information Displays. His interests at ATS are with the computer generated image and its future as an information bearing medium.

COMPUTROL - A New Technique in Computer Image Generation

Abstract

Four years in the making, ATS COMPUTROL CGI system has emerged from its third generation with an approach to computer imagery that relies on new techniques. The separation of three specific functions into nearly stand alone systems has yielded an array processor for the projection analysis which extracts the perspective of the gaming area from the modeled world, an array processor for the visible surface calculation, and a terminal processor for the output function.

The emphasis has been on hardware dedication without the system being dominated by software. The increase in speed by utilizing ECL chips, array processors, cache memory and specific function logic has produced a 30-K edge machine with a 30 cycle update.

This paper addresses the subject of edges and treats the manipulation of the modeled world from points to lines to surfaces to edges to segments as the image is built from the data base to the display.

Parameters

When the subject of Computer Generated Images is introduced, the following question is inevitable, "how many edges?" Every visual system has its main standard of performance--television has its resolution, computer graphics has its matrix count, photography has its line pairs, printing has its screen number, and xerography has its contrast ratio.

A visual display has more than a single parameter to account for its quality. There are the factors of color saturation, contrast, linearity, smear, highlight brightness, and another dozen quantities generated by the human factors people. In CGI, there is no stickiness of a pick-up-tube, there is no Kell factor for the random selection of an element on a scan line, there is no smear or overshoot of video, there is no non-linearity of the generated video, there is no color bleeding in fast motion scenes, and there is no Gaussian function of a scanning electron beam. What you generate is what you get. The criterion of CGI has been, and is now, the number of edges (and anti-aliasing, a point considered later). This criterion has evolved an "edge war".

Is this "edge war" a conflict or a confusion? Is a 2000-edge system only half the scene content of a 4000-edge system? Counting edges is a precarious game. Which edge do you count? There are the modeled edges in the data base, mathematical lines in the co-ordinate system connecting points of the model which can easily exceed 20 million. There are the projected edges extracted from the model of terrain and targets. The COMPUTROL offers 200,000 of these as wire frames and polygon edges. There is the subtraction of hidden edges, which in a good design are discarded after the viewpoint is made so as not to clutter up further processing. Already we have a variability in edge count since a target of 2000 modeled edges may have 1000 surviving edges in one perspective or may have 100 in another perspective (or as little as 20, if scaling down the detail with range reduces the count). There are chunked edges, whereby 2 edges crossing 2 edges to form a pound-sign may have to be processed as 12 edges. There are intersection edges, created by CGI in the example case of two 9-edged cubes intersecting to make 20 edges. There are clipped edges which may be processed up to the point of border or depth determination that they're out of the pyramid of view, and thence discarded. There are texture edges which lend a realism but do not emanate from the model, and finally there are the visible edges--at last an edge count that can be quantified. But

the output edges can be restricted by their preceeding operations in the projection processor or visible surface processor, where the time element in the complexity of computations may be the limiting factor.

With visible edges as the measure of scene detail, why not add on more processors, larger memory, a bigger frame buffer and increase the edge count? The design philosophy at ATS has been to maximize the number of edges that can be processed by three cabinets containing the function of the projection analysis, the visible surface determination and the conversion to a raster format. That is, how many edges per 225 cubic feet of cabinet space? (This volume does not include the space for model data base or display components).

It is the visual display that is the final product. Since it is a digital substratum upon which the analog color is projected, we have a pixel count, a scan line count and the color variations of each element to construct the parameters of a computer generated image. An area can be formed by the maximum number of edge crossings per scan line (approaching the limit of horizontal resolution) and the number of scan lines (the limit of vertical resolution). This area can be viewed as a pixel-squared quantity containing the single frame output of a CGI.

The number of channels producing a simultaneous output of different views must have all of the visible edges distributed amongst them. That is, the sum of edges in each output equals the total edge count. The pixel-squared area is now lengthened along the horizontal dimension by the number of channels.

A determining factor in edge count is the image update rate, or the number of times a second the scene is re-calculated and presented. The third dimension of time (really, frames per second of update), when stacked on the area of pixels produces a volume representing the display limit to the number of edges per second. Given a CGI system supporting say, five channels of 1023-line outputs with a maximum of 800 edge crossings per scan line, and a 30-cycle update rate, we have a capacity of the raster system to support a theoretical edge count of roughly 24.5 million edges per second.

Now to define an edge more closely before examining the limits imposed by edge processing time. In the COMPUTROL a visible edge is a straight-line defining the location and color of the surface to its right. The edge is defined by its height and top position (x,y) along with its slope and color information. To put this surface on a raster, it is broken down to scan line segments, each segment commencing with an edge describing the surface to its right and extending along the scan line until the next edge defines another surface. The segment is constructed by a scan line number y, an intercept point along the x-direction of the scan line, a delta-x to the next edge, a flag to determine flat or smooth shading, and the color to its right, in a simultaneous RGB. With the pixel-raster system to support the presentation of all edges, the maximum edge density in a frame display is the edge crossing limit in the x-direction and the scan line count in the y-direction. The total number of edge-crossings for a scan line defines the horizontal resolution of a CGI frame as the minimum width of a surface, and the scan line count defines the vertical resolution as the minimum height of a surface.

Comparing the representation of a scene with edges versus the same scene represented in polygons, we find that polygon surface boundaries, if counted as edges, would double the edge count when meeting another surface. That is, the three visible faces of a cube are counted as 9 edges, but three surfaces of 4 edges each would be counted as 12 edges. The accepted ratio is 3.67 edges per polygon. It is unknown where they found a polygon of 3.67 edges.

As to the aliasing solution and the edge count, the COMPUTROL in the F-18 configuration computes eight resolution elements in the x-direction for each output pixel width. These eight values are averaged to form the color

components of the pixel containing the edge transition. Also eight times the number of scan lines (8000 in one frame) are used in the computation to average out the vertical value for the pixel assignment. This computation visually minimizes the aliasing effect, but it is expensive in computation time and reduces the number of visible edges. The F-18 sky-earth generator calculates the detail of 8000 x 8000 element frame and then mathematically smoothes the discrete points to a 1000 by 1000 matrix of pixels.

Before getting into a quantification of the maximum number of edges which can be produced by COMPUTROL, and the possibilities and limitations to this figure, it is necessary to explore the mechanism of edge processing.

The COMPUTROL Approach

The creation of images representing all possible fields of view to a pilot whose aircraft is at a specific attitude over a specific terrain has led to the development of a technology requiring innovation in design and innovation in hardware. The COMPUTROL approach has been to develop equipment reflecting three specific functions of the process.

Between the digitized model residing in the on-line disks and the analog output of color video, there are three distinct functions of processing. In a first order analogy, and at a risk of being anthropomorphic, one could say that a cameraman takes a picture of the model as a wire frame connecting points in space, that this perspective is passed to a draftsman who removes the hidden lines, and the final view is rendered by an artist who adds color and presents the view. The first function is accomplished by the projection processor, the second function by the visible surface processor, and the third function by the terminal processor.

The logic of dividing the processing among three functions lies with the nature of handling information. The projection processor receives data base points, transforms them into perspective points, calculates color on the basis of polygon surfaces and outputs data in the form of edges. The visible surface processing uses the edge list to determine the occulting, thence the structuring of edge crossings for sorting on each resolution line and outputs encoded visible edges. The terminal processor averages the resolution lines in x, calculates and stores the segments, decodes to a raster format and outputs an analog signal in simultaneous RGB. If there is a change in requirements of any section (say, the scan line or frame rate or points of perspective, or number of channels) the change is made at the cabinet level in hardware and the rest of the system is unaltered.

The first function of the projection processor is to extract the designated coverage of the modeled world from the data base and arrange the elements of the scene into the perspective of the viewer. It is as if a hypothetical camera with a selection of lenses from narrow field to wide angle (up to 360°) could move to any location of the modeled world, and at any angle record with nearly instantaneous shutter speed the terrain along with any selected targets placed in their appointed position. This function is the projection processor and occupies the first cabinet. The function is more complex than picture taking. Actually, in the two dome configuration of the F/A-18, there are 512 perspectives, each with a pyramid of view to provide accurate mapping to a curvilinear surface divided into 512 theoretical facets. The co-ordinate system of the model (x,y, z location of points) is transformed to an image plane with the object rotated, translated and scaled to reflect the perspective view. Then another transformation places the image in the eye coordinate system with the intervening "window" (the viewed display) receiving it's projection of the scene.

The color information in the modeled data base contains the polygon surface normals, optical properties, intrinsic color, and a flag for flat or curved surface shading. Since edges contain the color to their right, a visibility and sun direction must be calculated in the projection processor. The combination of the surface normals, their reflectivity, the sun direction, the visibility, the modeled color, the sun color and the gradient shading can be used to assign the color component to the edge, depending on its orientation in the viewed space.

The polygons are decoded into edges (since this is the medium of processing) and now the geometrical points can be addressed to determine if they fall into the viewing window. The edges at the borders of the window are clipped and, with the Z-direction component known, the edges falling on the viewer's side of the window are also clipped. The surviving edges receive computations to determine their height, their slope and their depth gradient. With this attendant information, the edges are assembled and sorted on the basis of the y-top (that is, the highest top point of an edge). This data is buffered for use by the second function, the visible surface processor.

All the edges in the perspective scene are placed in the main memory in y-sorted order. The visible surface processor searches its own "current edge" buffer of previous scan lines for new edges which are sent to a bucket sort of the x-intercepts. Now in x-order, an occulting algorithm is invoked to ascertain the overlay. The winning edges at each x-intercept point are added to the current edge list. If a new edge is required by the intersection of two surfaces, it is created at this time and placed with the current edges.

An occulting or Z-clipped fog can be generated by the visible surface processor: the general fog is created in the projection processor as a visibility restriction to all objects, but a Z-clipped fog starts at a scene depth like a fog patch, and therefore it is treated as an overlay of a translucent surface.

During the second stage of x-sorting, color data for terminating scan line segments are calculated. The end point colors are used in the smooth shading algorithm.

The visible edges are assembled in blocks of 1024 intercepts and stored in two frame buffers in which each can hold 64 thousand visible edges to be distributed across all the output channels.

A detection of impending image overload (that is, approaching maximum intercepts in the buffer or the maximum 16.7 millisecond computation time for a frame) is monitored by the CPU.

The encoded visible edges in the frame buffer are formatted in 89 bits as follows:

FUNCTION	BIT REPRESENTATION
Color (R,G,B), C (at top)	21 (7 bits each color)
Color Gradient, G (along edge)	27 (9 bits each color)
Top Scan Line Position, Y	9
Reciprocal Slope, S	12
Edge Height, H	9
Position of X (top)	10
Smooth, Shade Flag, F	1

The terminal processor receives data in the above format and derives an edge-to-segment calculation to transcribe the edges into their representation on scan lines. This process (1) calculates the x-intercept and color intercept of each edge: (2) generates a segment width of delta-x, a delta color, C, and smooth shade flag, F: (3) deletes segments of zero width: and (4) stores the results in a ping-pong buffer cache. This buffer is a sequential wrap-around write and serial read memory.

The smooth shader and raster generator decodes the read side of the ping-pong buffer data on a scan line time basis and digitally produces three colors at a 16 nano-second rate (2000 units in x for each channel). The D/A converters (three for each output channel) complete the transformation to video of simultaneous red, green, and blue to the color display system.

The Architecture of COMPUTROL

Intrinsic in the design philosophy of generating the maximum number of edges in three cabinets is the special purpose processor. To incorporate the peak efficiency for a specific function in digital processing, a custom design had to be developed. To wit, there has been no general purpose computer and its program which could play master chess until a special purpose processor was designed.

The three functions each have an array processor. This pipelining of the computation requires dedicated hardware arranged so that each processor does one operation of the general algorithm. A string of these processors then outputs a specific function--like a matrix transformation--in each cycle time. Because a function is repetitive, like the scaling, rotation and translation of a point or the depth determination of an edge, the operation on data requires no system commands. With the increased speed comes the need for short data paths, and with the specific format and content of each piece of information, the memory cache is utilized. These are local memory units, located in the same cabinet as the array processor and serving the input/output storage needs. Simplification of the addressing of memory results. That is, a place for each datum and each datum in its place--the epitome of organization.

As developed in the discussion of the function in each processor, each array handles information in a different form. The projection array processor does matrix transformations and operates on floating point numbers from the data base model. The visible surface array processor does a computation for overlay (depth of an edge) and operates with a fixed point number. The terminal array processor decodes a formatted data word and stores scan line segments in a frame buffer. In each case an array processor is responsible for a unique function and does its own thing without a program command, or an interrupt or a wait time for main memory addressing.

The fact that COMPUTROL, with its pipelined array processors, is not software dependent introduces a new concept to a digital computation. The task of the CPU is to manage main memory and provide timing signals to the processors. If a change in system parameters is mandated, this usually results in a board swap or a hardware alteration. A lengthy program patch and software modification is not required.

Now that the functions and the methodology of the computer generated image have been touched upon, the subject can turn to the quantitative question, "yes, but how many edges?"

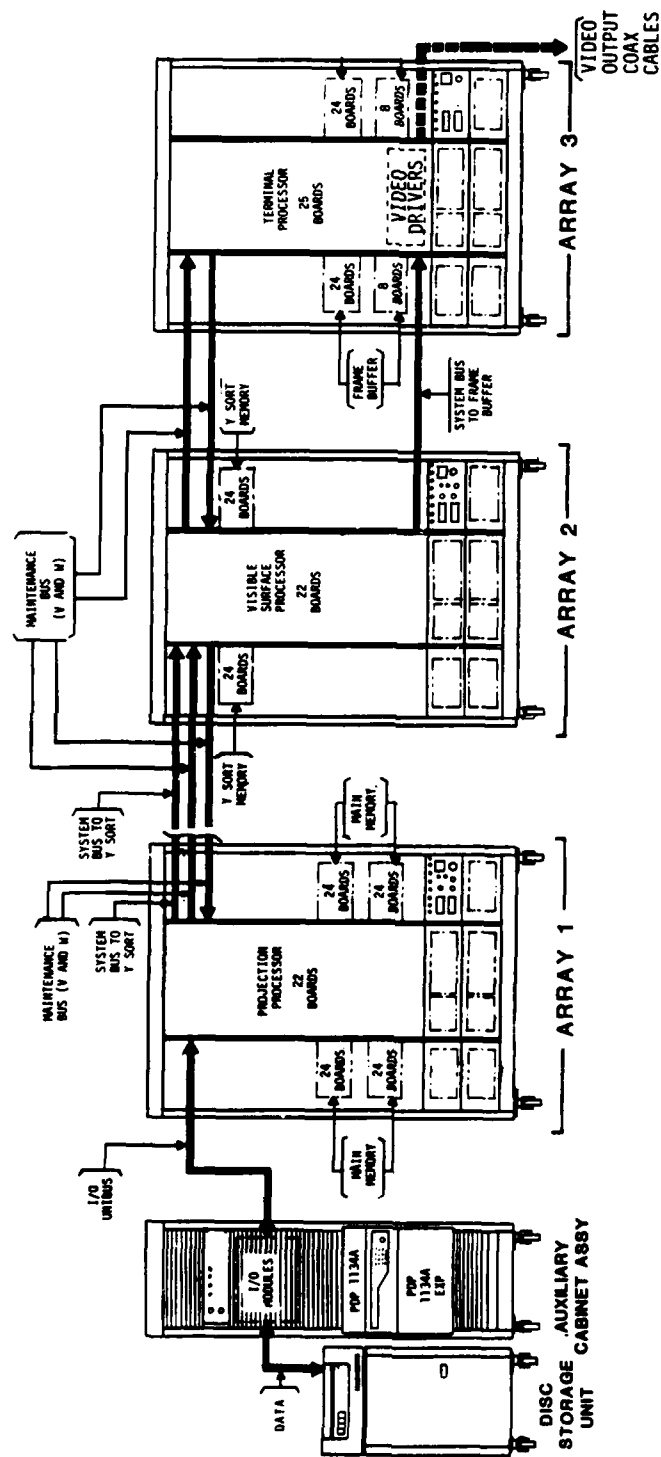
The limit on processing for the current system is not a fixed and absolute number, but is dependent on the scene composition.

In the model, a nearly unbounded area can be frozen in the data base. A 600 by 600 nautical mile area with detailed terrain and extensive target models may amount to 300 megabytes, placed on ten discs. The selected area in the total field of view (a composite of the sum of possible instantaneous fields of view) may comprise 400,000 points when placed in main memory. The projection processor is limited by the y-sort memory (that's the assembly of edges for its output) to 64-k edges. These are the wire-frame edges, the total for all channels, already clipped for the pyramid of view, but containing hidden edges which later may be obliterated. The visible surface processor has a limit due to the holdings of the current edge buffer, and its work load depends on number of

edges, the crossings per scan line, and the overlays per crossing. The terminal processor has two 64-k edge frame buffers to accommodate the odd and even fields, and this capacity is therefore dependent on frame time. The theoretical upper limit associated with a 30-cycle update system would be 64-k visible edges. However, the overall edge limitation lies in the scene complexity, and for an average view of terrain and a few targets, the number of visible edges can be taken as 30 thousand.

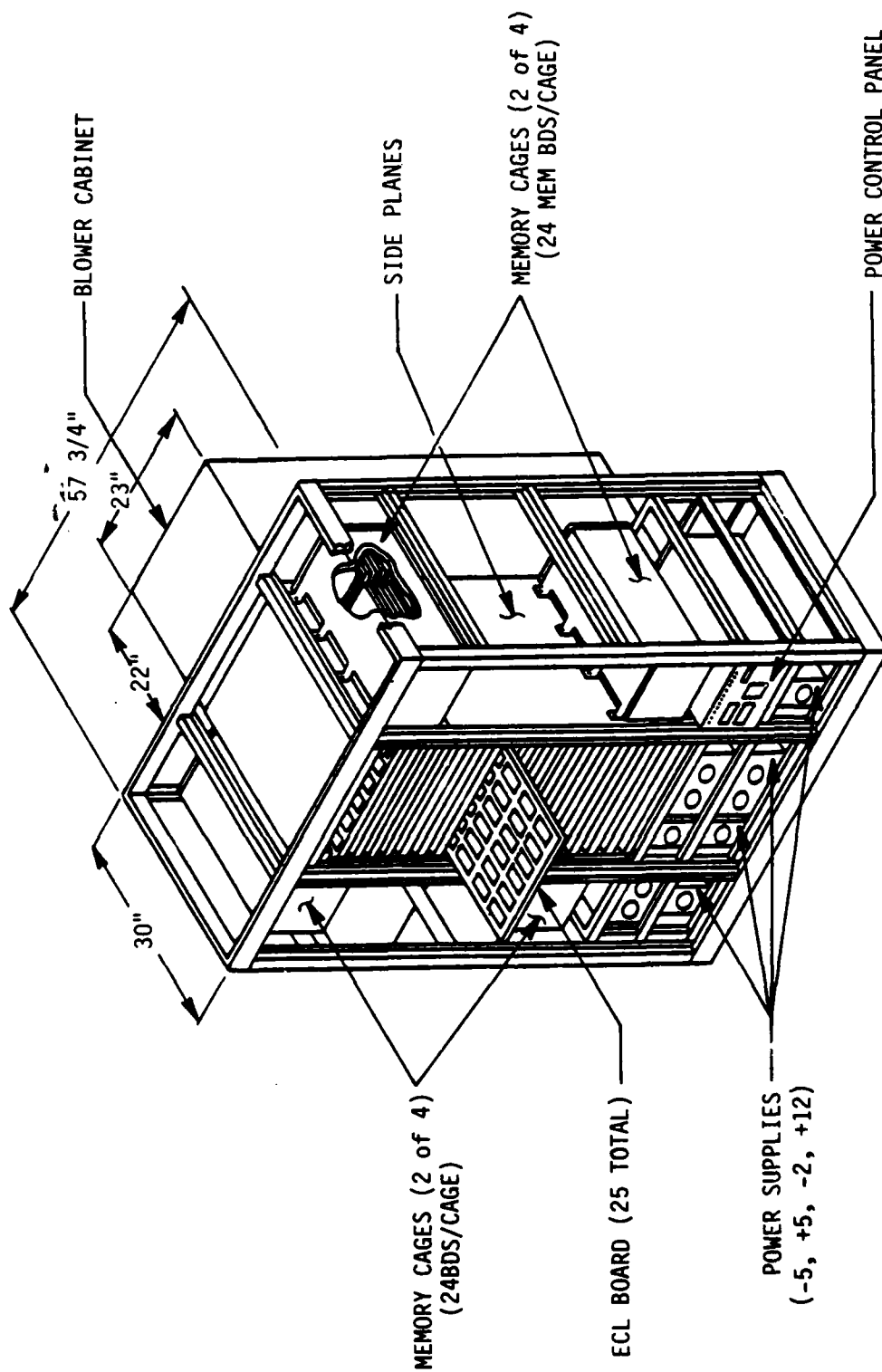
Summary

It has been shown how three cabinets can produce a picture worth 30-thousand edges. The packing density of 140 edges/cubic foot is yet to be increased in the fourth generation of CGI. But, as to the moment, COMPUTROL can supply to, say, five channels in a canopy of virtual image lenses, or to a 5-projector dome configuration, about 700 cubes in each projector, or roughly the limit of the resolution of the display device.



CGI COMPUTROL® ARRAY LAYOUT

Figure 1



ARRAY PROCESSOR RACK (TYP)

Figure 2

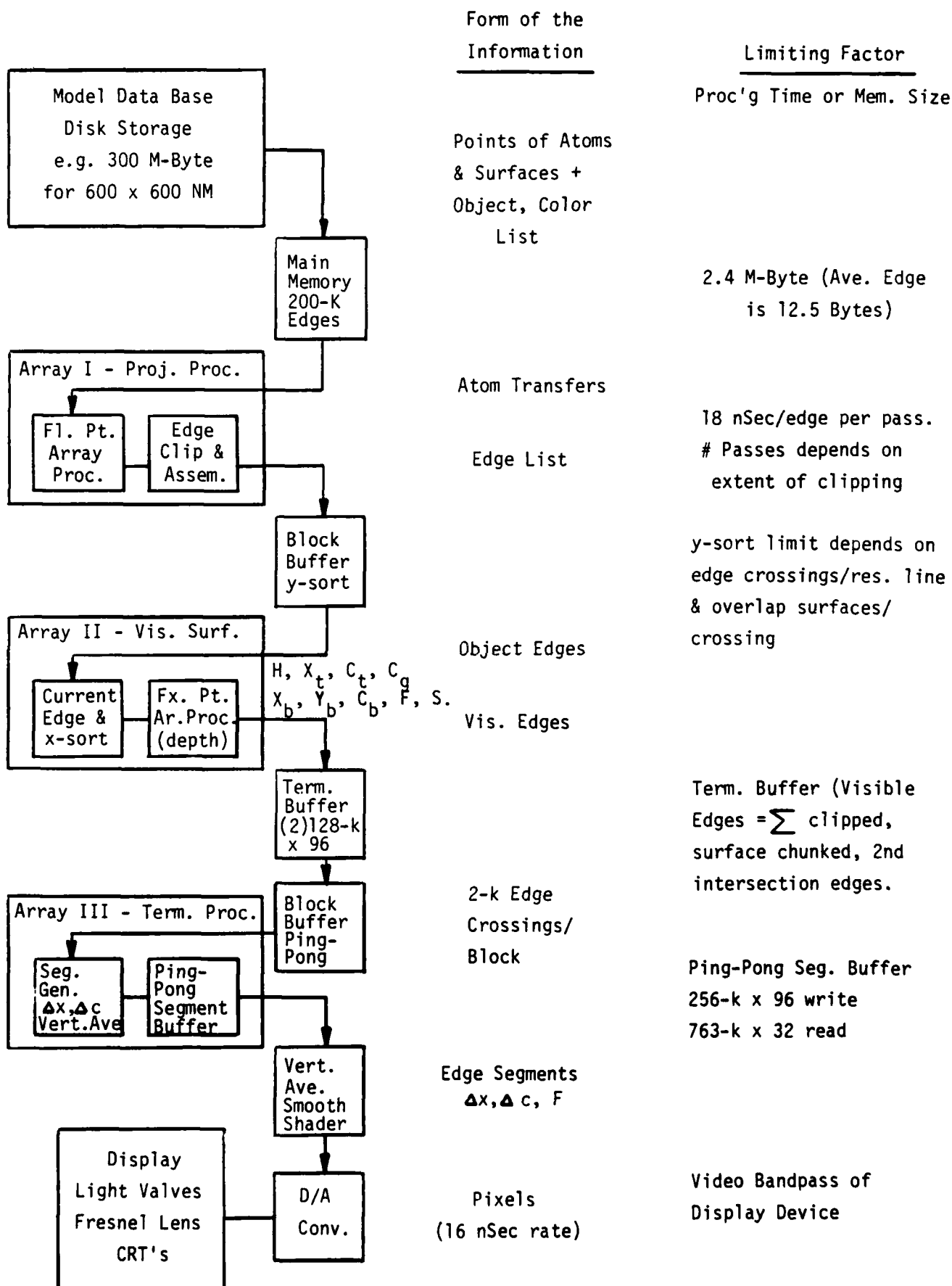


Figure 3 429

A CONTINUOUS WIDE-ANGLE VISUAL SYSTEM USING SCANNED LASERS



Paul M. Murray,
Manager,
Research Projects,
Rediffusion Simulation Ltd

Paul M. Murray obtained his M.Sc in Aviation Electronics from the Cranfield Institute of Technology. His 19 years of professional experience has been in industry. His 14 years at Rediffusion have included visual and sensor simulation techniques and systems and he has a number of patents in these areas.

He is a Member of the Institution of Electrical Engineers, London, and is a Chartered Engineer.



Bruce W. Barber,
Consultant,
Laser Visual Systems,
Rediffusion Simulation Ltd

Bruce W. Barber obtained his degree in Applied Physics when with the Royal Aircraft Establishment, Farnborough, England. He has worked since in industrial R & D in various fields, including 6 years with Rediffusion Simulation on visual systems. For the majority of that time he has acted as Project Manager for the RSL Scanned Laser Visual Development.

A CONTINUOUS WIDE-ANGLE VISUAL SYSTEM USING SCANNED LASERS

ABSTRACT

A wide-angle high resolution visual system is described which is specifically designed for the helicopter nap-of-the-earth flight training role, where good depth of focus and high scene detail are required.

INTRODUCTION

The need to develop a wide-angle visual system having the capacity for producing a very detailed scene over the whole field was originally considered by RSL more than ten years ago. The training application was at that time, and still is today, the low-level mission pilot in fixed wing or rotary wing aircraft. Typical mission programmes for these aircraft types are fairly well known and need not be described here^{1,7}. However, there are perhaps three primary aspects of such missions which can be usefully considered separately.

Firstly, the take-off and flight to a pre-determined position during which the aircraft will descend to contour flight and finally, in the case of a helicopter, to NOE flight.

As low-level flight is potentially very hazardous, there would be great advantage in a pilot gaining as much experience as possible of contour and NOE flight on a simulator, both before and during real flight exercises. Indeed, some flight patterns and certain manoeuvres considered essential under real battle conditions, may not be learnt safely in the aircraft. In addition, the experienced pilot could be checked out thoroughly and more conveniently on a low-level flight simulator.

The visual display for such a simulator would require a FOV of at least 120° horizontal by 60° vertical, and a scene rich in content, texture, colour, and structural detail. Resolution should be preferably as high as practicable, but need not approach human eye performance.

The second aspect to be considered is reconnaissance and target acquisition. True target identification training may require real world conditions, although even for this purpose some improvisation should be possible. For instance, objects may be artificially moved closer, or made larger in a visual system in order to compensate for reduced resolution, without loss of training value. Where telescopes or infra-red vision aids are used however, a secondary image generator could be incorporated to provide fairly realistic 'magnified' direct view or head-up images. It may not be essential for a ground target

to be seen to move in every case, but clearly a variety of target positions would be needed. Aerial targets may also have to be catered for.

The third aspect is the weapon aiming and delivery phase of a mission, if applicable. The chief requirements for simulation here are to have good correlation between aircraft pointing attitude and the displayed target and a reliable method of measuring fire accuracy. In addition, the display of weapon traces, weapon strikes, smoke, dust, etc, would be desirable.

It is worth summarising the performance of current visual systems in relation to the needs of the low-level flight mission.

TV camera-model techniques

The terrain modelboard provides very high scene detail, but the resolution obtained from a TV camera is only 10 arc min/OLP at best and degrades to much less than this in the near scene due to limited depth of focus in the optical probe. This effect is accentuated in the wider FOV probes (120°H x 60°V) which also suffer closeness of approach limitations, both horizontally and vertically. Tilt focus has been used in an attempt to improve the apparent depth of focus, but is only applicable to relatively flat terrain such as air fields or general terrain viewed from high altitudes. Thus in low-level flight where it is most important to see close three-dimensional objects, conventional TV probe systems are least effective. Moving targets and weapon effects would need to be superimposed CGI.

Computer generated imagery

FOV, resolution and gaming area are not limited for any fundamental reason in CGI and the whole scene is always in focus. FOV can be made large by using multiple channels, and resolution should be adequate if suitable display devices are used. However, the basic problem is in providing sufficient scene detail for terrain flight over a large area and maintaining a sufficient level of detail as various terrain features are approached. Systems using shading and texture have been produced, but severe problems have been encountered in the development of practical systems for low-level flight.

In addition the cost of development and purchase of an adequate CGI system threatens to be prohibitive.

Display devices

Increasingly it is becoming accepted that a projected display has several significant advantages over collimated CRT displays. For example, it allows a cab change to be made more easily and a variety of cab configurations to be used. Of particular importance for very wide-angle displays is the potential for pitching and rolling the displayed field such that the horizon and the terrain image remain

visible to the pilot at any roll angle, and throughout a large pitch range.

With current projectors there are usually significant penalties to pay for these advantages, such as increased cost and complexity of hardware, poorer resolution, increased colour misregistration, and often, reduced brightness. For multi-projector arrays there is the added problem of edge and colour matching, and the consequent high maintenance costs.

RSL Wide-Angle Scanned Laser Visual System

It is not difficult to specify a visual system that would be completely satisfactory for all low-level flight training applications. It would in effect have a performance approaching real world conditions in many basic parameters. For instance:

FOV	- Limited only by aircraft structure, say 240°H x 90°V
Resolution	- 1 - 2 arc minutes
Scene content	- Realistic detail and texture on all features, trees, ground buildings, pylons, wires, etc
Time of day/weather	- Fully variable
Targets/weapon effects	- Moving vehicles in variable formations, accurate weapon trajectories, exploding shells, etc

Obviously current technology and many practical limitations, including cost, prevent this ideal from being achieved, however the current development of the RSL Wide-Angle Visual System is aimed at achieving a substantial step toward this ideal.

The system employs TV raster principles, but through the use of laser beams and novel scanning methods, the usual inherent limitations imposed by lenses on FOV and resolution are avoided².

The target specification for the system is as follows:

FOV	175° horizontal x 60° vertical, continuous
Raster	5,280 vertical lines/frame
Refresh rate	60 fields/sec interlaced
Scene content	Approximately 1200 pixels/line and 6.25×10^6 pixels/frame
Resolution (limiting)	Vertical 3.5 arc minutes, Horizontal 4.0 arc minutes
Effective depth of field	5 mms - 5 metres
Colour	Red, green, and blue, separately modulated
Minimum eye height	1.8 mms
Horizontal clearance	5 mms
Motions -	
Heading	Accel 200°/sec ² ; rate 180°/sec; continuous 360°
Pitch	Accel 150°/sec ² ; rate 50°/sec; range to ±85°
Roll	Accel 350°/sec ² ; rate 120°/sec; continuous 360°
Gaming area	As required - typically 13 Km x 5 Km for 1000:1 scale
Display brightness	5 fL
Modulation depth	> 50:1
Moving targets) Weapon effects)	Superimposed CGI

The system specified therefore will produce a large FOV from a single projector giving little image distortion and a very high scene content. The image being continuous will be free from the usual colour and edge discontinuities to which multi-channel displays are prone. The camera can provide a minimum pilot's eye height of 6 feet at 1000:1 scale, and an electro-optic fast focussing device produces an effective depth of field from 5 mms to the far distance.

Resolution is approximately twice that of CCTV systems and with the use of the focussing device, the very near scene will show a level of detail and texture that is probably unobtainable on any other system.

The specification, as stated, will therefore very comfortably meet the need for a detailed scene which should enable the pilot to adequately carry out low-level flight training.

Full mission training capability would demand the simulation of moving targets, sights, night vision, weapon effects, etc. Unmagnified night vision and direct view optical systems could be simulated by using a small part of the wide-angle scene as defined by the required look direction, or with magnified targets being produced by a separate image source. These images could be two-dimensional only against a suitable background, in most cases, and might be CGI or photographs stored on video discs. A more difficult aspect to achieve would be the creation of moving targets and weapons within the wide-angle scene. Schemes for superimposing CGI on model-board scenes have been studied and some possibilities identified.

The display might, for example, be divided on a range basis between a CGI scene and a modelboard scene, with any near scene video overriding the more distant CGI. Obscuration of CGI targets by near scene features would thus be achieved.

However, in most cases, targets and weapons are observed only through head down vision aids and therefore it would probably not be cost effective to simulate the dynamic features of a battlefield environment for the 'out of the window' scene.

LASERS IN VISUAL SIMULATION

As is well known, lasers have many possible uses in science and engineering and the name laser has now become associated with much 'state of the art' technology, such as nuclear fusion, holography, ranging, weapon aiming, and data recording and transmission. Against this perhaps confusing background, it may be helpful to outline the reasons for using lasers in the RSL visual system and consider the main implications of operating these devices.

The laser is able to emit an almost parallel beam of light of high power density which can be put through almost any chosen aperture. If a conventional light source, such as an incandescent lamp were used for example, only a fraction of the total light could be directed into a narrow beam.

In the laser camera, this narrow beam allows a very good compromise between resolution limit and depth of field to be achieved with the added possibility of varying the beam convergence dynamically to give optimum focus over a very wide object range. By comparison, in a conventional probe and television camera system, the aperture size is normally sized to retain picture quality and therefore typically, produces a small depth of focus. Also focus changes must operate on the whole image at once so that no allowance for variation in scene depth can be made. In the case of a projector where light is always at a premium, the laser can provide increased power without causing a change in spot size and consequent loss of image quality that is typical of CRT devices. The laser is in effect a very efficient light source for the type of imaging systems required in simulation.

Colour

The RSL laser visual system, from initial conception, has been designed to provide a full colour display. Colour is generated by red, green, and blue laser beams which are combined and scanned as a single beam and then separated. Single lasers do exist that provide the three primary colours, but a high conversion efficiency is possible using an argon ion laser for green and blue and a krypton ion laser for red. Unlike the phosphors used on CRT's, laser emission lines are highly monochromatic and spectrally pure, but the power available in different lines varies widely and also some lines do not occur at convenient wavelengths.

The three most appropriate lines are 476 nm (blue), 514 nm (green) and 647 nm (red). The chromaticity diagram shows that the triangle defined by these three wavelengths includes the chromaticities of most natural features and is considerably larger than the triangle for the phosphors of colour television tubes. However for this colour potential to be achieved in practice, a suitable distribution of power between the three laser lines must be achieved. In particular, the low luminosity of the red line must be compensated for by using higher power in krypton than in argon, or alternatively a proportion of the argon light may be employed to produce red by exciting fluorescence within a suitable dye.

Safety

The type of laser employed in the described system will have an output power in the order of several watts and is described as a Class IV laser. If a stationary unmodified beam from such a laser entered the eye directly, permanent damage to the retina could result. This is the chief potential hazard from these devices, although only a very few such accidents have been recorded.

The laser visual system described will incorporate a number of features which will provide complete safety for the user. In brief, these will be as follows:

1. The beam emerging from both camera and projector is not stationary, but is in fact scanned rapidly over large angles. The pupil of the eye, even if quite close to the frame scanner, subtends a very small angle compared to the total scan angle and therefore only receives incident illumination for a fraction of the scan period. The averaging effect produced effectively reduces the intensity of the laser beam by a large factor. Should scanning begin to slow for any reason, the lasers will be rapidly switched off. The inertia of the scanning systems does not allow instantaneous loss of scanning.
2. The observer of the display will be prevented by suitable masking and structure, from placing his eye within the volume that is scanned by the laser beam (between the projector and the screen). This will apply both inside and outside the fuselage structure. Only the reflected light from the screen will be visible and even if the laser spot was stationary on the screen, the intensity at the observer's eye point would be several orders below the damage threshold.
3. It is a basic system requirement that the laser camera be located in a light tight enclosure. By incorporating door interlocks the area will also provide laser safety.
4. Maintenance and adjustment of the system will be carried out using eye safe laser power levels of the order of 1 milliwatt. Power reducing filters could be automatically inserted on removal of safety covers.
5. The team involved in the development of the scanned laser system are being monitored at regular intervals by Dr Brennan of the Institute of Aviation Medicine³.

SYSTEM CONCEPT

Introduction

The system, as shown in Figure 1, is based upon simultaneously scanning a pair of tri-colour light spots, one over a modelboard and the other over a front projection screen: A video signal is produced by collecting the light instantaneously scattered from the model surface on a photo-electric detector, and using the resulting voltage to modulate the projected spot to form an image.

During the conceptual phase a number of decisions were made related to field of view format orientation, raster orientation, collimated or non-collimated display, etc. Some of these are discussed below:

Field of view orientation

Flight simulator visual systems usually have the field of view defined with respect to aircraft axes. In a wide-angle system where the ratio of picture width to picture height is large, this results in a large variation in, for example, the length of the horizon line. In a low-level role, where the use of terrain features for concealment is important, this can result in an obstruction at the edge of the field of view disappearing from view as the pilot turns. The provision of an horizon stabilised picture prevents this loss of information and studies have shown that the provision of an horizon stabilised display 120° wide by 60° high permits obstacle avoidance¹.

From the practical point of view the implementation of an horizon stabilised display permits the inclusion of the pitch and roll mechanism at the projector where there is more room than at the camera probe.

Line scan orientation

A wide-angle system can be designed using lenses of moderate field angles by arranging the frame scanner to rotate as shown in Figure 2. The maximum field angle required in such a system is that of the line scan which in this case is 60°. If the projection lens is rotated with the frame scanner, then each scan line follows exactly the same path through the projection lens and frame scanner and so gives uniformity of resolution across the scan lines. The adoption of this approach in the system developed has resulted in vertical scan lines which enables the apparent depth of field of the camera to be improved.

Display screen

A wide-angle picture produced by a single projector is conveniently projected onto the inner surface of a hemispherical screen from the centre of radius. In the system developed, this screen is viewed directly, and, due to the very large field angles subtended at the viewer's eyes, gives a high degree of subjective realism and depth perception.

System description

The technique employed is essentially a form of CCTV in that scanning is used to generate and display the image. The method of producing the camera and projector raster scans is by deflection of laser beams using rotating mirrors which are very accurately synchronised. This

general approach has been in use for many years in film recording applications, but has previously been limited to broadcast television scanning standards and narrow field of view format.

In this case a vertical line scan was chosen operating in synchronism with a continuously rotating frame scan optical system. The line scanner produces a 12° scan which is expanded to 60° by the optical system, with successive line scans rotated about the vertical axis by the frame scan prisms to give a total horizontal angle of 180° as illustrated in Figure 2. In this way the use of very wide-angle optics is avoided together with the potentially severe aberrations which are normally associated with them. In fact the image quality does remain consistent throughout the horizontal field. In addition, the scan mechanisms and associated optics in each unit can be similar or identical, because both the camera and projector generate a raster scan.

When projected onto a terrain model the scan pattern emitted by the camera is seen to be radial and originates from a point immediately below the centre line of the probe.

The raster light is scattered from the model surface and detected by a number of photomultipliers arranged in a similar way as lamps would be in order to provide uniform illumination. However, the exit pupil of the camera, which emits the laser beam constitutes the point of perspective or look point as does the entrance pupil of a conventional camera.

The projector scans an identical raster onto a hemispherical screen, which is intensity modulated by an acousto-optic device that is driven by the video signals obtained from the photomultipliers. An undistorted image, in correct perspective, is then formed.

In producing a display in full colour, two ion lasers will be used in the camera and two in the projector. An argon laser will provide blue and green emission lines and a krypton laser, red. In the camera these three beams will be combined prior to scanning and then detected by the photomultiplier triads, each having a detector independently sensitive to red, green and blue light. In the projector the three beams will be separately modulated by three acousto-optic cells driven by the corresponding colour video signal and then combined for scanning as in the camera.

Production of the raster scan

In order to achieve high definition over 180° of horizontal field (line scan vertical), a much larger number of scan lines are required than in broadcast television systems.

A twelve faceted mirror polygon, operating in conjunction with an array of 10 roof prisms, produces 120 lines/revolution of the polygon.

Rotational frequency is 1320 Hz (79,200 rpm) giving a line rate of 158,400 per second.

The polygon of Beryllium is an integral part of a motor which is supported on air bearings and is powered by a three-phase synchronous drive system.

The frame scanner consists of three independent rotating optical systems which operate downstream of the line scanner.

The pupil switch plate moves the exit pupil of the system from one frame scan to the other, every half revolution of the frame scan tube. In this way, each frame scan prism projects alternate fields into the same 180° sector. Successive fields are displaced slightly to provide interlace. The de-rotation prism rotates at precisely half the speed of the frame scan tube to prevent the line scan from rotating within the raster.

The frame rate was selected to be 30 per second which minimises flicker and allows 5,280 lines per frame. This line density is equivalent to less than 4 arc minutes per line pair.

Synchronisation of the camera and projector scanning systems is controlled by a common pulse generator that limits line and frame jitter to a level which is not detectable by the viewer.

Wide bandwidth video system

To achieve the high picture content that is considered essential for low level flight training over the large field angle available, a particularly wide video bandwidth system is required, compared with the 5.5 MHz currently used on 625 line TV. The system bandwidth chosen was from DC to 100 MHz. This means that the constituent components (ie, photomultipliers, head amplifiers, mixers, video channel, and finally the acousto-optic modulator) must have responses individually in excess of this bandwidth. The advantage of this exceptionally wide bandwidth video system is that 6.25 million picture points per frame are produced. This gives approximately twice the resolution of conventional CCTV systems, but of course over a much larger field of view.

IMAGE GENERATION

The image displayed by the projector can be derived from a modelboard, from computer generated imagery, or a combination of both.

Modelboard with laser camera

The chosen scale for a NOE modelboard is 1000:1 and as stated earlier, the laser camera probe allows closely representative vertical and horizontal approach distances at this scale. Modelboard development at RSL has shown that very detailed models may be produced at 1000:1 which give a variety of ground texture and tree detail, these should enable accurate height, distance and speed judgements to be made.

In addition, pylons, wires, buildings, and vehicles, have been modelled with sufficient realism to allow examination at close range, eg 10-20 mm actual, 10-20 metres visual.

Conventional camera systems are unable to focus on such close objects without blurring the more distant scene, due to the limited 'depth of focus' imposed by a finite entrance pupil, together with the fact that the lens system operates on the whole field of view. The laser has similar limitations, but in this case there is a technique available which can overcome the problem. As the laser beam scans across the terrain board it is possible to re-focus the laser spot rapidly during the line scan to keep all objects in focus and hence provide a large effective depth of field.

This fast focussing device incorporates electro-optic cells that are able to switch the plane of polarisation of the laser beam which when operated in conjunction with bi-refrangent lens, has the effect of selecting one of the two focal states of the lens. By using three cells, eight different focal states are provided to give a smooth change of focus with distance, with an operating speed fast enough to optimise the resolution, within a single scan line for objects from 5 mm to the far distance.

A range finding device, which would probably use a triangulation method will be required to provide the focussing device with the appropriate switching information.

Light gathering, comparable with modelboard illumination in a conventional camera/modelboard system, is provided by photomultiplier tubes and will be produced primarily by those detectors which move with the camera. These will be arranged in a series of concentric circles around the probe and will extend for a radius of perhaps two metres scale, corresponding to two kilometres visual range. If more distant scenes are required, these will be provided by fixed photomultipliers arranged in much the same way as the fixed lamp bank on conventional systems.

Photomultipliers are extremely sensitive to light and will produce a video signal which has much less noise content than a typical CCTV camera. Also the electrical power required to drive the camera lasers is only a fraction of that used in supplying a lampbank.

The combination therefore of a laser camera, photomultiplier detectors, and advanced terrain modelling at 1000:1 scale, can produce a highly detailed, in focus, wide-angle image that should provide a unique visual capability for many low-level training applications.

Aircraft that may require this type of image generator would include attack, scout and supply helicopters, anti-tank and ground attack fixed wing aircraft and VTOL.

COMPUTER GENERATED IMAGERY

The projector described above has the capacity to display over six million picture points (for comparison, a 525 line television will display 1/4 million).

The technology of CGI has now advanced to the stage where a high quality continuous tone image extending over a number of juxtaposed conventional displays can easily be produced⁴.

The scanned laser system is a continuous wide-angle display. The 180° by 60° image can, however, be formed by segmenting the viewing volume and dedicating a single CGI channel to each segment. In the case of the Rediffusion/Evans and Sutherland CT 5 image generator, it would be desirable to use six channels and to increase the pixel count to one million per channel. Now the scanned laser system scans in spherical polar co-ordinates, and conventional CGI assumes a display plane. There is, therefore, a need to either convert the standard image to spherical polar form, or to compute the image directly in the required form. The goals set for the design of a CGI system compatible with the scanned laser system were:

- a) Preservation of scene and pixel capacity with respect to available flat plane image generation
- b) Assure the straightness of edges
- c) Assure the continuity of scenery across computational channel boundaries
- d) Assure the preservation of fog and intensity gradients to the extent that they reveal or suggest shape and distance, and that Mach banding is not introduced
- e) Assure that a given level of scene quality achieved by anti-aliasing is not significantly reduced
- f) To not permit any increase in CGI throughput delay

All the above goals can be met by redistributing the scan on the image plane so that spherical pixels are generated directly. This can be achieved with little impact on hardware and processing capacity by a simple change of parameters in the nested interpolation formula used to convert analytic descriptions of scene elements into imagery. Such an approach preserves the in-built anti-aliasing measures and the continuity of imagery between computational channels without adding to the throughput delay.

By adopting this technique it is possible to configure a CGI system in which several computational channels can be combined to produce a high quality wide-angle image stored in a frame buffer. This store can then be read out at a video rate compatible with the scanned laser projector.

THE FUTURE

Computer generated imagery

Wide-angle displays such as the scanned laser projector have an enormous appetite for pixels if the images are projected with a uniform high resolution. The eye acuity curve only permits the viewer to see a high resolution image over a very narrow angle about the fovea, with a rapid fall off in acuity as the eccentricity is increased. An image generator which produced imagery matched to the resolution capability of the eye would, in principle, use the minimum amount of hardware to produce the image. In practice, the production of eye limited resolution image would require very accurate tracking of the eye pointing direction and an image generator with an effective zero throughput delay. This is unlikely to be achieved but a compromise solution in which a high resolution area of interest is moved within a larger field of view with lower resolution imagery is possible in the near future.

Display devices

There is a trend, for air combat training, for example, towards large field of view systems with resolution as good as the unaided eye. The design of such systems poses interesting interactions between factors such as resolution, system bandwidth, visibility of projectors, image distortion, brightness, etc.

As discussed in the previous section, the system bandwidth can best be utilised by an area of interest type display. If a lightweight projector is mounted on the pilot's helmet, then it will move with his head and will always present an image in the direction the pilot is looking. It will therefore have the same mobility as the pilot's head and will enable a training simulator to be built in which the total field of view will be limited only by the cockpit structure. Such a projector will almost certainly be laser based to give the required resolution and will present separate right and left eye images on a small dome screen to give the correct vergence cues⁵.

SUMMARY AND CONCLUSIONS

The Rediffusion scanned laser system (Figure 3) has a unique potential for displaying continuous wide-angle scenes from either a modelboard or CGI. When using the laser camera and 1000:1 modelboard as the image generator, a very detailed image will be produced that should have particular relevance to NOE flying training⁶.

CGI is more likely to be used for ground attack or air-to-air combat situations. The visual system would also appear to be suitable for simulating narrow angle, head directed vision aids, requiring a large field of regard.

Rediffusion has, through several separate development programmes funded by PM Trade, USAF, MoD, and PVR & D, proved and demonstrated a large part of the technology required to build a practical visual training aid.

REFERENCES

1. Mission environment simulation for Army rotorcraft development
- requirements and capabilities
D. Key, B. Odneal and J. Sinacori, AGARD - CP-249
2. Wide-angle visual system developments
C.R. Driskell, AGARD - CP-249, April 1978
3. Insidious ocular effects of laser radiation
Dr Brennan, RAF Institute of Aviation Medicine, Farnborough, UK,
May 1980
4. A new visual system architecture
R.A. Schumaker, Proceedings 2nd Interservice/Industry Training
Equipment Conference, November 1980
5. UK Patent Application - 7 944 045
6. Analysis of the design of an AH-64 combat mission simulator
P. Caro, W. Spears, R. Isley, E. Miller, Seville Research
Corporation, December 1980
7. Conceptual design of a rotorcraft advanced visual system
A. Deel, Proceedings 2nd Interservice/Industry Training
Equipment Conference, November 1980

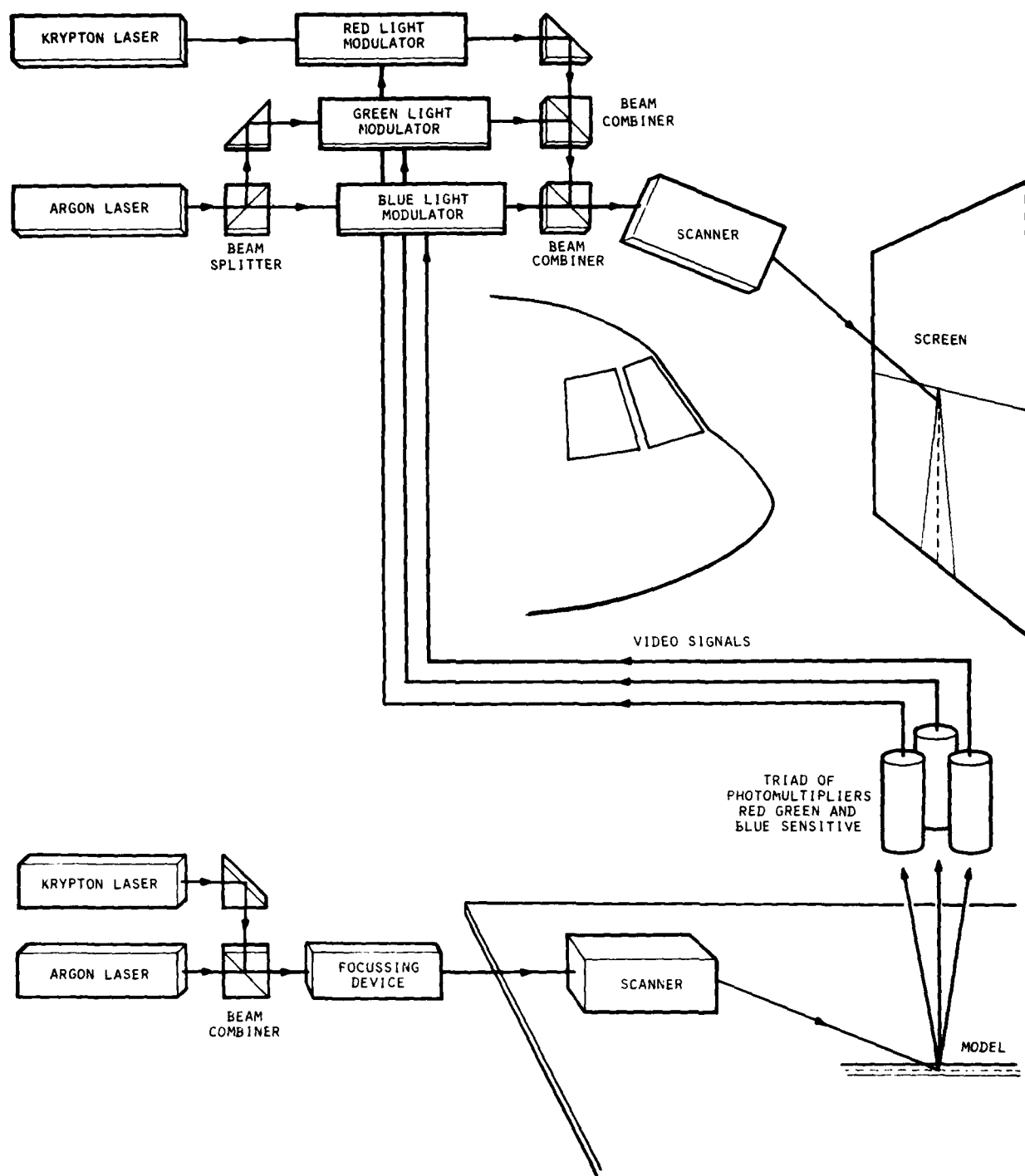


FIG 1
Laser T.V. System for Visual Simulation

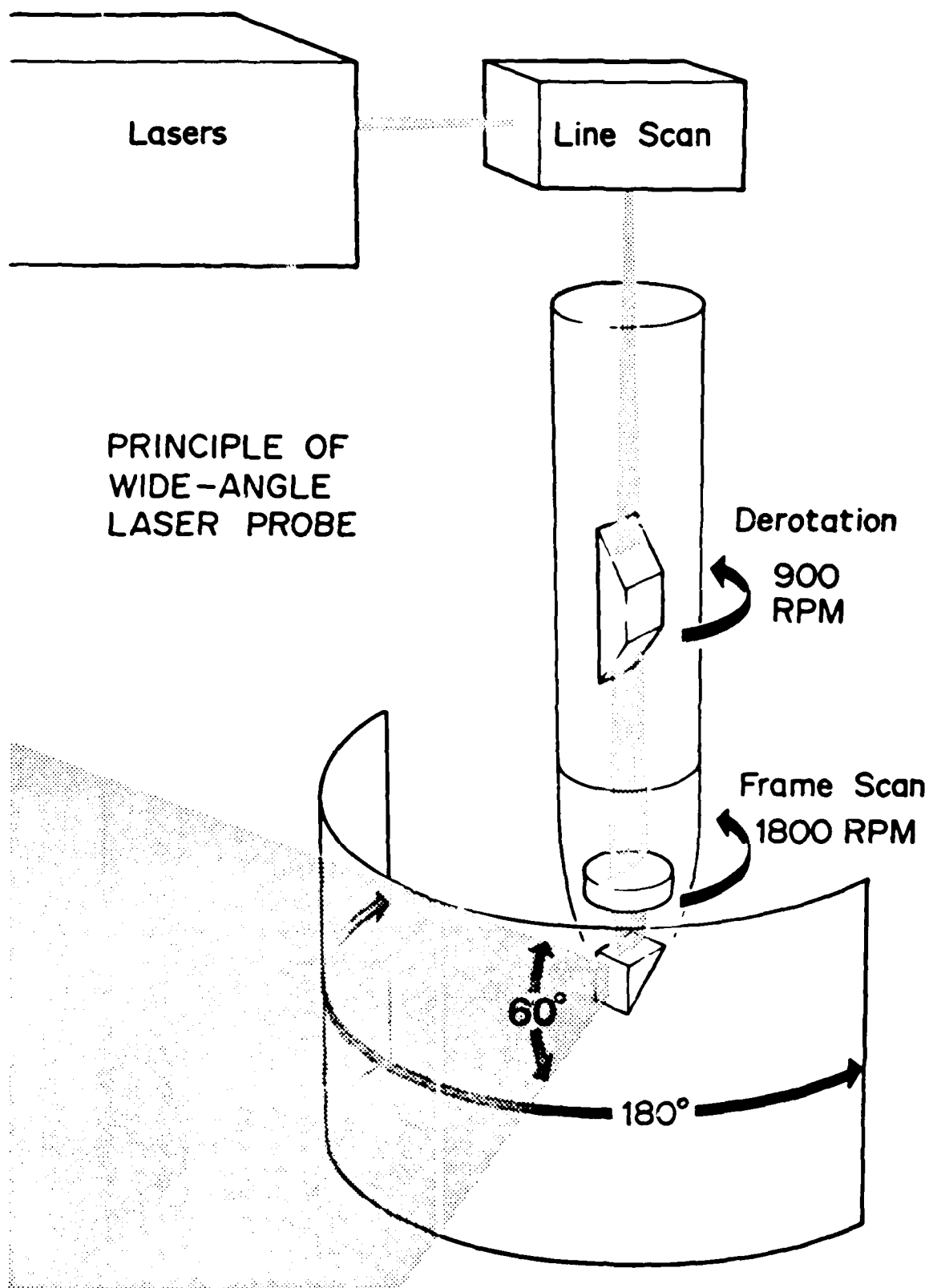
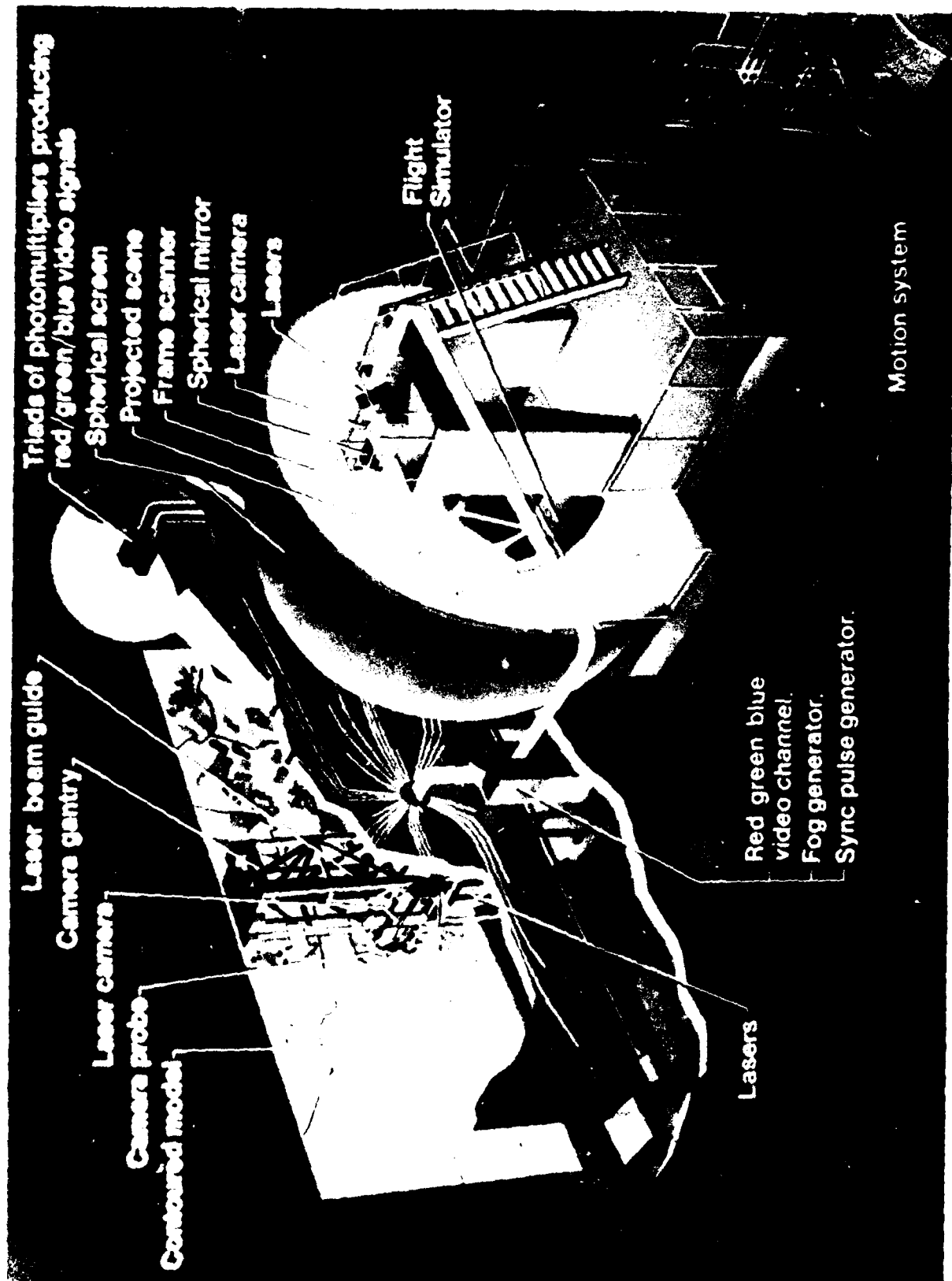


FIG 2

FIG. 3



INVESTIGATION OF SIMULATOR
DESIGN FEATURES
FOR THE CARRIER LANDING TASK



Daniel P. Westra
Staff Scientist
Canyon Research Group, Inc.

Daniel P. Westra earned his Ph.D. in Human Factors Psychology from the University of South Dakota in 1978. Since being employed at Canyon Research Group, Inc., he has been at the Naval Training Equipment Center's Visual Technology Research Simulator. He is currently involved with a multifactor research program investigating simulator requirements for the carrier landing task. His interests include economical multifactor experimental strategy.



Charles W. Simon
Senior Scientist
Canyon Research Group, Inc.

Charles W. Simon obtained his Ph.D. from Ohio State University in Engineering Psychology. His 34 years of professional experience has been in industry and academia working primarily on military problems. During his 28 years at Hughes Aircraft Company he did experimental studies on equipment design, particularly visual displays. In 1970, he began to develop a new methodology for conducting large scale multifactor controlled experiments economically. He is currently at Canyon Research Group, Inc. applying the methodology on several research programs.

(No photograph available)

Stanley C. Collyer
Engineering Psychologist
Naval Training Equipment Center

Stanley C. Collyer received his Ph.D. in Experimental Psychology from John Hopkins University. He has spent the past 13 years in university, industrial and Government behavioral research laboratories. He has published in the areas of visual perception, information processing, learning and memory. Since joining the Naval Training Equipment Center in 1973, his interests have been primarily in determining perceptual requirements for effective training of flying skills.

(No photograph available)

Walter S. Chambers
Head, Visual Technology
Research Simulator
Naval Training Equipment Center

Walter S. Chambers is manager of the Visual Technology Research Simulator at the Naval Training Equipment Center. He has served on a variety of visual-technology coordinating and working groups sponsored by DoD, NASA, and NATO. He is a graduate of Marshall University.

INVESTIGATION OF SIMULATOR DESIGN FEATURES FOR THE CARRIER LANDING TASK

ABSTRACT

The effects of eleven factors on carrier landing performance in the Visual Technology Research Simulator (VTRS) at the Naval Training Equipment Center (NTEC), Orlando, Florida, were investigated within a single multifactor experiment. Subjects for the experiment were eight experienced naval aviators. Nine display and simulator factors (Fresnel Lens Optical Landing System image, ship detail, field of view, visual lags, seascape, brightness, TV line rate, motion and engine lags), one environmental factor (turbulence) and subjects as a factor were studied. The purpose was to determine and rank order the sizes of effects, identify factors having no effect, and to obtain information for making decisions about future transfer-of-training studies. Results indicated small to null effects for equipment factors. As these factors were manipulated over a wide range of interest representing expensive vs inexpensive simulation options, the implication is that simulation for carrier landing skill maintenance and transition training does not require the more costly levels of fidelity for these features. Simulator requirements for training at the undergraduate level are currently being examined.

INTRODUCTION

The Visual Technology Research Simulator (VTRS) at the Naval Training Equipment Center (NTEC), Orlando, Florida, has been designed for research on flight simulator requirements for training and skill maintenance. The VTRS consists of a fully instrumented Navy T-2C jet trainer cockpit, a six-degrees-of-freedom synergistic motion platform and a wide angle visual system that can project both computer-generated and model-board images onto a spherical screen. The visual system is capable of displaying images via target and background projectors subtending 50° above and 30° below the pilot's eye level and can display 160° of horizontal field (Collyer and Chambers, 1978).

The current phase of effort at VTRS involves research to define simulator requirements for the carrier landing task. There was a need to investigate a large number of visual and other simulator features of interest to simulator designers because of their large cost implications. It was considered necessary to search for a more economical and organized method of investigation than has traditionally been employed in human factors research. A research program was therefore planned around the holistic experimental philosophy and paradigm discussed by Simon (1977; 1979). Fundamental to this approach is the importance of studying as many factors of interest as possible within a single experiment. In so doing, the information obtained will generally be more accurate and comprehensive, can be generalized to more operational situations, and will have been obtained more economically than would otherwise be possible. This holistic approach not only involves the data collection plan, but also covers the preparation, analysis, and interpretation phases of a program.

The experiment reported here, which investigated the performance of experienced pilots, provided information regarding the absolute and relative effects of eleven factors and their critical interactions. It also provided

a vehicle for exhaustively testing and debugging the simulator (both hardware and software), developing new performance measures and refining the methodology. The information acquired in this effort is directly relevant to the design of simulators for skill maintenance and transition training, and is also useful for the study of requirements for undergraduate training. This experiment culminated the first stage of a three-stage program that is an efficient and systematic way to investigate flight simulator design features. In such a program, performance studies are followed by "quasi-transfer" studies (the simulator is the criterion device as well as the training device) and finally by actual transfer studies (training in the simulator is followed by testing in the airplane). Information acquired at each stage can be used to make decisions regarding research strategy and selection of factors to be investigated at following stages. In addition, the information here could be reexamined later when transfer-of-training data were obtained from less experienced pilots in order to see the relationships that exist between these two bodies of data, thereby beginning to establish general principles relating performance to transfer.

METHOD

Task

The task was to land the simulated T-2C training jet on the aircraft carrier Forrestal, as depicted by a computer image generation (CIG) system. A trial consisted of a straight-in approach flown from just over a mile from the ship with the aircraft initialized on glideslope, on centerline, and at the proper angle of attack. Although a circling approach is part of the day-time carrier landing task, the decision was made to separate it from the final straight-in segment. The turn and final approach are in fact two tasks separated by the factors likely to be important, the nature of the psychomotor skills required of the operator, and the measurements that are critical. Including a study of the turn with the final approach would only add variability to performance which would mask the information of interest. A separate study with the final turn was done for factors selected as potentially having an effect on turn performance and is reported in Westra, *et al.* (1981).

The carrier approach and landing task involves a family of visual cues external to the cockpit. The principal cues come from a visual landing aid called the Fresnel Lens Optical Landing System (FLOLS) for vertical glideslope control; carrier deck runway, centerline and dropline markings for lineup control; and the sky, horizon, and seascape for general aircraft attitude control.

Factors

Many factors originally designated as candidates for study were pared down by a panel of engineers and psychologists into the set of ten factors shown in Table 1.¹ This final list of factors represented a number of design

¹Two other simulator factors with large cost implications which were part of the first research effort but not included in the experiment presented here were G-seat (on or off) and ship type (computer-generated image or model-board). Results for these two factors are reported in Westra, *et al.* (1981).

TABLE 1. FACTORS AND SUMMARY OF LEVELS SELECTED

FACTOR	LEVEL SETTINGS	
	"low"	"high"
FLOLS	TV/CIG	Optical/Model
Ship Detail	Night point-light	Day Solid Surface
Field of View	-27° + 9° Vertical + 24° Horizontal	-30° to 50° Vertical + 80° Horizontal
Visual Lags	200 msec Total Delay	100 msec Total Delay
Seascape	Gray Homogeneous Background	Wave Pattern
Brightness	Ship: 0.40 fL Sea: 0.04 fL Sky: 0.02 fL	2.80 fL 0.50 fL 0.16 fL
TV Line Rate	525	1025
Motion	Fixed Base	Six-Degrees-of-Freedom
Engine Lags	7½ Hz Update	30 Hz Update
Turbulence	Close to Maximum Flyable	No Turbulence

considerations relevant to carrier landing trainers. They were considered to be the most important in terms of cost implications and potential effects. These factors could generally be categorized as display and simulator hardware fidelity variables. Seven of these factors were visual system parameters which directly affected the quality of the visual cues. Training aids or augmented simulation features were not considered for this performance study as they cannot be meaningfully studied apart from their effect on learning and transfer of training.

The goal in choosing the factor level settings was to bracket the reasonable range of interest. Thus "high" and "low" levels for each factor were set with this in mind. Most factors had their high levels set at the "best" or optimum engineering levels attainable while the low levels were chosen to be the most degraded form of the factor still within the reasonable range of interest. Some factor level settings cannot necessarily be placed in the above categories and were simply comparisons of two design options differing in cost.

The FLOLS high level was an optical projection of a scale model of the FLOLS providing essentially real-world duplication of the 24 ft. wide array of lights except for a constant magnification of 1.5X. This high resolution direct optical projection was specially built for this test to represent maximum realism. It is not in current trainers and would be a high cost additional subsystem. The FLOLS low level was a TV projection of a CIG FLOLS data base defined by 96 edges. The two datum bars (stationary elements used as reference lines for the moving element known as the "meatball") which normally consist of six lights each were represented by two solid bars. At long range the FLOLS was magnified three times normal size, gradually shrinking to 1.5X at the ramp. The large magnification was required to compensate for limited TV resolution so that the pilots could discriminate meatball position for glideslope guidance at a range similar to the real world. This FLOLS magnification technique is regularly used on Navy carrier landing trainers with the TA-4J trainer (device 2B35) using magnifications as large as 7X. This technique involves no added cost to CIG carrier landing visual equipment.

The ship detail high level was a daytime solid model CIG carrier whose surfaces were defined by 985 edges. It contained all landing deck markings and was scaled normal size. This detail level was representative of that available from daytime CIG systems costing several million dollars such as the 2B35 trainer, although displayed at higher resolution than available in the 2B35. The ship detail low level was a night point-light CIG carrier deck consisting of 137 lights. It contained all deck outline, runway, centerline and drop lights, with the runway surface becoming visible during the final 1600 ft. of the approach. Its image is representative of a night CIG system costing less than a million dollars which is used on several Navy Night Carrier Landing Trainers (NCLT's).

The field of view high level was a 160° H by 80° V wide angle display which is costly and is representative of that currently available for carrier landing training only on multitask trainers such as the 2B35 and the F-14 Wide Angle Visual System (WAVS). The field of view low level was a 48° H by 36° V narrow angle display which is representative of the lower cost NCLT's used for F-4, F-14, A-6, A-7, and S-3 transition training.

The visual lag high level of 100 msec from stick input to the completion of the first field of video output is representative of a 30 Hz update computer simulation and a 60 Hz CIG update. This response time is faster than available on current Navy trainers and represents increased computer capacity and cost. The visual lag low level of 200 msec is representative of a 15 Hz update computer simulation and a 30 Hz CIG update. This response time is representative of the lowest level normally considered in simulator acquisitions with visual systems.

The seascape high level was a water texture pattern generated by a flying spot scanner readout of a photographic film plate of a seascape wave pattern. It provided translation and ground growth as well as attitude (i.e., roll, pitch, yaw) information considered to be potentially useful as cues for improved aircraft control and visual realism. The seascape low level was the absence of the texture pattern and the use of a uniform grey level below the horizon, providing roll and pitch information only. This, of course, represents a reduced cost by eliminating the seascape image generator.

The brightness high level of 2.8 foot-Lamberts (fL) for the target is representative of most narrow angle visual systems used on trainers. The brightness low level of 0.4 fL is representative of most wide angle dome displays such as the F-14 WAVS. To increase the wide angle display brightness to the higher level, if found advantageous for carrier landing training, would be very expensive and would require considerable development time.

The TV line rate high level of 1025 is the maximum available in standard TV equipment. The TV line rate lower level of 525 provides only half the resolution but represents low cost commercial equipment. This factor as used in this experiment relates only to narrow angle projectors which use zoom magnification to provide high resolution displays such as in the F-14 WAVS.

Three additional factors not involving visual equipment were included in the study. A six-degrees-of-freedom 48 inch synergistic motion platform was fully operational for the high level and stationary for the low level. This platform is similar to those on the Navy's 27 T-2C Instrument Trainers (device 2F101) used in Undergraduate Pilot Training (UPT) except that VTRS computation rates are higher for reduced cuing time lag. While it is representative of many older platforms on existing trainers, it does not have the low noise and improved response of new platforms.

Engine computation time lags were set at 30 Hz and 7.5 Hz for high and low levels. This factor was included because the rather large engine computations are typically done at low rates such as 7.5 Hz to minimize computer size and cost. Preliminary testing had generated positive reactions by pilots that the 30 Hz engine updates caused the simulator response to feel more realistic. This was considered important since Navy carrier landing approach procedures for jet aircraft typically require frequent throttle changes for glideslope control.

Turbulence was included in the experiment to allow examination of factor effects under two difficulty levels. The high level was set at no environmental turbulence (in this case the no turbulence level was called "high")

as it was presumed to result in better performance). The low level setting was turbulence in the form of wind acting on the longitudinal, lateral and vertical aircraft axes. These "winds" were generated by the summation of sine waves varying in frequencies and amplitudes. They were strong enough to create a degree of turbulence judged by Navy pilots to be near the maximum level under which operations would proceed at sea.

Subjects

The eight pilots were experienced naval aviators with at least one tour at sea. The average number of military flight hours for these pilots was 2254, ranging from 630 to 4500. The average number of carrier landings (non-simulator) was 346, ranging from a low of 50 to a high of 800. Five of the pilots had most recent flight experience in the A-7 aircraft, two in the S-3 and one in the A-4. All were volunteers stationed at Naval Air Station Cecil Field, Florida, at the time of the research.

Design

The basic design was one-sixteenth of the fully crossed full factorial 2^{11} and required 128 experimental conditions separated into four blocks. This design permitted each main effect and each two-factor interaction to be isolated from one another. Main effects were confounded with some three-factor interactions, but the effect of some other three-factor interactions (in strings) could be estimated. The design was modified by dividing the conditions within each original block into two blocks of 16 conditions each in order to test a different pilot on each block, two trials per condition. No main effects and only one two-factor interaction were confounded with blocks, i.e., mean differences among the pilots.²

The replication employed in the design as well as its resolution and size is normally not in keeping with the multifactor strategy of economy at this stage of a research program. No new information is obtained regarding factors by replicating and more isolation of higher-order effects would have been obtained had a different fraction of the total been employed. However, preliminary investigations pointed out several problems that showed the need for replication and fairly large sample size. First, observed trial-to-trial reliability was low and examination of two trials both separately and combined would provide better understanding of the data. Second, it became apparent that many of the factors studied were having little or no meaningful effect on performance. As a number of these had large cost implications, it was considered important to be able to accept the null hypothesis with confidence. The large sample size was needed to decrease the probability of being wrong when stating that certain factors had no practical effects.

Performance Measures

A great many performance measures were examined. These measures included outcome scores defined in terms of the task itself such as glideslope, lineup,

²The interaction of engine lags with brightness was chosen to be confounded with blocks as in the authors' opinion it has one of the lowest probabilities of being important.

and angle of attack deviations for various approach segments as well as touch-down performance. Intermediate aircraft measures of roll and pitch control and input measures of stick activity were also taken. Deviations for glide-slope, angle of attack, lineup, roll, and pitch were summarized over approach segments with root mean square (RMS) scores which were further broken down into the independent bias and variability components of RMS. This follows from the relationship $\Sigma e_t^2/n = \bar{e}^2 + \Sigma(e_t - \bar{e})^2/n$ where e_t is error at time t , n is the number of samples taken and the square root of the term on the left is RMS error. Bias and variability components were subjected to square root transformations. Deviations were measured both in feet and degrees for glide-slope and lineup. Stick summary measures for aileron, elevator, throttle, and pedal were taken simply as total stick movement (unscaled) over a segment. The segments were broken down roughly into distances representing "in the middle", "in close", and "at the ramp" (aft end of landing deck) which the Navy has traditionally used to define segments. These distances were 4000' to 2000' from the ramp, 2000' to 500' from the ramp, and 1000' to the ramp, respectively.

A number of quality scores were created in an attempt to provide information that could be interpreted directly in terms of "goodness" of performance, that is, measures that are clearly related to how accurately and safely the aircraft arrives at the landing deck. Quality of landing scores were created for touchdown lineup, roll, pitch, vertical velocity, and wire trapped. These scores were scaled from zero to 100 with zero indicating performance that was at the point of causing damage to the aircraft or was totally outside of acceptable limits. A score of 100 indicated performance within a fairly narrow range defining "perfect" touchdown. The wire trapped score was based partially on Britton's (1973) Landing Performance Score (LPS). Additionally, percent Time-on-Target (TOT) Scores were created for glideslope, lineup, and angle of attack for the "at the ramp" segment of 1000' to the ramp. Based on recommendations by Navy Landing Signal Officers (LSO's), tolerance bands for on-target glideslope, lineup, and angle of attack performance were $\pm .3^\circ$, $\pm 1.5^\circ$, and $\pm .5$ unit, respectively.

RESULTS AND DISCUSSION

Both univariate and multivariate analyses were performed. Since space limits the amount that can be presented here, only some of the more important and interesting findings will be discussed. The interested reader is urged to consult Westra, et al. (1981) for a detailed presentation of results. Univariate results will be presented for two measures, RMS vertical glide-slope error and roll variability, both in the segment between 2000' to 500' from the ramp. Multivariate results will be shown for seventeen measures which are directly interpretable in terms of the quality of performance.

The columns in Tables 2 and 3 are defined as follows. "Effect" is the difference obtained when subtracting the mean of the low level condition from the mean of the high level condition. "Percent total variance" indicates the relative contribution each source made to the total variability of performance within the experiment. It is obtained by dividing the sum of squares for that source of variance by the total sum of squares. "Mean square" is the variance, or the sum of squares per degree of freedom for the particular source. "F" is the ratio of the specific variance for a source

TABLE 2. RESULTS FOR RMS VERTICAL GLIDESLOPE DEVIATIONS
IN DEGREES 2000' TO 500' FROM THE RAMP

SOURCE	DF	MEAN SQUARE	F	EFFECT	PERCENT TOTAL VARIANCE
Equipment Factors					
Main Effects	9	.051	2.43		6.19
FLOLS	1	.356	16.97*	.075°	4.81
Ship Detail	1	.042	2.01	-.026°	0.57
Seascape	1	.019	0.92	.017°	0.26
Engine Lags	1	.017	0.81	-.016°	0.23
Brightness	1	.013	0.60	-.014°	0.17
Motion	1	.007	0.32	.010°	0.09
Visual Lags	1	.003	0.14	-.007°	0.04
Field of View	1	.001	0.07	.005°	0.02
Line Rate	1	.000	0.00	.000°	0.00
2-Factor Inter. ¹	44	.017	0.83		10.35
3-Factor Inter. ²	59	.036	1.71		28.65
Turbulence	1	.387	18.45*	-.078°	5.23
Subjects	7	.120	5.70*		11.31
Residual (error) ³	135	.021			38.27

*Probability $\leq .004$. This results in $\alpha \approx .05$ for 13 simultaneous independent F tests.

¹Includes all two-way interactions except engine lags by brightness.

²Includes all three-way interactions or strings of three-way interactions not confounded with lower order terms.

³Includes trial differences and all interactions with trial plus four-way interactions not confounded with lower order terms.

over the residual variance. The residual variance is actually a composite of all effects of trials as well as four-factor and higher interactions that could be isolated. (The trials effect was examined initially for the presence of systematic differences and none was found to exist.) It was used as is conventionally done as the error term.

RMS Glideslope Deviations

Table 2 shows the results of the analysis of the RMS vertical glideslope deviations in degrees in the flight segment between 2000' and 500' from the ramp. The analysis of variance reveals that turbulence, subjects, and the FLOLS are the only sources of variance with effects larger than one might expect by chance. The analysis also shows that while the cumulative effects of two- and three-factor interactions account for a good deal of the variance in this experiment, this variability had a high probability of occurring purely by chance. Furthermore, with the large number of interactions involved (44 two-factor and 59 three-factor) on average the contribution of each is small, being 0.23 and 0.49 percent of total variance, respectively. Two-factor interactions were examined separately and summed into a single term only after determining that none was large enough to be considered important.

Neither the large turbulence effect nor the subject effects come as a surprise since turbulence was designed into the experiment to provide at least two levels of task difficulty and individuals ostensibly from the same population do differ. The experimental design was constructed so that differences among each subject's average performance would not be confounded with any of the main effects or interactions of interest.

Of the equipment factors, only the FLOLS effect stood out from the rest for this measure. The magnitude of the FLOLS effect is $.075^\circ$ of RMS glideslope error which is approximately 1/4 of the angle subtended by one of the five separate columnar FLOLS lenses. The sign of the effect indicates that the "low" condition which was the CIG FLOLS had a lower mean RMS glideslope error than the optical FLOLS. This result was surprising since the optical FLOLS was considered the "better" higher fidelity display. However, the CIG FLOLS had been increased in size to compensate for its poorer resolution such that it would be visible from approximately the same range as the optical FLOLS. The CIG FLOLS was then gradually reduced in size until it was the same relative size as the optical FLOLS at the ramp.

Roll Variability

Table 3 shows results for the measure of roll variability in degrees from 2000' to 500' from the ramp. This is a more sensitive and less global measure of an intermediate control loop and has a smaller proportion of "error" variance associated with it. Considering the large sample size involved, the relative power for this measure is very high. Examination of the percent variance column shows field of view and visual lags had the largest effects of the equipment variables accounting for 4.27% and 3.51% of the variance in the experiment, respectively. The narrow field of view resulted in greater roll variability than the wide field of view. Results agree with expectations here since it was felt that the wide horizon on a

TABLE 3. RESULTS FOR ROLL VARIABILITY IN DEGREES
2000' TO 500' FROM THE RAMP

SOURCE	DF	MEAN SQUARE	F	EFFECT	PERCENT TOTAL VARIANCE
Equipment Factors					
Main Effects	9	2.882	9.03*		11.26
Field of View	1	9.836	30.82*	-.392°	4.27
Visual Lags	1	8.086	25.34*	-.355°	3.51
Brightness	1	2.972	9.31*	-.215°	1.29
Ship Detail	1	1.843	5.78	-.170°	0.80
Engine Lags	1	1.728	5.41	-.164°	0.75
Line Rate	1	0.553	1.73	-.092°	0.24
Motion	1	0.345	1.08	.073°	0.15
Seascape	1	0.322	1.01	-.071°	0.14
FLOLS	1	0.253	0.79	-.064°	0.11
2-Factor Inter. ¹	44	0.599	1.85		11.30
3-Factor Inter. ²	59	0.484	1.54		12.60
Turbulence	1	46.326	145.18*	-.851°	20.11
Subjects	7	8.569	26.85*		26.03
Residual (error) ³	135	0.323			18.70

*Probability $\leq .004$. This results in $\alpha \approx .05$ for 13 simultaneous independent F tests.

¹Includes all two-way interactions except engine lags by brightness.

²Includes all three-way interactions or strings of three-way interactions not confounded with lower order terms.

³Includes trial differences and all interactions with trial plus four-way interactions not confounded with lower order terms.

straight-in approach could be useful to the pilot as peripheral information to aid in keeping wings level. Preliminary investigation also had indicated that increased visual lags would cause increased roll variability (until the delay is so long that the pilot stops trying to make precise corrections) and results confirm this. Whether these effects are of practical importance is another issue which must take into account their effect on the outcome of the task among other things.

Brightness shows up as a statistically significant effect in Table 3 but it only accounts for 1.3% of the variance and the magnitude seems small (although there is no good barometer for determining "small" or "large" for this measure). Thus this effect was judged real but relatively minor. Roll variability is sensitive to turbulence effects and also to subject differences as noted by the large amounts of variance accounted for by these factors. The size of subject effects is an item that an investigator wishing to interpret results should not ignore. When other effects are small relative to subject effects, even though statistically significant, generalizability is restricted until the causes of subject variability are better understood.

Quality of Performance

An attempt was made to provide some information for interpreting results in a general or overall sense in terms of the quality of the approach and landing. Multivariate analyses were performed for seventeen quality indices including: RMS glideslope, lineup, and angle-of-attack error for segments 6000' to 4000', 4000' to 2000', and 2000' to 500' from the ramp; percent time on target for glideslope, lineup, and angle of attack for 1000' to the ramp; and the touchdown performance scores described earlier for touchdown lineup, roll, pitch, vertical velocity, and wire trapped. One-factor discriminant analyses were performed for each factor to provide a multivariate ranking of the magnitude of effects. In each discriminant analysis, the levels of the factor were designated as "groups" and the discriminant procedure finds the linear combination of the dependent measures which maximally discriminates between groups. The relative degree to which groups can be discriminated then provides for a multivariate ranking of the factors.

Table 4 shows the results of the discriminant analyses. The factors are listed in the order of greatest differences between levels of factors. Ranking was based on the percent of cases correctly classified into groups based on the discriminant function. A jackknifed procedure was used to predict group membership which helps reduce bias by making a prediction for a trial based on all information except information from that trial. Note that a two-group correct classification of 50% would be expected by chance alone. The multiple R is the multiple correlation between the dependent variables and the levels of the factor and the multivariate F is an approximation based on Wilks' Lambda. (The ranks based on R and F do not correspond exactly to the rank based on percent classification because the jackknifed procedure removes some of the bias inherent in multiple R with correlated measures.)

As Table 4 shows, of the equipment factors, only the FLOLS has an overall effect which is clearly greater than chance as indicated by the multivariate F. Most of the effect was in glideslope control which was better for the CIG FLOLS. Lineup control was also better with the CIG FLOLS

TABLE 4. DISCRIMINANT ANALYSES RESULTS
USING SEVENTEEN QUALITY INDICES

<u>FACTOR</u>	<u>JACKKNIFED % CORRECT CLASSIFICATION</u>	<u>MULTIPLE R</u>	<u>MULTIVARIATE F¹</u>
FLOLS	61.4	.41	2.80*
Ship Detail	57.0	.32	1.44
Seascape	51.4	.28	1.12
Line Rate	51.0	.26	0.99
Motion	49.4	.26	1.12
Engine Lags	48.2	.28	1.15
Field of View	47.0	.22	0.71
Brightness	45.0	.22	0.71
Visual Lags	44.6	.22	0.67
Turbulence	68.5	.50	4.67*
Subjects ²	40.6	.66	4.13*

¹Approximate F based on Wilks' Lambda with 17 and 233 degrees of freedom.

²First discriminant function only. Since there were 8 pilots, the expected percent correct classification is 12.5. F is based on 119 and 1490 degrees of freedom.

*Probability $\leq .05$

in the middle of the approach. Touchdown performance was not affected by FLOLS type to an appreciable extent. Ship detail ranks next in terms of overall effect with 57% correct classification. This is slightly better than chance and although the multivariate F is not significant it must be kept in mind that all other sources of variance are in the "error" term including turbulence and pilots. Thus ship detail was judged as having a real effect on the quality of performance. The effect was most noticeable in lineup control which was better with the highly detailed ship in the middle and in close. Angle-of-attack control at the ramp and the wire-trapped score were moderately better with the high detail ship. No other equipment factor appears to be operating at more than chance in terms of overall quality of the task.

SUMMARY AND CONCLUSIONS

The results for the measures presented here as well as for many other measures examined reveal that, generally, equipment effects were small relative to subject differences. Since the pilots were all experienced naval aviators with at least one tour at sea and their differences in performance still overshadowed equipment differences, there is an implication that a point of diminishing returns with regard to further simulator fidelity improvements has been reached for this task. Only one of the nine equipment factors studied was judged to have meaningfully affected the quality of performance and one other was judged to have marginally affected the quality of performance. Seven other equipment factors were shown to have no effect on the quality of performance although some of these did have specific real effects on some dimensions of performance. A brief summary of these effects by factor follows.

FLOLS - The CIG FLOLS resulted in improved glideslope control compared to the optical FLOLS. Touchdown performance was not affected.

Ship Detail - The night point-light ship seemed to cause a lineup bias to the left. This bias decreased in close to the ramp although touchdown performance for both lineup and wire trapped was slightly worse than with the fully detailed CIG ship.

Field of View - The narrow field of view increased roll variability throughout the approach relative to the wide field of view. Although this was a real effect and may suggest increased workload, no effect on the quality of performance was noted.

Visual Lags - The longer visual delay also increased roll variability throughout the approach. No effect on the quality of performance was noted.

Motion - Pilot and aircraft activity in general seemed to be increased with the motion on, particularly elevator input and pitch variability. This increased activity did not meaningfully affect the overall quality of performance. However, analyses of some specific measures suggested an interaction of motion with turbulence. With turbulence, the motion system improved the touchdown lineup and wire-trapped performance moderately while with no turbulence, motion had no effect or a slightly deleterious effect.

Engine Lags, Seascape, Brightness, and Image Line Rate - Although in a few cases there were specific effects which were statistically significant, generally no more than 1% of the variance was accounted for in any measure by any of these factors. There was no evidence that they had a meaningful effect on performance.

As factors were manipulated over a wide range of interest generally representing expensive vs inexpensive alternatives, the implication is that simulation for carrier landing skill maintenance and transition training does not require the greater fidelity represented by the high levels tested in this experiment. The lower levels tested resulted in little or no performance decrement, and represent relatively low cost options for dedicated part-task carrier landing trainers such as NCLT's. Multitask trainers providing higher levels of fidelity (which may be necessary for other tasks) would not be expected to provide better carrier landing skill maintenance or transition training.

The implications for training at the UPT level will be verified in research now underway. Results of this experiment have been used to make decisions about the next phases of the carrier landing program, including the selection of factors to be carried forward into transfer-of-training research. Experiments using quasi-transfer and actual transfer-of-training paradigms with inexperienced undergraduate pilots will determine the effects of ship detail, field of view, FLOLS size, motion, and other factors.

This multifactor approach provided much information not available from typical few-factor experiments. In particular, the overview that was obtained put the relative importance of the factors into a better perspective. Results are more generalizable because of the many conditions under which performance was investigated, all of which were of interest and concern. The existence of two-factor interactions has been examined far less expensively and more completely than had any subset of factors been studied a few at a time. The approach is recommended to others concerned with identifying the necessary and sufficient characteristics of training devices.

REFERENCES

- Bricton, C.A., Burger, W.J., and Wulfeck, J.W. Validation and application of a carrier landing performance score: the LPS. Arlington, VA: Office of Naval Research, Technical Report NR 196-115, Contract No. N00014-72-C-0041, 1973.
- Collyer, S.C., and Chambers, W.S. AWAVS, a research facility for defining flight trainer visual requirements. Proceedings of the Human Factors Society 22nd Annual Meeting, Detroit, Mich.: Human Factors Society, 1978.
- Simon, C.W. Applications of advanced experimental methodologies to AWAVS training research. Orlando, FL: Naval Training Equipment Center, Technical Report NAVTRAEQUIPCEN 77-C-0065-1, January, 1979.
- Simon, C.W. New research paradigm for applied experimental psychology: a system approach. Westlake Village, CA: Canyon Research Group, Inc., Technical Report CWS-04-77A, October, 1977.
- Westra, D.P., Simon, C.W., Collyer, S.C., Chambers, W.S., and Nelson, B. Investigation of simulator design features for the carrier landing task. Orlando, FL: Naval Training Equipment Center, Technical Report NAVTRAEQUIPCEN 78-C-0060-7, 1981.

SYSTEM STRATEGIES TO OPTIMIZE

CIG IMAGE CONTENT

M. Cosman
R. Schumacker

Evans & Sutherland
Salt Lake City, Utah

(no photo available)

Mr. Robert A. Schumacker is Director, Advanced Visual Systems at Evans and Sutherland. He has been active in the development of CIG visual systems for over 15 years and holds BS and MS degrees from the Massachusetts Institute of Technology.



Mr. Michael A. Cosman has provided technical support to the development of CIG visual systems at Evans and Sutherland for over 7 years, working primarily on image quality and system architecture issues. Mr. Cosman holds a bachelors degree from Brigham Young University.

SYSTEM STRATEGIES TO OPTIMIZE CIG IMAGE CONTENT

M. COSMAN and R. SCHUMACKER
Evans and Sutherland Computer Corporation

ABSTRACT

Along with the rapidly increasing capability of computer image generation equipment has come an increasing appreciation of the role of database design, structure, and management in providing effective training imagery. This paper describes the techniques used in CT-5 image generation systems to organize and manage the database, and to efficiently focus the system resources on producing images of maximum complexity and quality. Approaches to database design that exploit these system characteristics are discussed and illustrated by photographs taken from production equipment.

INTRODUCTION

As computer image generation technology moves into an era of intense and accelerated development, the requirements placed on such training equipment seem always to outpace the available capability. The quest for systems and techniques which provide a meaningful and realistic training environment is intensifying, and increased emphasis is being given to the issues of image quality and image usefulness. The CT-5 systems now in production at Evans & Sutherland address these basic issues by incorporating a comprehensive solution to the problem of image quality, while implementing an approach which provides dramatic improvements in routinely achievable image complexity. Special attention is given to the problem of managing extremely large databases, while making sure that the image generation hardware spends a maximum amount of its resources processing scene details which are relevant to the training mission.

Several basic philosophies and concepts guided the development of the CT-5 architecture. One was the belief that simulated imagery should be as free as possible from any distracting visual artifacts which reduce the impression of realism, or, worse yet, constitute negative training cues. Thus image quality, particularly lack of any of the symptoms of aliasing so characteristic of some previous systems, was a prime design goal. Another was the notion that system capacity must be more cleverly used in order to be maximally effective, hence a database development and management strategy which emphasizes providing scene details of greatest visual significance.

This paper will discuss three main areas of the CT-5 technology in some detail: The display processor and its impact on image quality; the viewpoint processor and its role in providing relevant scene details; and an approach to database structure, design and development which effectively supports and exploits the capabilities of the first two.

SYSTEM OVERVIEW

Figure 1 shows a basic configuration of CT-5 components that provides a single channel capability at standard (525-line) resolution. The major sections include a general purpose computer (a Digital Equipment Corporation PDP-11), special purpose hardware called an image processor, and a display.

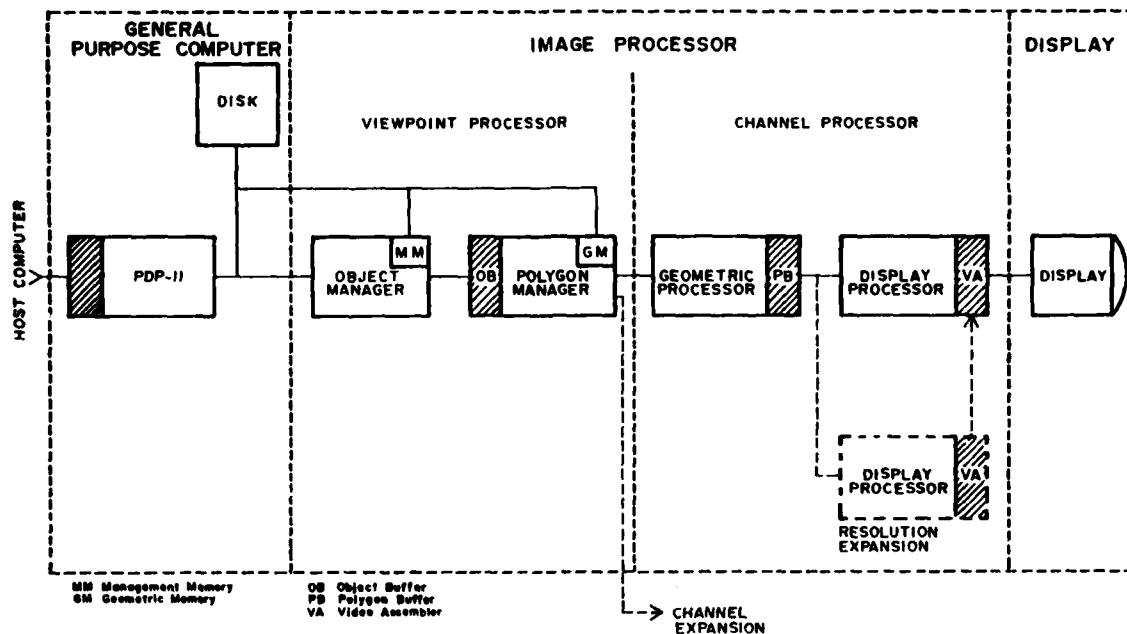


Figure 1 Basic CT-5 Configuration

The general purpose computer interfaces to the image processor and to the host computer, and monitors and manages the visual system. It hosts the magnetic disk on which the database is stored, and provides support for database development, system maintenance and hardware diagnostics.

The image processor in this simplest configuration consists of one each of four basic unit types, and would occupy two standard equipment racks. The addition of system units to increase resolution or add channels is accomplished as indicated in the figure. The system is structured as a pipeline of processing units where computing tasks are distributed along a sequence of dedicated computing elements. The cross-hatched areas in Figure 1 represent the several field buffer memories in the system. One television field time is allocated to transport and process data from one field buffer to the next, thus each device can operate at its own pace and be designed to accommodate only the average complexity of an image field.

The object manager and polygon manager comprise what is called the viewpoint processor. They perform image computation functions which are system-wide (i.e. channel independent). These functions include the processes required to identify the necessary subset of the database required for a specific eye position, and fetch and process this data to an appropriately selected set of scene elements which are potentially on-screen, front-faced and at their proper level of detail.

The geometric processor performs all computations required to transform the incoming model-space description of scene elements into a two-dimensional perspective image in display space. These steps include rotation, clipping and

perspective division. The result of this process is an image-plane description of all scene data, which is stored in the polygon buffer.

The remaining steps to generate the final image are accomplished in the display processor, which performs hidden-surface removal and "scan conversion", although both operations proceed in significantly different ways than heretofore. The display processor also applies the effects of fog, illumination, shading and color.

THE OBJECT MANAGER

The object manager performs three main functions: management of the database from the magnetic disk to the management and geometry memories; culling of the database to extract the minimal set of required scene elements for a given eyepoint; and ordering of the scene elements into visual-priority order (front to back). Its main parts are the management memory, the cell processor, and the priority processor.

The cell processor traces a database tree, discovering and outputting pointers to collections of scene elements as branches of the tree are traversed. The local depth of tree tracing depends on the results of the various database management tests, and the order of tree tracing is determined by the priority processor, which orders the scene elements into visual priority order according to the procedure specified in each local collection of scene elements. In order for this process to be better understood, we pause here and discuss the database structure itself.

Database Organization and Structure

The database is a hierarchical tree structure of geographically organized nested levels of detail. Embedded within the database structure is information required to perform a variety of culling tests. The inter-relationship of the tree parts provides a structure which is self-managing. The nature of this structure will become more apparent as we define and use the following terms:

A scene element is either a polygon or a light. The modeler can specify the reflectance at each vertex of a polygon, or he can have the image generator calculate each vertex reflectance by performing a sun calculation once per polygon (flat shading), or once per vertex (smooth shading). The modeler also specifies a color for each polygon, and may specify special features such as color blending. Lights may be specified individually or as strings, where a string may be straight or curved. The modeler can also specify directional, flashing, rotating and strobing characteristics for lights.

An object is a collection of scene elements. The scene elements within an object are usually related by structure or geographic proximity, and the order-of-encounter of scene elements within an object is assumed to be their visual priority order. Objects can be specified as transparent. Several levels of transparency are provided, giving the modeler great flexibility in representing important cues such as the pilots helmeted head inside a canopy.

A cell is a volume in model space represented by a decision node in the database tree. A cell can have up to two option pointers and a transition range which is used to choose between them. Associated with the cell is sufficient information to perform a coarse field-of-view test. This FOV test is done so as to be valid for all database elements that subsequent portions of the database tree may invoke.

An option pointer is a pointer to either an object or a mesh. If the pointer references an object, then the tree structure along this path is finished. If the pointer references a mesh, then more tree tracing may be done. As the cell processor traces the tree, object pointers encountered are output to the polygon manager while mesh pointers cause the cell processor to reenter its mesh processing algorithm.

A mesh is a collection of cells. Included within the mesh is information which allows the visual-priority ordering of the cells to be accomplished. They can be fixed-ordered, range-sorted (by the real-time software), or ordered by the structure of planes and relationships contained within the mesh. This last approach, while using some common notions such as separating planes and priority relationships, is far more flexible than the usual binary tree method. Modeling constraints are considerably relaxed, since priority structure is confined to local geographic regions, limiting priority interactions to relatively small collections of scene data. In addition, complex three-dimensional geometry which would be impossible to resolve with binary trees is easily done without the need to perform artificial subdivision of polygons and objects along various separating planes.

Culling tests are performed to eliminate, as early as possible and in pieces as large as possible, those portions of the database which will not appear in any display channel. These culling tests include level-of-detail (only the simplest representation of an object necessary for a given viewing distance is used), field-of-view testing (does the item impinge on any display channel), backface test (polygons whose visible sides face away from the eyepoint), and perspective area (polygons whose projected screen area is smaller than a system-controlled threshold). Level-of-detail and field-of-view tests are applied in the object manager in a nested hierarchical fashion; field-of-view, backface and perspective-area tests are done in the polygon manager on a scene-element basis.

The database tree is the structure of meshes and objects organized by their association into cells. Each item in the database is uniquely associated with both its parent (calling) item, and items it references (its sons). The structure thus provides for a hierarchical processing of the database, controlled by level-of-detail considerations, culled by field-of-view constraints, and ordered into visual priority.

The Cell Processor

The cell processor traces the database tree once every field, outputting the proper sequence of object pointers to the polygon manager to draw the image. A field is initiated when the cell processor is given an eyepoint and

the database visual environment mesh pointer. When a mesh is processed the priority processor determines the output order of the cells while the cell processor performs field-of-view and transition-range calculations. Cells which don't impinge on any channel are not output and all further processing on these cells ceases. The remaining cells are output in their priority order, and the transition range calculations are used to determine, for each cell, which option pointer will be pursued. Since the visual-priority ordering of cells in each mesh applies to the scene elements which the cells will ultimately invoke, when a mesh pointer cell is output the new mesh must be processed before resuming the output of cells in the current mesh. Thus the algorithm must be reentrant. When a mesh is completed (i.e. when all of its cells have been output and none invoked new meshes), the algorithm "pops" back to the previous level of processing to resume the previous mesh. The processing of the database tree proceeds in this manner until all branches specified by the level-of-detail tests have been traced, and all object pointers have been output to the polygon manager.

The Pager

Implemented within the object manager as a background task is an algorithm whose function is to manage the physical memory so that potentially required database scene elements are resident. The pager embodies many of the database management concepts from previous Evans & Sutherland systems, but executes those processes within the hardware at greatly increased efficiency. A consequence of this is the ability to manage databases whose actual size is limited only by the fixed storage medium (the disk), and with speed limited only by the disk seek/transfer rate.

The pager traces the database tree in much the same fashion as the cell processor; however, no consideration is given to the visual-priority ordering of database elements, and no field-of-view rejection is performed. A pager pass is initiated when the PDP-11 sends the pager an eye vector and the database input mesh pointer. The database tree is processed for level-of-detail decisions, and the pager checks that each item required is resident in physical memory. As it traces the tree it discovers items needed but not resident. These are requested from the PDP-11 and are sent from the disk via "direct-memory-access" mode. The pager also identifies database blocks which are resident but not required, and such memory blocks are "garbage-collected" for later use.

This approach to managing the disk/memory interface has several advantages over software based methods. First, the amount of work that the pager must do is related not to the total database size, but only the portion of the database required for a specific viewpoint. Thus the pager load is tied to the local database density, and order-of-magnitude increases in database size cause almost insignificant increases in pager work-load. Second, the process of tracing the tree is very fast—typically the entire on-line database can be traced and update requests identified in much less than a second. Thus the system responds very rapidly to changing database scene-element needs, and the total amount of data required to be on hand can be reduced to a minimum. Third, the process is entirely driven by the database structure itself—the

real-time software needs to know very little about the database to support its management.

THE POLYGON MANAGER

The polygon manager performs sun illumination calculations as well as a number of additional, increasingly discriminating database culling tests. Included within the polygon manager is the geometry memory, which contains the vertex and structural data for the scene elements, as well as information needed for the various inclusion tests.

Processing in the polygon manager is directed by the information stored in the object buffer. This field buffer contains pointers to the various objects required for each channel, as well as control and transformation information. The nature of this structure allows constants, control and geometry to be processed in an intermixed mode, making it possible to accommodate special requirements such as split screen and multiple eyepoints. Also, objects can be preceded by offset vectors to allow instancing (multiple use of scene details).

The polygon manager does the series of tests mentioned above to attempt to discard each scene element. Scene elements which survive all tests continue processing as appropriate to their type. For polygons, the shading type is determined and sun illumination calculations are performed for either smooth, flat or fixed shading. Each scene element is then output to the geometric processor. The required channel-specific transformation matrices are sent to the geometric processor prior to any scene elements that need them.

THE GEOMETRIC PROCESSOR

The geometric processor receives polygons in model space coordinates; it also receives eye vectors and rotation matrices specific to its channel. The geometric processor first transforms the scene element to channel coordinates, then performs clipping to eliminate portions of the polygon or light string which lie off-screen. Light strings are expanded and the directionality of each individual light is calculated according to specific lobe parameters. On-screen vertices undergo perspective division and are scaled to the resolution of the screen, which is much higher than the number of lines or elements. The resultant image-plane description of all the scene elements is stored in the polygon buffer.

THE DISPLAY PROCESSOR

The display processor performs the set of tasks required to transform a display-plane representation of the image into a composite picture with hidden portions removed, image quality preserved, special effects applied, and T.V. formatting accomplished. In CT-5, the display processing function abandons the notions of scan-line processing, and capitalizes on the considerable advantages of area-processing, feature-sequential image processing, and analytic handling of image descriptors to avoid aliasing and greatly extend performance.

The display processor operates on rectangular areas of the screen called spans. A span may be thought of as a collection of display pixels which are computed in parallel. Individual scene elements are submitted to the span processor in visual priority order, and the span processor calculates the image for each span which is thus influenced. The time to compute a span is not a significant function of the complexity of the scene element internal to the span, thus the time to compute a scene element is nearly proportional to its size. One can see how the principal processing functions are accomplished by referring to Figure 2.

Three memories participate in the process. The polygon buffer contains image-plane descriptions of all the scene elements (such as polygons and lights) that are to appear on the display. The video assembler is a dual video field buffer with storage for the red, green and blue components at pixel resolution. This "ping/pong" memory is written into on one side by the span processor while the other side provides video output to the display. The mask memory contains a high-resolution composite record of all prior image regions processed in a field, but it includes only the geometric details delineating the presence or absence of scene data.

As each new polygon is submitted to the span processor, an analytic description of the polygon within each touched span is prepared. The mask memory is used to "erase" portions of this analytic description which correspond to portions of the span which are already occulted. The remainder, which denotes the visible part of the current polygon, is convolved with the spatial filter to derive the display video contribution of this polygon within the span. The incremental effects of the polygon are summed into the video assembler memories after accounting for visibility effects, smooth shading, color blending, transparency, and color. The analytic description of the geometry is then added to the mask memory to occult future submissions to this span.

Several important concepts embodied in this process account for the exceptional image quality thus achieved. First, since the image presented to the spatial filter is a faithful, high resolution rendition of the actual geometry involved, errors due to quantization of the image to scan-line resolution are avoided. Second, since image processing proceeds on the basis

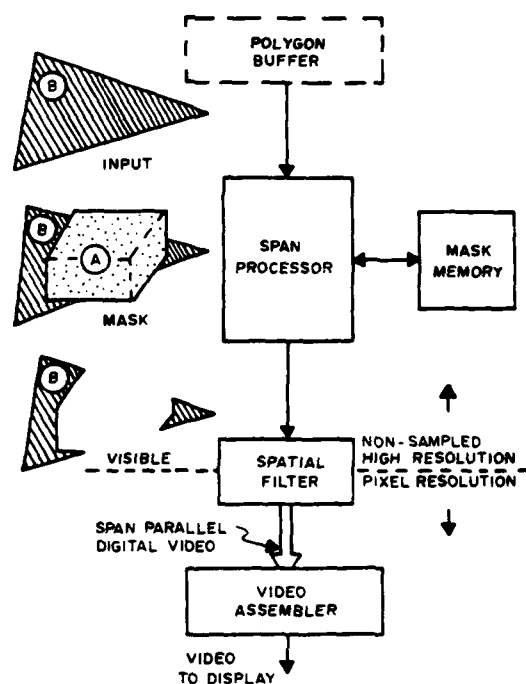


Figure 2

AD-A110 226

AIR FORCE HUMAN RESOURCES LAB BROOKS AFB TX
1981 IMAGE II CONFERENCE PROCEEDINGS.(U)

F/G 14/2

NOV 81 E G MONROE

UNCLASSIFIED

AFHRL-TR-81-48

NL

6-6

4 0204



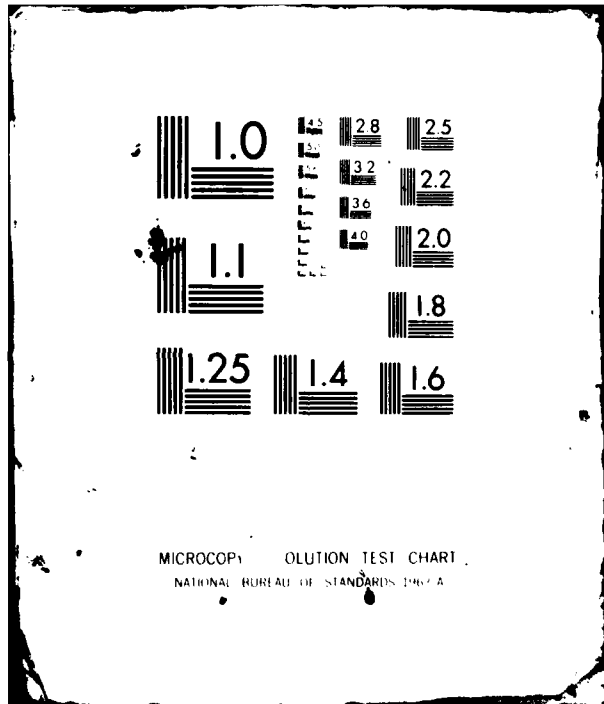
END

DATE

FILED

2 82

DTIC



of rectangular areas on the screen, all imagery is treated identically, without complexity limits, and without directional biases related to raster orientation. Third, spatial filtering, which is performed at the pixel level with a filter approximately two pixels wide, attenuates the higher spatial frequencies smoothly and without loss of phase information. These image processing techniques produce images with high subjective resolution, allowing useful presentation of scene details with dimensions much smaller than the pixel size.

Capacity Characteristics

The area-based nature of the display processing algorithm gives rise to an interesting capacity-versus-time relationship. We can gain an intuitive insight into the nature of this relationship by imagining a basic image which we wish to make more complex, and by observing the way in which the display processor responds.

We can increase the richness of an image in two basic ways. One is to increase the detail of an existing object. In this case, the image area of the more detailed object will be about the same as the simpler one. Although the span processing is based on area, some additional time is required due to the fact that, as scene elements become smaller, the efficiency with which they fit the spans decreases. In this situation, then, the processing time grows somewhat as surfaces are added, but much less than linearly.

The second way we can increase scene richness is to add more objects. In this case, the depth complexity of the scene increases (i.e. the image has, on an average, more layers). However, since we are building the image up from nearest to farthest surfaces, we can skip over portions of the image which have previously been totally occulted. Such a "full-span" mechanism can help to bring the net processing time for a frame significantly closer to that for a tiled image which has no occulted parts.

The net effect of these characteristics is to give rise to a capacity versus processing-time relationship with the general characteristic shown in Figure 3. The interesting property of this timing function is that its slope is appreciably steeper than one; i.e. that small percentage increases in processing time allow large percentage increases in visual complexity. This characteristic makes it very attractive to trade field time for image complexity when needed.

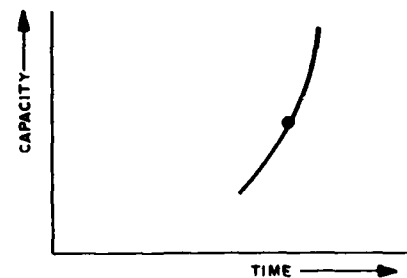


Figure 3

USING LEVEL-OF-DETAIL

Figure 4 shows one potential use of multiple levels-of-detail. Although five levels were used in the example, the system can effectively support an unlimited number of levels of detail. The modeler provides the number of

levels needed for each specific application to optimize tradeoffs between scene fidelity and load requirements. He specifies the transition ranges based on the various compromises that apply to the geometry, color and contrast of adjacent levels of detail, focusing the system resources where they are most needed.

The pager builds the database tree into memory beginning with the lowest levels of detail (i.e. the simplest representations), and it retains in memory all levels up through the ones currently needed. As is evident in the example, the relative cost of keeping around all simpler versions of something is about equal to the cost of the most complex version stored. This cost in memory space is a bargain, since it allows the system to fall back instantaneously to less complex representations of scene elements that are already in memory. The practical advantage is that there is effectively no restriction on how fast the system can respond to load management needs, while traffic at the disk interface is minimized. Note that levels of detail more complex than currently required are not brought into memory, so only the memory needed to actively support the current image (and its fallback lower levels of detail) is in use. Thus the system effectively uses the available memory, closely relating memory usage with the displayed scene complexity rather than the total database size.

The extensive use of level-of-detail, and the rapid response time of the system to changing database scene element needs, provide the capability to manage very large databases while providing high local scene complexity. These characteristics are important prerequisites to effectively performing some simulation tasks which are of particular importance in military applications. For instance, high-speed low-level flight over mountainous terrain or heavy forest can be effectively supported by CT-5 while maintaining high scene complexity and image quality.

RESULTS

The architectural concepts described above lead to some interesting and useful system properties. The following sections summarize the resulting system characteristics that may be of particular interest to those who plan, specify and apply CIG systems.

Overload Response

Overload in CIG visual systems is inevitable. Regardless of the specified capacity of a system, the user will, in time, exceed it. Thus the manner in which a system responds to overload is very important to the user. Two systems with the same nominal capacity can prove to be quite different in practice when compared on the basis of effective performance. Some systems are characterized by having absolute capacity limits which are at or near their nominal performance limits. Breaching these limits, even by a small amount, can result in drastic image errors. The only available strategy in such cases is to tune the model so that overload does not occur—even briefly. This tuning is accomplished typically by limiting model density and by carefully structuring the level of detail transitions to prevent overload - a costly undertaking that generally results in under-utilization of the system.



Figure 4A: 220 Polygons



Figure 4B: 132 Polygons



Figure 4C: 69 Polygons

Figure 4 Frames A, B, C

A C-135 military transport modeled to various levels of complexity. The polygon counts are for the aircraft only, and are the front-faced on-screen (i.e. displayed) polygons. Frames A to C are the highest complexity levels.



Figure 4D: 32 Polygons



Figure 4E: 16 Polygons



Figure 4F: 439 Polygons

Figure 4 Frames D, E, F

Frames D and E are the lowest two levels of detail. Frame F shows a formation of C-135's in which all five levels are represented. The aircraft are at about 500, 1500, 2500, 3500 and 5000 feet. When viewed "in-context", the various compromises in aircraft complexity and geometry are not evident.

CT-5 systems automatically manipulate image generator resources to produce controlled responses over a broad range of impending and actual overload conditions. Thus, the system may be operated at much higher average load levels, and model tuning requirements can be relaxed or adjusted to suit the training mission needs. This fortunate impact on modeling requirements will become increasingly important with the advent of larger and larger data bases as automated modeling techniques are employed and hand tuning becomes prohibitive.

Three principal mechanisms are employed to accomplish load management objectives:

1. CT-5 capacity increases with available computing time. This characteristic, previously described for the display processing functions, also holds for the remainder of the system, where the only limits beside computing time are certain memories, and they are generously sized relative to nominal requirements.
2. Polygons are rejected based on their perspective size. This size threshold can be adjusted to provide continuous control over the number of polygons presented to the pipeline.
3. Overall scene loading can be controlled by level-of-detail selections and the range thresholds at which switching occurs. These thresholds can be changed dynamically.

The general purpose computer monitors load at various points in the image processor and also controls the field time. Under normal conditions the field time is kept constant. Impending overload conditions are sensed and regulated by changing the thresholds on perspective size and level of detail.

If scene conditions should change so rapidly that units cannot complete their tasks in the allotted field time, then the field time is simply extended to provide immediate relief for the problem. Thus the instantaneous penalty for overload is a lower field rate.

Field rate reduction is viewed as a temporary measure to be used while more gradual adjustments are made on level of detail and perspective size parameters. These changes reduce the load by rejecting increasingly larger polygons. Thus the long term penalty is that potentially perceptible polygons are rejected and alternate scene definitions come into use sooner.

At intermediate values of these thresholds it becomes preferable to accept operation at a lower field rate rather than to reject scene details of obvious and useful size. The principal effect of a lower field rate is to introduce the possibility of perceptible flicker. Field time extension is therefore limited to preclude excessive flicker.

Under still more severe conditions the strategy resorts to frame rate update. This doubles the processing time (and capacity) for all units up to the display processor. As a final measure, the display processor can resort to a frame rate update cycle with field rate display.

In summary, the overload response of CT-5 is designed to fit the penalty to the crime. The result: graceful overload response and more useful imagery on the screen more of the time.

Image Quality

One of the principal objectives for CT-5 was to improve image quality well beyond that available from the best existing CIG systems. The CT-5 system approach implements a fundamentally sound and comprehensive solution to aliasing problems. In the course of developing and evaluating these concepts we designed a test pattern that was found to be quite discriminating in issues of image quality. A photograph of the pattern as generated by a CT-5 system on a 700 line color display is shown in Figure 5.

The pattern consists of triangles radiating from a common center. The triangles are defined as maximum intensity polygons against a black background. At the periphery of the pattern each triangle is one pixel wide and the space between neighboring triangles is four pixels. The pattern reveals much about system performance.

The first thing to note from the photograph is that there is very little variation in the appearance of the triangular spokes as a function of their orientation. The system tends to treat scene details equally, without directional biases.

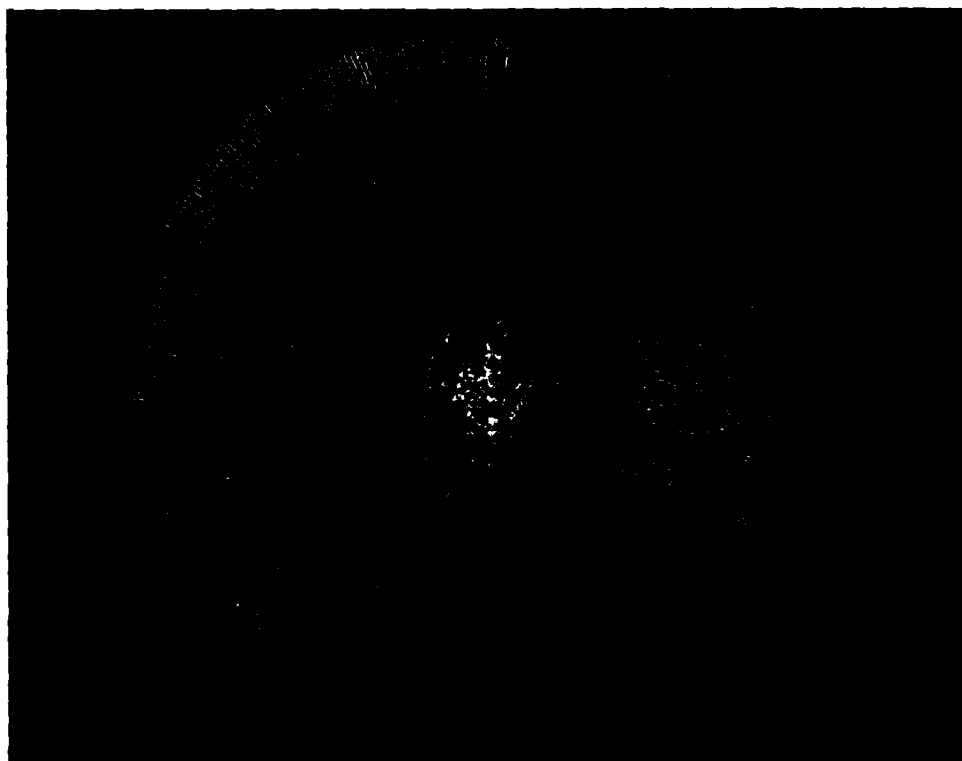




Figure 6

The individual spokes are resolvable towards the center well beyond the half-way point. Thus we see that the system is able to consistently resolve detail that measures less than one half pixel in size, and the detail appears in proper positional relationship (phase) with similar neighboring elements. This aspect of the pattern indicates that high effective resolution is achieved and that small, generally isolated segments of scene detail can be visually tracked down to fractional pixel size.

The final observation about the test pattern performance is that the spokes blend uniformly into the central region. The central part of the pattern maintains a generally constant character and average intensity. Pattern modulation decreases uniformly and no coherent patterns arise toward the central area as would be characteristic of aliased spectra. This property allows small objects to be portrayed and recede unobtrusively into their background.

Figure 6 shows all this theory being applied to a typical modeling situation, and illustrates the detail and quality of images drawn by the CT-5 display processor. Note particularly the runway cracks, which are modeled .05 feet wide (about 5/8 of an inch) on 30 foot grids. The cracks toward the right side of the runway image are still clearly evident and well behaved, even though they are only about 1/7 of a pixel wide.

Expansion

The basic CT-5 system can be expanded both in display resolution and in number of channels by simply adding more units of the types already described. Part of the overall system strategy was to provide an approach to expansion which did not cause degradation of individual channel capacity as resolution or number of channels was increased. The modularity of CT-5 building-block components allows easy and direct expansion with negligible impact on per-channel performance.

Channel Expansion. Channel expansion in CT-5 is achieved by the addition of channel-specific parallel hardware at an early stage in the processing pipeline. These modular system increments provide independent computing capacity for each channel, thereby decoupling the performance of any one channel from that of the other channels. This also makes it possible to conduct simultaneous independent simulations within one CT-5 visual system without the danger of unpredictable interactions among the simulations. CT-5 is designed to accommodate a variety of other special requirements of this type. Independent channels also greatly simplify fault isolation and make it highly probable that failure effects will allow training to continue on the remaining channels.

The parallel channel approach used in CT-5 contrasts with the organization commonly employed by most other CIG systems, wherein a single image processing resource is shared among all channels. That architecture minimizes the channel specific hardware, but the available system capacity must be divided in direct proportion to the number of channels served. Thus, both model and scene densities must be reduced as channels are added. Furthermore,

secondary system constraints such as edge crossings per scanline or total segments often remain constant with increasing channels, and become serious limits when applied to the composite of all channels.

Increased Resolution. Increased raster resolution is accomplished by the modular addition of display processing units. The single DP unit used in the basic configuration provides a raster of 1/4 million pixels - equivalent to a 525 line T.V. standard. Expansion to 700 line resolution has been accomplished, and provision has been made to accommodate 1000 line requirements. The relative distribution of available pixels between lines and elements is quite flexible, thus permitting a wide variation in the aspect ratio of the chosen display. DP units are designed to operate in parallel configurations that divide the span processing load so that there is no attendant sacrifice in channel capacity as resolution is increased.

CONCLUSION

A system strategy has been presented which addresses the problem of optimizing CIG image content. This strategy relies on carefully considering the interrelationship of all the parts that make up a computer image generator, from the database to the display. It includes some novel concepts that offer effective solutions to perennial problems encountered in real-time visual systems. CT-5 applies these concepts in an integrated approach that capitalizes on an increased understanding of the intimate relationship between the image generator and the data structures that drive it.

A hierarchical nested database architecture provides the driving structure for a novel approach to database management. This approach not only frees the modeler from many previously troublesome constraints, but allows the image generation hardware to make optimum use of its resources in providing training imagery of maximum complexity. Special attention is given to the problem of managing extremely large databases, while insuring that images of maximum detail are continuously displayed, and performance limitations imposed by software management algorithms are removed. The hardware implementation of some very powerful database management concepts enables CT-5 to satisfy simulation needs which heretofore have gone unmet, expanding the sphere of effectiveness of the simulation exercise.

The CT-5 display processor makes a substantial departure from the scan-line approaches currently used, and sets new standards of image quality and capacity. The rigorous approach to the preservation of image quality, and the avoidance of aliasing by analytic methods allows CT-5 to provide imagery of unexcelled quality and resolution, while the parallel area processing of scene features eliminates complexity limits imposed by scan-line based systems.

The architectural properties which govern the performance parameters of the system relate processing time, degree of area parallelism and capacity in an intriguing way. This behavior has made possible the provision of an extremely elastic overload response within the context of high basic capacity. The power of the integrated CT-5 approach to load management suggests new directions in database design. In the future, perhaps the objective will be to provide appreciably more model detail than usual, while allowing the load

management capability of the system to keep the displayed complexity of the visual environment at the nominal system performance limits. As database generation processes become more and more automated, and as suppliers and users of CIG visual systems gain increased insight into the complex problem of supplying the important training cues relevant to each mission, the value of this approach will increase.

ACKNOWLEDGEMENT

Many individuals contributed in major ways to the realization of the concepts presented in the paper. The basic genius for many key ideas belongs to Ace Erdahl, John Mason and John Robinson, without whose friendship and tireless creativity the effort might not have succeeded.

AREA OF INTEREST - INSTANTANEOUS
FIELD OF VIEW VISION MODEL



Dorothy M. Baldwin
Physicist, Advanced Simulation
Concepts Division
Naval Training Equipment Center

Dorothy M. Baldwin obtained her M.A. in Physics from Kent State University in 1968 and her B.A. in Physics from Hartwick College in 1965. Her 13 years of professional experience has been in government and academia. Her 3 1/2 years at Naval Training Equipment Center include work on the 360° Laser Scan Display System, the Helmet Mounted Display System and the Annular Projection System. Her current assignments include: Principal Investigator on the Multi-Spectral Image Simulation Project and Principal Investigator on the Active Screens Project.

Area of Interest - Instantaneous Field of View Vision Model

ABSTRACT

Experiments have been carried out using a limbus eye tracker and a static projected scene with a servo driven high resolution area. The results of these experiments are being used to define vision model specifications for a Helmet Mounted Display under development at the Naval Training Equipment Center.

INTRODUCTION

The ultimate goal of the Helmet Mounted Display (HMD) is to provide a pilot with a displayed scene which is indistinguishable from the real world in terms of pilot performance on the required task. Vision model tests have been conducted at NTEC which led in part to the specifications of an optimum HMD. (See Figure 1). The optimum HMD specifications also included trade-off considerations among all the system parameters. The HMD concept is discussed in detail in another paper in these proceedings.

Present visual simulation technology does not provide for all the necessary variables to simulate the real world completely. Therefore, the actual display obtained must be a trade-off among the available parameters. One important parameter is the physical limitation of the human in the loop. For example, it is not necessary to provide a high detail scene in a non-look direction. In fact, psycho-physical experiments are indicating that realism can be obtained by providing a high resolution Area of Interest (AOI) insert within a larger Instantaneous Field of View (IFOV) to match the resolution capabilities of the human eye. The visual acuity of the human eye is one minute of arc in the fovea of the retina. Outside the fovea, the acuity drops rapidly reaching approximately 1/10 of the foveal acuity at 20° from the fovea. Also, indications are that the IFOV does not need to cover the Total Field of View (TFOV) available to the observer. The intention of the HMD system is to apply these concepts to a Computer Image Generator (CIG) which is limited by the throughput delay and number of edges which can be processed in real time. The intent is to use two channels of CIG for the HMD. One channel will be used for the small field AOI and thus have high edge density. The second channel will be used for the larger field IFOV and thus have lower edge density.

The tests conducted at NTEC considered the following as variables: size of AOI, size of IFOV, resolution drop from AOI to IFOV, edge matching between boundaries, brightness fall off, eye tracker AOI, eye tracked AOI and IFOV, and throughput delay variation. The boundary conditions for these variables are defined by considering human visual characteristics, input from our own and other laboratories, and HMD-CIG requirements. Head tracking experiments have not been completed as yet.

EXPERIMENTAL PROCEDURES

The system that was used for vision model tests is a modification of the SURNOT (Surface Navigation and Orientation Trainer). SURNOT is a wide angle display system designed and assembled at NTEC. It consists of a Xenon arc light source, a unique 360° annular projection lens, and a 12.5' radius spherical screen. Figure 2 shows an example of the imagery produced by this annular projection lens. Figure 3 shows the format of the annular image projected through the lens system.

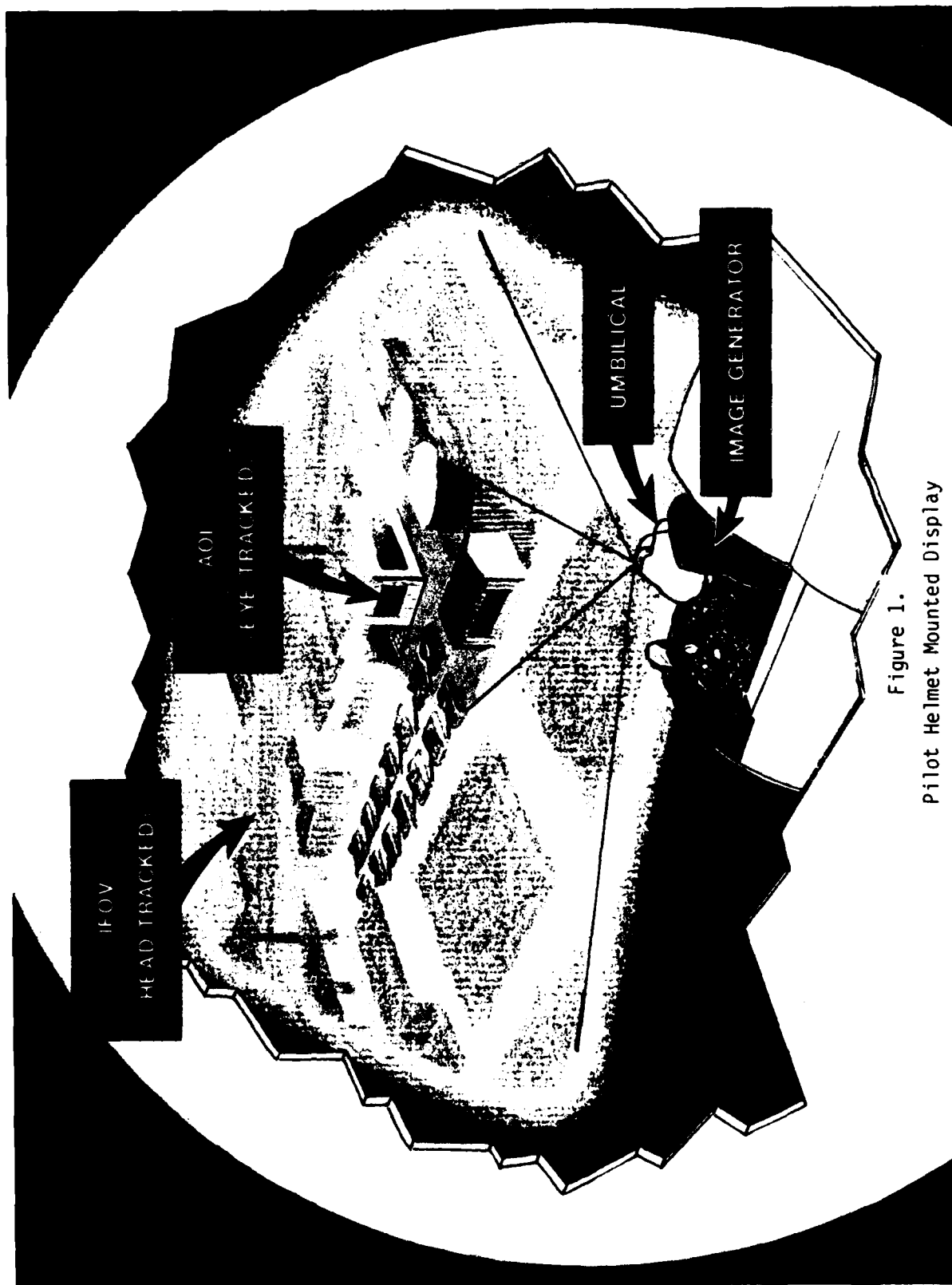


Figure 1.
Pilot Helmet Mounted Display



Figure 2.
Annular Projection Lens Imagery



Figure 3.
Annular Image Format Through the Lens

The system has been modified by placing a servo driven, variable resolution mask near the image plane as shown in Figure 4. The mask is made of acrylic and is designed to reduce the resolution away from the line of sight. The servo, which rotates the mask horizontally, can be controlled by the output from the eye tracker which is a Biometrics Model 200. The servo system was designed and built according to specifications for use with the eye track system. The servo responds to an input of 55 mV/deg and has the following limitations: position error $< .2^\circ$; maximum angular velocity $\geq .6^\circ/\text{msec}$; dynamic jitter < 5 percent; and throughput delay ≤ 12 msec. The servo can rotate $> \pm 90^\circ$.

A block diagram of the entire Vision Model Test System is shown in Figure 5; Figure 6 shows a photograph of the entire test system. For each test, a subject was positioned in a chair facing the screen, head resting in the restraint. The glasses used were calibrated for the individual. Eye movements were sensed by the eye tracker which has a pair of silicon photo-transistors operating in conjunction with a gallium arsenide IR source mounted in front of each eye. The dominant eye was tracked based on recent information from the literature which indicates that the dominant eye can be as much as 100 to 500 msec behind the non-dominant eye for certain types of eye movement (example: vergences). Eye dominance may not be a factor in these tests, but since only one eye can be tracked horizontally, the decision was made to track the dominant eye. The test used for eye dominance is the "hole-in-the-card-test" which is as follows: a hole, two to three inches in diameter is cut in an ordinary piece of cardboard and the subject asked to sight an object at about four meters distance through the hole (both eyes open). Closing one eye and then the other should make it obvious by observing parallax effects, which eye is dominant for that subject. The eye tracker was then adjusted to track the dominant eye horizontally. The operating principle of the eye movement monitor depends on detecting the changes in reflected light between the white sclera and the left and right sides of the iris. The eye tracker can track $\pm 20^\circ$ horizontally to an accuracy of $1/4^\circ$ depending on calibration.

The output from the eye tracker was fed into the electronic delay circuit which can vary the delay from 17 to 125 msec. This signal was then transmitted to the servo which rotated the mask the required amount to keep the high resolution area along the line of sight.

The image generation system to be used with the HMD has a given delay time before a new scene is presented to the observer. Throughput delay measurements were made because an indication of the objectionability of this delay time is highly desirable. It may be necessary to compensate for this delay in the final system. Parallel studies are underway dealing with methods of compensating for the CIG delay.

Twenty one masks were used in these tests. The characteristics for the various masks are shown in Table 1. Fourteen subjects were used, two of whom were pilots.

Resolution profiles were obtained for each mask by projecting an annular, high-contrast bar chart and reading the limiting resolution at one point on the screen while the mask was rotated. Figure 7 shows the resolution profile for mask 2C. The luminance profile was also obtained for each mask by using a Spectra Pritchard Photometer set up at eye viewing position and rotating the mask. Figure 8 shows the luminance profile for mask 2C. This luminance profile shows the extreme of brightness falloff which the eye finds acceptable, but it is not recommended for the final systems.

Judgements were obtained by asking each subject to rate the display on a scale of 1-4 with the following rating designations: 1 = ideal; 2 = noticeable degradation; 3 = objectionable degradation; and 4 = degradation

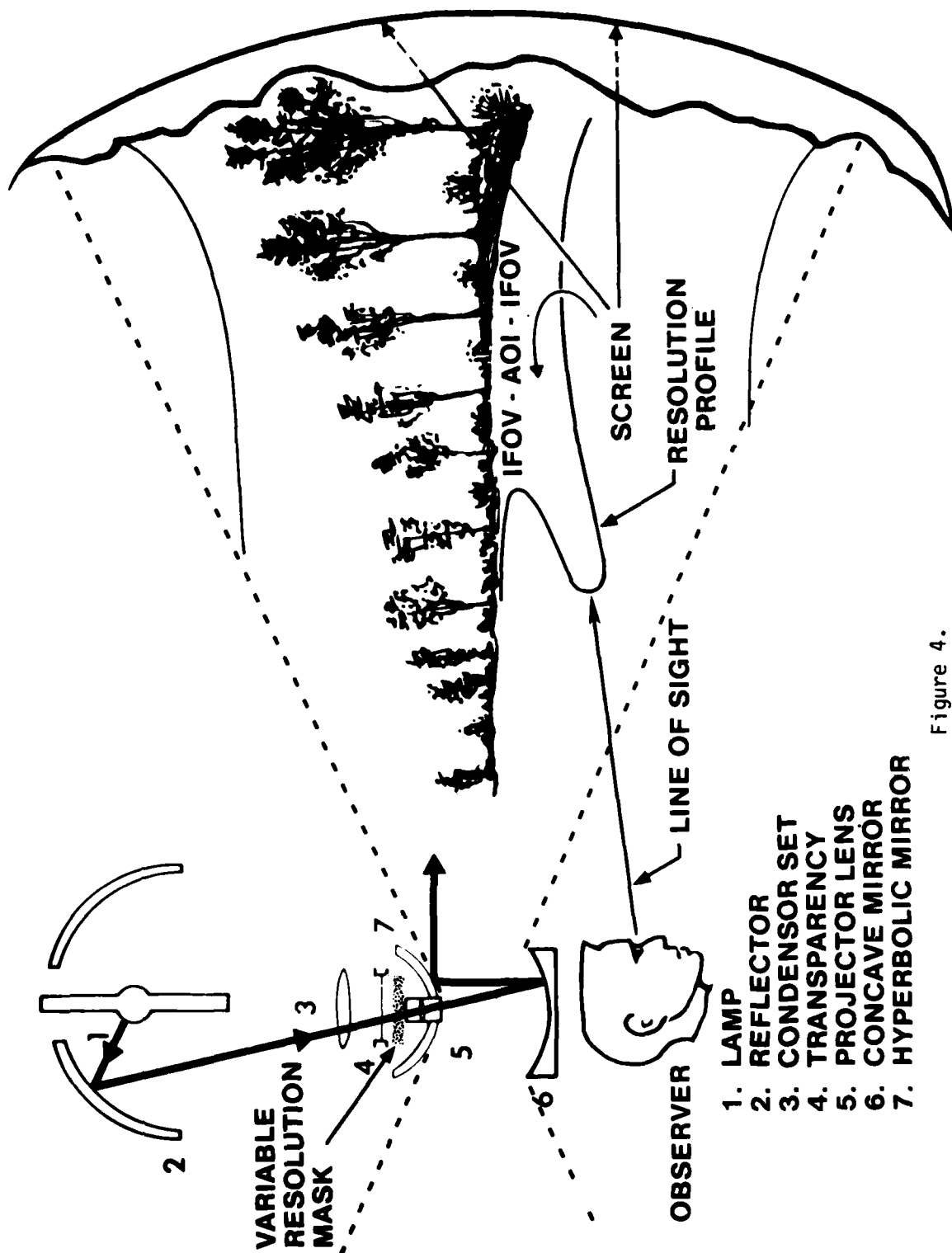


Figure 4.

Annular Panoramic Projection Devices with Modification

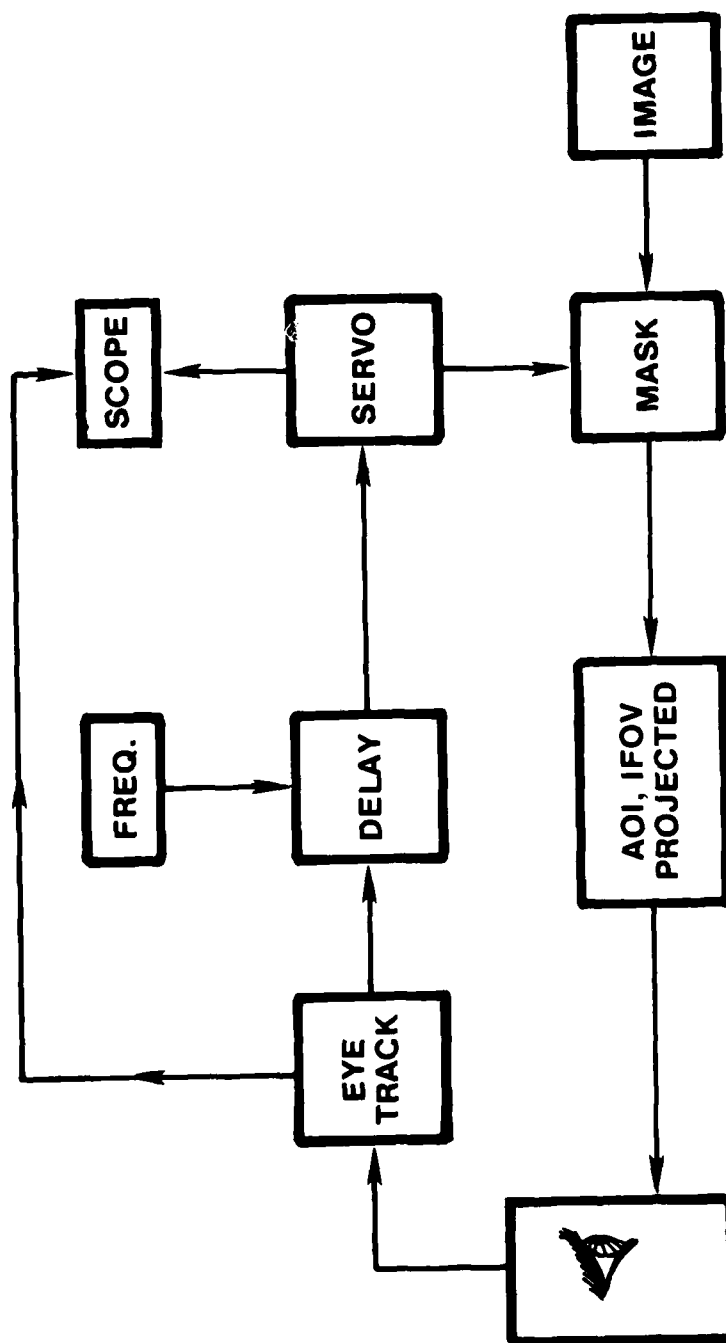
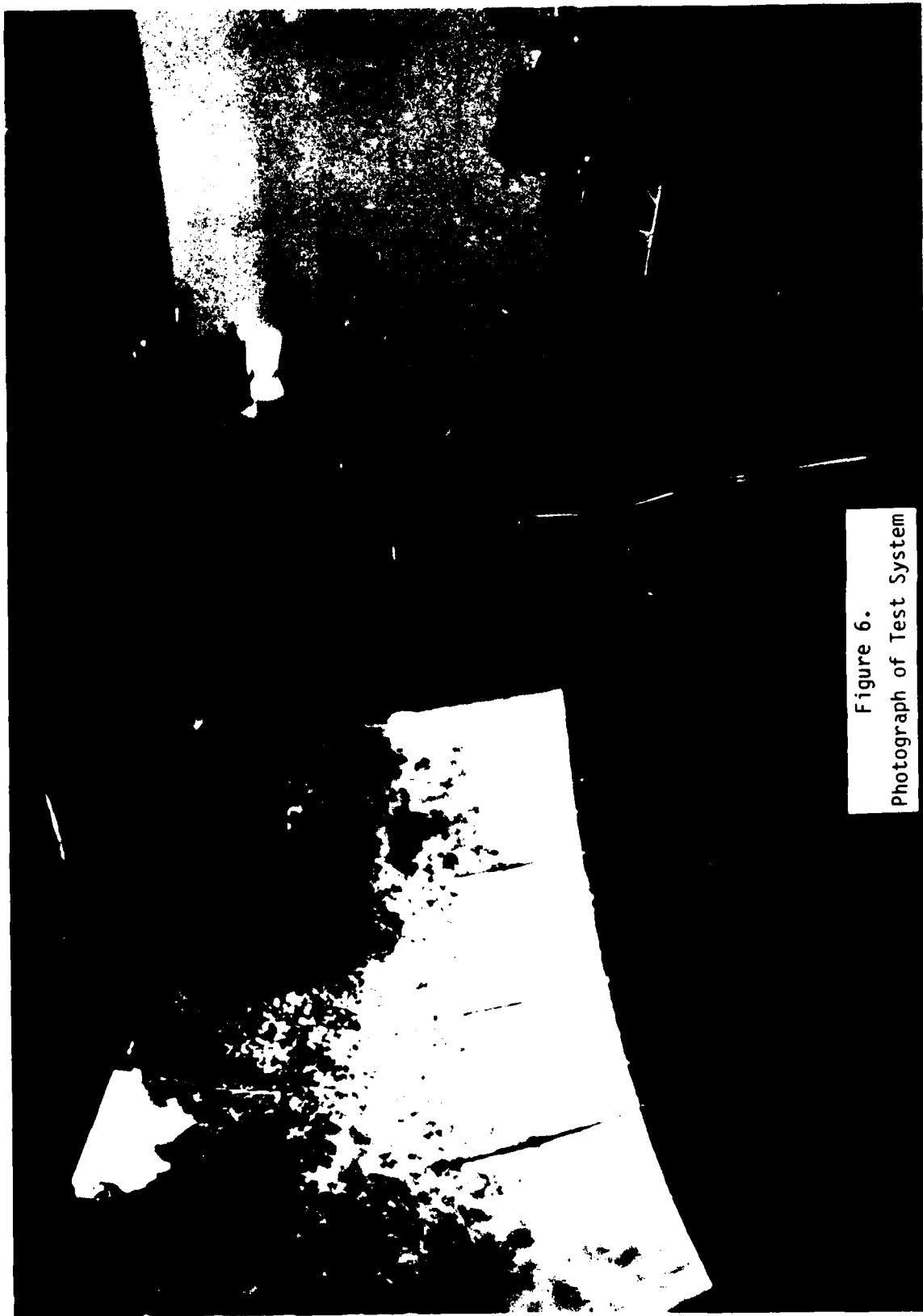


Figure 5.
Vision Model Test System



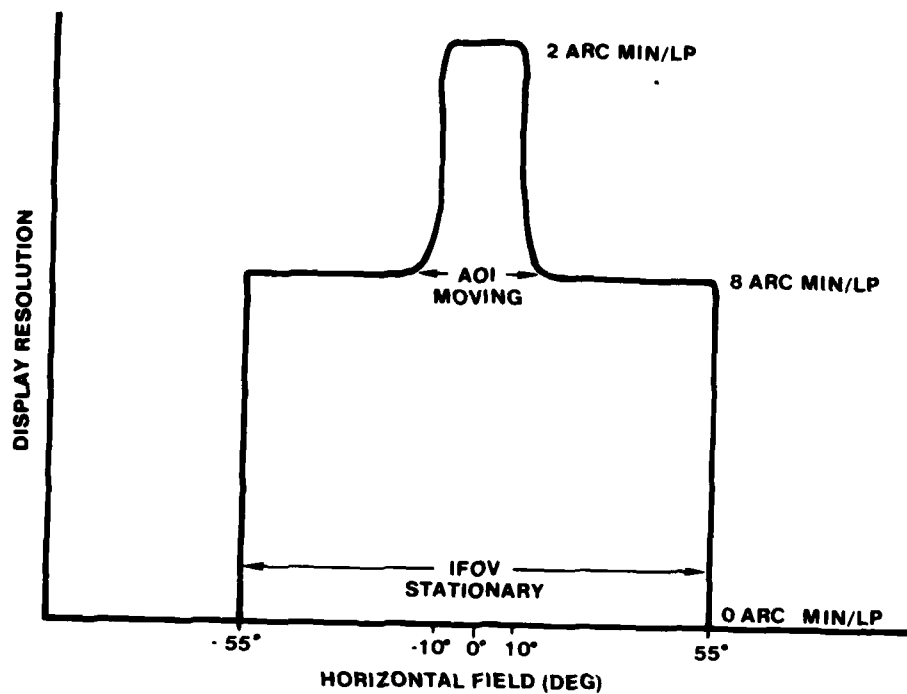


Figure 7.
Mask Resolution Profile

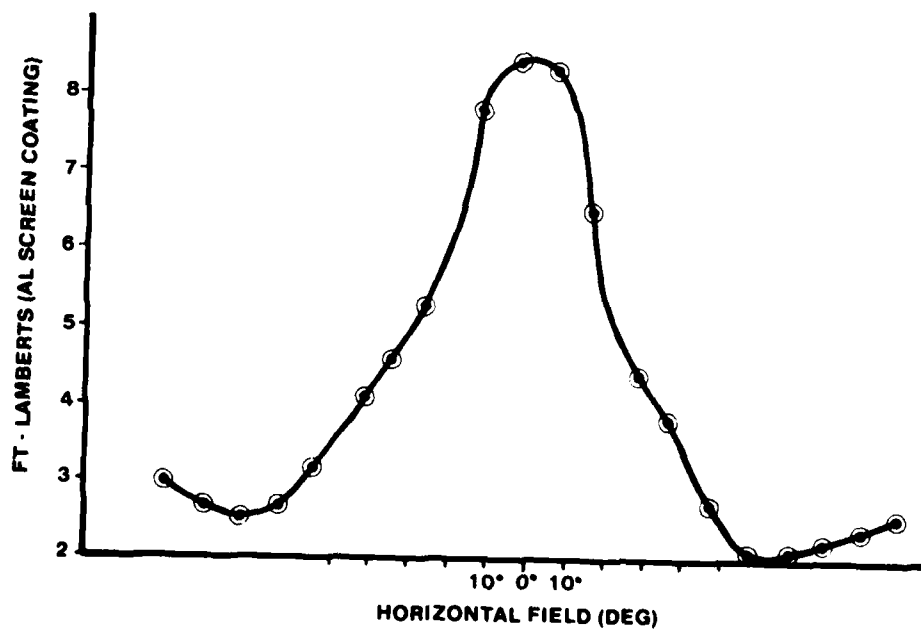


Figure 8.
Mask Luminance Profile

TABLE 1. MASKS USED

MASK Number	SIZE AOI	SIZE IFOV	SURROUND
1a	15°	70°	Black
1b	15°	90°	"
1c	15°	110°	"
1e	15°	180°	"
2a	20°	70°	"
2b	20°	90°	"
2c	20°	110°	"
2d	20°	130°	"
2e	20°	180°	"
3a	30°	70°	"
3b	30°	90°	"
3c	30°	110°	"
3d	30°	130°	"
3e	30°	180°	"
4	40°	Same as AOI	"
5	90°	"	"
6	90°	"	Grey
7	110°	"	Black
8	20°	90°*	Grey
9	20°	90°*	Black
10	20°	110°*	"

* Eye tracked with AOI

expected to impair operator performance. At the start of each test, the subject observed the display without the mask but with all other test conditions in use, i.e., glasses on, etc. This was done to give the subject a baseline for judging the degradation in the display as various masks were used. The subject was not told the characteristics of the mask or the delays being used while tests were in progress.

A subjective analysis of discriminable kinds of degradation phenomena was also made. Degradation phenomena were described by the phrases: edges AOI visible; drop in resolution visible; edges IFOV visible; granularity of mask in low resolution area visible; and brightness fall-off visible. Additional subjective comments were solicited from subjects and recorded.

CONCLUSIONS

In analyzing the parameters used and the results of these experiments, it must be kept in mind that these tests were designed and conducted for a very specific purpose, i.e., to aid in defining acceptable input specifications for the Helmet Mounted Display being developed at NTEC. The tests should not be viewed as comprehensive vision model tests. In order to reduce the range of vision model parameters requiring testing, HMD system constraints were used based on simultaneous effort on, for example, design of an acceptable projection lens. In addition, the following test equipment limitations are noted: (a) tests were conducted with a high detail static scene; (b) only horizontal servoing of AOI, IFOV was possible; (c) real imagery, not CIG imagery, was used (additional tests are required to test CIG images, i.e., "popping" in of CIG edges as the level of detail changes needs to be addressed); and (d) conclusions here are based on eye tracking - resource limitations have not allowed for head tracked experiments to be completed as yet.

The averaged ratings obtained from test subjects for two groups of masks are given in Figure 9 and Figure 10. Figure 9 shows the results for IFOV held constant and stationary at 130° with the AOI varying to 15°, 20°, and 30°. As can be seen from the graphs, the larger AOI resulted in more favorable overall responses. Figure 10 shows the results for masks where AOI was held constant at 30° while the IFOV varied from 70° to 130°. Statistical analysis indicates that there is a significant difference between the graphs shown. To illustrate that the range of ratings and the masks are compatible, Figure 11 shows the range of response for various masks from an individual.

Subject comments were also recorded. Some of the more pertinent comments related to various masks are:

Masks 4, 5, 6 and 7: The motion of a black, sharp edge tracked by eye movement was very annoying and apparent, more so with smaller IFOV, but still noticeable with larger IFOV. Masks 4, 5, and 7 went from a four rating to approximately 2.5. When the area surrounding the IFOV was grey, the motion was less annoying (mask 6).

Masks 1a, 1b and 1c: AOI not bad except as delay increases. This results from the requirement to track the eye more closely when AOI is smaller. Because of CIG delay (~ 80 msec), this AOI (15°) is most likely not acceptable unless some method is used to compensate for this delay.

Masks 2a, 2b, 2c, 2d and 2e: 70° and 90° IFOV could be seen by all subjects. With small delays AOI was somewhat noticeable, but not objectionable to most observers. One subject commented, "Judgements apply only to non-task loaded situation. A minor distraction, such as short lag, might be noticeable when I have nothing better to do than to look for it, but

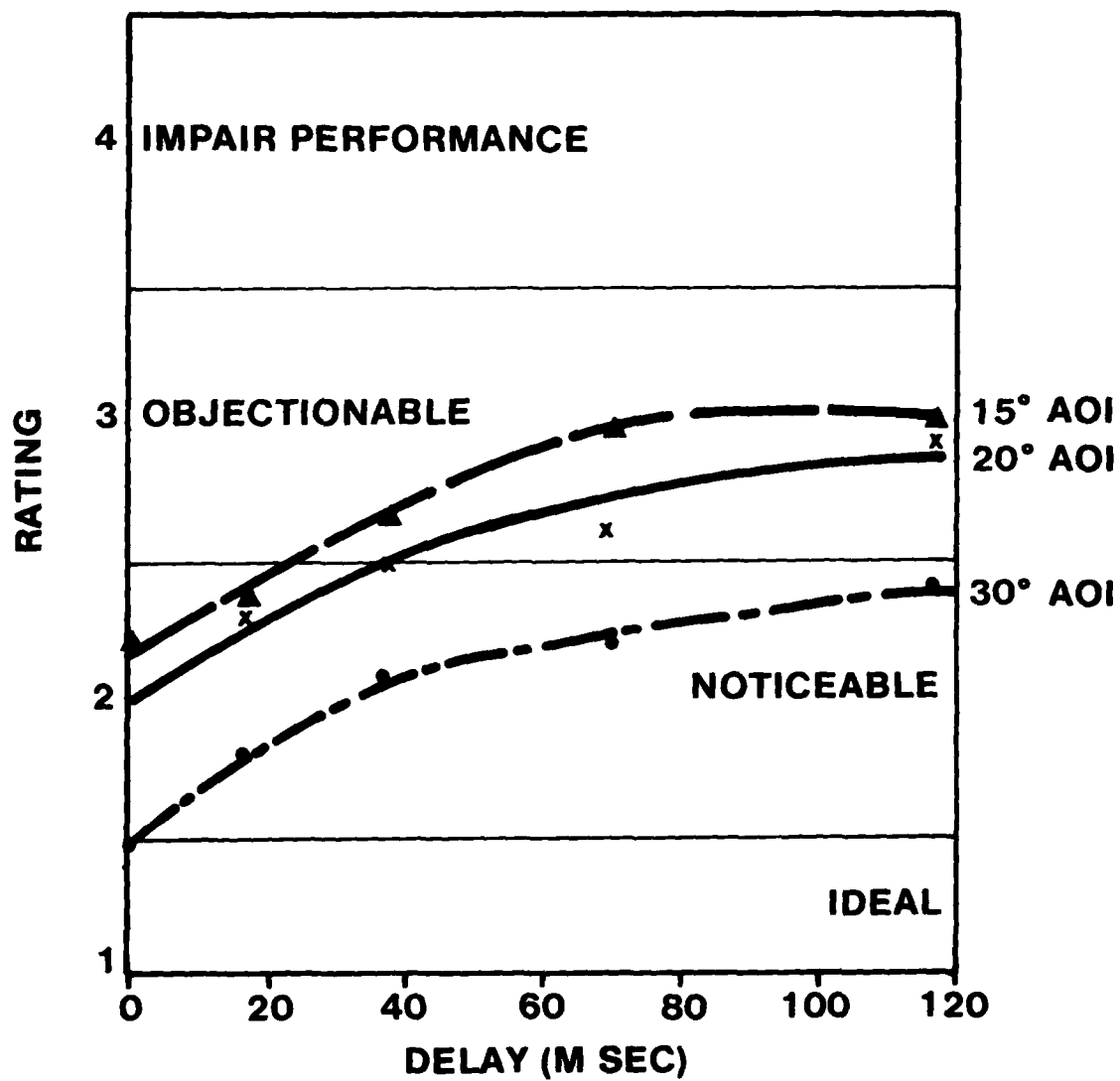


Figure 9.
Average Rating (IFOV Constant)

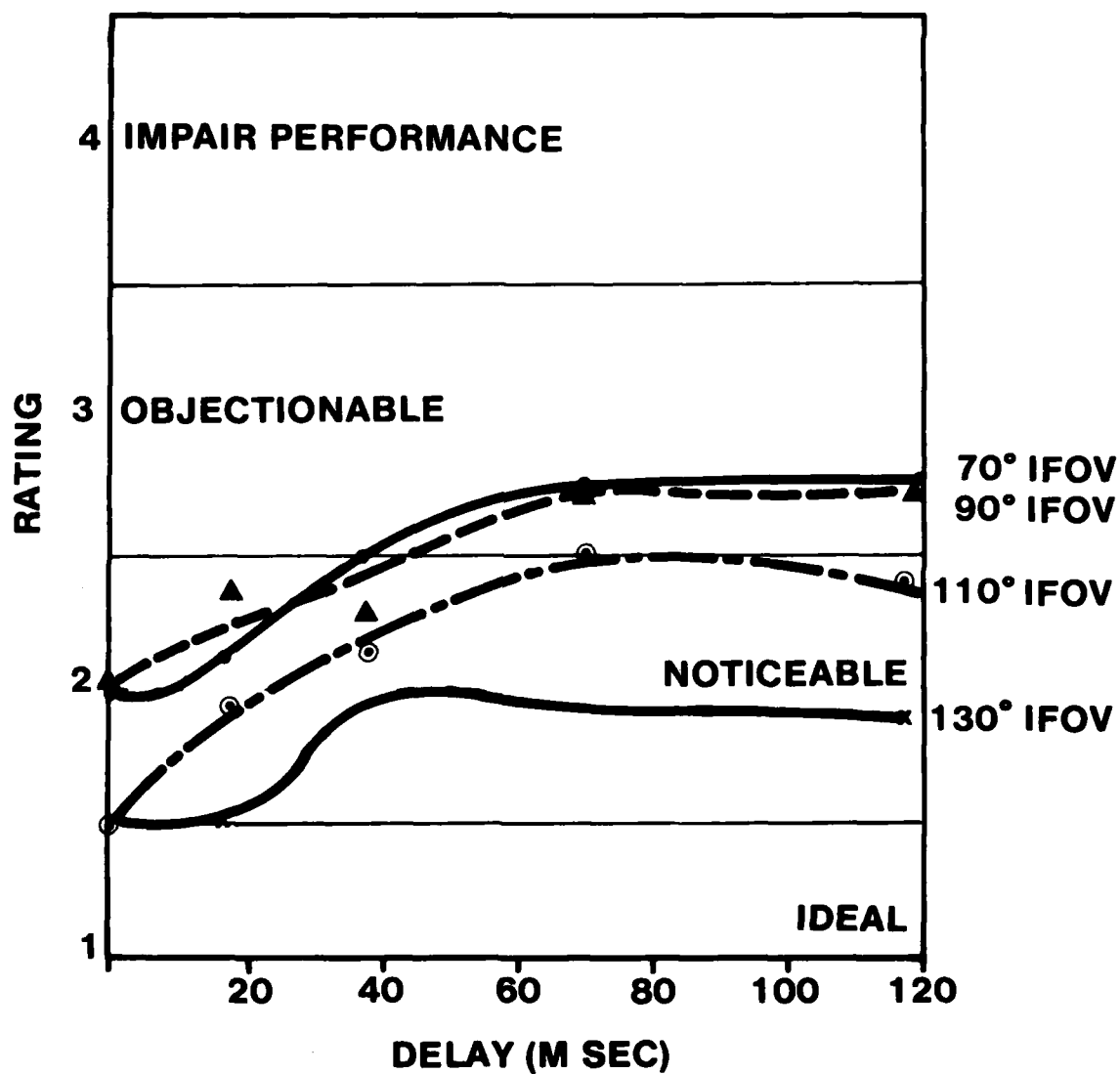


Figure 10.
Average Rating (AOI = 30°)

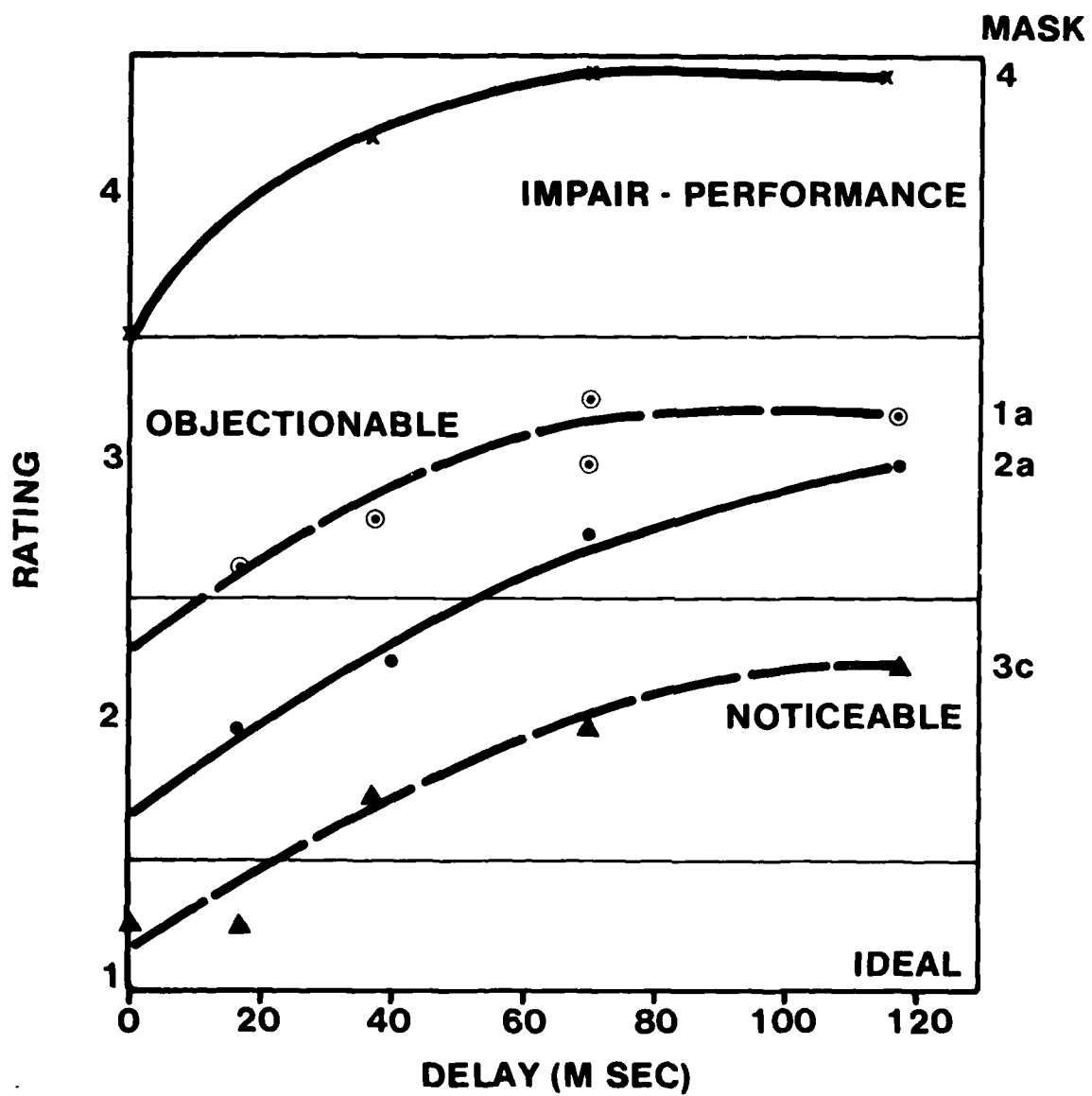


Figure 11.
Range of Responses

might go unnoticed if I were involved in a task . . ." A second subject commented, "Good for a simulator display--looks as good as a camera model board system (up to 70 msec delay). Resolution drop was no problem, but brightness drop and mask granularity were noticeable at longer delays." A third subject commented, "The picture is so detailed that its easier to pick up a drop in detail. Eye movements are so fast that "motion" can be picked up when mask is eye tracked." A fourth subject commented, "Brightness drop and granularity of mask were more of a problem than resolution drop." It should be noted that granularity in the low resolution area was a function that the mask used to drop the resolution off axis, and will not be present in the final system.

Masks 3a, 3b, 3c, 3d and 3e: 70° and 90° IFOV could be seen by all subjects. Even with maximum delay, the degradations were noticeable but not objectionable to subjects.

Mask 3d: One subject commented, "No problem using." A second subject commented, "I'm impressed." A third subject commented, "I can see the degradation, but it wouldn't be a problem for most tasks in a simulator."

In conclusion, based on these vision model tests and other system design constraints, the following performance parameters were chosen for the HMD system: AOI = 25° with soft, blended edges; IFOV \geq 120° with soft, blended edges; acceptable resolution drop, AOI/IFOV \geq 5/1; acceptable luminance drop, AOI/IFOV \geq 2.9/1. These parameters are compatible with other system constraints and are being incorporated into the Helmet Mounted Display System.

ACKNOWLEDGEMENTS:

Many people at NTEC have contributed to the tests described here. In the Simulation Technology Branch (Code N-731) of the Advanced Simulation Concepts Laboratory (Code N-73): Rich Hebb developed techniques to fabricate the masks and conducted tests; John Dillard aided in setting up the test equipment and conducted tests; John Allen designed and assembled the delay circuit; Paul Grimmer did mechanical design and drawings for various subsystems. In the Human Factors Laboratory (N-71), Stan Collyer and Gil Ricard provided consultation on the test procedure and data analysis. NTEC's Shop (N-72), under the direction of Joe Porthouse, fabricated and installed many of the subsystems.

CLOSING REMARKS

Dr. Earl A. Alluisi
Chief Scientist, Air Force Human Resources Laboratory
Brooks Air Force Base, San Antonio, TX



Earl A. Alluisi is Chief Scientist of the Air Force Human Resources Laboratory, Brooks Air Force Base, San Antonio, Texas, on assignment since January 1979 under provisions of the Intergovernmental Personnel Act of 1979, from Old Dominion University (university professor of psychology). He was awarded the Ph.D. degree in psychology by The Ohio State University in 1954. He has held appointments at the University of Louisville, the Lockheed-Georgia Company, Emory University, Stanford Research Institute, the Lockheed Missiles and Space Company, the Army Medical Research Laboratory, and the Aviation Psychology Laboratory at The Ohio State University. He was corecipient of the Jerome H. Ely award of the Human Factors Society in 1970, and received the Franklin V. Taylor award of the Society of Engineering Psychologists in 1971. He is a past president of Divisions 19 and 21 of the American Psychological Association, the Southern Society for Philosophy and Psychology, the Kentucky Psychological Association, and the Tidewater Chapter of the Human Factors Society. He is (1980-1981) president of the Human Factors Society, and author or coauthor of more than 180 research reports and publications.

